University of Alberta Library
0 1620 2701888 4

THE UNIVERSITY OF ALBERTA

Design of Shallow Tunnels in Soft Ground

by

Arsenio Negro Jr.

VOLUME II

A THESIS

SUBMITTED TO THE FACULTY OF GRADUATE STUDIES AND RESEARCH
IN PARTIAL FULFILMENT OF THE REQUIREMENTS FOR THE DEGREE
OF Doctor of Philosophy

Department of Civil Engineering

EDMONTON, ALBERTA

SPRING 1988

Ex Libris
Universitatis
Albertensis

THE UNIVERSITY OF ALBERTA

Design of Shallow Tunnels in Soft Ground

by

Arsenio Negro Jr.

VOLUME II

A THESIS
SUBMITTED TO THE FACULTY OF GRADUATE STUDIES AND RESEARCH
IN PARTIAL FULFILMENT OF THE REQUIREMENTS FOR THE DEGREE
OF Doctor of Philosophy

Department of Civil Engineering

EDMONTON, ALBERTA
SPRING 1988

UNIVERSITY LIBRARY
UNIVERSITY OF ALBERTA

estimates of the factor of safety. The stability verification is preferably performed by traditional plasticity solutions, such as those derived from the Lower Bound Theorem, which in theory, furnishes safe estimates of the collapse loads.

A fairly large number of plasticity solutions appeared over the last decade, most of them resulting from research work conducted in Cambridge, U.K. These solutions have been mainly tested through physical modelling, where they showed considerable potential for practical application. Notwithstanding this, their use in practice is conditional on the validity of the assumptions made in their development. A more detailed discussion on some of these assumptions is presented in Section 6.5.2, where these solutions are used to assess the limiting conditions for the application of a design procedure whose development is presently projected.

Briefly, in the application of the Lower and Upper Bound Theorems of Plasticity (see Calladine, 1969) to the shallow tunnel problem, it is customary to introduce the following assumptions:

a) the soil is homogeneous;
b) the problem is time independent;
c) the collapse load is unique;
d) the soil has an associated flow rule;
e) the soil has a perfectly plastic behaviour.

There are solutions that relax some of these assumptions. For example, Gunn (1984:13), developed a lower bound solution for a frictionless heterogeneous soil with an undrained strength increasing linearly with depth. Also, there are solutions that introduce other simplifying assumptions, such as a soil with zero body forces (the driving force being a surcharge at the surface), a uniform internal tunnel pressure, etc.

The solutions available do not recognize time dependent effects resulting from changes in pore pressures and effective stresses, as they operate in terms of total stress changes. A rather simplified assessment of this problem was made in Section 3.3.4.4, where it was analysed in mere qualitative terms. Some of the problems related to assumptions (c) and (d) are discussed in Section 6.5.2.

It appears that very little has been investigated regarding the consequences of assumption (e). Muhlhaus (1983) was one of the few who attempted to study the effect of the soil deformations prior to collapse of the shallow tunnel. A specially designed finite element code was developed to study the problem, which seems to have avoided numerical difficulties normally encountered as the collapse condition is approached. He presented results suggesting that collapse loads assessed by the method of characteristics (a lower bound solution) may be larger, thus less safe, than those calculated including the effect of ground displacements prior to collapse. Muhlhaus (Op.cit.)

used a non-linear elastic homogeneous material to represent the soil. He noted that a better agreement between the plasticity solution collapse load and that given by his solution is found as the soil becomes stiffer, and therefore closer to the rigid-plastic assumption.

These limitations indicate that the use of the plasticity solutions in practice should be undertaken with due care and be understood as an approximation, which is not unlike many other similar procedures normally used.

In the present section, an attempt is made to survey the available shallow tunnel plasticity solutions. No attempt is made here to review in detail or to apply the existing methods to practical situations. A more detailed description, as well as examples of applications of some of these solutions are presented in Chapters 6 and 7.

Accordingly, Table 4.12 was prepared to summarize the survey undertaken. In it, each method of shallow tunnel stability assessment is identified by its author. The types of stability problems addressed were classified into five groups, following the more important instability mechanisms discussed in Section 3.2:

a) face instability;
b) face and heading instability;
c) heading instability;
d) plane strain (P.S.) tunnel instability;
e) local instabilities.

	Author/Year	Stability Problem	Type of Solution	Soil Self-Weight	Strength Condition	Geometric Approach	Solution Presentation	Comments
1.	Casarin (1977:67), Mair (1979:134)	Face	UB	No	U	3D	Equation	Circular shaft failure
2.	Davis et al (1980:409)	Face	UB	Yes	U	3D	Chart	Elliptical and inclined shaft failure
3.	Davis et al (1980:408, 409)	Face	UB	Yes	U	2D	Equation	Long wall face; liner roughness does not affect
4.	Britto and Kusakabe (1985)	Face	UB	No	U	3D	Chart	Composed circular shaft failure
5.	Davis et al (1980:407, 409)	Face	LB	Yes	U	2D	Equation	Smooth lining
6.	Davis et al (1980:409)	Face	LB	No	U	3D	Equation	Thick cylinder approximation
7.	Davis et al (1980:409)	Face	LB	No	U	3D	Equation	Thick sphere approximation
8.	Casarin and Mair (1981)	Face	LB	No	U	2D	Chart	Long wall face; stress characteristics solution
9.	Casarin (1977:68)	Face and Heading	UB	No	U	3D	Chart	Square tunnel
10.	Muhlhaus (1985:50)	Face and Heading	LB	No	D	3D	Equation	Thick sphere approximation; zero tunnel pressure
11.	Casarin (1977:66)	Heading	UB	Yes	U/D(c=0)	3D	Equation	Approximate solution
12.	Caquot and Kerisel (1956:478)	P.S. Tunnel	LB	Yes	U/D	2D	Equation	Consider internal fluid pressure
13.	O'Escatha and Mandel (1974)	P.S. Tunnel	LB	Yes	U/D	2D	Charts	With and without fluid pressure; stress characteristics
14.	Seneviratne (1979:76)	P.S. Tunnel	LB	No	D(c=0)	2D	Equation	Corrected Atkinson and Cairncross (1973:203); solution not complete
15.	Muhlhaus (1985:44)	P.S. Tunnel	LB	Yes	U/D	2D	Equation	Uniform internal pressure

Table 4.12 Features of some Methods for Ground Stability Verification

Author/Year	Stability Problem	Type of Solution	Soil Self-Weight	Strength Condition	Geometric Approach	Solution Presentation	Comments
16. Atkinson and Potts (1977:210)	P.S. Tunnel	LB	No	D(c=0)	2D	Equation	Complete solution
17. Atkinson and Potts (1977:211)	P.S. Tunnel	LB	Yes	D(c=0)	2D	Equation	Complete solution
18. Seneviratne (1979:75)	P.S. Tunnel	UB	No	D(c=0)	2D	Equation	Correction of Atkinson and Cairncross (1973:204) solution
19. Atkinson and Cairncross (1973:203)	P.S. Tunnel	LB	No	U	2D	Equation	Also at Davis et al (1980:400)
20. Seneviratne (1979:79)	P.S. Tunnel	LB	Yes	U	2D	Chart	Stress characteristics; also at Davis et al (1980)
21. Gunn (1984:12)	P.S. Tunnel	LB	No	U	2D	Equation	Retangular tunnel
22. Gunn (1984:13)	P.S. Tunnel	LB	No	$U(C_u(Z))$	2D	Equation	C_u varying linearly with depth
23. Mair (1979:119)	P.S. Tunnel	UB	Yes	U	2D	Chart	Solution independent of self-weight; 4 mechanisms
24. Atkinson et al (1975:84)	Local collapse-roof	UB	Yes	D(c=0)	2D	Equation	Wedge failure; also at Atkinson and Potts (1977:212)
25. Davis et al (1980:411)	Local collapse-face	UB	Yes	U	2D	Equation	Long wall face
26. Davis et al (1980:411)	Local collapse-face	UB	Yes	U	3D	Equation	Circular tunnel face
27. Davis et al (1980:412)	Local collapse-face	LB	Yes	U	2D	Equation	Solution is depth independent; long wall face
28. Davis et al (1980:411)	Local collapse-P.S.	UB	Yes	U	2D	Equation	
29. Davis et al (1980:411)	Local collapse-P.S.	LB	Yes	U	2D	Equation	Solution depends on relative tunnel depth

Table 4.12 Features of some Methods for Ground Stability Verification (Continued).

For the face stability assessment, it is always assumed that the tunnel contour is entirely lined, up to the plane vertical tunnel face. All solutions in this group assume the tunnel to be full face excavated and that the lining is perfectly rigid. Some of them assume the lining-soil interface to be 'smooth', but most assume it to be 'rough'. They all furnish a critical internal tunnel pressure (for example, a fluid pressure), uniformly applied to the face, in problems where the driving forces are represented by surface surcharge loads and/or the ground self-weight. A discussion on the effect of the uniformly applied internal pressure at tunnel face is presented by Davis et.al. (1980:413).

The second group treats the combined stability of the face and of the unlined heading zone and the third focuses only the stability of this unlined zone. In all case, once more, the rest of the tunnel is supposed to be fully supported by some stiff lining. The solutions assume that an internal tunnel pressure acts against the unlined heading, except in that by Muhlhaus (1985:50), which assumes this pressure to be zero. The latter furnishes the critical unsupported heading length causing ground collapse.

The fourth group treats the case of the two dimensional stability of an unlined tunnel in plane strain condition, and furnishes the value of the internal tunnel pressure causing collapse.

While the former solutions postulate a complete collapse of the ground mass, the fifth group addresses the problem of localized instabilities, which may occur even though the overall stability of the ground mass is secured. Three sub-classes are assigned within this group according to the place where this instability process is identified: at the tunnel face, tunnel roof and tunnel walls in a plane strain condition. In undrained conditions, local instabilities may develop regardless of the value of the uniform tunnel pressure, and in some cases, regardless of the relative tunnel depth. Local collapses in these conditions, are found to be mainly dependent on the undrained strength ratio, $c_u/\gamma D$. The size, D, of the excavated opening is controlled by local collapse conditions.

Table 4.12 also identifies the type of plastic solution used in each method. Typically, two classes of solutions are included: lower bound (LB) and upper bound (UB). These solutions are sometimes derived analytically when they are presented explicitly through an equation, or numerically when they are defined for certain ranges of variables and are usually presented in charts. For simpler situations, stress fields can be postulated and explicit lower bound solutions can be found. Complex cases, for instance when the soil body forces are taken into account, require numerical approaches, usually implementing the method of stress characteristics. Upper bound solutions always require a critical tunnel pressure to be found, associated with a certain collapse mechanism. This is achieved after maximizing the value of the tunnel pressure with respect to the variation of a dimension or an angle that geometrically defines the mechanism. This optimization process can be done either analytically or numerically, depending on the complexity of the problem.

Two classes of geometric approximations are involved in the solutions included in Table 4.12. For instance, the face stabiliity problem can be approached three-dimensionally, as it should, or a two dimensional approximation may be considered. If this is the case, the actual 3D problem is reduced to that of the stability of a long wall mining face.

Two types of ground strength conditions are usually considered: undrained (U) or drained (D). In the first case, the soil is assumed to be frictionless with its strength defined by its undrained cohesion. In the second case, the soil is assumed to be frictional and the cohesive strength component (c) may or may not be considered.

In most cases, the tunnel cross section is assumed to be circular, though some solutions assume other tunnel shapes (square, rectangular, long wall).

None of the above methods yield the correct collapse conditions, which is theoretically approximated by maximizing the upper bound tunnel pressure and by minimizing the lower bound solution.

A definition of the factor of safety was introduced in Chapter 2 and its calculation, using the above methods is exemplified in Section 6.5.2.

This survey indicates that though a large number of solutions is available for a variety of stability problems, some important conditions are not covered by these existing methods. For instance, there are no upper or lower bound solutions for the 3D face stability problem under drained conditions (i.e. for a frictional and cohesive soil). This particular situation could be approximated by the stress field solutions put forward by Mandel and Halphen (1974) (not included in Table 4.12). By this approach, the tunnel face would be approximated by a spheric cavity in a plastic domain with drained or undrained strengths, under the action of gravity that these authors considered.

Among those that treat the two dimensional tunnel stability problem (P.S. tunnel), the solution by D'Escatha and Mandel (1974) is the most general. It considers both drained and undrained strength conditions as well as the soil self weight. For this reason, this particular solution will be presented later in this thesis (Chapters 6 and 7). As it derives from the method of stress characteristics, it is a lower bound, and therefore 'safe' solution.

A serious limitation of all these solutions is the fact that they are unable to consider the effect of pore pressures in the ground stability problem. Under certain circumstances, it is known that the stability of the ground is totally controlled by the groundwater condition. Seepage action may have a controlling role in the three dimensional tunnel face and heading stability. This class of problem is usually treated in practice, using simplified limit equilibrium analyses, with pore pressure calculated from flow nets (see Sections 3.3.4.2 and 4.2.3).

4.4 Survey of the Current Design Practice

4.4.1 Foreword

In this section an attempt is made to analyse some aspects of the current practice in geotechnical design of shallow tunnels. Two of the three major design activities (see Section 4.2) are reviewed herein: the prediction of lining loads and the prediction of ground displacements. The third activity, the ground stability verification, is not covered by the present survey. This exclusion reflects a decision to focus on topics directly related to the aims of the present research, and should not be understood as a disregard of this equally important design activity.

For the first design aspect, the review of the current practice on lining load prediction was based on a survey carried out earlier by the International Tunnel Association. A similar survey was conducted by Sgouros (1982:36). The results of this study, however, were of limited value as they represented only the design practice in the United States. In addition, this survey was largely based on personal interviews, which did not seem to have been arranged in a format that would allow comparative or statistical analyses of the results.

For the second design aspect, a specific inquiry was organized to cover the current practice on ground settlement prediction, in a large segment of the international designer's community.

The following sections present the details on how the inquiries were undertaken, the results of the surveys and, finally, their interpretations.

4.4.2 Prediction of Lining Loads

4.4.2.1 Survey of Practice

The lining design practice as it stood in the late seventies and early eighties was surveyed by a working group on structural design models for tunnelling, set up by the International Tunnelling Association (ITA). This was done by means of a questionnaire sent to ITA member nations in December 1978. The questionnaire focussed not only on shallow tunnels in soil, but also cut and cover tunnels and deep tunnels in moderately hard rock. The results of the survey, including the questions formulated, a summary of the answers, and the list of the respondents were presented in a report by Duddeck (1982). He was the co-ordinater of the working group, "Views on Structural Design Models for Tunnelling: Synopsis of Answers to a Questionnaire, May, 1981 " (published in "Advances in Tunnelling Technology and

Subsurface Use", Vol. 2, no. 3, 1982, Pergamon Press).

This section will review and re-interpret some of the results of this survey solely on what is pertinant to the practice related to soil tunnelling. It should be pointed out that the analyses and subsequent syntheses to be presented in the next items, resulted from the writer's interpretation of the responses to the ITA questionnaire as they appeared in descriptive form, (Duddeck (Op.cit)). This, in turn, is a condensed form of the original replies as prepared by the ITA working group. Although it had been submitted and proofed by the original respondents in August, 1980, (Duddeck, Op.cit.:161), it may include some interpretation by the working group members who prepared the condensation. Despite all attempts made by the writer and most likely by those who prepared the condensation, to depict an unbiased and faithful picture of the original responses, some inaccuracy might have been introduced in the condensation process. It is believed however, that, if any inaccuracy exists at all, it should not affect the main conclusions or the broad statistical trends that will be discussed.

The questionnaire was preceded by a statement on general motivations, and to get replies as specific as possible, the respondents were invited to answer the questions twice, for two ideal tunnelling situations. The first situation referred to a 6 m diameter tunnel with 8 m of ground cover, driven by a shield machine in a soil with properties shown in Table 4.13. This could represent a subway tunnel driven through a fairly cohesive soil, with a strength and stiffness greater than those of the overconsolidated Frankfurt clay. The second situation referred to a tunnel mined through a stronger and stiffer soil, with identical geometry. The stiffness of this soil is not dissimilar to that observed in the clay marl layers of Munich Tertiary Sediments, however at a higher depth. The strength properties, though, are appreciably higher than Munich "Flinzmergel", particularly regarding the cohesive component. Also dissimilar to Munich's condition is the absence of ground water. Tunnel construction in this second condition was done using shotcrete and steel arches for support, as in the NATM.

Only 47% of the respondents answered the questionnaire for the two situations envisaged. The remaining 53% provided answers to either one or other condition. Hence, differences in the answers to each question, as applied to the shielded or mined tunnel, may reflect different views in treating the design of tunnels built by distinct construction methods, as well as different design attitudes for distinct ground conditions. It may also be a reflection of different personal views, as distinct individuals replied to the questions associated with each tunnelling situation. To some extent this was an unfortunate circumstance regarding the survey preparation and results. It partly impaired a definite identification of distinct design attitudes (if

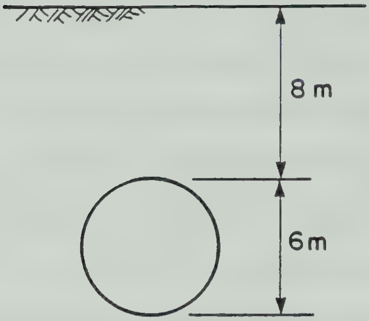

Ground Conditions and Properties	Shielded Tunnel Situation	Mined Tunnel Situation
Friction Angle	25°-30°	30° -35°
Cohesion (kPa)	100-200	300-400
Modulus of Soil Stiffness (MPa)	30-40	100-200
Density (KN/m^3)	20	20
Groundwater Level	2-15 m below surface	no groundwater (only small amounts of seeping water)

Table 4.13 Envisaged Ground Conditions for Response of Questionnaire on Lining Design (modified after Duddeck, 1982:173)

any) regarding distinct construction techniques. These facts should be borne in mind when analysing the results that follow. It could be said that in both cases, the tunnelling conditions are very favourable. Both grounds show high cohesive strength which reduces the risk of stability problems during excavation, and high stiffness whicha allow one to anticipate relatively small ground displacements upon standard tunnelling construction.

The questionnaire was prepared, including motivation and explanations, with 25 questions. Most of these demanded descriptive answers. but 4 questions were prepared in a multiple choice form, allowing the respondents to mark more than one answer per question. These questions were reproduced by Duddeck (1982:163) and will not be included here. Only those questions deemed relevant to the present work will be discussed. These refer mainly to the procedures for lining load prediction, including the statical system used for calculation and the ground loads. Questions related to other types of loads, site investigations, structural safety of the support and field monitoring will not be addressed here. Their answers can be found in Duddeck (Op.cit.)

The questionnaire was replied to by 19 respondents from 12 countries. The return rate is not known, as the number of questionnaires sent was not disclosed. Nine of the total number of respondents answered the questionnaire for both types of tunnelling situation. Five of them replied to the questions as it applied to shielded tunnels and another five answered the questionnaire for mined tunnels. Table 4.14 lists the number of respondents and responses for both tunnel situations and shows the representation of each country and region in the survey conducted. As it is seen the survey on lining design for shielded tunnels represents mainly the European practice (57%). On an individual country basis, the answers coming from the U.S.A comprise 21% of the total responses, followed by the United Kingdom and West Germany, each contributing 14%. Regarding the lining design for mined tunnels, the results of the survey represent, again, mostly the European practice (71%) and the two countries that mainly contributed with answers were West Germany (21%) and the United Kingdom (14%).

As noted by Duddeck (1982:165), the questionnaire was intended to be answered by "those engineers who prepare tenders and who actually design tunnels, not from scientists who may tend to say what ought to be done". However, it was not possible to assess with accuracy the actual type of practice of the respondents, since their technical background was not clearly identified, from the information made available. Nevertheless, it is believed that more than half of the responses reflect the intended view of consultants and contractors (in more or less equal parts).

Region/Country	No. of Respondents	Shielded Tunnels No. of Responses	Shielded Tunnels % of Total	Mined Tunnels No. of Responses	Mined Tunnels % of Total
Europe					
Austria	1	1	7	1	7
Belgium	1	1	7	-	-
France	1	1	7	1	7
W. Germany	4	2	14	3	21
Poland	1	-	-	1	7
Spain	1	1	7	1	7
Switzerland	1	-	-	1	7
United Kingdom	2	2	14	2	14
	12	8	57	10	71
North America					
U.S.A.	3	3	21	1	7
Australasia					
Australia	1	1	7	1	7
China	2	1	7	1	7
Japan	1	1	7	1	7
	4	3	21	3	21
TOTAL	19	14	100	14	100

Table 4.14 ITA Questionnaire Response on Lining Design

4.4.2.2 Results of the Survey

One of the questions involving an aspect which is highly consequential regarding the lining loads, asked "what are the values chosen for the primary stress-field before the tunnel is excavated" (Duddeck, Op.cit.:167). All respondents but two, provided answers to this question indicating that they take the overburden vertical total stress as a major principal stress, but different assumptions were evident regarding the horizontal total stress. Figure 4.7 shows that most of the respondents estimate a ratio horizontal to vertical total stress from the coefficient of earth pressure at rest, K_o, as determined from measurements (in situ tests inclusive) or from local experience. The second most popular approach is to arbitrarily assume a fixed value for K, usually between 0.4 and 0.6. A third group assumed that the coefficient K is a function of Poisson's ratio.

At another point, the practitioners were asked "what would be the loads or ground pressures assumed" for the design of the lining of a shielded or mined tunnel (Duddeck, Op.cit.:167). As shown in Figure 4.8, the answers were classified into four categories. For the shielded tunnel situation, the majority of the responses (54%) indicated full overburden, which implies the assumption that the lining is already installed before the ground is excavated. A second group of responses indicated the use of the full or reduced overburden, depending on whether the tunnel is very

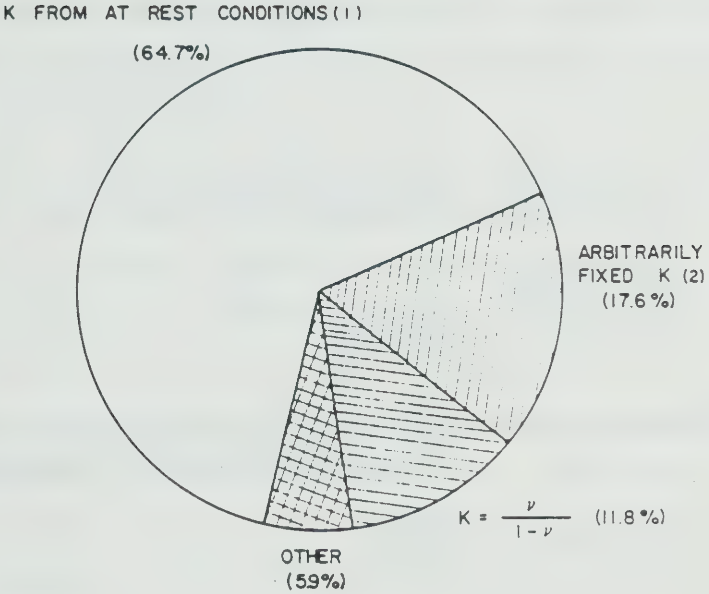

NOTES: (1) Determined from measurements of K_o or from local experience
(2) Typical K value ranging from 0.4 to 0.6
(3) 17 respondents

Figure 4.7 Assumed Ratio Horizontal to Vertical In Situ Stresses used for Design of Shielded or Mined Tunnels in Soil

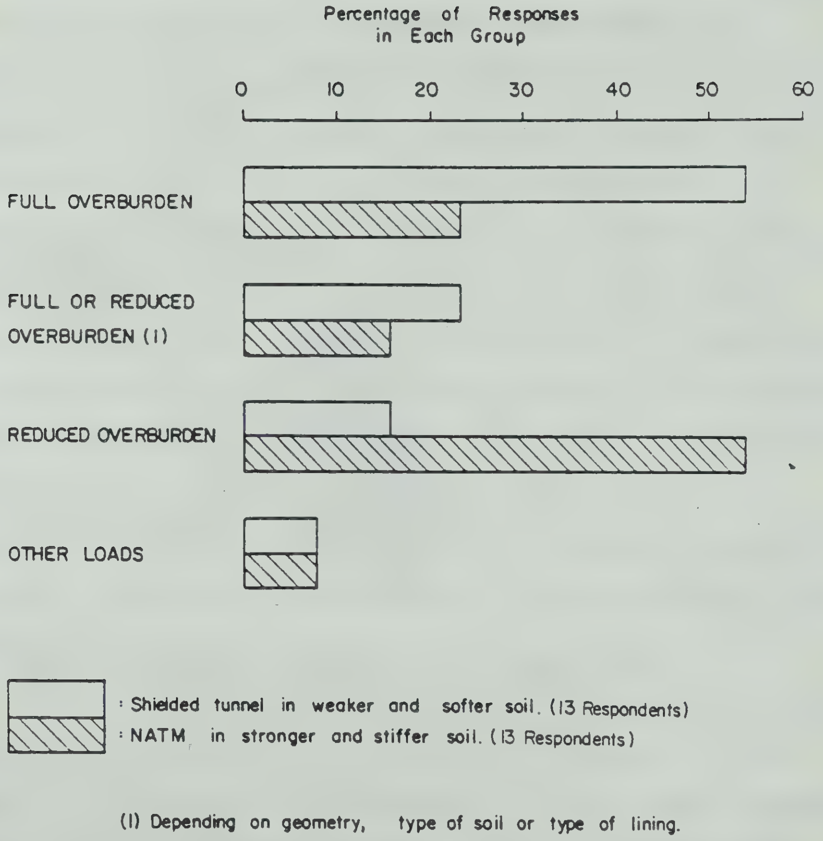

Figure 4.8 Ground Load Assumption Considered in the Responses for the Design of Shielded and Mined Tunnels

shallow or not, or on the type of soil (sandy or clayey). Just two responses indicated the use of a reduced overburden to account for ground stress relaxation before lining installation. One response revealed that ground load should not be considered in the lining design, but simply loads developed in handling the prefabricated lining, as well as other construction loads.

For the mined tunnel situation, the majority of the responses (54%) indicated a reduced overburden assumption for the lining design. Following this group were those postulating the full overburden hypothesis and those favouring either one of the other, depending on the particular case (relative depth and soil type). According to one respondent, it depends on whether the lining being designed is the primary or the secondary one (reduced load for the former or even for the latter if the tunnel is deep). Unfortunately, it is not very clear if the differences in the assumed ground load conditions for the two tunnelling situations, are due to the different construction technologies, soil properties,r ground conditions, or personal views of the respondents, as noted earlier.

It could be speculated that the predominant assumption of a reduced overburden load for mined tunnels results from the respondents probable understanding that the shotcrete and steel arch lining usually acts as a primary support. On the other hand, as most shielded tunnels use, nowadays, prefabricated linings as combined primary and secondary support, the respondents could have understood that a full overburden load assumption would be more adequate for the long term performance of this lining system. This interpretation was adopted by P. Gesta, who prepared the conclusions for mined tunnels of the ITA survey (Duddeck, Op.cit.:219). He concluded that there is a tendency towards designing primary supports using a reduced ground load, and secondary supports with the full (in situ) ground loads. He cautioned, however, that this is not a unanimous philosophy of the practitioners. Indeed, a careful review of the 13 responses on the subject revealed that only P. Gesta himself indicated that the ground load assumption depends on whether the support is the primary or the secondary. Other responses did not indicate this, possibly because the questionnaire did not invite this point to be answered. Although his interpretation might be correct, his conclusion cannot be supported by the explicit answers of the respondents. Although not requested to explain how the reduction in the ground loads would be estimated, the 14 responses (5 for shielded and 9 for mined tunnels) that indicated this assumption, provided indications about the procedure to be used for such an estimate. Figure 4.9 shows that the majority for both tunnelling situations combined (64%), favour the use of Terzaghi's arching theory for this purpose. This group is followed by those 21% who estimate the stress reduction on an arbitrary basis (founded on previous experience). The remaining group of responses use some sort of empirical approach based on classification systems, to evaluate the ground load reduction.

Further on, the questionnaire asked, "what kind of statical system is used for determining the inner stresses, the deformations ..." for the lining design (Duddeck, Op.cit.:167). For each tunnelling situation, 14 respondents offered answers to this question. Some respondents mentioned more than one method for lining load prediction. Considering only those responses that clearly answered the question, the 13 responses for the shielded tunnel situation mentioned 17 lining design methods. For mined tunnels, 13 responses mentioned 26 methods (some applied to the primary and some others to the secondary lining). If all 26 responses for both tunnelling situations are combined, 43 references to lining design methods are evident. The combined statistical results are shown in Figure 4.10, with the design methods classified into four main groups. The percentage of responses was calculated in relation to the total of 26 responses, and the value calculated for each group method gives an indication of how frequently this method was indicated in the responses.

As shown, the methods most frequently referred (69.2%) are those that represent the lining by a ring and the soil by springs. In these models, the structure is submitted to prescribed loads independent of lining deformation, and the ground reaction results from displacement dependent spring

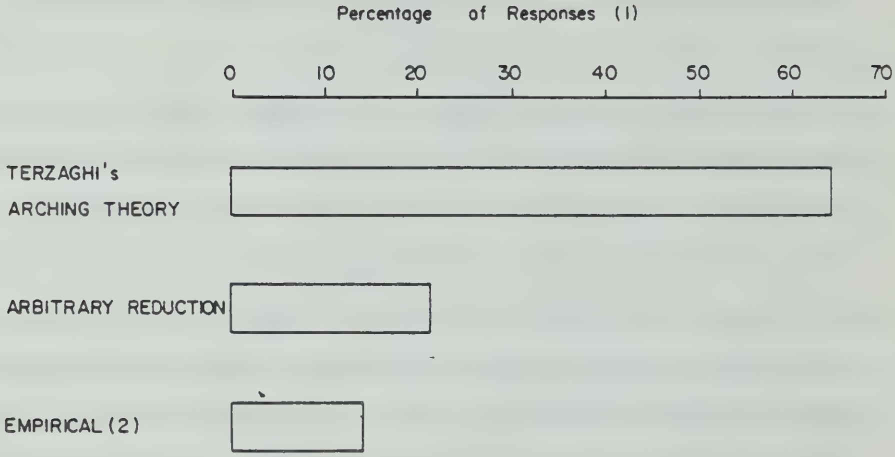

NOTES: (1) Total of 14 responses, combining 5 that reduce ground loads in shielded tunnels and 9 in mined tunnels.

(2) Ground load reduction by Geomechanics classification methods.

Figure 4.9 Criteria Indicated in the Responses for Ground Load Reduction both in Shielded and Mined Tunnels

loads. Some responses indicated methods based on continuous solutions (namely, Schulze and Duddeck, 1964 method), and others seem to use discrete solutions, numerically obtained for an embedment with a finite number of springs. Moreover, 8 responses (4 for the shielded and 4 for the mined tunnel situations), which represents 44% of the responses in this group, or 31% of the total responses, mentioned that they neglect the embedment of the lining in the crown region. In other words, they assume a "gravity load" condition, which is associated with a poor ground control assumption. Most of these came from German speaking respondents, and this is conversant with the local practice or tradition which has been incorporated in the design directives of the German Society for Soil Mechanics and Foundation Engineering (Duddeck, 1980).

The second most indicated procedure (39%) are the empirical methods, followed by ring and plate analytical models (31%) which include closed-form solutions such as Muir-Wood's and the convergence-confinement method. Finally, 27% of the responses indicated the finite element method, in most cases as an alternative approach and sometimes simply to check the solution provided by the simpler models.

Figure 4.11 presents the same data, but this time identifying the distributions of design procedures with respect to the different tunnelling situations. No significant differences are noted, except a tendency towards a more frequent use of empirical procedures and the finite

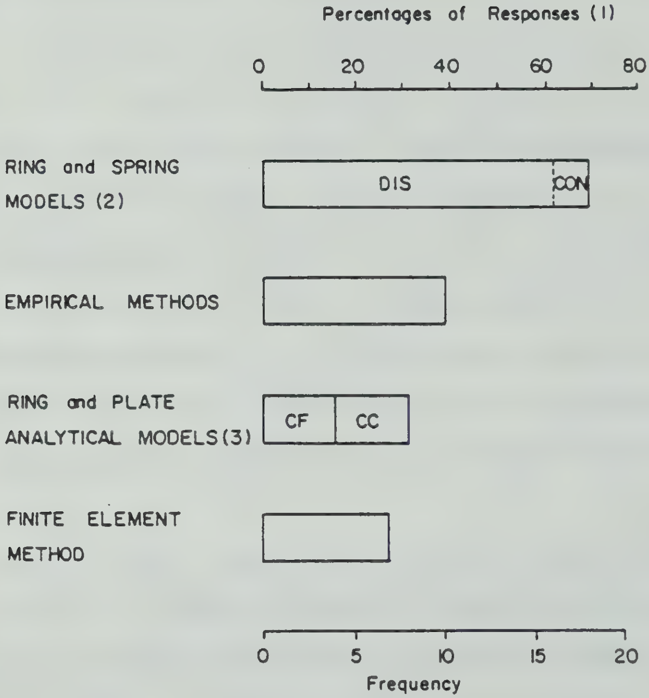

NOTES: (1) Some of the 26 responses indicated more than one design method (some for primary support, for secondary support or for both). 43 design methods were mentioned.

(2) The answers did not allow clear separation between numerical (NUM) and analytical (AN) solutions.

(3) Include closed-form (CF) solutions and convergence-confinement (CC) models.

Figure 4.10 Types of Statical Systems used for Assessment of Lining Loads in Shallow Tunnels

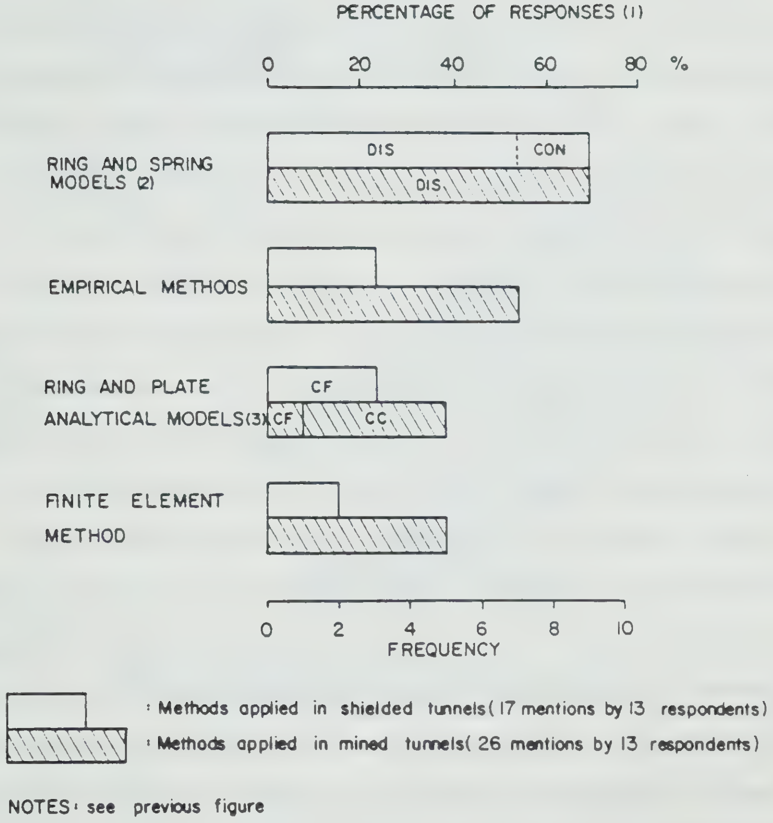

Figure 4.11 Statical Systems Applied in Shielded and Mined (NATM) Tunnels

element method for the mined tunnel situation. For both tunnelling situations, the ring and spring models are most popular.

All respondents were asked if there is "any method determining the ground reaction modulus by the measured characteristic of the ground", to be used in ring and spring models. From the 28 responses received for both tunnelling situations, 21 procedures were mentioned that could be classified as shown in Figure 4.12. The remaining 11 responses did not provide an answer or indicated that there is no simple method for this. The most referred to procedure (52%) was the indirect calculation of the radial spring constant (K_r) through elastic parameters (E and ν) obtained from laboratory tests. Included in this group are most of the German speaking respondents, who relate K_r to the constrained modulus of the soil, which is primarily obtained by oedometer tests (see Section 4.3.2.4). A second group of responses mentioned the direct estimate of K_r in situ by plate bearing and pressuremeter tests. The remaining group use spring constants from back analysis of monitored field performance.

Although the respondents were clearly asked to answer if "are the same models employed for 'lining' and for the 'temporary' supports" (Duddeck, 1982:167), 11 of the 14 responses for the shielded tunnelling situation provided no answer to this question. Most of the latter felt that the question was not applicable to this situation, since the

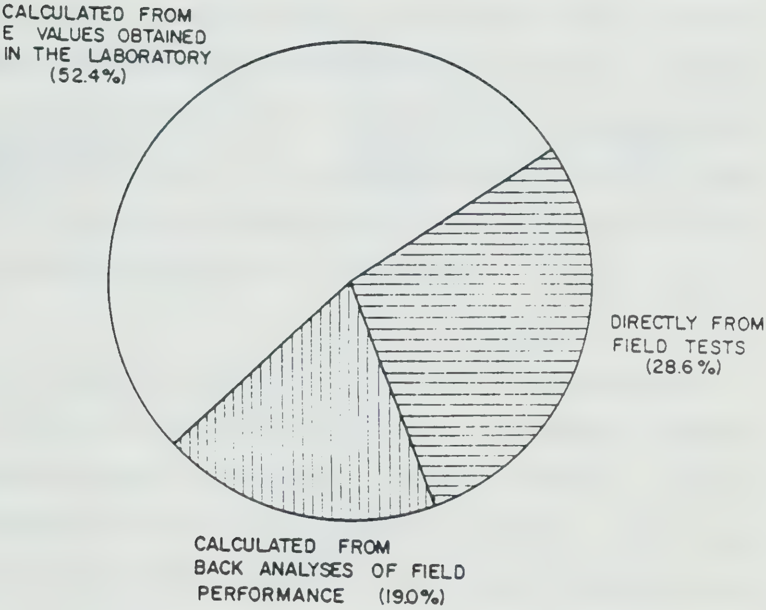

NOTE: 11 responses provided no answer; remaining 17 mentioned altogether 21 procedures. Percentages shown refer to the latter.

Figure 4.12 Procedures for Evaluation of the Spring Constant to be used in Ring and Spring Models for Lining Design of Shielded or Mined Tunnels

support normally used acts as a primary and a secondary lining. Considering only the answers for the mined tunnel situation, in which it is usual to apply a primary and secondary lining, the answers given in the 14 responses (Figure 4.13) indicate a slight tendency towards the use of different design methods for each lining type. Among the 6 respondents who use different lining calculation models, there was a general preference for employing an empirical and simple approach for the design calculations of the primary lining, combined with ring-spring models for the secondary support.

Another question posed was, "is the designing engineer obliged to take into account non-linear behaviour as for example, of the structural elements, of the ground, plasticity, rheology, large deformations?" (Duddeck, Op.cit.:169). From the 28 responses received, two of them (one for each tunnelling situation) were not clear, and could not be classified. Figure 4.14 summarizes the result of the survey for both shielded and mined tunnels. Half of the responses indicated that there is no obligation to take into account non-linearities of the soil or the support. Almost 27% said there is such an obligation, either for the support or for the soil. The remaining indicated that in some instances there would be a need to take that effect into consideration.

It may be questioned whether this statistical result is fully representative of the current practice. The question

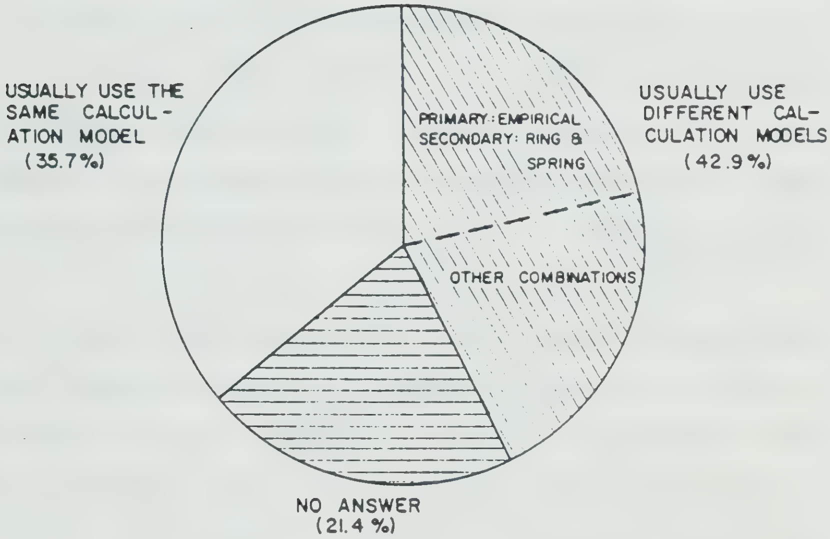

NOTE: 14 responses to the question for mined tunnels.

Figure 4.13 Distribution of Respondents on the Statical System used for the Design of the Primary and Secondary Linings in Mined Tunnels

asked if practitioners are obliged to take the effect into account, and not if they usually do.

Despite this, if the results are separated into shielded and mined tunnels (Figure 4.15), one notes slightly different trends for each. While only 15% of the responses agree that designers are bound to take into account non-linearity effects (for the soil only, however) in the shielded tunnelling situation, 38% of the responses for the mined tunnel and indicate that non-linearity of the soil (23%) is slighly more important than that of the support.

At another point (Duddeck, Op.cit.:169), the questionnaire asked "what kind of statical models are used checking the support actions at the working face? Are three-dimensional effects considered?". All 14 responses for the shielded tunnel situation could have been classified into three categories, as shown in Figure 4.16. However, only 10 responses for the other tunnelling situation could be properly classified.

As shown, the large majority for the shielded tunnel case do not consider any three-dimensional effect. A smaller group stated they may consider it for some occasional and non-specified condition. Only one response indicated that the only three-dimensional effect considered is the stress relaxation of the ground stress reduction by the 3D arching around the face.

For the mined tunnel case, a slightly higher tendency to consider 3D effects is apparent, but still the major part

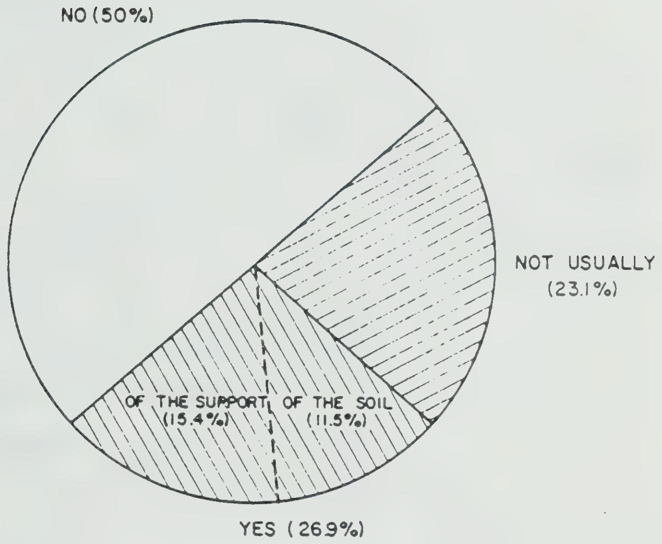

(26 responses ; shielded and mined tunnels combined)

Figure 4.14 Obligation to Account for the Non-Linear Behaviour of the Soil or the Support, in the Design of a Shallow Tunnel in Soil

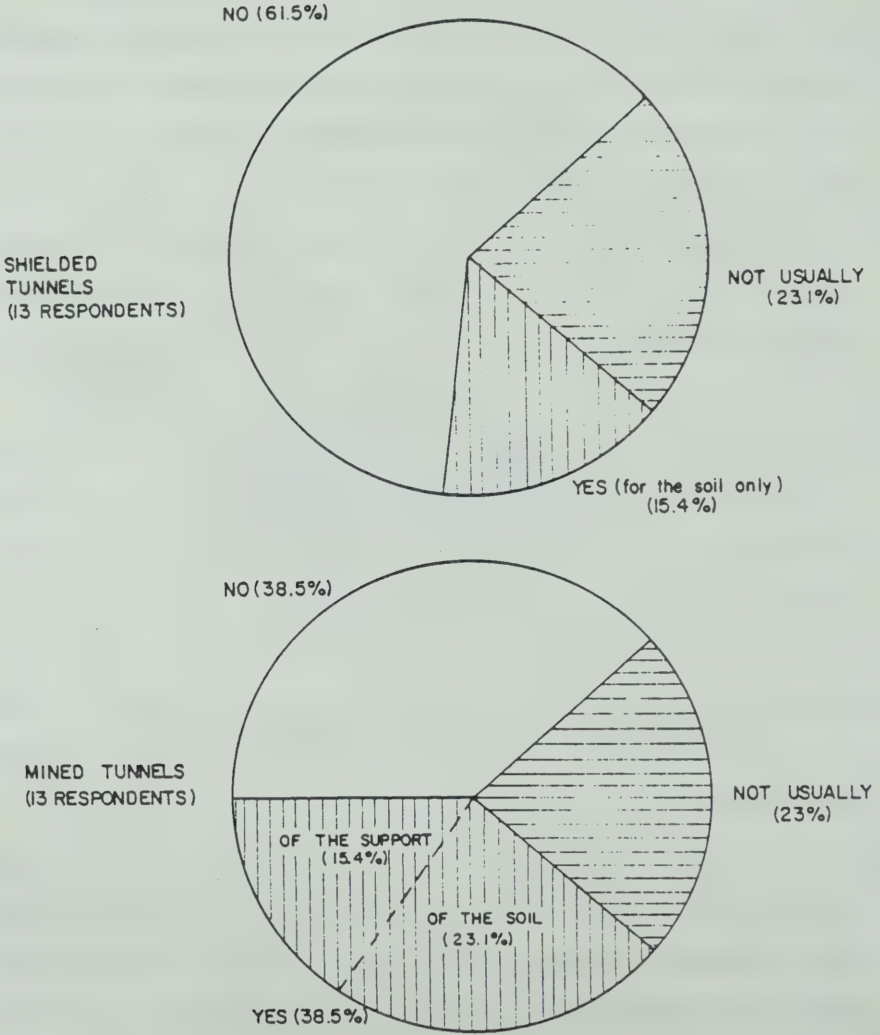

Figure 4.15 Obligation to Account for Non-Linear Behaviour of the Soil or the Support in Shielded and Mined Tunnels

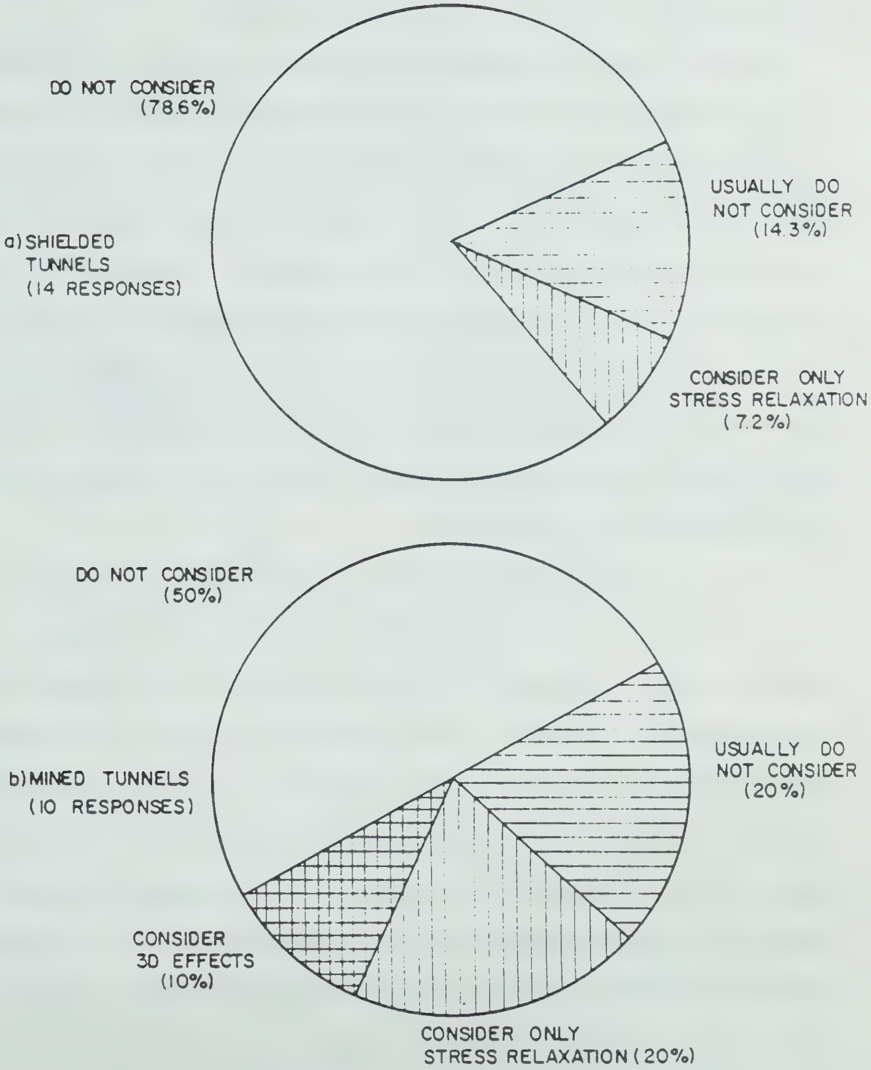

Figure 4.16 Consideration of Three-Dimensional Effects in the Lining Design of Shielded and Mined Tunnels

of the responses indicate no account is taken of these effects. Only one respondent stated that he does consider these effects, but on an empirical basis.

None of the respondents made any mention of possible load concentration in the leading edge of the lining that may result from the 3D soil arching around the unsupported heading. An assessment of the practitioners attitude towards this effect appeared to be the original intention of those who prepared the questionnaire. The responses seem to indicate that this effect is not considered in practice and when some three-dimensional action is considered, it is restricted to the ground stress relaxation induced by the face and heading excavation.

Finally the questionnaire asked (Duddeck, 1982:169) how factors of safety are employed in the lining design practice. Ten responses provided unclear or no answer to this question, and only the remaining 18 can be considered for the statistical analysis (Figure 4.17). No differences in distributions were detected for the mined or shielded cases, so the results are given in a combined form. One notes that the majority of the responses favour the use of partial factors of safety to the support section and to the soil loads. Another group of responses pointed out the use of both partial or global factors depending on the case.

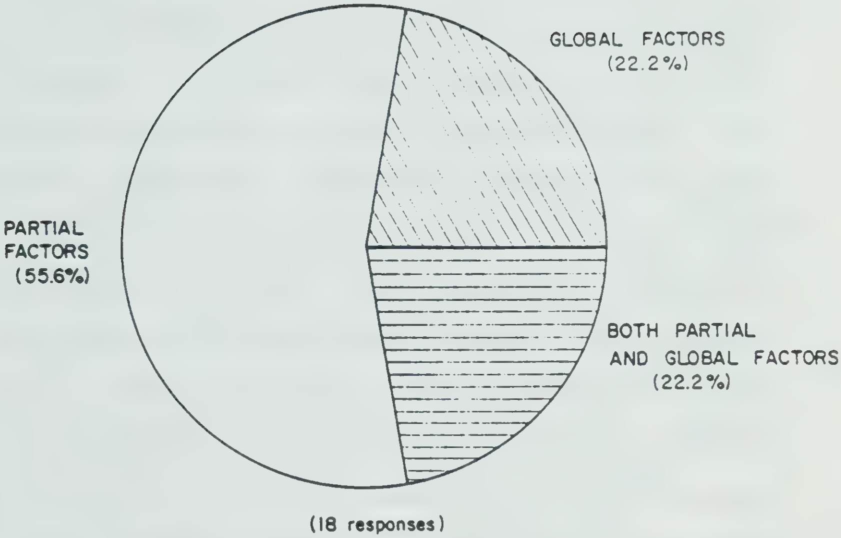

Figure 4.17 Factors of Safety used in the Design of Shallow Tunnels in Soil

4.4.2.3 Final Comments

Despite being recognized that the state of the in situ stresses has a major role in the design of the tunnel lining, a significant number of practitioners seems to believe that, for design purposes, it is sufficient to select a certain stress ratio (K), and use it for design. In so doing, the designer tends to select a conservative value for K, incorporating at the onset, an inbuilt and unknown margin of safety for the design. This reveals considerable departure from a typical design attitude, which is that of anticipating the actual behaviour of a structure under foreseen (even extreme) conditions, and providing it with a known , if possible amount of safety. Moreover, the practice of selecting an arbitrary K value, may in some cases be unsafe. This would be the case of those who fix a low K value, or who estimate it from the Poisson's ratio, if they were to design a tunnel in very overconsolidated soils, like London Clay, at shallow depths where K values in excess of 1.5 (in total stresses) can be observed.

For the shielded tunnel situation, practitioners tend to use a full overburden assumption for the lining design, whereas for the mined situation, they favour a reduced overburden assumption. Other respondents may or may not use the latter assumption in both tunnelling cases, depending on the type of soil, the relative depth of the tunnel or the type of lining. Unfortunately it was not possible from the answers collected, to identify the reasons for the different assumptions made. Parallel to the differences in construction technology in the two situations posed, including different lining systems, the two reference cases involved distinct ground conditions (more competent and water free ground in the mined case). Moreover, not necessarily the same individual replied to the questions for both situations, so that different personnal views might have affected the results. In addition, no details of the construction technology in each case were provided in the questionnaire. The respondents, therefore, were left unbound without a uniform view of how the two tunnels were to be built, and inconsistent interpretations of each situation posed, might have had a role in the results obtained. The conclusions included in the ITA report (Duddeck, 1982:219) suggested that the differences in the ground load assumptions depends on whether the support under consideration is the primary (shotcrete and ribs in the mined case) or the secondary or final lining (possibly prefabricated lining in the shielded case - not explicitly mentioned in the questionnaire, however). Although the writer was also tempted to draw the same conclusion, there is no firm indication from the data gathered that this is the case.

Also not answered by the survey are the reasons why or how those favouring the full overburden assumption support this reasoning. Does it reflect a belief that a shielded driven tunnel does not induce ground movements or stress release before lining application? Does it reflect a belief that the ground strength will be reduced to zero in a long term process? Most practitioners assuming a full overburden assumption take into consideration the interaction between the lining and the soil in the support design. This is in direct conflict if the shear strength of the soil supposedly fully deteriorates with time. Does it reflect an attitude towards providing an additional, built in, and somewhat hidden factor of safety to the structure being designed? Does it reflect an understanding that possible savings in the lining, otherwise designed with inconsistent and conservative assumptions, are marginal with respect to the overall cost of the tunnel (known to be mainly controlled by excavation and ground control costs)? Unfortunately, these questions remained unanswered by this survey and may be suggested as points to be included in similar investigations in the future.

Although empirical methods are still largely used for lining design, the survey indicated that ring and spring models are those most frequently used by the practitioners. This can be attributed to the facility of using available design charts for the continuous solutions, or to the current availability of microcomputers, which allow easy implementation of discrete solutions. These models can furnish good results, provided ground loads and spring constants are properly estimated. The constants usually seem to be calculated from elastic constants obtained through laboratory testing and using some approximate expressions. Not disclosed by the survey was how the elastic parameters are determined from the non-linear responses observed in the testing results. The success in applying these lining calculation models rely heavily on the correct assessment of some 'equivalent' elastic properties, which is not a simple task, especially in a problem in which the non-linear response of the soil is likely to play an important role.

It is interesting to note (particularly in the mined tunnel case), that most practitioners use a reduced overburden assumption for ground loads, combined with a ring and spring model to represent the lining and ground interaction. The usual criterion adopted to estimate the reduced ground loads is Terzaghi's arching theory. This appears to be somewhat inconsistent with Terzaghi's (1943:194) original ideas:

> "Part of the yield of the sand toward the tunnel occurs while the working face passes the section ... and the remainder takes place after timbering has been constructed. Owing to the imperfect fit of the timbers at the joints and the compressibility of supports of the footings of the vertical posts, the yield of the timbering is usually sufficient to reduce the pressure of the sand on the timbering almost to the value corresponding to the state of incipient shear failure in the sand. This state is similar to the state of stress in a mass of sand above a yielding strip."

In other words, Terzaghi suggested that the ground pressures derived from his trapdoor theory would include the effect of ground yielding both before and after lining installation, and the pressures it provides would approximate the final equilibrium pressure against the support.

By applying Terzaghi's reduced ground loads on an elastically embedded frame of a ring and spring model, the active loads will be shared between the latter and the former, according to their relative stiffnesses. The lining will end up sustaining a load at equilibrium which is lower than that given by the arching theory. Moreover, the combination of a limit state type of condition, represented by Terzaghi's theory, with an elastic model for soil-lining interaction analysis can be questioned or at least debated.

The reasons behind the slight trend towards the use of different lining calculation models for the primary and secondary supports were not fully grasped. Since the latter is usually installed far behind the advancing face, probably after the former attains a full equilibrium with ground loads, the secondary support is commonly designed to withstand any long term change in loads, as discussed in Section 4.2.1. Formally there is no apparent reason to require different calculation models. Perhaps that attitude still reflects the old design posture to treat the primary lining simply as a 'temporary' support, relegated in the overall design to a less important role and designed according to any simple empirical rule. At least 20% of the respondents (see Figure 4.13) seem to still share this view which nevertheless, is being changed, as noted in Section 4.2.1.

Most of the respondents did not feel any need to take into account the non-linear behaviour of either the soil or the lining in the shielded tunnel case. For the mined case, it was found that the account was felt to be more necessary, which is slightly surprising as far as the soil non-linearity is concerned. Indeed, in the second case, tunnelling conditions are more favourable and the magnitude of ground deformations are likely to be smaller. The more competent nature of the ground will also help this trend. If a linear elastic analysis was to be adopted in any of the cases, the chances are that the mined case could be better depicted by this approach.

It is apparent from the survey that no account is taken in practice regarding the possible concentration of loads on the lining close to the advancing face. If any three-dimensional effect were considered, it was the stress relaxation of the ground by arching or shear transfer around the face that ultimately reduces the lining loads.

Preference for the use of partial factors of safety was evident among practitioners. This is done by applying a factor to the ground loads and a capacity reduction factor to the lining section (or support strength), as recommended by some codes. Although not disclosed by the responses, it is believed that no fixed load factor is normally established for the ground loads, due to the varying degrees of conservatism frequently included in their evaluation, as noted by Paul et.al. (1983:134). Some factor is usually required to keep stresses and deformations in a structural member within tolerable limits when it is subjected to the operational ground loads. If the loads adopted in the design are the extreme envelope loads, and possibly conservatively estimated, the over-load factor could be less than that required when the lining is designed for the working ground loads which are expected to act on the support. This is so because the component of the load factor that accounts for the uncertainties in the loads, would already be implicitly included in the conservative estimate of the design ground loads. The other load factor which contributes to the overall safety margin, accounts for possible understrength of materials in the lining under operational conditions, and clearly should always be considered. Having this in mind, it seems preferable both in technical and economical terms, to estimate as simply as possible, the ground loads within a given range that are actually expected to act on the lining, rather than to work with a conservative assumption of this load as is frequently done.

4.4.3 Prediction of Ground Settlements

4.4.3.1 Survey of Practice

The principal purpose of this section is to report on the state-of-practice as it exists, regarding the prediction of ground settlements caused by shallow tunnelling. Although the writer was familiar to some extent with this practice in a few countries, both in South and North America as well as in Europe, it was decided to carry out a formal inquiry. This was done in order to avoid reporting the practice as the writer perceives it should be, and to avoid any other possible biased interpretation. Unlike the practice on lining design, which had already been formally surveyed, no inquiry had covered the present topic, to the writer's knowledge.

The inquiry was designed to cover the practice mainly in Western countries, as it stands presently within the designer's community. This was done by means of a questionnaire sent to practitioners known to be actively involved in designing underground urban systems at the time of mailing.

Similar surveys conducted previously by other authors, revealed that a reduced reply rate would be expected if the number of subjects or topics addressed was too large or if the number of questions was too many. For example, an inquiry recently conducted by Focht and O'Neill (1985:188), on the design of deep foundations, required answers to 36 questions, either in multiple choice form or in descriptive form. The questionnaire was sent to 66 active consultants but disappointingly only 11 (17%) of them were returned. Since one of the goals of the present survey was to have a representative reply, it was decided to limit the questionnaire to a single page, including only five questions with multiple choice answers, but allowing free comments. It was suggested to the respondents to indicate only one answer per question, but mulitple answers and any comments included by some were interpreted in the subsequent analyis. To further boost the reply rate, a self addressed envelope was included in the mail. It is believed that these combined measures justified the fairly high return rate of nearly 70%. The price paid for it, however, was that the survey had to cover the subject in a fairly circumscribed and simple manner, since more involved questions, demanding detailed answers were intentionally avoided. Nevertheless, it is believed that the results fulfilled the intended goals.

The questionnaire prepared is reproduced in Table 4.15. As is seen, the questions included a focus on ground displacements caused solely by the construction of shallow tunnels driven in soft ground in urban environments, by means of any type of tunnelling procedure. When answering the questions, the respondents were invited to disregard all components of time dependent movement due to soil consolidation or creep.

The questions were sent to 50 practitioners in 17 countries, where active urban tunnelling practice was evident during the first half of the current decade. Table 4.16 lists the number of questionnaires sent to all those countries, mostly located in Europe and secondly North and South America. Table 4.16 also shows the number of questionnaires returned, the percent returned of number sent, and the percent distribution of total questionnaires returned. The latter provides the weight of each country surveyed on the global results obtained. Therefore answers coming from West Germany affect the statistical results that will be shown, by 18%, followed by Brazil (15%), Canada and the U.S.A. (12% each). Regionally speaking, the survey results will represent firstly the European practice (47%) followed by North and South American practices (26 and 18% respectively).

The returns were approximately in proportion to the number sent, except for a few countries such as Belgium, Argentina, England and Japan, that end up being underrepresented in the survey by their lower return rate.

As noted previously, the questionnaire was sent basically to those involved with routine design practice of shallow tunnels. As indicated in Table 4.17, most of the respondents (74%) are connected with consulting engineering firms or have their private consulting practice. The remaining respondents work in other types of organizations, but also in design related activities. This is notably the case of contractors in West Germany and Japan, which include an in-house consulting or design group to whom the

The questions below focus on ground displacements caused by construction of a shallow tunnel driven in soft ground (including soft rock), in an urban environment, using any type of tunnelling method (TBM, NATM or other). Time dependent settlement components due to consolidation or creep are not part of this research and as such should be disregarded in answering the questions. Please mark only one answer per point.

1) In the design of a tunnel as defined above, do you normally perform a quantitative prediction of settlements induced in the ground?

a) ☐ Yes
b) ☐ No

2) If the answer to question 1 is "Yes", then, what procedure or method do you most often use for your settlement prediction?

a) ☐ Judgement or simple analysis based on past experience in similar conditions

b) ☐ Empirical method using some mathematical function

c) ☐ Peck-Schmidt method

d) ☐ Numerical procedures such as the finite element method

e) ☐ Method developed from parametric numerical analyses (e.g. Reséndiz and Romo, 1981). (Specify which: ....).

f) ☐ Other (Specify: ....).

3) If you could specify just one single most significant factor of the method you indicated above, it would be:

a) ☐ its simplicity
b) ☐ its reliability
c) ☐ its theoretical rigor
d) ☐ its widespread acceptance or use
e) ☐ other (Specify: ....)

4) Under favourable ground control conditions, the loads that finally act on the (primary) support system appear to be related to the magnitude of the displacements induced by tunnelling (concept of the ground-support reaction curves or the convergence-confinement model). In your normal design practice, do you estimate ground settlements according to the estimate of the loads on the primary lining (or vice-versa)? In other words, do you couple settlement and loads predictions?

a) ☐ Yes

b) ☐ No

5) If the answer to question 4 is "Yes", then, how do you do it?

a) ☐ By using the finite element method
b) ☐ By using other numerical methods
(Which? ....)
c) ☐ Other (Specify: ....)

Respondent: ....

Address: ....
....
....

Table 4.15 Questionnaire on Ground Movements Caused by Shallow Tunnels

Region/Country	Number sent	Number returned	Percent returned of number sent	Percent of total returned
Europe				
Austria	3	2	67	6
Belgium	1	0	0	0
Czechoslovakia	1	1	100	3
England	3	1	33	3
France	2	1	50	3
W. Germany	6	6	100	18
Hungary	2	2	100	6
Spain	3	2	67	6
Switzerland	1	1	100	3
	22	16	73	47
North America				
Canada	5	4	80	12
U.S.A.	6	4	67	12
Mexico	1	1	100	3
	12	9	75	26
South America				
Argentina	2	0	0	0
Brazil	6	5	83	15
Venezuela	1	1	100	3
	9	6	67	18
Africa				
Egypt	1	1	100	3
Asia				
Japan	6	2	33	6
TOTAL	50	34	68	100

Table 4.16 Questionnaire Response on Ground Movements

questionnaires were sent. The global distribution of the type of practice of respondents is illustrated by the chart in Figure 4.18. The names and affiliations of all contributors are listed in Appendix B.

4.4.3.2 Results of the Survey

The first question asked whether or not a quantitative prediction of ground settlements was normally performed by the practitioner in his tunnel design routine. As shown in Figure 4.19, the vast majority of respondents said yes to this question. A minority group seems to limit their practice in shallow tunnel design to the structural definition of the support system.

The next question asked what procedure or method the designer mostly used in his routine settlement prediction. Although asked to answer only one answer, some respondents (23.5%) marked more than one, without an indication of which is the procedure they most used. These were grouped as "multiple answers", being identified as those who combine different empirical or semi-empirical approaches and those who combine numerical and empirical approaches. The result of the statistical analysis on replies to this question is summarized in Table 4.18. Procedures 1 to 4 in Table 4.18 could be gathered as an "empirical or semi-empirical approach" group. Procedures 5 and 6, could be termed as a "numerical approach" group. Therefore the results could be re-arranged as shown in Figure 4.20. Fifty percent of the respondents favour an empirical or semi-empirical approach.

Region/country	Consulting Engineering	Other (owners, contractors, researchers)
Europe		
Austria	2	-
Czechoslovakia	-	1
England	1	-
France	1	-
W. Germany	2	4
Hungary	2	-
Spain	1	1
Switzerland	1	-
	10	6
North America		
Canada	4	-
U.S.A.	4	-
Mexico	1	-
	9	-
South America		
Brazil	5	-
Venezuela	1	-
	6	-
Africa		
Egypt	-	1
Asia		
Japan	-	2
TOTAL	25	9
	(74%)	(26%)

Table 4.17 Type of Practice of Respondents

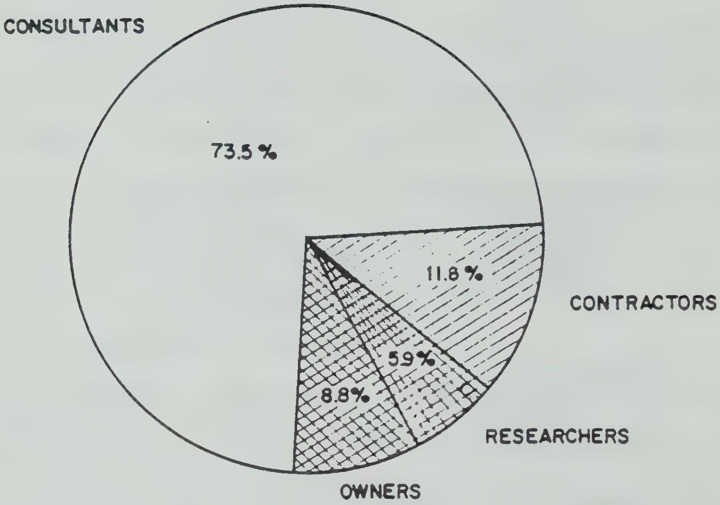

Figure 4.18 Type of Practice of Respondents

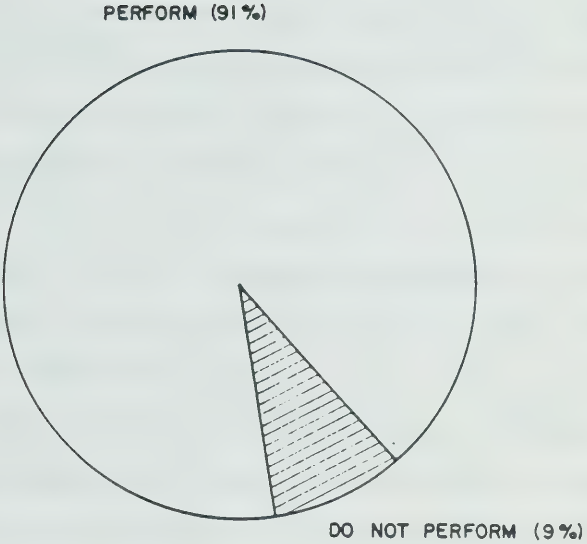

Figure 4.19 Distribution of Respondents that Normally Perform Quantitative Prediction of Settlements Caused by Shallow Tunnelling

That percentage is even higher (62.5%) among European practitioners.

Only 18% of the respondents showed sole preference for a fully numerical prediction. Among this group, the majority (83%) indicated that their preference lies in the finite element method and one respondent indicated the boundary element method as his most frequent choice. Those respondents who indicated that their preference, in routine practice, lies on an equal combination of numerical and empirical approaches amounts to 18% of the total. Among these, only one uses a numerically derived method combined with some empirical procedure. Therefore, 32% of the respondents declared that they normally use a fully numerical approach for ground settlement prediction, either solely or associated with some empirical method. This percentage is lower in Europe (19%) and higher in South America (50%).

Out of the larger group favouring an empirical approach (17 respondents), 35% do so by using judgement or some simple analysis based on past experience in similar conditions. These respondents are followed in number by those who use the Peck-Schmidt method (29%). The use of this method seems to be more frequent in Europe than elsewhere.

The third question asked the practitioner to single out one quality he would ascribe to his most used prediction method, which could be understood as a key attribute explaining the reason for preference. Figure 4.21 shows that

	Procedure/Method	No. of Respondents	Percent of Total
1.	Judgement based on past experience	6	17.6
2.	Empirical with some mathematical function	4	11.6
3.	Peck-Schmidt method	5	14.7
4.	Combined empirical methods	2	5.9
5.	Numerical procedures	6	17.6
6.	Numerically derived method	2	5.9
7.	Combined numerical and empirical methods	6	17.6
8.	No answer or do not predict	3	8.8
	TOTAL	34	100

Table 4.18 Preferred Approaches Indicated by Respondents for Ground Settlement Prediction

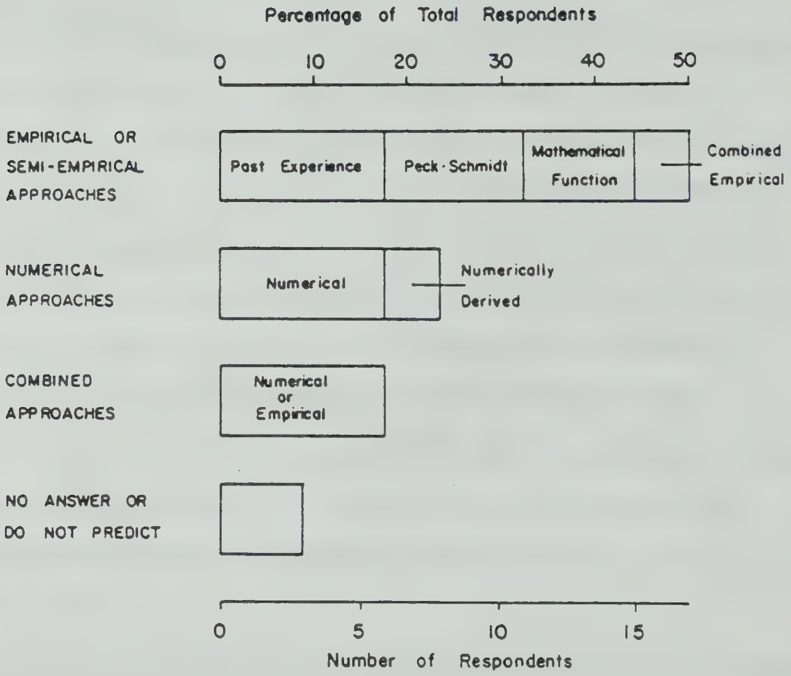

Figure 4.20 Distribution of most often used Methods for Settlement Prediction among Respondents

the leading attributes of a predictive method are its reliability (26.5% of respondents) and its simplicity (23.5%). Hence if a method is proved reliable and simple, it would possibly be accepted by 50% of the practitioners. Moreover, 15% of the respondents did not specify a particular attribute, but follow what is widely accepted or used in practice. In other words, any predictive tool being reliable and simple would be used by almost two-thirds of the design community. On the other hand, a mere 3% of the respondents indicated that their preference lies in the theoretical rigour of the prediction method. Some of the respondents (15%) could not simply select one single quality and pointed out more than one attribute among those listed. Additionally 12% made reference to some non-listed qualities.

If one cross-analyses the answers to the second and third questions, it is possible to identify what method or procedure each attribute is addressed to. The results of this assessment are shown in Table 4.19 and Figure 4.22. The latter summarizes the noted qualities of the "empirical" and of the "numerical" approaches for prediction normally made by the practitioners (17 and 14 individuals respectively). It is interesting to note that the distribution of attributes within each of these two groups of approaches are very different. While reliablity and simplicity is responsible for 76.5% of the qualities preferred by the respondents within the "empirical group", those favouring

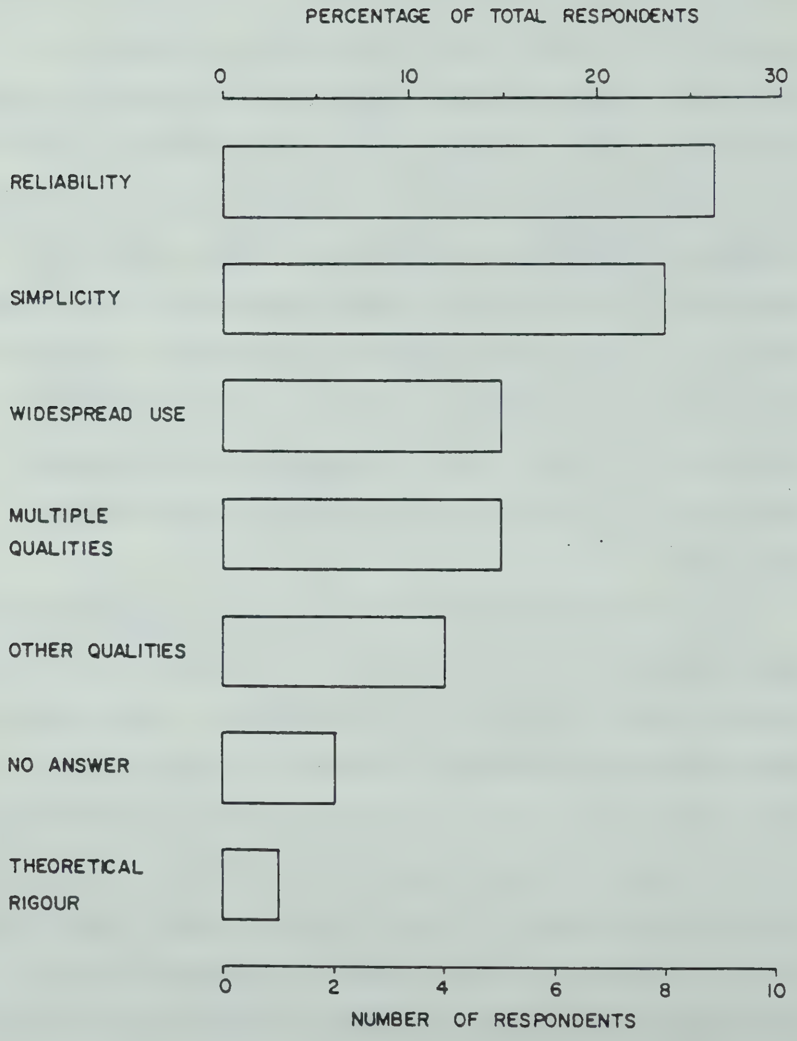

Figure 4.21 Basic Qualities of any Settlement Prediction

the numerical approaches made reference to "multiple qualities", to "widespread use" and to other qualities. Some of the latter qualities referred to were the possiblity of the numerical methods to allow sensitivity studies of certain parameters, to investigate the effect of the staged excavation of the tunnel, or of the effect of non-circular profiles of the tunnel cross section, as well as the possibility of obtaining settlements at points of the ground other than at the surface. Contrary to those who favoured an empirical approach, reliablity is a quality rarely referred to by those preferring a numerical approach. Also interesting is the fact that "theoretical rigour" is a quality seldom noted by those using a numerical approach. Very few respondents admitted that this approach is simple.

The next question asked whether the practitioner does or does not couple ground settlement and lining load prediction in his normal design practice, provided good ground control conditions are anticipated. The question was formulated after being stated that if these conditions prevail, it has been noted that the loads on the (primary) support appear to be related to the magnitude of induced ground displacements. Figure 4.23 shows that the larger part of the respondents (59%) declared that they either do not ever couple lining loads and settlement predictions, or do not usually do it, except under some special circumstances, as for NATM applications or for relatively deep tunnels as quoted by some respondents of the latter group. Among the

Group Method	Simplicity	Reliability	Theoretical Rigour	Widespread Use	Other	Multiple Attributes	No indication of attribute	Total
Empirical or semi-empirical	6	7		2	1	1		17
Numerical	1		1	1	2	1		6
Numerically derived	1				1			2
Combined numerical and empirical		1		2		3		6
No indication of method		1					23	2
Total	8	9	1	5	4	5	2	34

Table 4.19 Noted Qualities for Different Settlement Prediction Procedures

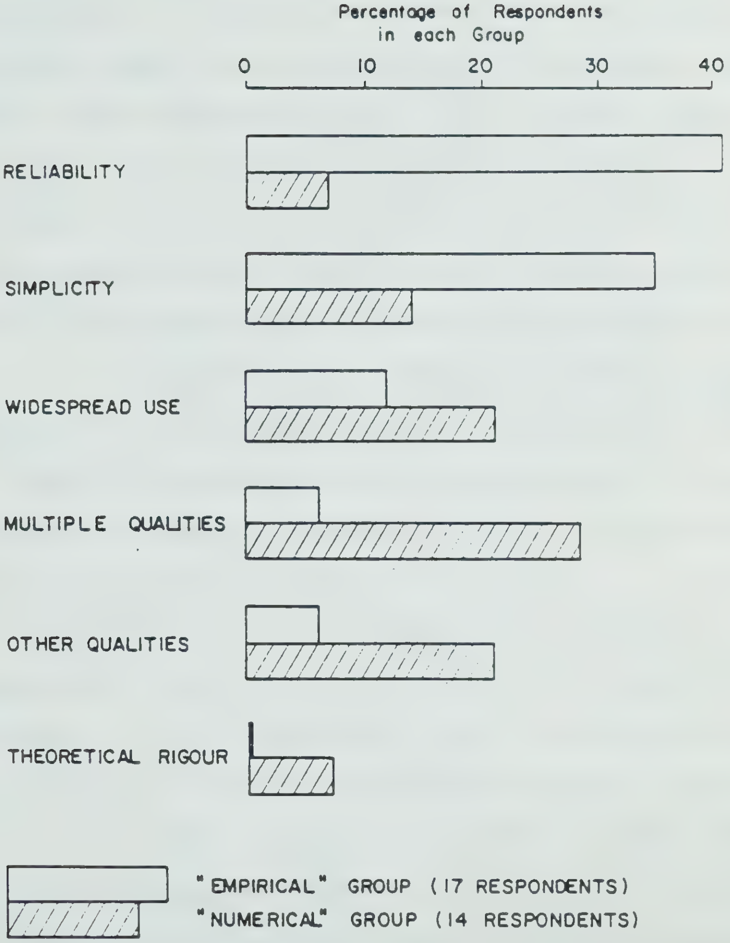

Figure 4.22 Noted Qualities of the "Empirical" and "Numerical" Approaches for Settlement Predictions Routinely Performed by Practitioners

remaining group declaring that they couple load and settlement predictions, one respondent suggested that his normal practice is to design the tunnel for "unfavourable" or "poor ground" control conditions. For these, the stated relationship between loads and displacement may no longer hold, as discussed in Chapters 2 and 3 of this thesis. It will be seen later, that inconsistency has been detected in some replies which makes one think that the number of practitioners actually coupling settlements and lining load prediction to be even smaller than indicated.

The last question asked the practitioner to explain how he does the coupled prediction. The answers by those 14 practitioners who said they usually perform the coupled prediction, are interpreted in Figure 4.24. The majority of those respondents (64%) declared they do it using the finite element method, 21% said they also use the finite element method combined with other procedures, and the remaining individuals declared they use other numerical methods (the boundary element method, for example). Hence, all respondents said that they perform the couple prediction, making use of some numerical tool, the finite element method being most commonly used (86%).

By cross-checking the answers to questions 2, 4 and 5, a few inconsistencies were detected in the replies of six respondents. Typically they admitted in answering question 2 that in their routine practice they favour some simple empirical analysis for ground settlement predition. By

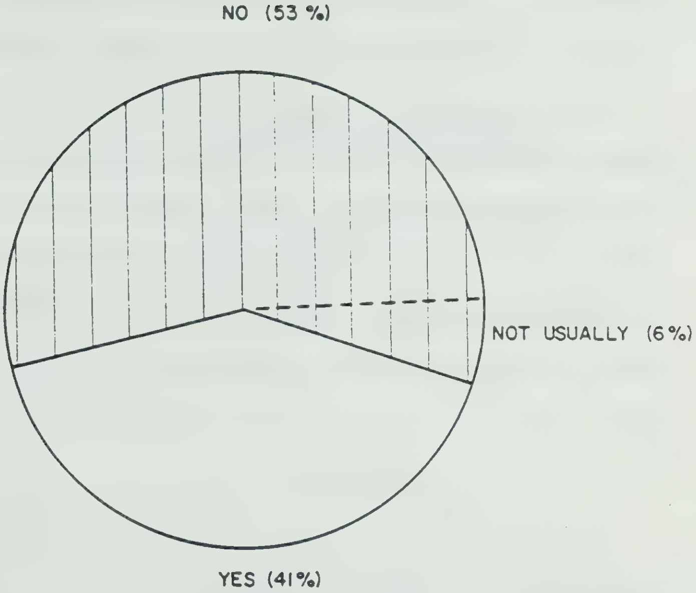

Figure 4.23 Distribution of Respondents Affirming they Couple Settlement and Lining Load Prediction in their normal Design Practice

possibly misunderstanding the statement of question 4, which also invited an answer regarding their routine practice these respondents apparently and contrary to their reply in question 2, admitted in answering question 5 that they use a numerical approach (the finite element method in all cases) to couple settlement and load predictions. Since no further elements were available to ellucidate this point, the answers were accepted as they were and thus included in the statistical analyses. However, if they were to be excluded, then the percentage of practitioners performing coupled prediction of loads and settlement would decrease from 41 to 29%.

4.4.3.3 Final Comments

The survey conducted revealed that quantitative prediction of ground settlements caused by shallow tunnelling in soil is routinely done in practice by almost all designers. It also showed that despite the significant developments in basic and applied soil mechanics, a great deal of empiricism remains in tunnelling design practice. This became apparent through the answers of 50% of the practitioners that still use empirical approaches for the solution of the ground settlement prediction problem. However, it could be expected that this amount may decline with the increasing availability of computer facilities and with further development of other numerically derived design procedures. In fact, the two procedures referred to by respondents, that belong to the latter class of solutions

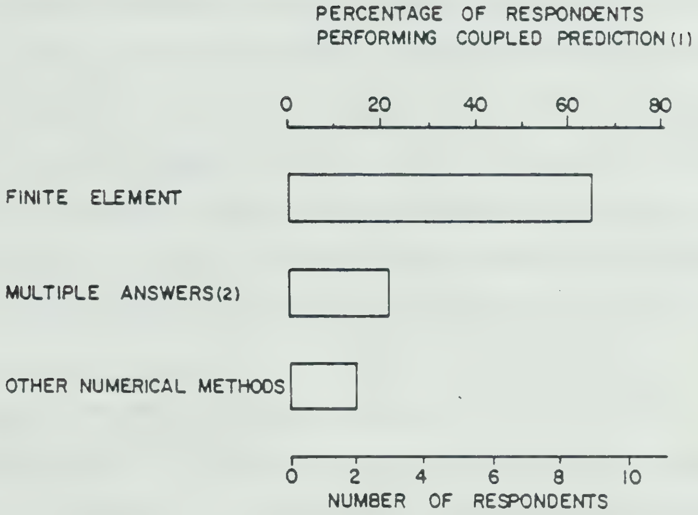

NOTES: (1) 14 RESPONDENTS
(2) ALWAYS INCLUDED FINITE ELEMENT

Figure 4.24 Distribution of Approaches Used for Coupling Ground Settlements and Lining Load Predictions

were developed recently and were made available in the early years of this decade (Resendiz and Romo, 1981 and Oteo and Sagaseta, 1982). Regardless of this, it is believed that none of the numerical approaches will ever preclude the use of knowledge based on previous experience.

Reliability and simplicity are the basic qualities required by the majority of practitioners for any method of settlement prediction. These are the two attributes noted by most respondents favouring empirical approaches. It seems commonly accepted that only the methods validated by past experiences are deemed acceptable in practice. Practitioners are not highly demanding with respect to the theoretical rigour of a prediction method.

Innovation in contruction practice tends increasingly towards a better ground control condition, represented by reduced ground movements. Although the dependence between the latter and the magnitude of lining loads is widely recognized particularly under the above conditions, certainly more than half of the practitioners (possibly more than two-thirds of them) do not couple the predictions of settlements and the support loads. Those who couple these predictions do so by means of finite element analyses, generally without claiming that this numerical procedure is either reliable or simple. It seems that the way to proceed is towards the use of simple numerically developed methods, calibrated against and possibly coupled with past experience, to render to the required attribute of reliability.

4.5 Summary and Conclusions

This chapter presented a review of available methods for the geotechnical design of shallow tunnels and a survey of the current design practice.

There are certain features specific to tunnels in soil that make their design slightly dissimilar from the design of other geotechnical structures. Included among these features are the definition of the loads acting on the lining, the need to take into account the lining-ground interaction, the acceptance of fairly low factors of safety, and the rapid development (in time) of deformations induced by the tunnel advance.

Basic Design Requirements

The basic requirements for the geotechnical design of a shallow tunnel were reviewed and discussed as related to the lining design, to the prediction of ground movements and assessment of the damage potential to neighbouring constructions, and to the verification of the excavation stability.

The tunnelling performance, defined by the response of the ground and of the support system, is directly related to the quality of the construction. In the discussion of the design requirements, it was assumed that the tunnel is to be built under what has been termed 'good ground control conditions'. These are represented by controlled and limited ground movements, avoidance of instability processes, limited soil overcutting in TBM excavated tunnels, minimized delay of support activation, good lining-ground contact, and minimized groundwater drainage into the tunnel and the associated consolidation settlements. Although described here in rather qualitative terms, some effort was directed in Chapters 2 and 3, to tentatively define quantitative criteria allowing the identification of such conditions. Under poor ground control conditions, the tunnelling performance may not be entirely predictable.

Regarding the lining design requirements, the discussion was mainly confined to the primary lining, where the geotechnical component of design is more evident. Though the design requirements focussed predominantly on the operational loads for the primary lining, some attention was paid to transient loading conditions that may represent a controlling design factor in certain cases. Under operational loads, for good ground control conditions and good lining-ground contact, the structural failure of a circular tunnel lining can result from the combined action of thrust and bending. Other modes of failure are possible, but are not usually observed.

In the design, it is customary to assume a linear elastic behaviour for the lining. This assumption is usually a conservative one, with respect to the assessment of the lining capacity. In modern design of linings with small eccentricities (and associated small bending moments), the linear elastic assumption does not lead to excessively conservative results.

The requirements for lining design also include the assessment of the lining capacity, of lining response to possible external loading conditions (excavations, parallel tunnel construction, etc.) and of lining deformations.

The design requirements for the secondary lining were also briefly discussed, with comments being made regarding current trends to integrate the design of primary and secondary linings.

The requirements for ground displacement prediction was then discussed, as related to the need for evaluating the potential risk of damage to neighbouring structures and utilities. Similar to the basic lining design requirement, an estimate of relevant quantities is required as well as an assessment of the appropriate capacity (damage potential to existing structures). Unlike lining design, the interaction between the ground and nearby structures is not fully accounted for in usual practice. An exception to this is the procedure presented by Attewell et.al. (1986:237), but it treats the tunnelling induced ground movements in an empirical and oversimplified way.

The existing criteria for assessment of the onset of damage to existing construction at the ground surface were reviewed. Most were derived from observations made in prototypes and are mainly empirical. The different approaches available to evaluate the building performance subjected to ground movements were discussed. Most originated from observations of building damage related to settlement caused by the structure selfweight. Cording et.al. (1976), proposed an empirical criterion derived from field observations made in structures adjacent to tunnels and open cuts, which is more appropriate to the present case. The damage magnitude was related to the average angular distortion of the ground surface (discounting the structure tilt). The need to investigate in future research, the three-dimensional distortional effects on existing constructions upon tunnel advance, was pointed out.

Finally, a brief review was made of the criteria and methods for assessment of the consequences of tunnel induced ground movements on buried pipelines. Considerable advances in the subject have been achieved over the last decade. It is worth mentioning that most methods available take into consideration the interaction between the ground and the buried pipeline. The main limitation of the above procedures is that the tunnel induced displacements are estimated using rather arbitrary assumptions which are predominantly empirically formulated. There is a clear need to supplement these methods with a more adequate treatment of the tunnelling induced ground movements.

The verification of tunnel stability is usually circumscribed to the stability of the unsupported excavation of the heading and face. The problem is three-dimensional and its solution involves considerable approximation.

Plasticity solutions are usually preferred to limit equilibrium approaches, unless the mode of failure is well known. Available plasticity solutions do not allow a treatment in terms of effective stress, so that the influence of pore pressures cannot be explicitly assessed. Two classes of solutions are available, where the soil response is represented either by an ideal undrained condition or by an ideal drained condition (with no pore pressures). Hence, it is important to identify the pore pressure responses in terms of the rate of dissipation, compared with the anticipated rate of tunnel advance. The stability assessment under steady state ground water flow is usually done for idealized two-dimensional conditions, with no solution being available for the actual three-dimensional problem.

The minimum acceptable factor of safety is defined in terms of maximum tolerable ground deformations. An interpretation of tunnel model test data undertaken in Chapter 2 indicated that good ground control conditions are achieved whenever the dimensionless crown displacement (U) is less than 1. This condition corresponds to factors of safety typically greater than 1.5, but this figure is not a rigid reference, since different displacement magnitudes are expected for different soil types, for the same factor of safety. Thus, lower values may be accepted for stiffer or denser soils (possibly 1.3 to 1.4) and higher values may be required for softer or looser grounds (e.g. 1.6 to 1.7).

Another requirement for the stability evaluation is the assessment of the soil strength. This point deserves special consideration when dealing with some stiff fissured clays. An example of this assessment was provided.

If the stability condition is not acceptable, or if ground displacements are excessive, ground control measures should be considered as an integral part of the geotechnical design of the tunnel. These control measures were classified into six groups. The techniques available for each group type were described and the action of each type of measure was identified. Reported examples of application of these control measures in soil tunnelling were furnished.

Having established the main requirements for the geotechnical design of a soil tunnel, a review of available design methods was undertaken.

Available Methods for Prediction of Lining Loads

The methods for prediction of lining loads were classified according to the basis of their development.

The empirical and semi-empirical methods include the earth pressure theories and the methods in which the lining performance is specified beforehand.

In the earth pressure theories, the ground loads are usually independent of the ground displacements and typically, the lining-ground interaction is disregarded. The ground loads to be applied to the lining are normally derived from considerations or theoretical models that imply substantial shear strength mobilization in the ground. This 'external' load (also referred to as 'gravity' load) approach corresponds to conditions of poor ground control, represented by large ground displacements, a large degree of 'loosening' and poor lining-ground contact. Though reflecting conditions commonly found in the past when these methods were developed, they correspond to conditions which are hardly acceptable for present requirements of urban tunnelling. By neglecting the ground-lining interaction, a conservative lining design is attained. However, the displacement independent earth pressure load assumption, may or may not lead to conservative lining design, in cases where the construction quality is good.

The methods that specify tunnel lining performance were developed in the U.S.A. by Peck and co-workers. They represent a development with respect to the older empirical methods just described, as they recognize (in an approximate way) the lining-ground interaction. They are more consistent with modern tunnelling practice, asking for flexible lining design and good construction quality. According to these methods, a circular tunnel lining should be designed for a uniform ring compression, corresponding to the overburden pressure at the springline, plus an arbitrary imposed distortion measured as a percentage change in the lining radius. As noted in Chapter 3, the full overburden assumption is debatable, since in most cases, it is not substantiated by practical or theoretical evidence. The arbitrarily imposed distortion generating bending stresses, is not consistent with the uniform lining compression assumption, since this calls for an ideally flexible and incompressible lining which does not generate bending moments. According to this approach, lining bucking is examined for a uniform load condition, under which, this type of instability is a rare occurrence, for usual tunnel depths and sizes.

The second group of methods reviewed for lining load prediction, included the ring-and-plate analytical solutions.

These solutions are divided into two categories, according to whether the type of in situ stress field they assume is uniform or non-uniform. In both cases, they are analytically developed as closed-form solutions which are very easy to handle.

The uniform stress field solutions include the so called convergence-confinement models. The particular state of stress they assume and the assumption of material isotropy, allow an independent assessment of the ground and of the support reactions. The evaluation of the interaction process, is therefore, greatly simplified, since no distortion of the lining occurs. This simplification allowed the treatment of the ground response using fairly complex constitutive relationships. For that they can be very useful in qualitative design estimates, but the impossibility to account for the lining bending in non-uniform stress conditions, makes the use of these solutions very restrictive for practical use in shallow tunnel design.

The non-uniform stress field solutions assume a state of plane strain and all, but one, assume the circular tunnel to be ideally deep, so that the action of gravity is disregarded. The non-uniformity due to stress ratios different from unity, gives more generality to these analytical solutions, but at the price of having to assume simpler linear elastic material behaviour for the lining-ground interaction analysis. Fourteen different solutions were reviewed, focusing on their assumptions, abilities and limitations. Some assume an external overpressure loading condition which is not applicable to the tunnelling problem. The lining-ground interface is usually treated by a full or non-slip condition. In Chapter 2, it was contended that the latter condition usually represents an assumption closer to reality.

Among the solutions in this group, the most useful, although least used or referred to, it that by Hartmann (1970, 1972). It is the only one that fully accounts for the action of gravity. However, like other approaches, it neglects the presence of the ground surface, but, as indicated in Chapter 2 and further discussed in Chapter 7, this is not a very restrictive assumption, provided the cover to diameter ratio is greater than 1.5. For deep tunnels, the effect of the ground surface on the lining-ground interaction is immaterial, though the influence of the gravitational stress field is not.

The major deficiency of this group of solutions is the lack of ability to account for the effects of delayed lining installation. These are represented by the stress and stiffness changes in the ground prior to lining activation, and are always present in real problems (see Chapter 2). In particular, even if an initial homogeneous ground condition could be accepted, by the time the support is installed, a non-homogeneous ground condition would have been developed, as the non-linear soil at different points around the tunnel, would have undergone different degrees of straining, implying different degrees of stiffness degradation.

The third group of methods for lining load prediction included the ring-and-spring solutions. In these solutions the ground is represented by an infinite or finite number of springs (continuous or discrete ground reactions). Twelve different solutions were reviewed, with emphasis on their assumptions, features and limitations. These closed form solutions were either analytically or numerically approached, through the use of design charts or else requiring a computer program code for application.

Most solutions within this group assume a partial ground embedment, with no ground reaction considered at the crown region. This representation is derived from the assumption that a fully developed failure zone will always be generated above the tunnel, confined by two slip surfaces rising upward from the opening and intercepting the ground surface. This assumption implies accepting an extreme collapse condition, which will not prevail if adequate ground control measures are ensured, as they should be in urban tunnelling. The absence of ground embedment is assumed in the upper 90° or 100°, on the assumption of a tunnel roof collapse. This is also a very arbitrary assumption, as it is known (see Sections 2.2, 3.2 and 4.3.4) that, depending on the soil strength and on the geometry, other modes of collapse may develop. Accordingly, the partial embedment assumption would have to be further extended to the tunnel walls. For normal conditions, the assumption of 'embedment absence' could more sensibly be replaced by a 'weakened' or 'softened embedment' assumption.

In most solutions of this group, only radial springs are considered. Tangential springs are considered in a few cases in an attempt to obtain a better correspondence with the ring-and-plate solutions. The assumption of radial springs only will normally lead to safer estimates of the lining loads.

Some solutions are inaccurate, in that they neglect to consider the shear stresses at the lining-ground interface as an active load. Hence, as in Muir Wood's (1975) original ring-and-plate solution, they do not take into consideration the deformation components due to the full slippage condition.

Two main types of ground load assumptions are normally made: in situ stress and localized gravity loading. In the first, the lining is assumed to be installed in the ground before excavation takes place. This assumption of full ground loads is not consistent with the assumption of partial embedment, which requires considerable ground movement (thus, in situ stress relaxation) to realize it. The acceptance of these two assumptions combined implies assuming zero shear strength and zero shear stiffness along the two slip surfaces in the tunnel cover. This is clearly not realistic and is overconservative. The localized gravity loading at the crown (see Chapter 3) imply an acceptance of localized roof collapse and stable tunnel walls, and once again, these are conditions which are not compatible with good ground control and good lining-ground contact required in urban tunnelling.

Most of the ring-and-spring solutions assume that the tunnel profile is circular but some treat non-circular cross sections. This is one of the features that makes these solutions very attractive for practical use.

Other features reviewed referred to the account of geometric non-linearities and of the gravitational stress field in shallow tunnels.

It was shown that it is possible to find a complete correspondence between ring-and-plate and ring-and-spring solutions, provided in the latter, an infinite number of springs (continuous ground reaction) and that both radial and tangential springs are considered. The equivalence between the two types of solutions was illustrated for an unlined circular tunnel under a gravitational stress field.

The equivalent spring constants were found to depend on the position on the tunnel contour, on the in situ stress ratio, on the relative depth of the tunnel and on the elastic parameters of the corresponding continuum. The equivalence for a lined tunnel could also be found but was not attempted.

It was also shown that a complete correspondence between ring-and-plate and ring-and-spring solutions, with discrete ground reactions is not possible.

The deficiencies of this group of solutions are similar to those discussed for the ring-and-plate since no account of delayed lining activation (ground loads and stiffness reduction) is undertaken. The present solutions seem to show slightly more potential, in that with them, it is possible to account for different ground stiffness changes at the instant of lining activation, by ascribing different spring constants at different points of the tunnel contour. The differential stiffness changes around the tunnel were discussed in Chapter 2.

The fourth group of methods for lining load prediction included the numerical solutions, where the ground is treated as a continuum. The finite element method is the one most frequently used within this group, though other numerical solutions could be included. By treating the soil as a continuum, lining loads and ground displacements can be obtained simultaneously, which is one of the most important features of this group of models. The problem can be treated by two or three dimensional analyses, but the latter tends to be too complex for practical use. The use of finite element techniques in shallow tunnel design was not covered in this chapter but in other sections of this thesis. In Section 5.2.1.1 a brief review is presented on lining representation and on lining material modelling. In Section 5.2.1.2, an attempt is made to assess the ability of two-dimensional finite element analyses to predict lining loads in existing tunnels. Further comments on the subject are included in Section 5.2.2.1 and three-dimensional modelling is discussed in Section 5.3.

Two-dimensional finite element analyses present more potential practical use, though they are still involved and time consuming for routine usage. Putting aside aspects related to the material constitutive laws, the main difficulty involved in two-dimensional simulation is how to account for the actual three-dimensional effects of the tunnel advance. This problem is common in other two-dimensional methods for lining load prediction and the subject is treated separately.

The fifth group of methods for lining load prediction included solutions derived from parametric numerical analyses (numerically derived methods). Five methods within this group were reviewed. All of them used the finite element method as the numerical modelling tool. Most of them treated the ground and the lining as linear elastic materials. Just one assigned an elasto-plastic constitutive law to the soil, but assumed fixed strength parameters which reduced the generality of the results. Three of the methods assumed plane strain conditions. Another assumed a three-dimensional axisymmetric condition with a non-axisymmetric and non-gravitational stress field. The fifth assumed an actual three-dimensional representation of a shallow tunnel with non-circular cross section.

Additional assumptions and features of each method were described and discussed and these included the type of loading assumed in the two-dimensional methods, consideration of the in situ stresses, the presentation of the solution, etc.

The three-dimensional axisymmetric solution with non-symmetric loading by Erdmann (1983) deserves some comment. Though designed as a linear elastic analysis of a deep tunnel, with non-unity in situ stress ratio, the author included a representation of the shotcrete lining hardening with face advance. Support rings closer to the face were assigned lower stiffnesses in some analyses. If the results of these analyses are compared to those where a constant lining modulus was assumed, one concludes that the influence of the increasing shotcrete stiffness with increasing distance to the face, on the lining loads, is nearly equivalent to a net increase in the delay of application of a constant stiffness lining. Though requiring further investigation, it is believed that, for all practical purposes, the influence of the shotcrete lining hardening can be accounted for by using an increased unsupported heading span and a constant stiffness liner. It seems worth investigating in the future some criterion to define this increased span, taking into consideration the rates of shotcrete hardening and of lining placement.

The main deficiency of the available numerically derived methods is related to the usually strict range of validity of their assumptions. The parametric analyses they were based on usually cover conditions (geometric or geotechnical) which are fairly narrow, so that their application in practice is fairly restricted. Moreover, the linear elastic ground response they normally assume is another important limitation. Further limitations of each method were discussed on a case by case basis. However, it is believed that this type of method presents great potential for development in the future.

It is customary to introduce into the two dimensional models for lining load predictions or ground displacement estimates, some sort of approximation in order to get results which are closer to those obtained by three-dimensional methods. The actual three-dimensional longitudinal arching effect is represented in two-dimensional models by the introduction of some balancing internal stresses in the unsupported opening. Four procedures are available to simulate this, of which none are rigorously correct. As faint approximations of the actual three-dimensional condition, these procedures should be interpreted in terms of their degree of simplicity in use and of their ability to offer results that better approximate reality.

Eighteen methods were reviewed, some of them applicable only to numerical (finite element) solutions, but others also applicable to analytical (ring and plate) solutions. According to their development, these procedures are empirical, analytical or numerical. Moreover, according to the type of representation used, they were classified into four groups: core stiffness reduction, progressive core removal, imposed tunnel convergence and ground stress reduction. The advantages and limitations of each approach were discussed.

The core stiffness reduction introduces ficitiously created unknowns: a softened core stiffness and its rate of softening. The progressive core removal is only meaningful in staged tunnel construction and usually underestimates the lining loads. The imposed tunnel closure may be meaningful in TBM excavated schemes, when the soil closes the overcutting gap. Its application for other conditions is not as clear. It always requires an estimate of the closure at the face, which is not known. The ground stress reduction is the more usual procedure, and possibly the simpler one. It introduces one unknown, the amount of ground stress release prior to support activation. This stress release, defined as a fraction of the in situ stress is usually assumed to be uniformly applied to points of the tunnel contour. There is some evidence, however, suggesting that different stress releases may occur at different points of the contour. Even so, the constant release fraction is a simpler and usually safer assumption, as far as the lining design is concerned.

Unfortunately, most of the procedures available are applicable to numerical simulations only. Moreover, the others are to be used mainly in uniform stress field ring-and-plate solutions. The survey indicated that except for some fully empirical procedures, there is not a single solution to account for the three-dimensional effects in non-numerical two-dimensional models, such as the ring-and-plate or ring-and-spring, which could be applicable to shallow tunnels.

Available Methods for Prediction of Ground Displacements

A less extensive survey was made regarding the methods for ground displacement prediction. This is due to the much smaller number of methods available. These methods were classified according to the type of development on which they are based: empirical, semi-empirical, numerical and numerically derived. Numerical methods were not reviewed in this chapter since the use of finite element modelling for ground displacement prediction is covered in detail in Chapter 5 of this thesis.

Twelve methods were reviewed, the output of each were described, their assumptions presented and discussed. The input requirements were also given and the conditions for application of the methods reviewed.

Most of the methods were empirically or semi-empirically developed. The empirical methods have the least general application, as they cannot be used or extrapolated to conditions other than those assumed in their development.

The semi-empirical methods may allow a wider range of application, since they take into account some more or less fundamental parameters that control the phenomenon. However, many fundamental aspects are neglected.

Two types of semi-empirical procedures are distinguished: those that treat the soil as a continuum and those that approximate it by a particulate medium. The last group is the more popular one, in which the ground subsidence is treated as a stochastic problem. The number or volume of particles at a certain location being lost into the tunnel, is related to the probability of these particles moving down into the tunnel. This enables the ground subsidence profile to be approximated by a normal probability curve.

For good ground control conditions, in which local collapse of the ground is prevented, no ground particles are 'lost' and the fundamental soil behaviour is not probabilistic (de Mello, 1981). The essence of the soil response is better portrayed by a continuum mechanics approach, in which stresses and displacements can be related, which is a feature not allowed by the stochastic approach.

For these conditions, the stochastic solutions are reduced to fully empirical methods, with the normal probability function understood as a single curve fitting tool to adjust measured settlement profiles.

All methods within this class require an independent (usually empirical) estimate of the total volume of surface settlement or of the maximum surface settlement.

An extension of these empirical approaches was recently presented, in which the longitudial distribution of settlement was approached by a cumulative probability function. By assuming a zero volume change in the ground and by taking the ground settlement at the face as equal to half the total displacement, Attewell and co-workers further extended the method which can now be used to approximate the distributions of the entire displacement field in the cover of a tunnel being advanced. The ground displacement magnitudes, however, are estimated in an empirical manner.

The numerically derived methods approach the problem by two or three dimensional representations. The latter were developed with very restrictive assumptions, and can be applied only to a narrow range of conditions that make their potential practical use too limited. The limitations of each method were discussed on a case by case basis. A common limitation of available two-dimensional methods is that they always require some empirical assessment of certain parameters and in none of them, are the settlement predictions coupled with the lining load estimate.

Available Methods for Ground Stability Verification

The ground stability verification is usually performed using Plasticity solutions. Twenty-nine methods were reviewed. These were classified according to the stability problem they address. The main assumptions made in each method were identified, as well as the type of solution used (Upper or Lower Bound). The assumptions within the various solutions include the soil being weightless, approximating the problem by two or three dimensional representations, and treating the stability problems in terms of undrained or drained soil strength parameters. The format of each solution was described as well as its development(analytical or numerical).

The limitations of these solutions can be apprehended by their individual features and assumptions. Globally speaking, most of the available methods are strictly valid for homogeneous ground conditions and they do not account for time dependent ground responses. Effective stress stability analysis, with explict account of the pore water pressure effects, cannot be undertaken. The solutions are strictly valid for materials with the associated flow rule, showing a perfectly rigid-plastic type of response. Some of these limitations are further discussed in Chapter 6.

The most general 2D stability solution is that by D'Escatha and Mandel (1974), which is presented in detail in Chapter 6. No solution is available for the 3D tunnel face stability for drained soil strength parameters.

Survey of Lining Design Practice

The current practice of lining design was assessed through a survey carried out by the International Tunnelling Association in the late seventies and early eighties. The answers related to the soil tunnelling section of the survey were reviewed and re-interpreted by the writer.

Details of the survey procedures and its representativeness were given. The answers were provided mainly by designers, consultants and contractors, from 12 different countries. The questions were presented for two tunnelling situations: a TBM driven and a mined (NATM) tunnel, in different but very favourable geotechnical scenarios.

No conclusive answer was found in terms of the use of different design attitudes regarding distinct construction techniques.

A significant number of respondents use rather arbitrary approaches to define the in situ stress ratio, a factor which has an important role in the lining design.

Over half of the practitioners (54%) use a full overburden assumption when designing linings for shielded driven tunnels. On the other hand, a reduced overburden assumption is adopted by the same percentage of the respondents when designing the shotcrete lining of the mined tunnel case. It was not possible to clearly identify the reasons for these different design criteria.

For predictions of the thrust forces and bending moments, ring-and-spring models are those most frequently used (69%). The least frequently used is the finite element method (27%). In 31% of the responses the crown embedment is neglected.

Terzaghi's arching theory is the procedure more frequently used (64%) to define the reduced overburden ground load. The remaining responses indicated a preference for empirical approaches. It was noted that the commonly found use of a ring-and-spring model, with the semi-empirical earth pressure theory by Terzaghi, is somewhat inconsistent. According to his original ideas (Terzaghi, 1943:194), his theory approximates the actual pressures on the tunnel support after yielding of the soil upon the face passage and upon lining deformations under the ground loads. Thus, it approximates the final loads on the support and was not intended for use in a lining-ground interaction analysis.

The survey indicated that the spring constants of the ring-and-spring models, are usually obtained from results of laboratory tests, but did not disclose how this was done.

Some trend was noted towards the use of different design methods for different lining types. Empirical methods were preferentially used for primary lining design, while ring-and-spring models were used for secondary lining.

The majority of respondents do not take into consideration the non-linear behaviour of either the soil or the lining in their practice. They also do not take into account any three dimensional effect in the lining design, except for ground stress relaxation accounted by a few respondents.

Survey of Practice on Ground Settlement Prediction

A questionnaire was prepared and sent to active practitioners in 17 countries. Almost 73% of the respondents were active consultants. Simple questions were prepared to ensure a high return rate, which resulted in 70% of the 50 questionnaires sent. The questions were related to time-independent ground movement only.

The survey showed that 50% of the respondents use solely empirical or semi-empirical approaches for settlement prediction. Those using numerical methods only represented 18% of the respondents.

Reliability and simplicity are the basic qualities required by the majority of the practitioners in the selection of any settlement prediction method. The least demanded quality was the theoretical rigour.

Though the correspondence between ground movements and lining loads is widely recognized, more than half (possibly two-thirds) of the practitioners do not couple settlement and lining load predictions. These two predictions are usually done separately. Those who couple the predictions do so by means of the finite element method, though without claiming that this method is either reliable or simple.

It is apparent that if a new design procedure is to be developed, it would have to be a simple numerically based procedure, and it would have to be validated or calibrated against past experience to render it compatible with the required attribute of reliability.

5. SHALLOW TUNNEL MODELLING

5.1 Introduction

In Chapter 4, the available design procedures and the current design practice for shallow tunnels in soil were reviewed. It was noted that most existing procedures and the most common practices, even in the so called 'good ground control' conditions, do not take into consideration some important features of the ground behaviour or of the ground-support system. These features can be, but not always are, incorporated in designs based on numerical procedures, such as the finite element method. The survey of the practice revealed that only 27 and 32% of the responses to the questionnaire on lining design and on ground movements, repectively, use numerical approaches for design (normally combined with other procedures). Also, possibly two thirds of the practitioners do not couple the predictions of lining loads with ground settlements. This state of affairs seems to result, not so much from lack of knowledge or understanding of the mechanisms involved in a shallow tunnel construction, but rather, on the availability of adequate design tools that allow consideration of these mechanisms.

Practitioners are bound to introduce simplifications in their calculation models that tend to transform the design activity into an exercise of the anticipation of the most adverse conditions (possibly unattainable in the field), rather than an attempt to estimate more closely the likely response of the structure. In other instances the simplifications introduced are inadequate as they are possibly, unsafe.

Therefore, it seems desirable to attempt the development of a design procedure that may improve current practice, allowing for instance, the simultaneous estimate of lining loads and ground movements. Moreover, it seems crucial that this procedure take into consideration those important factors that always affect the tunnel behaviour. It appears that, if such a venture is to have some practical significance in present times, it should not be aimed at the development of a numerical model such as a new FEM code, but rather at a self-contained and simple method that avoids the use of a main frame computer facility. This is particularly important if such a procedure is to be used as an expiditious design tool for a preliminary design assessment, allowing sensitivity studies on the influence of these dominant factors that control the tunnel behaviour.

A method such as the one described above, can result from a systematic modelling of the tunnel behaviour, leading to a process of generalization. The limits of the generalization will clearly depend on the limits of the modelling tool and on its capacity for handling the controlling variables. Further comments on the process of generalization will be be included in the following chapter of this thesis. Otherwise the subject is covered in a paper by Resendiz (1979).

The knowledge accumulated from theory and the experience gathered from laboratory testing and modelling, as well as from field observations in prototypes, allow the identification of the relevant factors or variables that control the behaviour of a shallow tunnel in soil. The influence of some of these factors was discussed in Chapters 2 and 3 of this thesis. Although the inclusion of a very large number of variables in an analysis is theoretically possible, in practice this may not be feasible, particularly if the procedure is to retain simplicity. Therefore, a decision has to be made on which factors should be included and which should not. In order to render the problem tractable and yet to ensure some generality in the proposal, the number of factors or variables to be considered has to be reduced using some sort of criterion. For instance, those factors known to have an important role in most or all cases should ideally be considered. On the other hand, variables, regardless how of influential they might be, that may affect the tunnelling behaviour in one instance, but not in another, may momentarily be put aside and perhaps studied independently.

Following this criterion, it was decided to limit the development to full face excavated circular tunnels under time independent conditions with no ground failure. By excluding the effect of ground pore water pressure changes, the influence of soil consolidation does not have to be addressed and the influence of the tunnelling technology, in terms of the effect of the tunnel advance rate, is somewhat reduced. If ground failure is not involved, hence, on the assumption of good ground control conditions, there seems to be no need to address the effects of shear localization, as suggested in Chapter 2. It was also suggested there that, under those conditions, the effects of shear dilatancy may not be very pronounced, especially if the so called 'loosening' process is inhibited. Evidence shows particularly, that the volumetric strains in overconsolidated clays are very small even for tunnels at a near collapse situation. As additional simplifications, it will be assumed that the ground does not exhibit pronounced anisotropic behaviour or strain softening response. Moreover, non-geostatic loading conditions, represented by existing construction at the surface or subsurface, will be disregarded.

On the other hand, it was decided to include in the development of the design procedure, factors whose actions are known to be present in most common shallow tunnel situations. These are:

a) the effect of the relative position of a horizontal and stress free ground surface (H/D);

b) the action of gravitational body forces generating a stress gradient in the soil across the tunnel profile;

c) the non-uniformity of the in situ stresses generated by a horizontal to vertical stress ratio, K, different from unity;

d) the non-linear response exhibited by soils in terms of their stress-strain relationships, including the dependence on hydrostatic and deviatoric stress levels;

e) the delayed installation of the lining, generating ground movement and stress changes prior to support installation;

f) the interactive nature of the load transfer process developed between the soil and the support system.

Despite the simplifications assumed a priori, and a few others to be discussed later, it is believed that a design procedure that includes the influence of the factors listed above, is still sufficiently general for potential use in practice.

After identifying and reducing the factors or variables to be included in the development, the next step is to model the shallow tunnel problem. The purpose of the present chapter is to select, implement and test a modelling procedure, which allows the influence of these relevant factors to be considered separately. Yet, it must permit a simple representation of the problem, which may ultimately lead to a simple generalized solution for a prescribed range of conditions, without the recourse of additional modelling.

For the purpose envisaged, numerical modelling is the convenient approach to follow. Despite the considerable advance in physical modelling of shallow tunnels (e.g. Schofield, 1980), the ability and ease of studying the controlling factors separately, is far more limited in physical models than in numerical ones. Moreover, finite element simulation presently seems to be the most versatile tool available, widely accepted and used in tunnelling research and practice. It also seems convenient to depict the tunnel performance by some combined two and three-dimensional finite element simulations, in order to simplify the representation and yet still account for the relevant variable involved.

In the next section, overviews of previous studies on finite element modelling of shallow tunnels under time independent conditions will be included. No attempt, however, will be made to review the theoretical aspects of the subject, which are beyond the scope of the present work.

5.2 Two-Dimensional Modelling

5.2.1 Review of Previous Studies

An appreciable volume of contributions on two-dimensional modelling of shallow tunnels using finite element analyses has been observed over the last 20 years. Some of them were directed towards the understanding of the mechanisms associated with tunnelling and to the identification of the controlling factors that govern the tunnel behaviour. This is done by means of sensitivity studies. Some others were aimed at the development of design procedures, by generalization modelling, as shown in Sections 4.3.2.6 and 4.3.3, for lining loads or ground movement predictions, respectively. Finally, others focused on the finite element technique as a modelling tool for a prediction of the behaviour of actual tunnel structures or small scale physical models.

In the present section, an attempt will be made to briefly review previous studies, with emphasis being given to the latter class. The subject was of interest to other workers (for example, Katzenbach, 1981:34, Eisenstein, 1982, Heinz, 1984:78), who reviewed it to a considerable extent. The present assessment will focus on numerical modelling from the user's point of view, and will summarize former works which are mainly related to prediction exercises in time independent situations. Intentionally left out of this review are the theoretical aspects related to the solution techniques of linear and non-linear finite element equations. This subject lies beyond the scope of this thesis.

5.2.1.1 Modelling Aspects

There are no firmly established criteria for modelling a shallow tunnel and, typically, the practical approach is to follow precedents. This task is partly guided by some rules or guidelines established from sensitivity studies, such as those by Kulhawy (1974) for deep tunnels, by Heinz (1984:80) for shallow tunnels and others.

Mesh Design

The finite element mesh is usually designed following guidelines that have resulted from parametric analyses. Most of them assume linear elastic stress-strain relationships for the materials involved. Therefore, they are strictly valid for this condition. Table 5.1 summarizes some of these guidelines, regarding the size of the domain to be discretized, the density of elements and the choice of boundary conditions. Available indications regarding the ideal position of the lateral boundary are not conclusive. During the course of investigations with the numerical model to be presented in Section 5.2.2, it was noted that the position depends not only on the size of the opening, but also on the ratio of cover to diameter, and on the Poisson's ratio of the ground. These facts were also noted by Seneviratne (1979:87). No attempt was made to generalize these findings, although some systematic investigation on the subject would be very useful. The location of the lateral boundary was defined in a case by case basis in the present study. In analyses where the ground is homogeneous with a constant stiffness with depth, the amount of heave at points below the tunnel will depend on the location of the lower boundary. Unrealistic heaves result in this case, unless stiffness-depth variations are considered or the correct location of a 'rigid' boundary can be assumed. The positioning of the lower boundary becomes immaterial when ground stiffness increases with depth.

Some authors (e.g. Kulhawy, 1974:465) advocate the use of elements with linear strain capabilities for the ground representation. Others (e.g. Orr et.al. 1978:123, Medeiros,

Representation Aspect	Case	References	Comments
Mesh discretization	Shallow and deep tunnels	Kulhawy (1974:469) Oteo & Sagaseta (1982:653) Ahrens et al (1984:87) Heinz (1984:87)	Element density affects tunnel convergence more and surface settlements less. Increase density where stress gradients are higher. Discretize tunnel half contour with more than 8 elements (lower order).
Boundary location	Deep tunnels	Kulhawy (1974:470) Almeida & Pereira (1978)	Boundary location affects displacements more than stresses. Locate 'infinite' boundary at more than 3 diameters away from tunnel centre. Location effects depend also on boundary condition.
	Shallow: Lateral Boundary	Oteo & Sagaseta (1982:653) Ahrens et al 1982:264) Heinz, (1984:94)	Effect of boundary negligible when located at more than 8 diameters away from tunnel centre.
	Lower Boundary	Ho (1980:49) Rowe et al (1981:271) Oteo & Sagaseta (1982:654) Rowe et al (1983:14) Heinz (1984:94)	Lower boundary located at 'infinity' result in unrealistically high ground heave below tunnel if ground is elastic and homogeneous. Magnitude and distribution of ground displacements are thus affected. Heave effect mitigates if realistic variation of ground stiffness with depth is assumed or if a higher operating ground modulus is assigned to elements below tunnel floor.
Boundary conditions	Deep tunnels	Almeida & Pereira (1978)	A fixed displacement boundary condition affects the numerical results more than a free boundary, for the same boundary location.
	Shallow tunnels	Heinz (1984:94)	Magnitude and distribution of surface settlements unaffected by type of boundary condition at the lower boundary.

Table 5.1 Some Guidelines for Two-Dimensional Finite Element Mesh Design, Derived from Sensitivity Studies

1979) favour the use of the simpler lower order constant strain elements, despite the need of a higher element density to provide sufficient accuracy. For the lining representation, beam elements are sometimes favoured (e.g. Ahrens et.al., 1982:264, Paul et.al., 1983:85), for their ability to directly furnish the lining internal forces. In this case the integration of element stresses is avoided. Otherwise, layered systems of plane elements may also suffice (e.g. Fleck and Sonntag, 1977,1978).

As noted in Section 2.3.5, while a full slip condition between the ground and the lining is hardly realistic, and a no-slip situation is a better representation, there might be some interest in investigating intermediate slip conditions. For this, interface elements such as those reviewed by Brandt (1985), are adequate. Applications of these element types to tunnelling problems are not abundant but can be found in Rodriguez Roa (1981), in Saha (1982) and in Paul et.al. (1983:86).

Excavation Simulation

The need to take into account the gravitational in situ stress field in shallow tunnel analyses was stressed in Section 2.2. This was also pointed out by Kulhawy (1975:47) who performed numerical analyses considering the action of gravity. He concluded that the latter should be considered for openings at 150 m depth or less. His conclusion, however, cannot be readily generalized since no indication of the size of the opening was given.

The initial stresses are computed directly as a function of depth below ground surface, assuming the vertical and horizontal stresses to be principal stresses. The vertical stress is taken as the overburden stress and the horizontal stress is calculated as K times the vertical. This requires a horizontal ground surface and horizontally layered deposits, with constant lateral earth pressure coefficient K. This approach was favoured by Medeiros (1979:158) and is the most commonly used procedure to introduce the initial stress condition with horizontal ground surfaces (Kulhawy, 1977:531). Otherwise, the initial stress state is implemented by the "switch-on-gravity" approach, in which K is dependent on Poisson's ratio. This restricts the generality of the approach, unless an unbounded Poisson's ratio can be assumed initially in order to render the desired K value, and amended in a second step to comply with the bounds imposed by elasticity. The latter approach was favoured by Chan (1985) and Wong (1986:48) for shallow tunnel simulations.

Three procedures are usually used to simulate the excavation of an underground opening. These are listed in Table 5.2, where some indications of their main features are also included. The limitations of these techniques can be inferred from the comments. The so-called general approach is a more rigorous method, furnishing results which are insensitive to the number of steps or phases into which a staged or incremental excavation is divided. However, for single phase excavation, as for a full face tunnel excavation, the errors involved in the other procedures tend to be small and the results are virtually the same (Kulhway, 1974:467, Ghaboussi and Pecknold, 1984:2061). In this case the discussion on the adequacy of the simulation procedures is merely academic.

In Section 4.3.2.7, a variety of approximate methods to account for three-dimensional effects in two-dimensional models were reviewed. Some of them are strictly applicable to finite element numerical simulations. A summary of the latter is reproduced in Table 5.3. For further examples and specific details of these procedures one is referred to Table 4.10. The procedures in Table 5.3 were classified into four groups, according to particular features and also where each are usually applied: staged (or incremental) and full face tunnel excavation. Moreover, each procedure employs more or less distinct numerical techniques to simulate the excavation. This is also shown in the table.

As suggested in Section 4.3.2.7, all procedures should be taken as rough approximations to bring the 2D solutions closer to the actual conditions. Their qualities should not be analysed in terms of the generality of their assumptions or of their rigour. Rather they should be evaluated by their degree of simplicity and their ability to furnish results closer to reality. For full face, single stepped excavation schemes, procedures 2, 3 and 4 in Table 5.3 are equally applicable. Procedure 1 is inappropriate as it leads to an

Procedure	References	Comments
1. Gravity turn-on	Kulhawy (1974:466)	Require two analyses, with and without the opening. Results furnished by the differences between the analyses. K is not an independent variable but a function of Poisson's Ratio. Do not model a construction sequence. Adequate for one step full face excavation in linear elastic materials.
2. Conventional approaches		
a) Stress reversal	Kulhawy (1974:465) Medeiros (1979:163) Chandrasekaran & King (1974)	Apply equivalent nodal forces with reversed sign along excavation contour and reduce modulus of excavated elements (to at least 10^{-6} times its original value). Forces calculated for instance, by lumping element stresses adjacent to the contour, using different approximate procedures. Results are step number sensitive.
b) Relaxation	Kulhawy (1974:466)	Excavated region not represented in the finite element mesh. In situ stresses applied as nodal forces on tunnel contour to represent action of non-existent core. Contour loads relaxed to simulate excavation. Difficult to follow a stepped construction sequence with simplicity. Procedure reduces approximately to the previous for single step, full face tunnel excavation.
3. General approach (Activation and de-activation)	Ghaboussi & Ranken (1981:254) Ghaboussi & Pecknold (1984:2052) Heinz (1984:83)	Equivalent nodal forces calculated consistently with interelement stress discontinuities across element boundaries that do not form part of the excavation contour, and accounting for weighted element residuals, arising from local equilibrium errors. Excavated elements are deactivated, being omitted in equilibrium equation. More rigorous approach involving less approximations. Insensitive to number of excavation steps. No major differences in relation to previous procedures, for single step, full face tunnel excavation.

Table 5.2 Excavation Simulation Procedures for Tunnel Modelling with Finite Element Techniques

	Procedure	Where Usually Applied	Main Features	Excavation Simulation Procedure	Examples of Use[(1)]
1.	Progessive Core Removal	Sequential excavation schemes	Gradual removal of elements within tunnel cross section (core), normally following the actual sequence of tunnel excavation. The stresses around the contour of the portion being excavated are usually zeroed and the partial application of the support takes place in the subsequent excavation step.	Stress reversal or general approaches	Baudendistel (1972) Sagaseta (1973) Kulhawy (1975) Wanninger & Breth (1978) Negro et al (1984)
2.	Ground Stress Reduction	Full face excavation schemes (non staged)	Complete 'removal' of elements within the entire tunnel cross section with their stiffness reduced to a near zero value or excavated area not represented in the finite element mesh. Boundary stresses at tunnel contour gradually reduced to a prescribed value or until a certain value of section convergence is achieved. At this stage support is installed and remaining boundary stresses are released.	Stress reversal or relaxation approaches (2)	Tan (1977) Rowe et al (1981) Zagottis (1981) Heinz (1984) Baumann et al (1985) Wong (1986) Ng et al (1986)
3.	Core stiffness Reduction	Both full face or sequential excavation schemes	Stiffness reduction of elements in certain area within tunnel section. Reduction factor empirically assessed, being usually calibrated by back analyses. Then partial or complete reduction of in situ stresses around the contour of softened area.	Stress reversal and general approaches	Swoboda and Laabmayr (1978) Van Dillen et al (1979) Schikora (1982) Baumann et al (1985)
4.	Imposed tunnel Convergence	Full face excavation schemes (non staged)	Imposed displacement boundary conditions at tunnel contour derived from independent numerical simulation accounting for face advance effects or from field observations.	Pre-determined displacement boundary	Negro and Eisenstein (1981) Ohta et al (1985)

Notes: (1) For further examples see Section 4.3.2.7 and Table 4.10.

(2) General approach can be used but it is reduced to the conventional approach, if boundary stresses and equivalent nodal forces at tunnel contour are inconsistently determined from element boundary tractions or are independently fixed.

Table 5.3 Numerical Procedures to Account Approximately for Three-Dimensional Effects of a Tunnel Advance in Two-Dimensional Finite Element Analyses

unstressed support. Procedure 3 (core stiffness reduction), has the virtue of automatically furnishing the boundary balancing stress around the softened area without a prefixed assumption on the rate of the in situ stress release around the tunnel contour. However, it introduces an additional unknown variable, which is the degree of stiffness reduction (referred to herein as 'softening') of the tunnel core. The assessment of this parameter is inevitably empirical.

Procedures 2 and 4 are basically equivalent. They both require an independent assessment of the degree of stress release at the tunnel contour or of the amount of tunnel convergence. This is to account for the 3D stress transfer and the delayed support application. This can be done with some degree of formalism using few existing methods, but a large amount of empiricism or informal judgement is always required. Available simplified methods (e.g. Ng et.al., 1986:48, Ohta et.al. 1985), are conceptually inadequate as they infer that the losses of ground of a shallow tunnel can be approximated by deep tunnel solutions, with uniform stress field (K=1). In essence, no 2D procedure is presently available to properly relate the degree of stress release or tunnel cross section convergence occurring in the 3D advance of a shallow tunnel. Moreover, in cases where the construction technology used does not make use of a shield machine, the simplified procedure such as that by Ng et.al. (1986) and others, are not readily acceptable.

Lining Material Modelling

As in the ring-and-plate or the ring-and-spring solutions (Sections 4.3.2.3 and 4.3.2.4), most finite element modelling assumes the support as a linear elastic, isotropic and homogeneous material. This is a simpler and usually conservative assumption, for prediction of the working loads on the lining. However, as noted by Paul et.al., (1983:137) and Duddeck and Erdmann (1985:257), if the analysis aims at the assessment of the ultimate capacity of a concrete lining, the assumption of linear elasticity may lead to an overconservative design. Paul et.al., (1983:139) showed that if the actual non-linear behaviour of a reinforced concrete lining is taken into consideration, the capacity thrust value for large eccentricities is typically 1.8 to 2.8 times that estimated from linear elastic analysis. Recognizing however, that a non-linear lining analysis will hardly be carried out routinely, these authors proposed a simplified procedure, applicable to cases where the load eccentricity is large (load path intersecting the moment-thrust interaction diagram below the balance point). Linear elasticity is assumed to obtain the eccentricity and the thrust load, but the ulimate thrust value is obtained from Paul et.al., (1983:142), taking the non-linear effect fully into consideration. For smaller eccentricities, results from linear elastic analyses will not provide overconservative ultimate loads and the lining non-linearity may be neglected.

The case of shotcrete lining represents a special case, as its stiffness changes with time. Hence, with a gradual advance of the tunnel, lining sections at different distances from the face will show different stiffnesses. The net response of the lining will be non-linear, and the degree of non-linearity in its stress-strain behaviour will depend on the rate of the shotcrete stiffness increase in time, on the rate of tunnel advance and shotcrete placement. The subject was studied by Erdmann (1983:185) and by Schikora (1984) who used three-dimensional finite element modelling. As explained in Section 4.3.2.6, Erdmann (Op.cit.) assumed a constant shotcrete modulus in one analysis, and made two assumptions of the variation in the modulus with distance to the face. In both cases, the shotcrete modulus was assumed to increase from a near zero value at the leading lining edge to its final value one diameter behind. In any case, the lining behaviour was assumed to be linear elastic. Two distances of delayed lining installation were considered, measured from the tunnel face to the leading edge; 0.5 and 0.25 times the tunnel diameter. Erdmann's results strongly suggest (Op.cit.:193-195,202-206) that the effect of this variable stiffness on radial displacements, radial stresses, thrust and bending moments, can be quite reasonably taken into account by assuming a constant shotcrete modulus (in a linear elastic analysis) and a nominally increased distance of delayed lining installation. Although Erdmann did not pursue the subject, it seems likely that one could propose some useful rule relating the rate of shotcrete stiffness increase with time and distance, to an equivalent distance of delayed lining application, for a constant shotcrete modulus.

Lining-Soil Interface Modelling

Most of the finite element modelling conducted for soft ground tunnelling assume a non-slip condition between the soil and lining. Few studies assumed a full-slip interface condition, with zero shear transfer from soil to lining (for example, Ranken, 1978:96 and Ahrens, 1982:266, see Section 4.3.2.6). Fewer treated the interface as a non-linear material. Rodriguez Roa (1981) and Saha (1982) modelled it using an interface element, with very high normal stiffness and an elasto-plastic tangential shear-deformation relationship, with failure described by the Mohr-Coulomb criterion.

Soil Modelling

A review of the stress-strain relations applicable to soil modelling is beyond the scope of the present work. The subject was covered comprehensively by Christian (1982), Wroth and Houlsby (1985), Dyer et.al. (1986), among others. Some aspects of these relations which have been used to model tunnels in soil will be briefly discussed.

Figure 5.1 lists examples of different stress-strain relations for soils, which have been used in shallow tunnel modelling for the assessment of stress and displacement, under time independent conditions. Three classes of relationships are identified. The two most commonly used are the elastic and the elasto-plastic models, which are mainly used in connection with finite element applications. A third class of soil model is included, that is used in associated field solutions, which are less popular than finite element for stress-displacement analyses. This class includes rigid-plastic models, which usually satisfy the normality condition of the associated flow rule. But the associated field solutions have been extended to cases where the soil is not at failure everywhere and therefore the flow rule is not associated (Atkinson, 1981:262). Atkinson et.al. (1975:8) presented solutions using the latter approach with a hardening law for shallow tunnels in sand.

For the reasons exposed in Sections 2.3.4.3 and 4.1 linear elastic analyses applied to shallow tunnelling tend to furnish results that are poorer than those from non-linear analyses. Good correspondence may be found between linear elastic prediction and actual performance, if the comparison is defined in terms of a limited number of parameters (e.g., maximum surface settlement). However if a complete comparison is proposed, including vertical and horizontal displacements in the ground mass as well as lining deformations and loads, then a good correspondence between linear elastic prediction and performance seems unlikely for most soils and usual ground control conditions. Consideration of soil anisotropy in these analyses may

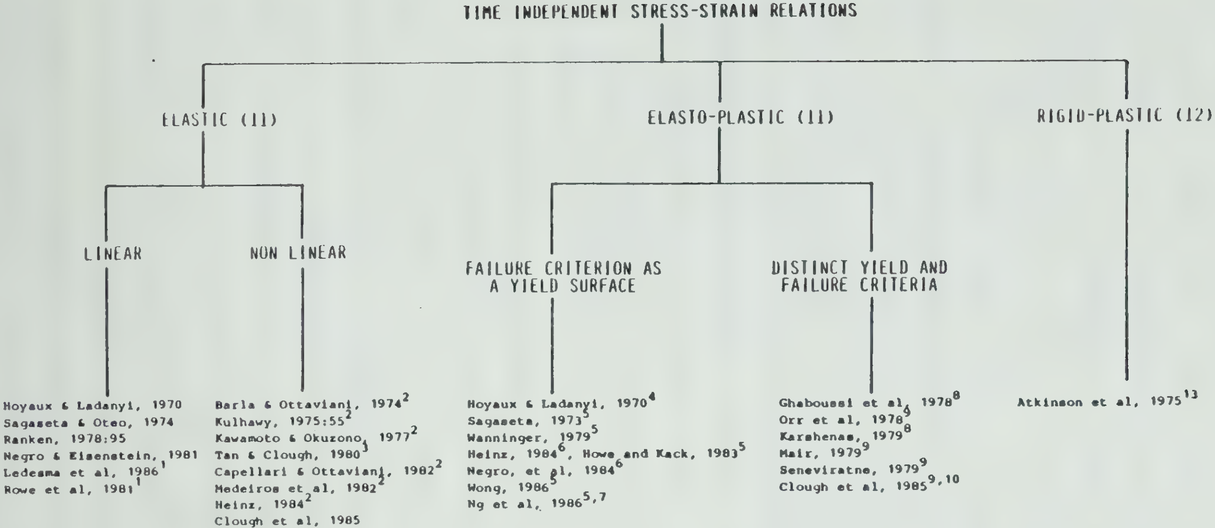

Notes:

1. Elastic anisotropic model
2. Duncan & Chang (1970) hyperbolic model
3. Hyperbolic model in terms of bulk and shear moduli
4. Tresca's failure criterion
5. Mohr-Coulomb failure criterion
6. Von Mises failure criterion
7. Elastic anisotropic model; parameters defined according to stress path
8. Ghaboussi & Karshenas, 1977 critical state model
9. Modified cam-clay model
10. Prevost, 1980 critical state model
11. Finite element applications
12. Associated field solution
13. Non classic plasticity solution, with limited failure, non-associated flow rule and hardening law.

Figure 5.1 Examples of Stress-Strain Relations for Soil used in Shallow Tunnel Modelling

improve the correspondence, for instance with respect to the maximum slope of the surface settlement trough (e.g., Rowe et.al., 1983:17), but it is improbable that a complete correspondence of all aspects involved would be achieved. Besides, proper assessment of cross anisotropic material properties (e.g., Lo et.al., 1977, Ng and Lo, 1985) involves testing and evaluation procedures which are not routinely used, except in cases where the ground anisotropy is of prime concern and likely controls the tunnel performance.

Potentially the most useful relationships for soil tunnel modelling are non-linear, and are either elastic or elasto-plastic. As it will be seen in the following section, the latter seems to be widely used in numerical predictions for soil tunnelling. This fact would appear to reveal a general belief that for this type of geotechnical structure, the soil non-linearity is an aspect of concern.

Among the linear elasto-plastic models, those in which the failure criterion is adopted as a yield surface are more frequently used. Normality is often assumed, but non-associated flow rules have also been employed. If the construction of the tunnel being simulated is performed under good ground control conditions, so that soil failure is fully prevented or the failed zone is rather limited, these models will mainly portray a linear elastic response. This is a shortcoming of this class of stress-strain soil relationships.

In fact, accurate strain measurements with displacement transducers in the laboratory (Costa-Filho, 1980), have shown that even stiff soils like London Clay, exhibit a clear non-linear stress-strain behaviour at very small deviatoric strains. The study of small strain behaviour of soils (up to 0.1%) under undrained conditions as observed in triaxial testing, has advanced considerably by the use of electrolevel gauges (Jardine et.al., 1984) or of magnetic flux density gauges (Clayton and Khatrush, 1986), that allow the local measurement of strain as opposed to the global one. Jardine et.al. (1985) observed that the undrained stiffness of a stiff clay can show a drop of two-thirds for an increase in strain from 0.01 to 0.1%. A similar response can possibly be anticipated in terms of the drained stiffness.

The results of the laboratory testing by Jardine et.al. (1985) suggest that, at least for London Clay, the account of the non-linear behaviour at small strains is more important than the influence of stress relief due to sampling and of the stress path applied to the sample. Indeed, while the stiffness of this particular clay may change by a factor of two when subjected to undrained compression as opposed to extension, the stiffness at small strains (say at 0.01%) as obtained from external measurements, can be an order of magnitude smaller than the value derived from local strain measurements (Jardine et.al., 1984:331 and Jardine et.al., 1985:511).

Moreover, the large mass of soil in a number of geotechnical structures including excavations, is strained to less than 0.1% deviator strain (Jardine et.al., 1986:394). Therefore, it is not possible to accurately depict soil behaviour before yield by ascribing linear elastic deformation moduli, even if the parameters are backanalysed from field measurements of similar structures (Fourie et.al., 1986:233).

Elasto-plastic stress-strain relations with distinct yield and failure criteria, represent an improvement with respect to other elasto-plastic models. The use of critical state models such as the Modified Cam-Clay model may ameliorate predictions, especially for normally consolidated soils. However, for lightly or overconsolidated clays, Cam-Clay models will still predict an elastic response for the soil at stress levels below yield, both for drained and undrained loading (Bolton, 1979:220, Wroth and Houlsby, 1985:19). The criticism applied to the other elasto-plastic models is also valid here: no account is taken of the pre-yield non-linear response of overconsolidated soils.

Non-linear elastoplastic models (e.g. Evgin and Eisenstein, 1985) would solve this problem. Apparently the use of these models in shallow tunnels has not been reported. Few constitutive models available take into account the complete non-linearity of the stress-strain response of soils. The most popularly used model for analyses of tunnels in soil are those with non-linear elastic incremental formulations of a hyperbolic type (see Figure 5.1). This empirical model will be described and discussed in following sections of this thesis. It is formulated in different ways and it is popular because it is simple and requires a small number of parameters which are easy to obtain.

Jardine et.al. (1986:380) proposed a new non-linear elastic formulation for undrained loading. The stress-strain relation was empirically derived from curve fitting of laboratory results and is represented by a periodic logarithmic function, requiring 5 parameters for its definition. While designed to provide a more accurate fit of the stress-strain relation in the small strain range, it increased the number of required parameters compared with that needed for the more traditional undrained hyperbolic formulation. The new model was tested in a retained excavation scheme and furnished improved predictions of horizontal and vertical displacements of the ground, as compared to an elasto-plastic analysis with the failure criterion as a yield surface. Nevertheless, the merits of this formulation for shallow tunnel modelling remain to be seen.

Figure 5.2 furnishes results of tests on a reconstituted glacio-marine sediment of low plasticity, anisotropically consolidated and subjected to undrained shearing in a Bishop and Wesley triaxial cell (Jardine et.al., 1984:327 and Jardine et.al., 1986:379). The clay had an OCR of 2.05 before shearing, and K_o equal to 1.47. The dots represent results of the triaxial test with locally measured axial strains. The dashed curve corresponds to a simulation using the non-linear elastic-perfectly plastic model of Jardine et.al. (1986). A good agreement with the experiment is obtained using this five parameter model. The full line shown represents a best fit hyperbola described in this case (anisotropic test) by three parameters. A fairly reasonable agreement is also obtained, despite the latter being a simpler model. From this , it can be seen that the hyperbolic formulation can provide an adequate representation of the stress-strain relation of this lightly consolidated clay in the small strain region.

Another example of the suitability of the hyperbolic formulation is shown in Figure 5.3. The dots represent results of an unconsolidated undrained triaxial test in an undisturbed Blue London Clay sample, taken from a depth of 7.3 m below surface the at Canons Park (Jardine et.al., 1985:511). The soil was heavily over-consolidated and had an estimated K_o of 3. The axial strains were also measured locally. A fitted hyperbola accommodates the data reasonably well over a considerable range of deviator strains. An initial tangent modulus from the hyperbola was found to be 91.5 MPa. Had the axial strains been measured externally, with all due corrections included (e.g. cell compliance), the stress-strain curve obtained would be that shown by the chain-dotted line. An initial 'linear elastic' portion would

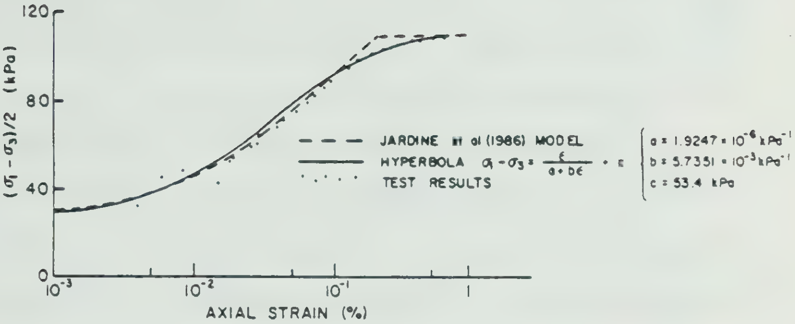

Figure 5.2 Triaxial Test Results on a Lightly OC Clay and Predictions by the Hyperbolic and Jardine et.al. (1986) Models

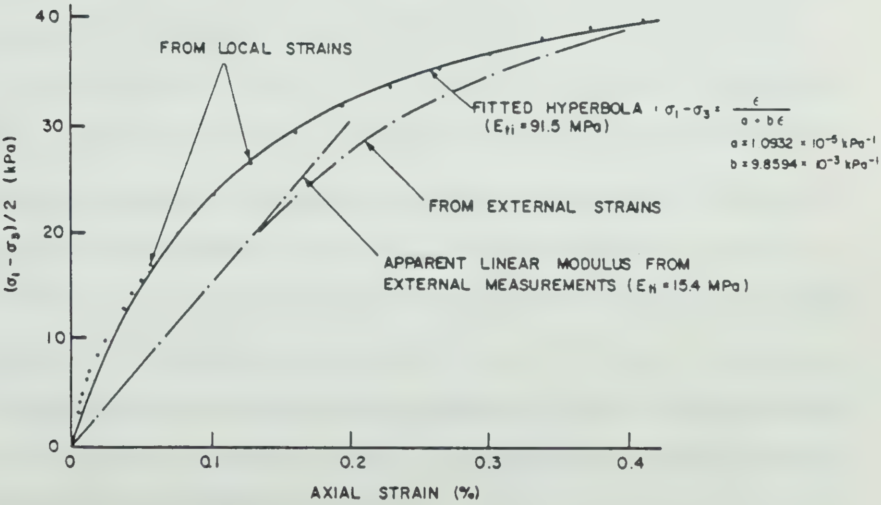

Figure 5.3 Stress-Strain Relations for OC London Clay under Unconsolidated Undrained Triaxial Test (after Jardine et.al., 1985:512, modified)

have been identified giving a Young's modulus of 15.4 MPa. This is about one-sixth of the initial modulus given by the locally measured strain data.

In summary, a good prediction of ground behaviour could be ensured if the complete non-linear stress-strain relation was to be accounted for and if an accurate assessment of the initial tangent modulus was possible. The hyperbolic stress-strain formulation is a simple and adequate way to describe the non-linearity of soil. Assessment of the soil stiffness at the small strain range can be made in the laboratory with good quality undisturbed samples, by means of specially designed strain meters. It can also be evaluated through in situ testing (e.g. Jamiolkowski et.al., 1985:113). Recent studies on seismic or geophysical measurements for the evalution of elastic parameters provided encouraging results (for instance, Abbiss, 1986).

5.2.1.2 Prediction of Performance by Finite Elements

In this section, an attempt will be made to evaluate the capabilities of finite element techniques as a prediction tool for soil tunnelling problems. The role of predictions in soil engineering practice was examined by Lambe (1973) who proposed a classification that is reproduced in Table 5.4.

A comprehensive, but not exhaustive, list of prediction exercises applied to shallow tunnels was prepared and is shown in Table 5.5. The review covers only works published over the last decade, where comparisons between numerical results using two-dimensionsal finite element analyses and field measurements were made available. The list provides brief details of the tunnel location, construction method and type of soil. Laboratory tunnel models are also included. Furthermore, the type of prediction mode is indicated, according to the classification shown in Table 5.4. Each case was classified according to details and descriptions provided by the authors. A relative degree of uncertainty was involved in the classification of a number of cases (38% of the total) and these are marked accordingly.

Table 5.5 also includes some indications of how the numerical simulation was performed, especially how the 3D effects were accounted for in the 2D analyses. The type of stress-strain relation used for the soil is also given. Lining representation was not always included, but when it was, lining material was assumed to be linear elastic, and a no slip condition at the lining-soil interface was assumed.

Finally, Table 5.5 provides a qualitative comparison between the predicted and measured performances. The aspects of performance that were inspected included:

a) surface settlements: magnitudes of the maximum settlement and maximum distortion, plus the overall aspect of the transverse settlement profile;

b) subsurface settlements: magnitudes of the maximum subsurface settlement and the overall distribution of settlements with depth;

Prediction Type	When Prediction Made	Results at Time Prediction Made
A	Before event	-
B	During event	Not known
B1	During event	Known
C	After event	Not known
C1	After event	Known

Table 5.4 Classification of Prediction According to Lambe (1973)

	Author/Year	Tunnel	Soil	Construction Method	Prediction Type$^{(1,2)}$	Numerical Simulation	Stress-Strain Model for Soil	Surface Settlement			Subsurface Settlement		Horiz. Displ.		Lining Loads	
								Mg.	Dist.	Dtr.	My.	Dtr.	Mg.	Dtr.	My.	Dtr.
1.	Takemoto et al 1977	Odawara-Atsugi	Loam	Side drift	B1? (w)	Progressive core removal	Linear elastic (with creep)	≈		G	>	R	<	R	>	P
2.	Kawamoto & Okuzono 1977	Nagoya Subway	Sands	Shield	C1 (w)	Ground stress reduction	Non linear elastic	≈	≈	G						
3.	Gartung & Bauernfeind 1977	Nuremberg Subway	Keuper Sandstone	NATM	B (z)	Ground stress reduction	Elasto-plastic	>	≈	G						
4.	Swoboda & Laabmayr 1978	Munich Subway L8/1	Marls	NATM	B1 (z)	Stress & stiffness reductions	Elasto-plastic								>	G
5.	Ghaboussi et al 1978	Univ of Ill. model	Ottawa sand	Self weight model test	C1 (x)	Imposed tunnel convergence	Elasto-plastic (with cap)	≈	>	G						
6.	Orr et al 1978	Cambridge Univ static model	o.c. kaolin	Ext. load drain. test (a)	C1? (x)	Ground stress reduction	Elasto-plastic (mod. Cam-clay)	>	<	R	>		>			
7.	Karshenas 1979	Cambridge Univ static model	Leighton Buzzard sand	Ext. load model test	C1 (x)	Ground stress reduction	Elasto-plastic (with cap)	≈	<	R	>					
8.	Mair 1979	Cambridge Univ centrifuge model	O.C. kaolin	Gravit.undr. load (2DP,2DV)	C1? (x)	Ground stress reduction	Elasto-plastic (mod. Cam-Clay)	<	<	R	<					
9.	Seneviratne 1979	Cambridge Univ static model	N.C. kaolin	Ext. load undr. test (UDC)	A? (x)	Ground stress reduction	Elasto-plastic (mod. Cam-clay)	<	<	P	<					
10.	Negro & Eisenstein 1981	ABV water tunnel	Clayey sand	Full face hand mined	C1 (y)	Imposed tunnel convergence	Linear elastic	<	<	R	≈	G				
11.	Schikora 1982 and 1983	Munich Subway S6, LW2	Gravel	NATM	C1? (z)	Stiffness & Stress reduct.	Elasto-plastic	≈	≈	G	≈	G			≈	R
12.	Garcia C. et al 1984 Sagaseta 1973	Madrid Subway L6	Hard Clay	Belgian method	C1 (y)	Progressive core removal	Elasto-plastic	>			≈	G			≈	P

Table 5.5 Review of Some Numerical Predictions of Shallow Tunnel Behaviour Using Two-Dimensional Finite Element Analyses

							Surface Settlement			Subsurface Settlement		Horiz. Displ.		Lining Loads	
Author/Year	Tunnel	Soil	Construction Method	Prediction Type$^{(1,2)}$	Numerical Simulation	Stress-Strain Model for Soil	Mg.	Dist.	Dtr.	Mg.	Dtr.	Mg.	Dtr.	Mg.	Dtr.
13. Imaki et al 1984	Narita Airport Skinkansen tunnel	Fine Sand	NATM	A? (w)	Progressive core removal	Visco elasto-plastic	>	=	G	>	G	>	R	<	G
14. Negro et al 1984 Eisenstein et al 1986	Sao Paulo Subway North Extension	Fissured silty clay	NATM	A (x)	Progressive core removal	Elasto-plastic (with harden.)	=	=	G	=	G				
15. Katzenbach 1985	Munich Subway S2, L5/9	Marls	NATM	C1 (w)	Progressive core removal (and dewater)	Elasto-plastic	<			<	G				
16. Clough et al 1985	San Francisco Water Tunnel (N2)	Soft silt and clay	Earth Pressure Balance Shield	C1 (w)	Ground stress reduction	Elasto-plastic with consol. (Mod. Cam Clay)	=	<	R			<	P		
17. Ohta et al 1985	Sewage tunnel	Sands	Slurry Shield	C1? (y)	Imposed tunnel convergence	Elasto-plastic with consol (Mod. Cam Clay)	=	<	G	>	R	>	P		
18. Baumann et al 1985	Munich Subway U5/9-7	Marls	Twin NATM (compr. air)	C1? (w)	Ground stress reduction	Elasto-plastic	=	<	R	<	G			<	R
19. Ng et al 1986	Thunder Bay (Array 1)	Soft silty clay	Shield	C1 (w)	Ground stress reduction	Elasto (anis.) plastic (stress path drain.)	=	>	R	=		>	G		
20. Ledesma et al 1986	Barcelona (Sect C)	Stiff clay	Mined	B (z)	Ground stress reduction	Linear elastic (back anal. param. used)	=			=	G	=	G		
21. Tan (1977:166)	Washington, DC Metro	Ungrouted sand	Shield	C1 (y)	Ground stress reduction	Non linear elastic	=	=	G	>	P	>	P		

Notes: (1) Types of prediction according to Lambe (1973:158) classification. The question mark indicates a certain degree of uncertainty.
(2) x: actual prediction; y: back analyses; z: prediction with previously calibrated model; w: any of the former x, y or z.
(3) Meaning of abbreviations and symbols: HORIZ. DISPL: horizontal displacements; MG: maximum magnitude; DIST: maximum distortion; DTR: overall distribution; =: calculated value approximately equal or equal to measured value; >: calculated value greater than measured value; <: calculated value smaller than measured value; G: good; R: regular; P: poor.

Table 5.5 Review of Some Numerical Predictions of Shallow Tunnel Behaviour Using Two-Dimensional Finite Element Analyses (Continued).

c) horizontal displacements: magnitude of the maximum displacement and the overall distribution of displacements with depth;

d) lining loads: magnitude of the maximum loads defined in terms of either radial ground stresses onto the lining, or thrust, and in a few cases, bending momements.

The calculated value is said to approximately equal the measured value, whenever the latter is within 20% of the former. Otherwise the calculated value is said to be greater or smaller than the measured value. The spatial distributions of displacement or loads were arbitrarily defined as good, regular or poor, after a liberal comparison between prediction and measurements was made.

Most of the literature covering the reviewed cases does not provide a complete set of information regarding both the case history (including construction details) and in depth details of the numerical simulation. The majority of cases fail to include an accurate assessment of the soil properties and their constitutive modelling. This alone could hinder any careful assessment of the models used to simulate the tunnel performances. Moreover, even if this were not the case, there is strong evidence that differences in the application of judgement (always required) between different individuals doing the prediction, are as significant as the different features involved in each modelling tool (Poulos, 1982:2). Ideally, a proper assessment of the modelling capabilities would be done by a single individual carrying out the prediction before the event (type A prediction), using different numerical simulation tools applied to a large number of case histories and covering all aspects of tunnel performance. The only exercise carried out closer to this ideal condition, was that by Clough et.al. (1985). However, they conducted a type C1 prediction, using basically one simulation procedure, three constitutive models for the soil in just one case history and restricted their comparison to ground displacements only. For this particular case (number 16 in Table 5.5) they were able to claim that the critical state model seems to provide the most adequate prediction. However, a brief inspection of their results, described in qualitative terms, shows that they are no better than the results obtained by other individuals, using different simulation procedures or stress-strain models in other locations.

Notwithstanding these facts, an attempt was made to identify the capabilities of the simulations, as related to the soil type, the construction method, and the prediction class, for each group of numerical simulation of tunnel construction and for each group of stress-strain model used. For that, a point rating criterion was tentatively established, and total points recorded for each case. Not suprisingly, the attempt was a fruitless one. Some of the most complete or powerful modelling procedures provided both some of the best and some of the worst predictions. No clear correlation was found between the prediction quality and the soil type, the tunnel construction method or the prediction type. The analysis was partly affected by the fact that, except for the magnitude of the maximum surface settlement, the predictions were compared to different aspects of measured tunnel performance. This is possibly due to the unavailability of field monitoring data on some performance aspects or failure to publish a complete set of comparative data.

Furthermore, it should be noted that most likely, some of the predictions classified as type C1, could actually be labelled as back-analyses of field performance, although not always clearly identified as such by the authors. A tentative identification is appended to the prediction type in Table 5.5, indicating which of the cases are actual predictions, back-analyses, predictions done with previously calibrated models and which are the unidentified cases. It is then observed that even a very simple numerical model, like that by Ledesma et.al. (1986), using a linear elastic relation with parameters derived from back analyses of similar conditions, can rank among those providing the best predictions. In this case, however, the lining installation was not simulated (Ledesma et.al., Op.cit.:337), and therefore the model cannot provide predictions of lining loads.

Because of the noted difficulties in evaluating the modelling abilities in each case, an overall appraisal of the numerical predictions was attempted. A similar assessment was done by Eisenstein (1982) on surface settlement predictions. Here the assesssment is extended to include other aspects of performance.

As a guideline to future interpretation, Table 5.6 has been prepared. It is noted that almost half of the cases studied originated in Europe and that 67% of the soils involved showed a cohesive nature. More than 50% of the cases refer to mining methods of tunnel construction, as opposed to TBM schemes that accounted for 24%. This distribution reflects the trend noted in Section 4.4.2.2 towards a more frequent use of finite element analyses in design practice for mined tunnels. With respect to the numerical simulation, most of the predictions accounted for the 3D effect of tunnel advance by utilizing a ground stress reduction procedure. This is followed in preference by the progressive core removal technique. Regarding the stress-strain model adopted for the ground representation, preference is given to elasto-plastic models (43%), with yield and failure coinciding. These are seconded by elasto-plastic models with distinct yield and failure conditions (33%).

As indicated in Figure 5.4, the majority of cases (67%) refer to type C1 predictions, including cases of actual back-analyses. This is not the ideal type of prediction to evaluate a simulation procedure, but nevertheless, it can provide some insight if this fact is fully appreciated.

Aspects	Percentage of Cases
(1) Case History Aspects:	
a) Tunnel location and study origin	
Europe	48
Asia	19
North America	24
South America	9
b) Type of soil	
Cohesive	67
Cohesionless	33
c) Construction Method	
Mined tunnel	52
Model tests	24
TBM schemes	24
2. Simulation Aspects:	
a) Account of 3D effects in 2D analysis	
Ground stress reduction	52
Progressive core removal	24
Imposed tunnel convergence	14
Core stiffness reduction	10
b) Stress-strain model for soil	
Elasto-plastic (yield=failure)	43
Elasto-plastic (yield≠failure)	33
Linear elastic	14
Non-linear elastic	10

Table 5.6 Overall Aspects of Reviewed Numerical Predictions of Shallow Tunnel Performance

Figure 5.5 shows that in the majority of the cases reviewed (72%), the comparison between calculated and observed performance was limited to ground displacements. A full comparison of the complete ground displacement field and lining loads, which is ideally required for the proper evaluation of a simulation, was achieved in only two cases (10% of total). Whenever one aspect of the performance is not assessed in the comparison, the prediction (or even a back analysis) becomes more flexible and more easily adjustable to the observations, especially those of types B1 and C1.

The results of comparisons between calculated and observed surface settlements are shown in Figure 5.6. The magnitude of the maximum observed surface settlement is very closely matched by the numerical predictions in 60% of the cases. Overprediction or underprediction are observed in equal proportion. This may indicate that finite element simulations are good enough for estimating the magnitude of surface settlement. This is confirmed by the result of the predicted overall distribution of the transverse settlement profile. This is seen to be good to regular, and seldom poor. However, one may also speculate that in those predictions where the result of the performance is known (B1 or C1), the calculation might have been biased towards that result. As noted by Eisenstein (1982), regardless of the type of the analysis or which type of stress-strain model is used, and regardless of the type of soil or construction

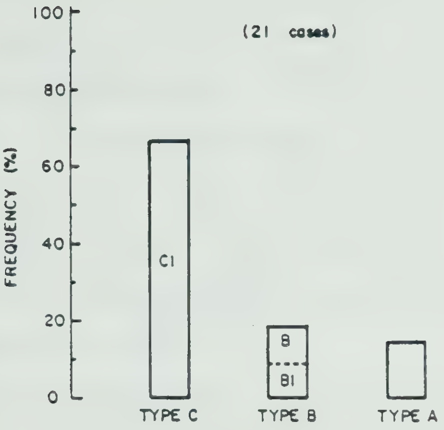

Figure 5.4 Types of Numerical Prediction of Shallow Tunnel Behaviour made by Two-Dimensional Finite Element Analysis

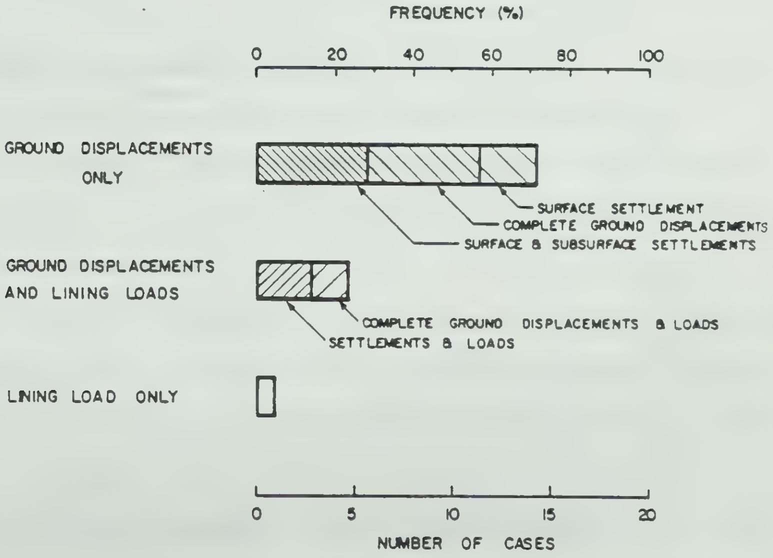

Figure 5.5 Performance Aspects Compared in Numerical Predictions of Shallow Tunnel Behaviour by Two-Dimensional Finite Element Analyses

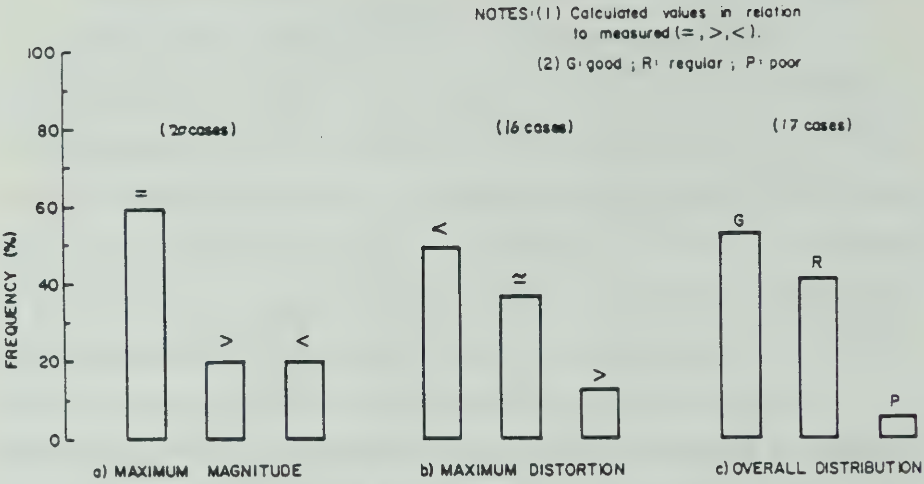

Figure 5.6 Comparison of Surface Settlements Calculated by Two-Dimensional Finite Element Analyses and Measured Values

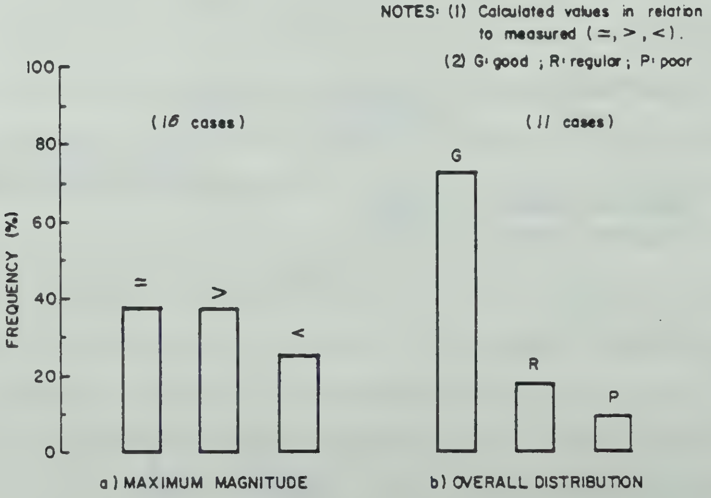

Figure 5.7 Comparison of Subsurface Settlements Calculated by Two-Dimensional Finite Element Analyses and Measured Values

scheme, the numerical simulations appear to furnish smaller surface distortions (maximum slope of the settlement profile) or wider settlement troughs than observed. Some authors (Mair, 1979:132, Eisenstein, Op.cit.) attribute this to the concentration of shear strains into relatively narrow zones. This aspect of soil behaviour is not adequately modelled by most finite element codes and constitutive models presently available.

An immediate consequence appears to be that a finite element approach would underestimate the damage potential to structures located at the ground surface. However, in practice, this may not be as consequential as initially thought. The estimate of surface distortion is only required when there are neighbouring structures. However, the estimate is usually performed ignoring the existence of buildings at the surface. As shown in Section 4.2.2, this simplification leads to an overestimate of the ground distortion, which may compensate the shortfall from the finite element analyses.

Figure 5.7 summarizes comparisons between calculated and observed subsurface settlements with depth. An even trend is noted towards matching or overestimating the maximum magnitude at points closer to the tunnel. As noted in Section 4.1, linear elasticity will hardly provide a good match of displacements at the tunnel contour and at the surface, unless the ground is very stiff or the ground control conditions are extremely good, so that the effect of the always present non-linearity in the stress-strain response of the soil is minimized. It will be shown in the next chapter (Section 6.3.2.3) that depending on the in situ stress ratio, on the relative depth of the tunnel and on the nature of the soil strength (purely cohesive or purely frictional), a match in the crown displacement in a linear analysis may lead to either an overestimate or an underestimate of the maximum surface settlement. Correspondingly, a match in the surface settlement with a linear elastic model, will also be followed by either an over or an underestimate of the crown settlement. Similar trends will be observed in linear elastic-plastic analyses if the amount of soil yielding is limited. Hence, if the cases reviewed in Table 5.5 involved mainly this type of analysis in providing a good match of the maximum settlement at the surface, the results shown in Figure 5.7(a) make sense provided soil yielding has not been extensive.

The calculated overall distribution of subsurface settlements is usually good, as shown in Figure 5.7(b). However, it should be pointed out that this interpretation requires clearer definition, since there are few cases where sufficient field measurements are taken at points very close to the tunnel contour where the strain and displacement gradients tend to be appreciably high. The noted agreement is, broadly speaking, good at points located at more than 30% of the tunnel radius away from its wall.

No immediate explanation is found for the noted trend on the calculated maximum horizontal displacement transverse to the tunnel. In most of the cases where this comparison was available, the results from analyses tended to be greater than the measured values (Figure 5.8). This tendency is noted even in anisotropic elastic-plastic analyses (Ng et.al., 1986:43). This displacement is very dependent on the initial stress ratio and one could speculate that inaccurate estimates of this ratio might explain the observed departures. However, this reasoning would lead to an equal frequency of over and underestimated displacements, which was not observed. Moreover, the noted feature could not be explained in terms of the numerical simulation procedures adopted or of the constitutive models used, as the same procedures or models resulted in both over and underestimates in different cases. Among them, the best agreement noted was in the linear elastic analysis by Ledesma et.al. (1986), using elastic parameters and a stress ratio which had been backanalysed from an instrumented section at the early stages of the tunnel construction.

The comparison between calculated and measured lining loads furnished mixed results (Figure 5.9). Equal frequencies of matched values, overestimates and underestimates were found, regarding the magnitude of the loads. Similarly, the distributions of these calculated loads were found to be equally good, regular and poor, with respect to the measurements. Again, no clear justification

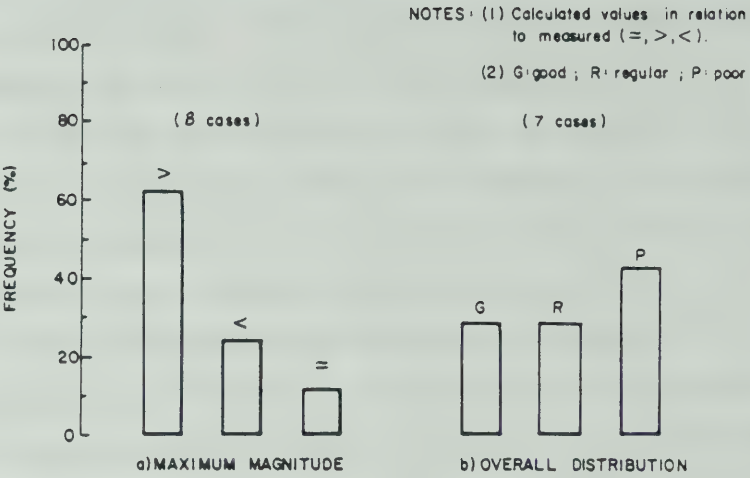

Figure 5.8 Comparison of Horizontal Displacements Calculated by Two-Dimensional Finite Element Analyses and Measured Values

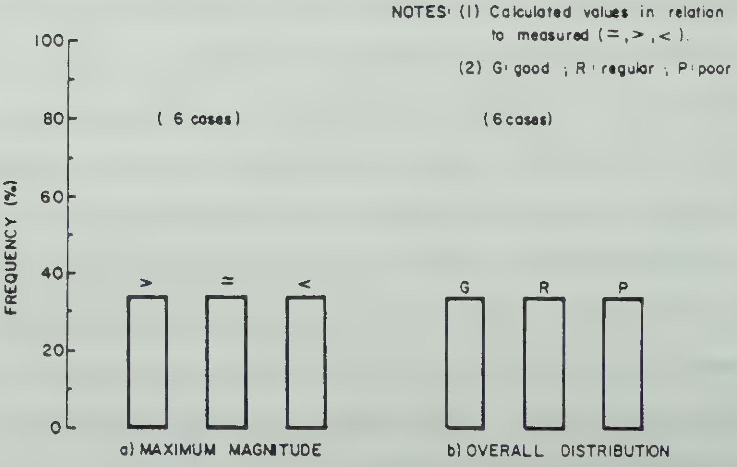

Figure 5.9 Comparison of Lining Loads Calculated by Two-Dimensional Finite Element Analyses and Measured Values

is found for this finding. On purely speculative grounds one could suggest that in most of the cases reviewed, the authors were mainly interested in evaluating the capabilities of their numerical simulation in terms of the ground response, which was usually expressed in terms of ground movements. Since in most of the cases, the results of field measurements were already available at the time the analyses were performed, the calculations could have been manipulated to achieve a better agreement in terms of soil displacement. Lining loads would have resulted as a by-product of the study with not much emphasis being placed on them. This is somewhat confirmed by the results provided by Ng et.al. (1986:45) as well as other authors. On the other hand, the well known difficulties associated with monitoring lining loads should not be overlooked. Consequently, measured loads are frequently treated more suspiciously than measured displacements, and differences between load calculations and measurements are attributed to unrepresentative or erroneous measurements (e.g. Duddeck and Stading, 1985), particularly if pressure cells are used. Moreover, in cases where the ground control and the lining-soil contact are poor, it is very unlikely that any correspondence between calculation and measurements is found. The reasons for this were exposed in the discussion on the idealized action of a support with poor contact with the ground in Section 2.3.5 of this thesis. It was shown there that if the lining contact is poor, and if the so-called loosening condition with "gravity" loads develops, then the support performance is likely to be unpredictable in formal terms.

5.2.2 Numerical Simulation Applied

Having in mind the capabilities of finite element simulations of shallow tunnels as reviewed in Section 5.2.1 and considering the goals of the present study established in Chapter 1, it was decided to make use of a simple finite element program which could incorporate and simulate the factors that most affect the tunnel performance. These were discussed in Chapter 2 and summarized in Section 5.1.

An open finite element code prepared by Medeiros (1979) was found suitable for the proposal. It is based on a simple constant strain triangle formulation, originally developed by Murray (1971) and extended by Medeiros for the solution of incremental supported excavations, allowing non-linear elastic analyses to be performed. This program was modified and implemented to allow the analysis of a shallow tunnel problem.

5.2.2.1 General Description of the Solution

The plane strain tunnel problem is solved by a displacement formulation, allowing the calculation of nodal displacements as primary unknowns and element stresses as secondary quantities. The finite element equilibrium equations are solved directly by the Gauss elimination technique. Constant strain triangles are the element type used.

The initial vertical and horizontal stresses are assumed to be principal stresses (ground surface assumed horizontal). They are specified directly at each element, as the overburden vertical stress and K times this value for the in situ horizontal stress. The former is taken as the bulk specific weight (assumed constant) times the difference in elevation between the ground surface and the centre of the element being considered. A single and constant stress ratio, K, is assumed in the analysis.

The problem is solved in stages, in order to represent different construction phases (typically two). In the first stage, ground excavation is simulated. This is done using the conventional approach (Section 5.2.1.1), in which all elements within the tunnel cross section have their elastic constants reduced to very small values to represent air and have their stresses zeroed to represent a full face excavation. This is followed by the application of boundary loads at the excavated contour, designed to cancel (gradually) the nodal loads equivalent to the initial stresses. These boundary loads correspond to boundary stresses with magnitude equal to a fraction, a, of the in situ stresses, but with a reversed sign. This boundary stress reversal simulates a partial in situ stress release, designed to approximately account for the true three-dimensional stress transfer mechanism in the two-dimensional analysis. To implement this procedure, referred to as 'ground stress reduction' (see Table 5.3), the finite element method requires the boundary stresses to be imposed as equivalent nodal loads. These forces are calculated by integration of the in situ stresses within the elements being excavated. In the first stage of the solution simulation, the fraction, a, of the load magnitudes are applied with reversed sign to partly reduce the initial in situ loads. This is necessary as the excavation should not be left unsupported, as explained in Section 4.3.2.7. The amount of in situ stress reduction, a, is a key issue in the simulation, and has to be independently assessed. The fraction of the stress release is equal to

$$a = 1 - \Sigma \qquad [5.1]$$

where Σ is defined in Section 2.3.2. The same stress reduction factor is uniformly applied to all points around the tunnel profile, and this produces a proportional reduction of the radial and shear stresses along the contour.

The reversed nodal loads applied to reduce the ground stresses are divided into a number of steps of equal magnitude and are applied incrementally. This allows the material non-linearity to be taken into account. The piecewise linear incremental displacements are accumulated to give the total displacement. After each load step the element stresses are updated and new elastic constants are obtained for the next load increment. This procedure is called 'past stress solution', since it uses elastic constants determined from stress levels obtained in the previous load increment. The stiffness matrix is formulated in terms of the tangent moduli. No attempt was made to redistribute the unbalanced loads within each increment.

The stress-strain relationship assumed for the soil is hyperbolic, following the original formulation by Duncan and Chang (1970). The soil is thus treated as a hypoelastic [13] isotropic time-independent material, defined by a variable and stress dependent tangent modulus and a constant Poisson's ratio. As an incremental constitutive model, the state of stress depends on the current state of strain as well as on the stress path followed to reach that state (Chen and Saleeb, 1982:217). As it will be shown in Chapter 6, in order to reduce the number of variables and to make the process of generalization simpler, an incrementally reversible (unique) stress-strain behaviour was assumed. Since no distinction is made between loading, unloading and reloading behaviours, the stress path dependency with respect to loading and unloading is not represented. The hyperbolic model was originally derived as a fitting function for conventional triaxial tests results (Kondner, 1963). Because of this, the shear stress component is simply approximated by the difference between the major and minor principal stresses acting in the plane being considered, and the mean normal stress component is approximated by the minor principal stress in that plane. The out of plane stress is not taken into consideration, as far as the constitutive model is concerned. The present model allows both effective or total stress analyses to be performed, by using the appropriate set of parameters. Details of the hyperbolic stress-strain formulation are given by Duncan and Chang (1970) and are reviewed by Chen and Saleeb (1982:516). A summary of its development is given in Figures 5.10 and 5.11. In its current configuration, the program allows the representation of just one layer of soil with the hyperbolic stress-strain relations, but this can easily be extended to include more than one soil layer.

---

[13] The term 'hypoelastic' model is used to describe the incremental elastic constitutive relations. Such models are used to represent the behaviour of materials where the state of stress is generally a function of the current strain state and of the stress path followed to reach it (Chen and Saleeb, 1982:148).

Once the last load step of the first simulation phase is applied, the remaining boundary stresses acting on the tunnel contour maintain equilibrium, and are equal to a fraction, Σ, of the original in situ stresses. At this stage, the support is applied by assigning properties of the lining material to appropriate elements. The balancing boundary stresses are no longer needed to ensure the 'stability' of the opening and therefore, they are reduced to zero. This is done by applying opposite and equivalent nodal loads incrementally and the reaction provided by the balancing stresses is gradually substituted by the support reaction. The final equilibrium between soil and lining is reached in an interactive form, after the complete removal of the fictitious balancing boundary stresses corresponding to Σ equal to zero or α equal to one (full stress release). No special provision is made to represent the interface between the lining and soil, and therefore, a no-slip contact is assumed.

The support is represented by layered rings of constant strain triangles. The reduced thickness of the lining ring (about 3% of the diameter for a concrete lining) would require a large number of elements for the discretization. However, the stress distribution within the support is not of primary concern in the present study. The overall action of the support in the interaction process with the soil can, therefore, be adequately represented by an equivalent lining ring with slightly increased thickness. This ensures an adequate element aspect ratio (close to 1), but requires selecting artifical material properties, such that the resulting compressibility and flexibility ratios are close to the actual values. This approach is similar to that used by many authors in retaining wall analyses (e.g. Medeiros, 1979:175), by Medeiros et.al., (1982:929) in a complex station-shallow tunnel analysis, and by Kasali and Clough (1983:73) in 3D analyses of shallow tunnels. This expedient simplifies the mesh design since a smaller number of elements can be used to represent the lining, which is assumed weightless. Accordingly, the program sets the initial stresses to zero in the lining. The lining material is treated as homogeneous, isotropic and linear elastic. Lining radial joints are not represented directly in the

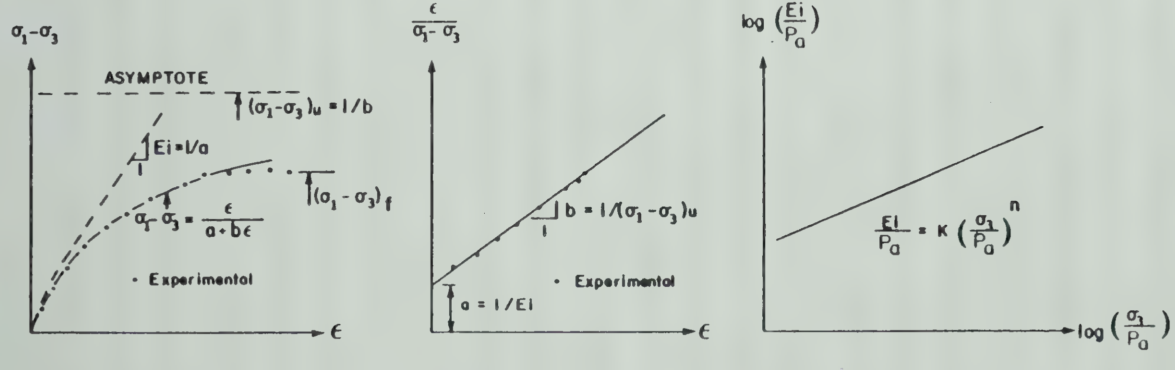
$\sigma_1-\sigma_3$
ASYMPTOTE
$(\sigma_1-\sigma_3)_u = 1/b$
$Ei = 1/a$
1
$(\sigma_1-\sigma_3)_f$
$\sigma_1-\sigma_3 = \frac{\epsilon}{a+b\epsilon}$
· Experimental
ϵ
$\frac{\epsilon}{\sigma_1-\sigma_3}$
$b = 1/(\sigma_1-\sigma_3)_u$
1
· Experimental
$a = 1/Ei$
ϵ
$\log\left(\frac{Ei}{P_a}\right)$
$\frac{Ei}{P_a} = K\left(\frac{\sigma_3}{P_a}\right)^n$
$\log\left(\frac{\sigma_3}{P_a}\right)$

Hyperbolic stress-strain curve by Kondner

Transformed stress-strain curve

Janbu's initial modulus confining stress relation

Figure 5.10 Hyperbolic Model Representation

Kondner (1963) hyperbola:

$$\sigma_1 - \sigma_3 = \frac{\varepsilon_1}{a + b\varepsilon_1}$$

with σ_1, σ_3: major and minor principal stresses and ε_1: axial strain. Material constants:

$$a = \frac{1}{E_i} \quad \text{and} \quad b = \frac{1}{(\sigma_1 - \sigma_3)_u} = \frac{R_f}{(\sigma_1 - \sigma_3)_f}$$

where E_i = initial tangent modulus; $(\sigma_1 - \sigma_3)_u$: ultimate or asymptotic stress difference; $(\sigma_1 - \sigma_3)_f$: stress difference at failure; R_f = stress ratio.

In conventional triaxial compression test σ_3 = constant. Hence the current tangent modulus is:

$$E_t = \frac{\partial}{\partial \varepsilon_1} (\sigma_1 - \sigma_3) \qquad \therefore \; E_t = \frac{a}{(a + b\varepsilon_1)^2}$$

But

$$\varepsilon_1 = \frac{a\,(\sigma_1 - \sigma_3)}{1 - b\,(\sigma_1 - \sigma_3)}$$

Thus

$$E_t = \frac{1}{a} \left[1 - b\,(\sigma_1 - \sigma_3)\right]^2$$

or

$$E_t = E_i \left[1 - R_f \frac{(\sigma_1 - \sigma_3)}{(\sigma_1 - \sigma_3)_f}\right]^2$$

Janbu (1963) relation:

$$E_1 = Kp_a \left(\frac{\sigma_3}{p_a}\right)^n$$

where p_a: atmospheric pressure, K and n: dimensionless constants.

Failure in conventional triaxial, with Mohr-Coulomb criterion:

$$(\sigma_1 - \sigma_3)_f = \frac{2c \cos \phi + 2\sigma_3 \sin \phi}{1 - \sin \phi}$$

with c: cohesion and ϕ: friction angle.

Therefore

$$E_t = Kp_a \left(\frac{\sigma_3}{p_a}\right)^n \left[1 - R_f \frac{(1 - \sin\phi)(\sigma_1 - \sigma_3)}{2c \cos\phi + 2\sigma_3 \sin\phi}\right]^2$$

Figure 5.11 Derivation of the Current Tangent Modulus

solution, but their effect in reducing the bending stiffness in the lining can be indirectly taken into account, by Muir Wood's (1975:126) approximation:

$$I_e = I \left(\frac{4}{n}\right)^2 + I_j \qquad [5.2]$$

where I_e is the equivalent moment of inertia (per unit length of tunnel) of a continous ring corresponding to the actual lining, with n joints or segments with moments of inertia equal to I_j and I respectively. Hence for an eight segment lining, with perfectly articulated joints ($I_j \simeq 0$), $I_e = I/4$.

The assumed plane symmetry simplifies the shallow tunnel problem, as it allows the analysis of only half of the plane strain section. The mesh design observed the guidelines presented in Section 5.2.1.1. The nodal points in the vertical boundaries were allowed to move freely in the vertical direction and were fixed horizontally (zero horizontal displacement). The nodes lying in the lower boundary, had both vertical and horizontal displacements fixed. The location of the lateral boundary varied from case to case, but typically it was located at 18 tunnel radii away from the tunnel centre. The lower boundary was located at a convenient location representing the position of rigid bedrock. The assumption of an increasing tangent modulus with increasing confining stress (or with depth) in the hyperbolic model formulation (Figure 5.11) lessens the effect of the unrealistic ground heave below the tunnel floor which is evident in analyses with a constant modulus profile. Therefore the position of the lower rigid base becomes irrelevant, as noted in Section 5.2.1.1. As much as possible the elements were designed to show aspect ratios close to unity, both in the ground and in the lining domains. Following the indications given in Table 5.1, a higher element density was adopted around the tunnel contour, where the stress gradients are higher. A typical finite element mesh used is shown in Figure 5.12a, and the details of the discretization around the tunnel are given in Figures 5.12b and c for clarity. This particular mesh contains 332 nodes and 609 elements. For a two phase construction simulation, with five load step increments each, the average CPU time to execute the complete solution using the present computer scheme at the University of Alberta, was 88 seconds with CPU storage of virtual memory integral (VMI) of 367 page-minutes. The band width for this mesh was 150. The program subroutine that reads the problem geometry (READGE) also allows the generation of intermediate nodal points and elements, and this simplifies the input preparation.

The complete listing of the computer program is not included herein, but can be found in the 'Tunnel Excavation' Computer Program Manual edited by Negro (1981), available in the Department of Civil Engineering at the University of Alberta.

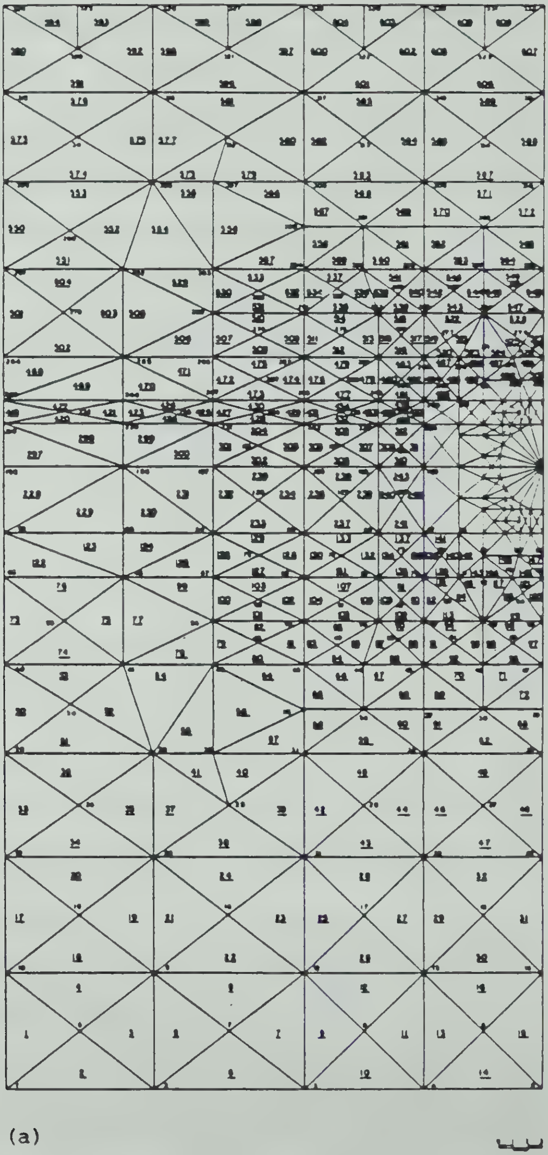

Figure 5.12 Details of the Finite Element Mesh

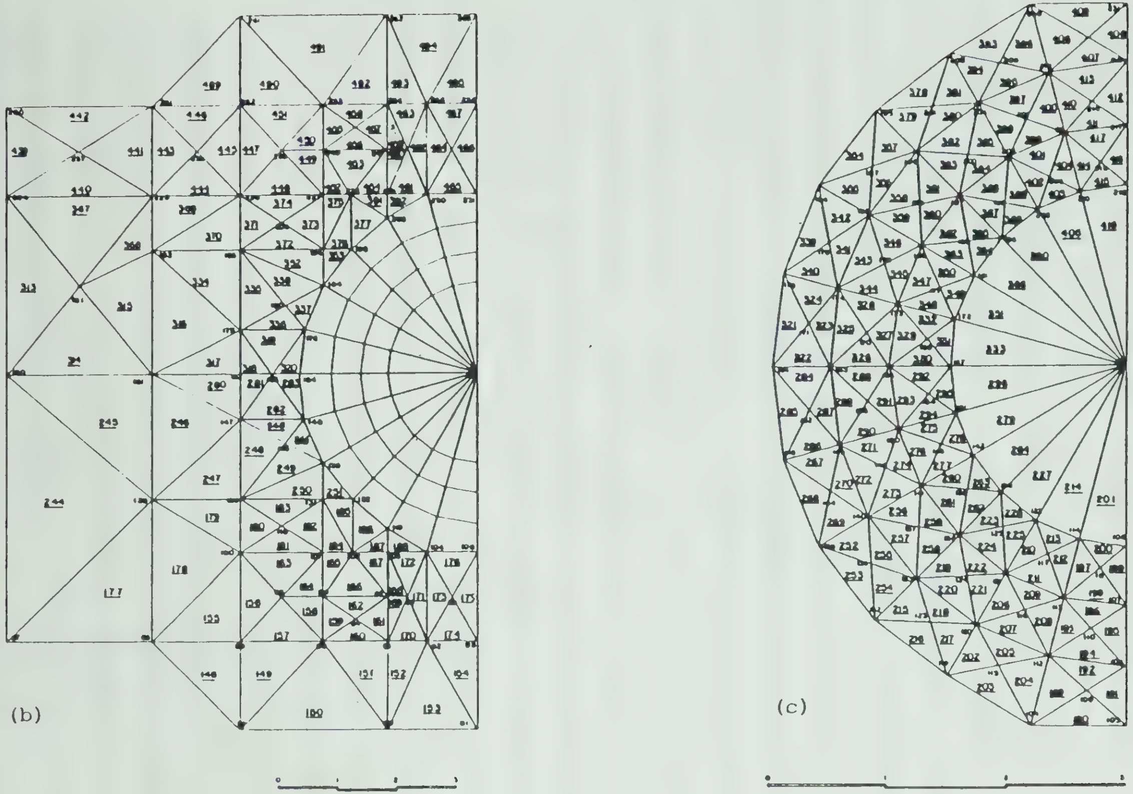

Figure 5.12 Details of the Finite Element Mesh (Continued).

The manual provides details of the program organization and structure, the flowchart of the solution, a description of the subroutines, a glossary of names of input variables, instructions for data input and an input data sample.

5.2.2.2 Discussion on the Solution Adopted

The justifications of the numerical solution adopted and of the underlying simplifications can be inferred from the discussions included in the former sections of this chapter. Moreover, they are largely supported by the understanding of the behaviour of shallow tunnels presented in Chapters 2 and 3, and by the detected needs of current design practice, as shown in Chapter 4. A few additional points are discussed in this section, in an attempt to better assess the limitations of the solution adopted.

The use of constant strain triangles involves clear limitations which are partly compensated for by employing a larger number of elements. While this enhances accuracy, it increases computing time and cost and adds inconvenience to input and output handling. The problem is less severe in terms of the ground representation than it is for the lining, where higher stress gradients can be anticipated. With respect to the latter, Evison (1987) using the present numerical solution, analysed the problem of a simple fixed cantilever with elastic response, subjected to axial compression and bending. In order to approximate the correct solution for pure bending, it became apparent that an extremely large number of elements would be required, thus rendering the solution impractical. However, for uniform compression it was found that even a coarse mesh could provide a reasonable approximation of the exact solution, both in terms of displacements and stresses. Notwithstanding this, Medeiros (1979) used this solution for a retaining wall analysis, a structure where the behaviour in bending dominates. To compensate for the stiffening effect of the finite element solution, Medeiros (Op.cit.:178) reduced the wall stiffness by 35%, a value derived from the solution equivalence of the fixed cantilever model. Despite these shortcomings, the interactive process between the wall and ground was successfully simulated and the ground response quite satisfactorily represented.

For the tunnel lining, the problem tends to be less severe since, unlike the retaining wall case, compression tends to prevail, particularly in modern designs, where bending is likely to be very small. Moreover load eccentricity will also be minimized in a large group of stiff soils which have an in situ stress ratio between 0.8 and 1.2. The use of an equivalent lining in the analysis, with increased thickness in order to render an adequate element aspect ratio, should not be a matter of concern, provided proper attention is given to the equivalence of the compressibility and flexibility ratios. Kasali and Clough (1983:73) used a similar approach in their three-dimensional analyses of a shallow tunnel. They considered, however, that it would be sufficient to ensure a bending stiffness in the equivalent (thicker) lining comparable to that of the actual support. Accordingly, the modulus of the thicker liner elements was reduced proportionally to the relation between the liner thickness and the bending stiffness (which is proportional to the cube of the liner thickness). Despite being simpler than the criterion selected in the present study, the results of the numerical back-analyses shown in Sections 5.2.4.2, 5.2.4.3 and 5.2.4.4 confirm that the Kasali and Clough (Op.cit.) suggestion is indeed quite reasonable. It will then be shown that the best correspondence between observed and calculated performances is achieved when the flexibility ratios of the real and equivalent lining are comparable. This condition implies, in fact, the equivalence of bending stiffness (EI), provided the average lining radii are equal (which may not be the case).

As noted in Sections 2.3.5.2 and 2.3.5.3, the assumption of a no-slip interface is not a critical one, as only very limited relative tangential displacement is to be expected in the soil-lining contact. Moreover, as shown in that section, the non-slip assumption will tend to furnish both the highest and lowest values of thrust, at different locations in the lining, depending on the geometry of the problem and on the in situ stress ratio.

The premise of a horizontal ground surface, constant specific weight and constant in situ stress ratio is not very restrictive. More so is the assumption of homogeneity of the soil profile. Provided the tunnel cross section is fully embedded in one single layer and the case in study does not involve a mixed face condition, the simplification adopted is quite acceptable.

The solution adopted assumes a full face tunnel excavation. While this may be a reasonable approximation for a TBM excavation scheme, one may argue that it may not be so for a staged excavation. However, in schemes where the tunnel invert is excavated and supported at a small distance behind the leading tunnel face (say, one diameter), it is believed that the effect of the staged excavation may simply be localized and possibly transient. In these cases, the final response of the ground and lining may not be very sensitive to the sequence in which the face is excavated. Although this aspect has not been fully proven so far, the analyses shown in this chapter and in Chapter 7 of this thesis tend to confirm this assertion. Broadly speaking, provided a good soil-lining contact is ensured, as in shotcrete support, and provided the excavation is stable both globally and locally, in either a full-face or in a staged face scheme, the final stress changes in the ground are not dissimilar if the distance between the heading face and the point of closure of the lining invert is the same. The overall final tunnel performance is likely to be similar.

As noted in Section 5.2.1, the use of the conventional approach here for excavation simulation does not induce too much approximation since a full face excavation is represented and it is performed in a single phase. Also, the numerical integration of the in situ stress around the tunnel profile is quite acceptable as the number of elements around it is fairly large.

The ground stress reduction procedure used to simulate the 3D arching process in a 2D analysis, is quite adequate for the problem at hand, as shown in Sections 4.3.2.7 and 5.2.1. As noted, despite some indications that the rate of stress release around the contour may not be uniform as assumed in the present solution, the use of a unique stress reduction factor, a, is simpler and possibly safer, as far as lining bending is concerned. The key issue in this aspect of the simulation lies in how this factor, a, is determined.

The merits and limitations of the incremental procedure, as compared to iterative or mixed procedures, were discussed by Desai and Abel (1972:226). Perhaps the main advantage is that the convergence problems, often associated with iterative approaches, are non-existent, and that it provides complete descriptions of the load-deformation behaviour, since information is rendered at each load increment. The difficulty is associated with the definition of an adequate increment of load. However, experience gained with the present numerical solution, as applied to pre-failure simulations of excavations in fairly stiff soils (Medeiros, 1979:166), indicate that a relatively small number of increments (around four) is sufficient in this past stress incremental solution.

The merits and limitations of the hyperbolic stress-strain model, as implemented in this solution are well known (see, for instance, Morgenstern, 1975:12, Duncan et.al., 1980:20, Duncan, 1980:456, Christian, 1982;193, Chen and Saleeb, 1982:523, Vaid, 1985). A brief summary of these points is presented below.

The model is rather simple both conceptually and mathematically. It requires a small number of parameters, which have readily understood physical significance, although some of them are not fundamental soil properties. As it has been used for more than a decade, a fairly wide data base is available, which facilitates the estimate of parameter values in cases where sufficient data is not available. These values can be determined from the conventional triaxial testing which is routinely performed in geotechnical projects. A considerable amount of experience has been accumulated with this model, in a fairly wide range of practical geotechnical problems, including shallow tunnels, foundations (e.g. Domaschuk and Valliappan, 1975), excavations and retaining structures (e.g. Clough and Tsui, 1977:520), culverts (e.g. Duncan, 1979) and dams (e.g. Kulhawy and Duncan, 1972). This explains to some extent, the degree of confidence yielded in using this simple model. Moreover, the model accounts for non-linearity and stress dependency of soil behaviour and is applicable to both drained and undrained conditions.

As the model is based on incremental elasticity, it is not suitable for conditions where the behaviour of the soil mass is largely controlled by those elements which have already failed. As noted by Duncan (1980:457), the model is useful for predicting movements in basically stable earth masses and not for conditions extending up to the stage of soil mass collapse. Numerical procedures allowing stress redistribution after an element of soil fails ("load shedding") according to some failure criterion, have been developed (Byrne and Janzen, 1984), but were not incorporated into the present solution. The soil behaviour in this model is represented through a variable tangent modulus and a constant Poisson's ratio, which adds difficulty to portraying the soil response at failure. As failure is approached with increasing deviatoric stress, the modulus E_t undergoes a pronounced decrease. If the Poisson's ratio is kept constant, the reduction in E_t entails a proportional reduction of the tangent bulk and shear moduli, which are defined as:

$$B_t = \frac{E_t}{3(1-2\nu)} \qquad [5.3]$$

$$G_t = \frac{E_t}{2(1+\nu)} \qquad [5.4]$$

respectively. While the reduction in G_t is supported by experimental evidence, the pronounced reduction required in B_t is not. The value of the bulk modulus of soils is essentially independent of the magnitude of the deviatoric stresses and depends only on the mean normal stress (Chen and Saleeb, 1982:523). Even after failure, soils are able to sustain additional increases in mean normal stresses. An improved representation of soil behaviour at failure is obtained through hyperbolic models formulated in terms of the tangent bulk and shear moduli as above (e.g. Domaschuk and Wade, 1969) or in terms of the tangent Young's and bulk moduli (e.g. Duncan et.al., 1980). This problem is more pronounced at higher mean normal stress levels. In a plane strain shallow tunnel representation, failure is reached at relatively low stress levels, with decreasing confining stress. Thus, the E_t, ν formulation may suffice, especially if an accurate failure representation is not aimed for.

The present solution is strictly applicable only to soils in which shear dilatancy is not significant. Since the model is incrementally elastic and isotropic, cross effects between hydrostatic and deviatoric response components are disregarded. By uncoupling these components, volumetric changes are solely due to changes in the mean normal stress and those volume changes which are observed in certain soils under pure shear, are not represented. Byrne and Eldridge (1982) extended the original hyperbolic formulation by including an additional dilatancy parameter, which allows shear-volume coupling. This model was tested against some laboratory controlled problems but its potential in actual field conditions remains to be seen.

It has been assumed that the strength parameters, c and ϕ, are constant and stress level independent. Although the variation of the friction angle with the mean normal stress level (Vesic and Clough, 1968) can be easily implemented in the present solution (e.g. Duncan et.al., 1980:30), the conventional approach of assigning a "working" strength parameter, for the expected range of stresses, has been preferred. This range is fairly wide in some geotechnical structures (in a medium sized dam, the mean stresses can vary from zero to more than 1 MPa) and thus, a single representative ϕ value is difficult to define (particularly in cohesionless soils, with pronounced curvature of the failure envelope). In most urban tunnels, especially if a good ground control is ensured, the variations of the mean normal stresses around the opening are usually small (say from 0.1 to 0.3 MPa in a typical subway tunnel). Therefore, a single representative value of the strength parameter can be defined with no major implications.

Results shown by Duncan and Chang (1970:1644, 1646) and by Chang and Duncan (1970:1675), on laboratory testing, foundation and excavation simulations, indicated that satisfactory results may often be obtained using a reasonable estimate for a constant value of Poisson's ratio. Moreover, the experimental difficulties of determining parameters related to Poisson's ratio, indicate that it may be sufficient to assume a constant value in the analyses (Chen and Saleeb, 1982:520).

The stress-strain relationship adopted in the present solution followed a formulation which is compatible with the triaxial compression test. This led to the use of the minor principle stress and of the stress difference (major and minor prinicipal stresses), instead of the formally more appropriate stress invariant components such as the octahedral mean, normal and shear stresses. The latter were used in the hyperbolic model formulation by Domaschuk and Wade (1969), but the triaxial test based formulation gained wider acceptance and popularity, despite its lack of formal rigour. More critical than this is the fact that it is formally applicable only to that particular state of stress, in which the minor and intermediate principal stresses are equal. But, this is not the case in a plane strain or in a more general three-dimensional representation. In the present solution, the effect of the out of plane stress is not included, despite its known influence on both deformational and strength characteristics of soil behaviour. Moreover, by using parameters usually derived from triaxial tests, both characteristics will normally be underestimated in a plane strain analysis, unless some independent correction is included. The effect of the intermediate principal stress in the stress-strain relation of a numerically simulated unconfined compression test, was investigated by Gopalakrishnayya (1973:111), who pointed out that for a lower range of strains, its effect is not significant, but increases with increasing straining. Nevertheless, this effect is possibly less significant than the hyperbolic fitting approximation of the actual stress-strain data.

For the reasons exposed in Section 5.2.2.1, the present solution does not include any unloading and reloading criteria. As noted in Section 2.3.4.1, certain points around the tunnel may experience a rotation of the principal stresses. Consequently, these points will experience a decrease in the stress difference, associated with an increase in the minor principal stresses as the boundary stresses are reduced. This is the case of soil elements above the crown and below the floor of a tunnel, when the in situ stress ratio K is smaller than one. As a result, these elements become less stiff than they would have if an unloading-reloading feature had been implemented. It will be shown, however, that for stiff soils with K not far from unity, this simplification is not critical, as the stress reversal is achieved quite rapidly, and is followed by a monotonic increase in the stress difference. The major asset with this simplification is the allowance of a simpler generalization process as will be seen in Chapter 6.

The inability of the stress-strain model implemented in the present solution to predict the soil response under certain types of stress paths is well known. One of them is the constant stress-ratio paths (σ_1/σ_3) (Duncan and Chang, 1972:497), similar to that experienced in the central part of embankment dams. For these conditions, the strains are overpredicted for primary loading modulus values (Eisenstein, 1974). Another path is that of constant deviator stress under decreasing minor principal stress. For this, the present model would indicate expansion in all directions, while in actual fact compressive stains would be observed in the direction of the major principal stress. This anomaly was noted by many authors, for example, Duncan and Chang (1972) and Verruijt (1976). Chen and Saleeb (1982:524) suggested that this is due to the assumption of co-axiality of stress and strain increments, which result from the assumption of incremental isotropy and linear elasticity of this model. They recalled experimental evidence showing that the principal directions of strain increments coincide more closely with the direction of the principal stresses rather than that of the stress increments, notably at high stress levels and as failure is approached. Fortunately, none of these paths are typical for points around a shallow tunnel (Section 2.3.4.1).

Additional limitations to the present solution are its inability to account for the strain softening behaviour after peak and the fact that the parameters involved are not fundamental soil properties. However, these parameters have clear physical significance which facilitates the comparisons of different soil properties and the appreciation of their effects on the soil response.

Despite all the limitations described, the stress-strain model implemented in this numerical solution has shown its potential in a variety of situations, including the prediction of soil responses under quite unconventional loading conditions as shown by Duncan (1980:245). When used with judgement and making allowance for the uncertainties in the test data serving as input and in the approximations in the model, Duncan (Op.cit.) has shown that reasonable ranges of behaviour are predicted for different soil types.

5.2.3 Parametric Studies

The numerical model described in the previous section was tested for a variety of idealized conditions, before being used for the simulation of actual shallow tunnels. A number of sensitivity studies were undertaken in order to gain experience and to assess the influence of the intervenient parameters and variables.

It was felt that the results of these studies would be better appreciated in connection with the development of a model for generalized shallow tunnel performance. Accordingly, some of the results of these sensitivity studies are presented in Chapter 6. They include assessments of aspects related to the numerical simulation (size of mesh, number of load steps, etc.), to the effect of the in situ stress conditions (tunnel depth, in situ stress ratio), to the influence of the soil strength (cohesion and friction angle), to the influence of the soil deformation properties (Janbu's modulus and exponent, Poisson's ratio), and to the amount of stress release, etc.

5.2.4 Analyses of Some Case Histories

5.2.4.1 Opening Remarks

In order to assess the overall ability of the numerical solution adopted to simulate the performance of actual shallow tunnels, a few case histories were analysed. All analyses are type C1 predictions. Unlike the majority of similar studies reviewed in Section 5.2.1.2, the analyses shown in the following sections attempted a complete comparison between calculated and observed performance, including ground displacements and lining loads.

The selection of case histories for study was guided by a number of factors. Firstly, preference was given to well documented cases with comprehensive and numerous field data, and under well known geotechnical conditions. Secondly, the selected case histories should entail aspects which are understood as typical of the idealized conditions required for the application of the numerical solution. These include geometric aspects, soil properties and soil conditions, construction type, etc. Hence, tunnel cases where the construction quality and the quality of the ground control were recognized as good were intentionally chosen. Finally, preference was given to cases where the writer was directly or indirectly involved in the process of field observation, data acquisition and construction follow-up.

There were three cases chosen for analyses. The first is the 4 m diameter Alto da Boa Vista Tunnel, abbreviated to the ABV tunnel, built in Sao Paulo, through a clayey sand sediment, using the so called New Austrian Tunnelling Method (NATM). The second is the Southbound Edmonton LRT tunnel at Jasper Avenue, driven by a 6 m diameter TBM, through a stiff glacial till. The third is the Edmonton Experimental Sewage tunnel, also driven by a TBM, but with a 2.56 m diameter, through a softer glacial till. Further details of these case histories are summarized in Table 5.7 and will be furnished in the following sections.

In the three cases, soil conditions and properties were fairly well defined or bounded. The major unknown was the amount of stress release to be applied in the 2D analyses representing the 3D mechanism. With respect to this, the study conducted was a back analysis, in which the independent variable was the fraction of ground stress reduction, a, to be considered prior to lining installation, in order to obtain a reasonable match between the observed and computed performances. Besides this variable, some other properties were also varied, but to a lesser degree and covering their possible ranges of values.

The subject of back analysis as applied to geotechnical engineering has received considerable attention in recent years. Also referred to as calibration, characterization or identification processes, the back analysis problem can be solved by "direct" or "inverse" approaches. In the first approach, the solution is obtained by minimizing the differences between observed and computed performances, by correcting the trial values of the unknown parameter. In the

Case	1	2	3
Tunnel	ABV	Edmonton LRT	Edmonton Exper.
Reference	Negro & Eistenstein, 1981	Branco, 1981	El Nahhas, 1980
Soil Condition	Clayey sand (stiff-dense) above W.L.	Stiff glacial till, above W.L.	Softer glacial till, above W.L.
Construction	NATM	TBM	TBM
Primary lining	Shotcrete	Steel ribs and wooden lagging	segmented concrete
External diameter (D)	4.0 m	6.1 m	2.56 m
Cover (H)	6.20	9.0 m	22.5 m
H/D	1.55	1.48	8.79

Table 5.7 Case Histories Selected for Analyses with the Adopted Numerical Solution

second, the governing equations of the problem are "inverted", so that the observed performance quantities are set as input data and the unknown parameters become output of the inverted problem. Since the number of field measurements usually exceeds the number of unknowns, some minimization procedure is required to optimize the solution. The problem can be treated using either a deterministic or a statistical approach. The latter is applied whenever the influence of possible errors or uncertainties in the observed variables are believed to be significant in the results of the analysis. A general review on the subject was presented by Gioda (1985) who discussed different optimization procedures, and the advantages and disadvantages of direct and inverse approaches. Applications to the tunnel problem have been limited to simpler linear elastic constitutive relations (e.g. Gioda and Jurina, 1981:47, Ledesma et.al., 1986). The treatment of non-linear material responses is the subject of ongoing studies by different researchers.

The analyses presented in subsequent sections do not include any of the formalism just described. The best fit conditions were obtained by a direct trial and error approach, where the acceptance of the results relied simply on a balanced judgement of the aspects of the tunnel performance being inspected.

5.2.4.2 Alto da Boa Vista Tunnel

Introduction and Site Geology

This was a medium sized tunnel built in 1978 in the southern area of Sao Paulo, Brazil, to connect two water treatment plants. Details of this project were given by Negro (1979), Negro and Eisenstein (1981), Simondi, Negro and Kuperman (1982), Negro (1983) and were partly summarized by Heinz (1984:273). A very brief description is included herein for completeness.

This 73 m long tunnel was driven as an experimental project, to test the NATM procedure in the construction of an urban tunnel, for the first time in South America. It was driven with an almost circular profile of about 4 m external diameter, and with a soil cover of 6 to 6.5 m. A longitudinal cross section of the tunnel is shown in Figure 5.13, where a simplified geological profile is included which summarizes data from the logs of 7 boreholes.

The soils found at the site represent some of the upper layers of Sao Paulo Sedimentary Basin. This deposit resulted from the combined action of tectonics affecting the Pre-Cambrian metamorphic bedrock (gneiss, migmatite and mica-schist mainly) with simultaneous sedimentation processes. A depressed valley floor was formed and filled with sediments in the early Tertiary. The source of sediments was the residual soil mantle covering adjacent scarps, which was eroded, transported a short distance and finally deposited under an alluvial-lacustrine environment.

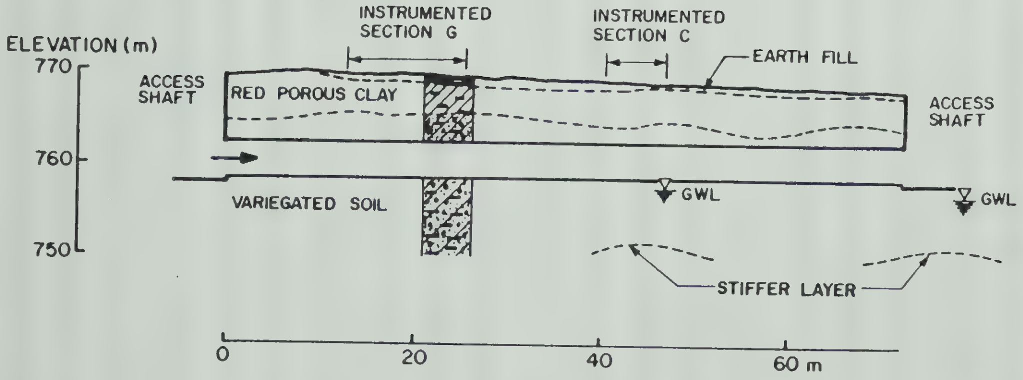

Figure 5.13 Longitudinal Profile Along ABV Tunnel

The soils thus formed were later subjected to pedological processes under a dry climate, involving chemical weathering of the upper layers.

Below an earth fill layer of some 0.5 m thickness a 3 to 4 m thick layer of a soft lateritic silty clay is found, which is locally called red porous clay. Underlying this is a thick layer of what is locally referred to as the variegated soil, thus named for its diversified colours. The tunnel was entirely driven through this rather heterogeneous material which was predominantly represented at this site by a silty and clayey fine sand of medium density with occasional gravel layers. The ground water level was found 1 or 2 m below the tunnel floor, and a stiffer horizon was detected at some 20 m below the surface.

Geotechnical Properties

The typical index properties of the soils given in Table 5.8 were obtained from samples collected at the site. Of particular interest are the mechanical properties of the variegated soil, which should govern the tunnel response. These are summarized in Table 5.9 and are derived from laboratory tests carried out on undisturbed block samples collected at the site and at other locations. This soil belongs to Groups II and III according to the classification system proposed by Sousa Pinto and Massad (1972), and by Massad (1980). The properties indicated are expressed in terms of effective stresses (drained parameters). While most parameters shown have been obtained from actual laboratory testing (triaxial compression and oedometer tests), the coefficient of earth pressure at rest was estimated from an empirical expression proposed by Mayne and Kulhawy (1982:863):

$$K_o = (1-\sin\phi')OCR^{\sin\phi'} \qquad [5.5]$$

The K_o range shown was calculated for a friction angle of 29°, for the given range of overconsolidation ratios.

The red porous clay overlying the variegated soil, although more homogeneous in appearance than the latter, is in reality very heterogeneous particularly in terms of deformation properties (Massad, 1974 and Massad et.al., 1981). Some mechancial properties of this material as found at the site are shown in Table 5.10. Additional data on this soil can be found, for example in Kupper (1983).

Possibly for a better evaluation of the in situ deformation properties, a few pressuremeter tests were conducted using the same probe and equipment used by Eisenstein and Morrison (1973). Figure 5.14 shows the variations of the Young's modulus, calculated from the pseudo-elastic testing stage on primary loading, using the Gibson and Anderson (1961) interpretation. Tests were conducted at three boreholes, but the results were superimposed for presentation. The considerable scatter of data noted may reflect the erratic nature of the sediments, but there appears to be an overall trend of the E modulus increasing with depth. Results marked with an asterisk were probably affected by the presence of gravels immersed in the

Soil Type	Red Porous Clay	Variegated Soil
Liquid Limit (%)	58 - 72	44 - 64
Plasticity Index (%)	27 - 38	17 - 31
Water Content (%)	30 - 39	13 - 26
Finer than 2 μm (%)	52 - 74	19 - 57
Coarser than 75 μm (%)	10 - 25	14 - 83
Total Unit Weight (kN/m^3)	14.3 - 16.0	17.8 - 19.4
Specific Gravity	2.69 - 2.85	2.68 - 2.84
Void Ratio	~ 1.55	~ 0.86
Degree of Saturation (%)	62	63

Table 5.8 Typical Ranges of Properties of ABV Soils

Cohesion intercept c' (MPa)	0.01 - 0.03 (1)
Friction angle ϕ' (°)	26 - 32 (2)
Failure ratio R_f	0.8 - 1.0
Modulus number K	300 - 400
Modulus exponent n	0.2 - 0.3
OCR	2 - 3
K_0	0.7 - 0.9 (3)
Posson's Ratio ν	0.3 (4)

Notes:
(1) For stresses above the overconsolidation pressure the cohesion intercept is zero.
(2) Range for stresses beyond the overconsolidation pressure. For that C' = 0.
(3) Estimated from Mayne and Kulhawy (1982) expression for $\phi' = 29°$.
(4) Estimated.

Table 5.9 Range of Geotechnical Parameters for the Variegated Soil at the ABV Site

Cohesion intercept c' (MPa)		0 - 0.07 (1)
Friction angle ϕ' (°)		22 - 30 (1)
Oedometer E moduli (MPa)		
Primary loading	(50 to 100 KPa)	5 - 10
Unloading	(100 to 50 KPa)	11 - 16
Reloading	(50 to 100 KPa)	25 - 30
OCR		2.5
K_0		0.8 (2)
Poisson's Ratio		0.2 - 0.4 (3)

Notes:
(1) Drained strength range for stresses below overconsolidation pressure. Data from other locations.
(2) Estimated from Mayne and Kulhawy (1982) expression for ϕ' = 26°.
(3) From Kupper (1983:118) measurements at low confining pressures.

Table 5.10 Range of Geotechnical Parameters for the Red Porous Clay at the ABV Site

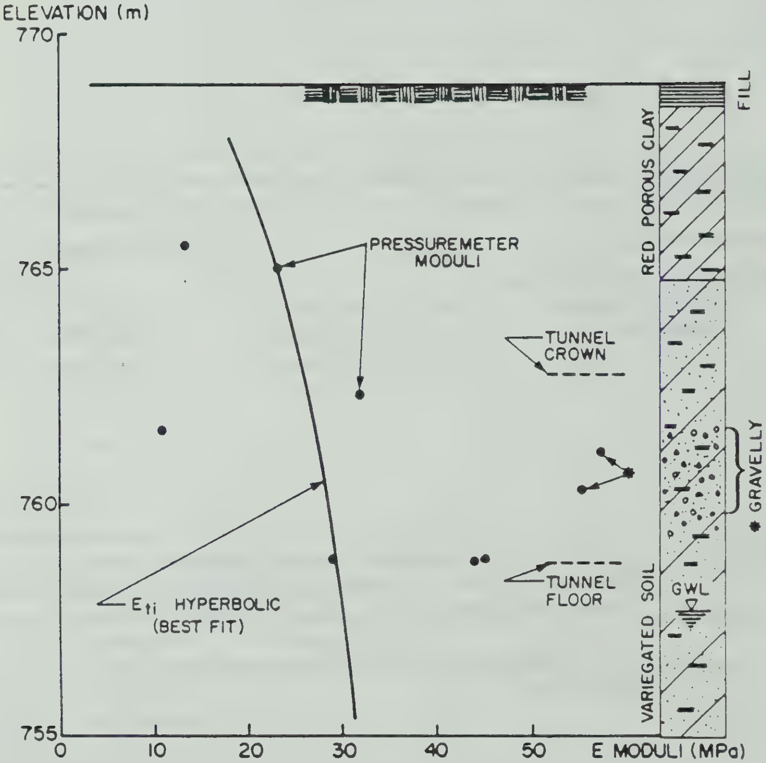

Figure 5.14 Profile of the In Situ Deformation Modulus at the ABV Site

clayey sand layer. Also shown, is the variation of the initial tangent modulus with depth as given by the hyperbolic model formulation (Figure 5.11), for the in situ stress conditions. This modulus distribution was the one used in the best fit back analysis as explained later. It corresponds to $K=400$, $n=0.25$, $\phi'=29°$, $c'=0$, $R_f=1$, $K_o=0.75$ and $\gamma=16$ KN/m^3.

Construction Details and Field Monitoring

Tunnel construction was undertaken with a three-stage face excavation (heading, bench and floor) with immediate shotcreting of exposed walls. Details of the transverse and longitudinal sections of the tunnel are shown in Figure 5.15. The cross section of 12.8 m^2 was fully hand mined, with the heading advance varying from 1 to 1.5 m. Lining invert closure at the instrumented section took place at about 2.6 m behind the heading face. The average construction rate was 1.6 m/day for a single 10 h/day shift and when passing the instrumented section, it peaked at a rate of 2.8 m/day.

The initial support system was a 10 cm thick shotcrete with a light wire mesh placed in the centre of the section. After tunnel completion, an additional 3 cm layer of shotcrete was applied at the lateral walls. This system worked as a primary and secondary support. Perfect material and structural conditions were revealed by a site inspection 40 months after completion. A complete set of information on the construction control and the shotcrete properties and

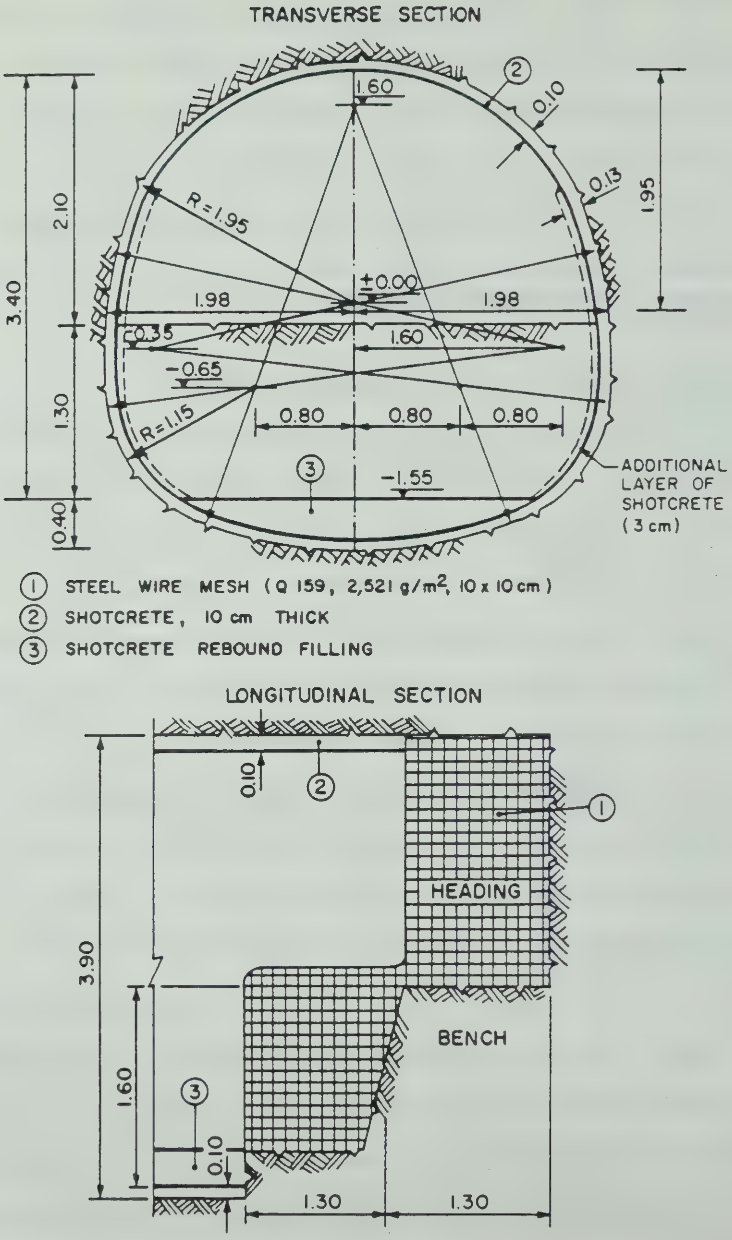

Figure 5.15 Construction Details at the ABV Tunnel

performance was published by Simondi, Negro and Kuperman (1982). From this data it can be estimated that the Young's modulus of the concrete increased from 2 GPa a few minutes after its application to 20 GPa about 24 hours later. The excavation of the heading and bench proceeded during concrete hardening, before it achieved its final strength. Field monitoring, which included convergence and levelling measurements inside the tunnel and ground movements near the opening, indicated that a substantial part of the lining deformations took place in less than 24 hours following the initial shotcrete application at the heading walls. Lining invert closure took place in less than 24 hours after the heading face reached the instrumented section. Most of the remaining lining deformations took place in the subsequent 24 hours, with the heading face advanced about one diameter ahead of the instrumented section. In other words, most of the interaction processes between the soil and lining took place while the shotcrete was young, at which stage it is difficult to assess its mechanical properties. Moreover, it is appreciated that within the same shotcrete ring, there are portions with different ages, which further complicates the assessment. If a single value of the secant Young's modulus of the shotcrete was to be chosen in order to be represented in a simplified interaction analysis, this value would have to be necessarily low. A reference value of 5 GPa was liberally selected, which is believed to have been the shotcrete secant modulus some 6 to 8 hours after its application. A Poisson's ratio of 0.25 was adopted for the shotcrete. This is slightly higher than is usually assumed for normal concrete. However, it is known that during hardening, the Poisson's ratio decreases from 0.4-0.5 to a final value of around 0.2. To be consistent with the lower reference modulus of deformation, a higher Poisson's ratio had to be assumed.

Field instrumentation comprised surface and subsurface settlement measurements, section convergence monitoring, tunnel crown levelling and contact pressure measurements. The latter was done using hydraulic pressure cells (Interfels type HPG077) located at the lining-soil interface, at the crown, springline and floor of the tunnel. Details of other measuring schemes are given by Negro and Eisenstein (1981), who also provide the results and interpretation of the field measurements.

Numerical Simulation

For the back analysis of this tunnel performance the numerical solution described in Section 5.2.2.1 was used, with a finite element mesh having 273 nodal points and 500 elements. A surficial porous clay layer of 4.2 m thickness and with linear elastic behaviour was initially considered to overlie the non-linear elastic variegated soil layer. A few runs revealed that the results of the analyses were not very sensitive to the elastic properties assigned to the upper layer, for the ranges given in Table 5.10. It will be shown later in Section 6.2.4.2 that the tunnel response is basically controlled by the properties of ground extending a half tunnel diameter above and below the opening. In this case, only variegated soil exists within those limits. It was decided to simulate the problem as a single soil layer, with selected properties representing the variegated soil.

Figure 5.16 furnishes the assumptions that were made and the values of the soil parameters that were used and kept constant in the analyses. Field monitoring indicated that the ground response was basically time-independent and the location of the ground water level below the tunnel floor led to the assumption of a fully drained soil response. The soil parameters were selected accordingly from the range of values shown in Table 5.9. Furthermore, they were chosen so to approximate the in situ modulus distribution provided by the pressuremeter tests results shown in Figure 5.14, both for the variegated soil and for the porous clay. The specific weight shown is a weighted average value for the two soil layers combined. The only soil parameter allowed to vary in the analyses was the coefficient of earth pressure at rest. The range of variation considered for K_o was that shown in Table 5.9 (from 0.7 to 0.9).

A perfect equivalence between the actual shotcrete lining and the thicker lining ring used in the numerical simulation would be achieved only if the compressibility and flexibility ratios of both linings were equal. This, however, is not possible since there is one condition too

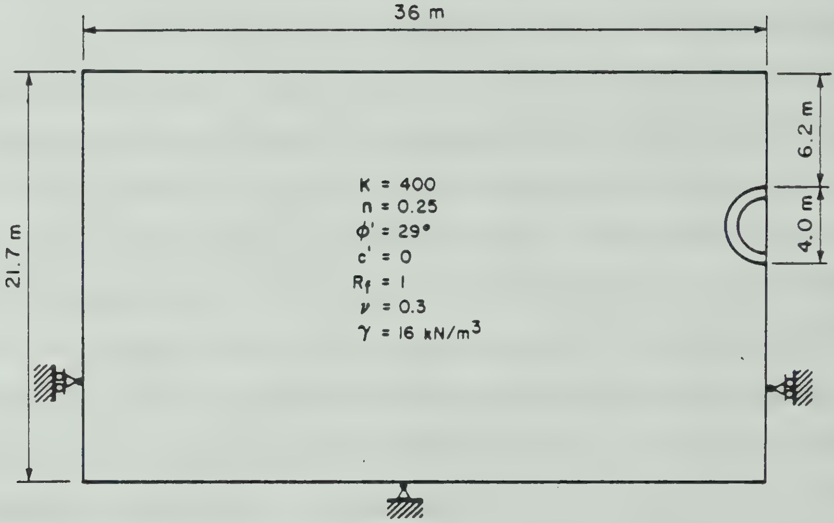

Figure 5.16 Assumptions and Fixed Parameters for ABV Tunnel Back Analyses

many. For the 10 cm thick shotcrete lining, an outside diameter of 4 m, a 5 GPa modulus, and a Poisson's ratio of 0.25, those ratios are equal to 0.11 and 507.8, respectively, using the Einstein and Schwartz (1979) definitions (equations 2.17 and 2.18). To approximate these figures, the 50cm thick equivalent lining of equal external diameter, would require a modulus of either 30 MPa to harmonize with the compressibility ratio or 900 MPA to equal the flexibility ratio. Accordingly, in the back analysis, the lining modulus was assumed to vary within these limits. It was later found that the best agreeement between measured displacements and stress is obtained when the flexibility ratios are similar.

The third and most important parameter to be varied in the analyses, is the amount of stress release taking place prior to the lining installation. An interpretation of the field measurements suggested that it would be sufficient to vary this parameter from 30 to 50%.

Results of the Back Analyses

After a few tentative runs it was concluded that five equal load increments, for each simulation phase (10 unloading steps altogether), allowed an adequate approximation. Table 5.11 summarizes the parameters that were varied in the analyses. Fourteen combinations of these parameters were required to give what was called the best fit case. For the higher lining modulus, the tunnel crown heaved rather than settled as observed in the field. The

Stress release α prior to lining installation (%)	30	40(1)	50	
In situ stress ratio K_0	0.7	0.75(1)	0.8	0.9
Equivalent lining E modulus (MPa)	50(1)	100	200	

Note: (1) Best fitted values

Table 5.11 Parameters Varied in ABV Tunnel Back Analyses

best fit analysis provided a reasonably good match between the calculated and observed performances, both at the final equilibrium situation and before lining installation. This condition was found for 40% stress release prior to the lining installation, for K_o=0.75 and for an equivalent lining modulus of 50 MPa. This modulus value corresponds to a flexibility ratio, F, equal to 293.7 or a shotcrete modulus of about 8.65 GPa. As noted previously, the in situ (initial) tangent modulus distribution with depth is that given in Figure 5.14, which roughly agrees with the pressuremeter test results.

Figures 5.17 and 5.18 compare observed and calculated vertical displacements in the ground, at the surface and below it, when the heading face reached the instrumented section. The calculated values correspond to a stress release of 32%. Figures 5.19 and 5.20 show in turn, the final vertical movements of the ground after full equilibrium between lining and soil. In both situations, a reasonable agreement between observed and calculated movements is found, in terms of the magnitude of the maximum displacements and in terms of their overall distribution, including ground heave below the tunnel floor.

Figure 5.21 compares the final radial stresses onto the lining as measured in the field and as calculated in the best fit finite element run. The latter was obtained by extrapolation of the averaged element stresses in the ground to the lining-soil interface. The contact stresses were

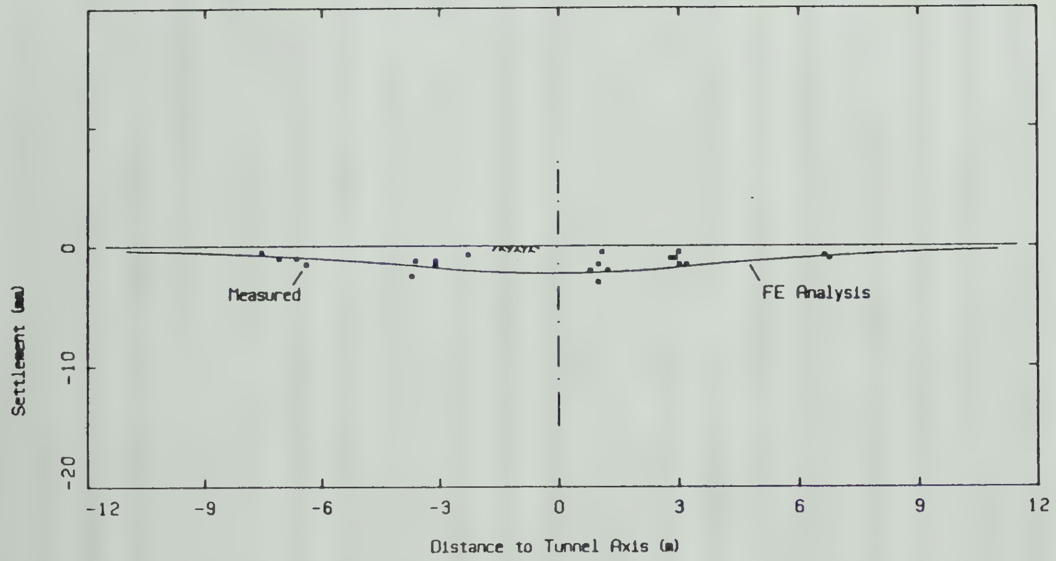

NOTE: MEASUREMENTS AT INSTRUMENTED SECTION C AND G

Figure 5.17 Measured and Calculated Surface Settlements at the Face of the ABV Tunnel

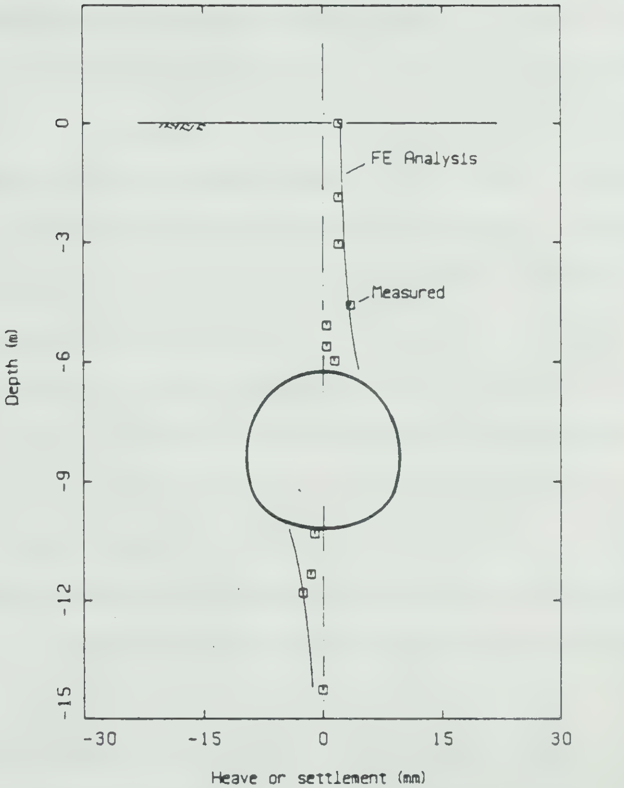

NOTE : MEASUREMENTS AT THE MAGNETIC EXTENSOMETER CCI (SECTION C)

Figure 5.18 Measured and Calculated Subsurface Vertical Displacements at the Face of the ABV Tunnel

measured by three Glotzel type pressure cells located at the crown, springline and floor. Notwithstanding the known difficulties associated with the installation of these type of cells notably at the upper arch of the lining, the agreement between the measured and calculated contact stresses is fairly reasonable. The radial stresses at the crown and springline are overestimated by the FE analysis, and slightly underpredicted at the floor.

Finally, Table 5.12 summarizes the comparisons between measured and predicted performances for this case history. It also includes additional data regarding measurements taken inside the tunnel, for convergence and crown levelling. The major discrepancies found refer to these latter measurements. The maximum horizontal convergence of the lining was appreciably overestimated while the lining roof settlement was underestimated. These disparities are not unexpected, when one considers the three-dimensional arching and ground-lining responses discussed in Section 2.3.6. It was suggested in that section that in heading and bench schemes with immediate application of shotcrete in the tunnel walls, some longitudinal bending of the upper shotcrete shell, which is open at springline elevation, may occur. The field instrumentation seems to support that this was the case in the ABV tunnel. The upper shell seemed to have worked as a cantilever, "fixed" in the closed section further behind. A partial rebound was noted once the invert was closed. The associated spatial squatting

Performance Aspect		Measured(1)	Calculated	C/M
1. Maximum surface settlement at tunnel face	mm	1.6	2.3	1.44
2. Maximum final surface settlement	mm	5.0	4.2	0.84
3. Maximum slope of final settlement trough at surface		1:1300	1:1790	0.73
4. Floor heave at tunnel face	mm	1 - 1.5(2)	3.2(3)	2.13 - 3.2
5. Final floor heave	mm	5 - 9(2)	8.2(3)	0.91 - 1.64
6. Maximum horizontal convergence of the lining	mm	0.85	5.7	6.71
7. Crown settlement at tunnel face	mm	1.5(4)	4.2(4)	2.80
8. Final crown settlement	mm	8.0(4)	7.7	0.96
9. Total settlement of lining roof	mm	4 - 5	2.6	0.52 - 0.65
10. Pressure on lining at the crown	kPa	30	44	1.47
11. Pressure on lining at the springline	kPa	35	49	1.40
12. Pressure on lining at the floor	kPa	55	47	0.85

Notes:
(1) Average values.
(2) Measured at 0.2m and 1.2m below tunnel.
(3) Calculated at 0.7 m below tunnel.
(4) At 0.2m above tunnel.

Table 5.12 Measured and Calculated Performance of ABV Tunnel

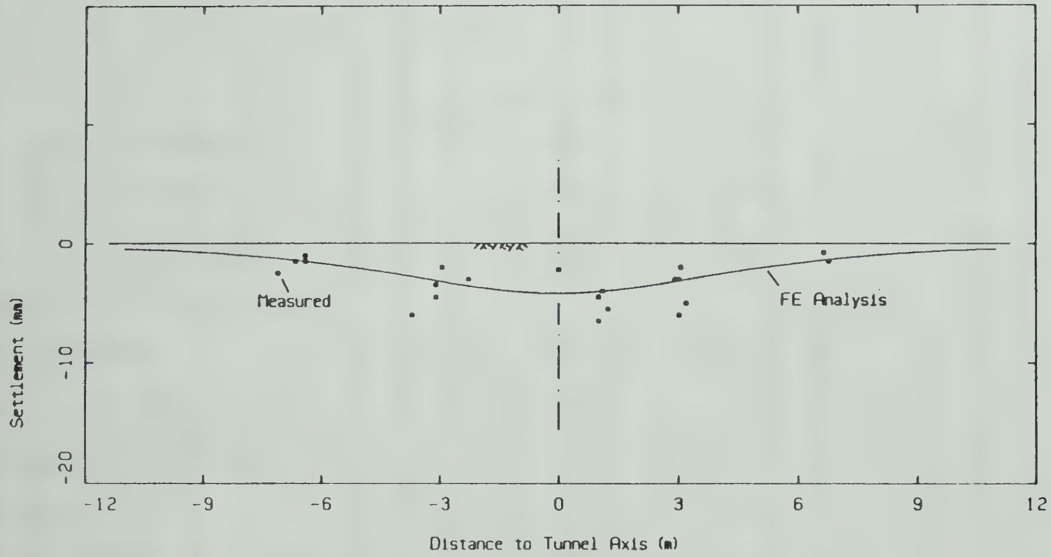

NOTE : MEASUREMENTS AT INSTRUMENTED SECTIONS C AND G

Figure 5.19 Measured and Calculated Final Surface Settlements at the ABV Tunnel

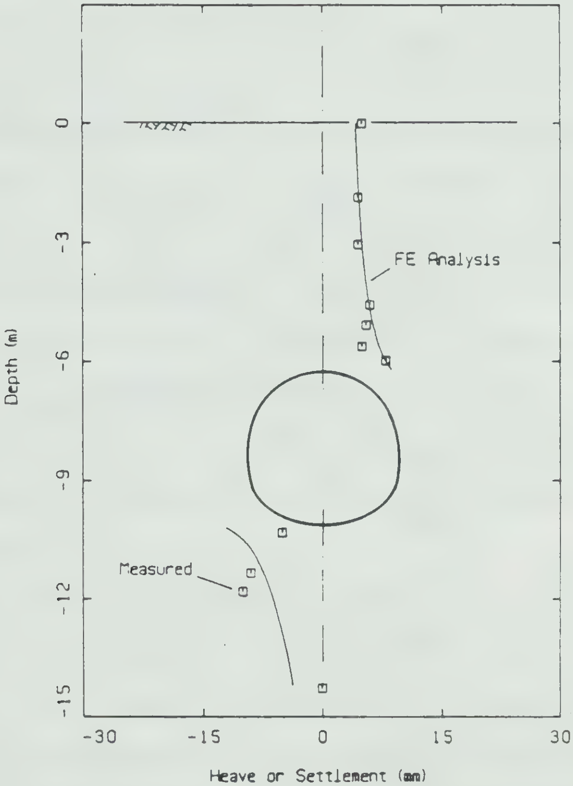

NOTE : MEASUREMENTS AT THE MAGNETIC EXTENSOMETER CCI (SECTION C)

Figure 5.20 Measured and Calculated Final Subsurface Vertical Displacements at the ABV Tunnel

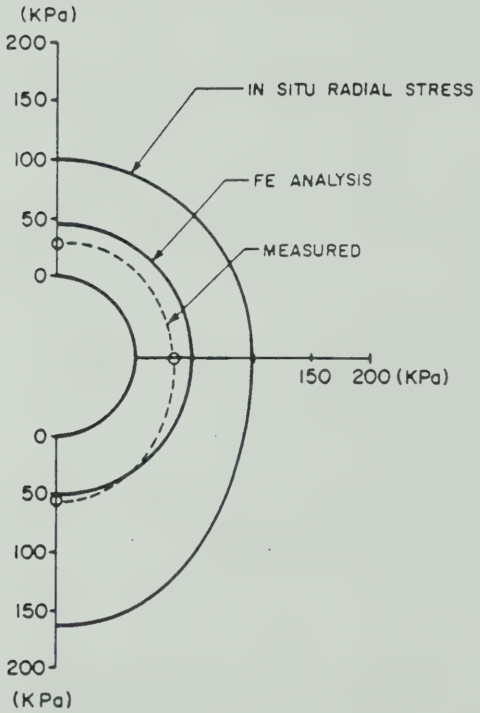

Figure 5.21 Measured and Calculated Final Radial Stresses on ABV Tunnel Lining

of the half cylinder shell which causes the crown to deflect downwards and springline points to move outwards, cannot be simulated with the present simple two-dimensional model, and this could explain the noted discrepancies.

Unfortunately, the readings in the contact pressure cells were not planned to monitor this type of response. It seems worthwhile to confirm this mechanism in similar projects in the future, using adequate monitoring equipment and planning. Moreover, it seems relevant to explore the consequences of this type of response, by using detailed three-dimensional numerical simulations in future research projects. The absence of an adequate treatment of this problem in lining design was indicated in Section 4.2.1. Also, the current lack of appreciation, by practitioners, of this mechanism as a possible source of problems was shown in Section 4.4.2.2.

The same reasons exposed above could explain the poorly predicted magnitude of crown settlement and floor heave at the moment the tunnel face reaches the instrumented section. A simple two-dimensional representation cannot portray with accuracy the ground-displacement field around the tunnel face. While in the present plane strain solution, the vertical displacements along the tunnel axis above crown, will always be shown as attenuating from the opening to the surface, it is known that this may not be the case (see for instance, Casarin, 1977 and Katzenbach, 1981:100). In the planes containing the tunnel face or ahead of it, settlements larger than the crown settlement can be observed above the crown elevation in an actual 3D case. Reciprocally, the same response may occur below the floor elevation. If the aspects of performance that are strongly influenced by the 3D nature of the tunnel problem are put aside (items No. 4, 6, 7 and 9 in Table 5.12), the others are fairly reasonably approximated by the numerical simulation. Although not formally attempted, it was felt in the course of these analyses that 3D dominated aspects could have been fully bracketed by the numerical solution, if allowance for extreme variations of the soil properties had been made.

Unfortunately, no measurements of horizontal ground movements were taken in this case history, and this allowed an additional degree of flexibility in fitting the observed performance. The best fitting process is also made easier by virtue of the fact that three parameters (K_o, E_s, a) were allowed to vary. It should be noted that the K_o value was only allowed to vary within fairly narrow limits. The same cannot be said regarding the lining properties but this does not affect the back analysis of the performance prior to support application, but only after. Hence, it can be accepted that the assessed amount of stress release before lining placement, has been reasonably approximated in this analysis. For similar studies in the future, it would be advisable to undertake careful investigation of the variation in the deformation modulus of the shotcrete with time and with the tunnel advance. This would be affected by means of some in situ monitoring or laboratory testing under variable strain rate control conditions. This would enable a narrower range of properties to be considered, which could improve the accuracy of the stress release estimate.

The back analysis furnished a final all round average radial stress onto the lining which amounts to 40% of the in situ radial stresses. This is compared with the 34% provided by the measurements. The mean thrust in the support was, therefore, overestimated by about 18%. If the bending moments are considered to be proportional to the radial stress difference between the crown (or floor) and the springline, it could be said that the analysis underpredicted the actual bending moments by about 11%. These figures should be taken with a word of caution, because of the known difficulties with pressure cells. It is worth noting that an almost uniform all-round radial stress distribution was obtained from the analysis. This seems to be consistent with the mode of behaviour, which is usually anticipated for unreinforced or lightly reinforced shotcrete linings. In these the final bending moments are expected to be negligible due to the singular process of ground load transfer while the shotcrete is hardening.

Finally, Figures 5.22 and 5.23 illustrate the amount of straining after final equilibrium is reached, that points around the tunnel should be subjected to according to the numerical simulation results. Figure 5.22 indicates that the soil next to the opening underwent compression in the major principal strain direction (up to about 1%) and extension in the minor one (up to about -0.4%), as expected. As a measure of shear straining, principal strain differences were plotted in Figure 5.23. The maximum strain difference is observed around the tunnel springline and amounted to 2%. At distances greater than about one radius from the tunnel the effect has dropped significantly to 0.1% or less. The difficulties in defining a "failure zone" from shear strain contours, was discussed in Section 2.3.4.3. Although no laboratory data is available on samples of the variegated soil tested under the stress path that prevails in this region, available results from conventional triaxial tests (Massad, 1980), suggest that this soil would fail under higher strain differences (around 3 to 6%). In fact, the numerical simulation indicated that no soil element experienced failure, as defined by the Mohr-Coulomb envelope, in any stage of the analysis. Despite this, a substantial decrease in the tangent elastic modulus was observed from its initial in situ value to that calculated for the final situation. This is also illustrated in Figure 5.23, where it is shown that near the tunnel walls, the tangent modulus decreased to about 1% of its original value.

Despite the fact that this tunnel had been built under very good ground control and favourable ground conditions (Negro, 1979, Negro and Eisenstein, 1981), a significant

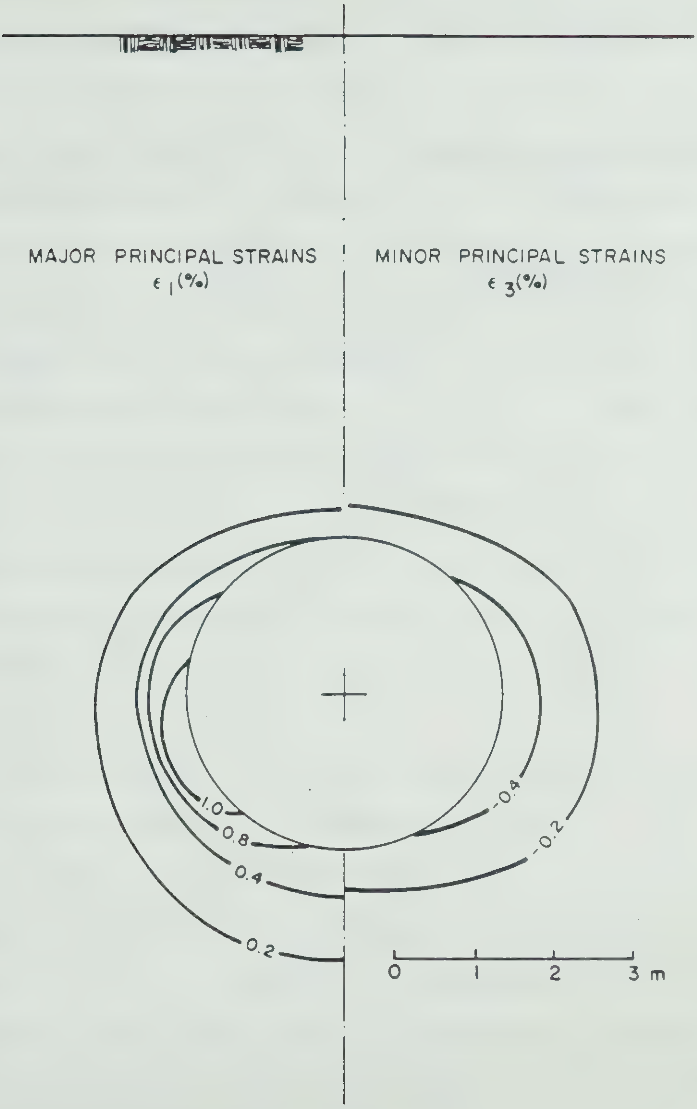

Figure 5.22 Calculated Contours of Major and Minor Principal Strains Around the ABV Tunnel

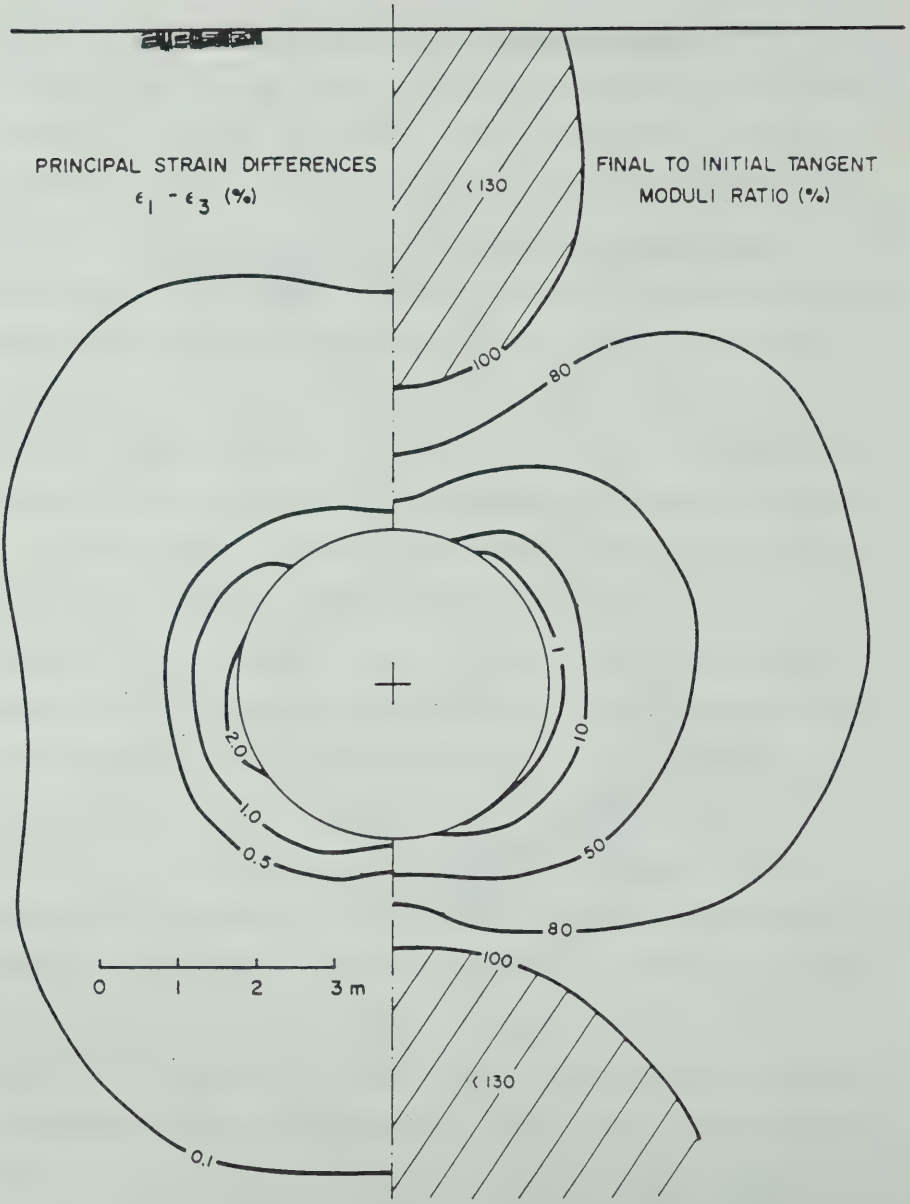

Figure 5.23 Calculated Principal Strain Differences and Changes in Tangent Modulus Around the ABV Tunnel

non-linear ground response seems to have occurred. This tends to confirm the aspects discussed in Chapter 2, where it was pointed out that, even if ground failure is avoided by adequate construction procedures, the non-linear response of the soil cannot be neglected when interpreting or simulating the observed the observed tunnel response. Consequently, the associated tunnel performance could not be adequately simulated by a linear elastic model or by some elasto-plastic models (Section 5.2.1.1), unless some aspects of the behaviour are disregarded. This was the case of the linear elastic analysis of the same tunnel carried out by Negro and Eisenstein (1981), where a full stress release was assumed at the excavated tunnel boundary and where the presence of the lining was not explicitly taken into account.

No concentration of shear straining was detected, although one would not expect to obtain this with the present finite element code. But even if the plastic behaviour of soil was represented by an elastic-plastic model, as for instance the Cam-Clay model, the concentration would not have been correctly simulated according to the discussion in Sections 2.3.4.3 (see also Mair, 1979:133 and Seneviratne, 1979:113).

If the action of the lining could be simply reduced to that of a uniform pressure acting against the walls, thus assuming the support to be a very flexible membrane then a factor of safety against global collapse of the tunnel opening could be estimated for the final equilibrium situation. The limiting tunnel pressure causing tunnel collapse could be assessed by the D'Escatha and Mandel (1974) method, (see Sections 4.3.4. and 6.5.2). Using the definition of the factor of safety given by equations 2.11 and 2.14, and working in terms of a uniform average in situ stress field and uniform tunnel pressures, a factor of safety of 1.42 is determined for the average stress produced by the FE analysis and FS=1.26 for the average measured stress. These values are less than the range of safety factors (2 to 3) proposed in Section 2.3.3, below which a non-linear ground response is to be expected. Thus, it tends to confirm the criteria established then.

With the final crown displacement as given by the back analysis or by the field instrumentation (both roughly equal to 8 mm), it is possible to calculate the dimensionless crown displacement, U, given by equation 2.16. This is found to be equal to 0.55, for an initial tangent modulus at the crown elevation, of about 26 MPa. According to the criteria proposed in Section 2.3.4.3, a value of U higher than 1.8 will generally mean a high shear strain concentration and conditions approaching tunnel collapse. In the present case a value of U well below this proposed threshold was found and it is actually lower than the reference unit value proposed for good ground control conditions. As such, it supports the criterion established then. For this condition, no "loosening" effects should be manifested and the numerical model used is adequate for the present simulation.

An additional interesting feature shown in Figure 5.23 is the increase in the tangent modulus at points above and below the tunnel. This aspect of behaviour was anticipated from Section 5.2.2.2, where it was explained that this results from the rotation of principal stresses in those regions. During the initial increments of stress release, it was noted that the shadowed areas touched the opening, and as the unloading proceeded they moved away after complete reversal of the principal stresses. In these regions, the ratios of final to initial tangent moduli varied from 1 to 1.3. Had the unloading-reloading feature of the hyperbolic model been implemented with a modulus solely dependent on the confining pressure, higher moduli ratios would have been found in those areas, since the Janbu's modulus number for unloading is greater than for loading (about 20% more for stiff soils , Duncan et.al., 1980:13).

5.2.4.3 Edmonton Light Rail Transit (LRT) Tunnel

Introduction and Site Geology

This was a large diameter tunnel, built in early 1981 along Jasper Avenue, in Edmonton, Canada, as part of the South Extension of the light Rail Transit System. This extension was about 600 m long and built as a twin tunnel. The case history described herein refers solely to the tunnel driven first, which was the Southbound line on the northern side of Jasper Ave. Details of this project, including field monitoring and its interpretation, were provided by Branco (1981), Eisenstein and Branco (1985), and Branco and Eisenstein (1985). Previous local experience was reported by Eisenstein and Thomson (1978), related to the performance of the first LRT line, thereafter extended through the length currently described.

The 6 m diameter tunnel was driven with a soil cover of 8.5 to 9.5 m. A longitudinal cross of the tunnel is shown in Figure 5.24, where a simplified geological profile is included which summarises data from 18 borehole logs.

The geological and geotechnical conditions of downtown Edmonton were reviewed recently by Thomson et.al. (1982). The bedrock, comprising clay shale, mudstones and sandstones, was uplifted during the Eocene and subaerial erosion led to the formation of a mature drainage system prior to glaciation. During Pleistocene epochs, the preglacial river systems began aggrading, as a result of the only recorded advance of the continental ice sheet into the area. Many of the preglacial valleys became partially infilled with a sequence of dense to very dense sands and gravels termed the Saskatchewan Sands and Gravels. Local advances and retreats of the Wisconsin Ice Sheet are said to have laid down two till layers (the Upper or Brown Till and the Lower or Grey Till). While the lower unit has been laid down on the Saskatchewan Sands and Gravels or on the bedrock by an ice lobe moving NW-SW, the upper one resulted from ice advancing from the NE direction. Both till sheets contain lenses of water-deposited sands with thicknesses varying

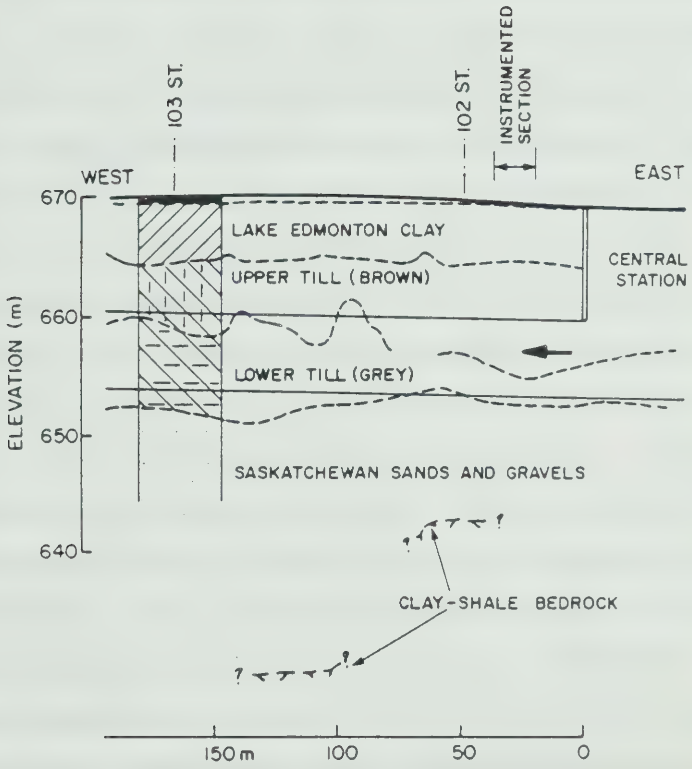

Figure 5.24 Subsurface Profile of Southbound LRT Tunnel along Jasper Avenue (after Branco, 1981:modified)

from a few centimeters to several metres, and range in extent from less than one to more than 10 metres. These lenses are frequently water-bearing and randomly located. The surficial deposit is a silty clay, glacial lake sediment, formed in the late Pleistocene and is covered locally by fill material.

As noted in Figure 5.24, the upper fill material is less than a metre thick. The Lake Edmonton Clay is 4 to 5 m thick. The combined till units appear at the site with a total thickness of 12 to 14 m, the upper till being thicker than the lower one at the instrumented section. As elsewhere in the area, the upper till was found to be columnar jointed with joint spacing in the order of some 20 to 40 cm. The lower till is also known to be jointed but in a rectangular fashion. The till body overlies the tertiary Saskatchewan Sands and Gravels, which in turn lie on a Clay-Shale bedrock located at an elevation which is not clearly defined at this site. The bedrock was detected at two locations at depths varying between some 30 to 40 m. Apart from some free water found in a few of the sand lenses detected within the till, a ground water level has not been identified in this site, and may be located well below the tunnel floor.

Geotechnical Properties

Basic geotechnical properties of these soils were given by a number of authors (for example, Thomson, 1969, Morgenstern and Thomson, 1971, Eisenstein and Thomson, 1978, Wittebolle, 1983). The results of tests on samples collected at this particular site were presented by Branco (1981:13, 268-273), and are summarized in Table 5.13. Apart from differences in colour and in the joint systems the two till materials are geotechnically very similar (Thomson et.al., 1982:176). For this reason, single ranges of properties are given for the stiff to hard Edmonton Till. Of particular interest are the mechanical properties of this material since the tunnel was entirely driven through this layer. Some of these properties are summarized in Table 5.14. With the exception of the K_o value and Poisson's ratio, the parameters were obtained from drained axial compression triaxial tests on block and cored samples, which were collected at nearby excavation sites, some 300 m northeast and 400 m west of the present site by Medeiros (1979) and by Wittebolle (1983) respectively. The hyperbolic model parameters were obtained from the drained conventional triaxial test results (confining pressures from 15 kPa to 34 kPa) furnished by Medeiros (1979:78). His data was reinterpreted by the writer who fitted hyperbolae to the stress-strain curves. Some of the curves obtained by Medeiros (Op.cit.) were not closely fitted by a hyperbola. These were the tests with cell pressures between 20 and 26 kPa and were therefore discarded following recommendations by Duncan et.al., (1980:22) on elimination of experimental inconsistencies. The range of modulus constants resulting reflects considerable scatter of data despite the elimination of inconsistent results. The scatter can be

Soil Type	Lake Edmonton Clay	Edmonton Till	Saskatchewan Sands and Gravel
Liquid Limit (%)	34 - 79	27 - 67	-
Plasticity Index (%)	8 - 48	10 - 46	-
Water Content (%)	21 - 39	10 - 29	5$^{(6)}$
Finer than 2 m (%)	9 - 62	8 - 55	0$^{(5)}$
Coarser than 75 m (%)	1 - 13	9 - 48	97.5$^{(5)}$
Total Unit Weight (kN/m^3)	18 - 20	19 - 23	18.5$^{(6)}$
Specific Gravity	2.76$^{(2)}$	2.65$^{(3)}$	2.67$^{(6)}$
Void Ratio	~0.9$^{(4)}$	~0.4$^{(4)}$	~0.5$^{(4)}$
Degree of Saturation (%)	95 - 100$^{(4)}$	90 - 100$^{(4)}$	28$^{(6)}$
Undrained Shear Strength (kPa)	44 - 141	94 - 662	-

Notes: (1) All data from Branco (1981:13), except where indicated.
(2) Average value given by Thompson (1969:14).
(3) Average value given by Wittebolle (1983:54).
(4) Calculated typical values.
(5) One sample only.
(6) From Medeiros (1979).

Table 5.13 Range of Basic Soil Properties Found Along LRT Tunnel Alignment at Jasper Avenue

Cohesion intercept c' (MPa)	0 - 0.035	(1)
Friction angle ϕ' (°)	35 - 40	(1)
Failure Ratio R_f	0.75 - 0.95	(2)
Modulus number K	550 - 800	(2)
Modulus exponent n	0.45 - 0.6	(2)
Poisson's Ratio ν	0.4	(3)
K_0	0.5 - 1.2	(4)

Notes:
(1) According to Medeiros (1979) and Wittebolle (1983) data.
(2) Based on Medeiros (1979) results from drained axial compression triaxial tests.
(3) Equal to estimated value by Eisenstein and Morrison (1973) and Medeiros (1979).
(4) From selfboring pressuremeter tests by Thurber Consultants (1980).

Table 5.14 Range of Geotechnical Parameters for Edmonton Till at the South LRT Tunnel Line

partly attributed to the fact that each stress-strain curve was obtained from samples taken at different depths in the till thickness (from 7 to 15 m, approximately). Each sample was tested with a confining pressure roughly equal to the overburden pressure at the point it was collected. This testing program exaggerates the effect of the soil variability, thus increasing the scatter of results, but the combined interpretation of these data better reflects the overall behaviour of the till mass. It may be fortuitous that the test results eliminated correspond to samples collected at elevations in the upper metre of the lower till, where the soil is known to be more fractured by the action of the overriding upper till (Eisenstein and Thomson, 1978:336).

Laboratory tests were not conducted on the Lake Edmonton Clay found at this site, but some selfboring pressure meter "quick" tests were available. Their results are given in Table 5.15, following the interpretation furnished by Thurber Consultants (1980).

Medeiros (1979:120) conducted also some conventional drained triaxial tests in block samples of Saskatchewan Sand, collected also at the site northeast of the present project location. The resulting parameters obtained are shown in Table 5.16. No clear relation was found between the initial tangent modulus of the hyperbolae fitted by the writer and the confining cell pressure. This was partly due to the fact that Medeiros (Op.cit.) used a narrow range of cell pressures (38 to 49 kPa), that again corresponded to the overburden stresses at the level of sampling. Hence, to obtain the modulus number K, a modulus exponent n of 0.5 was selected, which is believed to be reasonable for this granular material.

Although both the Till and Saskatchewan Sands have been tested in triaxial cells under stress paths other than axial compression, and in spite of the known influence of stress paths in these soils (Medeiros and Eisenstein, 1983), only results of conventional triaxial tests have been considered. The reasons for this decision bear on the discussion presented in Section 2.3.4.1. and also to be consistent with the aims of the present analysis, stated in Section 5.2.4.1. The numerical solution adopted is based on the original hyperbolic formulation, which in turn is based on parameters derived from conventional triaxial test results.

The deformation properties of these soils were investigated also by pressuremeter testing, conducted along Jasper Avenue by Thurber Consultants (1980). Two types of equipment were used. One is the self-boring pressuremeter and the other is the high pressure pressuremeter which requires a pre-drilled borehole. Details of the equipment, testing procedures and results interpretation are given by Worth and Hughes (1974), Hughes et.al. (1977) and Hughes and Ervin (1980). They are also summarized in Thurber Consultants (1980) report to this particular project. In the self boring equipment a fairly quick probe expansion is done

Friction angle ϕ' (°)	20 - 30
Cu (kPa)	50 - 150
Pressuremeter E moduli (MPa)	6 - 15
Poisson's ratio	0.4 - 0.5$^{(2)}$
K_0	0.5 - 2.0$^{(3)}$

Notes: (1) All data from Selfboring pressuremeter (quick expansion) tests by Thurber Consultants (1980) at 104th Street and Jasper Avenue.

(2) Estimated.

(3) Interpreted range. Higher values (in excess of 3) were not considered.

Table 5.15 Range of Geotechnical Parameters for Lake Edmonton Clay at the South LRT Tunnel Line

Cohesion intercept c' (MPa)	$0^{(2)}$
Friction angle ϕ' (°)	39 - 41
Failure Ratio R_f	0.7 - 0.8
Modulus number K	$730 - 940^{(3)}$
Modulus exponent n	$0.5^{(2)}$
Poisson's Ratio ν	$0.25^{(2)}$
K_0	$0.36^{(4)}$

Notes: (1) Data based on Medeiros' (1979) results from drained axial compression triaxial tests.
(2) Assumed
(3) Range calculated for the assumed modulus exponent.
(4) Estimated from Jaky's expression.

Table 5.16 Range of Geotechnical Parameters for Saskatchewan Sands and Gravels at the South LRT Tunnel Line

in discrete increments of air pressure. Pore pressure changes are also monitored during testing. Figure 5.25 shows the variations of the Young's modulus derived from the cell pressure expansion curves obtained in the field, for assumed Poisson's ratios. Tests were done in two boreholes at two locations along the LRT alignment about 200 and 700 m west of the instrumented section, but the test results were superimposed in Figure 5.25 for presentation. Also included in this figure are the results of pressuremeter tests carried out by Eisenstein and Morrison (1973) in the different soil units, at locations not far from the present site. A considerable scatter of data is noticed, reflecting the erratic nature of the locally occurring soils. This feature was referrenced earlier from Thomson et.al. (1982:179).

Also shown in Figure 5.25 is the variation of the initial tangent modulus with depth, as given by the hyperbolic model formulation (Figure 5.11) for the in situ stress conditions. This modulus distribution was the one used in the best fit back analysis, as will be explained later. It corresponds to an upper soil layer with constant E value of 5 MPa, and a lower one described by K=600, n=0.50, $\phi'=40°$, $c'=0$, $R_f=1$, $K_o=0.75$ and $\gamma=19.5$ kN/m³. The given distribution seems to work nearly as an envelope for the results gathered in the later investigation, and as a lower bound to those tests conducted earlier.

Construction Details and Field Monitoring

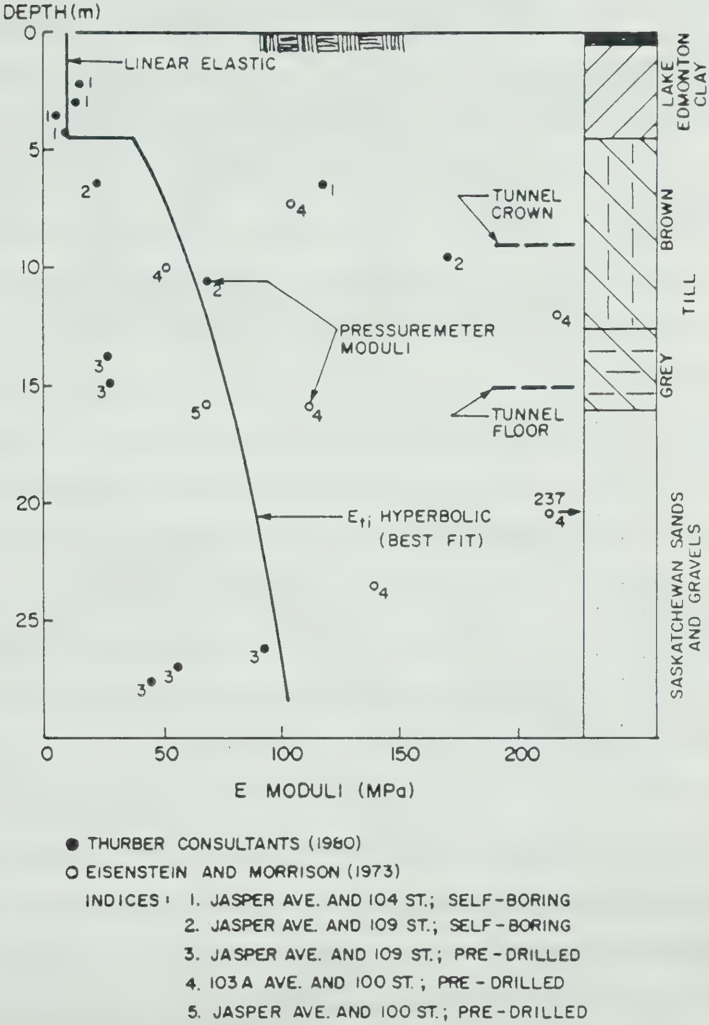

Figure 5.25 Profile of In Situ Deformation Modulus at the LRT site

Tunnel construction was carried out with a full face cutting wheel TBM (a Lovat M-246 Series 2100), whose details are given in Figure 5.26a. The TBM body is 5.5 m long and the cutting profile has a 6.17 m diameter. The cutting head is arranged in such a way that the soil at the face is indented and scraped by staggered teeth protruding outwardly and fixed at six spokes. Consequently, the fairly strong and stiff soil is cut at the heading in a nearly vertical face and left virtually unsupported. A detailed account of the tunnel construction was given by Branco (1981:17). The lining system used is shown in Figures 5.26(b) and (c). The primary lining comprised steel ribs spaced at 1.22 m, each one with four bolted segments, and wooden lagging in between. The support was expanded immediately after the ribs were exposed to the ground. Therefore, the maximum distance between the tunnel face and a fully expanded rib was about 6.7 m. Details of the secondary concrete lining is also given in Figure 5.26. However, they are not particularly relevant to the present study, as the performance of the tunnel being investigated is that observed before the secondary lining installation, which took place after completion of this tunnel. The average construction rate was 2.6 m/day while the TBM passed through the instrumented section. The field instrumentation included surface and subsurface settlement measurements, slope indicator readings, load cell measurements at loosely bolted joints of the steel ribs, load measurements in instrumented steel

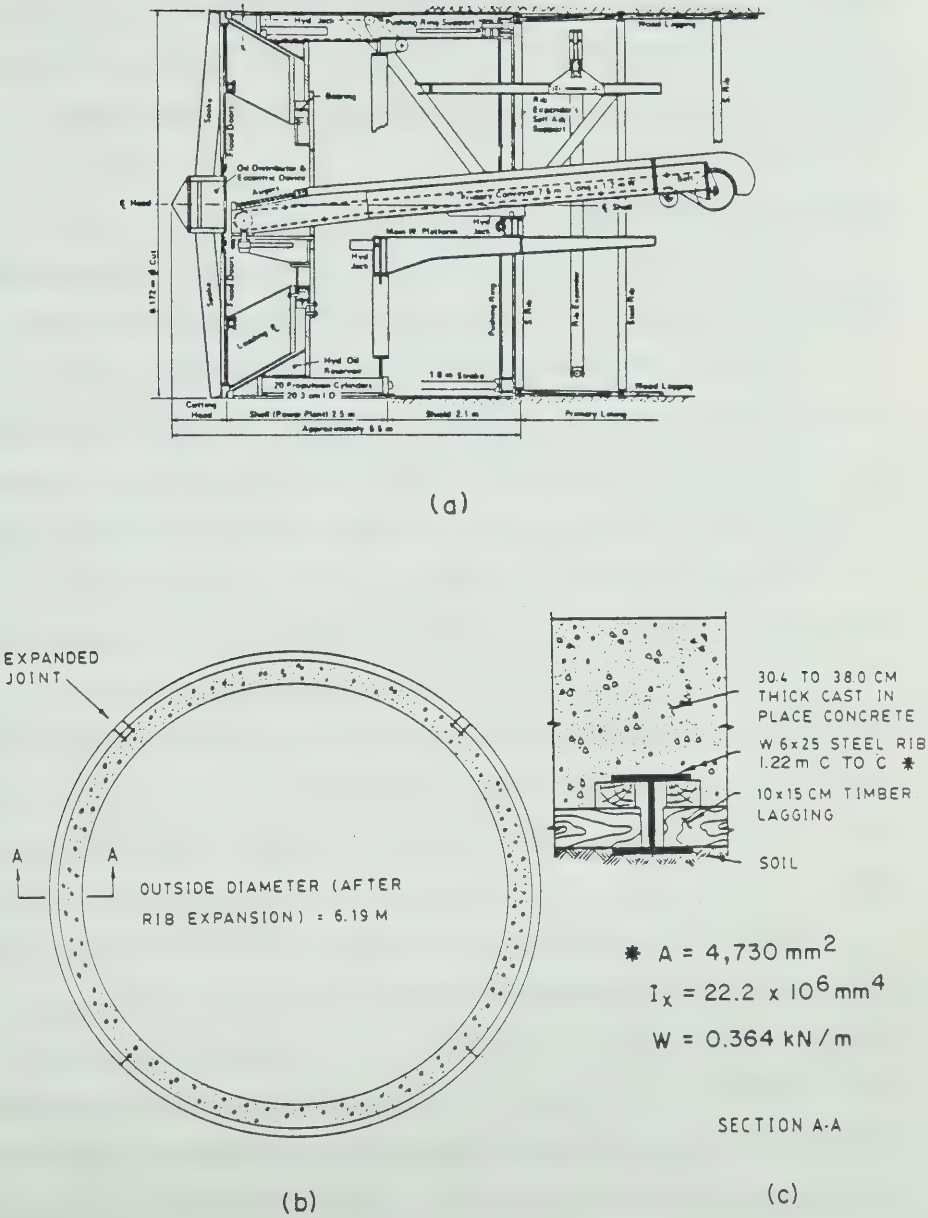

(a)

(b)

(c)

Figure 5.26 TBM and Lining System used at the Edmonton LRT Tunnel (after Branco, 1981:modified)

lagging with the same flexural rigidity (EI) as the timber lagging, convergence measurements of the steel ribs and levelling of two points of the steel set. Branco (1981) presented a detailed account of this rather involved monitoring program.

Numerical Simulation

For the back analysis of this tunnel, a finite element mesh of 298 nodes and 549 elements was used. A surficial layer of Lake Edmonton Clay with 4.5 m thickness and linear elastic behaviour was considered. As in the ABV tunnel case, it was noted again that the results of the analyses were not very sensitive to the elastic properties of this clay in the range given in Table 5.15. Also, it was noted that the deformation properties of the underlying Saskatchewan Sands (Table 5.16) are not dissimilar to those of the till (Table 5.14). As the tunnel was driven entirely through the till layer, it was decided to represent a single soil layer, below the surficial clay, with properties corresponding to that of the till.

Figure 5.27 presents the assumptions that were made and the values of the parameters that were used and kept constant in the back analyses. With the exception of the loads measured in the steel ribs which showed some increase with time, the ground response observed through displacement measurements seemed to be fairly time independent. This appears to be consistent with observations made in other projects in the area (Eisenstein and Thomson, 1978:343, Medeiros, 1979:75). However, the fairly high degree of saturation in the till, despite the fact that the ground water level was located well below the tunnel, may suggest that some pore pressure changes could have happened during tunnel advance.

Recent isotropic consolidation tests, carried out by Wittebolle (1983:56) on intact 10 cm diamter Edmonton Till samples, showed that the coefficient of consolidation (c_v) of this material as measured in the laboratory, for confining stress levels which occur around this tunnel, is about 10^{-3} cm²/s. This value can be used as a lower bound of the field values for the entire till mass. In fact, the presence of joints or fractures in the mass should considerably increase the rate of pore pressure changes with time. These discontinuities were not present in the laboratory samples (Wittebolle, Op.cit:41), and therefore a lower coefficient should have been obtained. Moreover, the existing sand lenses in the till will act to further accelerate any process of pore pressure equalization. A c_v value of, at least an order of magnitude higher that the laboratory value, can be said to better portray the overall till mass. A value of 10^{-2} cm²/s was suggested by Medeiros (1979:73) and is used here for discussion.

The tentative criteria developed in Chapter 3 for the identification of the ground response type for a shallow tunnel, in terms of time dependence (Figure 3.23), may be useful in this analysis. As noted by Branco (1981), the

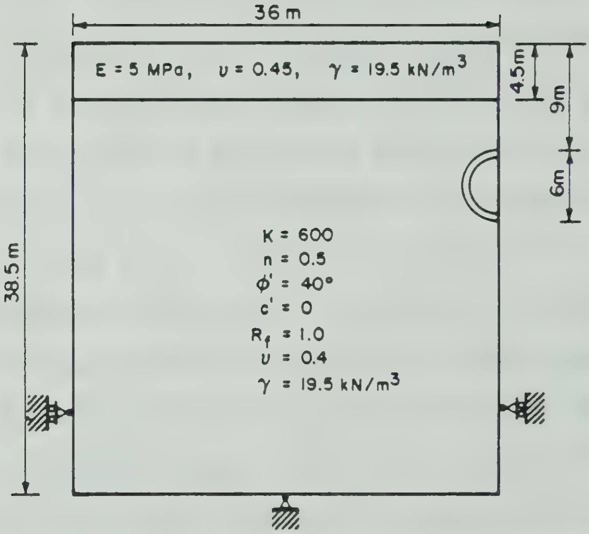

Figure 5.27 Assumptions and Fixed Parameters for the LRT Tunnel Back Analyses

"immediate" soil movements were observed over a time span of some 20 days, when the tunnel face advanced from a point about 1 to 2 diameters behind the instrumented section to a point 6 to 7 diameters past this section. The primary lining can be assumed to be fully permeable. If a till cover of some 5 m is considered with a c_v of $10^{-2}cm^2/s$, then over a period of time of 20 days, the consolidation of the soil due to drainage towards the tunnel will be partial, but closer to "appreciable" (see Figure 3.23). Had a c_v of $10^{-3}cm^2/s$ been selected, a partial consolidation condition would still result, but a larger percentage of the time dependent process would be occurring after the field measurements were taken.

From this simplified analysis, one would expect some long term ground response for this tunnel. Surface settlement measurements taken 282 days after the "short term" observations were completed (from February 26 to December 5 of 1981), confirmed that some additional ground movements had occurred. However, these movements were small in magnitude (and possibly not reliable). Unlike these, the load cell readings at the steel rib joints indicated a clear increase over the same time interval. The average thrust measured in the upper rib joints increased by 94%. A smaller increase seems to have occurred in the lower joints. Unfortunately not all lower joint cells were measured in the first measuring campaign, but 3 months after the "short term" observations (i.e. May 27) a 20% increase in the average thrust had already been measured for a 31% increase in the upper joints at the same time. Eisenstein et.al., (1983:19) attributed this increase in loads to a progressive loosening of the soil above the crown, associated with a succession of roof failures with time. Branco (1981:187), on the other hand, noted that there was no space left behind the primary lining, a couple of hours after it had left the shield. Furthermore, he noted that a soft and wet clay mixed with sand, had squeezed into and filled the space left behind the wooden lagging. Considering these facts, one could also speculate about the possibility of time-dependent lining load behaviour arising from some pore pressure equalization with time.

Although the reasons for the observed lining load increase with time in the LRT tunnel are not clear, the overall ground response observed should have been close to a drained one. Correspondingly, the soil parameters selected for the back analyses are consistent with those derived from drained tests and were chosen to roughly approximate the in situ modulus distribution provided by the pressuremeter test results, shown in Figure 5.25, both for the till and for the underlying sand. The only soil parameter allowed to vary in the analysis was the coefficient of earth pressure at rest (from 0.7 to 0.9).

An equivalent lining, 50 cm thick, was used in place of the actual primary lining. This gives compressibility and flexibility ratios of 0.3 and 600, according to the Einstein and Schwartz (1979) definitions and for the dimensions given in Figure 5.26. These values are for a soil modulus of 65 MPa and a Poisson's ratio of 0.4, and for a lining modulus of 200 GPa and its Poisson's ratio of 0.2. The contribution from the lagging is disregarded. If the compressibility and flexibility of the rib joints were considered, then the C and F values would be higher. To approximate these ratios, the equivalent lining with a 6 m external diameter would require a modulus of 0.25 or 1.40 GPa to equal either one or the other ratio. Accordingly, in the back analyses, the lining modulus was initially assumed to vary within these limits. However, it was soon found that modulus values lower than 0.25 would have to be investigated, in order to match the observed performance after lining activation. Therefore a new range of moduli from 0.09 to 0.7 GPa was considered. As in the ABV case, the best agreement was obtained when the flexibility ratio of the equivalent lining was set close to the "real" one, rather than matching the compressibility ratios.

The third solution parameter to be varied in the analysis, is the amount of stress release prior to the lining activation. An interpretation of the field measurements, followed by some preliminary computer runs, indicated that it would be sufficient to vary this amount from about 30 to 70%. These tentative runs indicated also that five equal load increments, for each phase of simulation (10 unloading steps altogether) would enable an adequate approximation.

Results of the Back Analyses

Table 5.17 summarizes the parameters that were varied in the analyses. Clearly, not all combinations of these parameters were needed to obtain the best fit case. This was found after fifteen computer runs. The runs using the higher lining modulus furnished unrealistic lining loads and deformations. The best fit analysis provided a reasonably good match between calculated and observed performances, at the final equilibrium situation and also before lining activation. This condition was found for 50% stress release prior to support application, for K_o=0.75 and for an equivalent lining modulus of 0.13 GPa. This modulus corresponds to a flexibility ratio F of 1114, which is almost twice as much the value initially estimated. If the joint flexibility and compressibility were disregarded, the flexural rigidity of the ribs (EI) per unit length of tunnel would be 3.64 MN.m. In the best fit case, EI corresponds to 1.71 MN.m, indicating that the rib joints do have an effect on the overall lining flexibility. It is worth noting again that the wooden lagging was assumed not to contribute to the support stiffness (in compression or bending).

As shown previously, the in situ (initial) tangent modulus distribution with depth is given in Figure 5.25. While this was obtained from drained triaxial test data, the pressuremeter moduli may reflect the soil stiffness under different drainage conditions (and of course, different

Stress release α prior to support activation (%)	33	$50^{(1)}$	67		
In situ stress ratio K_0	0.70	$0.75^{(1)}$	0.85	0.90	
Equivalent lining E modulus (GPa)	0.10	$0.13^{(1)}$	0.16	0.40	0.70

Notes: (1) Best fitted values

Table 5.17 Parameters Varied in the LRT Tunnel Back Analysis

stress paths).

Figure 5.28 compares observed and calculated settlements transverse to the tunnel axis at 3 m below the ground surface, just before lining activation. The measurements were taken when the tunnel face was located 6.3 m (1D) beyond the instrumented section, which is when support expansion was being undertaken. The finite element results correspond, accordingly, to the end of the first phase simulation after a 50% stress release had been applied, but before installation of the lining.

Similarly, Figure 5.29 compares observed and calculated final surface settlements. The measurements were taken when the tunnel face was located 37.6 m (6D) beyond the instumented section. The calculated displacements correspond to the end of the second phase simulation, after equilibrium was reached between the lining and soil.

In both situations depicted in these two figures, a fairly reasonable agreement between observed and calculated measurements is found, both in terms of the magnitude and the overall distribution of the surface settlements.

Figures 5.30 and 5.31 compare the vertical movement in the ground, along vertical lines located at approximately 10 and 4 m off the tunnel centre line, respectively. In each case, calculated and measured displacements are compared at the moment the lining was activated and when final equilbrium was achieved. Both magnitude and distribution of the final movements with depth are fairly reasonably

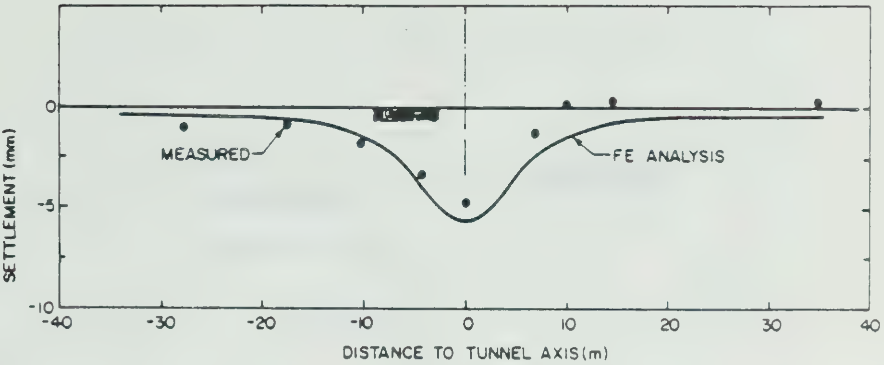

NOTES :

1. MEASURED AND CALCULATED SETTLEMENTS AT POINTS 3m BELOW SURFACE
2. MEASUREMENTS TAKEN WHEN THE TUNNEL FACE WAS 6.3m BEYOND THE INSTRUMENTED SECTION.
3. FIELD DATA FROM BRANCO (1981 : 67)

Figure 5.28 Measured and Calculated Surface Settlements before Lining Activation at the LRT Tunnel

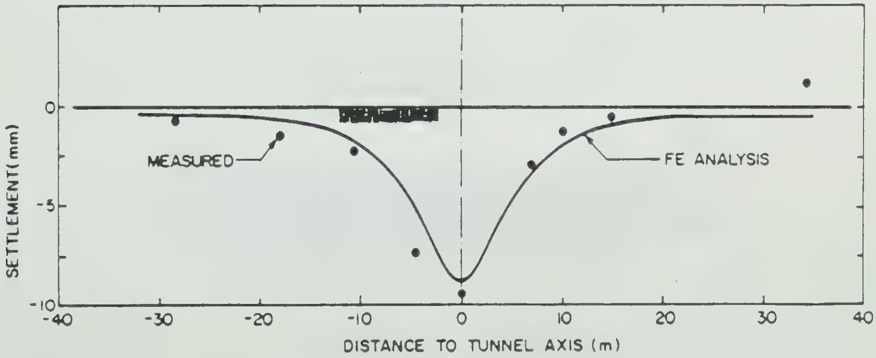

NOTES :

1. MEASURED AND CALCULATED SETTLEMENTS AT POINTS 3m BELOW SURFACE.
2. MEASUREMENTS TAKEN WHEN THE TUNNEL FACE WAS 37.6m BEYOND THE INSTRUMENTED SECTION.
3. FIELD DATA FROM BRANCO (1981 : 67)

Figure 5.29 Measured and Calculated Final Surface Settlements at the LRT Tunnel

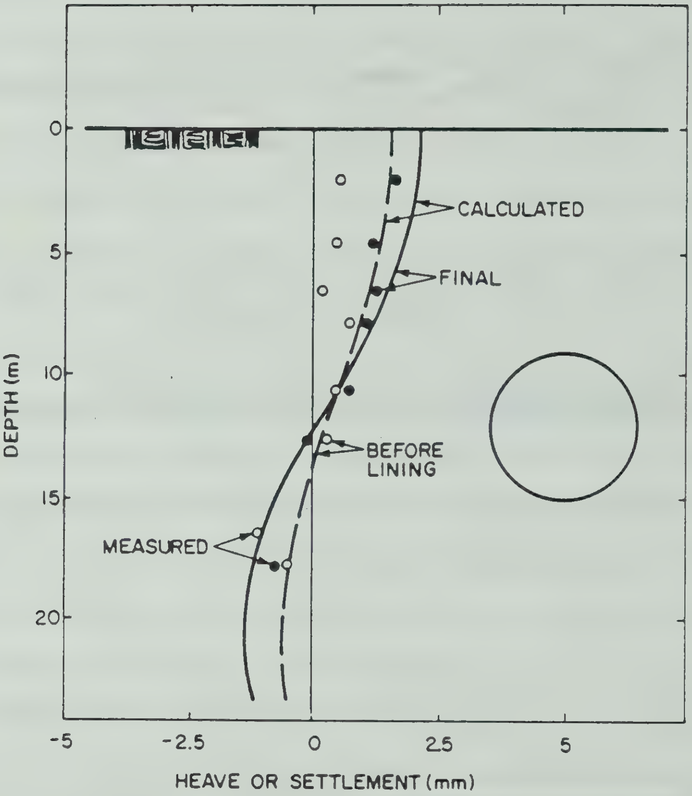

NOTES:

1. MEASUREMENTS AT ME5, 10.4m FROM TUNNEL AXIS.
2. CALCULATED DISPLACEMENTS AT 9.5m FROM TUNNEL AXIS.
3. MEASUREMENTS TAKEN WHEN THE TUNNEL FACE WAS ABOUT 1D AND 6D BEYOND THE INSTRUMENT STATION.
4. FIELD DATA FROM BRANCO (1981: 279 TO 287)

Figure 5.30 Measured and Calculated Vertical Displacements Along a Vertical Line 10 m off the Centreline of the LRT Tunnel

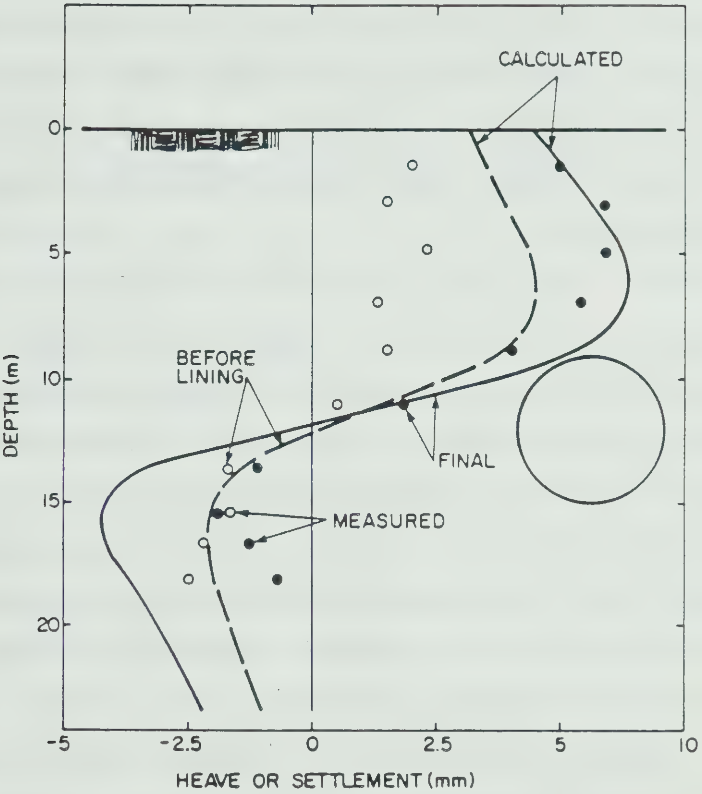

NOTES:

1. MEASUREMENTS AT ME9, 4.3m FROM TUNNEL AXIS.
2. CALCULATED DISPLACEMENTS AT 4m FROM TUNNEL AXIS.
3. MEASUREMENTS TAKEN WHEN THE TUNNEL FACE WAS ABOUT 1D AND 6D BEYOND THE INSTRUMENT STATION.
4. FIELD DATA FROM BRANCO (1981:288 TO 297)

Figure 5.31 Measured and Calculated Vertical Displacements Along a Vertical Line 4 m off the Centreline of the LRT Tunnel

predicted for points above the tunnel axis elevation, for points below, the analysis tends to overestimate the heave. This is possibly due to the simplifying assumption of introducing a single soil layer below the Lake Edmonton clay. The in situ modulus of the Saskatchewan Sands and Gravels may, in reality, increase faster with increasing confining stress than anticipated. Nevertheless, the results seem acceptable.

On the other hand, the movements predicted at the moment the lining was installed are, in both cases, overestimated for points above the axis elevation. A better agreement is found below it. This result is not suprising, since at a section one diameter behind the tunnel face, the actual displacement field is still affected by the heading advance, and non-zero longitudinal movements are present (see Section 2.3.6 and Eisenstein and Branco, 1985:58). But, when a near plane strain situation is met in the field, the numerical model seems to portray the observed behaviour quite satifactorily.

In Figures 5.32 and 5.33, measured and calculated horizontal displacements are compared along a vertical line beside the tunnel, before lining installation and after final equilibrium is reached. It should be noted that while the measurements refer to data from slope indicators located at 6.4 m and 4.3 m away from the tunnel centreline, the lateral movements were calculated along a vertical line between the slope indicators, some 5.5 m away from the centreline. Some difficulties were experienced with the zero readings of the slope indicators used in the comparison. Movements of as much as 5 mm were detected before the advance of the tunnel face (Branco, 1981:77). The measured displacements indicated in Figures 5.32 and 5.33 were assessed from the Branco (Op.cit.:101) data, but using as a zero reading, the measurements taken three diameters ahead of the face for the slope indicator SI6 and 4 diameters ahead for SI7.

The maximum magnitude of the calculated horizontal movements agrees fairly closely to the maximum observed. However, the distributions of movements are dissimilar. While the numerical models tend to yield maximum lateral displacements at the springline elevation, the observed maxima were noted to be always above the tunnel. This comparison is made with a word of caution since, as noted by Branco (1981:111), the measured movements were small compared to the accuracy of the measuring equipment. Hence, no assurance can be given to the trends of lateral movements observed.

In Figure 5.34, measured and calculated thrust forces at rib joints are compared. The load cell readings included the loads due to the support self-weight, as the zero readings were taken immediately before installation (Branco, 1981:142). The finite element analysis disregards the lining self-weight. For a consistent comparison, the self weight had to be excluded from the load cell readings. Through an

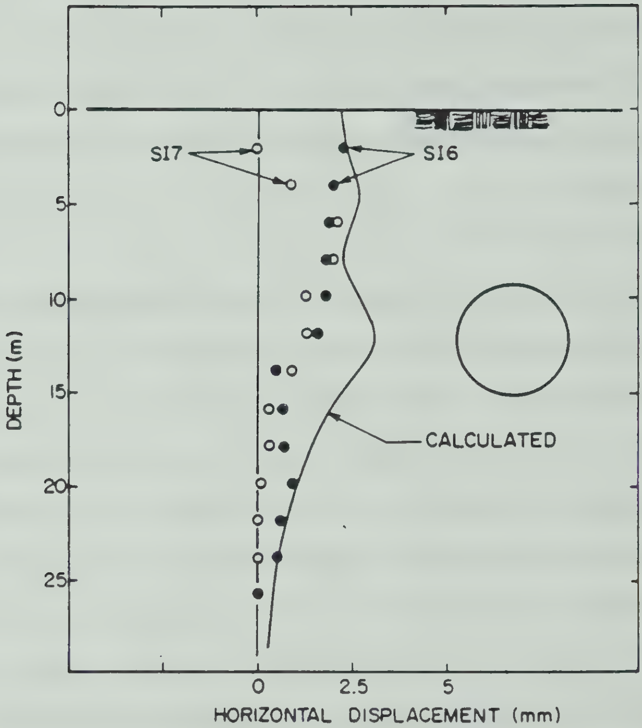

NOTES;

1. CALCULATED DISPLACEMENTS ALONG A VERTICAL LINE 5.5m AWAY FROM TUNNEL CENTRE LINE. SLOPE INDICATORS SI6 AND SI7 LOCATED AT 6.4 m AND 4.3m FROM TUNNEL AXIS.
2. MEASUREMENTS TAKEN WHEN THE TUNNEL FACE WAS ABOUT 1D BEYOND THE SLOPE INDICATORS.
3. FIELD DATA BASED ON BRANCO (1981: 102 AND 103)

Figure 5.32 Measured and Calculated Lateral Movements in the Ground beside the LRT Tunnel before Lining Activation

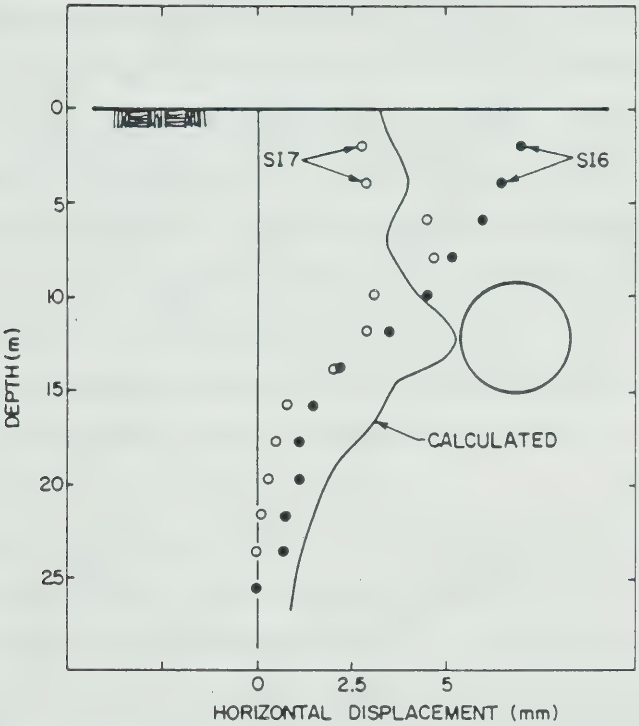

NOTES:

1. CALCULATED DISPLACEMENTS ALONG A VERTICAL LINE 5.5m AWAY FROM TUNNEL CENTRE LINE. SLOPE INDICATORS S16 AND S17 LOCATED AT 6.4 m AND 4.3m FROM TUNNEL AXIS.
2. MEASUREMENTS TAKEN WHEN THE TUNNEL FACE WAS MORE THAN 3D BEYOND THE SLOPE INDICATORS.
3. FIELD DATA BASED ON BRANCO (1981 : 102 AND 103)

Figure 5.33 Measured and Calculated Final Lateral Movements in the Ground beside the LRT Tunnel

approximate calculation, it was estimated that a 2.6 kN reduction in the upper joint thrusts and 7.7 kN in the lower ones were required in order to obtain the thrusts due to the ground loads only. As the calculated forces shown refer to a plane strain section of 1 m thickness, the measured loads in the ribs had to be divided by the rib spacing (1.22 m) to allow proper comparison. The "short-term" measurements are those taken when the shield tail was about 6 diameters away at 16 days after rib installation. The long term readings were taken 293 days after rib erection. The calculated thrusts were obtained at different sections of the lining, by averaging the computed tangential element stresses in those sections, and integrating them along the lining thickness.

As noted in Figure 5.34, the calculated forces tend to be higher than those measured in the "short term". But they seem to agree well with the long term measurements. To illustrate this more clearly, Table 5.18 was prepared. Here the measurements from all cells in the upper joints and in the lower joints were averaged out separately. Note that the values refer to the thrust in each steel rib. The numerical solution underestimates the long term load in the upper joints by only 3.6%. On the other hand, the long term load in the lower joint is underestimated by 7.7%. These results seeem to be quite reasonable, bearing in mind the limitations of the numerical code used, particularly those related to the lining representation, as discussed in

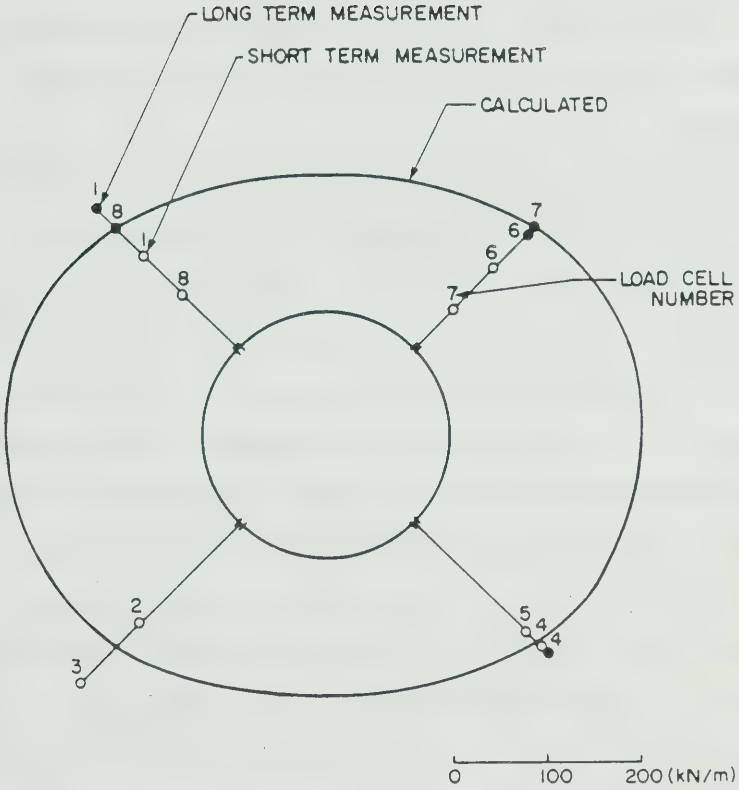

NOTES:

1. SHORT TERM READINGS 16 DAYS AFTER INSTALLATION; 36.4 m AWAY FROM SHIELD TAIL
2. LONG TERM READINGS 293 DAYS AFTER INSTALLATION
3. LINING SELFWEIGHT DISCOUNTED FROM READINGS
4. MEASURED AND CALCULATED THRUST VALUES PER UNIT LENGTH OF TUNNEL (1.22 m C TO C RIB SPACING CONSIDERED)
5. FIELD DATA FROM BRANCO (1981: 156) AND FROM EISENSTEIN ET AL (1983)

Figure 5.34 Measured and Calculated Thrust Forces at Rib Joints in the LRT Tunnel

Section 5.2.2.2. The favourable comparison with the load cell measurements was probably due to the small amount of bending carried by the support system in this case history. For this condition, the deficiences of the present finite element formulation in representing the lining are minimized.

Table 5.19 summarizes the comparisons between measured and calculated performances for this case history. It also includes some additional data regarding measurements taken inside the tunnel of convergence and invert levelling. The overall agreement seems quite reasonable. Even the lateral movements in the ground, which were not investigated in the ABV tunnel described before, show a favourable comparison, despite the difficulties experienced with the zero readings of the slope indicators. The maximum total heave of the lining invert segment was overpredicted by the calculation. However, as described by Branco (1981:192), the initial measurement was taken only after the TBM tail had been advanced 1.6 m beyond the instrumented rib. In other words, part of the heave occurring between the moment the rib was expanded and the moment the zero reading was taken was not included. The maximum horizontal movement of the lining at the springline was excessively overestimated by the calculation. Part of these movements were also not measured, again due to the delayed zero reading. Branco (Op.cit.:200) threw some doubt on the observed movements because of the reduced number of readings and the possible action of the

	Average Thrust in Rib Joints (kN)		
	Measured(1)		Calculated(4)
Joint	Short Term(2)	Long Term(3)	
Upper	119.3	224.7	216.6
Lower	229.4	242.3(5)	223.7

Notes:
(1) Lining selfweight discounted.
(2) 16 days after installation, 36.4 m away from shield tail.
(3) 293 days after installation.
(4) Considering a rib spacing of 1.22 m c. to c.
(5) Only load cell 4 was read. At 103 days after installation the average thrust was 268.3 kN.
(6) Data based on Branco (1981) and on Eisenstein et al. (1983).

Table 5.18 Measured and Calculated Average Thrust Forces at Rib Joints in the LRT Tunnel

	Performance Aspect		Measured(1)	Calculated	C/M
1.	Maximum surface settlement at lining installation	mm	4.8	5.8	1.21
2.	Maximum final surface settlement	mm	9.3	8.5	0.91
3.	Maximum slope of final settlement trough at surface	-	1:1000	1:1090	0.92
4.	Maximum lateral movement at ground surface	mm	2.5 to 7(2)	3.5	0.5 to 1.4
5.	Maximum total heave at the lower joints of the steel ribs	mm	3.6(3)(7)	5.4	1.5
6.	Maximum horizontal movement of lining at springline elevation	mm	1.2(4)(7)	8.3	6.92
7.	Maximum final deep settlement (4 m from axis)	mm	6.0(5)	6.5	1.08
8.	Final average thrust in upper rib joints	kN	224.7(6)	216.6	0.96
9.	Final average thrust in lower rib joints	kN	242.3(6)	223.7	0.92

Notes:
(1) Data from Branco (1981), Eisenstein et al (1983) and Eisenstein and Branco (1985).
(2) SI7 and 6.
(3) Observed by levelling joint B of ring 8 (Branco, 1981).
(4) At Ring 8
(5) At ME9
(6) Lining selfweight excluded
(7) Zero reading taken 1.6 m behind TBM tail.

Table 5.19 Measured and Calculated Performance of the LRT Tunnel

thrusting forces used to advance the TBM. From experience gained in other projects, using a similarly designed tape extensometer, it can be said that the accuracy of such measurement is frequently very low (up to a few millimeters). It is interesting to note that a poor comparison of horizontal convergence was also obtained at the ABV tunnel, where the same measuring device was used. The reasons for these noted departures require more detailed investigation.

Unfortunately the magnetic extensometer installed in the tunnel axis, was lost when it was hit by the cutting wheel. The distribution of subsurface settlements, above the tunnel crown was therefore not assessed, except ahead of the face where heave was noted throughout the tunnel cover. A second extensometer was intalled later, but a localized collapse of a sand lens at the roof occurred when the tunnel face reached the instrument station and again the measurements were lost (Branco, Op.cit.:110; see also Section 2.3.5.4).

Nevertheless, the larger amount of field data available in this case history, including a fairly complete picture of the displacement field around the opening, created a much more restricted condition for the back analysis than was the case with the ABV Tunnel. The variations allowed in K_o and on the lining properties, still offered some degree of flexibility in fitting the observed performance. But as in the previous case, it is believed that despite these variations, the assessed amount of stress release prior to lining installation was also reasonably approximated in this analysis.

The all-round uniform ground stress, corresponding to the average long term thrust measured in the steel ribs, is estimated to be about 30% of the in situ radial stress. The same figure is found with the numerical solution, noting that a slightly smaller tunnel diameter has been considered here (Figures 5.26 and 5.27). In this regard, a better agreement is found in this case, than in the ABV Tunnel. It is also noted that the present construction scheme led to a slightly higher ground stress reduction, than was observed in the NATM construction scheme. This was due mainly to a delayed support application in the LRT case, compared with the ABV case. In both cases the stress reductions taking place after lining installation are comparable.

The simplified stability assessment for the final plane strain situation, as explained in the former case (Section 5.2.4.2) can be repeated here. Similarly, the support action is reduced to that of applying a uniform internal pressure in the opening walls, so that a factor of safety against global collapse of the ground can be estimated. Both measured or calculated performances convey a factor of safety equal to about 1.3 which is comparable to that noted at the ABV tunnel. Again this figure is less than the range specified in Section 2.3.3, and once more a non-linear ground response would have to be expected. In fact, Figure 5.35 confirms this. Very low tangent moduli were calculated around the opening, but no soil element actually "failed" under the final equilibrium condition. The overall distribution of the elastic modulus around the LRT tunnel was very similar to that in the ABV case, including the increase in modulus above and below the tunnel (not entirely shown). This pattern tended to be not as intense as in the former case. The extent of the "softened" zone in the LRT was a bit larger than in the ABV, for points above and below the tunnel, and smaller in the lateral region. The distribution of the principal strains around the opening was also very similar. Once more, despite the fairly good ground control achieved in this tunnel (Eisenstein and Branco, 1985), a significant non-linear response of the ground appears to have occurred.

Using the final crown displacement of 15.9 mm given by the back analysis, it is possible to calculate the dimensionless crown displacement (U), given by equation 2.16. It is found to be equal to 0.86, for an initial tangent modulus of the soil at the crown equal to about 57 MPa. This value of U is smaller than the reference value of 1.8, set in Section 2.3.4.3, as a threshold figure for a near collapse condition. It was mentioned (Branco, 1981:110) that a localized roof collapse was triggered by a dry sand pocket and by an excessive overcutting. This event cannot be portrayed by this simplified numerical simulation. Had the sand lens been absent, or had a smaller overbreak been

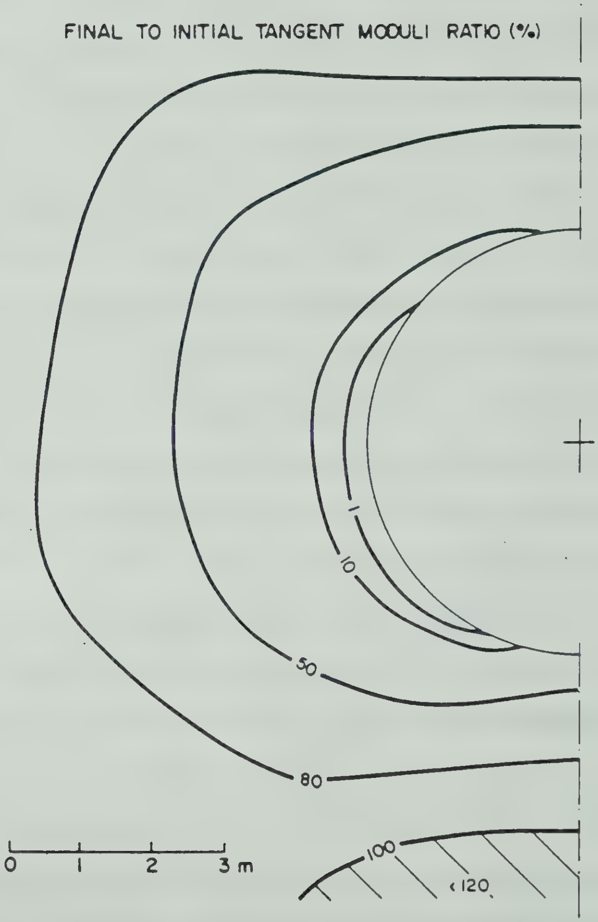

Figure 5.35 Calculated Changes in Tangent Modulus around LRT Tunnel

ensured, such an occurrence would not have been manifested. If this localized phenomenon is put aside then the criteria established seems to operate adequately.

5.2.4.4 Edmonton Experimental Tunnel

Introduction

The small diameter tunnel was built in 1979 as a main storm sewer for the Yellowhead Trail freeway, in northern Edmonton, Alberta. It includes a length of precast segmented concrete lining which was introduced on an experimental basis in the Edmonton area. This case history refers solely to the experimental portion of the tunnel, and does not deal with the remaining length, where a conventional two-phase support system was used. Details of this project are found in El-Nahhas (1980), Eisenstein et.al. (1981a) and in Eisenstein et.al. (1981b).

Site Geology

The 2.56 m diameter tunnel was driven under a soil cover of 22 to 25 m. A longitudinal cross section of the tunnel is presented in Figure 5.36, where a simplified geological profile is included.

A brief overview of the geological conditions in Edmonton was given in the previous section. At the time the present back analysis was initiated, the writer assumed that the geological and geotechnical conditions found in this case were similar to those of the LRT tunnel. A review of the former investigations and analyses then available on this case history did not indicate otherwise. Hence it was

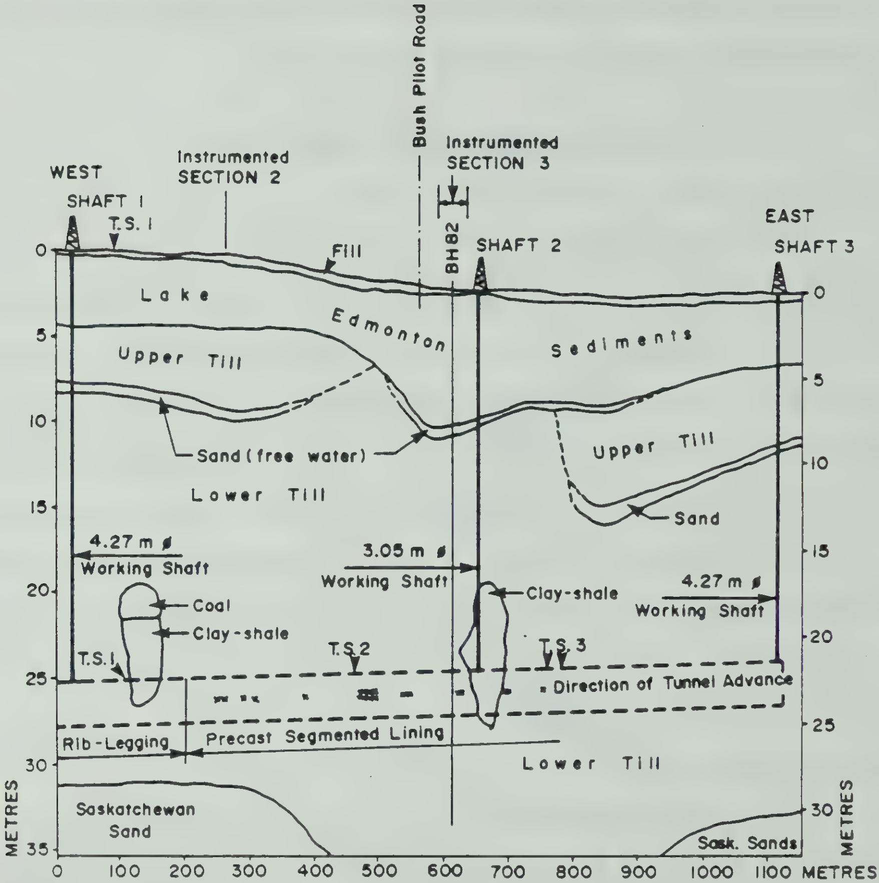

NOTE: ADDITIONAL BOREHOLE BH82 DRILLED IN 29th OCTOBER 1982, 19.7m SOUTH OF TUNNEL AXIS, 44.3 m WEST OF CONSTRUCTION SHAFT 2 (Current Manhole AA14)

Figure 5.36 Subsurface Profile of Edmonton Experimental Tunnel along 125 Avenue (Yellowhead Trail) (after El-Nahhas, 1980:modified)

accepted that the experimental tunnel had also been driven through a stiff, very stiff to hard till. Accordingly, the first preliminary numerical simulations assumed the same 'best-fit' parameters found for the LRT case. These calculations indicated ground movements that were typically five times smaller than that actually measured. This raised the question of whether the tunnel had been driven through one of the soft zones known to exist in the Edmonton till (Thomson et.al., 1982). Available geotechnical data was not sufficient to answer this question. It was thus decided to conduct additional field and laboratory investigations. An exploratory 8" diameter borehole (BH 82 in Figure 5.36) was drilled in late 1982, followed by a testing program. Results of this program will be presented later, but as was anticipated a softer till zone exists in the area.

An examination of the available data on the urban geology of Edmonton (Kathol and McPherson, 1975:20) reveals that the tunnel axis runs almost parallel to the thalweg of the Beverly Preglacial Valley. This is the dominant topographic feature of the Edmonton bedrock and is considered to be the largest and deepest valley present in the area. It shows a gentle downstream gradient to the east (about 0.05%), is locally 7 km wide, and it has a northern side slope of up to 10%. The tunnel runs about 500 m south of its northern flank and about 25 m above its floor. Thomson et.al. (1982) suggested that the commonly used description of two dense basal tills (lodgement tills) in

Edmonton is overly simplistic. They suggested that other types of depositional features could have been present such as rapidly accumulated flow till zones. A review of recently proposed models explaining the formation of glacial sediments was presented by Wittebolle (1983:5).

As noted in Figure 5.36, the fill layer is less than a metre thick (about 3 m at BH 82). At the instrumented section 3, which is of interest to the present study, the base of the lake sediments is 8 m below the surface. The additional borehole BH82 did not detect the free water bearing sand layer underlying the upper sediments as shown in that figure. Instead, small sand lenses or pockets were found in the lower portion of the lacustrine sediments and in the upper region of the subjacent till body. The latter was medium to dark grey in colour and comprised mainly a silty clay (CL), locally including shale pebbles and coal bits, as well as the sand lenses. A careful logging of the twelve 3" diameter shelby samples did not reveal the existence of any joints in the till. The compression tests later conducted did not indicate any fissure controlled mode of failure. The description of the subsurface profile by El-Nahhas (1980:56), who was able to inspect the material in place through a number of construction shafts, large diameter power holes and instrument installation boreholes, does not include any reference to discontinuities in the till mass. Unlike the LRT tunnel, there was no record of localized ground collapses or of failures that were structurally controlled by soil discontinuities. Therefore, it seems probable that the soft till in the area is not jointed. If joint genesis is associated with drying (May and Thomson, 1978:368), then this till may not be dessicated to the same extent as typical Edmonton tills.

Geotechnical Investigations

Some 18 disturbed samples and 12 shelby tube samples were collected and tested. The basic geotechnical profile and properties of the soils found are given in Figures 5.37 and 5.38. The Unified Classification of the grey till is CL. The bedrock and the ground water level were not encountered by the 30.25 m deep borehole, which was drilled using a hollow stem auger. However, the degree of saturation of the till was always found to be greater than 95% and was 100% in most samples. The measured average water content and the in situ void ratio are slightly higher than that found at the LRT tunnel. Very low SPT blow count numbers were detected which were even lower than those found in another soft till zone in downtown Edmonton (Thomson et.al., 1982).

Thin walled shelby tubes turned in to form a cutting edge, were used for 72.9 mm diameter sampling. Sampling locations are given in Figure 5.39. Samplers had an inside clearance (3.9%) and area (20.6%) ratios which were higher than that ideally required for soft to medium clays. Sample length was typically 45 cm. Some of the tube tails had bezel edges protruding inside the sampler close to the fixing holes. This caused two of the samples (I and V) to be

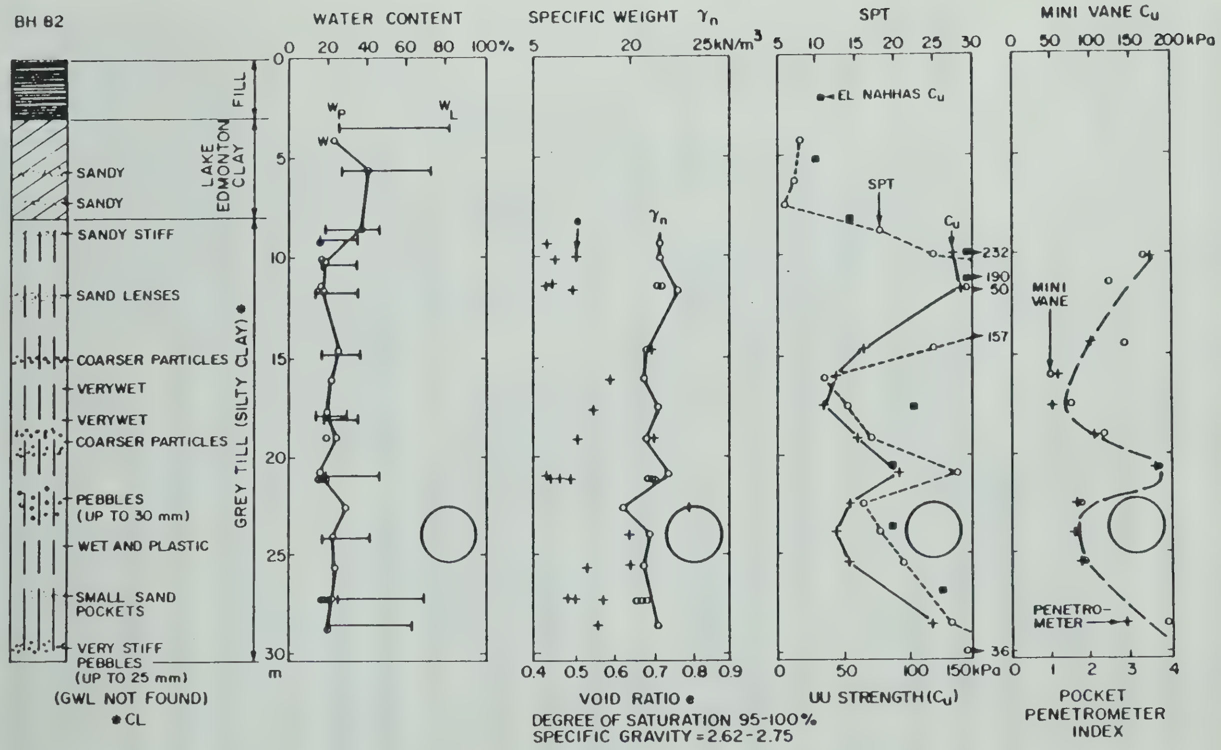

Figure 5.37 Geotechnical Profile at the Instrumented Section 3 of Edmonton Experimental Tunnel

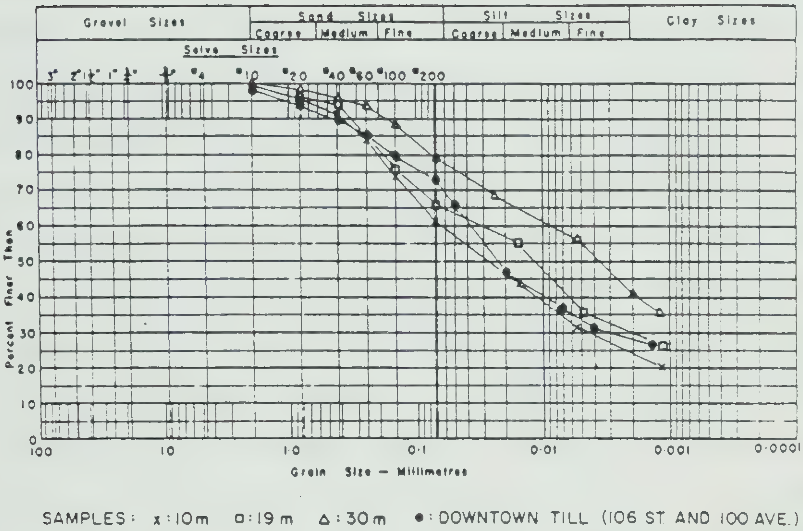

Figure 5.38 Grain Size Distributions

severely disturbed during extrusion. Therefore, it was decided to extrude the remaining samples against the driving direction, (as opposed to the recommended practice). The quality of these samples is regarded as low, and an unknown amount of disturbance would be inherent in the sampling and extruding operations.

Despite this, unconfined undrained tests, mini-vane tests and pocket penetrometer indices indicated trends of undrained strength variation with depth closely resembling that given by the SPT blow counts. Figure 5.37 includes data gathered earlier by El-Nahhas (1981), as well as from the instrumented Section 3. The relatively higher undrained strengths from the El-Nahhas data could be explained by the larger sample size (4") used or by a better quality sampling. Even so, one notes that from 9 to 15 m depth, which roughly corresponds to the very upper portion of the till, the soil strength is considerably higher than at other depths.

Laboratory Testing

Figure 5.39 also furnishes the types of laboratory tests carried out on the shelby samples. Except for the oedometer consolidation tests, conducted on 63 mm diameter samples, all triaxial tests were conducted on 70 mm diameter samples. Figure 5.40 and Table 5.20 furnish the results of some oedometer consolidation tests. The maximum past consolidation stresses at three depths were estimated according to Casagrande's method. As shown in Table 5.20,

Sample	Depth (m)	Compression Index C_c	Initial Void Ratio	Maximum Post Consolidation Stress (kPa)	OCR
II	10.0	0.164	0.50	280	1.33
VII	19.0	0.176	0.60	160	0.26?
XI	25.5	0.194	0.60	300	0.56?

Table 5.20 Results of Oedometer Consolidation Tests on Till for Edmonton Experimental Tunnel

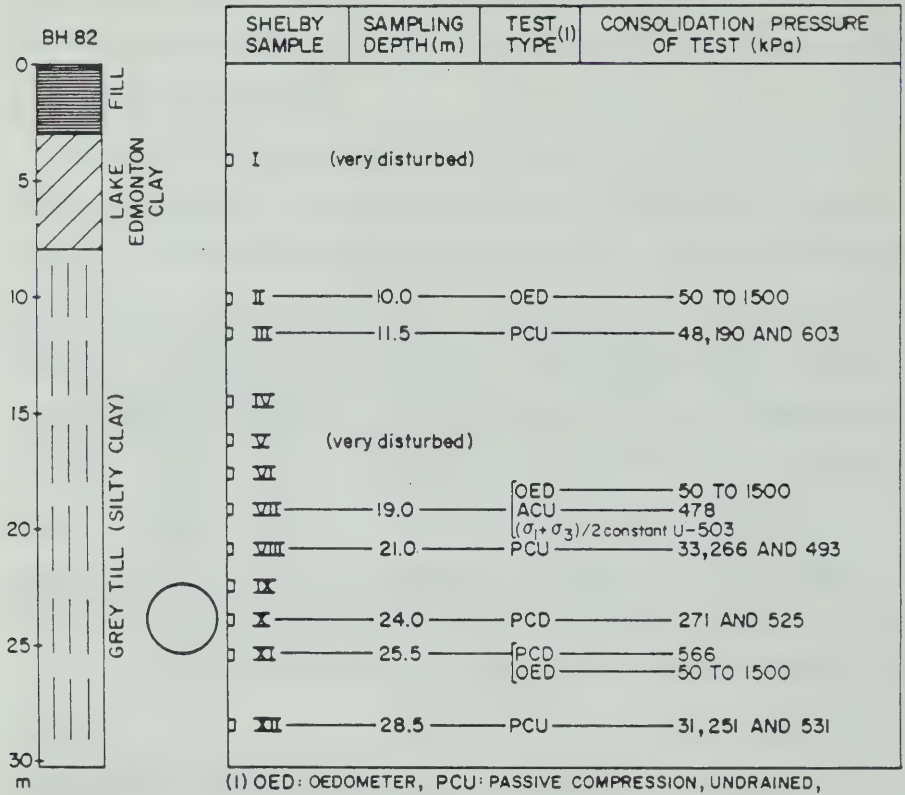

SHELBY SAMPLE	SAMPLING DEPTH (m)	TEST TYPE(1)	CONSOLIDATION PRESSURE OF TEST (kPa)
I	(very disturbed)		
II	10.0	OED	50 TO 1500
III	11.5	PCU	48, 190 AND 603
IV			
V	(very disturbed)		
VI			
VII	19.0	OED ACU $(\sigma_1+\sigma_3)/2$ constant U	50 TO 1500 478 503
VIII	21.0	PCU	33, 266 AND 493
IX			
X	24.0	PCD	271 AND 525
XI	25.5	PCD OED	566 50 TO 1500
XII	28.5	PCU	31, 251 AND 531

(1) OED: OEDOMETER, PCU: PASSIVE COMPRESSION, UNDRAINED,
ACU: ACTIVE COMPRESSION, UNDRAINED,
PCD: PASSIVE COMPRESSION, DRAINED.
TRIAXIAL TEST SAMPLES 10 cm HIGH AND 7 cm DIAMETER, ALL WITH BACKPRESSURE.

Figure 5.39 Location of Shelby Sampling and Types of Test in Edmonton Experimental Tunnel

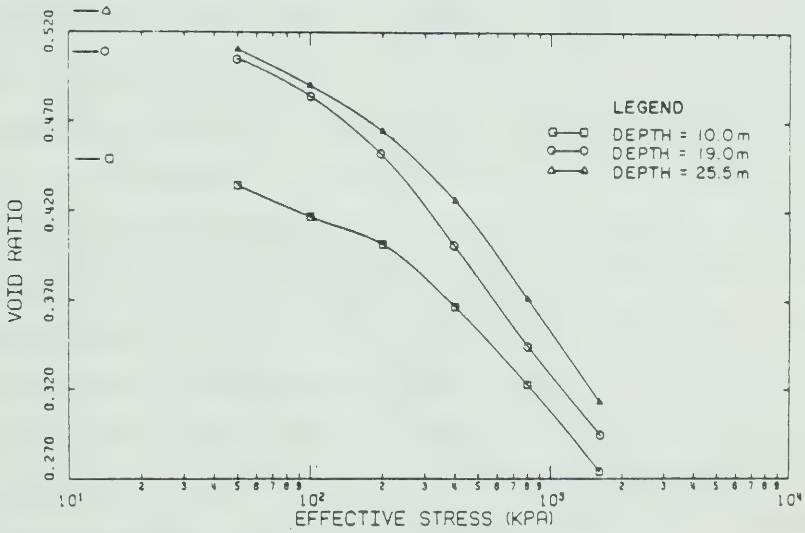

Figure 5.40 Void Ratio - Effective Stress Curves from Oedometer Tests for Edmonton Experimental Tunnel Through Till

sample II which was collected in the upper part of the grey till, is more consolidated than the deeper samples and confirms the higher strength detected in this horizon. The calculated overconsolidation ratios of the deeper samples were less than unity.

The apparent 'underconsolidated' nature of the lower samples could be attributed to localized arching of discrete zones within the till mass. In other words, the stress field would not be simply geostatic, where the vertical stress is equal to the overburden pressure. Wittebolle (1987) suggested that this process could be associated with differential thawing after the till was laid down. The distorted profile of the till surface between stations 450 and 750 m as shown in Figure 5.36, resembles a subsidence trough with a maximum distortion of about 1:20. This could be interpreted as an indication that some arching mechanism might have occurred when ice rich soils which possibly existed in the area, melted out. These zones arch against adjacent soil which act as buttresses. As a result, the ice rich soils would have been later consolidated under vertical stresses lower than the overburden. If this mechanism were correct, one would expect horizontal stresses and K_o values for these soils to be higher than those occurring for normally consolidated state under overburden loads. It is not clear however, if this proposed mechanism could explain the existence of the stiffer upper layer of till which is a feature that seems to be always associated with the softer till lying underneath (see, for instance, Thomson et.al., 1982:179).

On the other hand sampling disturbance effects could also explain, at least in part, the low maximum past consolidation stresses found at depth. Since no definite information is currently available regarding the actual stress field in the area, it will be assumed that the deeper soil samples are normally consolidated under the overburden stress and that the upper layer is lightly overconsolidated.

The coefficient of consolidation of the softer till was found to be 4 to 20 x $10^{-5}cm^2/s$. It will be later shown that even when the higher value of c_v is considered and applying the tentative criteria proposed in Chapter 3, the consolidation in the till induced by the tunnel excavation was probably negligible for several months after the TBM passed the section. Naturally, this is strongly dependent on the assumptions used to develop the simplified criteria, one of which is the soil is fully saturated.

It was decided to conduct both drained and undrained triaxial tests in an attempt to bound the observed field performance. This approach +as used by Chang and Duncan (1970:1674) to calculate the response of a 60 m deep open excavation for a pumping plant in California. Isotropically consolidated undrained tests, however, have been preferred in this study, rather than the unconsolidated tests favoured by Chang and Duncan (Op.cit.). This preference reflects an attempt to minimize the recognized sample disturbance. All

70 mm diameter triaxial test samples had a height to diameter ratio of 1.2 to 1.5 and were loaded with free ends at the top and bottom platens. This follows successful testing experience on glacial tills by Wittebolle (1983:47). All samples in the undrained and drained tests were saturated with back pressures ranging from 400 to 530 kPa. Saturation control, consolidation and strain controlled loading followed the procedures established by Wittebolle (1983:49, 147).

The testing program was set up to provide the required parameters for the hyperbolic model. Accordingly, a suite of passive compression tests (σ_3 constant, σ_1 increasing), both undrained and drained, were carried out. Twelve tests were performed (9 undrained and 3 drained) at the effective consolidation pressures given in Figure 5.39. The results obtained are shown in Figures 5.41 to 5.44. The drained tests showed contraction during loading. The initial sample volumes, after the consolidation stage are indicated in Figure 5.41. Bedding errors were observed in some of the undrained tests which resulted from an initial lack of fit between the sample surface and the lubricated platen. These errors had to be taken into account when the hyperbolic parameters were being obtained. As anticapted, the samples at 11.5 m depth, which is roughly at the midheight of the "stiffer" upper portion of the soft till, showed higher stiffness and strength than the samples below. Unfortunately in one of the tests at this depth, part of the data was lost due to malfunction of the recording system. Most of the samples at all depths considered showed positive pore pressure changes. One exception was the sample at 28.5 m depth, consolidated at 31 kPa (Figure 5.43), where a slight negative trend was noted. This could indicate that, despite sampling disturbance, this sample behaved as an overconsolidated material when reconsolidated in the laboratory at a low effective stress. A similar response was noted in the 11.5 m depth sample under low consolidation stress. All other samples reacted as normally consolidated soils under the test consolidation stress.

Hyperbolic Model Parameters

Using the procedure shown in Figure 5.10 and the recommendations by Duncan et.al. (1980:22), the basic parameters of individually fitted hyperbolae were obtained and are shown in Table 5.21. While the failure ratio result was expected, i.e., being independent of the confining effective stress, the initial tangent modulus was not. Figure 5.45 shows the relation between these two variables, normalized to atmospheric pressure. Two distinct variations of the undrained modulus with confining stress are proposed, one for the stiffer portion of the till (points 1 and 3 - refer to Table 5.21), and one for the softer layer underneath (points 4, 5, 6 and 8). Some of the samples were tested under a confining stress much less than the overburden stress (nominal OCR much greater than unity). Thus, a non-linear modulus-confining stress logarithimic

No.	Depth (m)	Type[1]	σ'_3 Conf. (kPa)	OCR[2]	σ'_3/p_a	R_f	E_i/p_a
1	11.5	Undrained	47.81	5.05	0.472	0.70	78.95
2	11.5	Undrained	189.93	1.27	1.874	-	-(3)
3	11.5	Undrained	602.99	1.00	5.951	0.86	724.06
4	21.0	Undrained	32.50	13.57	0.321	0.98	27.41
5	21.0	Undrained	265.72	1.66	2.622	0.91	217.61
6	21.0	Undrained	493.34	1.0	4.869	0.94	379.6
7	28.5	Undrained	31.21	19.18	0.308	0.96	170.2
8	28.5	Undrained	251.00	2.38	2.477	0.90	180.75
9	28.5	Undrained	530.85	1.13	5.239	0.90	343.87
10	24.0	Drained	270.99	1.86	2.674	0.90	186.20
11	24.0	Drained	524.73	1.00	5.179	0.90	290.27
12	25.5	Drained	566.10	1.00	5.590	0.89	215.28

Notes: (1) Passsive compression tests only.
(2) Nominal value assuming the soil normally consolidated under the overburden stress.
(3) Early portion of stress strain curve was lost.

Table 5.21 Parameters of Fitted Hyperbolae for Softer Till

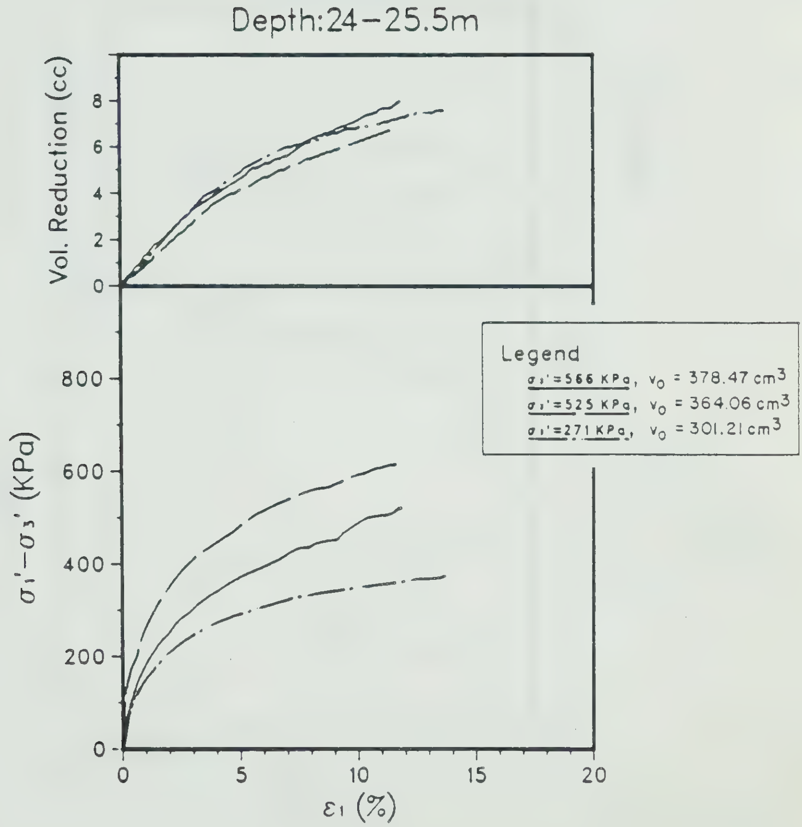

Figure 5.41 Drained Passive Compression Tests in Softer Till (24 - 25 m depth)

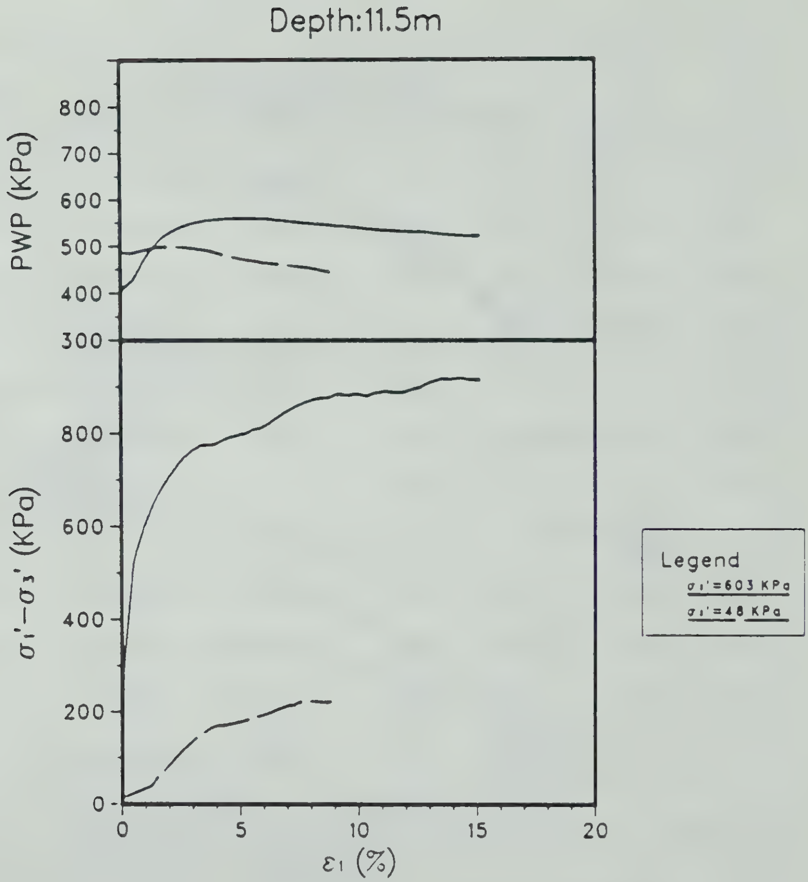

Figure 5.42 Consolidated Undrained Passive Compression Tests in Softer Till (11.5 m depth)

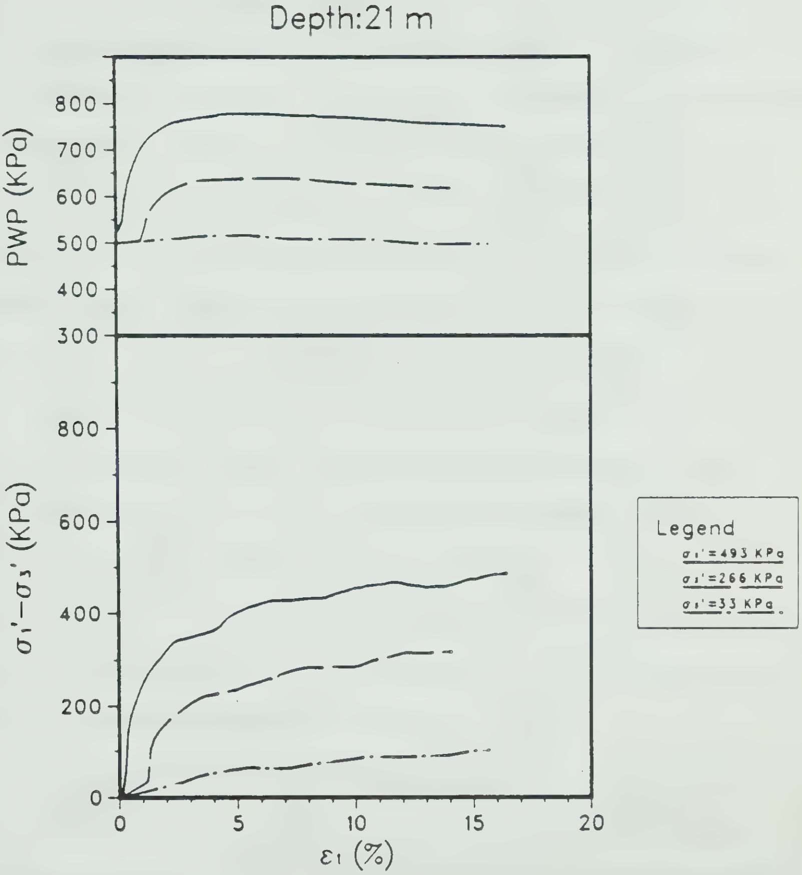

Figure 5.43 Consolidated Undrained Passive Compression Tests in Softer Till (21.0 m depth)

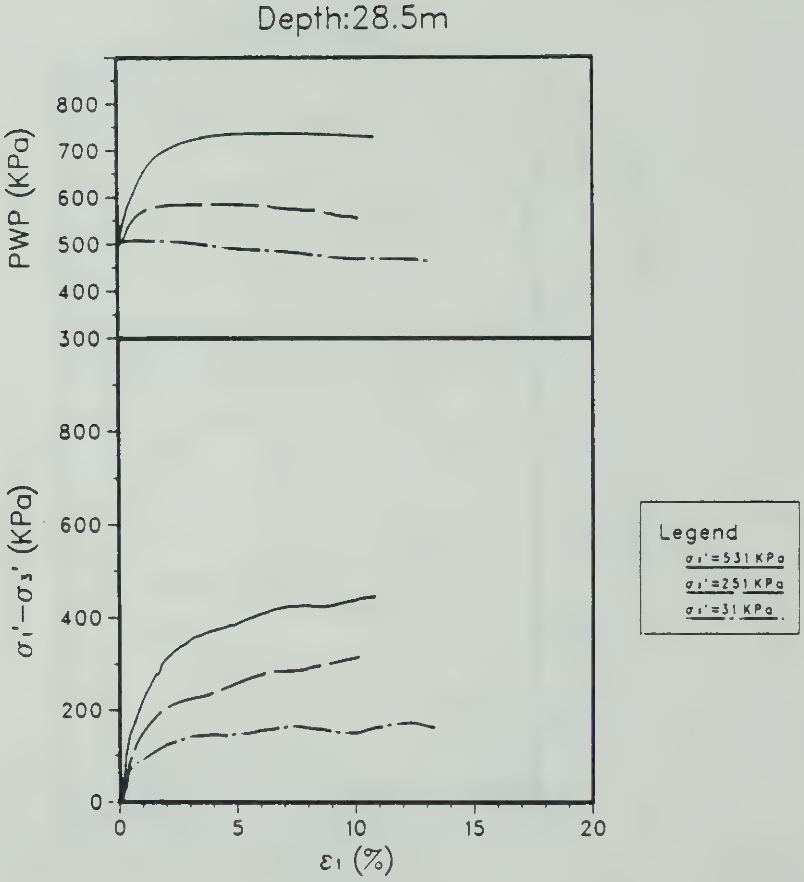

Figure 5.44 Consolidated Undrained Passive Compression Tests in Softer Till (28.5 m depth)

relationship was initially anticipated, as it was recognized that this relation would also depend on the maximum past consolidation stress. This feature, noted by Janbu (1963:21) when investigating the compressibility of natural deposits, was not clearly detected in the present case. A possible exception refers to point 7 in Figure 5.45 which corresponds both to the deepest sample collected and the minimum confining stress used. In this case, a modulus higher than that given by the linear relationship shown in the figure was obtained. This could indicate that the stiffness of this sample is controlled by a maximum past consolidation stress which was higher than the test confining stress. Excluding this point, a modulus number and a modulus exponent were found for the softer till for undrained and drained conditions. For the stiffer layer, a dimensionless initial tangent modulus of 345 (i.e. an elastic modulus of 35 MPa) was found for the average in situ stress at the midheight of the layer (12.35 m depth).

As the deviator stress did not level off or decrease in most tests, failure was defined in terms of the maximum principal stress ratio. This criterion was also favoured by Wittebolle (1983:50) when investigating other tills. As shown in Figure 5.46, two failure lines can be drawn, one for the stiffer and one for the softer till layers which allow the effective stress strength parameters (c', ϕ') to be defined. Similarly, total stress parameters (c, ϕ) can be defined, as shown in Figure 5.47. Despite knowing that the

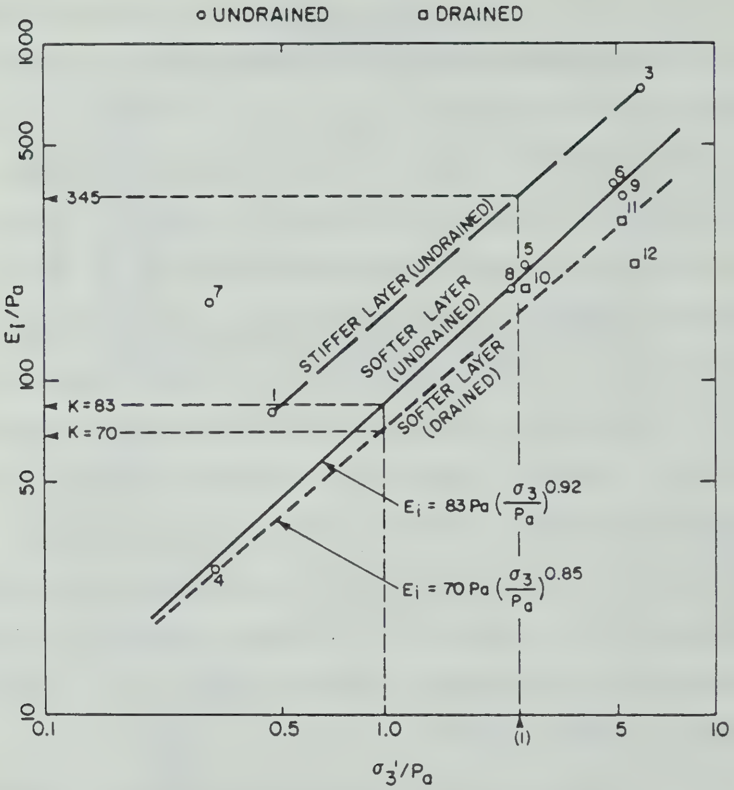

NOTES:

1. AVERAGE IN SITU STRESS AT THE MIDHEIGHT OF THE STIFFER LAYER EQUAL TO 2.56.
2. SEE TABLE 5.21 FOR TEST NUMBER IDENTIFICATION.

Figure 5.45 Variation of Initial Tangent Modulus with Confining Pressure for Till in Edmonton Experimental Tunnel

latter are arbitrary, since they are strongly path dependent, they are needed for an undrained analysis which is discussed later.

The failure ratios shown in Table 5.21 were calculated assuming a deviator stress at failure equal to the maximum observed during the test. As noted, this implied taking the deviator stress at the end of the test, as the stress difference did not level off or decrease. Despite this approximation, the failure ratios were usually greater than 0.90. Perhaps a better estimate of R_F would be a value closer to one. This implies that failure occurs at very high strains, as may have been the case in most samples.

Regarding the in situ stress condition, the coefficient of earth pressure at rest can be estimated from the Mayne and Kulhawy (1982:803) empirical expression. For a friction angle of 22° and an overconsolidation ratio possibly varying between 1 and 2, K_o should range between 0.6 and 0.8. On the other hand, El-Nahhas (1980:195) suggested that K_o should vary between 0.8 and 1.0 in this case, according to his interpretations of the observed ground response to tunnelling. For the present study, K_o was considered to vary from 0.5 to 1.0. It will be shown later that from the best fit analyses, K_o was found to lie between 0.8 and 0.9.

Figure 5.48 furnishes the variations of initial tangent modulus with depth, as given by the hyperbolic model formulation (Figure 5.11), for the most probable in situ stress conditions in both drained and undrained situations.

They were obtained from the data shown in Figures 5.45 to 5.47, and correspond to the analysis that provided the best fit of field performance. Note that the stiffer grey till horizon was represented by a linear elastic material with constant properties (E=35 MPa). The soil below and above this layer was represented by a single non-linear elastic material. Its undrained hyperbolic parameters are K=83, n=0.92, ϕ=16°, c=45 kPa and R_f=1. The drained parameters are K=70, n=0.85, ϕ'=22°, c'=30 kPa and R_f =1.0. The soil was assumed to be fully saturated, with γ = 20 kN/m^3, but with zero in situ pore pressure and K_o between 0.8 and 0.9.

Although the parameters above were obtained for the grey till, the resulting in situ modulus for the upper part of the profile shown in Figure 5.48 could well represent that of the Lake Edmonton Clay. This clay was found to have pressuremeter moduli varying between 6 and 15 MPa as reported in the LRT tunnel case (see Table 5.15 and Figure 5.25). These values agree well with the proposed E modulus profiles given in Figure 5.48.

Also shown in Figure 5.48 are the results of pressuremeter moduli obtained by Thomson et.al. (1982:179), in another softer till zone, found elsewhere in Edmonton (107 Str. and Jasper Ave.). It is interesting to note that fair correspondence seems to exist between the proposed in situ tangent modulus profile for the Edmonton Experimental site and the pressuremeter data. These were obtained in pre-drilled boreholes, using the same equipment and

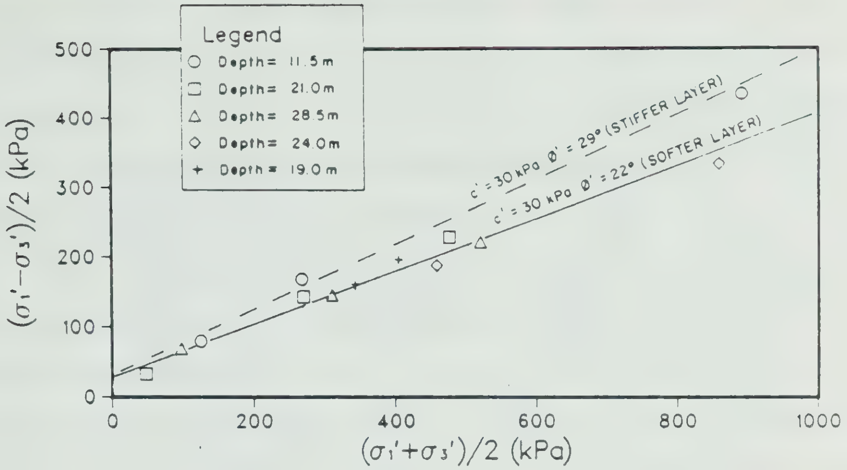

Figure 5.46 Effective Stress Strength Parameters for Till in Edmonton Experimental Tunnel

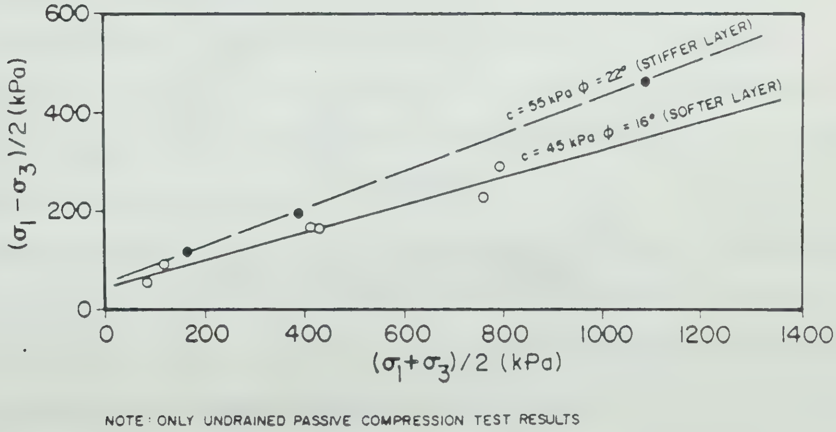

Figure 5.47 Total Stress Strength Parameters for Till in Edmonton Experimental Tunnel

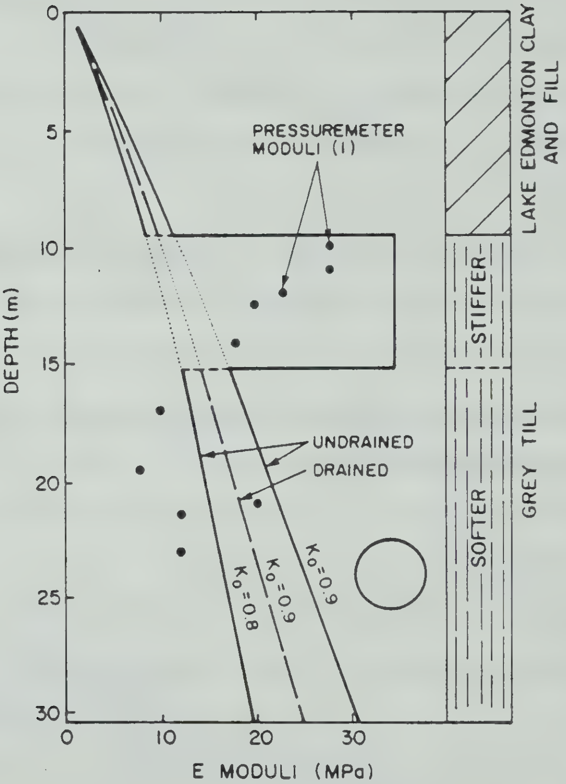

NOTE:
(1) PRESSUREMETER DATA FROM SOFT AREA AT JASPER AVE. AND 107 ST. (BH1A AND BH5A); THOMSON-ET-AL (1982 : 179)

Figure 5.48 Profile of In Situ Deformation Modulus at the Edmonton Experimental Tunnel

interpretation procedure described by Eisenstein and Morrison (1973). The correspondence applies even for the stiffer upper horizon of the till. Standard penetration test results exhibit similar trends in both sites. An explanation for the noted similarities has not been presented so far.

Stress Path and Drainage Effects

The input parameters for the numerical back analyses of this case history have been derived from conventional passive compression triaxial tests, despite the known dependency of the stress-strain relationship on stress path. Medeiros and Eisenstein (1983) showed that the stress path effect is well pronounced on the drained behaviour of Edmonton till. This dependency should be less pronounced in undrained loading, as the effective stress path of the saturated soil is less affected by the type of undrained shearing to which it is subjected. To illustrate this point, two additional undrained triaxial tests were performed on a sample collected at 19 m depth. In both tests, the till was consolidated by an isotropic confining stress of about 500 kPa. The testing procedure was the same as in the other tests including the strain rate, but the shear loading paths were different. In the first test, the soil was brought to failure by proportionally increasing the axial stress and decreasing the radial stress, so as to maintain a constant average total stress, $(\sigma_1 + \sigma_3)/2$. In the second test, the till was subjected to an active compression test, by keeping the axial stress constant and reducing the radial stress.

The results of these two tests are shown in Figure 5.49 and 5.50.

The stress-strain curves of these two tests are superimposed in Figure 5.51, together with those from two passive compression tests, one undrained and another drained. Both were consolidated to confining stresses close to 500 kPa, but the tests were conducted on samples collected at slightly different depths (see Figures 5.42 and 5.44). The solid lines shown in Figure 5.51 represent best fit hyperbolae to each test curve. The parameters for each fitted hyperbola are given in Table 5.22. From these, the variations of the tangent modulus with the axial strains can be obtained, as shown in Figure 5.52. Note that due to the particular total stress paths used and due to the fact that the soil is saturated, the Young's modulus in each case is equal to the slope of the deviator stress-axial strain curve. As is seen in Figure 5.52, differences are noted in the undrained modulus variation with strain, but they are appreciably less than that observed for drained moduli (see Medeiros and Eisenstein, 1983:126). The differences can be attributed to the unequal consolidation stresses used, to differences in the inital water content (or void ratio) of each sample, collected at slightly different depths, differences in the past stress histories as well as soil inhomogeneities or anisotropies. Apart from these, differences due to inaccuracies in fitting the curves by hyperbolae should also be considered. An entirely different

Type of Test	Sample Depth (m)	Conf. Stress (kPa)	a (10^{-5}kPa^{-1})	b (10^{-5}kPa^{-1})	$E_i = 1/a$ (MPa)	$(\sigma_1-\sigma_3)_u=1/b$ (kPa)
A. Passive Compression, Drained	24.0	525	2.72	146.0	36.76	685
B. Passive Compression, Undrained	21.0	493	1.85	213.8	54.05	468
C. Constant $(\sigma_1+\sigma_3)/2$ Test, Undrained	19.0	503	1.70	294.4	58.82	340
D. Active Compression, Undrained	19.0	478	1.35	245.8	74.07	407

Notes: (1) Hyperbola: $\sigma_1 - \sigma_3 = \varepsilon_1/(a + b\varepsilon_1)$; $E_t = a/(a + b\varepsilon_1)^2$

(2) Confining stress always greater than overburden stress.

Table 5.22 Parameters of Hyperbolae Fitted to Stress-Strain Curves of Till, Tested under Distinct Total Stress Paths and Drainage Conditions

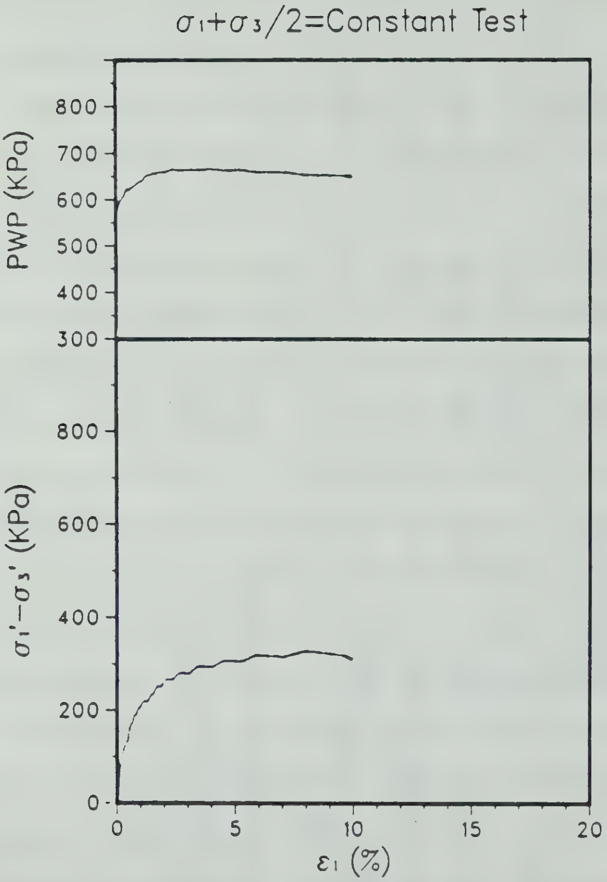

Figure 5.49 Consolidated Undrained Compression Test in Softer Till with Constant Average Stress

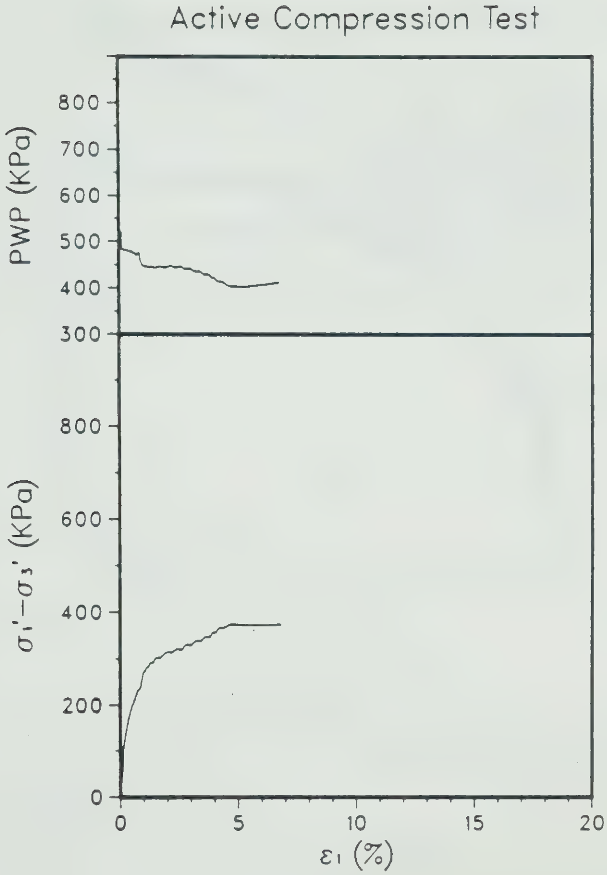

Figure 5.50 Consolidated Undrained Active Compression Test in Softer Till

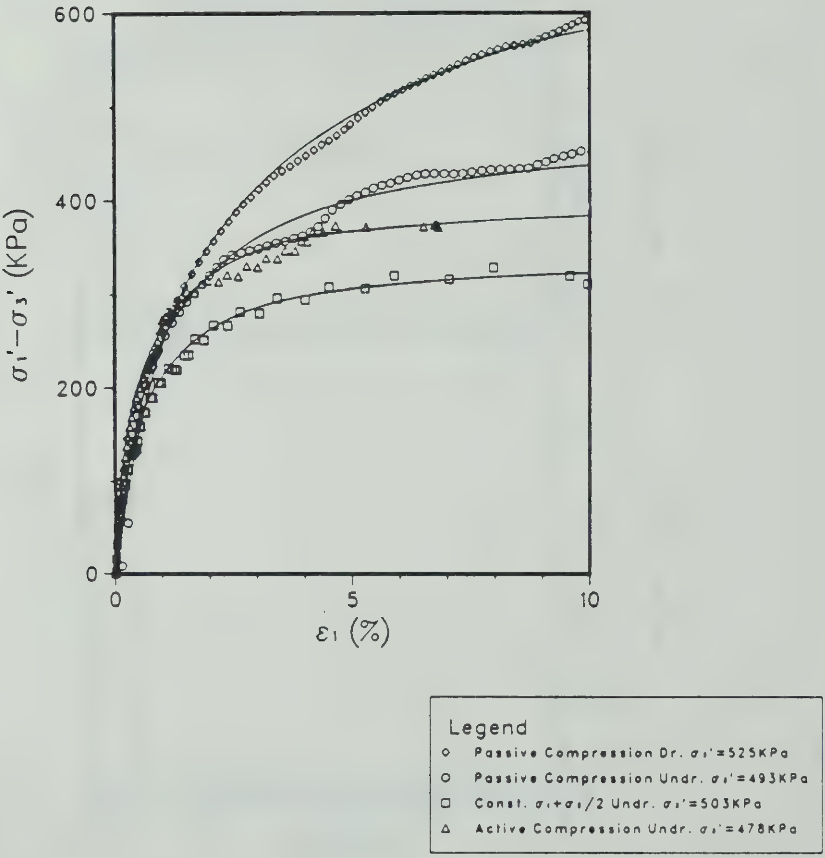

Figure 5.51 Stress-Strain Curves of Softer Till Tested under Distinct Total Stress Paths and Distinct Drainage Conditions

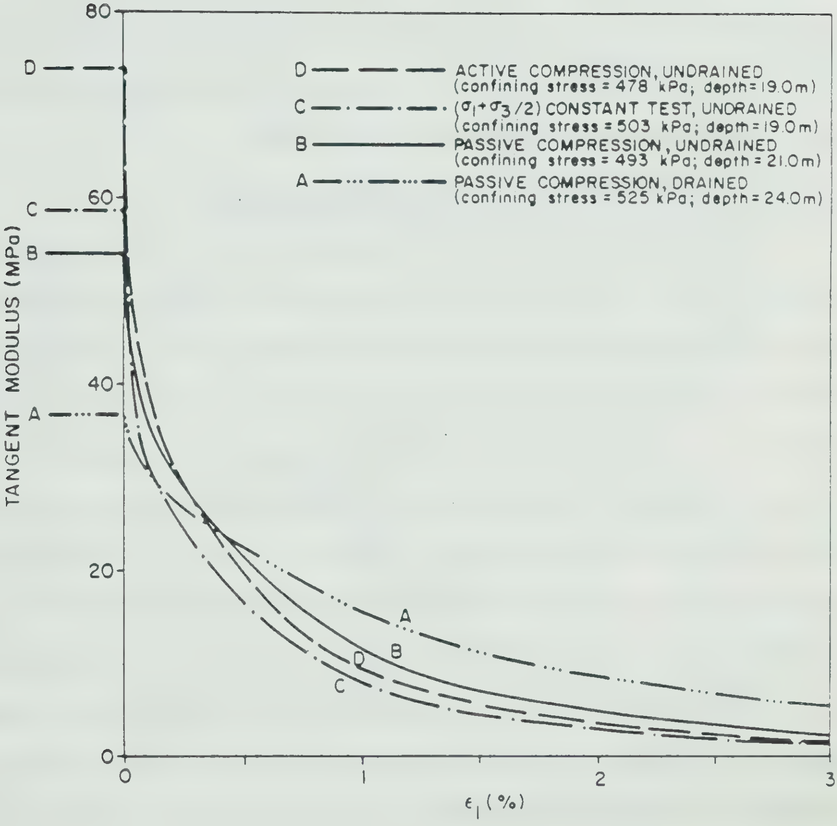

Figure 5.52 Tangent Moduli of Deformation of Till in Edmonton Experimental Tunnel for Distinct Total Stress Paths and Drainage Conditions

modulus variation is noted, however, for the drained test. As indicated earlier, the larger difference here is attributed to the very different effective stress path followed in this case. It is observed in Figure 5.53 that, despite the very distinct total stress paths in the undrained tests, their resulting effective stress paths are not entirely dissimilar, but they are very different from that corresponding to the drained test.

Tunnel Construction and Field Monitoring

Tunnel construction was carried out with a full face cutting wheel TBM (a Lovat M-100 Series 1900), whose details are given in Figure 5.54. The TBM body is 5.96 m long and the cutting profile 2.56 m diameter (including overcutting). Similar to the TBM used at the LRT tunnel, the soil at the face is indented and scraped by staggered teeth, protruding outwardly and fixed at three spokes. The soil is thus cut at the heading in a near vertical face which is left virtually unsupported. A detailed account of the tunnel construction was given by El-Nahhas (1980:60). The lining system used is shown in Figure 5.54. Each support ring, one metre wide, consisted of four trapezoidal precast concrete segments. Each segment was provided with a longitudinal stress raiser which locally reduces the segment thickness from 11 cm to 7 cm. These stress raisers are designed to act as a section of low moment resistance, ideally increasing the lining flexibility. The segments were lightly reinforced with steel mesh at the mid-section. Every ring was expanded radially to

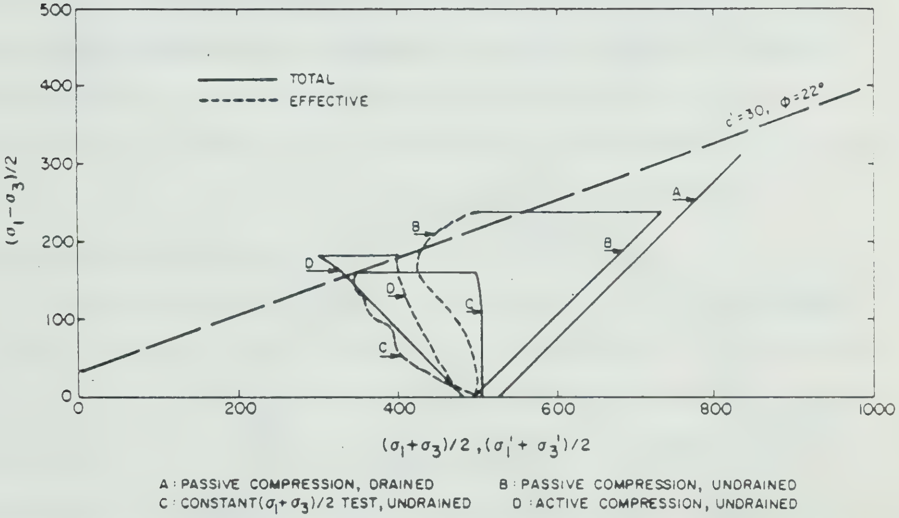

Figure 5.53 Stress Paths of Triaxial Tests on Till in Edmonton Experimental Tunnel

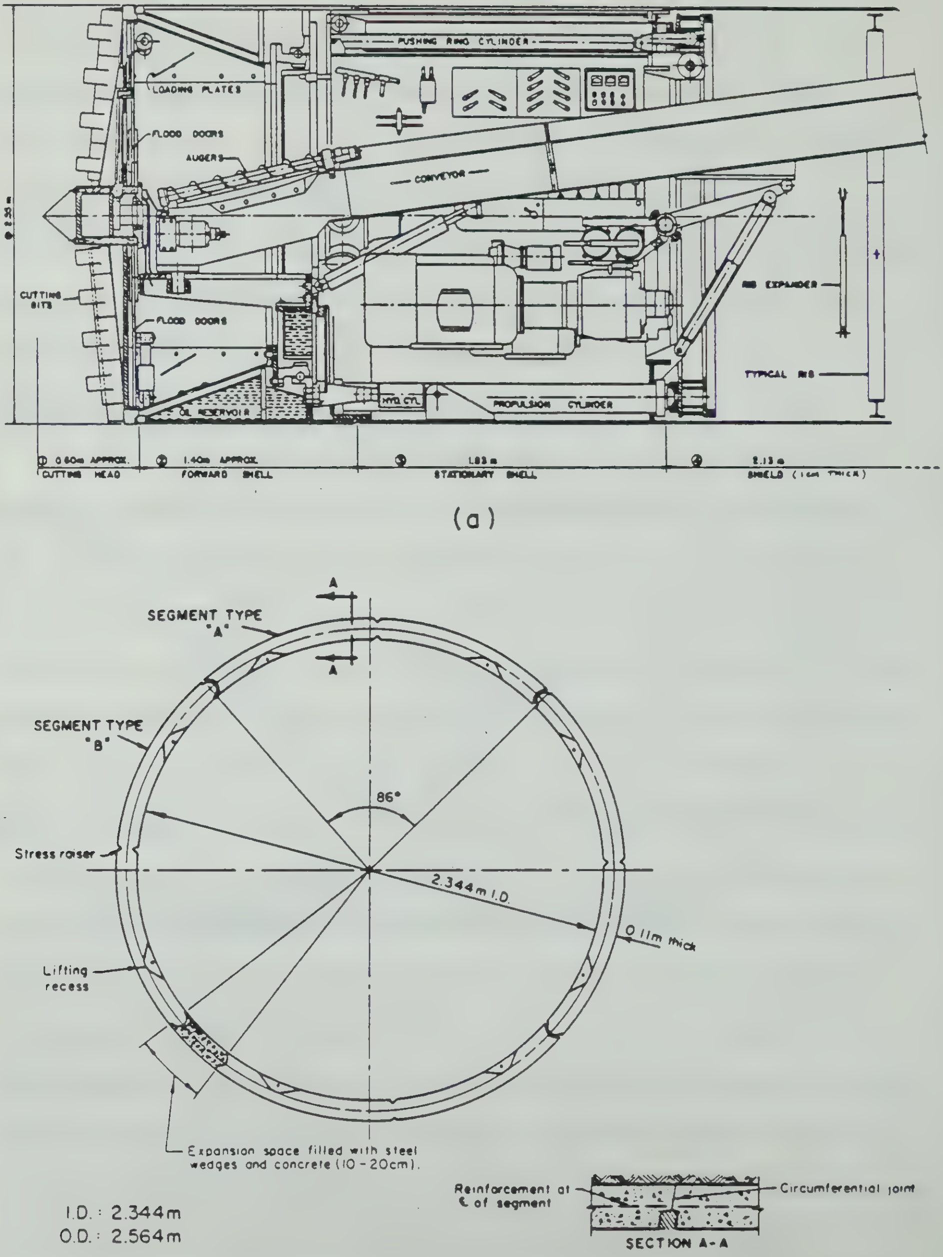

(a)

(b)

Figure 5.54 TBM and Lining System used at the Edmonton Experimental Tunnel (after El-Nahhas:1980:modified)

the excavated surface of the soil, as soon as the shield had advanced beyond that ring. Therefore, the maximum distance between the tunnel face and a fully expanded ring was about 7 m. The average construction rate within the instrumented section was 12.8 m/working day.

The field instrumentation included surface and subsurface settlement monitoring, slope indicator readings, load cell measurements at the lower tangential joints, a few surface and embedded vibrating wire concrete strain gauges (in instrumented section 2 only), tape extensometer measurements for the lining convergence, and levelling of one point on the lining. A detailed account of this field monitoring program is presented by El-Nahhas (1980).

Numerical Simulation

For the numerical back-analyis of this tunnel three finite element meshes were tested beforehand with variable element densities and widths. The maximum surface distortion seemed sensitive to the element density near the ground surface. The use of a slightly narrower mesh was favoured, but with a higher density of elements. This mesh included 388 nodes and 709 elements. The entire ground mass was modelled with properties representing the softer till, except for a 5.7 m thick layer located at 9.5 m below the surface, to which properties representing the stiff till layer was assigned. Figure 5.55 shows the assumptions that were made and the values of the soil parameters that were adopted and kept constant in all numerical analyses. A lower rigid boundary was assumed to exist at 32.42 m below surface.

Both ground instrumentation and lining load monitoring showed some minor but obvious time dependent component. The major part of the ground response in terms of displacements and load magnitudes, developed within 7 days after the TBM face passed the instrumented section. More than two months later the readings had not stabilized, although the increments over that period of time were not very large compared to the recorded "short-term" variations. The time dependent changes were slightly more pronounced in the lining loads. Despite the fact that the ground water level was located well below the tunnel, the grey till was literally saturated throughout its thickness. The observed time dependent responses could thus be attributed to induced pore pressure changes.

One may take as a reference, a liberal value of 10^{-3} cm^2/s for the coefficient of consolidation of the ground mass. This is five times larger than the maximum value found in the laboratory samples, and reflects the effect of macrostructural features in the soil mass that tend to accelerate the process of pore pressure equalization. Again, the approximate criteria shown in Chapter 3 proposed for the identification of the type of ground response, may be used. As noted above, the "immediate" soil movements or lining load build up took place within about one week after the TBM passed the instrumented section. Despite attempts to make it

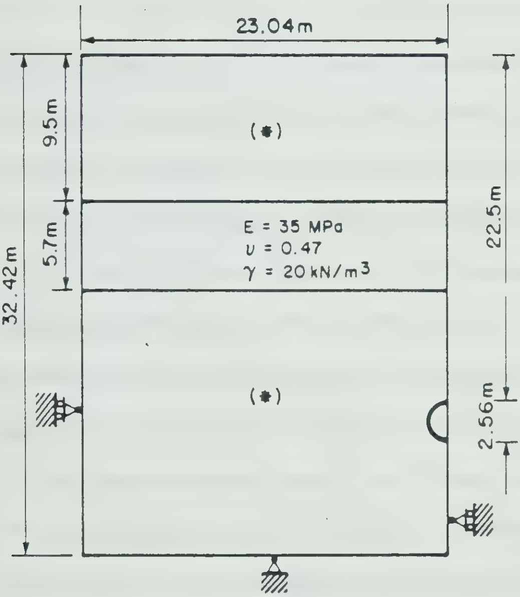

(*)

Parameters	Undrained	Drained
K	83	70
n	0.92	0.85
ϕ(°)	16	22
c (kPa)	45	30
R_f	1	1
υ	0.47	0.3
γ (kN/m^3)	20	20

Figure 5.55 Assumptions and Fixed Parameters for the Edmonton Experimental Tunnel Back Analyses

water tight, the segmented lining can be assumed to be fully permeable relative to the the soil. But even if it were not and if the tunnel were supposed to be ideally deep, Figure 3.22 indicates that for a period of time of one week after excavation, "negligible" consolidation may have developed. After two months, the consolidation process is incomplete which is confirmed by the field readings not being stabilized.

If the lining is assumed to be fully permeable (Figure 3.23), then for a till cover of 13 m and taking into account the presence of a continuous sand layer covering the till (actually undetected in BH 82), after one week or one month the consolidation process is virtually negligible.

From this simplified analysis, the ground response, particularly that observed up to a week after the TBM passed the instrumented section, was close to undrained. It was decided to perform both undrained and drained analyses, in order to bound the observed behaviour which may have actually been partly drained over the monitoring period. This would be a reasonable approximation if the soil behaviour was non-linear elastic. In reality, plastic strains may develop during the undrained loading of the soil, especially if failure or plastic yielding is locally induced. Hence, the final strains in the undrained case can be larger than those in a drained situation, in which local failure is less likely to occur. This type of path-dependence of strains is not accounted for in the numerical model being used.

An additional approximation refers to the way in which the undrained analyses were undertaken. Strictly speaking, an undrained analysis would imply $\phi=0$ and a constant strength c_u, for a soil element consolidated at a certain in situ stress level. Total stress changes produced by the undrained tunnelling operation would not cause changes in the undrained strength. Correspondingly, the numerical analysis would have to assign a certain strength c_u for each point of the soil mass, consolidated to a distinct mean effective stress. The present finite element code was developed mainly to portray time independent responses under drained conditions, making allowance for a single non-linear elastic material to be represented. If an adequate representation of an undrained response were to be made, then a very large number of non-linear elastic materials would have to be considered. One would be required for each element stress level with its associated undrained strength. Although the implementation of this feature could have been possible, it departed from the primary aim of the present study. Therefore, an approximation was favoured. This consisted of working in terms of a total stress failure envelope, defined by an undrained cohesion intercept and a friction angle (c, ϕ), obtained from the consolidated undrained passive compression tests shown in Figure 5.47. While this would give a reasonable approximation of the initial undrained strength, it would deviate from the "correct" undrained representation after a certain amount of stress release at the opening, since the current strength will change with changes in the minor principal stress. In other words, the "undrained" strength would have a frictional component depending on the "undrained" friction angle ϕ. The latter is a purely arbitrary parameter and is clearly path dependent. However, it is possible to anticipate the type of error involved in this simplification. Whenever the ground undergoes a decrease in the minor principal stress (for example, at points beside the springline region for $K_o<1$), the soil strength will be underestimated. It will be overestimated at points experiencing an increase in the minor principal stress (crown and floor regions, if $K_o<1$).

The relative stiffness of the segmented lining used can be estimated through the Einstein and Schwartz (1979) definitions. For the dimensions given in Figure 5.54, assuming a Young's modulus of 25.1 GPa (El Nahhas, 1980:166) and a Poisson's ratio of 0.2 for the concrete, and for an average soil modulus of 20 MPa and a Poisson's ratio of 0.47, the stiffness ratios can be calculated. The effect of the four joints and of the four stress raisers can be taken into account using Muir Wood's (1975:126) approximation (see Section 5.2.2.1). Assuming the 8 joints and stress raisers to be perfectly articulated, the equivalent moment of inertia of a continuous ring would be one fourth of the actual lining segment. The compressibility and flexibility ratios are equal to 0.011 and 65.408 respectively. In the numerical analyis, an equivalent liner of 0.32 m is used. To approximate the stiffness ratios, the equivalent lining would have to have a modulus of 0.19 GPa or 7.7 GPa, to equal either one or the other ratio. Accordingly, in the back analysis, the lining modulus was allowed to vary within those limits. As in the other two tunnel cases, the best agreement to observed performance was noted when the flexibility ratio of the equivalent lining was close to the "actual" value.

The only soil parameter allowed to vary in the back analyses was K_o (from 0.7 to 1.0). The remaining solution parameter that was allowed to vary was the amount of stress release prior to the lining activation. An interpretation of field measurements, followed by preliminary computer runs, suggested that it would be sufficient to vary this amount of stress release from about 50 to 70%. These initial runs indicated also that five equal load increments, for each simulation phase (10 unloading steps altogether) would yield an adequate approximation.

Table 5.23 summarizes the parameters that were varied in the analyses. Sixteen computer runs were made for the undrained analyses in order to obtain the best fit case. These corresponded to a 70% in situ stress release prior to lining activation, an equivalent lining modulus of 0.4 GPa and a K_o value of either 0.8 or 0.9. One drained analysis was performed, taking K_o equal to 0.9 after the undrained

Stress release α prior to support activation (%)	55	65	70(1)	
In situ stress ratio K_0	0.7	0.8(1)	0.9(1)	1.0
Equivalent lining E modulus (GPa)	0.1	0.4(1)	1.0	

Note: (1) Best fitted values

Table 5.23 Parameters Varied in the Edmonton Experimental Tunnel Back-Analyses

analyses were completed.

Results of the Back-Analyses

The best fit case provided a reasonably good match between calculated and observed performances before and after lining activation. The equivalent lining modulus found to fit the observed performance best furnished a flexibility ratio F equal to 30.241 which is approximately half the value theoretically estimated. In other words, the back analysed lining behaviour is stiffer than was assessed theoretically at the beginning. This could be partly attributed to assuming the lining joints and stress raisers were perfect articulations with zero moment of inertia and zero bending moments. Uncracked stress raisers in particular would carry moments. If both the joints and stress raisers had moments of inertia equal to that of the reduced concrete section in the stress raiser region (thickness equal to 7 cm), then Muir Wood's (1975:126) approximation would lead to an equivalent moment of inertia 2.03 times that calculated assuming perfect joints. The theoretical value of F for the actual lining would then be 32.21, and this is much closer to the back analysed figure. The flexural rigidity (EI) per unit length of the tunnel would then be equal to 1.41 MN.m, compared with the back analysed rigidity of 1.09 MN.m.

In the following, the comparisons between calculated and observed performances are presented and discussed. It should be noted that the measurements could represent a partial drainage condition in the field which was possibly closer to the ideally undrained situation. A complete comparison of the performance prior to lining installation was not possible. The reason for this was that the case history records (El-Nahhas, 1980) did not include an accurate account of the construction progress with time, or a precise identification of recorded readings relative to the position of the tunnel face. Unlike the previous two cases studied, only a few measurements are clearly identified as occurring just prior to lining activation. Only these were used to make a comparison for this condition. Some field data collected at instrumented Section 2 were included, although a slightly larger cover (25 m) exists, compared with Section 3 (22.5 m cover) where the back-analyses were actually applied.

In Figure 5.56, the final surface settlements transverse to the tunnel axis are compared. The measured range of settlements was that noted after the TBM cutting face had passed the section by more than 18 diameters. As is noticed, the observed maximum surface settlements are fully bounded by the approximate undrained analyses, taking K_o equal to 0.8 and 0.9. The calculated surface distortion, however, tends to be smaller than that measured. Vertical movements at the lateral boundary of the finite element mesh were not zero, indicating that the width of the mesh was too small. A much wider mesh was implemented (52 m width) and still the movements at the lateral boundary were non-zero. Moreover, both meshes produced very similar maximum surface

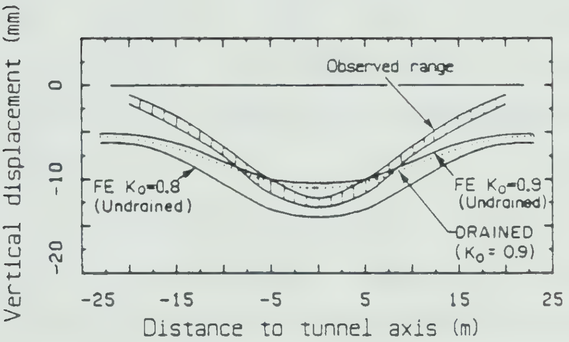

NOTES:

1. MEASUREMENTS AT POINTS 1.5 m BELOW SURFACE, AT SECTIONS 2 AND 3 (SOIL COVERS OF 25 AND 22.5 m RESPECTIVELY)
2. OBSERVED SETTLEMENTS 2 WEEKS AFTER TBM PASSED THE SECTION (TUNNEL FACE AT MORE THAN 18 DIAMETERS AHEAD)
3. CALCULATED (FE) SETTLEMENTS AT POINTS 1.9 m BELOW SURFACE
4. FIELD DATA FROM EL-NAHHAS (1980: 119 AND 125)

Figure 5.56 Measured and Calculated Settlements after Complete Passage of the TBM at the Edmonton Experimental Tunnel

distortions. The inability of the present model to simulate the observed surface distortion is not related to the boundary conditions used in the calculations but, possibly, to its inability to simulate adequately the concentration of shear strains that might have occurred in the soil. This type of problem was addressed in Section 5.2.1.2, where it was shown that it is a common feature in most finite element analyses applied to this type of problem.

The analyses with drained soil parameters furnished the settlement distribution indicated by the dotted curve (Figure 5.56). It gave a maximum "long term" settlement of only 4% larger than the corresponding "short term" value. Unfortunately "long term" readings were not available for most instruments installed. The final readings of the magnetic extensometers at Section 3 were taken almost 3 months after excavation (El-Nahhas, 1980:286). The magnets closer to the ground surface (from 2.24 to 4.19 m below it) indicated an average increase of 28% in the settlements. This is appreciably more than the drained analysis predicted. However, this discrepancy is not suprising, since plastic strains were probably induced in the ground, under the "undrained" loading. This should have led to long term ground movements larger than those given by the non-linear elastic drained analysis, as explained before.

Figures 5.57 and 5.58 compare vertical movements in the ground, along vertical lines at the tunnel centreline and about 2.5 m from it, respectively. The measurements were taken when the tunnel face was more than 20 diameters beyond the instrumented section. One notices that in both cases, the "undrained" ground movements show very good agreement both in magnitude and distribution, for the range of K_o considered. The dotted curves in both figures correspond to the analysis made with drained parameters. It furnished vertical displacements marginally larger than the corresponding undrained analysis, as noted for the surface settlements. The same comments made before regarding the influence of plastic straining in a long term situation, are also entirely applicable.

Perhaps a better view of the subsurface settlements above the tunnel is that seen in Figure 5.59. It includes measurements taken at all magnetic extensometers in Section 3, 8 days after the TBM passed it (tunnel face more than 20 diameters ahead). On the whole, good agreement between the "undrained" settlements is noticed. However, closer to the tunnel, 21.86 m below surface, the agreement is poorer.

A slope indicator located 2.33 m from the tunnel axis (SI33) had readings taken when the tunnel face was located 5 and 11 m past it. Assuming that the lining activation took place with the face 7 m ahead, it was possible to estimate by interpolation, the horizontal displacements that should have occurred at the moment the lining was expanded. A comparison between measured and calculated horizontal movements for this situation is shown in Figure 5.60. Similarly, Figure 5.61 compares measured and calculated

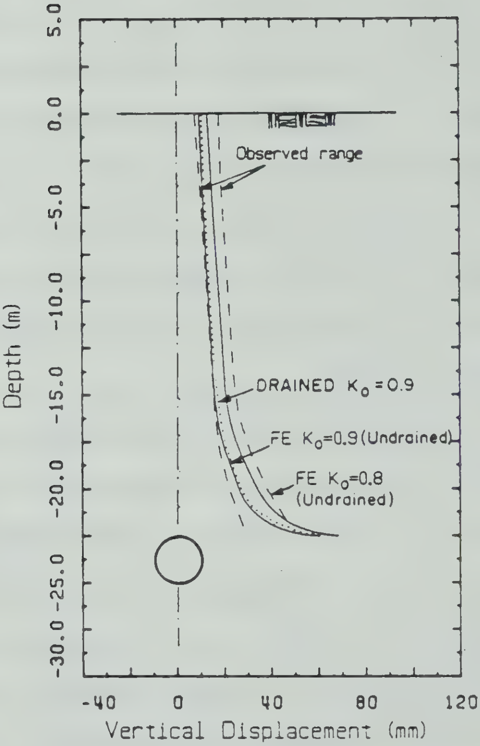

NOTES:

1. MEASUREMENTS AT SECTION 3 (MX 33, MX 38 AND SPX), ALONG TUNNEL VERTICAL AXIS.
2. MEASUREMENTS TAKEN 8 DAYS AFTER TBM PASSED THE SECTION (TUNNEL FACE AT MORE THAN 20 DIAMETERS AHEAD)
3. FIELD DATA FROM EL-NAHHAS (1980:122, 123 AND 124)

Figure 5.57 Measured and Calculated Subsurface Vertical Displacements along the Tunnel Centreline, after Complete Passage of the TBM at the Edmonton Experimental Tunnel

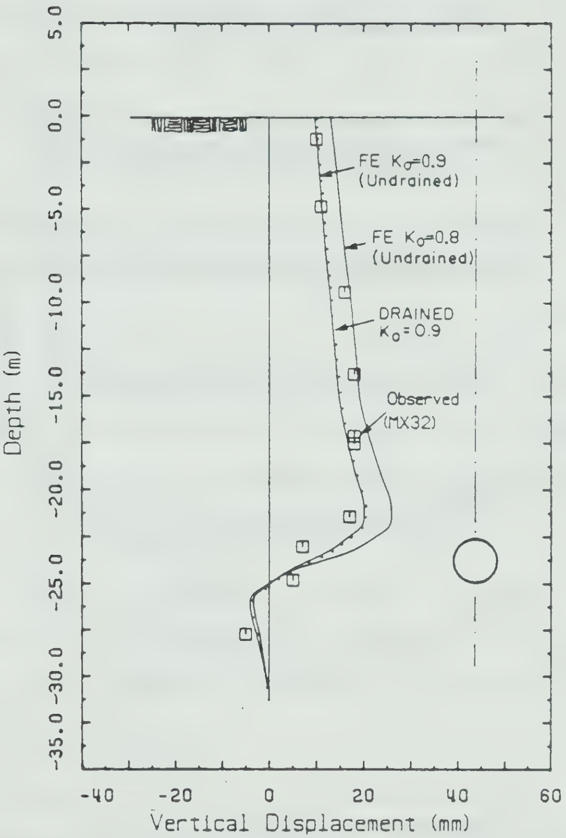

NOTES:

1. MEASUREMENTS AT MX 32 (SECTION 3) LOCATED 2.3 m FROM TUNNEL AXIS.
2. CALCULATED DISPLACEMENTS AT 2.56 m FROM TUNNEL AXIS.
3. MEASUREMENTS TAKEN 8 DAYS AFTER TBM PASSED THE SECTION (TUNNEL FACE AT MORE THAN 20 DIAMETERS AHEAD)
4. FIELD DATA FROM EL-NAHHAS (1980: 122)

Figure 5.58 Measured and Calculated Subsurface Vertical Displacements along a Vertical Line 2.5 m off the Centreline, after Complete Passage of the TBM at the Edmonton Experimental Tunnel

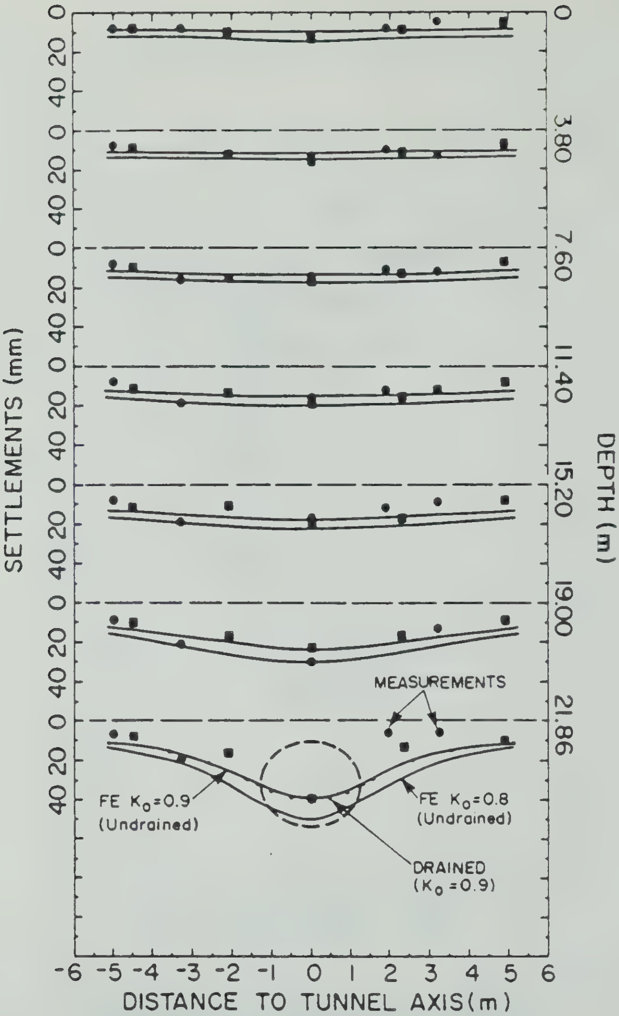

NOTES:

1. MEASUREMENTS TAKEN AT SECTION 3, 8 DAYS AFTER TBM PASSED IT(TUNNEL FACE AT MORE THAN 20 DIAMETERS AHEAD)
2. SQUARE POINTS OBTAINED FROM INTERPOLATION OF READINGS IN MX 31 TO 35 AT DEPTHS INDICATED. RING POINTS FROM MX 36 TO 310.
3. CALCULATED (FE) DISPLACEMENTS AT DEPTHS SHOWN BY DASHED LINES.
4. CALCULATED 'DRAINED' SETTLEMENTS SHOWN ONLY AT DEPTH 21.86m BY DOTTED CURVE. , AT OTHER ELEVATIONS THEY VIRTUALLY CONCIDE WITH 'UNDRAINED' SETTLEMENTS FOR $K_0 = 0.9$
5. TUNNEL CROWN AT ABOUT 22.5m DEPTH
6. ALL FIELD DATA FROM EL-NAHHAS (1980: 122 AND 123)

Figure 5.59 Measured and Calculated Subsurface Settlements after Complete Passage of the TBM, at the Edmonton Experimental Tunnel

lateral movements after the TBM had completely passed the instrumented section (tunnel face at more than 15 diameters ahead, 2 weeks after passing the section). In both cases the agreement is reasonable, especially in terms of the maximum magnitude of the horizontal movement. Above the tunnel crown elevation, the numerical model seems to underpredict the lateral movements, but the overall distributions of displacements seem to agree reasonably well.

It is believed that the load cell readings installed in Sections 2 and 3 provided the most reliable set of information regarding lining loads in this case history. The number of vibrating wire strain gauges embedded in the concrete was, perhaps, too small to allow a reliable picture of lining loads to be drawn. Therefore, only the data gathered from the segmented rings with load cells will be addressed herein. Each of these rings, with 1 m width, were instrumented with two load cells, installed at the lower longitudinal joint. This installation layout was somewhat unfortunate, since it did not allow formation of any conclusion about the distribution of thrusts around the liner. Figure 5.62 shows the measured thrusts in four instrumented rings. The cell readings included the loads due to the lining selfweight, while the finite element analysis disregards it. For a consistent comparison, the selfweight had to be excluded from the readings. Through an approximate calculation, a 5.3 KN/m reduction in the lower joint thrust was estimated, in order to obtain the thrusts due to ground

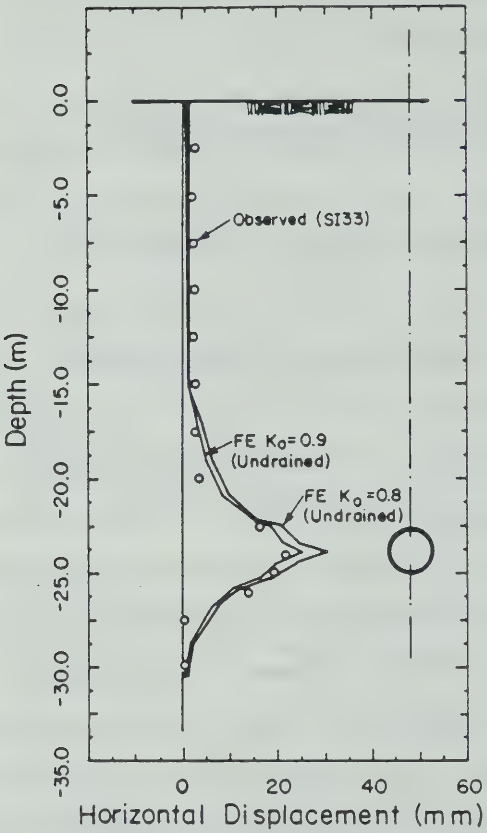

NOTES :

1. MEASUREMENTS AT SI33 (SECTION 3), 2.33m FROM TUNNEL AXIS.
2. CALCULATED DISPLACEMENTS AT 2.56 m FROM TUNNEL AXIS.
3. INTERPOLATED MEASUREMENTS FOR THE MOMENT THE LINING WAS EXPANDED (7m BEHIND TUNNEL FACE)
4. FIELD DATA FROM EL-NAHHAS (1980: 302)

Figure 5.60 Measured and Calculated Lateral Movements in the Ground beside the Edmonton Experimental Tunnel before Lining Activation

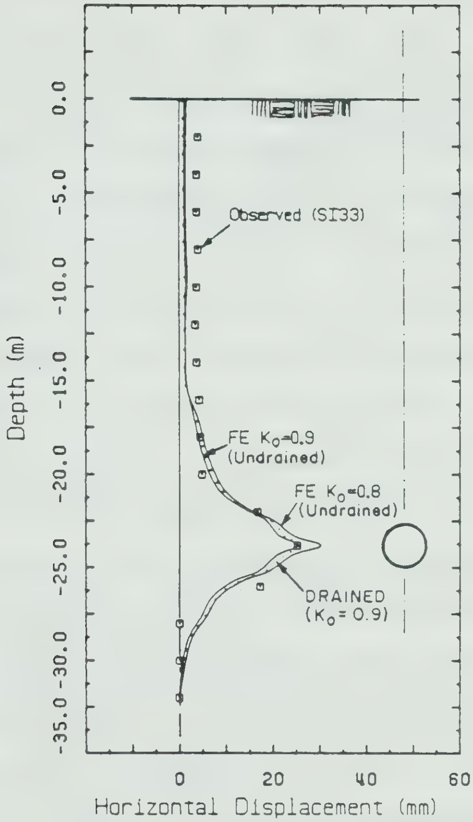

NOTES:

1. MEASUREMENTS AT SI33 (SECTION 3), 2.33 m FROM TUNNEL AXIS.
2. CALCULATED DISPLACEMENTS AT 2.56m FROM TUNNEL AXIS.
3. MEASUREMENTS TAKEN 2 WEEKS AFTER TBM PASSED THE SECTION (TUNNEL FACE AT MORE THAN 15 DIAMETERS AHEAD)
4. FIELD DATA FROM EL-NAHHAS (1980: 126 AND 302)

Figure 5.61 Measured and Calculated Lateral Movements in the Ground beside the Edmonton Experimental Tunnel after Complete Passage of the TBM

loads only. The "short term" measurements are those taken 7 days after lining installation, when the tunnel face was more than 22 diameters ahead. The "long term" readings were taken 2 months or more later. The calculated thrusts were obtained at different sections of the lining by averaging the computed tangential element stresses in those sections, and integrating them along the equivalent lining thickness. The calculated "undrained" thrusts provide a bound for the "short term" measurements, while the "long term" thrusts are bound by the calculated "drained" values. Table 5.24 furnishes values of the averaged measured thrusts in Section 3 for perhaps a clearer comparison. The reading at instrumented ring number 2 was referred to by El-Nahhas (1980:168, 194) as non-representative as the installation procedure of the load cells in this ring differed from the others. Nevertheless, the results of the comparisons are quite favourable, despite the limitations of the lining representation in the present numerical solution. As in the LRT tunnel, the support systems here seems to carry a small amount of bending and this minimizes the deficiencies of the lining representation.

Table 5.25 summarizes the comparisons between measured and calculated performances for the "short term" condition. It also includes some additional data regarding measurements taken inside the tunnel (convergence and invert levelling). The worst prediction aspect refers to the maximum slope of the surface settlement trough. Also lining convergence and

Condition	Average Thrust(1) (kN/m)			
	Measured		Calculated	
			K_0: 0.8	K_0: 0.9
Short Term(2)	137.0(4)	(149.5)(5)	157.9(6)	166.1(6)
Long Term(3)	158.7(4)	(177.2)(5)	-	172.0(7)

Notes: (1) Per unit length of tunnel. Section 3 only. Loads in the lower joint of the segmented ring. Lining self weight discounted.
(2) 7 days after installation of ring.
(3) 56 to 58 days after installation of ring.
(4) Excluding data from instrumented ring #2.
(5) Including data from instrumented ring #2.
(6) Using undrained parameters.
(7) Using drained parameters.

Table 5.24 Measured and Calculated Average Thrust Forces at the Lower Lining Joint in the Edmonton Experimental Tunnel

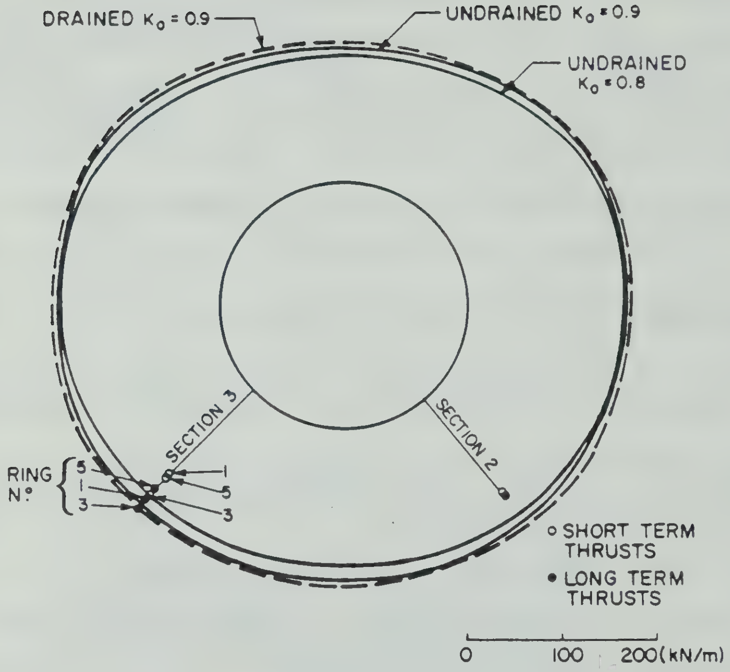

NOTES:

1. "SHORT TERM" READINGS 7 DAYS AFTER INSTALLATION; TUNNEL FACE AT MORE THAN 22 DIAMETERS AHEAD THE SECTION.
2. "LONG TERM" READINGS AT SECTION 2 TAKEN 90 DAYS AFTER INSTALLATION. AT SECTION 3 TAKEN 58 DAYS (RINGS 1 AND 3) AND 56 DAYS (RING 5) AFTER INSTALLATION. SOIL COVER IN SECTION 2-.2.5m AND 22.5m IN SECTION 3.
3. LINING SELFWEIGHT DISCOUNTED FROM MEASUREMENTS.
4. MEASURED AND CALCULATED THRUST VALUES PER UNIT LENGTH OF TUNNEL.
5. FIELD DATA FROM EL-NAHHAS (1980:167, 170, 172 AND 173).

Figure 5.62 Measured and Calculated Thrust Forces at Segment Joints in the Edmonton Experimental Tunnel

floor heave were not accurately estimated. The measured figure shown for these two aspects are indicative only, as suggested by El-Nahhas (1980:166).

As in the LRT tunnel, the large amount of field data available in this case history and the reasonable matching achieved in the back analyses, allowed a reasonable assessment of the amount of stress release, prior to the lining activation.

Assuming that the thrust distribution was uniform, the long term measurements in Section 3 (almost 2 months after lining installation) would indicate an all-round uniform ground stress acting on the lining of about 27% of the average in situ radial stress (for K_o=0.9). This construction scheme led to a ground stress reduction slightly higher than seen at the LRT tunnel. This was possibly due to the delayed support activation in the present case, resulting from the use of a relatively longer TBM. On the other hand, the stress reduction occurring after lining activation is smaller in this case, possibly reflecting the stiffer nature of the support used.

The simplified stability assessment for the plane strain (final) situation, as undertaken in the former two case histories, can be repeated here. The support action is one of applying a uniform internal pressure in the opening walls, so that a factor of safety against global collapse of the ground can be estimated. With that all round uniform ground stress, a safety factor of 1.4 is found. Once more,

	Performance Aspect		Measured(1)	Calculated(2)	C/M
1.	Maximum surface settlement	mm	12.5(3)	12.2	0.98
2.	Maximum slope of surface settlement trough	-	1:1300(3)	1:2100	0.62
3.	Crown settlement(4)	mm	39(3)	44	1.13
4.	Maximum deep settlement (2.5 m from axis)	mm	18(5)	22	1.22
5.	Maximum lateral movement at lining installation (2.5 m from axis)	mm	22(6)	27	1.23
6.	Maximum final lateral movement (2.5 m from axis)	mm	25(6)	27.2	1.09
7.	Horizontal diameter change of lining	mm	~2(7)	1.5(8)	0.75
8.	Floor heave after lining installation	mm	~2(7)	3.1(8)	1.55
9.	Thrust in lower longitudinal joint	kN/m	137(9)	162	1.18

Notes:
(1) Data from El-Nahhas (1980). "Short term" data only, after TBM had passed section 3 entirely.
(2) Averaged calculated response, using "undrained" parameters.
(3) Average value.
(4) About 1.5 m above crown elevation.
(5) At MX32.
(6) At SI33.
(7) At Section 2, according to El-Nahhas (1980:166).
(8) For $K_0 = 0.9$.
(9) Excluding instrumented ring No.2.

Table 5.25 Measured and Calculated Performance of Edmonton Experimental Tunnel

this figure is less than the range given in Section 2.3.4.3, and again, a non-linear ground response would be expected. Despite the good ground control conditions implemented in this tunnel, significant non-linear response of the ground is evident.

With the final crown displacement of 59.4 mm given by the drained back analysis, it is possible to calculate the dimensionless crown displacement (U) given by equation 2.16. This is found to be equal to 1.00, for an initial (drained) tangent modulus of the soil at the crown of about 19.5 MPa. This value is smaller than the threshold figure of 1.8 for a near collapse condition. In fact, although this dimensionless displacement is larger than that found in the other two cases, no sign of ground instability was detected in this case hisory.

Figure 5.63 illustrates the expected degree of straining of the ground around the tunnel after the "short term" equilibrium was reached. The shaded zones correspond to points subjected to maximum shear strains greater than 1%. The calculated shear strains shown on the left hand side correspond to the undrained analysis using K_o=0.9. The righthand side shows the shear strain distribution as deduced by El-Nahhas (1980:245) from his field measurements. The extent of the strained zone around the opening seems comparable but the shape of the zones are dissimilar. Figure 5.64 depicts similar information for maximum shear strains greater than 2%. The measurements indicate that points

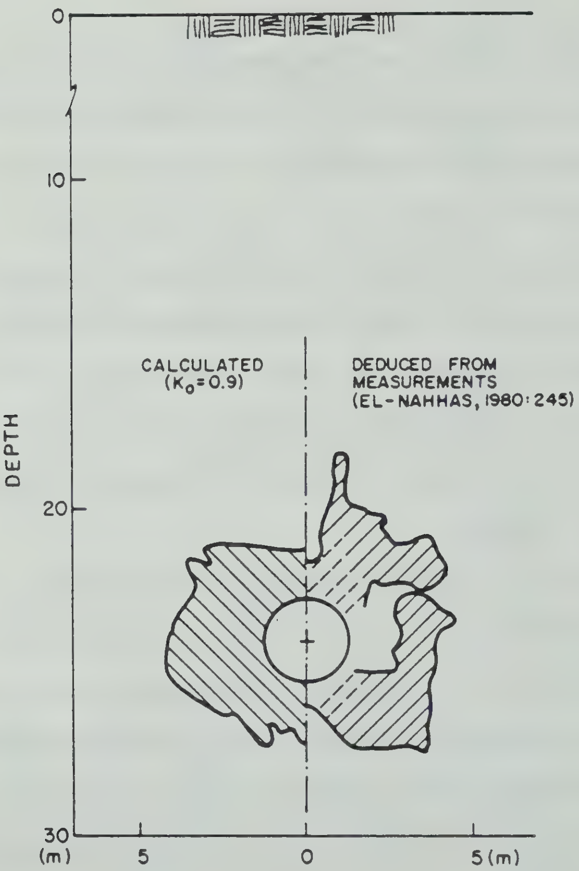

Figure 5.63 Calculated and Measured Zones with Maximum Shear Strain Greater than 1% in the Edmonton Experimental Tunnel

slightly farther away from the tunnel had been strained to that level and that, again, the strained zones show different shapes. In both figures one notes that the calculated straining pattern is more uniform and symmetric as compared to the pattern deduced from the field measurements.

The numerical simulation indicated that no soil element around the opening experienced failure as defined by the strength envelope. Nevertheless, a very pronounced decrease in the tangent modulus from its initial value was observed, particularly at springline elevation. In order to identify failure zones from the deduced field strains El-Nahhas (1980:250) suggested that maximum shear strains in excess of 1 to 2% would imply full mobilization of the shear strength. If the higher strain value is considered, and a major principal strain is estimated by using the stress-strain curves of the recent tests conducted, it can be seen that the degree of shear strength mobilization would vary from 40 to 70%, depending on the test stress path. In other words, the possible failure zone might have been much smaller in extent than it was originally thought.

The difference in the shapes of the maximum shear strain contours as given by the measurements and by the numerical model is not an unexpected feature. Variations in the predicted and observed shear strain contours have been noticed by Orr et.al., (1978:136), Mair (1979:131) and Seneviratne (1979:113). The calculated contours and the

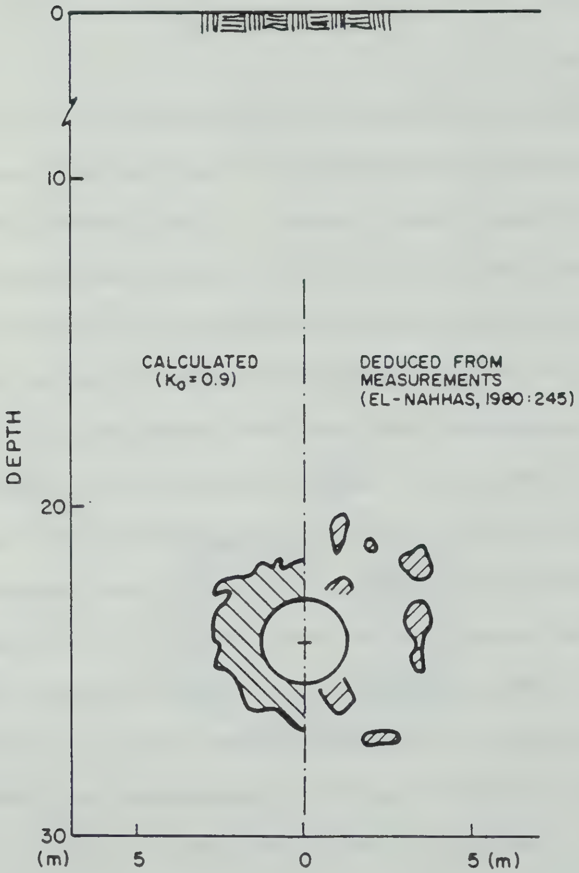

Figure 5.64 Calculated and Measured Zones with Maximum Shear Strain Greater than 2% in the Edmonton Experimental Tunnel

failure zones, tend to be more axisymmetric than those actually observed. Wong (1986:48,107) using a different numerical solution, also showed that a fairly axisymmetric yield zone would result for the Edmonton Experimental tunnel. As noted in Section 5.2.1.2, the current formulations of most finite element codes, regardless of their constitutive equations, are unable to properly model conditions that involve highly concentrated shear strains. Those preceding the collapse of a tunnel in soil are presented in Section 2.3.4.3. All things considered, the present numerical model was able to yield sensible results compared to the observed field performance of the tunnel.

5.2.5 Summary and Conclusions

This section reviewed the role of two-dimensional numerical modelling in predicting the behaviour of shallow tunnels under time-independent conditions. Relevant modelling aspects were examined, particularly the procedures for excavation simulation and methods to approximately account for the three-dimensional effects involved in the tunnel advance. Examples of stress-strain relations for soils that have been used in shallow tunnel modelling were reviewed and briefly discussed. The need to consider the non-linear behaviour of soils was stressed and some of the advantages of non-linear elastic relationships, such as the hyperbolic model, were assessed. One of these was the suitability of this model to represent the non-linear response of soil even in the "small strain" range of behaviour.

A comprehensive survey of predictive exercises on shallow tunnels using two-dimensional finite element analyses was presented. The survey included only those cases published over the last decade where the capability of the numerical solution to simulate actual behaviour could be evaluated by comparison with measurements. In each case, qualitative indications were provided on the results of these comparisons. Very few cases enabled a complete assessment of the predictive potential of the numerical models. Most cases fail to include a complete picture of the measured and predicted displacement fields and lining loads. It was not possible to relate the quality of the predictions made with the numerical model features or the constitutive relations used. No correlation was found between the quality of the predictions and the soil type, the construction method or the prediction class, as defined by Lambe (1973). Nonetheless, an overall appraisal of the numerical predictions was attempted in a global manner.

The majority of the cases reviewed (67%) referred to predictions after the event, with known results at the time the analyses were made. In most cases (72%) the comparison was limited to ground displacements and most frequently these were surface and subsurface settlements. Only 10% of the cases provided a complete comparison including all displacement fields and lining loads. The magnitude of the maximum surface settlement was closely matched by the numerical simulations in 60% of the cases, but in over half of the cases, the maximum surface distortions were underpredicted. The overall distribution of subsurface settlements was generally well estimated, but the maximum magnitude of these deep settlements was reasonably predicted in less than 40% of the cases. The magnitude of the maximum horizontal displacement in the ground was overestimated in more than 60% of the cases. No dominant trend was noted with respect to the prediction of lining loads. The above findings were discussed in detail and the reasons explaining these facts were either identified or suggested.

The numerical solution used for the present study was described and discussed. Its main features and limitations were analysed in detail in order to provide a basis for judgement and evaluation of its predictive capabilities. The three-dimensional effects of tunnelling advance are approximately accounted for by a partial release of the in situ stress, before the lining is installed. The amount of stress release to be considered in a particular case is unknown, but it should be related to the construction scheme, particularly to the distance between the tunnel face and the point of lining activation and also to the soil conditions.

Three well documented case histories were reviewed and were used to assess the capability of the simple numerical model selected to portray the main features of an actual tunnel performance. Moreover, the analyses of these case histories served as an opportunity to indirectly estimate the amount of stress reduction to be used in order to best fit the observed performances.

The geological and geotechnical aspects of each site were reviewed as well as the contruction details of the tunnels. In all three cases good ground conditions prevailed. A certain degree of uncertainty was present with regard to the in situ stress conditions and to the lining representation. Accordingly, these two additional parameters were included as independent variables in the back analyses. One of the cases, the Edmonton Experimental Tunnel, required additional investigations. These were carried out in order to supply the necessary input for the numerical simulation. The locally occurring till was found to be much softer than originally anticipated.

Despite the inherent approximation involved in the two dimensional simulation for the ground and lining representations, it was possible to find the amounts of stress release that had to be applied to the in situ stresses before support application, in order to yield good estimates of the performances in all three cases. The results of these studies are shown in Table 5.26, prepared in such a way as to allow a direct comparison with Table 5.5, which summarized the results of similar studies carried out with other tunnel cases. The results shown refer only to those aspects of the performance at the final equilibrium situation. As it is seen, the present numerical solution yielded results that compared very favourably with the measurements. Moreover, compared to the results of other simulations applied to other case histories (Table 5.5), it is noticed that the present numerical simulation ranks among those that showed the most favourable results. The fact that the predictions in this study are made after the performance is known (type C1), does not lessen its merit. Most of the analyses shown in Table 5.5 were performed under the same circumstances. Using the same point rating criterion referred to in Section 5.2.1.2, to evaluate the quality of the predictions, the analyses of the LRT and Edmonton Experimental Tunnel were ranked the best in all cases reviewed and were closely followed by the ABV case.

An additional point to be remembered is that in the three cases studied, besides the good agreement found between calculated and measured performances for the final equilibrium situation, fairly good agreement in the ground displacement field before lining installation was found. This agreement would not have been found had the lining been applied very close to the tunnel face. Indeed, the ground stress reduction expedient accounts only partly for the 3D effects involved in a real tunnel, as noted in Sections 4.3.2.7, 5.2.1.1 and 5.2.4.2. Fortunately most shallow tunnels are lined at some distance behind the face (0.5 to 2.0D) where conditions approach that of plane strain, as shown in Section 2.3.6.1.

Tunnel	Main Reference Source	Soil	Construction Method and Support	Cover and Diameter (m)	Distance from Support Appl. to the Face (m)	Back Anal.(2) Amount of Stress Release	Surface(3) Settlement			Subsurface(3) Settlement		Hor.(3) Displ.		Lining(3) Loads	
							Mg.	Dist.	Dtr.	Mg.	Dtr.	Mg.	Dtr.	Mg.	Dtr.
ABV	Negro & Eisenstein (1981)	Clayey sand above W.L.	NATM shotcrete	6.20/4.0-1.55	2.6m (0.65D)	40%	≈	>	G	≈	G			≈	R
LRT	Branco (1981)	Stiff glacial Till above W.L.	TBM, steel ribs and wood lagging	9.0/6.1-1.48	6.7 m (1.09D)	50%	≈	≈	G	≈	G	≈	R	≈	G
Edm. Exper.	El-Nahhas (1980)	Softer glacial till above W.L. but saturated	TBM segmented concrete	22.5/2.56-8.79	7.0 m (2.73D)	70%	≈	>	R	≈	G	≈	G	≈	G?

Notes:
(1) See Table 5.5 for the meaning of abbreviations and symbols used.
(2) Applied to the in situ stresses, prior to the support activation.
(3) All refer to the final equilibrium, after lining installation.

Table 5.26 Results of the Numerical Simulations of the Final Tunnel Performance in Three Case Histories

A major limitation is seen in this simulation procedure regarding it potential practical use for class A predictions. This refers to the need of an independent estimate of the amount of ground stress release taking place before lining activation. This stress release was brought into the simulation to represent the three-dimensional ground stress redistributions that take place during the tunnel face advance.

If the ground stress release was uniquely related to the ground displacement by some relationship then an estimate of these ground displacements including the three-dimensional effects of an advancing tunnel, could be a basis of an alternative approach to the solution of this problem. This approach presents several advantages. One is that, while the ground stress release is an artificial expedient without physical meaning, the corresponding ground displacements do have real significance. They would be the actual displacements developing around the opening at the section where the lining is activated.

This reasoning was followed by other authors seeking the solution of similar problems but for axisymmetric conditions. Most of these works have been reviewed in Section 4.3.2.7, and they include treatments by Daemen and Fairhurst (1972), Panet and Guellec (1974), Panet (1976). Baudendistel (1979,1984,1985) also followed this approach, but extended it for a specific non-unifrom stress condition (K_o=0.5) and for a particular cross section of a deep tunnel.

All these works have their value, but they are of little use for the solution of the present problem. They do not deal with the presence of the ground surface, the action of the gravitational stress gradients and the non-hydrostatic in situ stress conditions which are required for the solution of the problem.

In the following section, an attempt will be made to develop an approximate procedure to estimate ground displacements around a shallow circular opening making use of three-dimensional numerical modelling.

5. SHALLOW TUNNEL MODELLING (CONTINUED)

5.3 Three-Dimensional Modelling

5.3.1 Introduction

It was shown in Sections 5.2.4 and 5.2.5, that the two-dimensional numerical solution adopted in the present study may serve as a reasonable tool to anticipate tunnelling performance. This is so, provided the requirements for validating or applying the numerical solution are fulfilled. Moreover, it was shown that reasonable predictions of the behaviour will only be obtained if the amount of stress release allowed before lining activation is properly estimated. This is, perhaps, the major drawback of this two-dimensional modelling procedure. The model requires an independent estimate of this variable.

Clearly, in a particular case, the stress release should be related to the construction procedures as well as to the ground type. Regarding the construction procedure, the support activation delay seems to be the controlling factor. It is represented by the distance between the tunnel face and the point where the lining and the ground are brought into full contact.

As explained in Section 5.2.5, if the ground stress release was univocally related to the ground displacements, then an estimate of the ground displacements could lead to an evaluation of the stress release. In Sections 2.3.4.2 and 2.3.5.3, the relationship between the radial stresses and displacements in an opening was formulated in a 2D representation, by extending the concept of the ground reaction curve to shallow tunnel conditions. In Section 3.2.3 it was suggested that for this type of representation, an univocal relation between stresses and displacements may indeed exist, provided tunnel collapse and the associated "loosening" process is avoided. But even if these failure processes are present, the tunnel closure is associated with a single ground stress. In Section 2.3.6.2 and 2.3.6.4, it was shown however, that the actual three-dimensional response in terms of stress-displacement relations is far more complex, and that in fact an univocal relation may not exist. This seems to result from the three-dimensional stress redistribution mechanisms. The presence of the lining affects the stress-displacement relation even at unsupported sections between the face and the liner heading edge (see Figures 2.25 to 2.27). This effect is more pronounced for smaller support activation delays. It was suggested however, that a two-dimensional representation may serve to approximate or bound the final equilibrium between liner and soil.

If the final equilibrium condition is the only matter of concern, then the two-dimensional representation may still be useful. This was suitably demonstrated through the back analyses shown in Section 5.2.4. Thus, the lining influence would only be considered in the two-dimensional simulation when the support is activated.

By accepting this simplification, the amount of ground stress release can be directly related to the loss of ground occurring during tunnel advance (Cording and Hansmire, 1975 - see Section 2.3.4.3). If it were possible to identify each component of the ground loss, then one could apportion the stress release to each component within the simplified two-dimensional model. Each construction technology, as applied to a certain ground type or condition, may lead to different compositions of losses of ground, as shown by Negro and Eisenstein (1981). Figure 5.65 illustrates these concepts, making use of an idealized relationship between the amount of stress release and losses of ground for two types of construction scheme. This relation corresponds to an "averaged" ground reaction curve, since by definition in this work, the amount of stress release is related to the applied radial stress and the loss of ground is related to the radial displacements of the tunnel contour. It has been tacitly assumed that ground deformations are not uncontrolled and therefore, stress and strain changes in the ground are gradual and continuous. It has also been assumed that the ground-lining interaction will develop only when the contact between them is fully developed (stage 4 in the TBM scheme) or when the invert is closed (stage 3 in the NATM scheme).

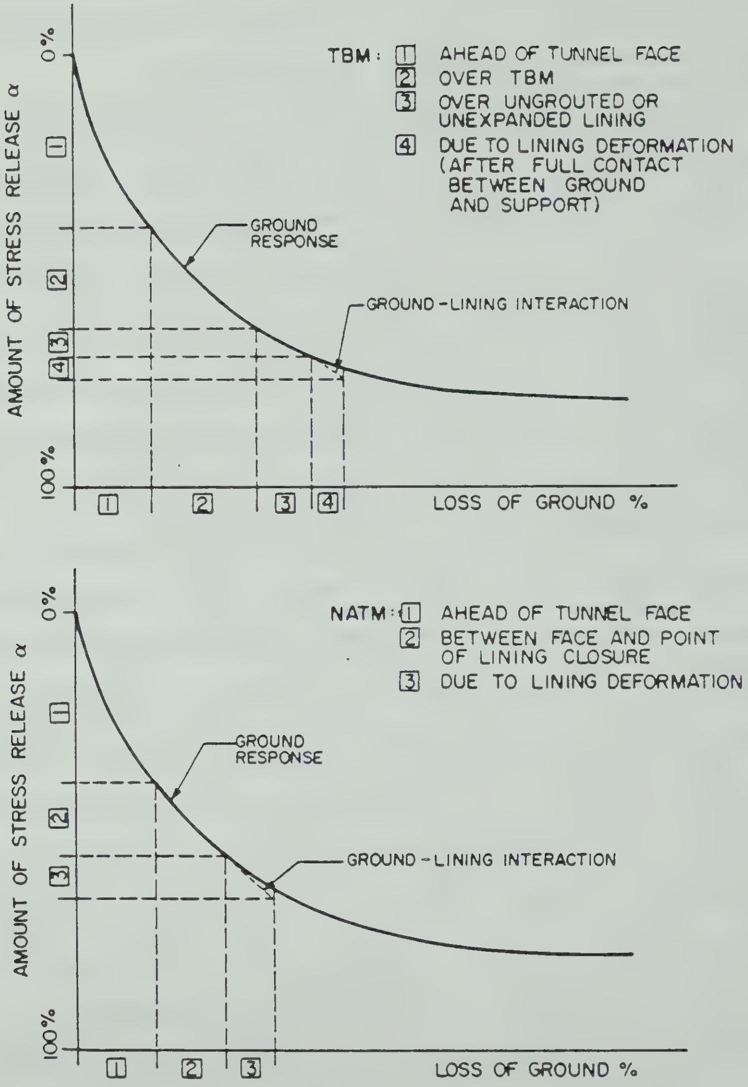

Figure 5.65 Conceptual Relations Between the Amount of Stress Release and Loss of Ground in a Two-Dimensional Representation

One may consider a few extreme situations. If the support was brought into full contact with the ground at the tunnel face, stages 2 and 3 would be non-existent in the TBM scheme, as well as stage 2 in the NATM case. In another situation, if the soil was highly deformable as in some soft clays, it would close the overcutting void left over the TBM body, and the amount of ground lost at this stage, would be equal to that void volume. Thus, if a full lining contact is ensured as soon as the liner leaves the TBM tail, the ground-support interaction would start after the occurrence of ground movements equal to those developing ahead of the face plus the void size behind the TBM. In these two extreme situations, the amount of stress release to be considered in a two-dimensional representation would be known, provided the ground response the accumulated movement at the tunnel face and the TBM overcutting size are all known.

However, if the soil is only moderately deformable and shows some stand-up time, like some stiff clays, then the overcutting space may not be closed. In this case, the losses of ground at stage 2 in the TBM scheme is, therefore, unknown and the amount of stress release would be undetermined. Nevertheless, portion 1 of the stress release would serve as a lower bound to the unknown release.

If the relationships like those shown in Figure 5.65 were available, then the amount of stress release prior to lining activation, which is to be used in a two-dimensional simulation, would be defined whenever the losses of ground or the total magnitude of ground movement are known at the section where the lining is activated.

Ground reaction curves derived from two-dimensional analyses, as those shown in Sections 2.3.4.2 and 2.3.5.3, could be used to obtain the type of relationships shown in Figure 5.65. The estimate of the ground displacements occurring ahead of the face or at the point where the support is activated, requires consideration of the three-dimensional nature of the problem. It seems therefore necessary to investigate available solutions of opening convergence with the advance of the tunnel face.

5.3.2 Available Solutions for Estimates of Tunnel Convergence

Many authors followed the reasoning exposed in Section 5.3.1 and tried to develop methods that would allow the estimate of the tunnel contour closure at different sections behind the advancing face for time independent conditions. Some of the early works were reviewed and discussed in Section 2.3.6.2. For completeness, Table 5.27 has been prepared. It supplements the former discussions and includes only those methods whose primary goal is the convergence estimate.

These methods were formulated following three main lines of development:

1. methods derived from finite element analyses (either axisymmetric or three-dimensional);

2. methods derived from three-dimensional boundary element analyses;
3. methods semi-empirically derived, using curve fitting techniques.

Unlike the first two classes of methods, the latter, represented by cases 10 and 12 in Table 5.27, are not actual prediction methods. Field data gathered at a certain site and under certain conditions are required for input, and this allows the extrapolation of convergence results for different conditions but at the same location. Therefore, they should be understood as ancillary techniques for the observational method.

Most methods were developed under the assumption that the opening was located far from the ground surface, so that the influence of the gravitational stress gradients could be neglected. The sole exception to this rule is the procedure given in reference 11, Table 5.27. This particular method, described in Section 5.3.5, furnishes the radial displacements of the tunnel contour at a section containing the tunnel face (assumed vertical). In following sections this method will be extended to allow estimates at other points along the tunnel alignment.

The methods developed by Baudendistel (1979, 1984, 1985) and by Erdmann (1983) (see Sections 4.3.2.6 and 4.3.2.7) have not been included in Table 5.27 as they do not explicitly provide the radial displacements of the tunnel contour at different sections along the axis, although these

Reference	Development	Factors Considered				Notes
		Tunnel Depth	In situ stress Ratio	Stress-Strain Rel. For Ground	Presence of Lining	
1. Daemen & Fairhurst (1972)	Axisymmetric finite element method	Deep	$K = 1$	linear elastic	unlined	
2. Descoeudres (1974)	3D finite element method (double symmetry)	Deep	$0.25 < K < 1$	linear elastic	unlined	
3. Ranken & Ghaboussi (1975)	Axisymmetric finite element method	Deep	$K = 1$	linear elastic and elastoplastic	unlined and lined	Account of non linearily and lining not generalized
4. Hocking (1976)	3D boundary integral equation method	Deep	$0 < K < 2$	linear elastic	unlined	
5. Niwa et al (1979)	3D boundary integral equation method	Deep	Any K	linear elastic	unlined	
6. Schwartz & Einstein (1980)	Axisymmetric finite element method	Deep	$K = 1$	linear elastic and elastoplastic	unlined and lined	Account of non linearily and lining not generalized
7. Ito & Hisatake (1981)	Curve fitting of axisymmetric FE solution	Deep	$K = 1$	linear elastic	unlined	
8. Hutchinson (1982)	Axisymmetric finite element method	Deep	$K = 1$	linear elastic	unlined and lined	Accounts of lining effect not generalized.
9. Hanafy & Emery (1982 and 1980)	Axisymmetric analysis with non symmetric loading	Deep	$K = 1$ and $0.75 < K < 1.25$	linear elastic and elasto plastic	unlined and lined	Accounts of non linearily and lining not generalized
10. Panet & Guenot (1982) Guenot et al (1985) Sulem et al (1987) Panet (1979) Gaudin et al (1981)	Curve-fitting of field data, semi-empirical	-	-	-	unlined	Observational method. Requires field data as input
11. Negro et al (1985, 1986)	3D finite element method (single symmetry)	shallow	$0.6 < K < 0.9$	linear elastic	unlined and lined	Convergence at the face only.
12. Barlow (1986) Barlow and Kaiser (1987)	Curve-fitting of field data. semi-empirical (similar to 10)	-	-	-	lined	Observational method. Requires field data as input.

Table 5.27 Some Solutions for Tunnel Convergence Estimates under Time-Independent Conditions

could be obtained indirectly.

Many methods assume a hydrostatic in situ stress condition, while others assume less restrictive field stresses (K_o not equal to 1). For a deep unlined tunnel, with axisymmetric geometric conditions, a single analysis with K_o equal to zero (uniaxial stress field) is sufficient to obtain a complete solution, provided the material is linear elastic, homogeneous and isotropic. The displacements for any K_o value can be obtained by using the principle of superposition. Therefore, the solutions derived from boundary integral equation analyses, presented by Hocking (1976:336) or by Niwa et.al. (1979:707) for K_o equal to zero, can be extended to any in situ stress ratio. This is summarized in Figure 5.66.

The numerical solutions available which have larger generality, thus applicable to a wider range of situations, are those which assume the ground behaviour to be linear elastic. Those which assume non-linear stress-strain relationships for the ground, cannot be readily generalized to conditions different from the original analyses, although they might be useful in providing insight on the effect of ground yielding.

Similarly, the methods that take into account the presence of the lining in the radial displacements of the opening are not generalized to conditions other than that studied. To achieve a broader generality, a larger number of parametric analyses, combined with components of

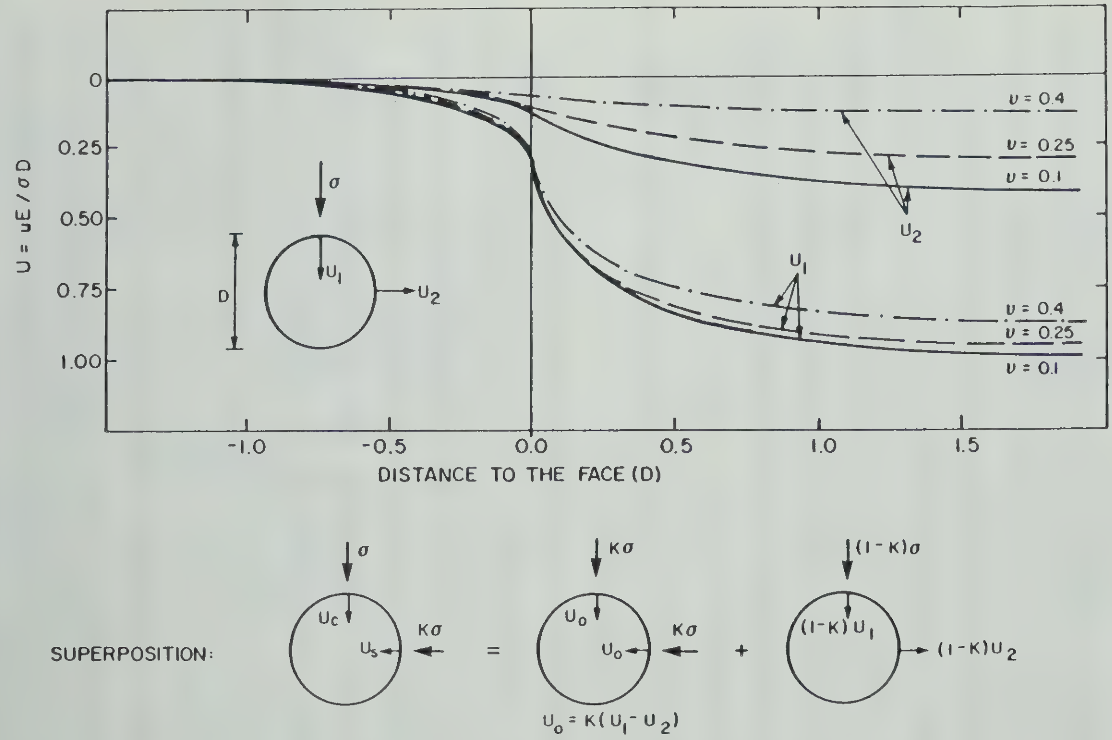

$$U_c = K(U_1 - U_2) + (1-K)U_1 \therefore \underline{U_c = U_1 - KU_2}$$

$$U_s = K(U_1 - U_2) + (1-K)U_2 \therefore \underline{U_s = KU_1 - U_2}$$

Figure 5.66 Radial Displacements of an Unlined Deep Tunnel in Elastic Ground (after Niwa et.al., 1979)

dimensionless analyses, would be required to obtain such a solution. Barlow (1986:45) achieved this to some extent. This author was able to introduce into the Guenot et.al. (1985) convergence solution, the influence of a lining installed at a certain distance behind the face of the tunnel. His procedure was developed from axisymmetric finite element analyses and, therefore, is strictly valid for hydrostatic in situ stress conditions. For these conditions the liner stiffness can be described in terms of its compressibility ratio only. A more general solution would require the flexibility ratio to be taken into account as well. Such a development is yet to be seen.

Nonetheless, Barlow (1986) has shown that for the conditions he studied (for instance, ground and support assumed elastic), the presence of the lining does have a strong influence on the radial displacements of the tunnel contour over the unsupported tunnel heading, as also shown by Eisenstein et.al. (1984) and as discussed in Section 2.3.6.2. This influence is more pronounced when the liner is placed close to the advancing face. The Convergence - Confinement method usually assumes that the opening deforms as in an unsupported tunnel, until the point of lining activation. The amount of stress release before lining installation can therefore be incorrectly estimated if this effect is neglected. Since the support tends to inhibit the ground movements around the heading, then neglecting the lining presence will likely result in an overestimate of the stress release. This means the support loads are underestimated and leads to an overestimate of the final ground movements. On one hand the assumption is unsafe and on the other it is too conservative. The errors involved in disregarding the lining-ground interaction however tend to be small for increasing distances between the face and the liner leading edge. For linear elastic materials, the results by Barlow (1986:59) showed that for support delays equal to, or greater than, 5/8 of the opening diameter, the tunnel closure at the leading edge of the liner is almost identical to that of an unlined tunnel for the same distance to the face. Since in most shallow tunnels in soil the lining is usually activated at distances from the face greater than this value, the errors involved in that simplifying assumption may not be very high. Moreover, for shotcret lining, its lower modulus at sections closer to the face, will further decrease the differences in the supported and unsupported tunnel closures, in the section the lining is activated. This fact was demonstrated by Erdmann (1983:189) for a non-uniform in situ stress condition. For these reasons, it is believed that possibly, a more critical issue is the linear elastic material assumption made by most of the available solutions.

Through this brief review, it is readily recognized that most of the methods available for the prediction of radial displacements at the tunnel contour which account for the 3D mechanisms involved, are of little help for the solution of the problem at hand. For instance, most methods disregard the presence of the ground surface and the action of the gravitational stress gradients which are always present in a shallow tunnel situation. A large number of solutions were developed to be used in connection with the Convergence - Confinement Method, and the assumption of uniform stress field is far too restrictive for application to the present problem. For the above reasons, it was felt that there was a need to develop another solution, especially designed to the purpose in mind. For convenience, it was decided to attempt this development, making use of three-dimensional finite element modelling. A concise evaluation of former studies using thise type of numerical simulation is included in the following section.

5.3.3 Review of Three-Dimensional Modelling by the Finite Element Method

Following the previous review of two-dimensional modelling studies presented in Section 5.2.1, this section attempts a comprehensive, but not exhaustive assessment of three-dimensional modelling of shallow tunnels driven in soil. Some of the studies referred to herein have already been discussed in Sections 2.3.6 and 4.3.2.6. In particular, Section 2.3.6 covered the main aspects of the three-dimensional stress redistribution and induced displacements associated with the advance of a tunnel. The approximate account for these processes in two-dimensional analyses was discussed in Sections 4.3.2.7 and 5.2.1.1.

In this section, the discussion will focus mainly on the applications of three-dimensional finite element solutions to shallow tunnels in soil. Reference will be made however, to other types of tunnelling conditions, whenever they present sufficient generality to contribute to the subject being focused on. Those studies involving fully axisymmetric assumptions, both in terms of geometry and loading conditions, will not be reviewed. Some of them (for instance, Daemen and Fairhurst, 1972, Panet and Guellec, 1974, Ranken and Ghaboussi, 1975, Schwartz and Einstein, 1980:47, Hutchinson, 1982, and others), have been referred to or partly reviewed (for instance, Sections 2.3.6.1, 2.3.6.2, 4.3.2.7 and 5.3.2). On the other hand, those axisymmetric analyses that consider non-axisymmetric loading assumptions will be referred to herein, as they provide some generality.

Table 5.28 summarizes some representative studies carried out over the last decade, where the use of three-dimensional finite element analyses was made. The studies were classified into three categories, according to their main purposes:

1. Prediction: cases where the aim of the study was mainly an attempt to anticipate the behaviour of a particular tunnel case history, allowing a comparison between calculated and observed performances.
2. Investigation of Behaviour: refers to the cases where

the analyses were conducted mainly to achieve or improve the understanding of some mechanisms or the features of behaviour of tunnelling under idealized conditions.

3. Generalization: cases where an attempt was made to develop some procedure or method that could be generalized and applied to conditions other than that assumed in the actual numerical analyses.

Although most of the cases reviewed could be classified in more than one category, the purpose of the analyses indicated in Table 5.28 reveals which was understood as the main objective of the study conducted.

Most of the cases reviewed used a linear elastic stress-strain model for the ground, assuming a constant elastic modulus or an increasing modulus with depth. The high cost of 3D analyses seems to be the main factor leading to this preference. Even so, a few studies took into account the non-linear behaviour of the ground, by using elasto-plastic or non-linear elastic models. In all cases, the lining was represented by a linear elastic material. In most cases, a constant liner modulus was assumed, but in cases 4, 12 and 14, a variable E modulus was considered, by assigning an increasing value for points at increasing distance from the face. This reflects an attempt to simulate the hardening of shotcrete with tunnel advance.

In the cases where the simulated tunnel was left unsupported and the ground was assumed to be elastic, there was no need to simulate the incremental construction as

Reference	Purpose of Analyses	Soil Stress-Strain Model	Simulation	Finite Element Features	Comments
1. Wittke et al. (1974) Wittke (1977:624)	Prediction (type A)	Linear elastic (constant E)	Single step excavation and simultaneous lining application(shallow circular tunnel)	Symmetric mesh, 3.1 x x 4.6 x 6.9D(1)	Analysis of initial length of the Altmuhl Tunnel in W. Germany (clay and sandstone). Poor agreement with measurements attributed to K_0 being higher than what was assumed. Moreover, construction sequence not simulated.
2. Descoeudres (1974)	Generalization	Linear elastic (constant E)	Unsupported full face excavation in a single step. No gravitational stress gradient (deep circular tunnel).	A quarter sector mesh, 2 x 2 x 4.8D; isoparametric elements; coarse discretization	Parametric analyses, K_0 varying from 0.25 to 1.0. Radial displacements at crown and springline, for sections at different distances to the face. A single elasto-plastic anlaysis was carried out for comparison.
3. Wittke & Pierau (1976)	Prediction (type C1)	Linear elastic-plastic (approx.) constant E	Single step excavation and simultaneous lining installation. Construction process accounted for by an interative procedure, where changing displacement boundary conditions are used (shallow tunnel).	Symmetric mesh 3.3 x 4.8 x 6.7D (525 nodes)	Analysis of the central length of the Altmuhl Tunnel in W. Germany (sandstone and clay). Simulation procedure allows the use of a smaller mesh. Anchoring and water level lowering considered. Ground displacement generally underestimated. In broad terms a favourable comparison with measurements.
4. Gartung et al (1979) Bauernfeind et al (1986)	Investigation of behaviour	Linear elastic brittle-plastic (increasing E with confinement)	Incremental construction simulation with heading and bench excavation, delayed shotcrete application (concrete modulus varying with advance) and and delayed anchor installation.	Symmetric mesh; 1.6 x 2.4 x 2.7D (816 elements) PAM-NL program	Evaluation of potential stability problems of a large cross section tunnel of the Nuremberg Subway, under reduced ground cover (Keuper sandstone). The effects of delaying shotcrete or anchor installation were studied. Results indicated the need to consider the 3D loading conditions of the shotcrete shell at the tunnel heading.
5. Baudendistel (1979, 1984, 1985)	Generalization	Linear elastic (constant E)	Unsupported non circular excavation in three steps: heading, bench and floor (each one in a single step) No gravitational stress gradient (deep tunnel).	Symmetric mesh; 3.5 x 3.5 x 3D (1326 nodes and 1012 isoparametric elements), SAP4 program	Analyses designed to develop ground stress reduction factors for lining design, as a function of the point of lining installation. $K_0 = 0.5$. Different factors for crown, springline and floor (see Section 4.3.2.7).

Table 5.28 Review of Some Three-Dimensional Finite Element Simulations of Tunnel Construction

Reference	Purpose of Analyses	Soil Stress-Strain Model	Simulation	Finite Element Features	Comments
6. Semprich (1980:161)	Investigation of behaviour	Elasto-plastic (Mohr Coulomb for failure and yield, assoc. flow rule) (constant E)	Simulation procedures similar to 3 above (non circular shallow tunnel)	Symmetric mesh; 3 x 4.2 x 3.6D (isoparametric elements); FEST03 program (Aachen) 704 nodes.	Evaluation of the effect of full face excavation with vertical and inclined tunnel face on the ground response. The effect of delaying the support application was also studied. Analyses applied to a particular tunnel case (a S-Bahn tunnel with 55 m^2 in silt).
7. Meister and Wallner (1977)	Prediction (type C1)	Elastoplastic	NA	Symmetric mesh; 2.4 x 3.2 x 2.6D (658 nodes, 444 elements).	Analysis of a test tunnel in the initial portion of the main Butterberg tunnel in W. Germany (sandy silty gravel). Poor agreement of lining loads and settlements.
8. Katzenbach (1981) Katzenbach & Breth (1981 and 1983)	Prediction (type C1) and investigation of behaviour	Non-linear elastic (Duncan & Chang, 1970)	Incremental construction simulation (stress reversal), with full face stepwise excavation and delayed shotcrete application (constant modulus).	Symmetric mesh; 5.2 x 5.2 x 8.8D, 990 elements with 6 or 8 nodes each; STATAN-15 program (Darmstadt)	Analysis performed to represent a typical NATM construction in Frankfurt clay. Despite simplified, non-staged sequence of construction, very favourable agreement with observations was obtained. No comparison made between calculated and measured lining loads.
9. Pierau (1981, 1982)	Generalization and investigation of behaviour	Linear elastic (constant E)	Simulation similar to 3 above. Shallow tunnel with non-circular cross section $K_0 = v/(1-v)$.	Symmetric mesh; 3 x 3.7 x 4D; isoparametric elements, lining forces and bending from plate elements loaded by calculated displacements, FEST03 program (Aachen), 666 nodes.	Parametric study designed to yield lining thrusts and bending moments at certain points of the lining, as well as maximum surface settlements. Generalization for certain ground covers, lining thicknesses, soil and lining properties, and for a fixed tunnel cross section (see Section 4.3.2.6).
10. Hanafy & Emery (1982, 1980)	Investigation of behaviour	Elastic-plastic (Von Mises, failure and yield criteria) with creep.	Incremental construction simulation, with full face stepwise excavation and delayed liner installation. One excavation step for unlined tunnel case. Axisymmetric analyses of a deep tunnel with plane symmetric (non-axisymmetric) stress field.	Axisymmetric mesh; 3.5 x 3.5 x 6.4D (equivalent solid dimensions); triangular axisymmetric ring elements.	Parametric study conducted for a particular tunnel geometry and ground properties typical for a siltstone. The effect of non hydrostatic initial stress field (both in longitudinal and transversal planes) on radial displacements was studied (K_l from 0 to 2 and K_t from 0.75 to 1.25). Also studied the influence of delayed lining installation and of different face advancement rates.

Table 5.28 Review of Some Three-Dimensional Finite Element Simulations of Tunnel Construction (Continued).

Reference	Purpose of Analyses	Soil Stress-Strain Model	Simulation	Finite Element Features	Comments
11. Kasali & Clough (1983)	Investigation of behaviour	Linear elastic (increasing E with depth)	Simulation starts with lining and THM already in place (tunnel partly built and no gravity). A single step advance is then made (stress reversal) Final displacement field by superposition of results of single step advance.	Symmetric mesh; 4.7 x 3.1 x 7D; isoparametric elements with variable number of nodes (8-21) for soil and lining; modified version of SAP IV program.	Comparative analyses of ground response to tunnelling by conventional THM, slurry and earth pressure balance shields in soft clay. Numerical solution is approximate as the superposition of displacement is not strictly correct. Losses of ground admitted to develop only at the face and at the tail void.
12. Erdmann (1983) Erdmann & Duddeck (1984)	Generalization	Linear elastic (constant E)	Axisymmetric analyses of a deep tunnel with plane symmetric (non-axisymmetric) stress field as in 10. Incremental construction simulation, with full face stepwise excavation, delayed shotcrete application (varying modulus with advance).	Axisymmetric mesh, with equivalent solid dimensions of 4 x 4 x 5D; program derived from multi-purpose code available in Braunschweig.	Analyses conducted to furnish reduction factors to be applied to the thrusts, bending moments and radial displacements obtained from ring and plate analytical models (see Section 4.3.2.6).
13. Eisenstein et al (1984); Heinz (1984:173) Present study (Section 2.3.6.4)	Investigation of behaviour	Linear elastic (increasing E with depth)	Incremental construction simulation (general approach), with full face stepwise excavation and delayed lining installation (constant modulus).	Symmetric mesh, 3.5 x 4.6 x 4.1D, 8 nodes solid elements for soil and lining; ADINA program (750 nodes).	Evaluation of the ground-lining response under 3D stress transfer conditions, in terms of radial stress-displacement relations, for points of the tunnel contour. Comparisons between 2D and 3D analyses (see Section 2.3.6.4).
14. Schikora (1984)	Investigation of behaviour	Elasto-plastic (constant E Mohr-Coulomb)	Incremental construction simulation, with full face and heading and bench stepwise excavation, delayed shotcrete application (varying modulus).	Not available.	Comparstive study of lining response to two different construction schemes, accounting for change in shotcrete modulus with the advance. Assessment of thrust variations in the longitudinal direction, in each support ring. Thrust concentration in leading edge of lining.
15. Heinz (1984:148)	Prediction (Type C1)	Linear elastic (increasing E in depth)	Incremental construction simulation with heading and bench stepwise excavation (general approach) and delayed shotcrete application (with constant modulus).	Symmetric mesh, 3.5 x 4.6 x 5.2D, 8 nodes solid elements for soil and lining; ADINA program (850 nodes).	Analysis applied to the ABV tunnel (clayey sand). Ground displacements at the tunnel face reasonably predicted. Final ground movements underpredicted.

Table 5.28 Review of Some Three-Dimensional Finite Element Simulations of Tunnel Construction (Continued).

Reference	Purpose of Analyses	Soil Stress-Strain Model	Simulation	Finite Element Features	Comments
16. Negro et al. (1985 and 1986) Present study (Section 5.3.5)	Generalization	Linear elastic (Increasing E with depth)	Unsupported circular excavation of shallow tunnel in in a single step. Incremental excavation as in 13 above for lined tunnel cases. Gravitational stress gradient.	Symmetric mesh, 3.5 x 4.6 x 4.1D, 8 nodes solid elements for soil (and lining), 750 nodes; ADINA program.	Parametric analyses yielding a procedure for estimating radial displacements at the tunnel face contour. Consider variable soil cover and variable K_0 values given by $(\nu/1-\nu)$. The procedure was applied to about 50 case histories and yielded reasonable estimates.
17. Swoboda (1985)	Investigation of behaviour	Linear elastic (?)	Incremental construction simulation with sequential face excavation and delayed lining application.	376 solid isoparametric elements for the soil and 84 shell elements for the lining. FINAL program (Innsbruck).	Investigation of ground movements immediately ahead of the tunnel face. Excessive soil heave below tunnel floor attributed to unrealistic material properties.
18. Pelli et al (1986)	Investigation of behaviour	Linear elastic (Constant E)	Incremental construction simulation with full face stepwise excavation (general approach) and delayed lining application (constant modulus). Deep tunnel and $K_0 = 2$ (constant).	A quarter sector mesh, 8 x 8 x 10D, isoparametric solid elements with 8 to 21 nodes; two slices of elements between tunnel face and liner; shell elements representing liner.	Study of mechanisms of stress redistribution process near the tunnel face, for a rock tunnelling situation. Detected radial stress and displacement reversals (to compression) are important for instrumentation analyses. Lining thrust concentrations detected in leading edge of liner, as in 14 above. Thrusts found to depend on round length (depth of advance).
19. Pelli (1987)	Investigation of behaviour	Linear Elastic (isotropic and anisotropic); non-linear elastic; elastic-plastic	Deep circular tunnel. Unlined opening. $K_0 = 2$. Incremental excavation for for non-linear rock.	Same as above except liner not represented.	Study to provide tools for monitoring data interpretation, including procedure for back-analysis of rock strength and deformational properties. Assessment of the influence of some factors such as the in situ stress state, anisotropy and non-linearity of the stress-strain relationship. Back-analysis of the Donkin-Morien Tunnel (Nova Scotia).

Note: (1) Dimensions of mesh in tunnel diameters (D): width x height x length.

Table 5.28 Review of Some Three-Dimensional Finite Element Simulations of Tunnel Construction (Continued).

explained in Section 2.3.6.4. The excavation was therefore simulated in a single step, on the assumption that the solution of the problem is unique. Ishihara (1971) formally proved the uniqueness of the solution of an excavation problem, assuming the ground to be linear elastic (for a loading which is not path dependent). However, as shown by Ghaboussi and Pecknold (1984:2052), depending on the numerical procedure representing the excavation, the resulting solution may be step-size dependent. As discussed in Section 5.2.1.1, strictly speaking, only the general approach of excavation simulation (see Table 5.2) is step-size independent.

Except for case 1, all other lined cases were simulated through an incremental advance of the tunnel heading followed by an incremental advancement of the lining, which resembles the actual tunnel construction. In order to reduce the cost of the analyses, cases 3, 6 and 9 made use of an expedient through which is avoided the continuously changing geometry of the problem (represented numerically by deactivation and activation of elements). The stiffness matrix of the problem is kept constant, but changing displacement boundary conditions are applied to the tunnel problem according to the displacement output obtained in the previous step, which are then used as an input for the following step. An interactive procedure was developed where the convergence of the solution is monitored through the differences between input and output displacements.

In case 1, a single step excavation and simultaneous lining application was performed. As noted by Wittke and Pierau (1976:1409) and Pierau (1982:1223), the ground displacements taking place before lining installation are not accounted for, and therefore the final calculated movements are too small and the lining stresses too high. To better portray the actual problem, an incremental construction simulation has to be performed for lined tunnels, even if the material behaviour is linear elastic. Having this in mind, the solution adopted in case 11, where the final displacement field was obtained by the superposition of results of a single step advance, is not accurate. Moreover, the numerical superposition is not rigorously valid, since there is a geometric non-linearity resulting from the changing geometry of the problem during the numerical incremental simulation. This inaccuracy however, does not invalidate the conclusions of the comparative study as the same approximation was applied to all cases of TBM performances considered.

With the exception of cases 2, 5, 10, 12, 18 and 19, the studies considered the gravitational in situ stress gradients across the opening, and are therefore actual shallow tunnel analyses. Among these, cases 10 and 12 represent a special type of 3D analysis. They assumed the problem to be geometrically axisymmetric, and made use of solid ring elements with triangular cross sections (Erdmann, 1983:150). However, as explained in Section 4.3.2.6, the solution considers that the stress field is non-symmetric (K_o not equal to 1), with the stresses and displacements being expanded into Fourier Series.

Very limited data are available to serve as a guide for a 3D mesh design. The 'German Recommendations for Underground Constructions in Rock' (DGEG, 1979:198) provide some indications on where to locate the boundaries in a three-dimensional analysis. According to them, for a symmetric mesh, the width should be greater than or equal to three times the opening diameter (D) and the length of the discretized block along the tunnel axis, should be greater than or equal to 4D. The meshes used in the cases included in Table 5.28, had widths varying between 1.6D (case 4) and 8D (cases 18 and 19), and lengths between 2.7D (case 4) and 10D (cases 18 and 19). In terms of element densities, case 2 is noted as an extreme case of a coarse discretization, and case 8 is one of a refined mesh.

Comments have been appended to each case reviewed in Table 5.28, including indications of some of the main findings. One of them refers to thrust concentrations in the leading edge of a lining ring, noted by Schikora (1984:160) and also by Pelli et.al. (1986). This feature was already discussed in Section 2.3.6.3. Unlike Schikora (1984) who found that the liner was always being compressed, Pelli et.al. (1986) found that the trailing edge of the support ring was submitted to substantial tension. The latter would have resulted from the radial rebounding of the leading edge of the support ring immediately behind. This effect, highly consequential in practical terms, may by attenuated by the limited ability of some actual linings to transfer shear through the circumferential joints, in for instance, segmented concrete linings, or in young shotcrete. It would be interesting to know whether this effect persists for different K_o values, for round lengths (depth of tunnel advance) and support activation delays closer to those found in a soil tunnelling situation. This would be represented by a round length of less than half the tunnel radius, and a delay of about two to four tunnel radii.

5.3.4 Numerical Solution Adopted

For developing a procedure to estimate the convergence of the opening behind the face of a shallow tunnel, a three-dimensional finite element solution was needed. The multipurpose program ADINA (Bathe, 1978) was selected for this purpose. For convenience, the modelling procedures including mesh design, stress-strain relationships, construction simulation, etc., used by Heinz (1984:143, 176) were maintained in the present study.

Briefly, the numerical model treated the soil and the lining as isotropic linear elastic materials. Yet, to better represent actual field conditions, the soil modulus was allowed to increase with depth. The tunnel was driven with a shallow soil cover and a gravitational stress field was considered. A non-hydrostatic stress field was assumed with the in situ stress ratio, K, different from unity.

Finite elements with eight nodal points were used to represent both the ground and the liner. As noted by Heinz (1984:144), lower costs and simulation simplifications were the reasons behind favouring this simpler element type. Since the purpose of this study was mainly limited to the displacements developing at the opening, the use of more convenient element types for lining stress evaluation was thought to be unnecessary.

The finite element mesh used is that shown in Figure 5.67, which is the same as used by Heinz (1984:180). The boundaries of the mesh were located following the German recommendations provided by DGEG (1979:198), as they are the only guidance available on the subject (see Section 5.3.3). The circular tunnel had an excavated diameter (D) of 3.9 m. The symmetric mesh had a width of 3.513 D and a length of 4.103 D. Two mesh heights were considered, the total element number being kept constant. The first, representing a shallower tunnel, had a cover to diameter ratio of 1.615 and is the one shown in Figure 5.67 (total height of 4.615D). The second mesh (not shown), representing a deeper tunnel, had a soil cover of 2.833D and a total height of 5.833D. This mesh was obtained from the former by shifting up the nodes located at the ground surface and on the horizontal plane immediately below. This was done in order to not increase the size of the problem and to avoid extremely elongated elements (the maximum aspect ratio allowed was

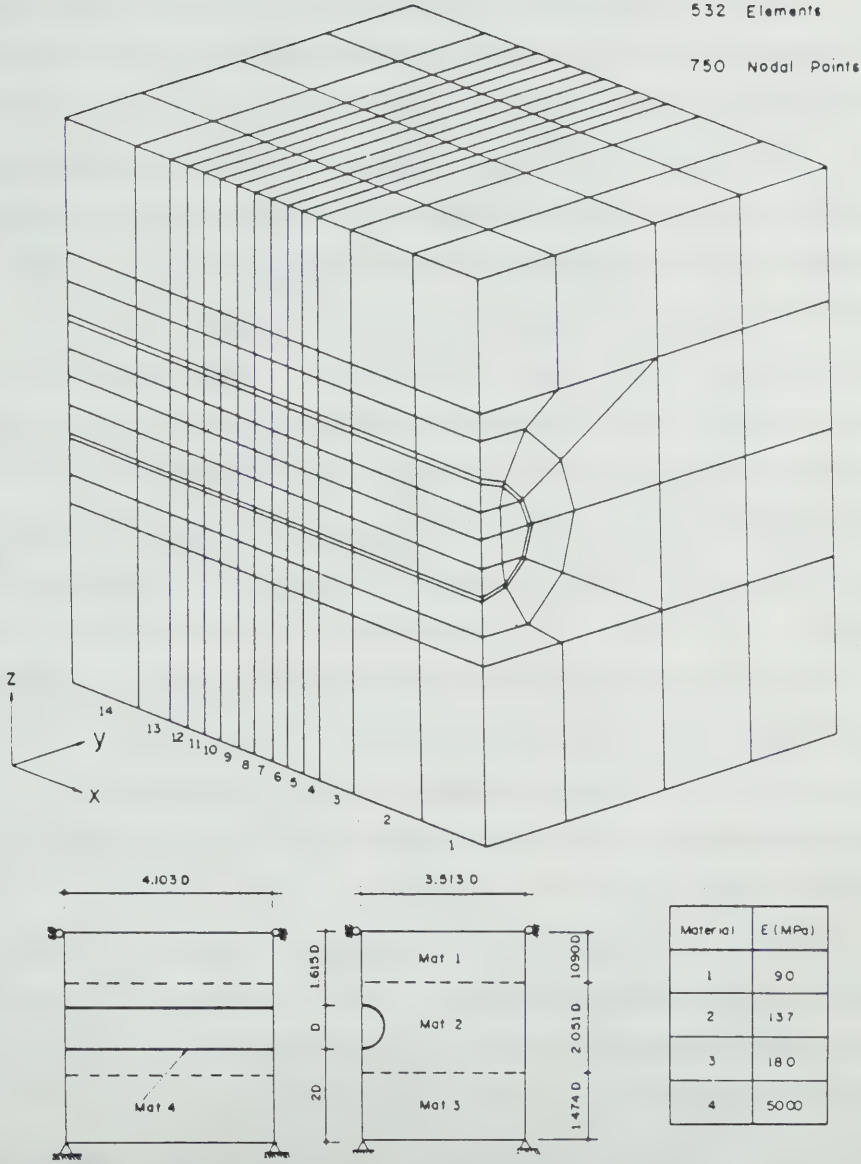

Material	E (MPa)
1	90
2	137
3	180
4	5000

Figure 5.67 Three-Dimensional Finite Element Mesh and Input Parameters

10).

Each "slice" had 38 solid elements and the full mesh was made out 14 slices (a total of 532 elements). The transverse face of each slice contained 50 nodes, resulting in a 750 nodal point mesh. Compared to the discretizations used by other authors (Table 5.28), and as noted by Heinz (1984:143), this mesh presents an element density which is a compromise between relatively coarser meshes (e.g. Descoeudres, 1974) and finer ones (e.g. Katzenbach, 1981 or Pelli et.al. 1986). The slice thickness decreased towards the centre portion to 1/6 of the tunnel diameter and increased agains towards the opposite end. This resulted in a simulation of the construction sequence in the central area.

All analyses were conducted with a premliminary step corresponding to the establishment of the initial conditions. This was performed by the application of gravity and the in situ stress ratio, K, results as a function of the Poisson's ratio, ν. From then on, two types of construction simulation were implemented depending on the tunnel being lined or unlined. Both simulations assumed a full face excavation. For the unsupported case, there was no need to represent the incremental construction. The excavation was thus simulated in a single step, where the elements within the excavated contour were de-activated from slice 1 to slice 7. For the analysis of the lined tunnel, a stepwise de-activation of excavated elements was implemented, followed by the gradual and delayed (in space) activation of the support. The central part of the mesh was reached after 6 additional steps. In each step, elements of one or two consecutive slices were simultaneously activated and de-activated. This simulation procedure was identical to that used in the work by Eisenstein et.al. (1984), by Heinz (1984:176) and also described in Section 2.3.6.4. In the lined tunnel cases, due to the irregular thickness of slices used, to the varying number of slices being cut through by the excavation, and to the proximity of the boundaries, the radial displacements calculated at the first three slices were found to oscillate irregularly and were thus neglected. The results to be presented refer to the central portion of the mesh more densely discretized with equal thickness slices, through which the face was advanced with constant depth of advance, or round length (always equal to D/3).

The activation or de-activation of elements was performed by the ADINA program using its 'birth-death' option, which allows an excavation simulation that follows the 'general approach' procedure referred to in Section 5.2.1.1 (see Table 5.2). While the excavation round length for the lined cases was kept constant and equal to D/3, the support activation delay was varied in the analyses. Two maximum unsupported distances, L, between the face and the leading edge of the liner were considered: D/2 and 2D/3.

The arbitrary modulus of the materials represented are shown in Figure 5.67, and these were kept constant in all analyses. As it is seen, the ground modulus increased with depth in a discrete manner. The tunnel was totally driven through the material 2 layer. In the supported tunnel analyses, a lining with a thickness of 15 cm was selected. If a Poisson's ratio of 0.25 is assumed for both support and ground, the relative stiffness of the support calculated according to equations 2.17 and 2.18 result in C=0.034 and F=64.2.

In the analyses performed, different in situ stress ratios were considered by varying the Poisson's ratio accordingly. The original version of ADINA used in this work (Heinz, 1984:83), did not allow other approaches besides the "switch - on - gravity" (see Section 5.2.1.1) to represent the in situ stresses in a gravitational stress field. This is a clear shortcoming of the simulation procedure adopted: in actual cases K is independent of ν. The effect of changes in ν alone is however, known to be small at the face or ahead of it, as shown in Figure 5.66 (see also Ranken and Ghaboussi, 1975:3.13).

The assumption of linear elasticity is another drawback of the simulation adopted. The numerical simulation would then be valid only in the case of limited development of yielding zones around the opening. Thus, the results to be presented would be mainly applicable to stiff or dense soils, where a good ground control construction is implemented. It could also be applied to softer or weaker grounds if an internal pressure (compressed air or slurry) is applied to the tunnel walls and face, which would ensure a limited degree of yielding around the tunnel. Results from axisymmetric analyses (Ranken and Ghaboussi, 1975:3.32; Panet and Guenot, 1982:199), have shown that this is the case with tunnels in cohesive soils with stability ratios of up to 1.5. Under these conditions the plastic behaviour of the ground, ignored in the present study, would increase the radial displacements by no more than 20%.

The assumption of linear elaticity is perhaps less restrictive regarding the behaviour of the ground ahead of the face. Under good ground control conditions the amount of straining ahead of the advancing tunnel is limited and the deformation modulus of the soil could be taken as the initial tangent modulus (E) of a representative stress-strain curve of the soil around the tunnel.

5.3.5 Parametric Analyses

5.3.5.1 Analyses and Results

In order to investigate the influence and significance of distinct factors affecting the tunnel convergence, some parametric three-dimensional analyses were conducted.

The tunnel diameter (D) and the ground modulus (E) profile were kept constant in all analyses. With respect to the unlined tunnel cases, the assumption of linear elasticity makes the variation of the ground modulus unnecessary, as the displacements are linearly related to it (for a proportionally changed modulus profile). In the analyses, variations in the unsupported tunnel length (L/D), in the depth of ground cover (H/D) and in the in situ stress ratio ($K=\nu/(1-\nu)$) were allowed. Table 5.29 summarizes the details of the parametric analyses.

It is convenient to express the radial displacements of the tunnel contour in the dimensionless form presented by equation 2.16 in Section 2.3.4.3:

$$U(\theta)= \frac{u.E}{D.\sigma_0(\theta)}$$

where θ defines the point considered at the perimeter of the tunnel, $U(\theta)$ is the radial displacement of this point and $\sigma_0(\theta)$ is the in situ radial stress at that point. The elastic modulus E is the one attributed to the second material layer which fully surrounds the tunnel.

Figures 5.68 to 5.70 present the distribution of the dimensionless radial displacements along the tunnel, at three points of the tunnel contour (crown, springline and floor, respectively) for cases 1, 2 and 3 combined (H/D=1.6). The distributions shown are confined to the central region of the finite element element mesh (about 2D in extent). As explained in Section 5.3.4, the calculated radial displacements at the first three slices in the lined tunnel cases (1 and 2) are not representative and were therefore, disregarded. Nevertheless, the lined cases exhibit some oscillation in the radial displacement distribution, which was a feature explained in Section 2.3.6.3, and was found by other authors in similar studies.

Case	H/D	Type	L/D	ν	K
1	1.615	Lined	1/2	0.430	0.75
2	1.615	Lined	2/3	0.430	0.75
3	1.615	Unlined	-	0.430	0.75
4	1.615	Unlined	-	0.375	0.60
5	1.615	Unlined	-	0.459	0.85
6	1.615	Unlined	-	0.474	0.90
7	2.833	Lined	1/2	0.430	0.75
8	2.833	Lined	2/3	0.430	0.75
9	2.833	Unlined	-	0.375	0.60
10	2.833	Unlined	-	0.474	0.90

Notes: (1) D = 3.90 m
(2) In all cases E = 13,694 KPa around opening (material 2).
(3) In all cases γ = 15.19 kN/m^3 for material 1 and 18.13 kN/m^3 for materials 2 and 3.

Table 5.29 Cases of Three-Dimensional Analyses

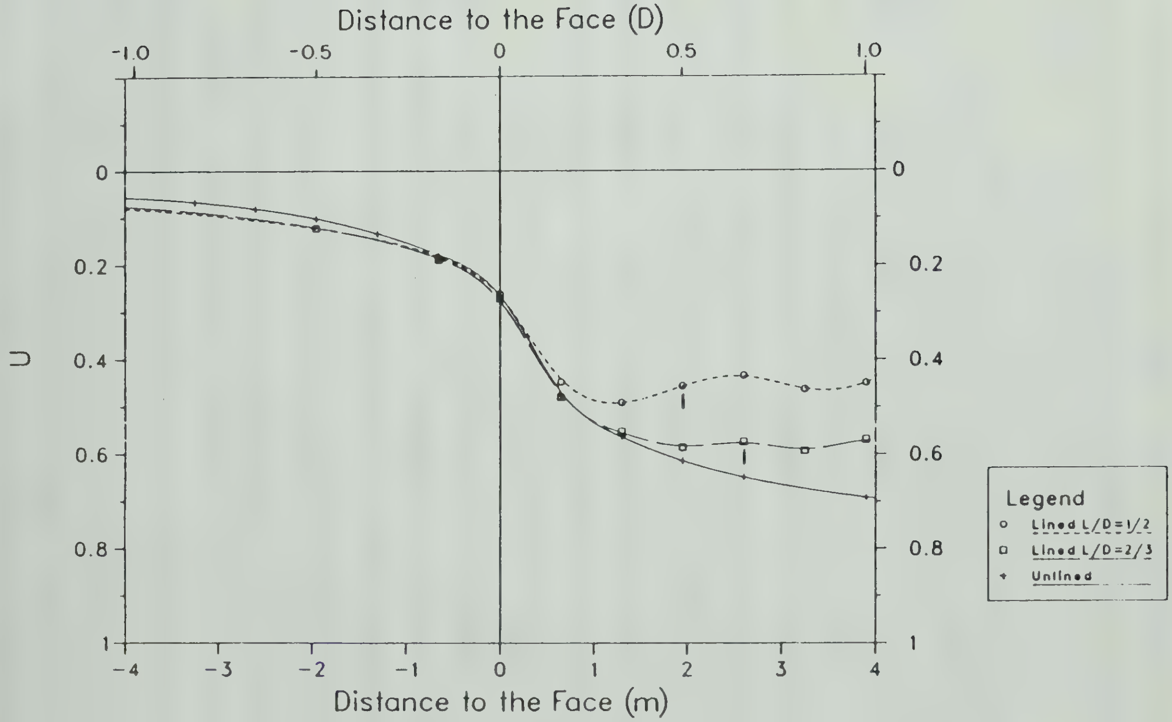

Figure 5.68 Dimensionless Radial Displacements at the Crown of a Lined and Unlined Shallow Tunnel (H/D=1.6 and K=0.75)

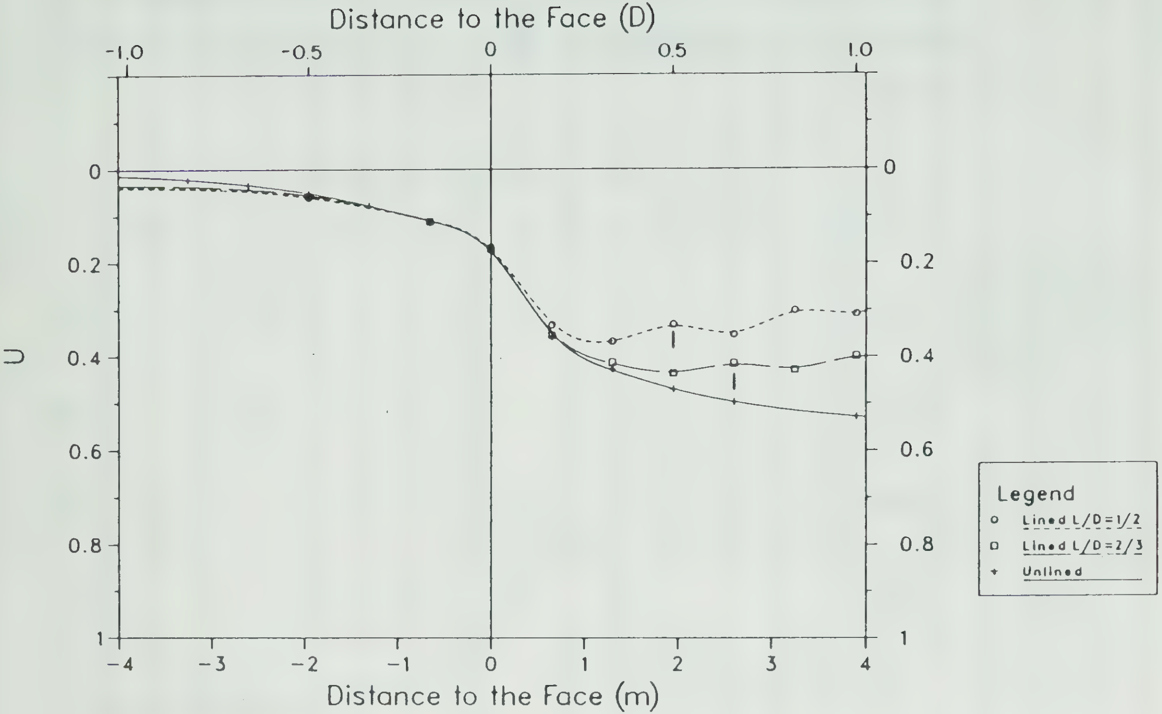

Figure 5.69 Dimensionless Radial Displacements at the Springline of a Lined and Unlined Shallow Tunnel (H/D=1.6 and K=0.75)

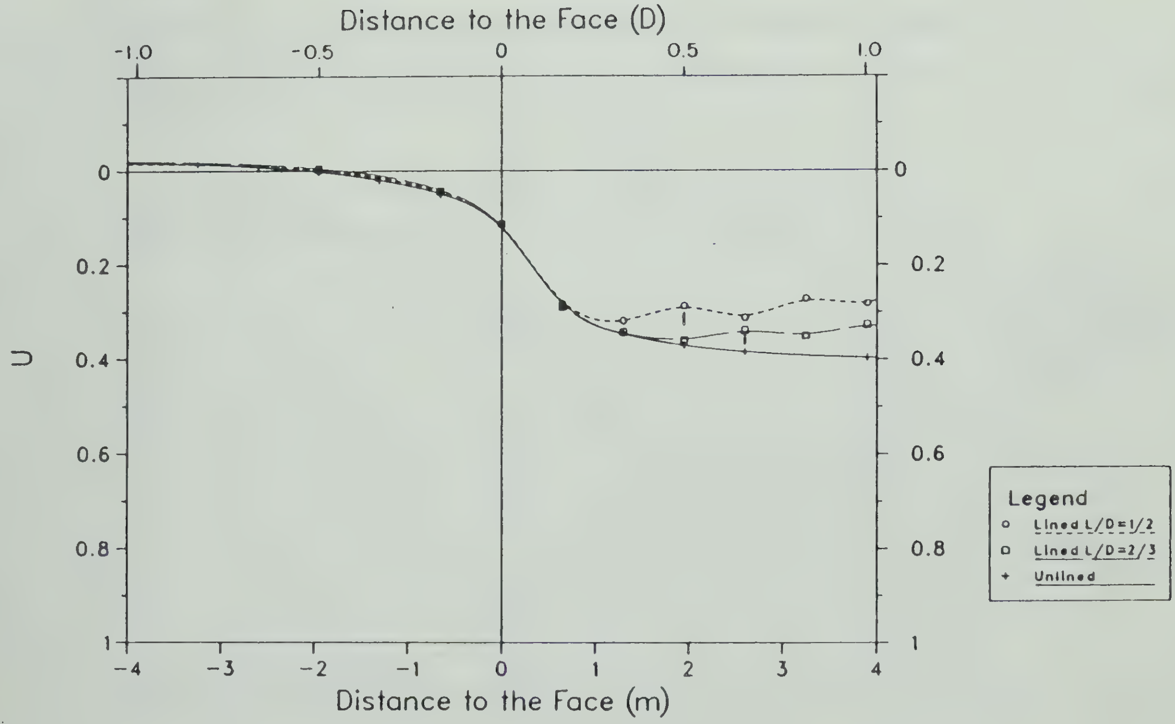

Figure 5.70 Dimensionless Radial Displacements at the Floor of a Lined and Unlined Shallow Tunnel (H/D=1.6 and K=0.75)

It is noted from these figures that the displacements ahead of the tunnel face are not affected much by the presence of the lining. The radial displacements at the face, in particular, are virtually unaffected by the distance to the point of lining placement. This finding confirms conclusions drawn by other authors. Ranken and Ghaboussi (1975:3.57, 3.58) showed that if the lining is installed at distances greater than half a tunnel diameter, the radial displacements at the tunnel face are not affected by the lining installation. Moreover, Erdmann and Duddeck (1984:180) showed that this seems to be correct irrespective of the lining stiffness. The results shown by Pelli et.al. (1986), who used a more refined finite element mesh, support these conclusions.

The same conclusions are drawn by comparing the results of cases 9 and 10, which refer to a deeper tunnel with H/D=2.8. These are shown in Figures 5.71 to 5.73. Note that in these figures, the solid lines represent the unlined case of the shallower tunnel (H/D=1.6). The only difference noted between the two sets of plots for the shallower and the deeper tunnel cases refers to the magnitude of the radial displacements, especially behind the face. Since the radial displacements were normalized to the in situ radial stresses, the effect of the stress level is fully accounted for. However, the effect of the ground surface is not. Therefore, the dimensionless displacements for the shallower tunnel would be expected to be larger than that for the

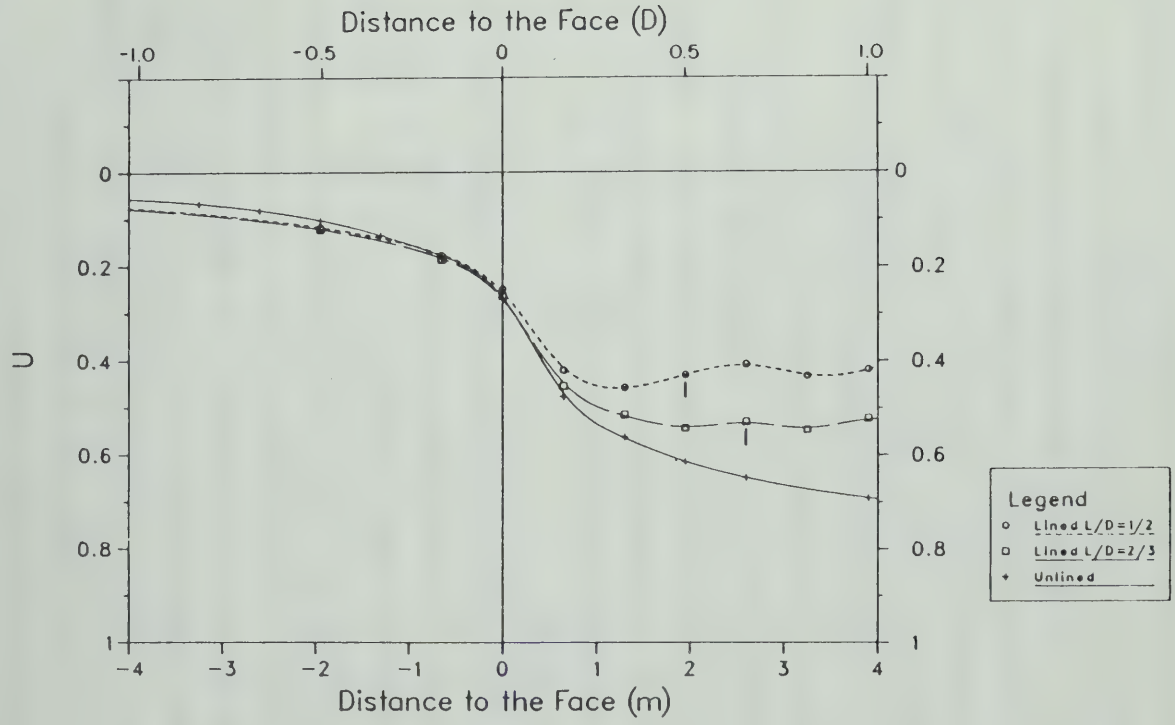

Figure 5.71 Dimensionless Radial Displacements at the Crown of a Lined and Unlined Deeper Tunnel (H/D=2.8 and K=0.75)

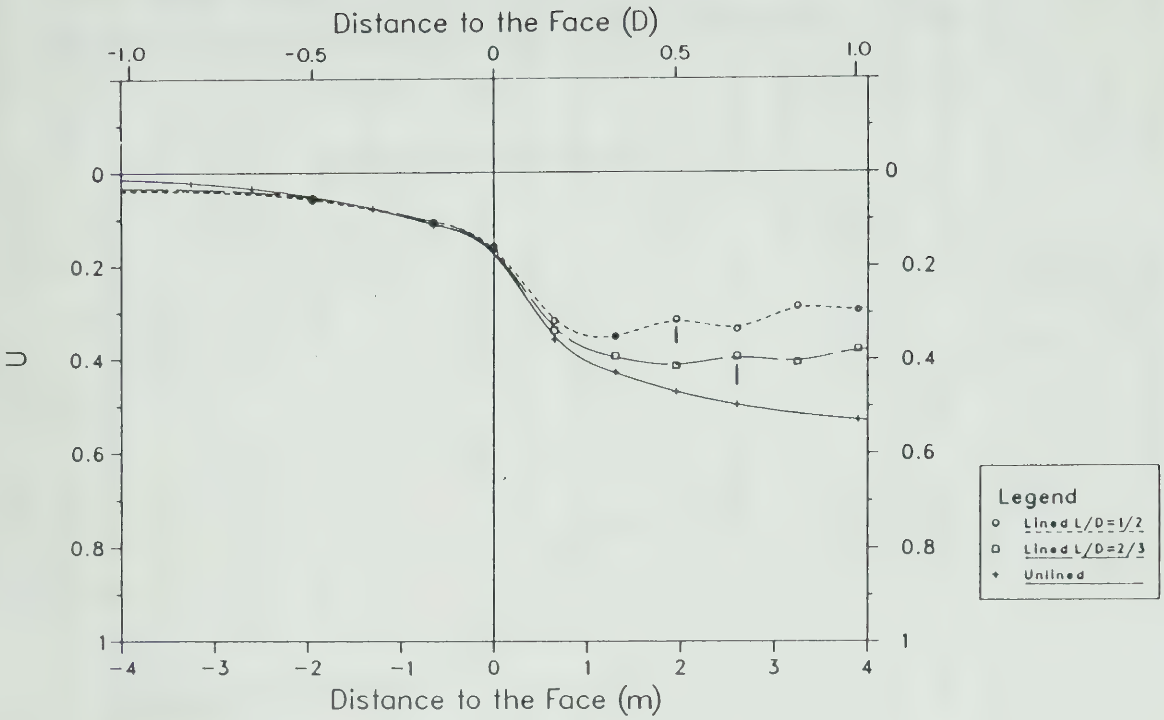

Figure 5.72 Dimensionless Radial Displacements at the Springline of a Lined and Unlined Deeper Tunnel (H/D=2.8 and K=0.75)

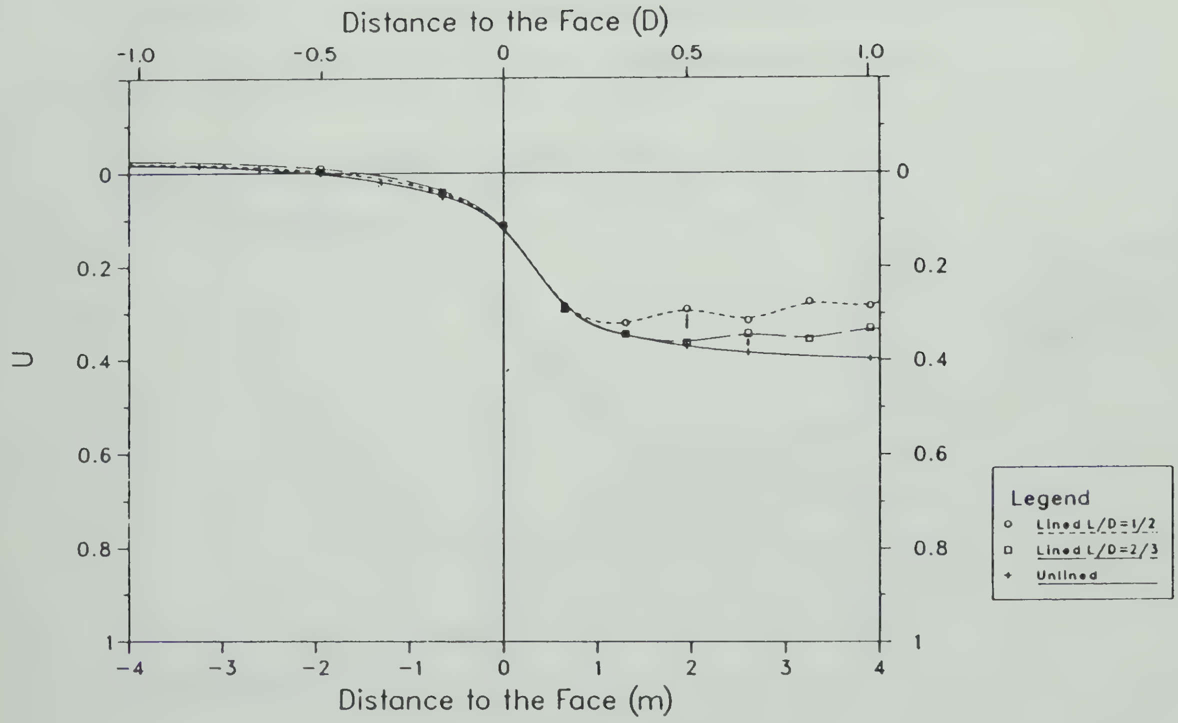

Figure 5.73 Dimensionless Radial Displacements at the Floor of a Lined and Unlined Deeper Tunnel (H/D=2.8 and K=0.75)

deeper configuration, as the thicker cover in the latter case offers a "stiffer" reaction to the stress changes. Notwithstanding this, it appears from the two sets of plots that the differences in the dimensionless displacements amount to less than 10%, for the range of cover to diameter investigated and for the other assumptions made. The difference in the displacements at the face are virtually nonexistent. These results are very much in agreement to what was discussed in Section 2.2. It was shown there that the influence of the ground surface on the behaviour of the lining or on the ground immediately around the opening is negligible for H/D greater than 1.5. The influence of the gravitational stress gradient, however, is evident. The latter is accounted for by using the radial stress at the point being considered, to normalize the corresponding radial displacement.

An additional conclusion from the last two sets of plots is that the tunnel closure at the point of lining installation is affected by the presence of the lining, as already discussed in Section 5.3.2. However, the relative error involved in estimates of the convergence assuming the tunnel is unlined, tends to decrease for increasing support delay lengths, L/D. If the unlined case results were to be used as a basis for evaluating the tunnel closure for a real situation, on one hand they would lead to an overestimate of the tunnel contour displacements. On the other hand, they could lead to underestimates, as the actual non-linear behaviour of the ground is not accounted for. A complete solution to the problem, including the lining action inhibiting the ground movements and the non-linearity of the soil behaviour which increases the movements with respect to the linear elastic solution, is not possible at the moment as it is too complex. As a compromise and as an ad interim solution, it will be assumed that those errors involved in a solution derived from linear elastic unlined tunnel analyses will be compensated for.

To illustrate the last point, Figure 5.74 has been prepared using data from Ranken and Ghaboussi (1975) axisymmetric analyses. The parameters used in these analyses are shown in the figure. The wall closures for an unlined tunnel assuming a linear elastic behaviour, are compared to that of two lined tunnels, with support installed at L/D=0.5 and where an elasto-plastic ground behaviour was assumed. In one case, a purely cohesive behaviour has been postulated and in the other, a c-ϕ material behaviour has been assumed. It is observed that at the point of lining application (0.5D), the dimensionless displacement of the unlined solution is almost equal to those obtained in the lined cases.

It should be pointed out, however, that the compensation for errors cannot always be conceded, as it depends on a number of factors. Thus, considerable caution should be exercised in any attempt to generalize the results of linear elastic unlined tunnel solutions to actual

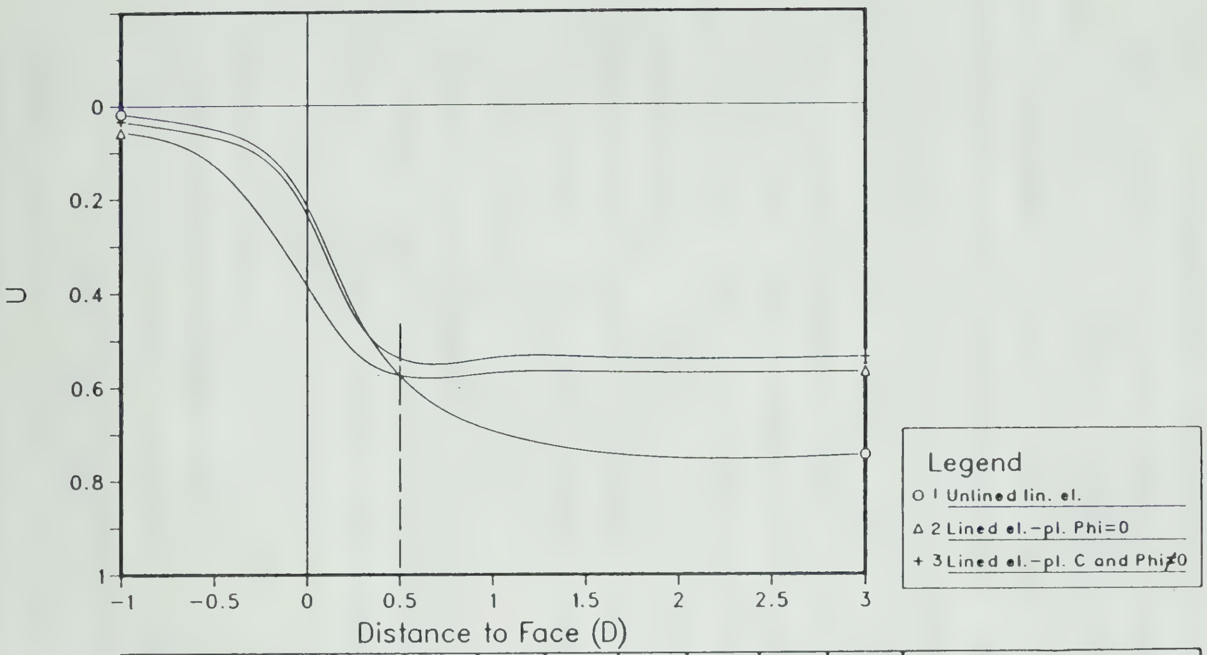

CASE	D (m)	σ_0 (kPa)	K_0	E (kPa)	ν	C (kPa)	ϕ (°)	t_s (m)	E_s (GPa)	ν	No. OF FIG. IN RANKEN AND GHABOUSSI (1975)
1	6.096	575	1.0	34.5	0.49	-	-	-	-	-	3.7
2	"	"	"	"	"	96.5	0	0.305	13.8	0.15	3.38
3	"	"	"	"	0.40	"	30	"	"	"	3.47

NOTE; IN CASES 2 AND 3 THE LEADING EDGE OF THE SUPPORT IS LOCATED 0.5 D BEHIND THE FACE.

Figure 5.74 Closure of an Unlined Tunnel in Elastic Ground Compared to that of Lined Tunnels in Elasto-Plastic Material

problems.

The calculated dimensionless displacements at the crown of an unlined tunnel are shown in Figures 5.75 and 5.76, for the shallower tunnel situation (cases 3, 4, 5 and 6 in Table 5.29) and for the deeper cases (9 and 10) respectively. The differences in the distributions of the radial displacements are due to the differences in the in situ stress ratio K, but they also reflect the variation in Poisson's ratio. The influence of the latter is less pronounced since it was varied within fairly narrow limits (from 0.375 to 0.474). The error involved in neglecting the effect of the variation of the Poisson's ratio can be estimated in an approximate way from the solution presented in Figure 5.66, developed the analyses of a deep tunnel (Niwa et.al., 1979). Since in that solution K and ν are independent variables, the influence of each parameter can be assessed individually. For instance, assuming a K value of 0.75, an increase in the Poisson's ratio from 0.25 to 0.4 will cause an increase in the dimensionless radial displacement at the crown or at the floor of about 1.5% for a section at the tunnel face, and of about 4.4% at a section a half diameter behind the face. It will be noted that the influence of the Poisson's ratio is more pronounced on the springline displacements (approximately 4 times larger than at the crown). However, considering the approximate nature of the solution being sought, it will be assumed henceforth that the differences in the displacements shown in the last figures are mainly

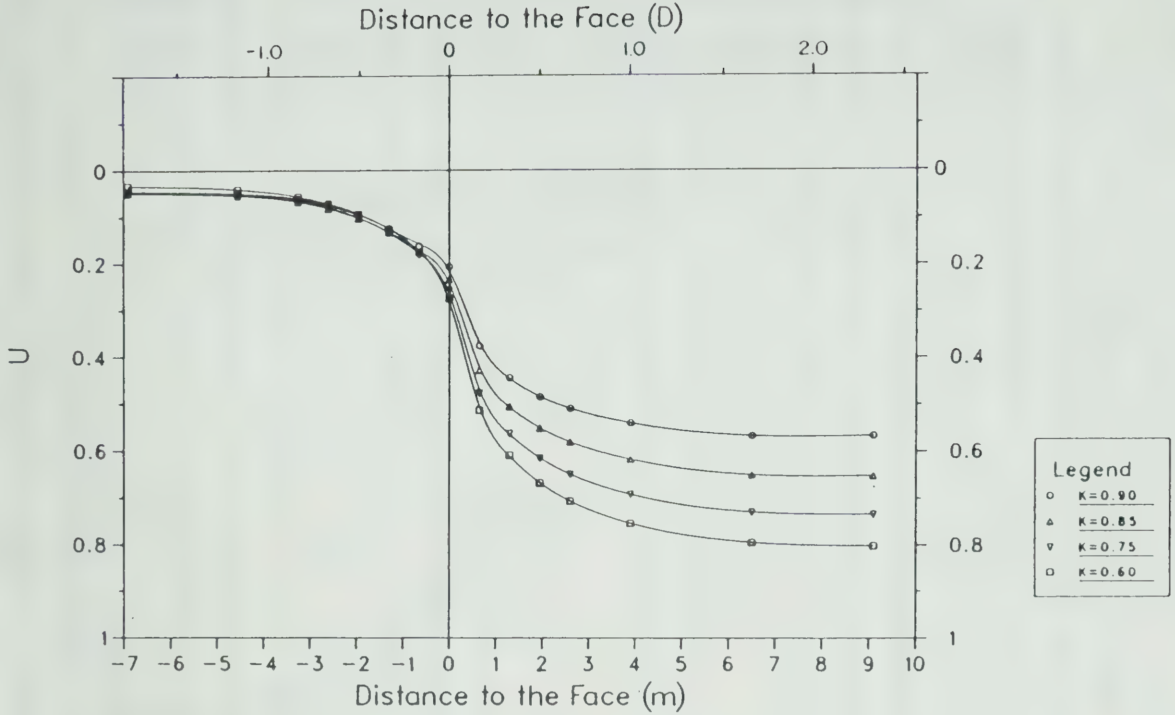

Figure 5.75 Dimensionless Crown Displacements of the Shallower (H/D=1.6) Unlined Tunnel for Different In Situ Stress Ratios K

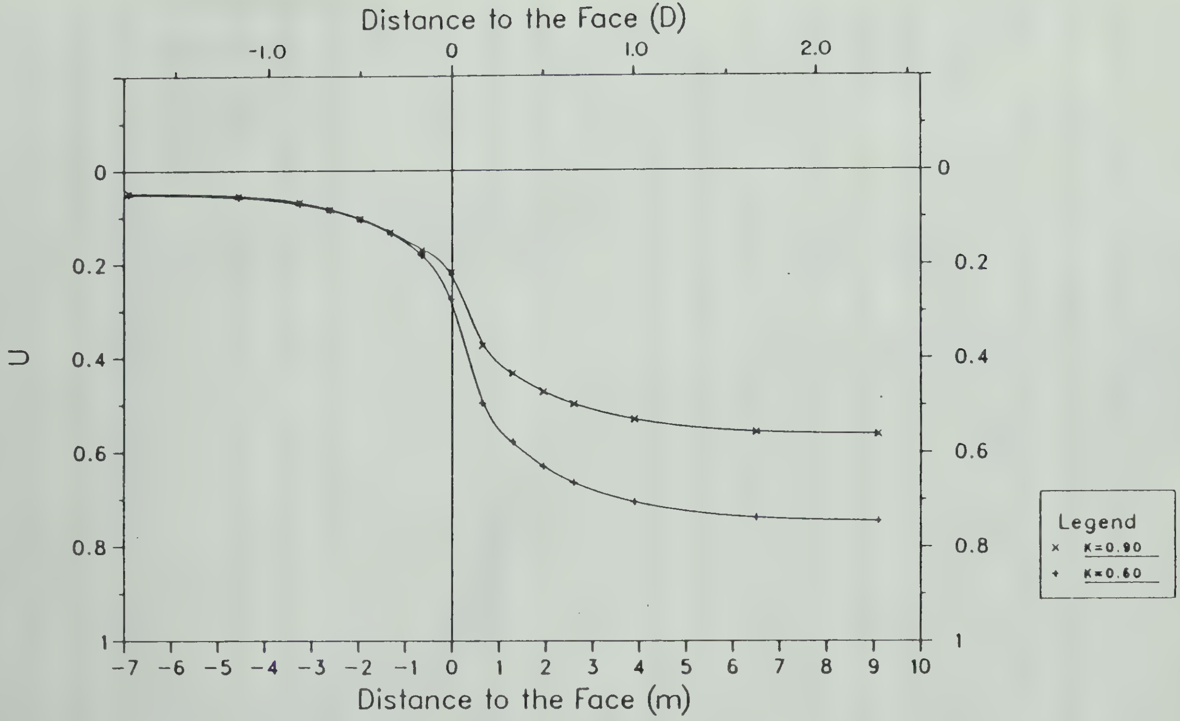

Figure 5.76 Dimensionless Crown Displacements of the Deeper (H/D=2.8) Unlined Tunnel for Different Stress Ratios K

due to the changes in the in situ stress ratio.

Similarly, Figures 5.77 and 5.78 present the dimensionless radial displacements at the springline of an unlined tunnel for the shallower and the deeper tunnel cases, respectively. It should be noted here that, unlike the deep tunnel solution for springline displacement shown in Figure 5.66, the present results of displacements have been normalized to the radial in situ stress at the tunnel springline. Therefore, if the present results are to be compared with those shown in Figure 5.66, they have to be multiplied by the corresponding K value.

Finally, Figures 5.79 and 5.80 furnish the dimensionless radial displacements at the floor of an unlined tunnel for the same cases.

The effect of the ground surface on the dimensionless displacements of the unlined tunnel can be evaluated by comparing the results obtained for the shallower and deeper tunnel cases. These comparisons are provided in Figures 5.81 to 5.83, for the crown, springline and floor of the tunnel respectively. As noted in the lined tunnel cases, the deeper the tunnel is, the smaller the dimensionless radial displacements are. The floor displacements are virtually unaffected by the position of the ground surface. Overall, the differences in the dimensionless radial displacements are relatively small for the two cover to diameter ratios considered, and these fairly well encompass the most frequent situations found in practice. Likewise, the range

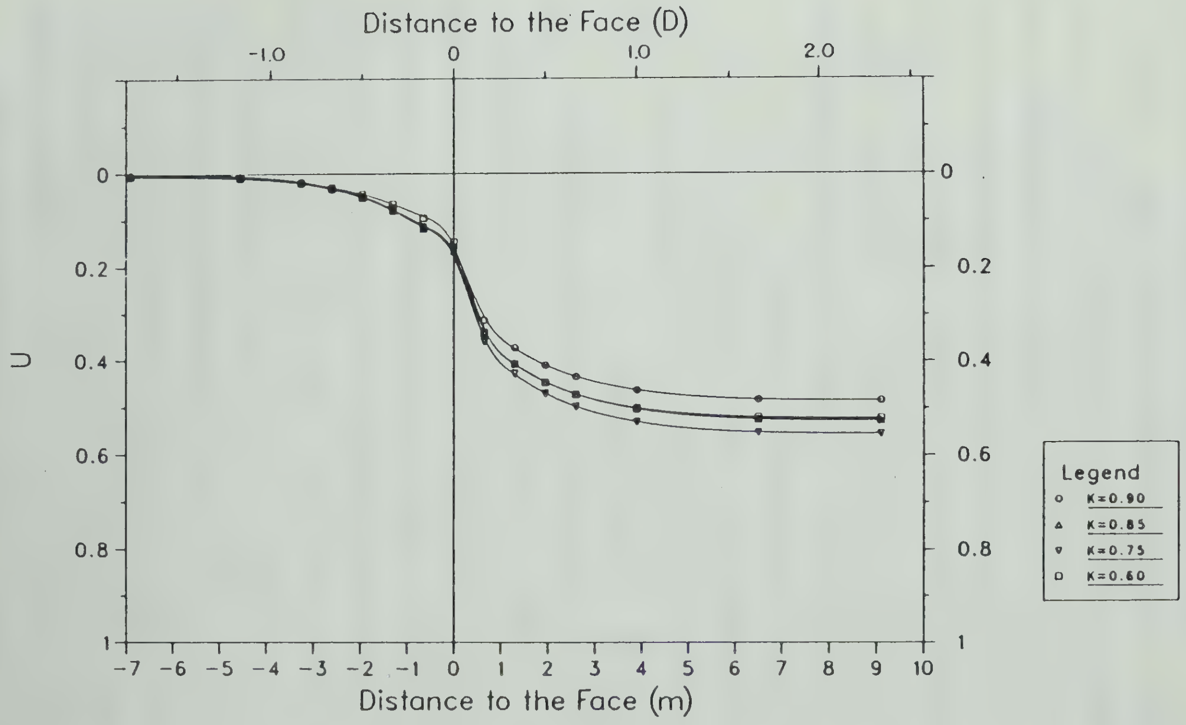

Figure 5.77 Dimensionless Springline Displacements of the Shallower (H/D=1.6) Unlined Tunnel for Different Stress Ratios K

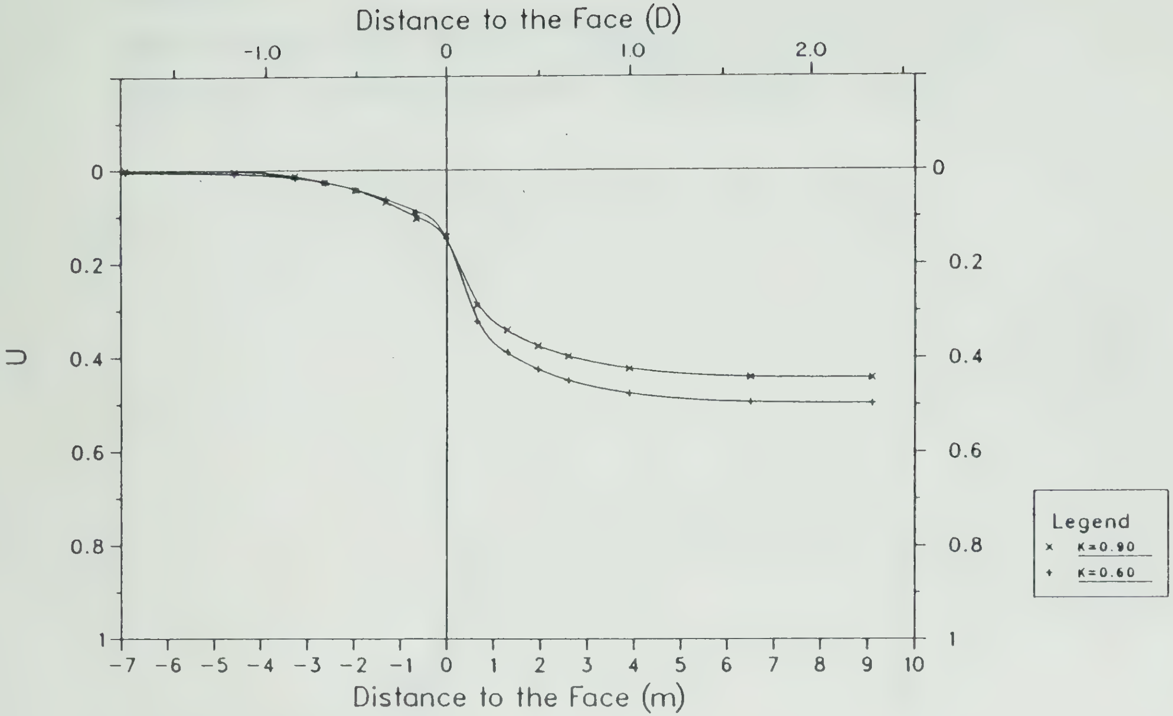

Figure 5.78 Dimensionless Springline Displacements of the Deeper (H/D=2.8) Unlined Tunnel for Different Stress Ratios K

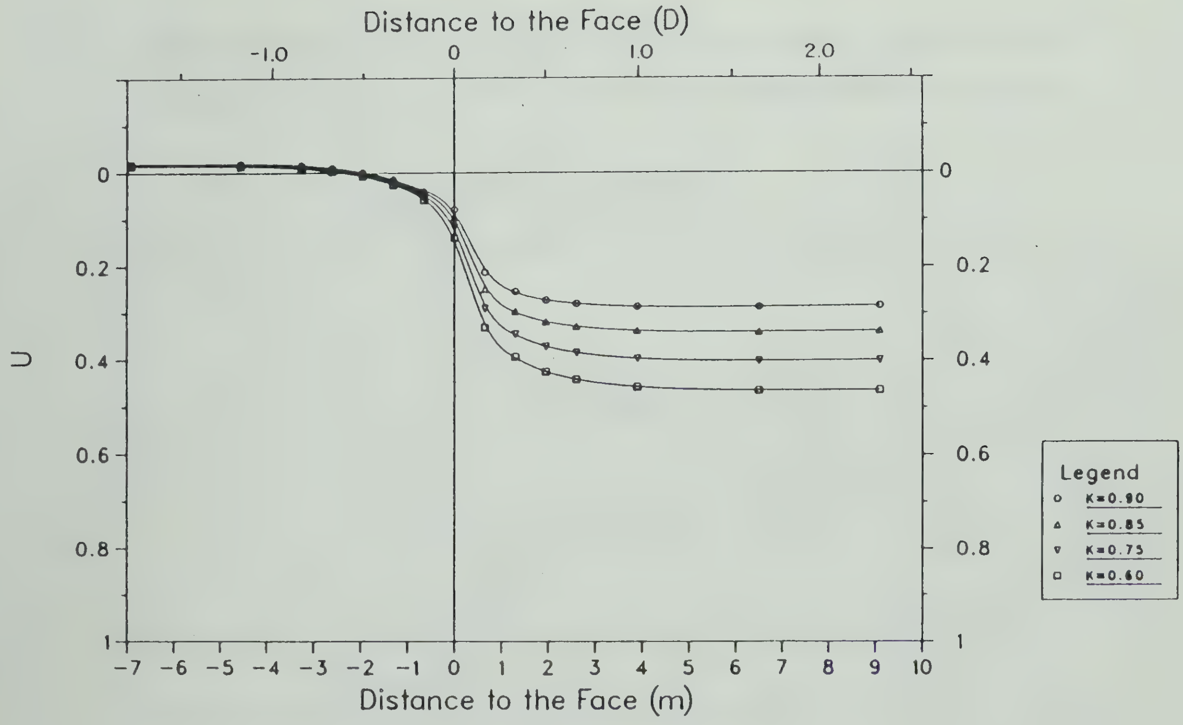

Figure 5.79 Dimensionless Floor Displacements of the Shallower (H/D=1.6) Unlined Tunnel for Different Stress Ratios K

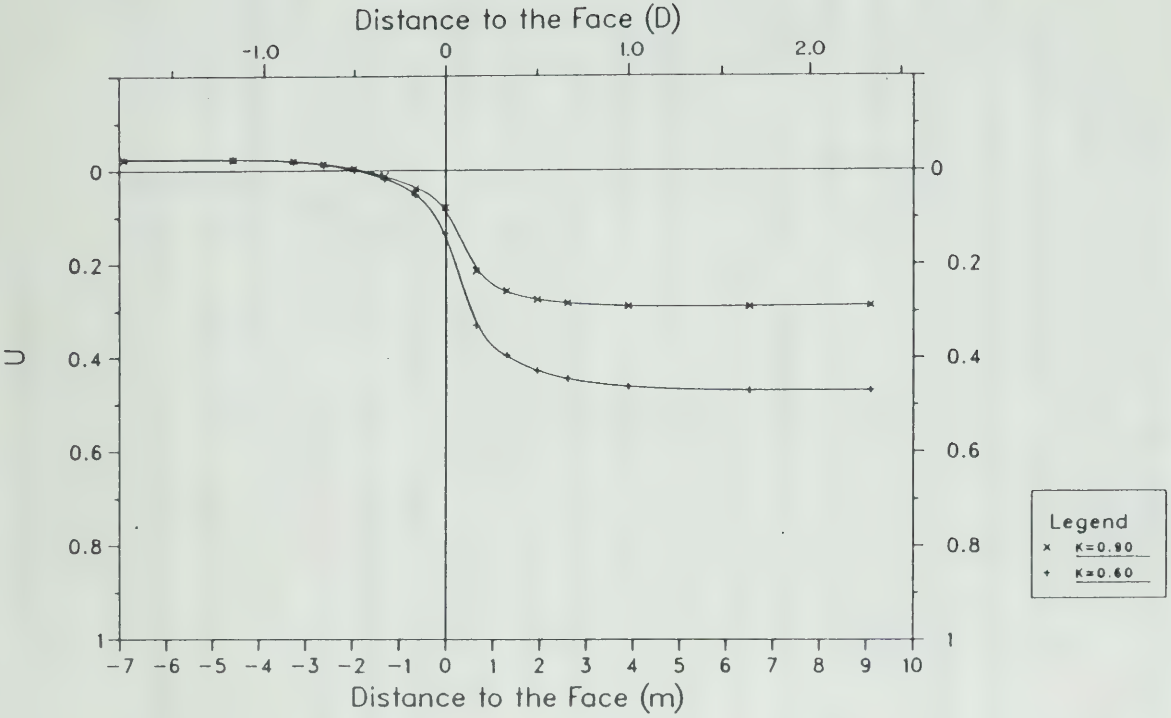

Figure 5.80 Dimensionless Floor Displacements of the Deeper (H/D=2.8) Unlined Tunnel, for Different Stress Ratios K

of the in situ stress ratio considered seems to also include a fairly large number of soil conditions found in practice.

So far the data presented refer to the radial displacement at the tunnel contour. To supplement this information, Figures 5.84 and 5.85 were prepared. They present additional data on the ground displacements around the unlined tunnels. For convenience, the displacements are presented in dimensionless form, and were normalized to the in situ radial stress at the crown of the tunnel. In these figures, the vertical ground movements, either settlement or heave, at four vertical sections are shown, as well as the longitudinal distributions of displacements at the ground surface and at the crown elevation, for the two extreme values of K considered in the parametric analyses. The horizontal displacements of the tunnel face are also presented. The effect of increasing the cover to diameter ratio is apparent by comparing those two figures. The dimensionless displacements tend to decrease everywhere. Ground distortions at the surface or at the crown elevation also decrease. A similar effect is noted by increasing the in situ stress ratio, except with respect to the face horizontal movements, which tend to increase with increasing K.

5.3.5.2 Interpretation of the Results

Closure of an Unlined Tunnel

It was shown in the previous section (Figure 5.65) that for an unlined and ideally deep tunnel, a linear

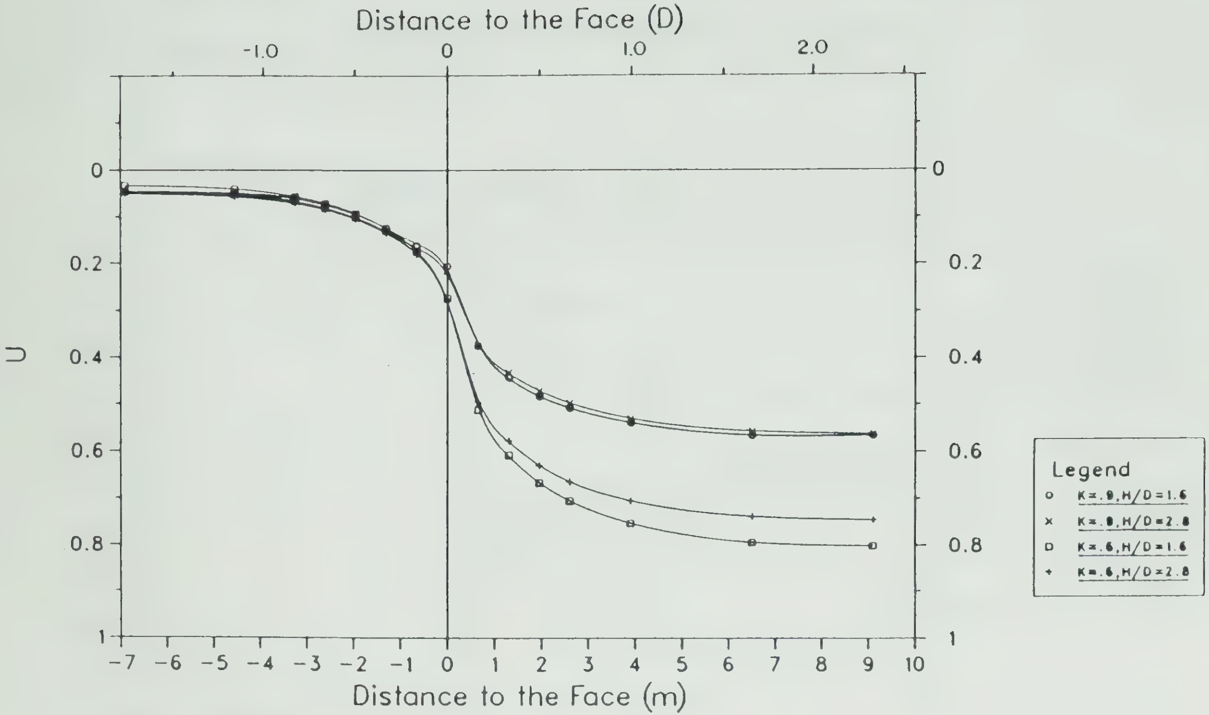

Figure 5.81 Comparison of Dimensionless Crown Displacements of the Shallower and Deeper Unlined Tunnels

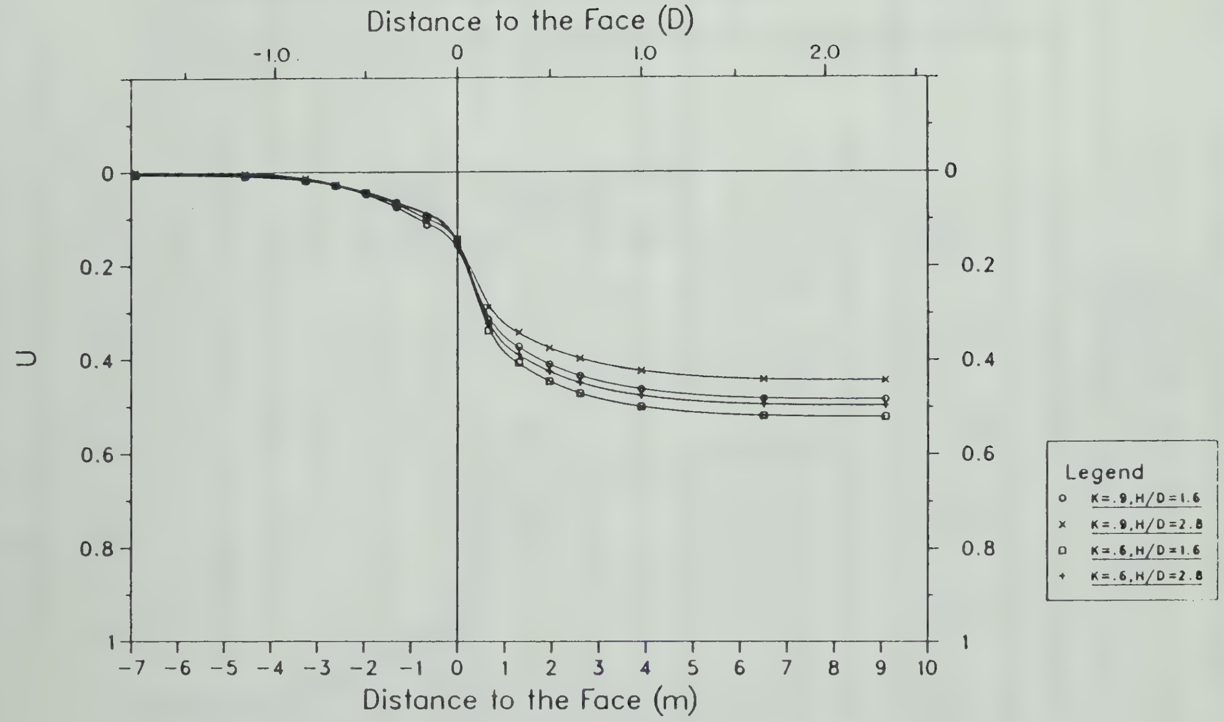

Figure 5.82 Comparison of Dimensionless Springline Displacements of the Shallower and Deeper Unlined Tunnels

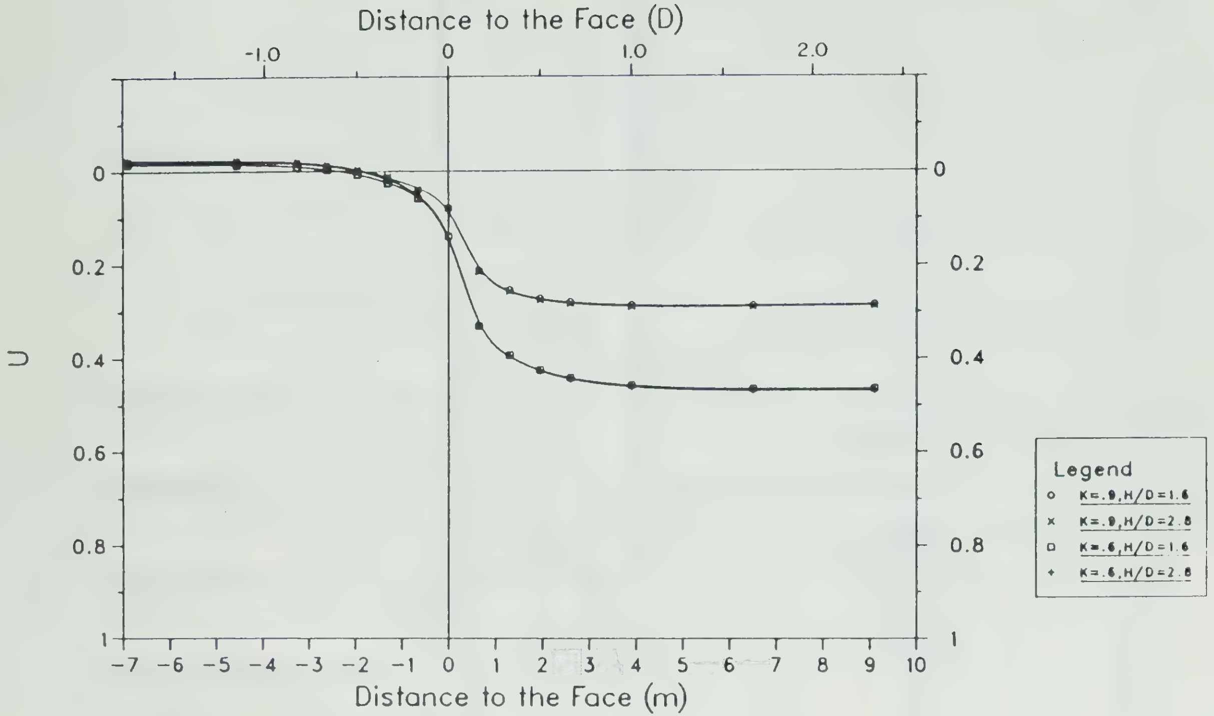

Figure 5.83 Comparison of Dimensionless Floor Displacements of the Shallower and Deeper Unlined Tunnels

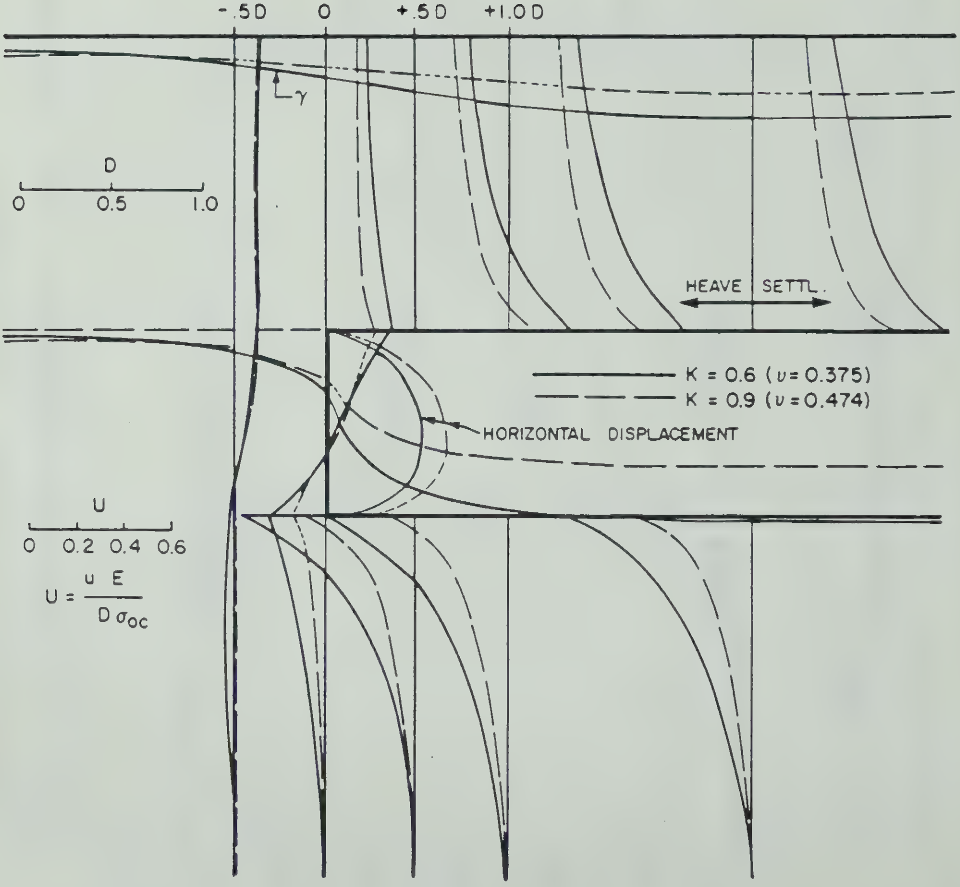

Figure 5.84 Ground Movements in the Vertical Longitudinal Plane of the Shallower (H/D=1.6) Unlined Tunnel

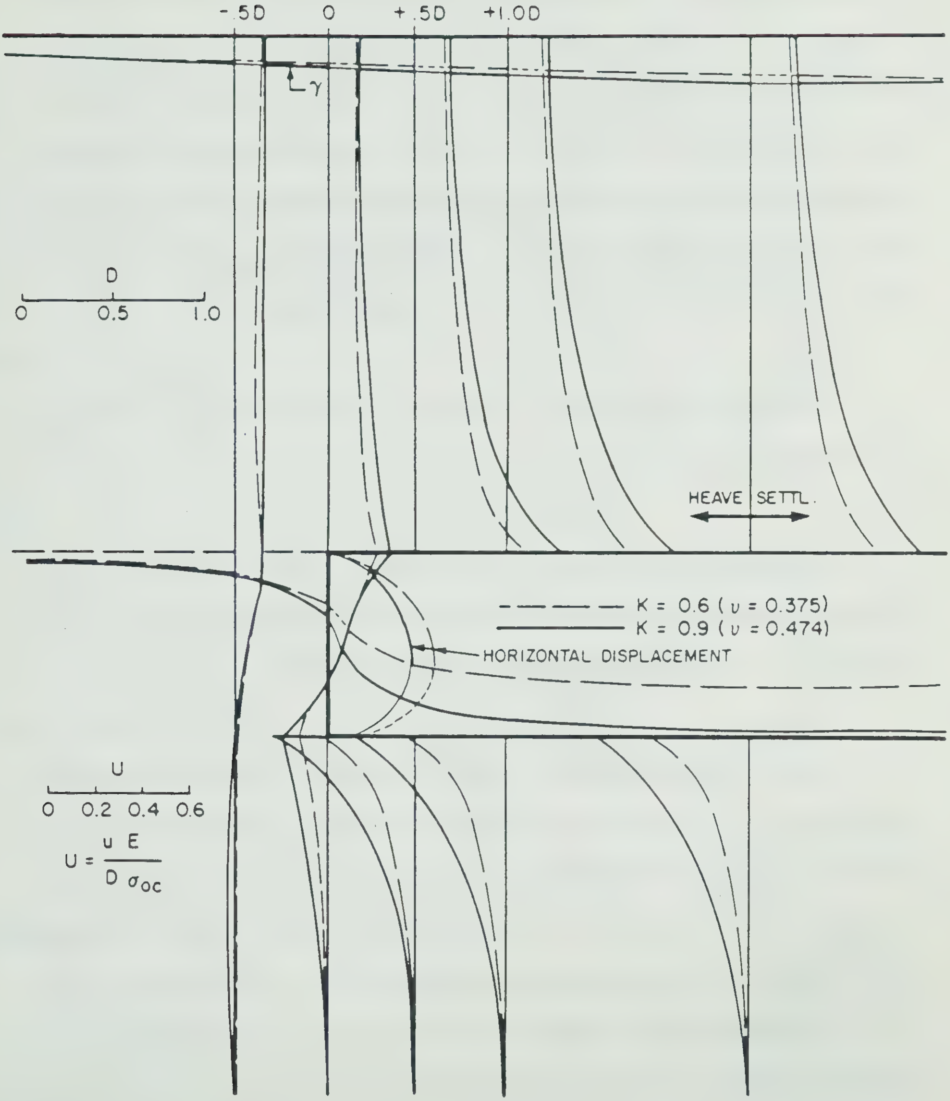

Figure 5.85 Ground Movements in the Vertical Longitudinal Plane of the Deeper (H/D=2.8) Unlined Tunnel

relationship exists between the dimensionless radial displacements of the tunnel wall and the in situ stress ratio, at a given section of the tunnel. If a linear relation is assumed to exist also for a shallow tunnel, one may be tempted to identify such a relationship, from the results obtained through the three-dimensional analyses of the unlined shallow tunnel. For the tunnel crown and floor, this relationship could be expressed as:

$$U = a - bK \qquad [5.6]$$

For the springline, the development shown in Figure 5.66 showed the following relation:

$$U_s = aK - b \qquad [5.7]$$

Considering however the distinct definition of the dimensionless displacement, U, being adopted herein, one obtains at the springline:

$$U = \frac{U_s}{K} \text{ therefore } U = a - b/K \qquad [5.8] \quad [5.9]$$

The coeffiecients a and b for the three particular locations of the tunnel contour (crown, springline and floor), can be obtained at different sections along the tunnel, which are defined in terms of the relative distance, X/D, between the face and the position of this section.

For sections located at X/D = 0 to 2, figures 5.86 to 5.90 present the dimensionless displacement U as a function of K, from the finite element analyses of both the shallower and deeper unlined tunnel cases. At the sections not coinciding with a face of the 3D mesh slices (X/D=0.25 and 2), the displacements were interpolated from adjacent nodal

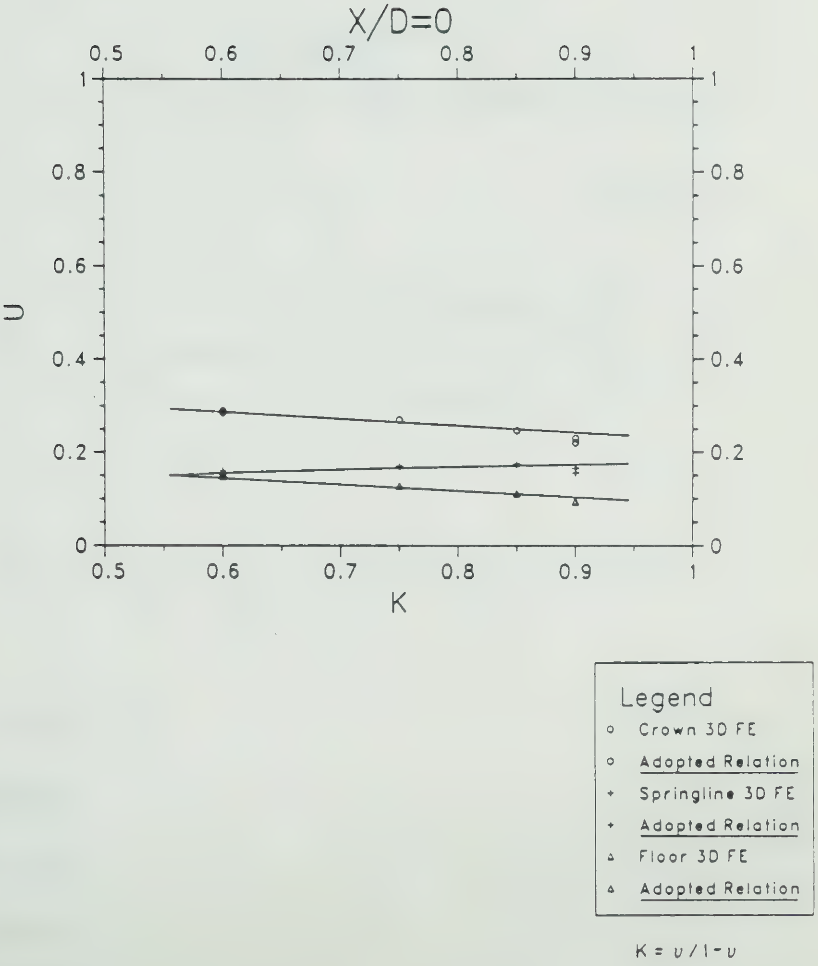

Figure 5.86 U and K Relationships for the Section at the Face

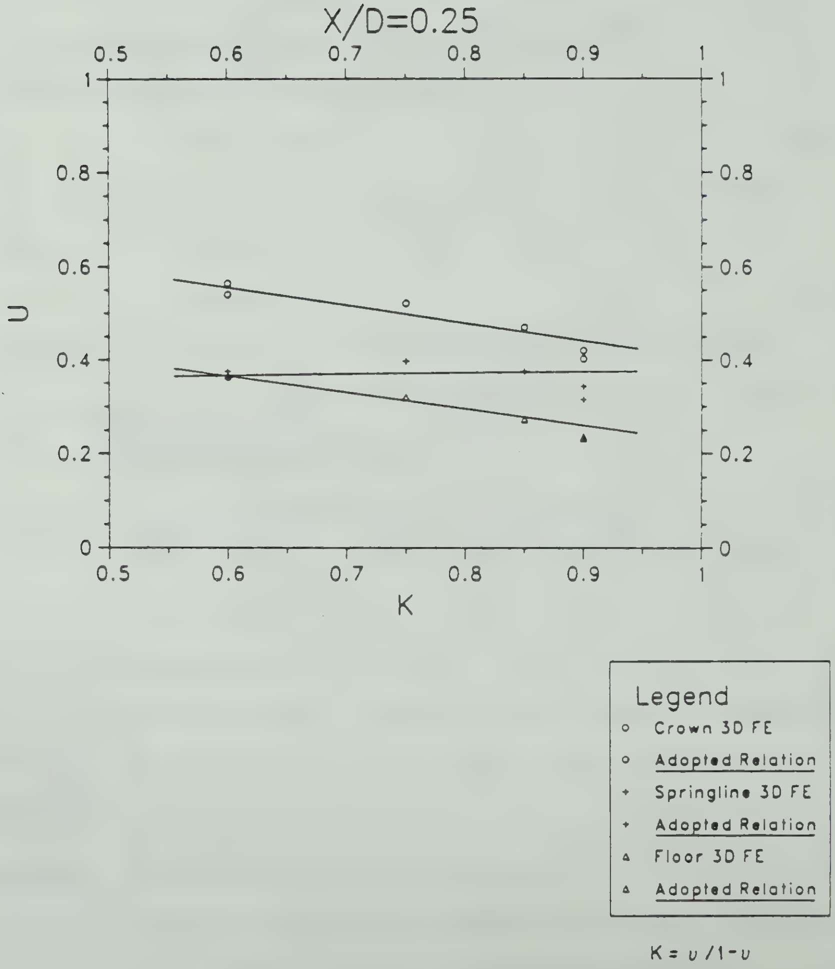

Figure 5.87 U and K Relationship for a Section D/4 Behind the Face

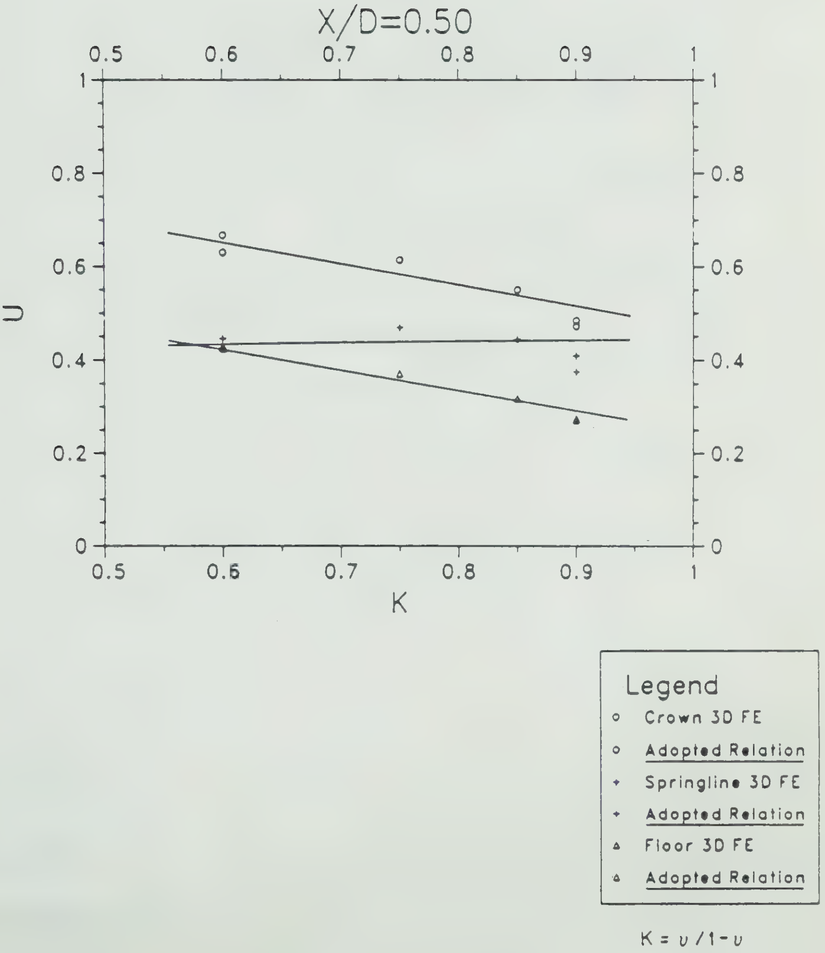

Figure 5.88 U and K Relationship for a Section D/2 Behind the Face

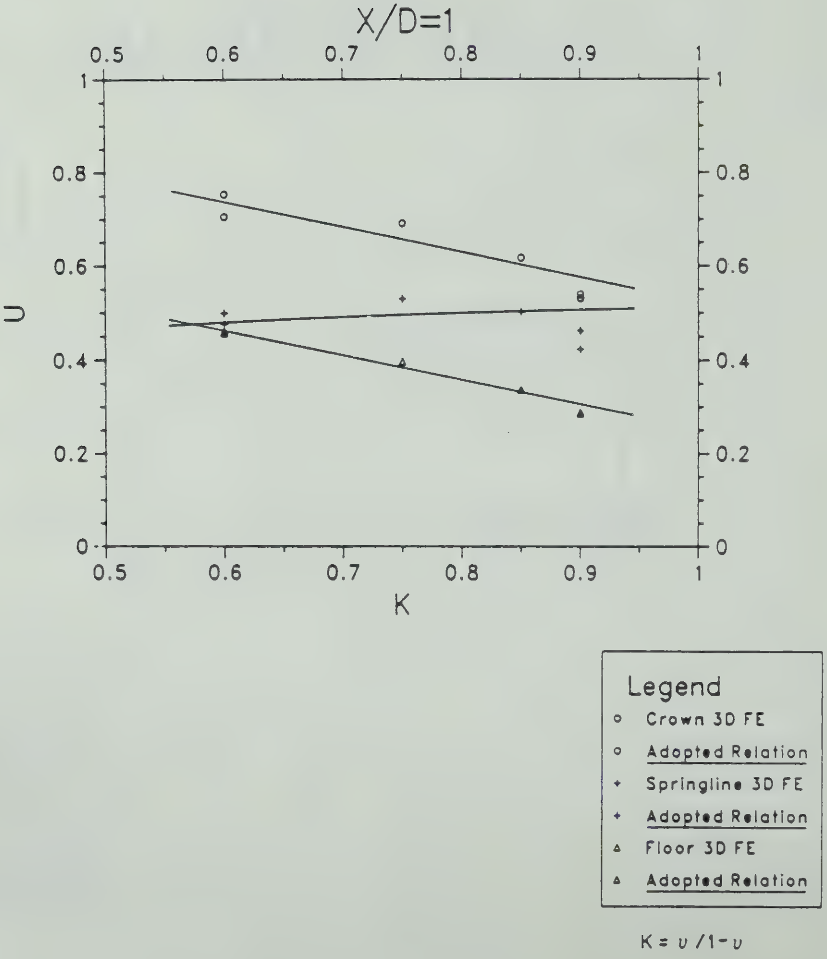

Figure 5.89 U and K Relationship for a Section 1.D Behind the Face

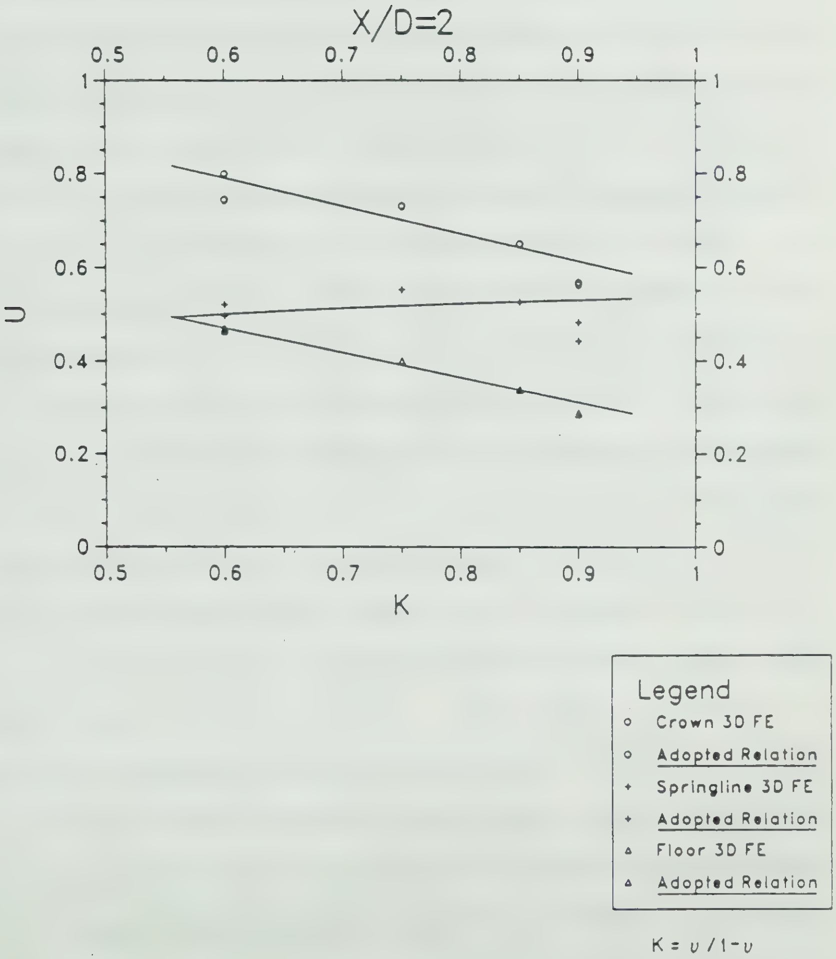

Figure 5.90 U and K Relationship for a Section 2.D Behind the Face

points using the smoothed curves shown in Figures 5.75 to 5.80. At X/D=2, the displacements are almost stabilized.

For each section considered, functions were fitted through the numerically obtained points. These functions are represented as solid lines in Figures 5.86 to 5.90. Since these curves were adjusted through points corresponding to the shallower and the deeper tunnel cases, they represent the typical U-K relationships for tunnels with cover to diameter ratios ranging from approximately 1.5 to 3.0.

Table 5.30 summarizes the values of the coefficients a and b obtained. To further illustrate the aspects of the fitted functions, Figures 5.91 to 5.93 have been prepared. These show for the considered points of the tunnel contour, how the U-K adopted relationships vary with the position of the section behind the tunnel face. One notes that the gradient of radial displacements along the tunnel axis are a maximum at sections just behind the tunnel face, and that is decreases rapidly at sections one to two diameters behind.

This is better seen in Figures 5.94 to 5.96, where the results of these interpretations are assembled in a compact form. From these three plots, one may obtain the coefficients a and b at any position X/D behind the tunnel face and, therefore, one may estimate the radial displacements at three points of the tunnel contour, for any value of K. The format of this solution is very similar to that presented in Figure 5.66, with the coefficients a and b corresponding to the parameters U_1 and U_2 of the deep tunnel

	Crown		Springline		Floor	
X/D	a	b	a	b	a	b
0	0.375	0.147	0.210	0.033	0.226	0.137
0.25	0.783	0.380	0.390	0.014	0.575	0.350
0.50	0.923	0.453	0.460	0.016	0.681	0.433
1.00	1.059	0.537	0.560	0.048	0.774	0.520
2.00	1.144	0.590	0.590	0.054	0.788	0.530

Notes: (1) Crown and Floor: $U - a - bK$

(2) Springline : $U = a - b/K$

Table 5.30 Coefficients of the Adopted U and K Relations for Sections at Different Distances Behind the Face

solution. The new solution is strictly valid for the conditions assumed: linear elastic ground (with modulus increasing with depth), unlined circular tunnel, ground cover to diameter ratio between 1.6 and 2.8 and in situ stress ratio K between 0.6 and 0.9, defined as a function of Poisson's ratio (varied beteen 0.375 and 0.474). Nonetheless it may be of some help in the evaluation of the closure behind or at the face of a shallow tunnel.

Face Displacements

Besides the vertical displacements above and below the unlined tunnels, Figures 5.84 and 5.85 also show the horizontal movements of the vertical tunnel face. The parametric finite element analyses revealed that the maximum dimensionless horizontal displacement of the centre point of the tunnel face depends on the relative depth of the tunnel and on the ratio K.

Figure 5.97 illustrates such a dependency. The maximum face movement towards the tunnel U_F is defined by:

$$U_F = \frac{u_f . E}{D . \sigma_{oc}} \qquad [5.10]$$

where u_f is the horizontal displacement of the face centre, E is the elastic modulus of the soil, D is the tunnel excavated diameter and σ_{oc} is the in situ vertical stress at the tunnel crown elevation. From Figure 5.97 one notes that U_F increases with increasing K and decreases with increasing H/D. Moreover, one notes that increasing the delayed support installation L/D, the dimensionless displacement of the face decreases. This result agrees with that found by Ranken and

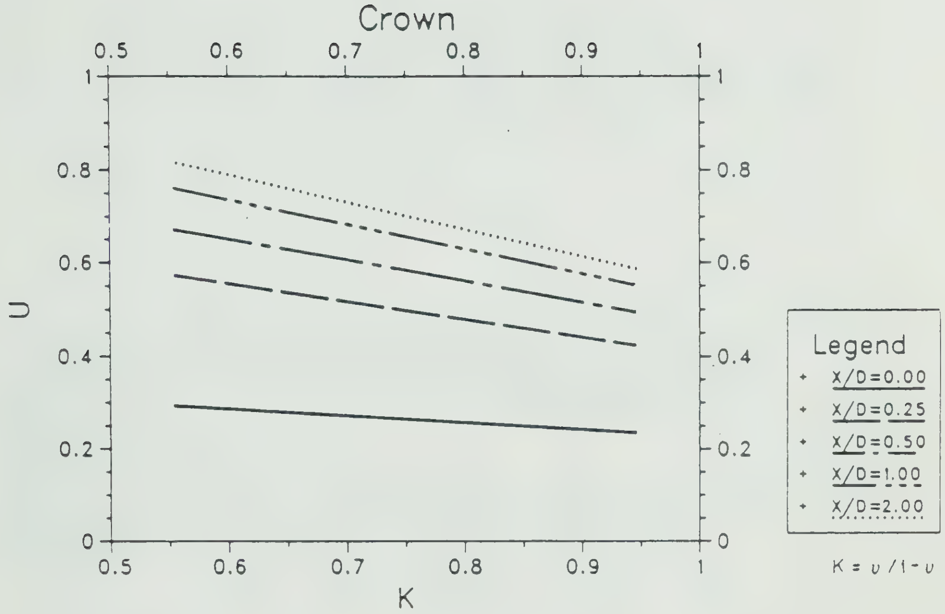

Figure 5.91 U and K Relationships for the Tunnel Crown

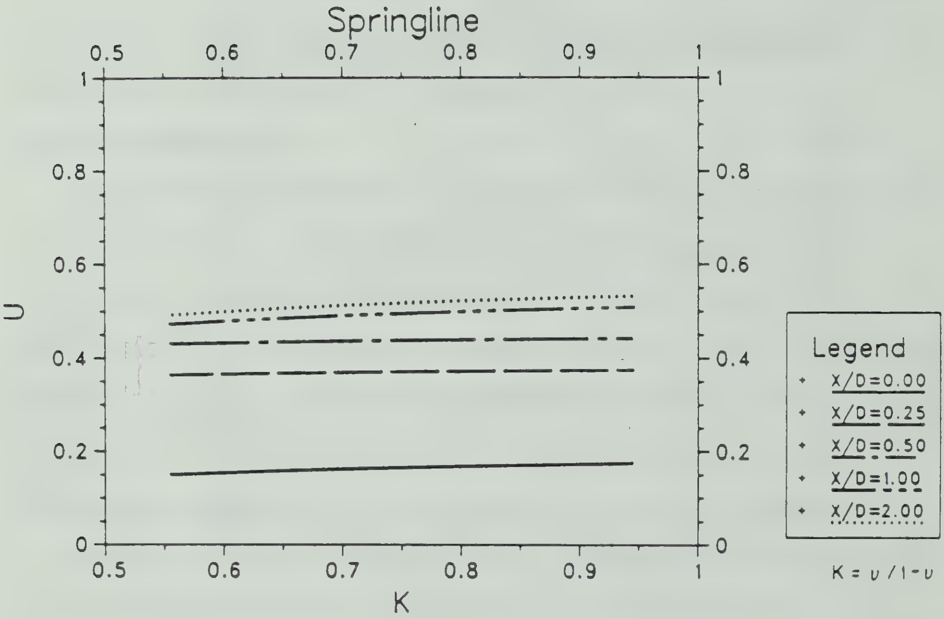

Figure 5.92 U and K Relationships for the Tunnel Springline

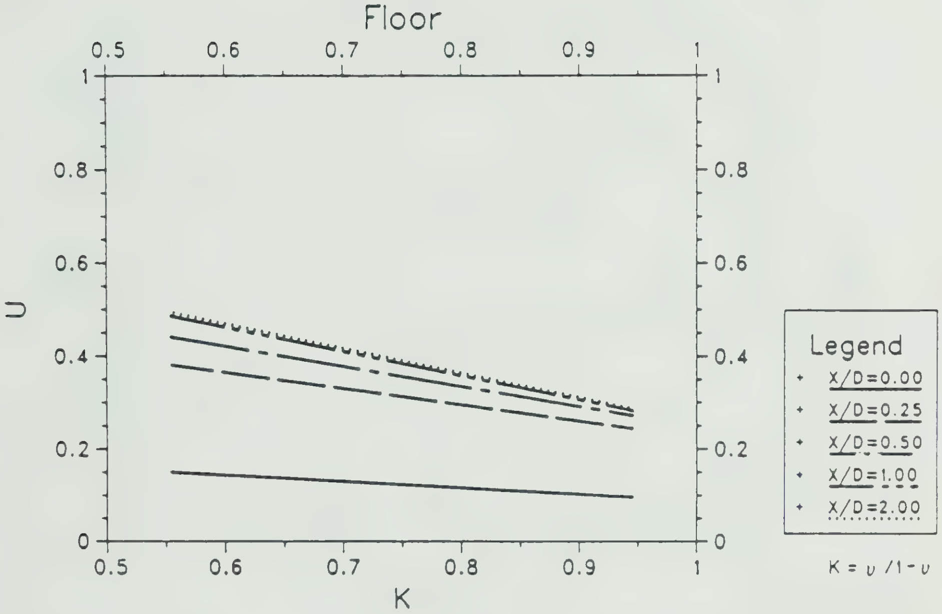

Figure 5.93 U and K Relationships for the Tunnel Floor

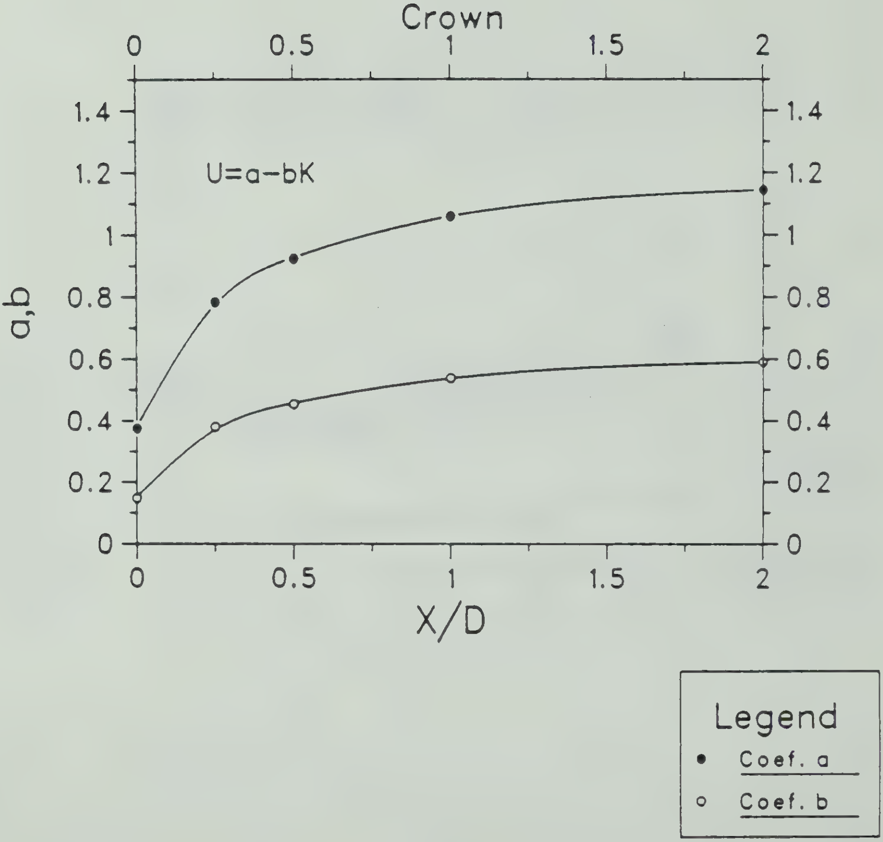

$K = \upsilon / 1 - \upsilon$

Figure 5.94 Coefficients of the U and K Relationship for the Crown of an Unlined Shallow Tunnel, (1.5<H/D<3.0) as a Function of the Distance to the Face

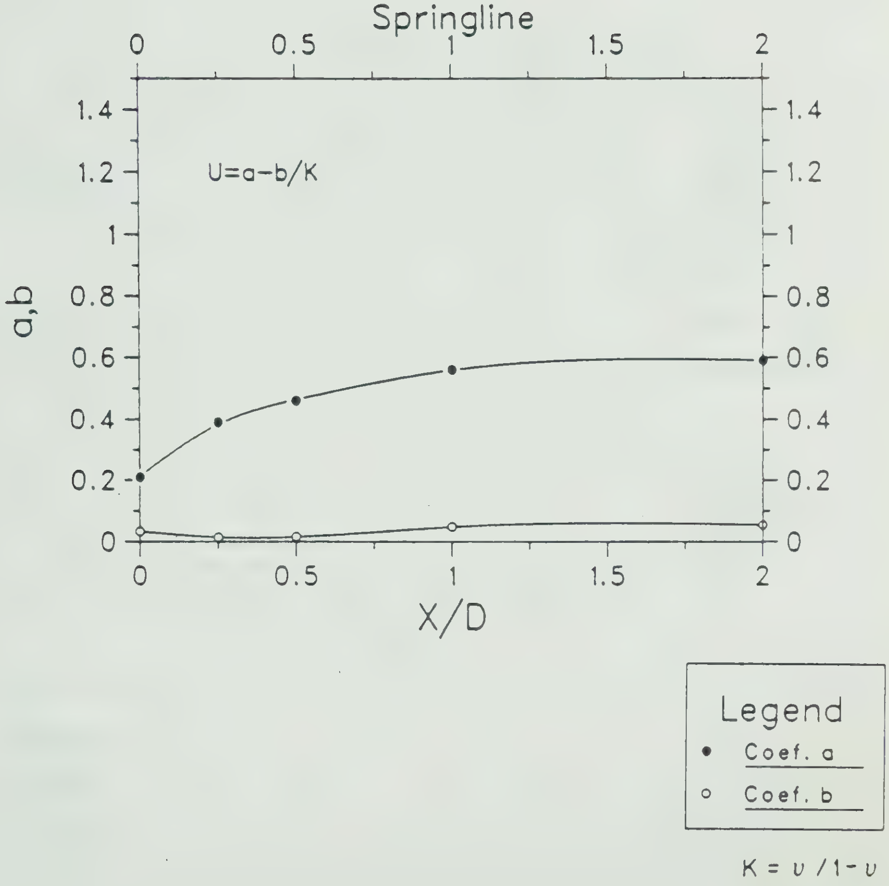

Figure 5.95 Coefficients of the U and K Relationship for the Springline of an Unlined Shallow Tunnel, (1.5<H/D<3.0) as a Function of the Distance to the Face

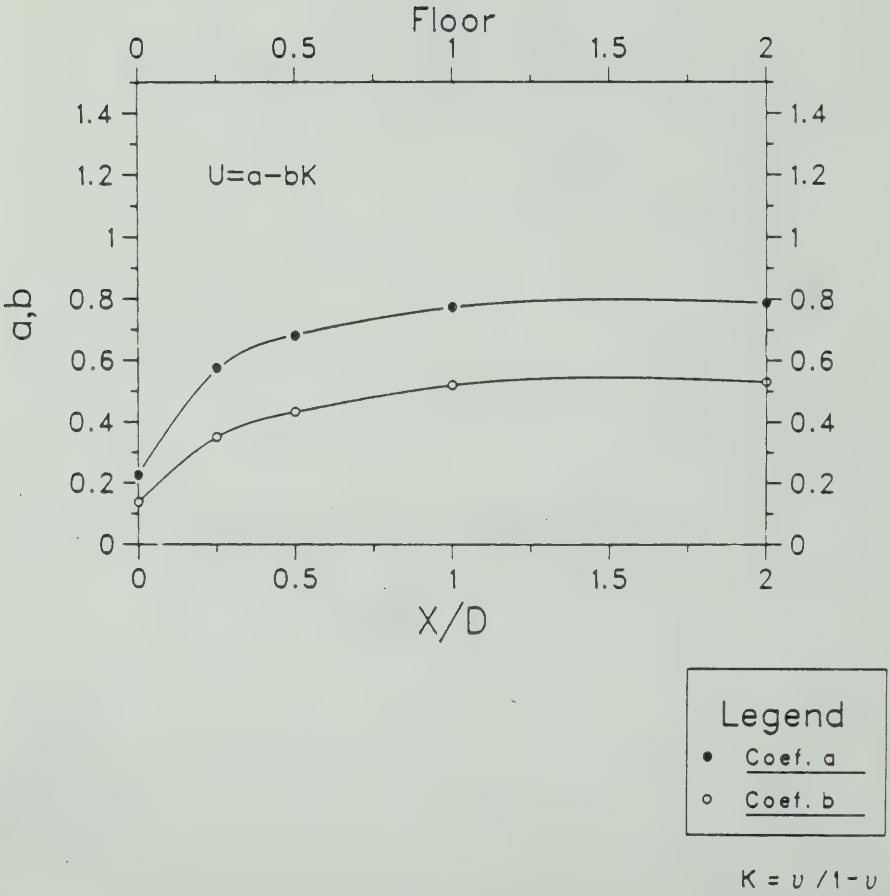

Figure 5.96 Coefficients of the U and K Relationship for the Floor of an Unlined Shallow Tunnel, (1.5<H/D<3.0) as a Function of the Distance to the Face

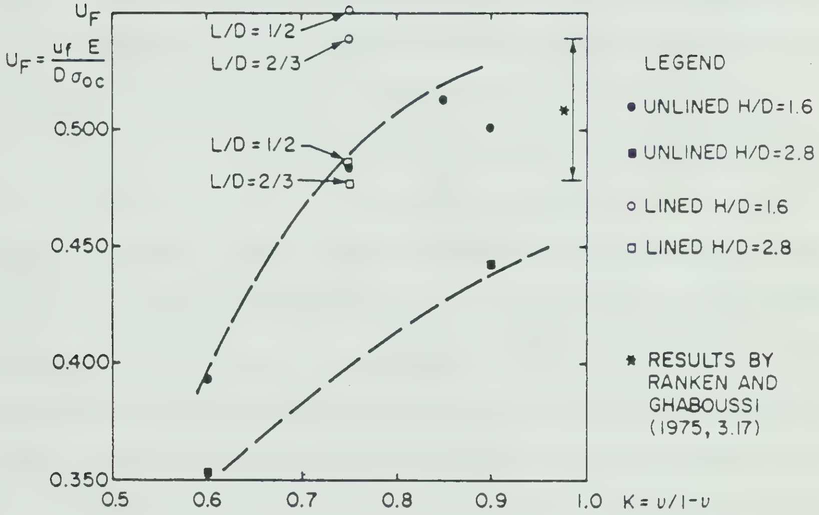

Figure 5.97 Maximum Horizontal Displacement of the Tunnel Face Expressed in Dimensionless Form, as a Function of the Stress Ratio K

Ghaboussi (1975:3.60). Also shown in Figure 5.97 is the range of U_F found by Ranken and Ghaboussi (Op.cit.:3.17), from axisymmetric finite element analyses (K=1) of unlined tunnels, with the Poisson's ratio varying between 0.3 and 0.49.

The dashed curves shown serve as boundaries for U_f estimates (the upper curve applied to shallower tunnels and the lower to deeper ones). Typically, the maximum horizontal displacement of the tunnel face could be estimated on a preliminary basis, by the expression:

$$u_f \simeq 0.5\ D\ \frac{\sigma_{oc}}{E} \qquad [5.11]$$

From it, one would conclude that for increasing tunnel depth (thus for increasing σ_{oc}), u_f would increase linearly. However, it should be remembered that for a large number of soils, E is also a function of the stress level (see Figures 5.10 and 5.11) and depending on this, u_f may even decrease with the increasing depth of the tunnel.

Longitudinal Distortions Ahead of The Advancing Tunnel

The results presented in Figures 5.75 and 5.76 show that the maximum gradient of the vertical displacements along the crown elevation develops at a section located about D/12 behind the face of an unlined tunnel. On the other hand, the results shown in Figures 5.68 and 5.71 indicate that if the tunnel is lined, the location of the maximum gradient is not affected and that the magnitude of this distortion is only slightly altered by the action of the support. The effect of the support is likely to decrease the distortion for a decreasing unsupported heading length (L/D).

The maximum longitudinal angular distortion at the crown elevation is given by the maximum gradient of the tunnel closure at the crown:

$$\gamma_{cmax} = \left| \frac{\partial u}{\partial x} \right|_{max} = \left| \frac{\partial U}{\partial (x/D)} \right|_{max} \cdot \frac{\sigma_{oc}}{E}$$
$$= \frac{1}{n_{\gamma c}} \cdot \frac{\sigma_{oc}}{E} \qquad [5.12]$$

The parameter $n_{\gamma c}$ is a measure of the inverse of the maximum longitudinal angular distortion and can be numerically determined from the results of the finite element analyses. Figure 5.98 is thus readily obtained. One observes, in fact, that the lining action is that of positively reducing the distortion. For usual support delays of about one diameter or so, and provided the ground is linear elastic, the longitudinal distortion at the crown can be safely estimated assuming the tunnel to be unlined and using the curves depicted in Figure 5.98. The distortion is found to depend on the ratio K, and decreases as this ratio increases. It is also found to depend on the relative tunnel depth (i.e. the proximity of the ground surface) again decreasing as the tunnel gets deeper. Note, however, that it is directly related to the vertical stress level σ_{oc} at the crown. A quick estimate of the magnitude of the maximum longitudinal distortion of the ground at the crown elevation could be made through the expression:

$$\gamma_{cmax} \simeq 1.5 \frac{\sigma_{oc}}{E} \qquad [5.13]$$

From it one sees that the distortion increases as the stress level increases and decreases as the ground becomes stiffer. The relation between the maximum distortion with the tunnel depth is not, however, obvious. It should be recalled, once more, that the modulus of the soil layer the tunnel is being driven through, may be also a function of the stress level. Accordingly, γ_{cmax} may increase, decrease or remain constant, for increasing depths of tunnel cover, depending on the type of soil.

In Section 3.2.2, a practical criterion for the detection of instability problems in the field was discussed. It consists of monitoring variations of the longitudinal distortion index (the angular distortion) with the tunnel advance, through the measurement of vertical movements of the ground just above the tunnel, at measuring points distributed along the tunnel alignment. Changes in the distribution of the longitudinal distortions may serve as an indication of incipient instability problems. It may be useful to know the maximum distortion as a reference for a stable condition. The features shown in Figure 5.98 may assist in this definition, provided the elastic modulus is taken as the initial tangent in situ modulus. However, more frequently than not, the deep settlement points used for this type of monitoring are not installed at the tunnel crown elevation, but rather some distance above it. Once more, the results of the numerical analyses of the unlined tunnel cases, may assist in obtaining the maximum angular distortion above the tunnel crown. Figure 5.99 furnishes the

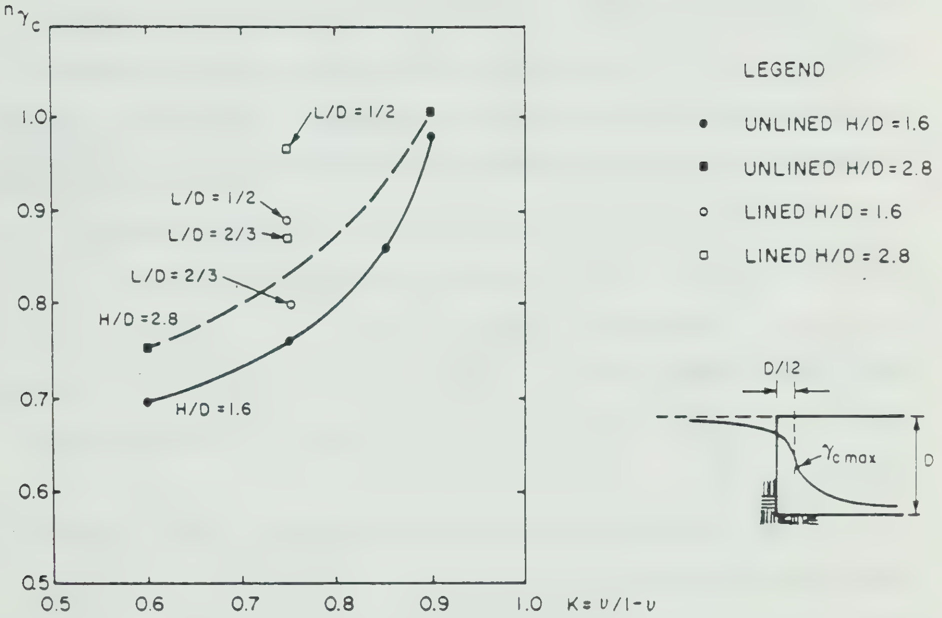

NOTE: MAXIMUM DISTORTION: $\gamma_{c\,max} = \frac{1}{{}^n\gamma_c} \cdot \frac{\sigma_{oc}}{E}$, AT $\frac{1}{12}$D BEHIND THE FACE

Figure 5.98 Maximum Angular Distortion Along the Tunnel, at Crown Elevation

ratio of the maximum distortion at crown (γ_{cmax}) to the maximum distortion of the ground at an elevation 0.3D above the crown (γ_{dsmax}). The latter distance is fairly typical for deep settlement points installed above the tunnel. One notes that, for the ranges of K and H/D investigated, the distortion ratio varies within a fairly narrow range. A typical ratio of 2.5 could be selected. Therefore, a rough estimate of the magnitude of the maximum angular distortion in the longitudinal direction, along an axis located 0.3D above the crown, could be made by the expression:

$$\gamma_{dsmax} \simeq 0.6 \frac{\sigma_{oc}}{E} \qquad [5.14]$$

The same comments made for γ_{cmax} are valid here. It was noted that γ_{dsmax} occurs at a section located D/12 behind the tunnel face.

Also of some interest is the maximum longitudinal distortion at ground surface, γ_{smax}, ahead of the tunnel face. Again the action of the support in this case reduces the angular distortion at the surface, by elongating the settlement profile and reducing the magnitude of the maximum movements. As the support is placed closer to the tunnel face, movements are noticed at greater distances from the face and the maximum angular distortion of the ground decreases. This fact was detected from the results of axisymmetric analyses by Ranken and Ghaboussi (1975:3.55), from results of field instrumentation by Negro and Eisenstein (1981) and was broadly confirmed in the present study.

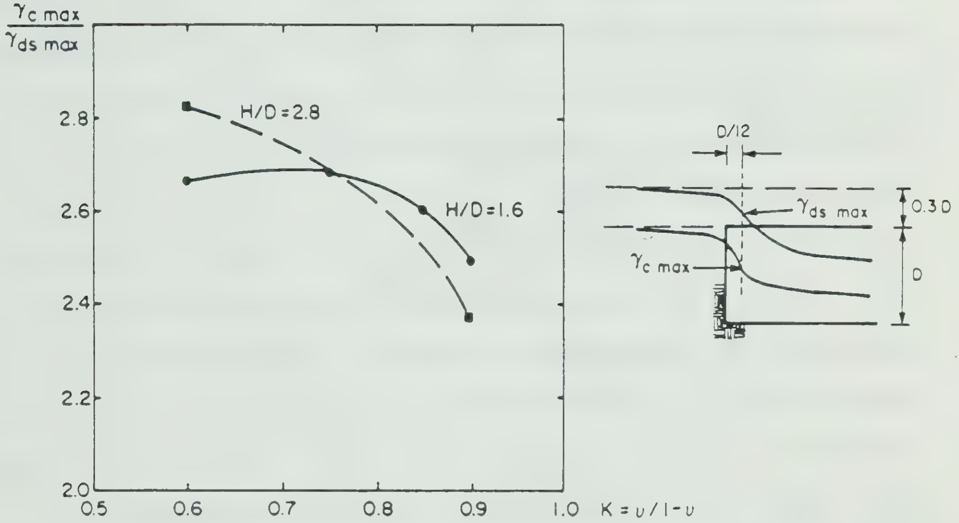

Figure 5.99 Maximum Angular Distortion Along the Tunnel, at an Axis 0.3D Above Crown Elevation, as a Function of the Maximum Crown Distortion

Having this in mind, the numerical results from the 3D analyses of the unlined tunnel, should provide a basis for a safe estimate of the maximum angular distortion ahead of the face. Accordingly, Figure 5.100 was prepared. The maximum surface distortion, γ_{smax}, is related to the maximum crown distortion, as a ratio. This ratio was found to vary with the cover to diameter ratio, increasing as the tunnel gets deeper, as expected. Obviously, when the cover tends towards zero, the ratio should tend towards unity. The in situ stress ratio K was also noted to affect this relationship. While the section where γ_{cmax} occurs was found to be always D/12 behind the face regardless of the depth of the tunnel and the K value, the section where the maximum surface distortion occurs seems to depend on the ratio H/D. For H/D equal to 1.6, γ_{smax} developed at D/4 ahead of the face. For H/D equal to 2.8, γ_{smax} developed further ahead at (21/36)D from the tunnel face. The results of the analyses with linings are also included in Figures 5.100 for comparison. The lined tunnel cases showed less distortion at the surface than the unlined cases, as expected. However, for H/D=2.8 and contrary to expectations, the case with the larger unsupported heading (L/D=2/3) yielded the smaller surface distortion. These results are somewhat suspect, as they may have been affected by the presence of the nearby lateral boundary of the finite element mesh.

Nevertheless, the results shown in Figure 5.100 may be of some help in the estimate of the maximum surface

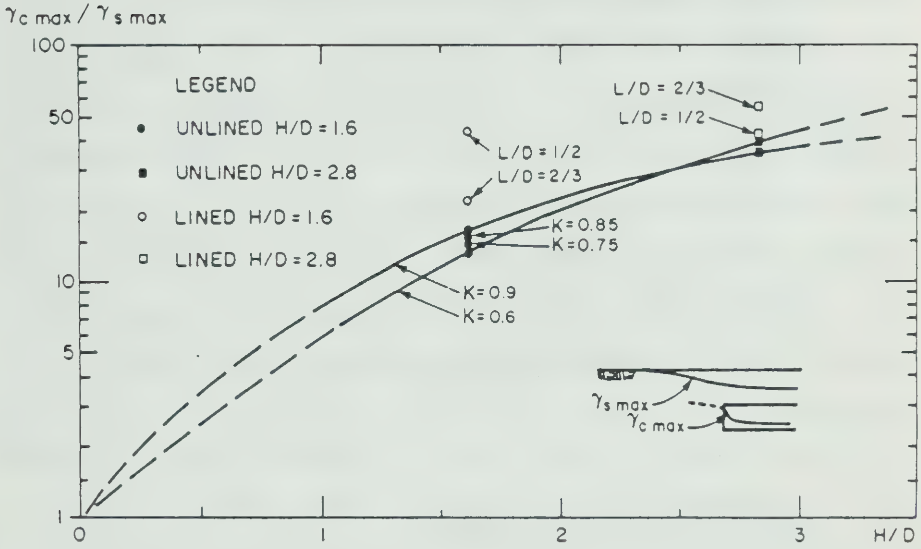

Figure 5.100 Maximum Angular Distortion of the Ground Surface Along the Tunnel Alignment as a Function of the Maximum Crown Distortion

distortion ahead of the tunnel. The use of this solution, or those shown in Figures 5.98 and 5.99, strictly depend on the validity of the simplifying assumptions made. For instance, they cannot be used in cases where substantial yielding develops ahead of the tunnel. An approximate assessment of this condition can be made by evaluating the face stability by using the solutions discussed in Section 4.3.4. Extending the concepts presented in Section 2.3.3 for a plane strain tunnelling situation, if the factor of safety for the face stability is larger than 2 to 3, then the simple methods for evaluation of longitudinal ground distortions ahead of the tunnel may be applicable. Since no other solutions are yet available to treat the present problems, the simplified methods just discussed can perhaps be of some help in practice.

5.3.6 Application of the Results

5.3.6.1 Tunnel Closure

Comparison with other Solutions

The solution developed and presented in Section 5.3.5.2 for estimating the convergence of an unlined tunnel presents a number of peculiarities. Despite this, one is invited to compare it with other solutions available. Among those reviewed in Section 5.3.2, the solutions by Hocking (1976) and Niwa et.al. (1979) display more generality with respect to accounting for the in situ stress ratio. Both solutions were derived from boundary element analyses and yield similar results. The one by Niwa et.al. (1979) however, has been presented in a slightly more convenient form, which allowed the generalization presented in Figure 5.66. Therefore it was selected for comparative purposes.

At least two problems emerge in comparing the presently developed solution with that by Niwa et.al. (Op.cit). The first refers to the nature of the development. The present solution was numerically derived from finite element analyses. The one by Niwa et.al. (Op.cit.) stemmed from boundary element analyses. Being both derived from numerical solutions, they involve numerical approximations, but these are dissimilar and depend on each type of solution. For instance, it has been shown that in the plane strain analysis of an elastic pipe under internal pressure (Brebbia, 1978:162), the displacement calculated by the boundary element method will be slightly larger than that by the finite element method, for equivalent degrees of "discretization". The same conclusion was found by Negro and Kuwajima (1985) in the plane strain elastic analyses of a deep tunnel. On the other hand, it is known that finite element solutions tend to yield displacements smaller than the exact (Zienkiewicz, 1983:36).

The second problem refers to the fact that while the Niwa et.al. (Op.cit) solution was developed for an ideally deep tunnel situation, the present one assumed the tunnel to be shallow, with certain cover to diameter ratios. To make the solutions comparable, the present solution had to be manipulated. In an attempt to "eliminate" the effect of the gravitational stress gradient across the shallow tunnel, the coefficients, a and b, of the proposed $\bar{U}$ versus K relationship shown in Table 5.30 were averaged in order to obtain the equivalent "deep" tunnel solution. Accordingly, the a and b coefficients for the springline were averaged with the mean values of a and b for the crown and floor, for each section of the tunnel behind the face. In so doing, these average values can be compared to the corresponding values of U_1 and U_2 of Niwa et.al. (Op.cit) solution presented in Figure 5.66. Consequently Figure 5.101 was obtained.

It should be noted that in the present solution, the in situ stress ratio was defined as a function of the Poisson's ratio. Moreover, the elastic modulus of the soil was assumed to increase with depth. These two facts alone would impede any equivalence between the two solutions. Notwithstanding this, the results shown in Figure 5.101 indicate some resemblance beween the solutions. The difference could be attributed to the different features of each case. Moreover, it is observed that the additive component, a, of the dimensionless displacement U given by the present solution is always smaller than that provided by the other solution. Inversely, the subtrahend component, b, is larger. As a result, the final dimensionless radial displacement given by the present solution will usually be smaller than that given by Niwa et.al. (Op.cit.).

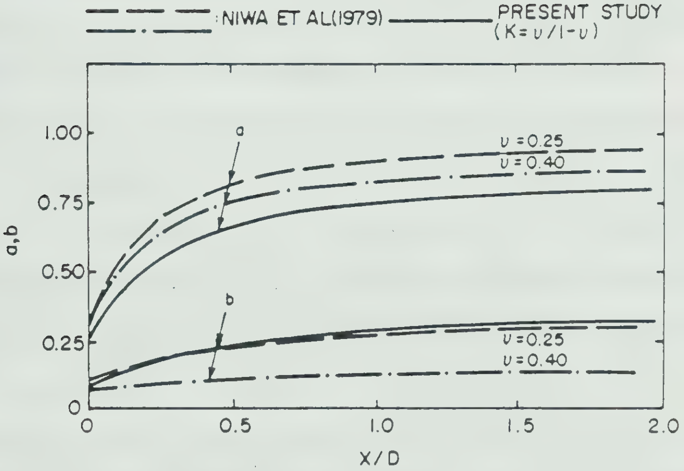

Figure 5.101 Comparison Between Niwa et.al. (1979) and the Present (Averaged) Tunnel Closure Solution

Comparison with Field Measurements

For a proper verification of the proposed method, calculations were performed for cases where field measurements were available. No special criterion was set up for case history selection. The basic requirement was availability of the required data to allow a comparison to be made. Therefore some cases were included which involved conditions lying outside the range those considered in the development of the present solution, either in terms of geometry (H/D) or in situ stresses (K). Not many cases of shallow tunnels in soft clays or sensitive soils were investigated, but at least some were included.

Tables 5.31, 5.32 and 5.33 list the cases investigated, where ground movements at the crown, springline and floor, respectively, have been measured. These tables present also the main source or reference for each tunnel case. They refer to those publications where most of the information shown was drawn from. Additional searches of the literature were undertaken in order to supply data on the ground properties, whenever necessary.

Besides identifying the case history, the tables indicate the instruments or the instrumented sections considered (second column). Indications of the construction method and lining type used are also included, together with a brief description of the ground type and the position of the tunnel with respect to the ground water level. The cases where the ground water level was lowered prior to tunnelling

No.	Tunnel and Section	Method	Lining	Ground	Water Level	Behaviour	D (m)	H (m)	E (MPa)	K	ϕ (°)	c (kPa)
1	Frankfurt 25 Romerberg	NATM$^{(1)}$	Shotcrete	Stiff clay marl CH MH	LO	DR	6.48	11.5	24	0.8	21	37
2	Frankfurt 25 Karmeliterg.	NATM$^{(1)}$	Shotcrete	Stiff clay marl CH MH	LO	DR	6.70	13.0	24	0.8	21	37
3	Frankfurt 25 Blauhandg.	NATM$^{(1)}$	Shotcrete	Stiff clay marl CH MH	LO	DR	6.70	12.5	24	0.8	21	37
4	Frankfurt 17 Bergerstr.	NATM	Shotcrete	Stiff clay marl CH MH	LO	DR	6.70	10.25	52	0.8	21	37
5	Frankfurt 23 Domplatz	Open Shield$^{(2)}$	Precast concrete	Stiff clay marl CH MH	LO	DR	6.70	11.75	24	0.8	21	37
6	Frankfurt 23 Fahrgasse	Open Shield$^{(2)}$	Precast concrete	Stiff clay marl CH MH	LO	DR	6.70	8.6	24	0.8	21	37
7	Butterberg-Osterode	NATM	Shotcrete	Sandy silty gravel GM	A	DR	11.5$^{(3)}$	14.6	150	0.5	33	20
8	Bochum A2 Bahndamm	NATM	Shotcrete	Stiff marl and sand	A	DR	9.03$^{(3)}$	12.2	70	0.8	25	64
9	Munich Los 6 West 2	NATM	Shotcrete	Sandy gravel	A	DR	6.85$^{(3)}$	6.0	100	0.4	37.5	4
10	Munich 8/1 - 18.2	NATM	Shotcrete	Hard marl and sand	LO	DR	6.91$^{(3)}$	22.0	200	1.0	25	40
11	Munich 5/9 - 6$^{(4)}$	NATM	Shotcrete	Hard marl and sand	LO ?	DR?	7.5$^{(3)}$	15.8	200	1.0	25	40
12	Munich 5/9 - 7 (MQ1)	NATM$^{(5)}$	Shotcrete	Hard marl and sand	B	DR?	6.95	20.8	200	1.0	25	40
13	Green Park ext. X1	Open Shield	Cast iron seg.	London clay - CH	B	UN	4.15	29.6	60	1.3	0	250
14	Green Park ext. Y1	Open Shield	Cast iron seg.	London clay - CH	B	UN	4.15	28.8	60	1.3	0	250
15	Green Park ext Z1	Open Shield	Cast iron seg.	London clay - CH	B	UN	4.15	28.2	60	1.3	0	250
16	Regent Park (Sth B) ext. H	Open Shield	Exp. concr. seg.	London clay - CH	B	UN	4.15	32.0	60	1.3	0	250
17	Regent Park (Sth B) ext. K	Open Shield	Exp. concr. seg.	London clay - CH	B	UN	4.15	32.0	60	1.3	0	250
18	Regent Park (Nth B) ext C$^{(7)}$	Open Shield	Exp. concr. seg.	London clay - CH	B	UN	4.15	17.8	30	1.6	0	200
19	Heathrow Cargo (U.K.)	Open Shield	Exp. concr. seg.	London clay - CH	B	UN	10.9	7.3	27	1.9	0	200
20	New Cross (U.K.) ext. B2	Bent. Shield	Cast iron seg.	Dense sand and gravel	A	DR	4.12	8.0	40	0.3	45	0
21	Chinnor (U.K.) ext. P2C	TBM	Steel ribs no lagg.	Lower chalk	A	DR	5.0	5.7	75	0.5	-	q_u=74,200
22	Chinnor (U.K.) ext. P5	TBM	Steel ribs no lagg.	Lower chalk	A	DR	5.0	6.2	75	0.5	-	q_u=74,200
23	Edmonton Exper. ext MX22	Closed Shield	Exp. concr. seg.	'Soft' till - CL	A$^{(10)}$	UN	2.56	25.6	17	0.8	0	100
24	Edmonton LRT (Sth) ext. 1	Closed Shield	Exp. ribs & lagg.	'Stiff' till - CL	A	DR	6.17	8.6	70	0.75	40	0
25	Edmonton Kennedale ext. ME1	Closed Shield	Exp. ribs & lagg.	Till - CL?	A	DR	3.2	12.0	60	1.0	35	10
26	S. Paulo Boa Vista ext. B	Closed Shield$^{(5)}$	Cast iron seg.	Clayey sand - SC	B	UN?	6.19	10.55	50	0.6	0	70

Table 5.31 Predicted and Measured Displacements at the Face and at the Point of Support Activation in Shallow Tunnels for the Crown

No.	σ_{r0} (kPa)	y (m)	Displ. u at the face (mm)			L/D	Displ. u at lining installation or closure (mm)			Face Position for Final u (x/D)	Final u (mm)		after Support	Main References
			Meas.	Extr.	Predic.		Meas.	Extr.	Predic.		Meas.	Extr.		
1	213	0.5	21.0	22.6	14.8	0.69	57.0	61.3	33.8	3.09	63.0	67.7	0.111	Edeling and Schulz (1972)
2	240	0.5	14.0	15.0	17.2	0.45	29.0	31.2	36.2	4.03	42.0	45.2	0.209	Stroh and Chambosse (1973)
3	231	0.5	13.0	14.0	16.6	0.22	22.0	23.7	29.0	4.48	34.0	36.6	0.200	Stroh and Chambosse (1973)
4	190	0.85	4.0	4.4	6.3	0.70	13.0	14.4	14.6	NA	19.0	21.1	0.274	Muller, Sauer and Chambosse (1977)
5	218	0.39	5.0	5.3	15.6	1.10	35.0	37.2	37.2	1.49	45.0	47.9	0.177	Chambosse (1972)
6	159	0.50	6.0	6.4	11.4	0.90	50.0	53.2	27.3	2.99	70.0	74.5	0.480	Chambosse (1972)
7	321	2.10	6.0	6.8	7.4	0.61	17.0	19.3	17.7	1.74	24.0	27.3	0.325	Meister & Wallner (1977)
8	244	0.50	8.0	8.5	8.1	0.70	16.0	17.0	18.8	1.74	20.0	21.3	0.137	Jagsch et al (1974), Hofmann (1976)
9	132	0.50	2.0	2.1	(2.8)	0.44	6.0	6.3	(6.5)	NA	7.0	7.4	0.122	Schikora (1983), Kriechke & Weber (1981)
10	462	0.60	2.2	2.3	(3.6)	0.87	7.0	7.2	(8.1)	NA	8.5	8.7	0.094	Laabmayr & Weber (1978)
11	332	0	1.9	1.9	2.8	-	-	-	-	-	-	-	-	Amstad and Kovari (1984)
12	376$^{(6)}$	0	2.1	2.1	(3.0)	0.72	-	-	-	-	--	-	-	Baumann et al (1985)
13	577	2.6	10.5	18.4	(7.3)	0.96	16.0	28.0	(14.4)	7.23	14.0	24.5	-0.088	Attewell and Farmer (1974)
14	562	1.5	8.5	12.0	(7.1)	0.96	12.0	16.9	(14.0)	9.64	15.0	21.2	0.111	Attewell and Farmer (1974)
15	550	1.5	7.5	10.6	(7.0)	0.96	12.0	16.9	(13.7)	12.05	16.0	22.6	0.150	Attewell and Farmer (1974)
16	625	7.15	3.5	9.8	(7.9)	0.96	5.0	14.0	(15.6)	12.05	9.0	25.2	0.259	Barrat and Tyler (1976)
17	625	2.75	6.0	10.2	(7.9)	0.96	7.5	12.8	(15.6)	14.46	11.0	18.7	0.136	Barrat and Tyler (1976)
18	347	1.98	10.0	15.6	(6.7)	0.96	14.0	21.8	(12.0)	10.84	19.0	29.6	0.162	Barrat and Tyler (1976)
19	153	0.91	10.0	11.1	(5.9)	0.33	12.5	13.9	(4.4)	0.55	14.0	15.6	0.028	Muir Wood and Gibb (1971)
20	120$^{(8)}$	1.30	5.0	6.3	(4.1)	1.33	21.0	26.6	(11.9)	1.82	23.0	29.1	0.152$^{(9)}$	Boden and McCaul (1979)
21	121	1.0	2.0	2.4	(2.4)	1.10	8.0	9.6	(6.5)	6.0	22.3	26.8	2.132	McCaul et al (1976), O'Reilly et al (1976)
22	132	1.5	3.0	3.6	(2.7)	1.10	8.0	9.6	(7.1)	7.0	18.0	21.6	1.364	McCaul et al (1976), O'Reilly et al (1976)
23	538	3.45	9.5	21.4	(20.9)	2.73	20.0	45.0	(54.4)	9.77	25.0	56.3	0.139	El-Nahhas (1980)
24	163	0.84	3.0	3.5	(3.8)	1.0	11.0	12.8	(9.5)	4.05	34.0	39.4	1.851	Thurber (1982), Branco (1981)
25	228	2.73	2.7	5.2	(2.8)	2.19	6.0	11.5	(6.7)	9.38	10.0	19.2	0.633	Corbett (1984)
26	108$^{(11)}$	4.36	3.0	5.0	3.8	1.29	18.0	29.9	10.2	4.85	56.0	93.0	3.226$^{(9)}$	Costa et al (1974)

Table 5.31 Predicted and Measured Displacements at the Face and at the Point of Support Activation in Shallow Tunnels for the Crown (Continued).

No.	Tunnel and Section	Method	Lining	Ground	Water Level	Behaviour	D (m)	H (m)	E (MPa)	K	ϕ (°)	c (kPa)
27	S. Paulo E.W. Line	Closed Shield$^{(5)}$	Cast iron seg.	Clayey sand - SC	B	UN?	6.19	21.6	80	0.6	0	120
28	S. Paulo Sanegran I	Open Shield	Precast conc.	Weathered gneiss	LO	DR	5.25	20.0	80	0.6	35	NA
29	S. Paulo Sangegran II	Open Shield$^{(5)}$	Precast conc.	Dense sand - SP	B	DR	5.25	18.4	80	0.6	40	0
30	S. Paulo Tamanduatei	Closed Shield	Precast conc.	Loose sand - SW	B$^{(18)}$	DR	1.79	6.2	5	0.5	30	0
31	S. Paulo ABV ext CC1	NATM	Shotcrete	Clayey sand - SC	A	DR	4.04$^{(3)}$	6.2	28	0.75	29	0
32	S. Paulo ABV ext GG1	NATM	Shotcrete	Clayey sand - SC	A	DR	4.04$^{(3)}$	6.45	28	0.75	29	0
33	S. Paulo ABV ext BB1	Hand mined	Steel ribs & lagg.	Clayey sand - SC	A	DR	3.99$^{(3)}$	6.70	28	0.75	29	0
34	S. Paulo N. Ext. S1.9$^{(14)}$	NATM	Shotcrete	Stiff silty clay CL CH	B	DR?	7.83$^{(3)}$	10.76	90	0.9	25	3
35	S. Paulo E. Ext. S1.3$^{(14)}$	NATM	Shotcrete	Stiff silty clay CL CH	B	DR	7.83$^{(3)}$	11.64	90	0.9	25	3
36	S. Paulo N. Ext. S1.2$^{(14)}$	NATM	Shotcrete	Stiff silty clay CL CH	B	DR	7.83$^{(3)}$	11.26	90	0.9	25	3
37	S. Paulo N. Ext. S1.10$^{(14)}$	NATM	Shotcrete	Stiff silty clay CL CH	B	DR	7.83$^{(3)}$	10.05	90	0.9	25	3
38	Rio Mangueira ext. 11N$^{(2)}$	Bernold Shield	Cast in place conc.	Residual soil SM SC	LO	DR	7.0$^{(3)}$	6.4	15	0.5	40	10
39	Rio Mangueira ext. 23N$^{(2)}$	Bernold Shield	Cast in place conc.	Residual soil SM SC	LO	DR	7.0$^{(3)}$	6.4	15	0.5	40	10
40	Washington C-line ext. 10	Open Shield	Exp. rib & lagg.	Sand&silty sand SP SM	B$^{(18)}$	DR	6.45	11.7	35	0.5	35	0
41	Washington C-line ext. 9	Open Shield	Exp. rib & lagg.	Sand&silty sand SP SM	B$^{(18)}$	DR	6.45	11.7	35	0.5	35	0
42	Washington L-Route ext. 1	Open Shield	Steel segments	Compact sand SM SP	LO	DR	5.5	17.4	115	0.4	40	0
43	Washington L-Route ext. 3	Open Shield	Steel segments	Compact sand SM SP	LO	DR	5.5	17.4	115	0.4	40	0
44	Washington L-Route ext. 9	Open Shield	Steel segments	Compact sand SM SP	LO	DR	5.5	19.6	115	0.4	40	0
45	Washington L-Route ext. 11	Open Shield	Steel segments	Compact sand SM SP	LO	DR	5.5	19.2	115	0.4	40	0
46	Winnipeg ext. P5	Hand mined	Cast in place conc.	Varved clay CH	B	UN	1.93	11.7	6	0.8	0	70
47	Winnipeg ext. P14	Hand mined	Cast in place conc.	Varved clay CH	B	UN	1.93	11.7	6	0.8	0	70
48	Thunder Bay I	Closed Shield	Precast conc.	Soft silty clay CH	B	UN?	2.47	9.6	7	0.9	0	30
49	Madrid Line 6, ext. 2	Belgian	Cast in place conc.	Hard fiss. clay MH	B	DR?	8.2$^{(3)}$	17.9	200	0.8	35	10
50	Seville Exp. Sect. 1 and 2	Mined	Brick and conc.	Clay marl CH	B	DR?	4.5$^{(3)}$	32.5	200	0.9	30	90
51	Mexico Siphon	Open Shield	Steel segments	Lacustrine clay CH	B	UN?	2.95	10.2	5	0.75	0	30
52	Japan B-2	Closed Shield$^{(5)}$	Precast conc.	Alluvial clay MH CH	B	UN	7.24	24.0	16	0.7	0	50

List of Symbols and Notes used in the table can be found in Table 5.33.

Table 5.31 Predicted and Measured Displacements at the Face and at the Point of Support Activation in Shallow Tunnels for the Crown (Continued).

No.	σ_{r0} (kPa)	y (m)	Displ. u at the face (mm)			L/D	Displ. u at lining installation or closure (mm)			Face Position for Final u (x/D)	Final u (mm)		After Support	Main References
			Meas.	Extr.	Predic.		Meas.	Extr.	Predic.		Meas.	Extr.		
27	254(12)	4.0	6.0	10.0	(5.6)	1.29	15.0	25.1	(15.0)	4.85	25.0	41.8	0.666(9)	Sozio (1978)
28	380	1.5	6.0	7.7	(7.2)	1.56	20.0	25.6	(19.3)	4.76	40.0	51.2	0.642	Azevedo (1983, 1985)
29	250(13)	3.9	3.0	5.7	(4.7)	1.56	5.0	8.2	(12.7)	13.33	8.0	13.1	0.187	Verski et al (1985)
30	112	0.21	13.0	14.2	(12.1)	3.91	80.0	87.0	(34.0)	8.38	110.0	119.9	0.821	Negro (1984)
31	101	-	3.3	3.3	3.8	0.6	7.4	7.4	8.7	1.50	8.8	8.8	0.096	Negro and Eisenstein (1981)
32	105	-	1.3	1.3	4.0	0.6	2.6	2.6	9.1	4.20	3.9	3.9	0.089	Negro and Eisenstein (1981)
33	109	-	3.3	3.3	4.1	0.25	5.6	5.6	7.7	4.51	17.7	17.7	0.779	Negro and Eisenstein (1981)
34	215	2.0	5.7	5.9	(4.5)	0.84	15.0	15.8	(10.5)	1.79	24.0	26.1	0.551	Negro et al (1985)
35	233	2.0	3.7	3.7	(4.9)	0.83	13.2	13.5	(11.4)	2.39	22.5	23.9	0.513	Negro et al (1985)
36	225	3.02	6.3	6.3	(4.2)	0.64	20.1	22.3	(10.4)	NA	24.9	26.0	0.189	Negro et al (1985)
37	201	2.0	6.3	6.0	(4.2)	0.42	16.1	16.0	(9.0)	NA	25.5	26.0	0.572	Negro et al (1985)
38	115	1.4	13.0(14)	15.0	(16.2)	4.5	350.0	402.5	(45.6)	NA	350	402.5	0	Massa (1981)
39	115	1.4	15.0(14)	17.3	(16.2)	NA	NA	NA	-	NA	120.0	130.0	-	Massa (1981)
40	234	0.46	15.0	15.0	13.0	1.23	280.0	280.0	35.1	2.33	335.0	335.0	1.275	Hansmire (1975)
41	234	0.46	10.0	10.0	13.0	1.23	230.0	230.0	35.1	2.33	320.0	320.0	2.087	Hansmire (1975)
42	347	1.8	2.0	2.7	(5.2)	1.16	18.0	23.9	(14.3)	2.18	30.0	39.9	0.964	Cording et al (1976), Tan (1977)
43	347	1.5	1.5	2.0	(5.2)	1.16	13.0	17.3	(14.3)	2.73	22.0	29.3	0.723	Cording et al (1976), Tan (1977)
44	391	1.7	7.0	9.3	(5.9)	1.16	39.0	51.9	(16.1)	2.36	51.0	67.8	0.850	Cording et al (1976), Tan (1977)
45	383	1.6	2.0	2.8	(5.8)	1.16	11.0	15.4	(15.8)	1.82	15.0	21.0	0.306	Cording et al (1976), Tan (1977)
46	199	1.2	10.0	20.0	(16.5)	2.0	12.5	25.0	(43.0)	5.0	17.0	34.0	0.141	Hardy & Associates (1980)
47	199	0.8	8.5	17.0	(16.5)	2.0	10.5	21.0	(43.0)	NA	16.0	32.0	0.172	Hardy & Associates (1980)
48	183	1.28	7.0	11.3	(15.7)	2.83	68.0	109.7	(39.6)	6.07	75.0	121.0	0.175	Belshaw and Palmer (1978)
49	358	1.40	3.1	3.7	3.8	3.0	10.8	12.9	9.9	NA	12.2	14.5	0.109	Sagaseta (1973), Sagaseta & Escario (1974)
50	649	3.46	2.0	3.6	(3.5)	0.53	~4.0	7.3	(7.7)	~4.0	18.5	33.7	1.808	Uriel and Oteo (1979)
51	115	1.2	40.0	58.8	(18.0)	2.70	-	-	-	NA	170.0	250.0	-	Saenz and Utesa (1971)
52	265(15)	4.0	42.0	75.0	(32.6)	1.25	105.0	189.0	(84.3)	4.5	120.0	216.0	0.166(9)	Hanya (1977)

Table 5.31 Predicted and Measured Displacements at the Face and at the Point of Support Activation in Shallow Tunnels for the Crown (Continued).

No.	Tunnel and Section	Method	Lining	Ground	Water Level	Behaviour	D (m)	H (m)	E (MPa)	K	ϕ (°)	c (kPa)
1	Frankfurt 25 Romerberg Sth I	NATM$^{(1)}$	Shotcrete	Stiff clay marl CH MH	LO	DR	6.48	12.0	24	0.8	20	20
2	Frankfurt 25 Romerberg Sth II	NATM$^{(1)}$	Shotcrete	Stiff clay marl CH MH	LO	DR	6.48	11.5	24	0.8	20	20
3	Green Park Incl. X2	Open Shield	Cast iron seg.	London clay CH	B	UN	4.15	29.6	60	1.3	0	250
4	Green Park Incl. Y2	Open Shield	Cast iron seg.	London clay CH	B	UN	4.15	28.8	60	1.3	0	250
5	Green Park Incl. Z2	Open Shield	Cast iron seg.	London clay CH	B	UN	4.15	28.2	60	1.3	0	250
6	Chinnor Incl. P4	TBM	Steel ribs no lagg.	Lower chalk	A	DR	5.0	6.5	75	0.5	0	q_u=74,200
7	Chinnor Incl. P6	TBM	Steel ribs no lagg.	Lower chalk	A	DR	5.0	6.1	75	0.5	-	q_u=74,200
8	Victoria Line Anchor A	Open Shield	Cast iron seg.	London clay CH	B	UN	4.11	24.0	60	1.4	0	250
9	Edmonton Exper. SI11	Closed Shield	Exp. ribs & lagg.	'Soft' till - CL	A $^{(10)}$	UN	2.56	25.7	17	0.8	16	45
10	Edmonton Exper. SI31	Closed Shield	Exp. conc. seg.	'Soft' till - CL	A $^{(10)}$	UN	2.56	23.2	17	0.8	16	45
11	Edmonton Exper. SI33	Closed Shield	Exp. conc. seg.	'Soft' till - CL	A $^{(10)}$	UN	2.56	23.2	17	0.8	16	45
12	Edmonton LRT Sth SI3	Closed Shield	Exp. ribs & lagg.	'Stiff' till - CL	A	DR	6.17	9.8	70	0.75	40	0
13	Edmonton LRT Sth SI7	Closed Shield	Exp. ribs & lagg.	'Stiff' till - CL	A	DR	6.17	8.9	70	0.75	40	0
14	Edmonton LRT Sth SI6	Closed Shield	Exp. ribs & lagg.	'Stiff' till - CL	A	DR	6.17	8.9	70	0.75	40	0
15	S. Paulo Sanegran I	Open Shield	Precast conc.	Weathered gneiss	LO	DR	5.25	20.0	80	0.6	35	NA
16	Rio Mangueira SI4$^{(14)}$	Bernold Shield	Cast in place conc.	Residual soil SM-SC	LO	DR	7.0$^{(3)}$	6.4	15	0.5	40	10
17	Washington C line SI16	Open Shield	Exp. ribs & lagg.	Sand&silty sand SP SM	B $^{(18)}$	DR	6.45	11.7	35	0.5	35	0
18	Washington C Line SI20$^{(2)}$	Open Shield	Exp. ribs & lagg.	Sand&silty sand SP SM	B $^{(18)}$	DR	6.41	11.7	35	0.5	35	0
19	Winnipeg SI	Hand mined	Cast in place conc.	Varved clay CH	B	UN	1.93	11.7	6	0.8	0	70
20	Mississauga SID1	Open Shield	Steel ribs & lagg.	Dense till CL	B $^{(18)}$	DR	4.27	11.5	120	1.0	35	30
21	Thunder Bay I left SI	Closed Shield	Precast conc.	Soft silty clay CH	B	UN	2.47	9.6	7	0.9	0	30
22	Hagenholz L7	Open Shield	Precast conc.	Glacial lacustr. sed.	LO	DR	11.4	28.7	200	0.8	NA	NA

List of symbols and notes used in this table can be found in Table 5.33

Table 5.32 Predicted and Measured Displacements at the Face and at the Point of Support Activation in Shallow Tunnels for the Springline

No.	σ_{r0} (kPa)	y (m)	Displ. u at the face (mm)			L/D	Displ. u at lining installation or closure (mm)			Face Position for Final u (x/D)	Final u (mm)		ΔU After Support	Main References
			Meas.	Extr.	Predic.		Meas.	Extr.	Predic.		Meas.	Extr.		
1	226	0.5	3.9	4.6	10.3	0.69	7.9	9.2	28.6	1.56	8.8	10.3	0.018	Chambosse (1972)
2	281	0.5	17.0	19.9	9.9	0.69	16.07	16.0	27.6	1.70	13.5	15.8	-0.003	Chambosse (1972)
3	814	1.73	1.0	1.7	(10.4)	0.96	6.0	10.3	(29.3)	9.0	7.0	12.0	0.030	Attewell and Farmer (1974)
4	792	2.15	4.0	6.8	(10.1)	0.96	6.0	10.2	(28.5)	9.0	7.5	12.8	0.047	Attewell and Farmer (1974)
5	779	4.23	1.5	3.9	(9.9)	0.96	2.0	5.2	(28.0)	9.0	3.0	7.8	0.048	Attewell and Farmer (1974)
6	96	0.5	0.6	0.9	(0.9)	1.10	5.7	8.0	(2.9)	6.0	8.9	12.5	0.703	McCaul et al (1976)
7	92	0.5	0.6	0.9	(0.9)	1.10	4.4	6.2	(2.8)	3.0	5.7	8.0	0.293	McCaul et al (1976)
8	710	0.49	2.7	3.3	(9.1)	0.87	9.7	11.8	(24.9)	1.86	12.3	15.0	0.066	Ward (1969)
9	454	0.61	9.0	15.4	(11.5)	2.73	23.0	39.0	(35.7)	NA	27.0	46.0	0.102	El-Nahhas (1980)
10	412	1.12	2.4	5.1	(10.5)	2.73	4.6	9.8	(32.4)	11.0	2.8	2.87	-0.113	El-Nahhas (1980)
11	412	1.05	6.5	13.4	(10.5)	2.73	18.0	37.1	(32.4)	6.0	25.3	52.2	0.243	El-Nahhas (1980)
12	183	1.91	0.5	1.0	2.7	1.0	0.8	1.5	8.0	15.0	3.8	7.4	0.366	Thurber (1982)
13	171	1.21(16)	0.5	1.0	2.5	1.0	2.5	5.0	7.5	4.0	3.1	6.0	0.066	Branco (1981)
14	171	3.31(16)	0.4	1.2	2.5	1.0	1.8	5.2	7.5	4.9	2.5	7.2	0.133	Branco (1981)
15	258	1.58(17)	4.0(17)	7.4	(2.6)	1.56	11.0	20.5	(8.4)	3.8	21.0	39.1	0.687	Azevedo (1983, 1985)
16	89	0.8	3.0	4.5	(6.0)	4.5	20.0	30.0	(20.0)	NA	20.0	30	0	Massa (1981)
17	149	0.03	8.0	8.0	4.0	1.23	25.0	25.0	12.6	6.0	18.0	18.0	-0.255	Hansmire (1975)
18	149	0.72	2.0	3.0	3.9	1.1	22.5	33.8	12.6	1.55	29.6	44.4	0.388	Hansmire (1974)
19	172	0.60	8.0	11.8	(9.3)	2.0	14.0	20.6	(28.9)	4.0	15.0	22.1	0.027	Hardy & Assoc. (1980)
20	327	0.91	2.0	3.0	2.1	1.75	4.0	6.0	6.2	5.27	5.0	7.5	0.129	DeLory et al (1979)
21	178	0.93	12.0	18.5	(10.9)	2.83	3.0	46.0	(33.3)	8.0	33.0	51.0	0.080	Belshaw and Palmer (1978)
22	550	1.92	2.2	3.0	5.3	1.0	NA	-	-	-	-	-	-	Andraskay and Attinger (1979)

Table 5.32 Predicted and Measured Displacements at the Face and at the Point of Support Activation in Shallow Tunnels for the Springline (Continued).

No.	Tunnel and Section	Method	Lining	Ground	Water Level	Behaviour	D (m)	H (m)	E (MPa)	K	ϕ (°)	c (kPa)
1	Heathrow Cargo (UK)	Open Shield	Exp conc. seg.	London clay CH	B	UN	10.9	7.3	27	1.9	0	200
2	Edmonton LRT (Sth) ME10	Closed Shield	Exp ribs & lagg	'Stiff' till CL	A	DR	6.17	8.9	70	0.75	40	0
3	Edmonton Exper. ext. MX37	Closed Shield	Exp conc. seg.	"Soft' till CL	$A^{(10)}$	UN	2.56	23.2	17	0.8	16	45
4	S. Paulo ABV ext. BH1 (B7)	Mined	Steel ribs & lagg.	Clayey sand SC	A	DR	$3.99^{(13)}$	6.7	28	0.75	29	0
5	S. Paulo ABV ext GG1 (G8)	NATM	Shotcrete	Clayey sand SC	A	DR	4.04	6.5	28	0.75	29	0
6	S. Paulo ABV ext. CC1 (C9)	NATM	Shotcrete	Clayey sand SC	A	DR	4.04	6.2	28	0.75	29	0

			Displ. u at the face (mm)				Displ. u at lining installation or closure (mm)				Final u (mm)			
No.	σ_{r0} (kPa)	y (m)	Meas.	Extr.	Predic.	L/D	Meas.	Extr.	Predic.	Face Position for Final u (x/D)	Meas.	Extr.	ΔU After Support	Main References
1	382	0.30	3.2	4.6	(-5.3)	0.33	NA	NA	-	NA	NA	NA	NA	Muir Wood and Gibb (1971)
2	286	-	2.7	2.7	3.1	1.00	NA	NA	-	NA	NA	NA	NA	Branco (1981)
3	542	$1.3^{(19)}$	2.0	12.0	(9.5)	2.73	2.4	15.0	-	5.4	3.0	19.0	0.049	El-Nahhas (1980)
4	171	0.46	1.0	1.2	3.0	NA	NA	–	–	1.5	3.0	3.6	-	Negro and Eisenstein (1981)
5	171	1.70	3.5	6.2	3.0	0.6	4.5	8.0	9.1	1.0	7.0	12.4	0.178	Negro and Eisenstein (1981)
6	165	1.24	1.5	2.1	2.9	0.6	4.5	6.3	8.7	2.22	9.0	13.5	0.302	Negro and Eisenstein (1981)

Table 5.33 Predicted and Measured Displacements at the Face and at the Point of Support Activation in Shallow Tunnels for the Floor

SYMBOLS	
LO	Water level lowered before construction
A	Tunnel above ground water level
B	Tunnel below ground water level
DR	Drained behaviour (and parameters) assumed
UN	Undrained behaviour (and parameters) assumed
D	Excavation diameter
H	Depth of cover to tunnel crown
E	Average initial tangent modulus of soil around the tunnel (drained or undrained)
K	In situ stress ratio (effective or total stresses)
ϕ	Friction angle (drained or undrained)
c	Cohesion (drained or undrained)
σ_{r0}	Radial stress at the point considered (effective or total stresses)
y	Radial distance between instrument and tunnel contour
Meas. u	Measured radial displacement at a point close to the tunnel contour
Extr. u	Radial displacement extrapolated to the tunnel contour
Predic. u	Predicted radial displacement
L/D	Relative distance between face and point of lining closure or activation

NOTES	
(1)	Twin tunnels driven simultaneously
(2)	Second tunnel built (excluding movements due to the first)
(3)	Equivalent diameter of excavation (non circular profile)
(4)	Data from side drift advance only
(5)	With compressed air
(6)	61 kPa of air pressure discounted
(7)	After southbound tunnel was driven
(8)	40 kPa of bentonite pressure discounted
(9)	Disregarding air or bentonite pressure
(10)	Tunnel above regional water table but possibly below perched water levels. Soil fully saturated
(11)	50 kPa of air pressure discounted
(12)	70 kPa of air pressure discounted
(13)	100 kPa of air pressure discounted
(14)	Tunnel heading only
(15)	95 kPa of air pressure discounted
(16)	Measuring point 0.4 m above springline elevation
(17)	Average of two inclinometers
(18)	Crown below water level. GWL lowered by drainage into the tunnel during advance
(19)	Measuring point 1.9 m off the centreline

Symbols and Notes for Tables 5.31 to 5.33

are also indicated. The geometric data of each case history is summarized in terms of the depth of the cover and in terms of the diameter of the excavation. An equivalent excavation diameter is provided in those cases where the tunnel had a non-circular cut profile. In a few cases, compressed air pressure or slurry pressure was used during construction. In these cases, the radial in situ stress at the point being considered was reduced by an amount equal to that pressure.

Attempts were made in each case to identify the probable response of the ground in terms of the generation and dissipation of pore pressures over the period of time the field measurements were taken up to the instant the lining was installed or closed. For this, the approximate criteria proposed in Chapter 3 were used, and these required an estimate of the coefficient of consolidation of the soil. Whenever this information was not available, that coefficient was evaluated indirectly through the coefficient of permeability and the deformation properties of the ground. To simplify the interpretation of data, only two extreme cases were considered: "drained" or "undrained" behaviour. Those cases where the ground response may have been situated between the two extremes, were labelled according to the extreme response closer to the one that most likely prevailed. A considerable degree of subjective interpretation might, therefore, have been included.

The ground properties were defined in accordance with the above classification. Drained or undrained deformation and strength properties were selected appropriately. Similarly, the in situ stress ratio K was defined in terms of effective or total stresses.

To account for the variations of the in situ deformation modulus with depth, an average E value was taken for points of the ground around the tunnel profile. Whenever the stress-strain data were available for a particular site, the selected E value corresponded to the initial tangent modulus defined at the early portion of a test result. In all cases where neither these nor laboratory tests were available, established correlations have been used to estimate the properties of the ground mass.

When dewatering preceded tunnel construction, the displacements associated with it have been deduced from the observed movements. Hence, the ground movements recorded in the tables refer, as much as possible, to those resulting from the tunnel construction and exclude those due to time dependent responses.

The displacements indicated in the tables are those measured by settlement points or slope indicators installed closer to the opening. Except where indicated, they can be taken as movements radial to the tunnel contour. In each case history, the displacements at three situations were identified: a) when the tunnel face (or the face of the heading in a staged excavation) reached the instrumented section; b) when the lining was activated or when the support ring was closed (in the staged application of a shotcrete lining) at the instrumented section; c) when the movements stabilized (in short term conditions). For situations (b) and (c), the tables provide the relative position of the tunnel face ahead of the measuring section. For shotcrete supports, cast-in-place concrete liners or expanded lining systems, no major difficulty was experienced in identifying the situation (b) at which the support was put in full contact with the ground. For grouted, pre-fabricated linings, however, it was not always simple to identify when this happened. In many cases, this depended on how much behind the face the grouting operation took place, but the information supplied by the references on this particular point are frequently vague or inaccurate. After a careful study of the construction procedures, the section at which the support activation possibly occurred was defined, but no assurance on the accuracy of its location is given, since it also depends on the quality of the grouting operation undertaken. If the grout failed to completely fill the void behind the lining, the support may have not have come in full contact with the soil at that section. Therefore, it cannot be said to have been fully activated there, but only at distances larger than the value shown. The displacements at situation (b) above would be those taking place just before ground-lining interaction starts at the instrumented section. Only when shotcrete is used does there exist some degree of confidence on the estimated distance of delayed support application (L/D), as its contact with the ground is usually "good" (Section 2.3.5). But even in this case, some uncertainty may exist as the records of the construction are not always given in sufficient detail.

Usually, field measurements of displacements are taken not at the tunnel perimeter but at a certain distance away. To allow adequate comparison between the proposed method of estimating the closure of the tunnel profile and the data from case histories, it was necessary to extrapolate the field measurements to the tunnel contour. To achieve this, the results of parametric non-linear elastic finite element analyses were used. These analyses are described and presented in detail in Chapter 6. Their results have partly presented by Eisenstein and Negro (1985:Figure 5). These analyses allowed the definition of the ratio between the perimeter displacement to that measured at a distance y from it (this distance is also shown in the tables). This ratio, as it will be shown in Chapter 6, is mainly a function of y, in relation to the tunnel diameter, of the ratio H/D, of the in situ stress ratio and of the ground properties (mainly ground strength). Clearly, the ratio would not be applicable to cases where localized ground collapse may have occurred. Since this condition could not be identified readily, the extrapolation was undertaken by this method in all cases investigated.

Besides the values of the extrapolated measurements to the tunnel contour, the tables provided the predicted radial displacements for comparison. These were estimated using the data shown in the tables, and the numerically derived solution for tunnel closure as proposed in Section 5.3.5.2 (Figures 5.94 to 5.96). Many of the predicted displacements are placed within brackets in the tables. This indicates that the input parameters used for the prediction lay beyond the formal range of validity of the proposed method of calculation (either in terms of K or H/D). Despite this, the predictions were made as if they were rigorously valid.

Note that the predictions were made only for displacements occurring at the tunnel face and at the point of lining activation. The tables, however, include the final radial displacements. Using the definition of the dimensionless radial displacement given by Equation 2.16, it was possible to calculate the increment, ΔU, of the dimensionless displacement after the support was activated and until the movements stabilized in each case history. This corresponds to the deformations that the support would ideally endure, provided a good lining-ground contact exists. A negative sign in the ΔU value reveals an outward movement.

Without exception, all observed radial movements taking place at the face, as well as the increments of displacement between the face and the section at which the support was activated, were positive (inwards). Most of the increments after the support was activated were also positive. A few exceptions to this were noted. One was the Green Park tunnel (extensometer X1), corresponding to case 13 in Table 5.31, where an outward crown movement was observed in this tunnel driven through London Clay. Further exceptions are indicated in Table 5.32 for the tunnel springline: cases 2, 10 and 17 also showed outward springline displacements after the lining was installed. Case 2 corresponds to a shotcrete lining, and cases 10 and 17 to expanded steel ribs and wooden lagging primary support.

Predicted and Measured Radial Displacements at the Face

The radial displacements of the tunnel crown at the face are compared in Figure 5.102 a and b. Figure 5.102 b is simply an enlargement of part of Figure 5.102 a. To help the comparison, the ground was classified into four groups as shown. The "stiff clay" group actually included clayey soils with consistencies ranging from medium to hard. The "soft clay" group includes soils with high clay content and with undrained cohesive strengths smaller than 50 kPa. The "granular soil" group comprises all soils with an appreciable content of sandy or gravelly fractions, with or without fines (silty or clayey). Finally the "soft rock" group includes both weathered and unweathered rocks.

Globally speaking, one notes that, within plus or minus 20%, the extrapolated measurements are approximated by the predicted values in about 50% of the cases. There is a slightly more pronounced trend of the predictive method to

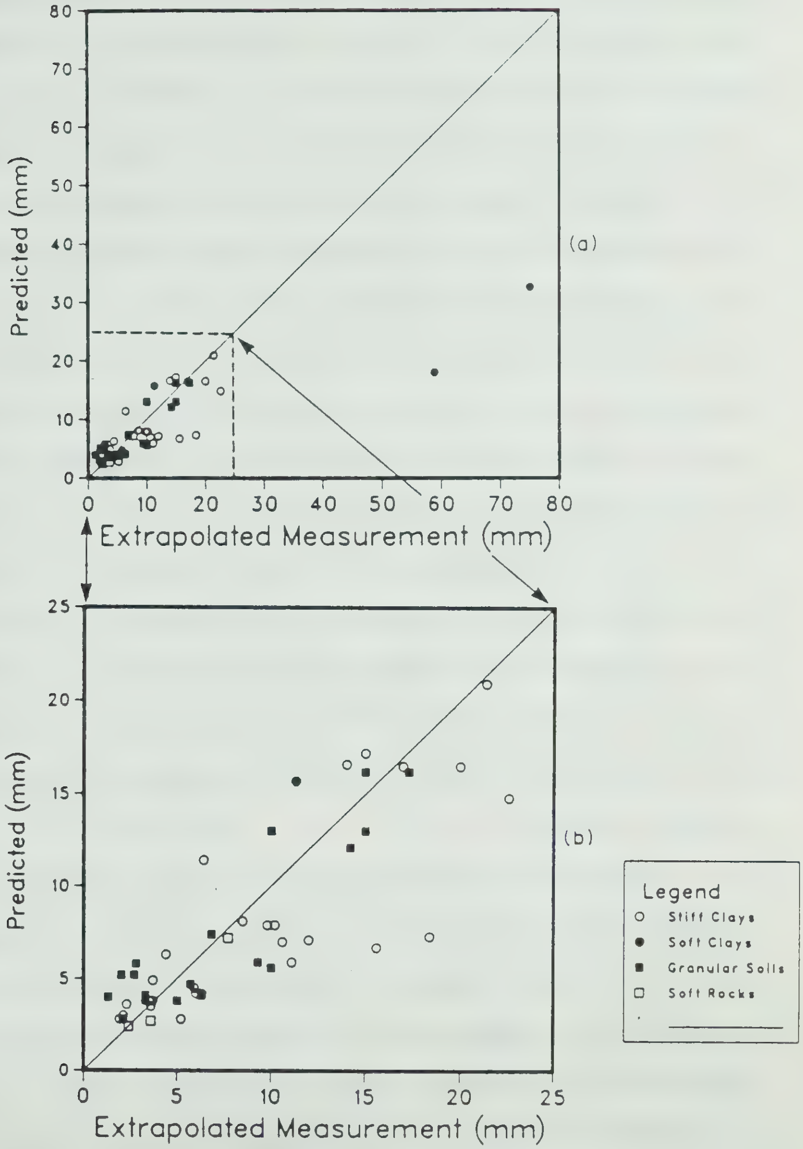

Figure 5.102 Predicted and Measured Crown Displacements at the Face for Different Ground Types

underestimate the displacements than to overestimate them (30% against 20% of the cases approximately). The predictions are based on a linear elastic numerical solution, and make use of the initial tangent modulus of the soil. Whenever departure from linear behaviour is observed in the ground, one would expect the simplified method to underestimate the field measurement. This could explain the noted trend. However, the frequency of cases where the displacements were overestimated is also high. Thus, one may suggest that the correct choice of the parameters of the soil, particularly the E modulus, is far more important than the simplified assumption of linear elasticity, as far as the estimate of displacements at the face are concerned. When applied to soft clays, the method shows a stronger tendency to underpredict the movements, which is explained by the more pronounced non-linear response likely to prevail in these cases.

A similar plot was prepared for the springline radial displacements, and is shown in Figure 5.103. An appreciable scatter is noted, despite the smaller number of cases available for comparison. A slightly more pronounced tendency of the present method to overestimate the displacements is noted. The reasons for this are not clear. One could speculate that the proposed method makes no allowance of ground anisotropy. Certain soils, such as London and Frankfurt clays are known to exhibit anisotropic behaviour, with horizontal deformation moduli larger than the vertical. On the other hand, the larger scatter of points could be explained in terms of the lesser accuracy possible in inclinometer results compared to the accuracy of settlement measurements by extensometers or levelling.

The lack of a sufficient number of case histories where floor heave has been measured does not allow an adequate evaluation of the predictions made for this point. Nevertheless, it is believed that the proposed method can yield sensible results (Table 5.33).

Another possible interpretation of the results presented so far, is to relate the displacement comparison with the construction method used. Accordingly, the data presented in the former two figures was replotted as shown in Figure 5.104 a and b. Three groups of construction methods were identified: (a) NATM construction, (b) Mechanized Construction Methods using TBM's and/or shields; (c) other mining methods. It is soon noticed that better agreement between predictions and measurements was obtained for methods (a) and (c). This is noted in spite of these methods do not always involve a full face excavation, as assumed in the development of the proposed prediction method. At least two reasons can be looked at to explain this. The use of non-mechanized and unshielded heading excavations are normally confined to fairly stable, stiffer and stronger ground. A linear elastic assumption, if applicable to any ground, would be more suitable for this type of soil. Secondly, and perhaps, more importantly, the

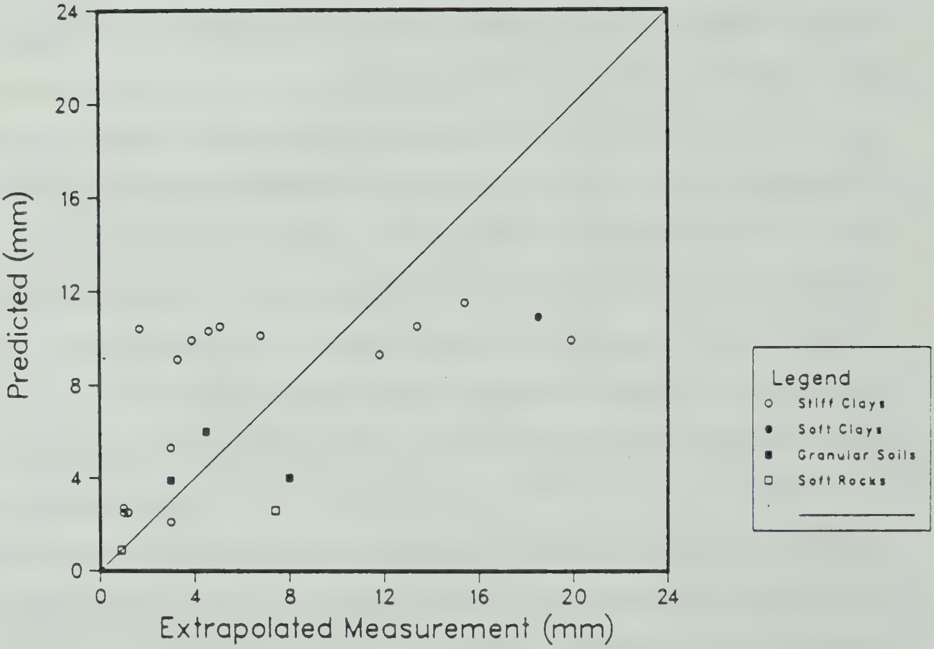

Figure 5.103 Predicted and Measured Springline Displacements at the Face, for Different Ground Types

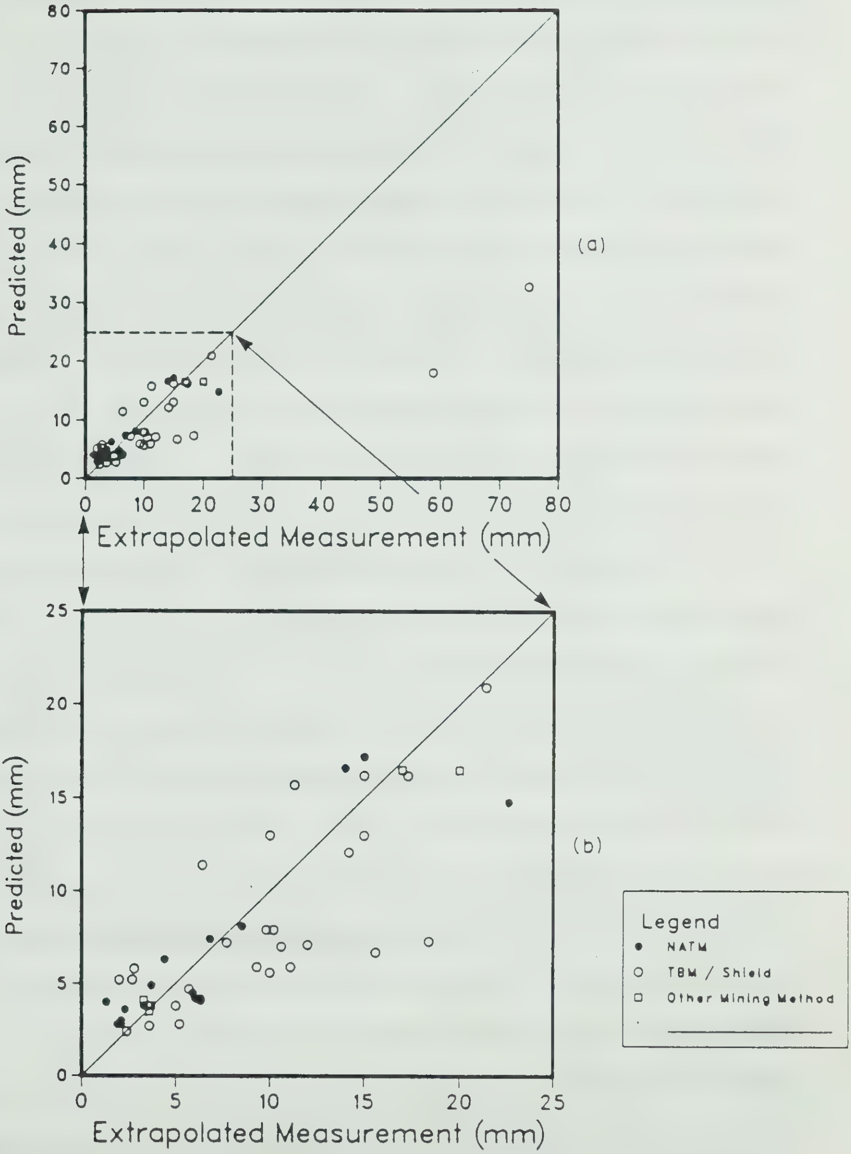

Figure 5.104 Predicted and Measured Crown Displacements at the Face for Different Tunnel Construction Methods

unprotected excavation requires for safety reasons, improved ground control measures. One of these is the earlier activation of the support. Tunnel convergence is restrained sooner by the support being activated closer to the face, and usually is without voids behind it. Most TBM or shielded excavated systems have residual void spaces behind the support. As a consequence, smaller ground stress release would be expected in (a) and (c), and possibly, less pronounced non-linear response in the ground. As for the springline displacements at the face, the results shown in Figure 5.105 do not permit any clear conclusion to be drawn.

The comparison between predicted and extrapolated measurements of radial displacement in the tunnel contour at the face show considerable scatter. It must be borne in mind that the data refers to case histories where a complete and accurate knowledge of ground properties and site conditions were not always available. Also, the predictive method encompasses substantial simplification, while still considering the most important factors. Under these circumstances the results obtained are not completely discouraging. The predicted value of displacement is particularly sensitive to the E modulus, and its correct value is not always known. The variation of this parameter alone for one particular deposit may be responsible to a significant extent, for the scatter observed in the last few figures.

Predicted and Measured Radial Displacements at the Section

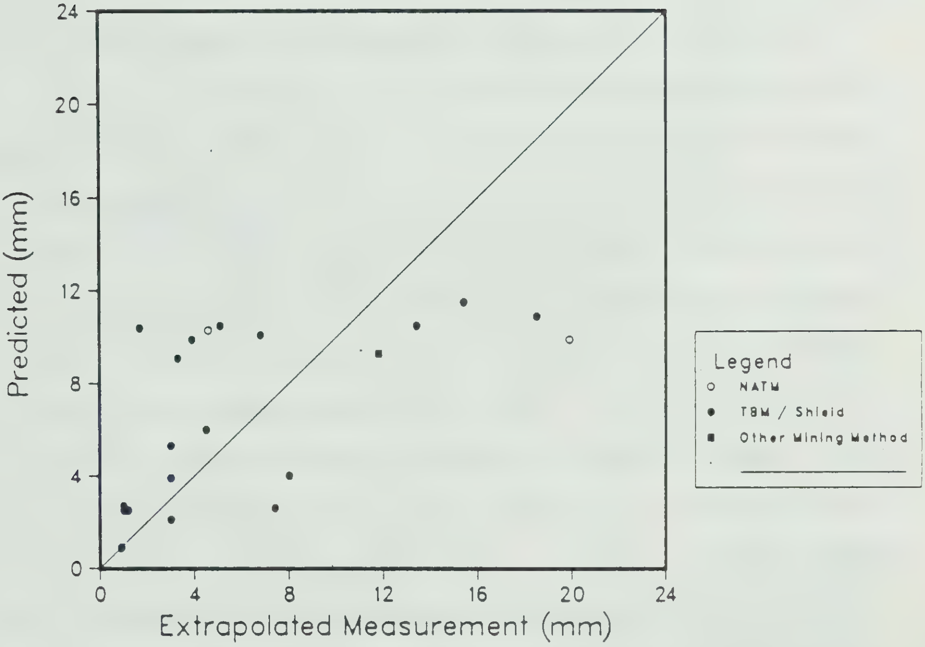

Figure 5.105 Predicted and Measured Springlne Displacements at the Face, for Different Tunnel Construction Methods

of Support Installation

The same interpretations presented for the displacements at the tunnel face were repeated for the ground movements at the tunnel sections where the support was installed. As noted before, these correspond to the sections where the shotcrete ring was closed at the floor in the NATM built tunnels.

Figures 5.106 a and b present the comparison of the crown displacements according to the different types of ground. Here one notes that for both soft clays and granular soils, the displacements tend to be underpredicted. An examination of Figures 5.107 a and b, in which the same results are presented according to the construction methods, reveals that those cases where this tendency was noted, correspond mainly to TBM or shielded excavation schemes. In other words, in TBM or shielded excavations of tunnels in soft clays and in granular soils, the proposed prediction method shows a trend to yield displacements which are smaller than those actually observed. This tendency could possibly be attributed to these soils squeezing in or collapsing to close the gap created by overcutting which is left behind the shield or the lining. In these construction schemes, the support is installed at a greater distance behind the face, and depending on the amount of overcut allowed, and on when and how efficient the grout or lining expansion operations are, the amount of stress release induced in the ground can be larger than in other

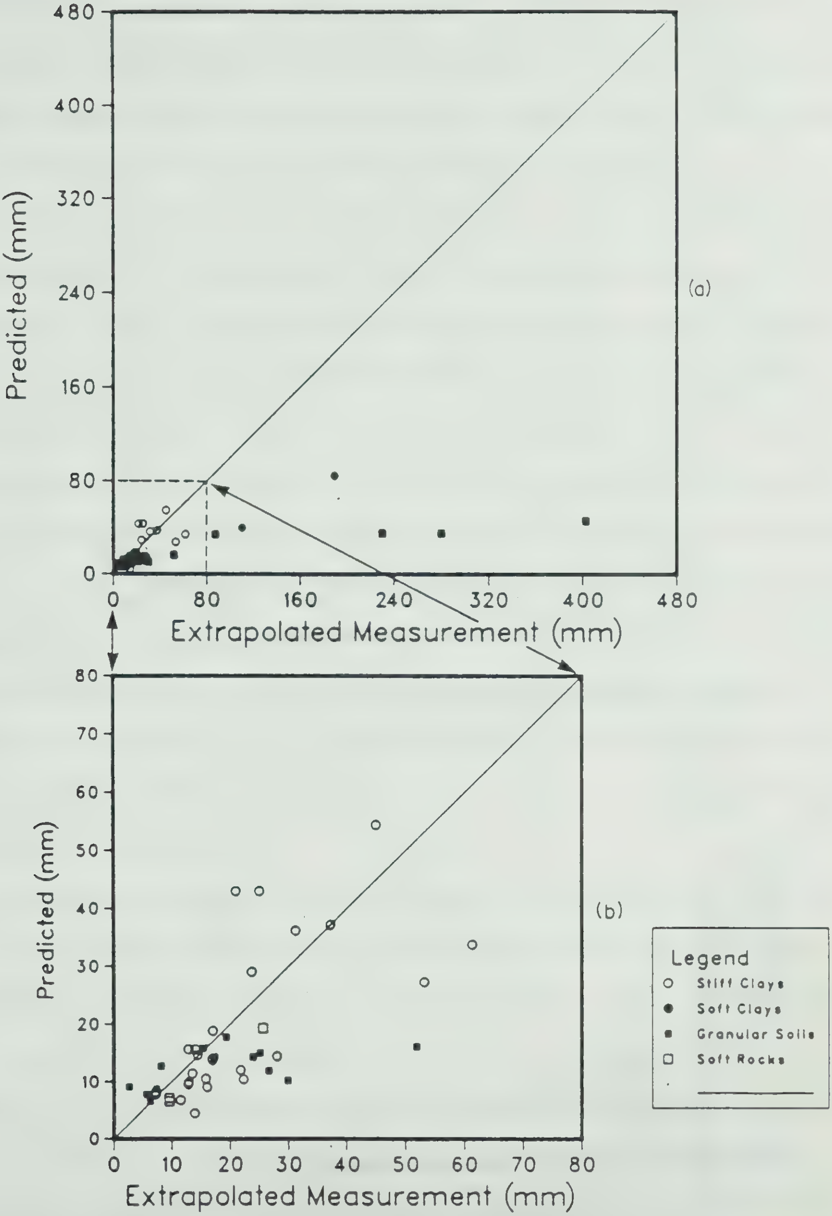

Figure 5.106 Predicted and Measured Crown Displacements at the Section the Support was Installed for Different Ground Types

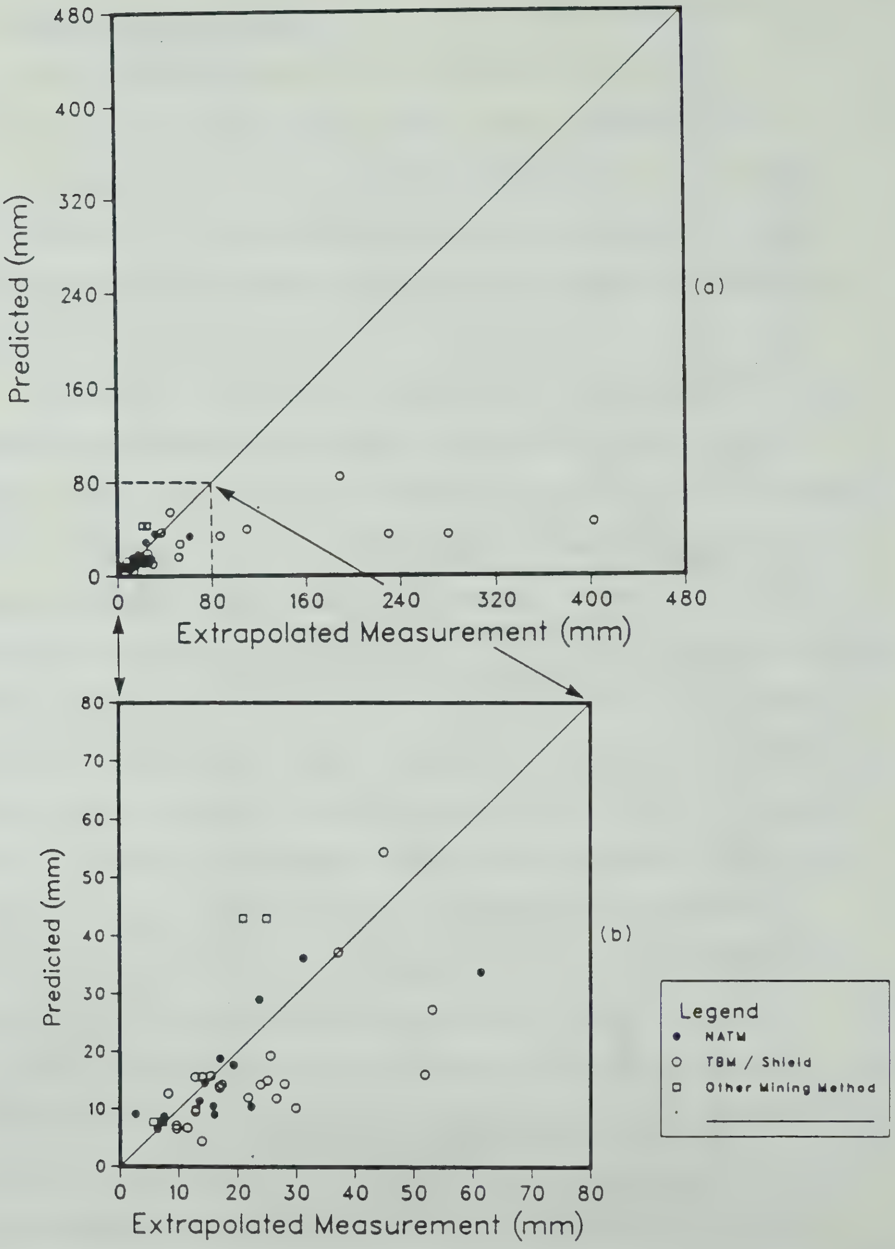

Figure 5.107 Predicted and Measured Crown Displacements at the Section the Support was Installed for Different Tunnel Construction Methods

construction schemes. Hence, a more pronounced departure from the linear response of the ground may be expected, and this leads to movements larger than those anticipated using the proposed method of tunnel closure calculation.

To illustrate this point further, Figures 5.108 a and b were prepared. The dimensionless crown displacements at the sections where the linings were installed, were calculated using the extrapolated measurements and other parameters provided by Table 5.31. These dimensionless displacements were plotted as a function of the distance X/D between the section where the lining was installed and the tunnel face. In (a), the observed data is presented according to the type of ground found in each case. In (b), the data is presented as a function of the construction method used. Included in both (a) and (b) is the distribution of the dimensionless radial displacement along the crown as given by the proposed solution, for K=0.5.

A quick examination of Figures 5.108 a and b confirms that the larger movements are noted for TBM or shielded schemes and are basically associated with soft or granular soils. This is particularly true when the support is installed at distances from the face greater than 1 to 1.2 D. In Section 2.3.4.3, a tentative criterion for ground collapse was proposed in terms of the dimensionless crown displacement. It was noted from tunnel model tests that whenever U exceeded 1.8, a near collapse condition was observed. If this criterion is correct, those points in

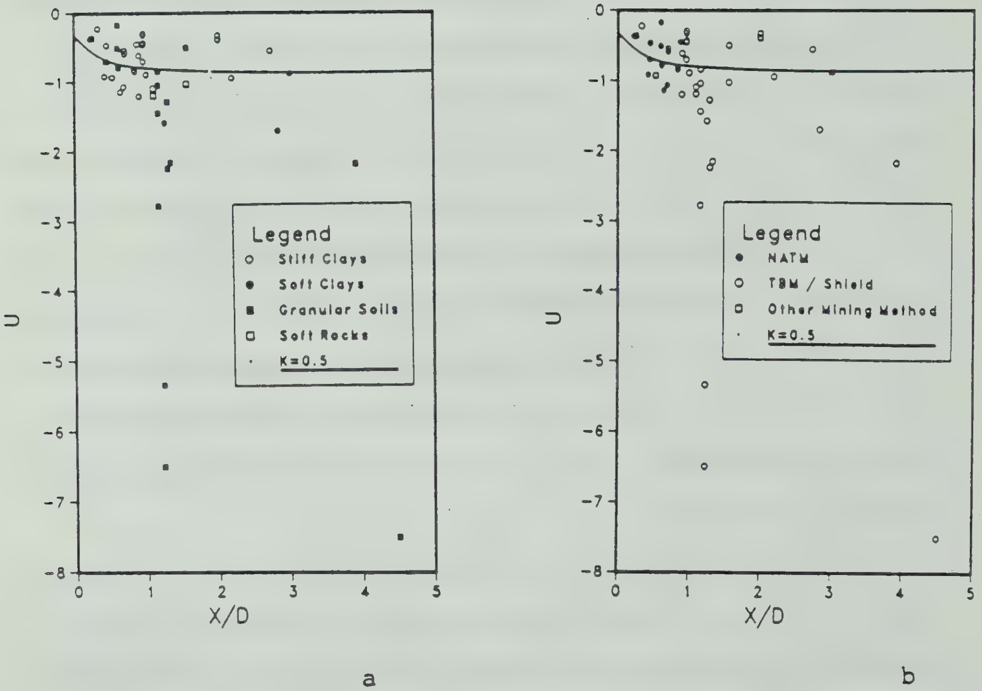

Figure 5.108 Dimensionless Crown Displacements Observed when the Support was Installed at Different Distances Behind the Tunnel Face

Figure 5.108 showing larger movements represent critical conditions where high shear strain concentration may have developed. These would involve substantial failure zones and ground instabilities such as running sand, fall-outs, etc. A review of the construction records of those case histories involved (e.g. Washington Metro), does reveal that these conditions may indeed have happened.

Recalling the discussion presented in Section 2.3.5.4, it is very likely that in those cases where the larger U values were noted, a poor lining contact may have existed which possibly resulted from excessive overcut. An overbreak larger than that set in Section 2.3.5.4 by the proposed limited overcut bringing about instability may have been the cause of the observed large movements.

While in TBM or shielded schemes the support is installed at distances greater than 1D behind the face, in NATM construction schemes, the shotcrete ring is closed at distances smaller than 1D behind the heading face (see Figure 5.108). Moreover, in the latter schemes, provided the face is stable, instabilities at the roof are seldom noticed, since the depth of unsupported advance of the heading (round length) is usually small (typically between 0.1 and 0.3D). Localized instabilities or collapse are prevented by the immediate shotcreting of the tunnel walls after the short advance. Despite the reduced strength and large deformation properties of the young shotcrete shell, it may be adequate to prevent local ground instabilities, although possibly not enough to completely restrain the ground movements. In other words, it does not impede the tunnel closure but it controls it, allowing the ground to relax without localized instabilities.

Despite the soil type, the NATM construction schemes seem to have yielded U values always smaller than about 1.0 at the section of lining closure. According to the material in Section 2.3.4.3, this value would correspond to factors of safety of about 1.5 or higher and be considered as "good ground control conditions". These conditions seem to have prevailed in all of the NATM constructions investigated, regardless of the ground type. To a great extent, these conditions seem to have existed in the NATM cases as a result of reduced overbreaks and good ground-lining contact.

To complete the picture, Figures 5.109 and 5.110 present comparisons between predicted and measured springline displacements before the support installation. Similar to the displacements at the tunnel face, a considerable scatter is noted, as well as a slightly more pronounced trend for overestimating the displacements at the section the support is installed.

In summary, if the simplified method presented herein for estimating the tunnel wall closure prior to the lining installation was to be successfully applied in practice, it would be only used in cases where good ground control conditions are specified and implemented in the tunnel construction. This seems to imply that this method may render sensible results in NATM construction schemes, regardless of the soil type (but provided the face is stable) and in TBM or shielded schemes when applied to firm grounds or even to less stable grounds, whenever the overcut is small and the lining is activated in full contact with the soil at a short distance from the face.

Measured Crown Displacements after Support Installation

The survey summarized in Table 5.31 allowed an additional set of information to be gathered. This refers to the increment of dimensionless crown displacement (ΔU) taking place after the lining is installed. This was calculated from the increment of the extrapolated crown displacement in the radial direction after the support was installed, until the ground movements stabilized (in the short term).

Figure 5.111 presents the data collected for three groups of support systems: (a) shotcrete; (b) prefabricated lining and grouted behind; (c) prefabricated lining, expanded against the soil. The prefabricated systems include precast segmented concrete linings, cast iron and steel segmented rings, as well as steel ribs and lagging. The data is shown in terms of frequency of cases for different ΔU intervals. The total number of cases for each different support group is shown in the figure.

The distinctions between these support systems are many, but within the present discussion, their main difference refers to what was defined in Chapter 2 as the

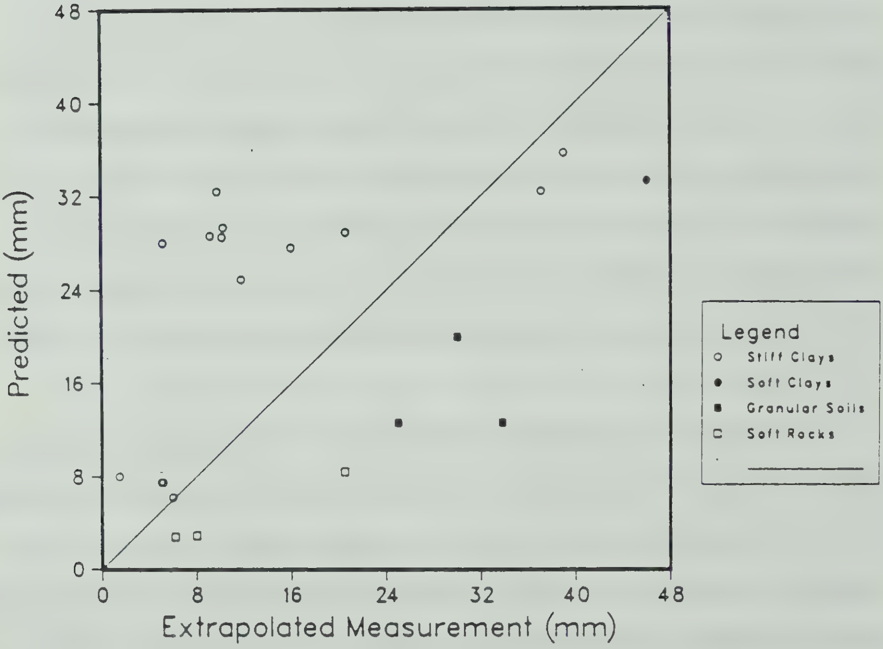

Figure 5.109 Predicted and Measured Springline Displacements at the Section the Support was Installed, for Different Ground Types

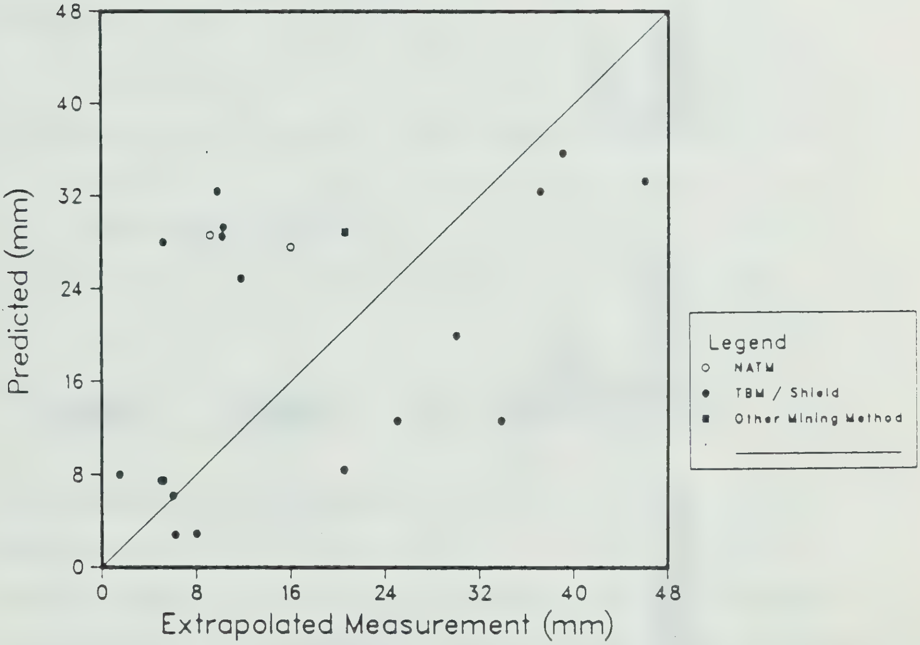

Figure 5.110 Predicted and Measured Springline Displacements at the Section the Support was Installed for Different Tunnel Construction Methods

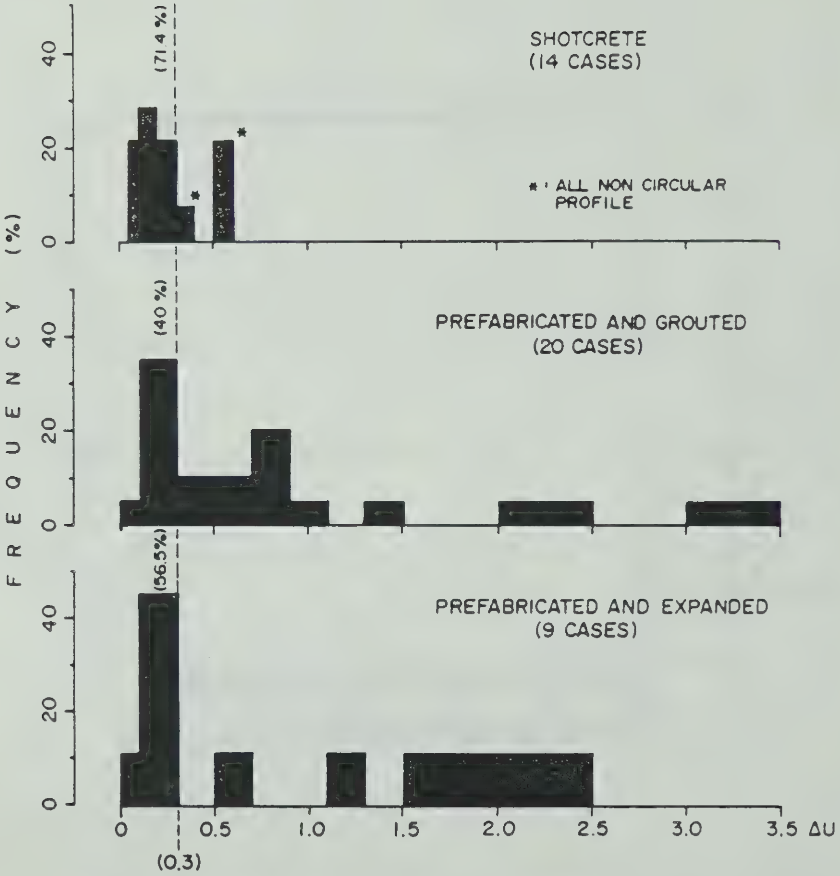

Figure 5.111 Distributions of Measured Crown Displacements after Support Installation

"quality" of the lining-ground contact. While in most shotcrete supports it is reasonable to assume that a full lining-ground contact may exist, in the other groups this may not be the case. The crown movements noted after lining installation in the last two groups may not be solely related to the relative stiffness of the support, but, are to a great degree, also affected by the size of the void left behind the lining.

For shotcrete linings, one notes that in more than 70% of the cases, ΔU is equal to or less than 0.3. If the cases in this group with a non-circular tunnel profiles (with width larger than height) were eliminated, then one could say that for circular shotcrete liners, the increment ΔU is always equal to or less than 0.3. If ΔU equal to 0.3 is taken as a reference value for limiting crown deformation of a lined tunnel with good support-soil contact, one would say that for prefabricated and grouted supports, only 40% of the cases responded as if having such a contact quality. A slightly higher accumulated frequency (56.5%) is noted for prefabricated and expanded supports. The slightly higher frequency would indicate that, in terms of ground control, expanded systems are marginally better than grouted systems.

Figure 5.112 presents the distributions of the frequency of the dimensionless crown displacement at the tunnel face, calculated from the extrapolated radial displacements which are indicated in Table 5.31. Separate distributions are shown for each ground group. One notes that, out of the total number of cases, the value of U at the face is equal to or less than 0.5, in more than 90% of the cases.

By recalling the limiting dimensionless crown displacement of 1.8 proposed in Section 2.3.4.3, a limiting increment of dimensionless crown movement can be established for between the tunnel face and the point of activation of the support in full contact with the soil. This would correspond to the total critical U less the maximum U taking place ahead of the face (0.5) and less the maximum U taking place after the support with good contact with the soil is installed (0.3). This results in the criterion of U=1.0 proposed in Section 2.3.5.4 for a maximum acceptable overbreak over a TBM or shield. The proposed approximate criterion was discussed and justified in that section.

5.3.6.2 Ground Movements Ahead of the Tunnel Face

In Section 5.3.5.2, an approximate equation was proposed to estimate the maximum horizontal movement of the face of a shallow tunnel. Table 5.34 lists a few case histories where that simplified expression was tested. In all cases the horizontal movements ahead of the tunnel face were monitored. It should be noted that while the calculated movements are those right at the face plane, the measurements were taken at some distance behind as indicated in the table. Thus, it would be expected that the predicted values would exceed the observed by some amount. To obtain the calculated maximum displacements, the information given

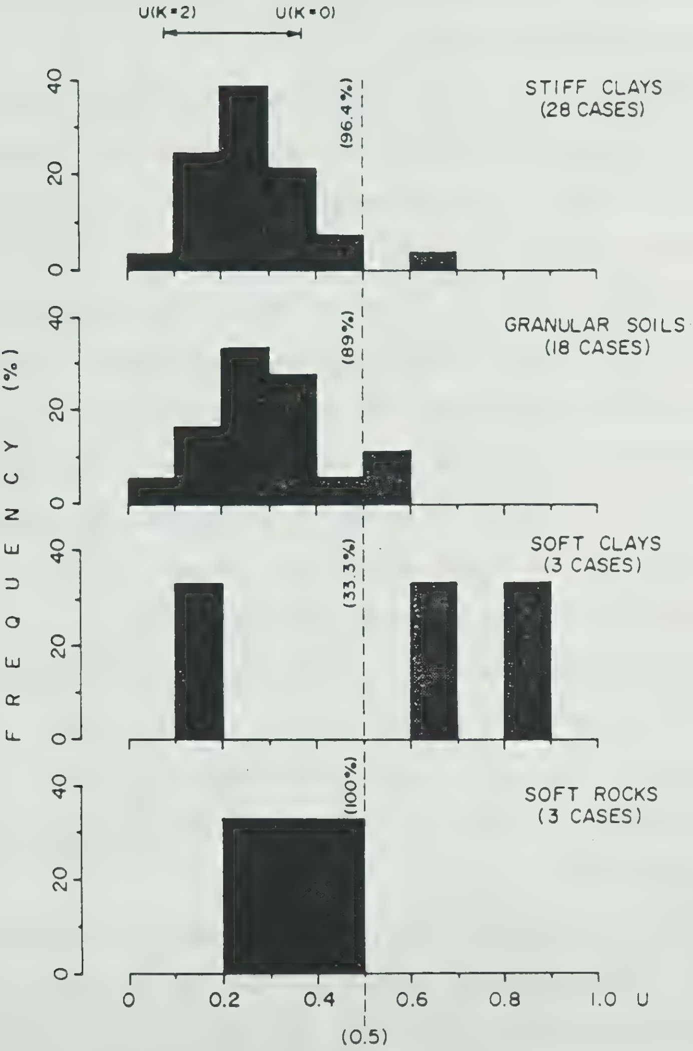

Figure 5.112 Distributions of Measured Crown Displacements at the Tunnel Face

in Table 5.31 was used. As it is observed in Table 5.34, the approximate equation yields fairly sensible results with calculated and measured horizontal movements being of the same order of magnitude.

Section 5.3.5.2 also proposed simplified procedures to evaluate the maximum longitudinal distortions ahead of an advancing tunnel. Unfortunately, not many case histories made this type of information available. In the cases listed in Table 5.35, contour lines of equal surface settlements ahead of the tunnel were presented. Therefore, the maximum surface distortion along the tunnel axis could be adequately estimated and are shown in the table. The calculated surface distortion was obtained by first ascertaining the maximum distortion at the crown elevation, using the approximate equation [5.13]. The maximum surface distortion was then obtained through the relation between the crown and surface distortions shown in Figure 5.100. In each case, the data presented in Table 5.31 served as input for the calculations. The approximate procedure proved to yield fairly sensible results.

The simplified methods for estimating ground movements ahead of the advancing tunnel should not be understood as being actual prediction tools, but rather as simple expedients whose merit is to avoid the need of expensive three-dimensional analyses otherwise required for such estimates. Accordingly, they should be only used to assess the order of magnitude of these movements. On a case by case

Tunnel	Distance to the face when reading was taken (m)	Max. inward movement (mm)		Reference
		Measured	Calculated(1)	
Washington C-Line (1st) SI 17	1.5	6	22	Hansmire (1975:52)
Edmonton LRT (Sth) SI 12	3.6	~4	7	Branco (1981:106)
Butterberg - Osterode	1.3	14	13	Meister and Wallner (1977:926)
Victoria Line anchor A	0	18	24	Ward (1969:323)

Note: (1) $u_f \approx 0.5D \frac{\sigma_{0c}}{E}$

Table 5.34 Calculated and Observed Maximum Horizontal Movements of the Tunnel Face

Tunnel	Maximum longitudinal distortion			Reference
	Calculated			
	At Crown$^{(1)}$	At Surface$^{(2)}$	Measured at Surface	
Washington C-line	1:100	1:1400	1:1200	Hansmire & Cording (1972:383)
Edmonton LRT (Sth)	1:290	1:3200	1:4000	Branco (1981:66)
S. Paulo ABV (NATM)	1:190	1:2500	1:4500	Negro and Eisenstein (1981)
S. Paulo N. Ext. (S1.3 to S1.9) (3)	1:260	1:2340	1:2000	Negro et al (1985)

Notes: (1) $\gamma_{cmax} \simeq 1.5\ \sigma_{0c}/E$

(2) From Figure 5.100

(3) Complete section with D = 9.84 m (non circular profile).

Table 5.35 Calculated and Observed Maximum Longitudinal Distortions at the Ground Surface, Ahead of the Tunnel Face

basis they should be tested and calibrated against field performance in order to make it reliable for predictive purposes within an observational metnod approach.

5.3.7 Summary and Conclusions

The need to estimate the amount of tunnel closure was explained within the present work, in terms of the need to estimate the amount of ground stress release in a two-dimensional tunnel representation.

Available solutions for estimating the tunnel convergence at and behind the face were reviewed. It was found that they are of little help for solving the shallow tunnel problem. Therefore, it was decided to attempt the development of a new and specific solution for the problem at hand. Moreover, it was decided to make use of three-dimensional finite element modelling for that purpose. Consequently, a brief review on the subject was undertaken, and the main features of previous 3D modelling of shallow tunnels were investigated and discussed. This review guided the selection and implementation of the numerical solution adopted in this study.

The details of the numerical modelling procedure used were presented and discussed. The assumptions, limitations and shortcomings of the solution adopted were examined.

Parametric numerical analyses were conducted and their results presented in terms of longitudinal distribution of dimensionless radial displacements at three points of the tunnel perimeter and at other points within the ground mass.

These results were interpreted and an approximate solution for estimating the tunnel closure of an unlined tunnel in an elastic medium was proposed. The solution allows the radial displacements at crown, springline and floor, to be obtained as a function of the Young's modulus of the soil, of the tunnel diameter and of the radial in situ stresses acting at those points of the tunnel contour, for different sections at or behind the face.

Another simplified solution was developed from the parametric analyses which permits estimates of the maximum horizontal displacement of the tunnel face.

Additional approximate solutions were proposed for the evaluation of the maximum angular distortion along the tunnel at the crown elevation, at some distance above it and at the ground surface. The validity of the approximations made were discussed.

The proposed solution for shallow tunnel closure estimates was compared to another method developed for a deep tunnel situation. Moreover, the presently proposed method was used to predict the convergence of actual shallow tunnels, observed for a number of case histories. Of interest were the radial displacements of the tunnel contour at the face and at the section where the support was installed. Details of each case history were presented.

The comparisons between predicted and measured radial displacements at the face and at the section where the lining was installed were presented and analysed. The ability of the proposed approximate method to predict actual tunnel closure was investigated for each ground type and for each construction method involved in the case histories. The reasons for departures between predictions and measurements were discussed. The ground and construction conditions where the proposed method is likely to yield better estimates were identified as well as the conditions where the method fails to provide good results. The approximate nature of the present solution was emphasized.

The extensive survey of case histories allowed an empirical evaluation of the maximum amount of crown settlement taking place after the installation of the support in full contact with the ground. Furthermore, it allowed the assessment of the maximum magnitude of the crown settlement developing ahead of the tunnel face. By combining the two evaluations with the tentative criterion proposed in Section 2.3.4.3, regarding the limiting crown displacement associated with a near ground collapse condition, the criterion for the maximum acceptable overbreak or overcut, proposed in Section 2.3.5.4 was justified.

Finally, a few comparisons were made available between measurements and approximate predictions of the ground movements ahead of the tunnel face. These include the maximum horizontal displacements of the tunnel face and the maximum surface distortions ahead of the advancing tunnel.

5.4 Conclusion

In Section 5.2, a two-dimensional finite element modelling technique was presented and applied to a few case histories. This modelling technique provided sensible results, if the amount of ground stress release allowed before lining activation was known.

If this stress release could be related to the radial displacements of the tunnel contour, then an estimate of the displacements could lead to an evaluation of the stress release. This approach was proposed and discussed in Sections 5.2.5 and 5.3.1.

In Section 5.3 an approximate method was developed for estimating the radial displacements at the section the lining is activated for three particular points of the tunnel perimeter. This method was developed from parametric three-dimensional finite element analyses. The applicability of this method in actual tunnelling situations was investigated.

To complete the picture, the method for estimating radial displacements should combined with results of the two-dimensional modelling, in order to assess the ability of the proposed procedure to provide estimates of the ground stress release required in the plane strain representation.

This was done for the three case histories analysed in detail in Section 5.2.4.

Alto da Boa Vista Tunnel

Using the parameters of the best fit analysis found for this case history as presented in Section 5.2.4.2, it is possible to obtain the ground reaction curves for points of the tunnel contour subjected to a gradual and complete stress release (in 10 steps). In this additional run, no support was applied to the opening. For convenience, these ground reaction curves can be expressed in terms of the stress release factor

$$a = 1 - \Sigma$$

where Σ is the ratio of the current radial stress to initial radial stress at the tunnel contour. Note that in the modelling technique adopted (Section 5.2.2), the same stress reduction factor is uniformly applied to all points around the tunnel profile and proportionally reduces the radial and shear stresses along that contour. The induced radial displacements can be expressed in the dimensionless form (U). As the in situ initial tangent modulus of the soil in this case history increases with depth (Figure 5.14), an average E value of 30 MPa was adopted to calculate the dimensionless displacement.

The curves presented in Figure 5.113 are thus obtained, for points at the tunnel crown, springline and floor.

The section where the shotcrete support of this NATM tunnel was actually activated is not easily defined. As described in Section 5.2.4.2 the support was installed in stages. The heading walls were immediately shotcreted after excavation (Figure 5.15). Immediate shotcreting also followed the bench excavation. The closure of the lining invert took place at about 2.6 m behind the heading face. From this one may say that the activation of the support system took place at some distance from the face between zero to almost 0.6D. The approximate solution for tunnel closure developed in Section 5.3.5.2 can be used to estimate the dimensionless radial displacements at those extreme situations ($X/D = 0$ and 0.6). The estimates of U at crown, springline and floor are thus shown in Figure 5.113. With these values, stress releases α at those three points can be obtained for each position of X/D considered. One notes that for a given distance behind the tunnel face, different α values are found for the different points of the tunnel contour. As noted above, the two-dimensional modelling technique uses a single reduction factor α for all points of the contour. Accordingly, those different α values obtained have to be averaged out, in order to allow a comparison with the best fit reduction factor found in this case history back analysis. This is easily determined, having in mind the plane symmetry of the problem, which requires the stress reduction computed for the springline point to be counted twice.

From this it is noted that had the lining been installed right at the face ($X/D=0$) the stress reduction factor to be used in a 2D analysis would have been 25.5%. On the other hand, had the lining been activated at 0.6D behind the face (approximately at the point of ring closure), the

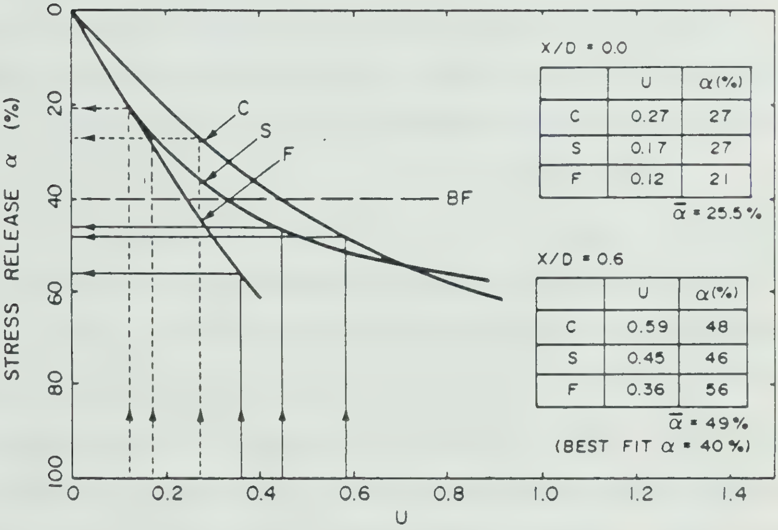

X/D = 0.0

	U	α(%)
C	0.27	27
S	0.17	27
F	0.12	21

$\bar{\alpha}$ = 25.5%

X/D = 0.6

	U	α(%)
C	0.59	48
S	0.45	46
F	0.36	56

$\bar{\alpha}$ = 49%

(BEST FIT α = 40%)

Figure 5.113 Evaluation of the Ground Stress Release at the ABV Tunnel for a Two-Dimensional Numerical Simulation

stress reduction factor to be considered would have been 49%. These two values are to be compared with the 40% stress release prior to the lining application found through the back analyses of this case history, presented in Section 5.2.4.2. The latter value lies within the extreme values given by the approximte procedure suggested, and, actually is closer to the α calculated for the section where the lining ring was closed at the floor. The latter finding seems to confirm that the actual activation of a support installed in stages, takes place at the point when the lining ring is closed.

Edmonton LRT Tunnel

The same reasoning and procedures applied to the ABV tunnel were also applied to the Edmonton Subway Tunnel. The main difference in this case refers to the definition of the section where the lining was activated. The construction procedures described in Section 5.2.4.3 indicate that the support came in full contact with the ground at a distance behind the face of 0.9 to 1.1 times the excavated diameter. Thus the tunnel closure is calculated for a section about 1D behind the face, using the best fit value of the in situ stress ratio found for this case (K=0.75). The ground reaction curves shown in Figure 5.114 were obtained as for the ABV case. Here an average initial tangent modulus of 70 MPa was considered (see Figure 5.25), to calculate the dimensionless displacements.

The radial displacements at the point of lining activation as calculated by the approximate solution are given in Figure 5.114. This enabled the stress reduction factors at the crown, springline and floor to be calculated from the corresponding ground reaction curves, which had been obtained from the 2D finite element analysis of the unsupported opening, using the parameters of the best fit case. Again the stress release factors are averaged out and a mean α value of 52% is found. This figure compares well with the best fit amount of ground stress release of 50% found in Section 5.2.4.3 for this case history.

Edmonton Experimental Tunnel

Once more the same procedures were applied to the third case history investigated. Figure 5.115 presents the ground reaction curves derived from a 2D finite element analysis of the unsupported tunnel, using the parameters of the best fit case (Section 5.2.4.4). It also assumes an undrained ground response and an in situ stress ratio, K=0.9. Correspondingly, an average initial tangent modulus of 25 MPa was considered (see Figure 5.48) to calculate the dimensionless radial displacements.

The construction details of the tunnel indicate that the lining was activated in this case, at a section located between 2.3D and 2.7D behind the tunnel face. The approximate tunnel closure solution given in Section 5.3.5.2 indicates however, that at distances greater than 2D behind the face the radial displacements are essentially constant

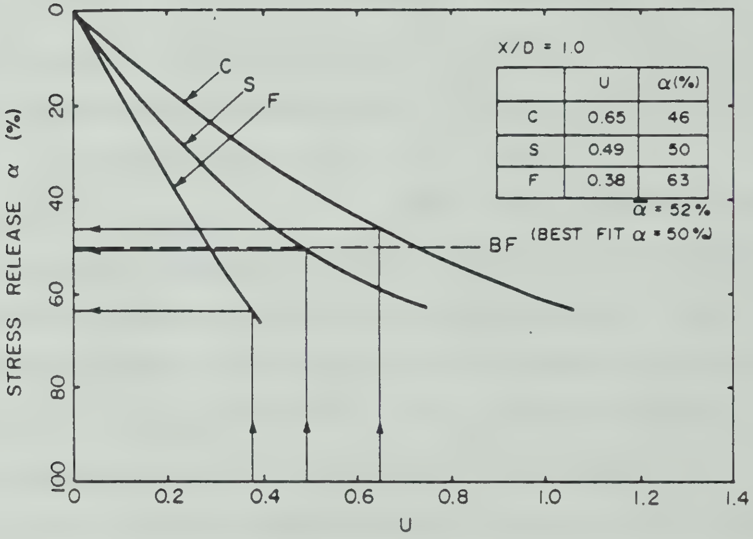

	U	α(%)
C	0.65	46
S	0.49	50
F	0.38	63

Figure 5.114 Evaluation of the Ground Stress Release at the LRT Tunnel for a Two-Dimensional Numerical Simulation

and fully stabilized. The dimensionless displacements are therefore calculated for X/D=2.0 and the values found are shown in Figure 5.115. The stress release α for the crown, springline and floor are thus determined and an average ground stress reduction factor of 50% is obtained. Unlike the former two case histories, a fairly poor agreement is found with the best fit reduction factor of 70%.

This result emphasizes the limitations of the proposed method for estimating the tunnel closure, as discussed in Section 5.3.6.1. It seems to render good results in tunnels built using the NATM regardless of the soil type but provided the face is stable, and to construction schemes using TBM and shields, where the support is activated at distances from the face smaller than 1 to 1.2 D. On the other hand the method tends to underestimate the tunnel closure when the support is activated at larger distances from the face (especially in softer soils) as in the present case history. As a consequence, the ground stress reduction it yields will be smaller than it should. A two-dimensional analysis using a smaller stress reduction will generally lead to smaller final ground movements and to larger lining loads.

Final Comments

It was shown in this chapter that a shallow tunnel construction can be adequately simulated through the two-dimensional modelling technique presented herein. This simulation requires, however, an independent estimate of the

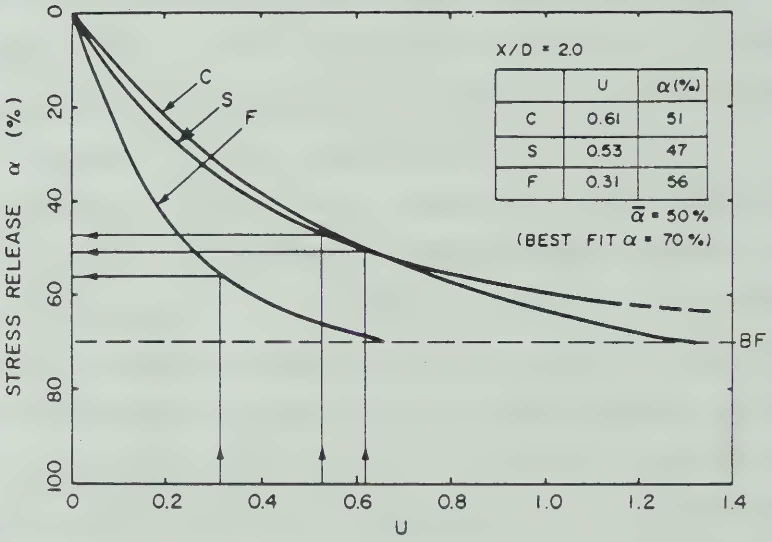

	U	α(%)
C	0.61	51
S	0.53	47
F	0.31	56

Figure 5.115 Evaluation of the Ground Stress Release of the Edmonton Experimental Tunnel for a Two-Dimensional Simulation

amount of ground stress release taking place before the support is activated.

An approximate procedure was developed to assess that amount of stress reduction. It requires an estimate of the radial displacements at the point when the support is activated. It also requires the knowledge of the ground reaction curve of the unsupported opening. This can be obtained from finite element analyses, using the two-dimensional modelling technique mentioned before. The radial displacements prior to supporting the tunnel can be estimated using the approximate method developed from three-dimensional numerical simulations. Combining those two procedures, the stress reduction factor can be assessed or bounded. Caution should be exerted, however, regarding the validity or limitations of the proposed procedure, since these may have an effect on the result of the analysis. Nevertheless, when applied judiciously, the proposed procedure leads to estimates of the ground stress reduction, that ultimately lead to reasonable predictions of the performance of the shallow tunnels, through the two dimensional numerical simulation technique presented in this chapter.

6. TWO DIMENSIONAL MODELLING FOR GENERALIZATION

6.1 Introduction

In Chapter 5, an approximate procedure was proposed to assess the amount of ground stress release to be applied before the lining is activated, in the two dimensional finite element simulation described in Section 5.2.2. This procedure was tested and evaluated in Section 5.4. It requires two basic components: (a) the ground reaction curves at three particular points of the contour of the unsupported opening; (b) the radial displacements of these points at the section the support is activated.

To a large degree, the three-dimensional modelling presented in Section 5.3 was devoted to supplying the fundamentals for requisite (b) above. An approximate solution allowing estimates of radial tunnel closure behind the face of a shallow tunnel was developed in Section 5.3.5.2 and was tested in Section 5.3.6.1. Despite its limitations, this solution presents sufficient generality for practical use.

The other requirement refers to the ground reaction curves of some points of the tunnel contour. In Section 5.4, these were presented in terms of relationships between a non-dimensional radial displacement (U) and a ground stress release factor (α) for the crown, springline and floor of the tunnel. An average stress release factor ($\bar{\alpha}$) is obtained by averaging the factors at these points. The ground reaction curves for three case histories shown in Section 5.4 were obtained through finite element analyses, using the numerical solution presented in Section 5.2.2, and the parameters used or derived from the back analyses presented in Section 5.2.4.

In this chapter, an attempt will be made to develop a procedure which would allow those ground reaction curves or stress release curves to be obtained, without the need of a finite element analysis. Obviously, the development of such a procedure requires a number of finite element analyses. Their results may lead to a generalized solution of the problem which would not demand additional numerical analyses. Through this process of numerical modelling, an additional effort will be made towards simultaneously obtaining the relevant ground displacements induced by the stress reduction at the opening.

To obtain a coupled solution for the ground response in terms of stress release curves and associated ground displacements, a process of generalization may be used. The application of this process to geotechnical problems was described by Resendiz (1979). According to this author, four steps are involved in this process: (a) the identification of the significant variables controlling the problem; (b) the reduction of the variables to a minimum set of mutually independent variables, sufficient to define the problem; (c) the derivation of quantitative relationships between the set of variables through modelling; (d) the validation and calibration of the proposed quantitative relationships against actual field cases.

The process of generalization makes use of similarity techniques through which a physical problem can be described by a set of relationships which are invariant with respect to the scale changes of the physical dimensions. To find these relationships, the theory of dimensional homogeneity or dimensional analysis is used. An application of these concepts to geomechanical problems involving material non-linearities was presented by Winter (1982). Resendiz and Romo (1981) applied these concepts to the solution of settlement over tunnels in frictionless soils exhibiting a hyperbolic stress-strain relationship. Dimensional analysis was also applied to obtain settlement over shallow tunnels in linear elastic soil by Sagaseta and Oteo (1974) and Sagaseta et.al. (1980). Kovari (1977:405) used a similar approach to obtain a solution for lining design on the assumption of linear elasticity for both the support and the ground. A common feature to all these works is the modelling step of the generalization process which made use of finite element analysis.

The steps described for generalization were liberally followed in this study, without the degree of formalism that a dimensional analysis should involve.

The identification of the significant variables controlling the problem at hand were largely discussed in Chapters 2 and 3. The reduction of the number of variables was discussed in Section 5.1 and further simplifications will be discussed in Section 6.2. Some of the variables involved were already reduced to a dimensionless form such as the radial displacements at the tunnel contour (U), or the amount of stress release (α). Other dimensionless variables will be presented later. This chapter will focus mainly on the third step of the generalization process. Having made the assessment in Chapter 5 of the capabilities of the selected modelling tool to simulate the behaviour of a shallow tunnel, the 2D numerical model will be used here to derive quantitative relationships between the reduced variables. The final step regarding the validation and calibration of the solution will be presented in Chapter 7.

A general solution for the ground reaction curves can be expressed in terms of the following equation, which reflects both the selected modelling tool and some simplifications already undertaken:

$$F=f(\sigma_r,u_r,\theta,D,H,\gamma,K_o,\nu,K,n,c,\phi,R_f) \qquad [6.1]$$

The symbols have the meanings established previously.

The next section will discuss some assumptions and simplifications, that will ultimately enable the definition of a minimum number of dimensionless and mutually independent variables which described the function f with sufficient generality.

6.2 Modelling Simplifications and Ranges of Variables

6.2.1 Foreword

Despite the simplifications set earlier in Section 5.1, equation 6.1 still includes a large number of dimensional and dimensionless variables. In order to further reduce this number and to make the modelling step simpler, one may explore some properties of the hyperbolic stress-strain relationship.

The original formulation of the hyperbolic model was presented in Figure 5.11. After inspecting that derivation, one may note that there are groups of hyperbolic relationships with a few peculiar properties as it will be seen in the next sections. Also included are discussions on the consequences of the simplifications introduced and on the ranges of parameters varied in the modelling step.

6.2.2 Cohesionless Soil Model

If the cohesive component of strength is set equal to zero and the Janbu's exponent, n, is also set equal to zero, a special group of hyperbolic stress-strain curves is found. An example of a family of curves of this group is shown in Figure 6.1. These curves present the property of homothety. The centre of homothety or of similitude of these curves is their origin, where the strain and deviatoric stresses are zero. The homothetic transformation maps a curved segment into a parallel segment with a length equal to the ratio of homothety times the length of the original segment. If the coordinates of the homothetic points on these curves (the intersection of the latter with an arbitrary axis through the centre of similitude) are used as reference values, $(\sigma_1-\sigma_3)_{ref}$ and $\epsilon_{1_{ref}}$, and if the deviatoric stresses and the major principal strains of each curve are respectively normalized to these reference values, a single normalized hyperbola is found for the entire ground mass, regardless of the value of the minor principal stress. This is demonstrated in Figure 6.2.

At homothetic points on these curves, the ratio of deviatoric stress to minor principal stress is constant as proved in Figure 6.2. Thus for c=0 and n=0, one gets for the tangent modulus at these points:

$$E_t = K\ p_a\ [1 - R_f \frac{1-\sin\phi}{2\sin\phi}\ \frac{\sigma_1-\sigma_3}{\sigma_3}]^2$$

Hence, for fixed K, R_f and ϕ values, E_t is a constant. This result is not suprising as it is known that a homothety preserves angles between lines of a polygon or gradients of a curve (Dodge, 1972:107). Furthermore, if the in situ stress ratio K_o is constant, the ratio $(\sigma_1-\sigma_3)/\sigma_3$ is constant and the in situ tangent modulus is also constant. This is apparent in Figure 6.1. The in situ or initial tangent modulus is thus given by:

$$E_{ti} = K\ p_a [\ 1-R_f \frac{1-\sin\phi}{2\sin\phi}\ \frac{1-K_o}{K_o}]^2 \qquad [6.2]$$

on the assumption that the ground surface of the soil mass is horizontal and that the major principal stress is vertical. For this ground mass, the initial tangent modulus

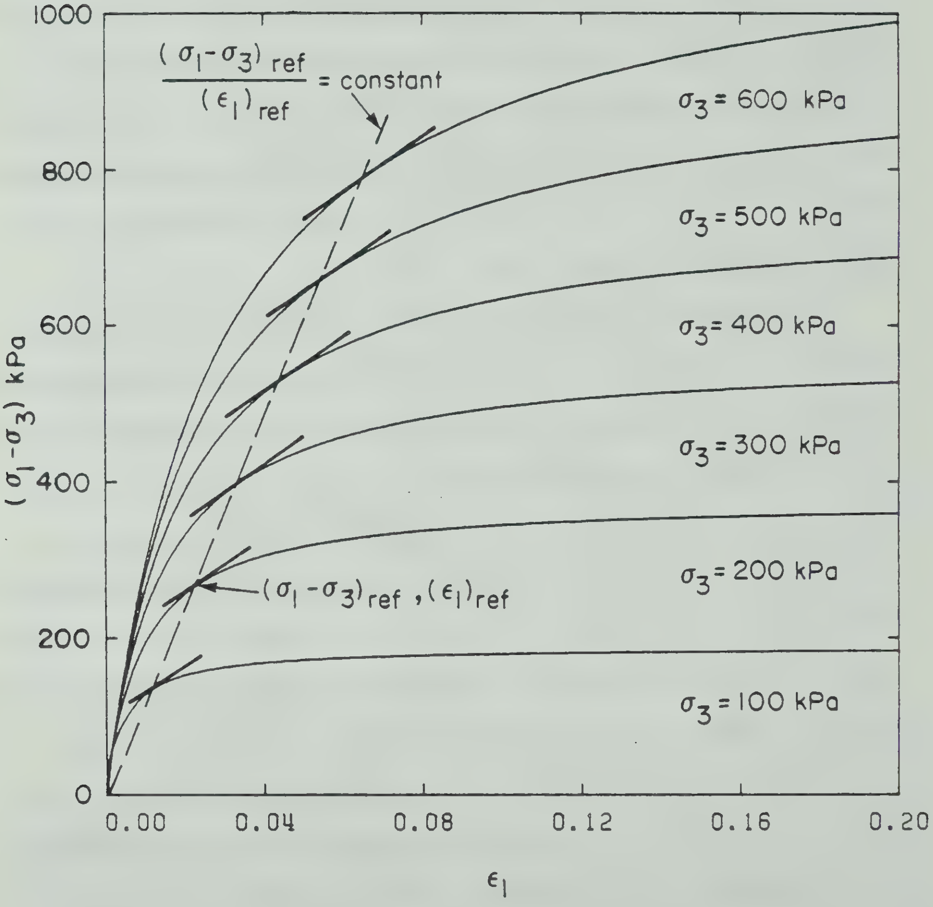

K=400 , n=0.0 , PHI=29 , c=0.0 , Rf=1.0

Figure 6.1 Example of Homothetic Hyperbolae

Hyperbola:

$$(\sigma_1 - \sigma_3) = \frac{\varepsilon_1}{a + b\varepsilon_1}$$

Dividing by $(\sigma_1 - \sigma_3)_{ref}$ and numerator and denominator of right hand side by $(\varepsilon_1)_{ref}$:

$$\frac{(\sigma_1 - \sigma_3)}{(\sigma_1 - \sigma_3)_{ref}} = \frac{\varepsilon_1/(\varepsilon_1)_{ref}}{a\,\dfrac{(\sigma_1 - \sigma_3)}{(\varepsilon_1)_{ref}} + b\,(\sigma_1 - \sigma_3)_{ref}\,\dfrac{\varepsilon_1}{(\varepsilon_1)_{ref}}}$$

If n = 0, then:

$$a = 1/Kp_a$$

Thus, for a given K and a fixed ratio $(\sigma_1 - \sigma_3)_{ref}/(\varepsilon_1)_{ref}$:

$$a\,\frac{(\sigma_1 - \sigma_3)_{ref}}{(\varepsilon_1)_{ref}} = a_0 \text{(constant)}$$

If c = 0, then:

$$b\,(\sigma_1 - \sigma_3)_{ref} = R_f\,\frac{1-\sin\phi}{2\sin\phi}\,\frac{(\sigma_1 - \sigma_3)_{ref}}{\sigma_3}$$

However

$$\frac{(\sigma_1 - \sigma_3)_{ref}}{\varepsilon_{1\ ref}} = \frac{1}{a + b\varepsilon_{1\ ref}}$$

But, for c = 0:

$$b = d/\sigma_3 \quad \text{(d constant for a given } R_f \text{ and } \phi\text{)}$$

Then for a fixed $(\sigma_1 - \sigma_3)_{ref}/\varepsilon_{1\ ref}$:

$$\varepsilon_{1\ ref} = e\,\sigma_3$$

Thus

$$\frac{(\sigma_1 - \sigma_3)_{ref}}{\sigma_3} = f \quad \text{(constant)}$$

Therefore

$$b\,(\sigma_1 - \sigma_3)_{ref} = b_0 \quad \text{(constant)}$$

Hence

$$\frac{(\sigma_1 - \sigma_3)}{(\sigma_1 - \sigma_3)_{ref}} = \frac{\varepsilon_1/(\varepsilon_1)_{ref}}{a_0 + b_0\varepsilon_1/(\varepsilon_1)_{ref}}$$

represents a unique hyperbola for a given K, R_f and ϕ.

Figure 6.2 Uniqueness of the Normalized Homothetic Hyperbolae for c=n=0

is therefore constant with the depth.

In a two-dimensional representation, unlined circular tunnels with different diameters will exhibit homothetic geometries if their ratios of cover to diameter (H/D) were the same. If geometrically homothetic tunnels are driven through a ground mass exhibiting homothetic hyperbolic stress-strain curves such as those defined, the ground mass response in terms of stress and strain changes should be also homothetic. If this is so, a unique normalized stress and strain response will be found at corresponding (homothetic) points around those tunnels. Therefore a unique normalized ground reaction curve (NGRC) should be obtained at corresponding points in these tunnels.

To illustrate this point, two finite element analyses were conducted, using the stress-strain parameters of the curves shown in Figure 6.1. Other input variables are given in Table 6.1. The two circular tunnels have different geometries but the same H/D ratio. The ground stresses at the opening were gradually reduced to zero in ten increments and no support was activated. After the 7th load increment, some elements close to the springline "failed" and the results after this event were discarded. In both cases, the in situ tangent modulus was equal to 27.414 MPa.

Figures 6.3 to 6.5 present the ground reaction curves at the crown, springline and floor calculated for both cases. The curves show the radial displacements at those points relative to the ratio of current to in situ radial stresses. Quite distinct curves were obtained for each case. However, if the displacements are normalized to the tunnel diameter and to the ratio of in situ radial stress to the in situ tangent modulus, such that

$$U=\frac{u_r . E_{ti}}{D . \sigma_{ro}}$$

then, single curves result for each point of the tunnel contour as indicated in Figure 6.6. As the in situ stress level at the deeper tunnel is twice that at the shallower one and as the diameter of the former is also twice that of the latter, the displacements in the deeper tunnel are four times larger than those in the shallower position. This is almost exactly the ratio of the displacement found through the numerical analyses.

Figure 6.7(a) presents the distributions of subsurface settlements along the tunnel cover calculated for a ground stress release of 50%. The settlements are plotted against the depth normalized to the tunnel diameter. The settlements for the deeper and larger tunnel are four times larger than those in the other tunnel. Hence, if the settlements are normalized to the settlement of the tunnel crown in each case, then a unique distribution of normalized settlements with depth is found as shown in Figure 6.7(b). Correspondingly, similar results are found for the surface settlements as indicated in Figures 6.8(a) and (b). When the surface settlements are normalized to the crown settlement, calculated for the same amount of ground stress release, once again, a single normalized distribution of surface

Diameter D (m)	4	8
Cover H (m)	6.2	12.4
H/D	1.55	
K	400	
n	0	
ϕ	29°	
c	0	
R_f	1.0	
ν	0.3	
γ (kN/m^3)	15.97	
K_0	0.75	
V/D(1)	2.875	

Note: (1) Definition in Section 6.3.1.2

Table 6.1 Input Parameters for Finite Element Analyses of Tunnels with the Same H/D and with a Homothetic Hyperbolic Stress-Strain Soil Model with c=0

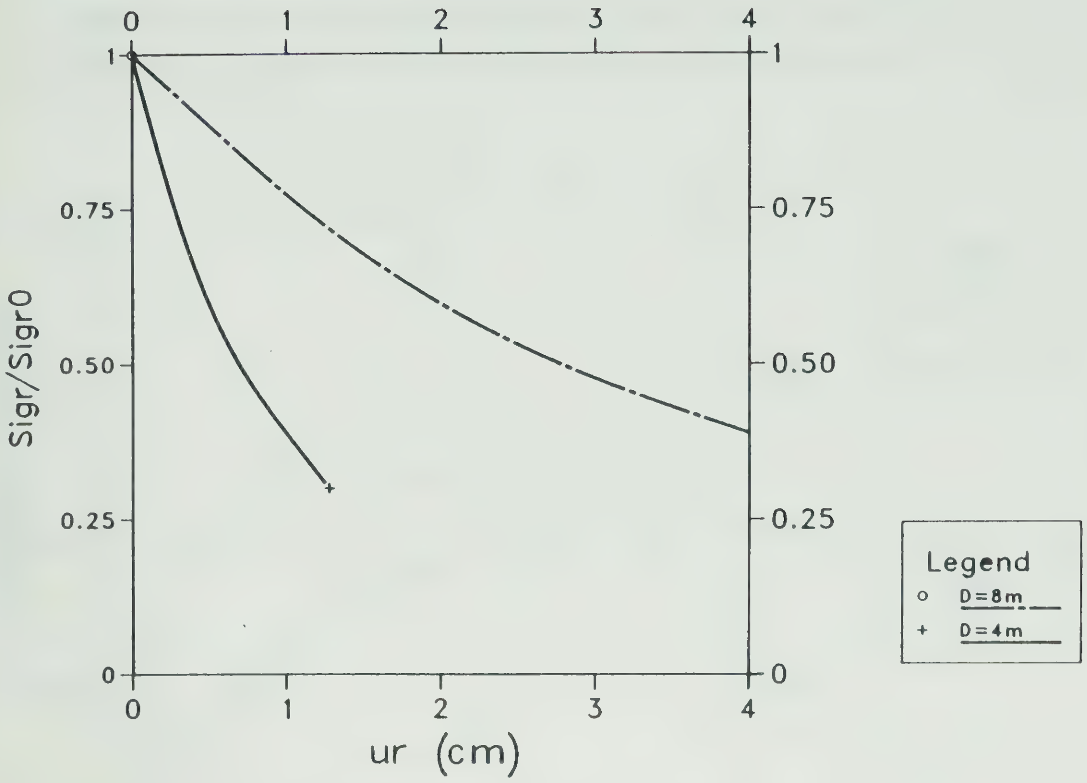

Figure 6.3 Ground Reaction Curves for the Crown of Geometrically Homothetic Tunnels in a Soil with a Homothetic Hyperbolic Stress-Strain Relationship (cohesionless model)

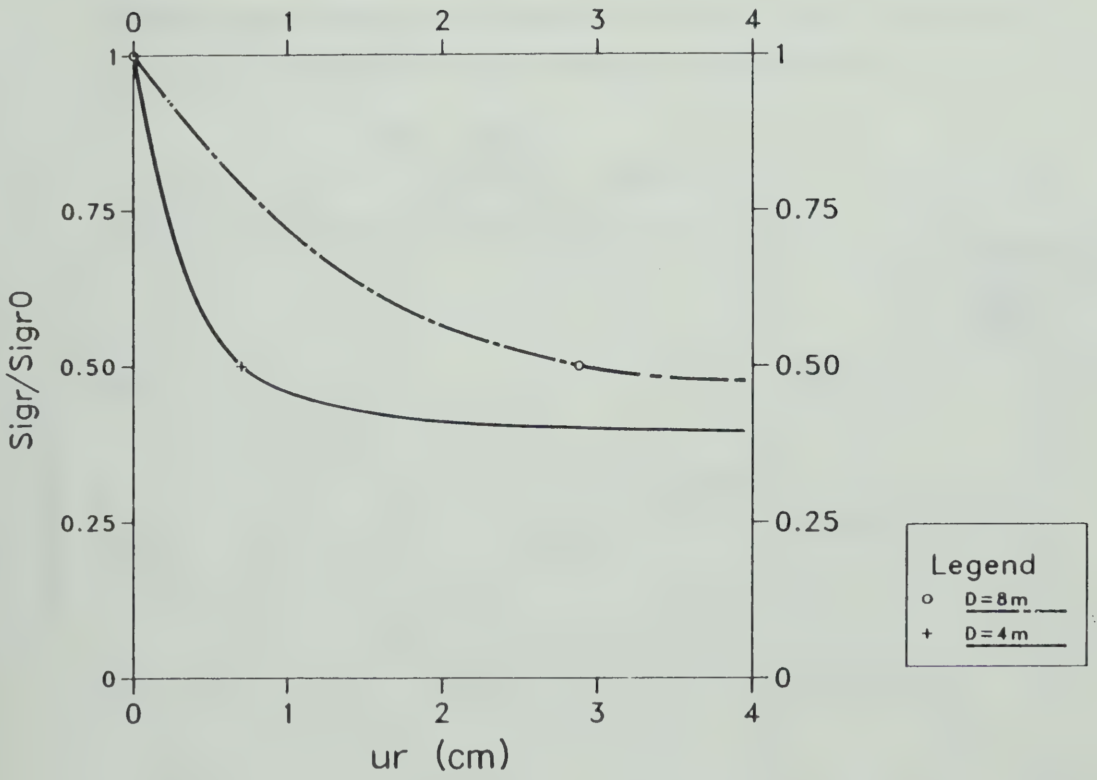

Figure 6.4 Ground Reaction Curves for the Springline of Geometrically Homothetic Tunnels in a Soil with a Homothetic Hyperbolic Stress-Strain Relationship (cohesionless model)

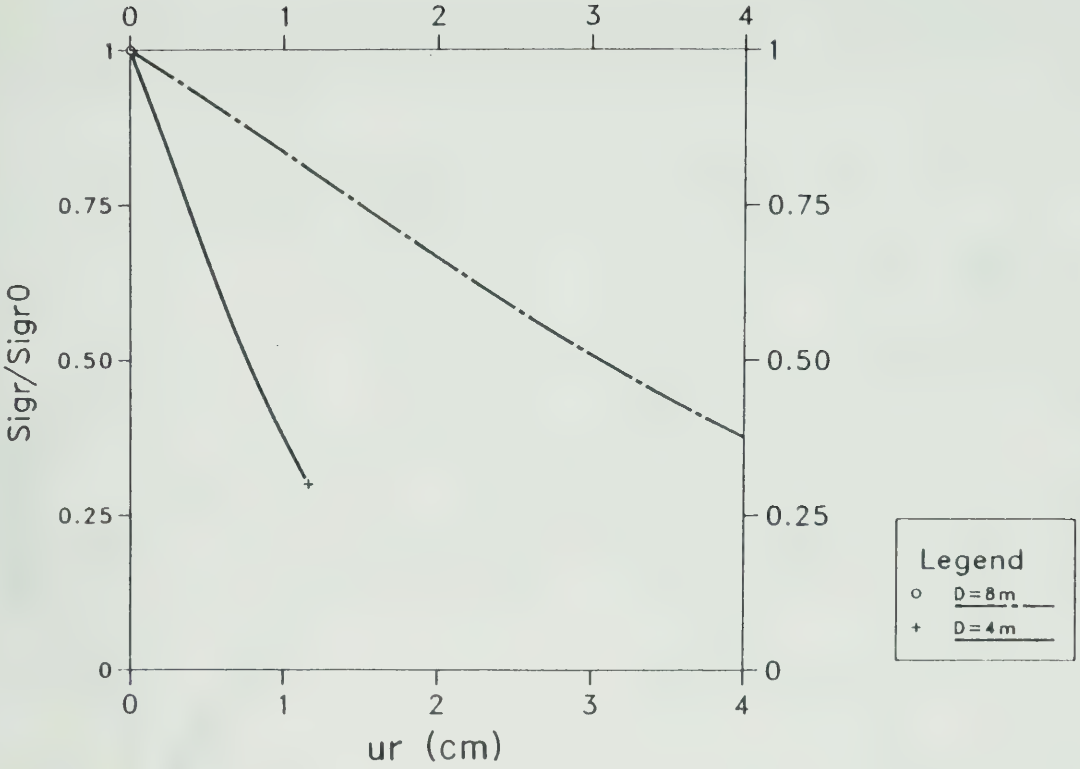

Figure 6.5 Ground Reaction Curves for the Floor of Geometrically Homothetic Tunnels in a Soil with a Homothetic Hyperbolic Stress-Strain Relationship (cohesionless model)

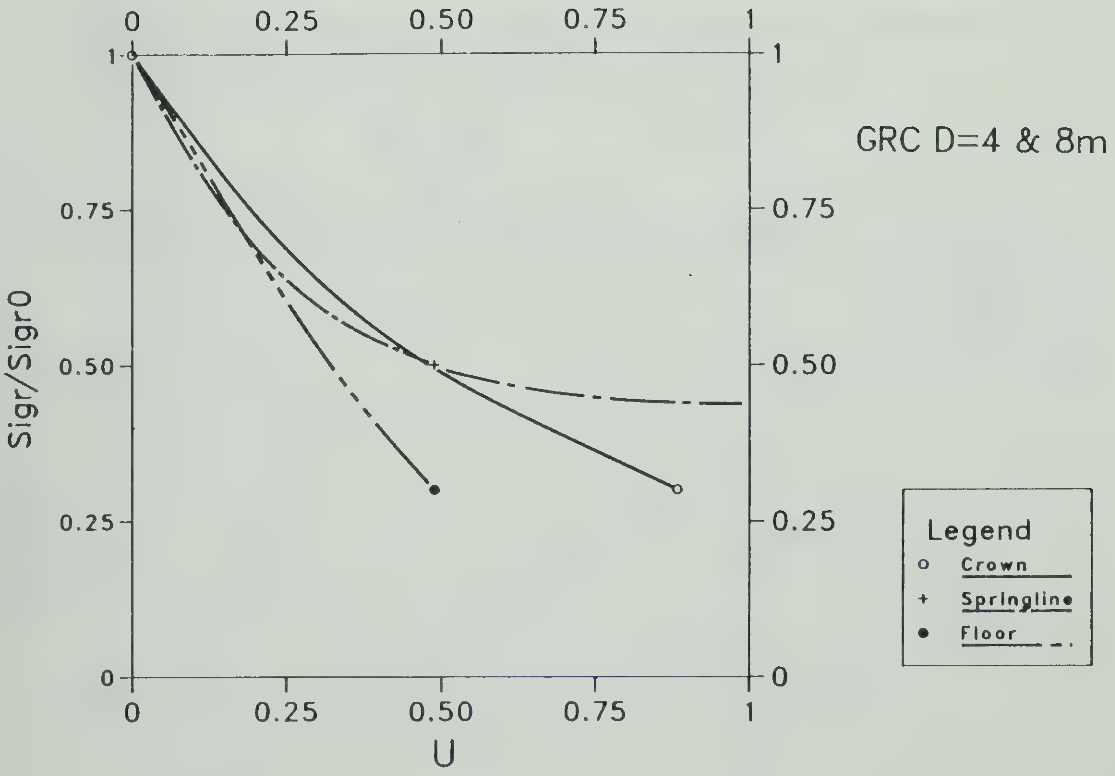

Figure 6.6 Normalized Ground Reaction Curves of Geometrically Homothetic Tunnels in a Soil with a Homothetic Hyperbolic Stress-Strain Relationship (cohesionless model)

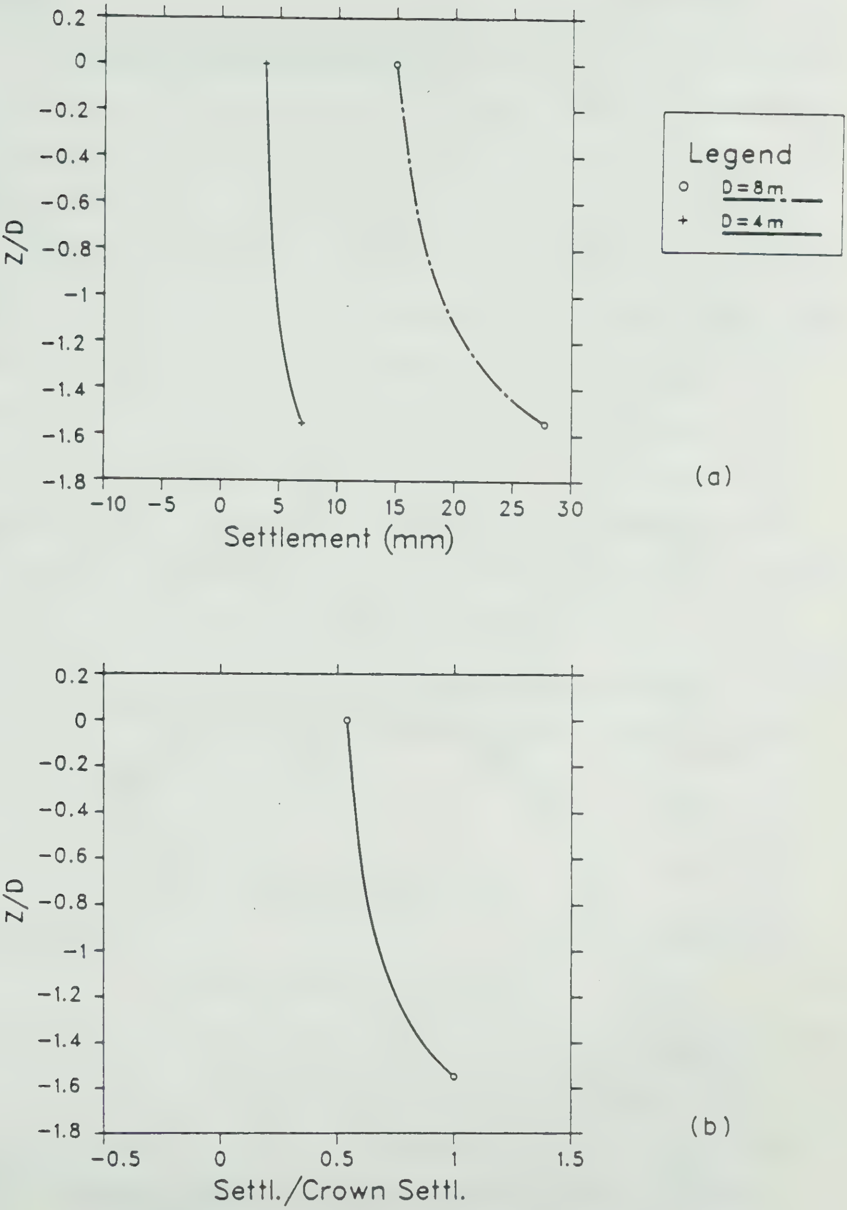

Figure 6.7 Subsurface Settlements along the Cover of Geometrically Homothetic Tunnels in a Soil with a Homothetic Hyperbolic Stress-Strain Relationship (c=0), for Stress Release of 50%

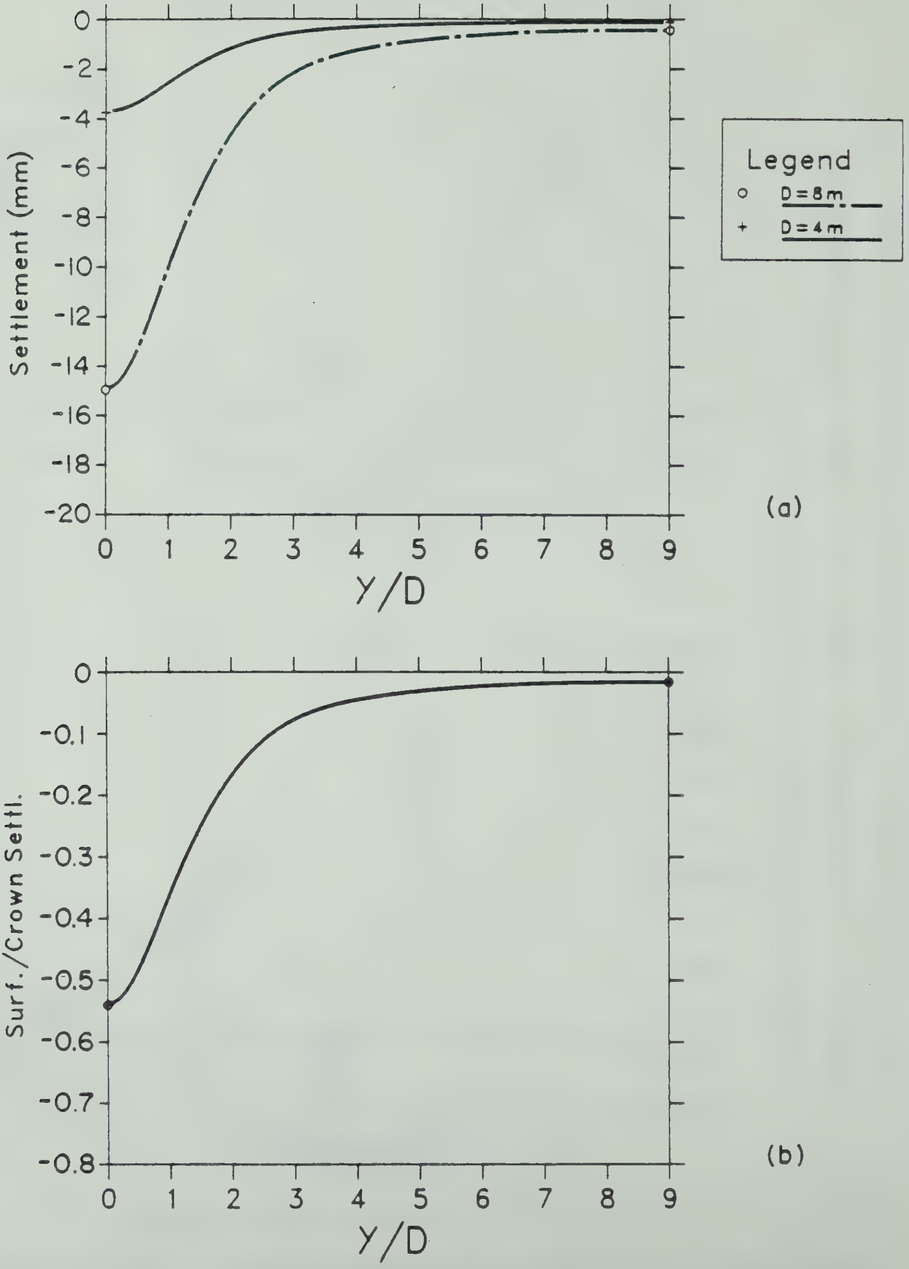

Figure 6.8 Surface Settlements over Geometrically Homothetic Tunnels in a Soil with a Homothetic Hyperbolic Stress-Strain Relationship (c=0), for Stress Release of 50%

settlements is found. Actually, the entire displacement field in one case differs from the other only in magnitude. Moreover, the ratio of displacement magnitudes is constant.

By using the property of homothety, the numerical analyses leading to the generalization of the projected solution will be greatly simplified, as one of the variables in equation 6.1, the tunnel diameter D, will not have to be varied in the parametric analyses, but only the ratio H/D. Furthermore, by making the soil cohesion equal to zero, there will be no need to vary the failure ratio, R_f, in these analyses. By examining Figure 5.11 or equation 6.2, one notes that for a soil with c=0 and with constant ϕ and R_f values, it is always possible to find an equivalent friction angle ϕ_e, associated with a failure ratio (R_{fe}) equal to unity which gives the same tangent modulus. Then:

$$R_f \frac{1-\sin\phi}{2\sin\phi} = R_{fe} \frac{1-\sin\phi_e}{2\sin\phi_e}$$

setting $R_{fe}=1$, then:

$$\sin\phi_e = \frac{1}{1 + R_f(1/\sin\phi) - R_f}$$

and therefore:

$$\phi_e = \arc\sin\,(1-R_f+R_f\csc\phi)^{-1} \qquad [6.3]$$

The stress-strain curves and thus the normalized ground reaction curves for a cohesionless soil, with $R_{fe}=1$ and with a friction angle ϕ_e, given by equation 6.3, are identical to that of a cohesionless soil, with R_f not equal to 1 and a friction angle ϕ.

One should also note that the unit weight, γ, of the soil of a homogeneous ground profile which appears in equation 6.1, does not affect the normalized ground reaction curve (NGRC) for n=0. This is because the NGRC is defined in terms of stress and displacements normalized to the in situ stresses. Also not affected are the displacements normalized to the crown settlement. This fact is demonstrated in Table 6.2, which presents the assumptions and results of two finite element analyses which considered identical input parameters except for different unit weights for the soil. The ratios of the normalized radial displacements and of the normalized surface settlements for the two γ values considered are very close to one. The deviations from unity are due to numerical inaccuracies of the calculations. The same results are found for displacements at other points in the ground mass and for other amounts of ground stress release. The invariance of the NGRC and of the ground displacement with respect to γ is in fact general for the simplified conditions considered in the analyses.

The simplifications introduced so far allow equation 6.1 to be expressed in a more compact form:

$$F= f(\theta,\frac{\sigma_r}{\sigma_{ro}}, \frac{u_r E_{ti}}{D\sigma_{ro}}, \frac{H}{D}, K_o, \phi_e, \nu) \quad [6.4]$$

Note that the variables in equation 6.4 are not mutually independent, as E_{ti} is a function of K_o and ϕ_e. They would been independent of each other had the displacements been normalized to Janbu's modulus, K, times the atmospheric pressure, p_a. However, there are some advantages in keeping the equation as shown. It will be shown later in this chapter that the NGRC for given K_o and H/D values, with

Assumptions:

$H = 12.0$ m
$D = 4.0$ m
$K_0 = 0.8$
$K = 400$
$n = 0$
$c = 0$
$\phi = 30°$
$\nu = 0.4$
$V/D = 1.5$
$\gamma = 15.68$ kN/m^3 and 19.60 kN/m^3
$E_{ti} = 31.015$ MPa (in both cases)
Full ground stress release in 10 equal increments
No lining installed

Results:

Displacements for 50% of stress release

a) Radial displacements at the opening

Point	$\gamma = 15.68$ kN/m^3		$\gamma = 19.60$ kN/m^3		$U (\gamma = 15.68)$ / $U (\gamma = 19.60)$
	u_r (mm)	U (-)	u_r (mm)	U (-)	
Crown	11.75088	0.48423	14.69135	0.48432	0.99981
Springline	10.18102	0.44951	12.72055	0.44931	1.00045
Floor	8.41449	0.26006	10.56987	0.26134	0.99510

b) Maximum surface settlement

	$\gamma = 15.68$ kN/m^3	$\gamma = 19.60$ kN/m^3
Settlement (mm)	4.40321	5.50558
Surface Settlement/Crown Settlement	0.37471	0.37474

(Settlement ratio $\gamma = 15.68$/Settlement ratio $\gamma = 19.60$) = 0.99991

Table 6.2 Invariance of NGRC and Normalized Displacements to Changes in the Unit Weight of the Soil

displacements normalized to E_{ti}, are homothetic curves for any ϕ value. This will provide a greater generality in the projected solution. Had the product Kp_a instead of E_{ti} been selected to define the dimensionless displacement U, the NGRC for different ϕ would not be homothetic.

6.2.3 Frictionless Soil Model

If the frictional component of strength is set equal to zero and the Janbu's exponent n is also set equal to zero, another special group of hyperbolic stress-strain curves is found. With ϕ=0, the stress-strain relationships become independent of the minor principal stress. For a given modulus K, different curves are obtained for different undrained cohesion (c_u) values. As in the previous case, it is simple to prove that these curves also present the property of homothety. Therefore, if the deviatoric stresses and major principal strains are normalized to the coordinates of arbitrary homothetic points, $(\sigma_1-\sigma_3)_{ref}$ and ϵ_{1ref}, on these curves then a single normalized hyperbola is found for the entire ground mass. A family of curves similar to that shown in Figure 6.1 is found, each one defined for a given c_u value.

The tangent modulus at homothetic points on these curves is given by:

$$E_t = K\ p_a[1 - R_f\frac{(\sigma_1-\sigma_3)_{ref}}{2c_u}]^2 \qquad [6.5]$$

Likewise to the case of cohesionless soil discussed in the previous section, it is easy to show that the ratio $(\sigma_1-\sigma_3)_{ref}/c_u$ is constant, and thus, for a fixed R_f value, E_t is constant at homothetic points in the stress-strain family of curves. As the stress-strain curve of a soil with a constant c_u profile does not depend on σ_3, the in situ tangent modulus profile for this soil is also constant with depth. For the special case of a hydrostatic stress field (K_o=1), the initial tangent modulus is:

$$E_{ti} = K\ p_a \qquad [6.6]$$

It can be shown that in a two-dimensional representation, unlined circular tunnels with different diameters, with the same cover to diameter ratio (H/D) and with the same strength ratio, defined as $c_u/\gamma D$, will exhibit a unique normalized ground response in terms of the ground reaction curves and of the displacement field. This will be so, once more, as a consequence of the homothetic property of the hyperbolic stress-strain curves of this particular soil group, with ϕ=0, n=0 and K_o=1.

To illustrate this fact, two finite element analyses were carried out using the parameters shown in Table 6.3. As indicated the two circular tunnels have different geometry but the same H/D ratio. The ground stresses at the opening were gradually reduced to zero in ten equal increments and no support was installed. After the 7th load increment some elements close to the tunnel contour, at about 45° from the crown, underwent tension and the results after this event were discarded. In both cases, the in situ tangent modulus

Diameter D (m)	4	8
Cover H (m)	6	12
H/D	1.5	
K	400	
n	0	
ϕ	0	
c_u (kPa)	98	196
R_f	1.0	
ν	0.49	
γ (kN/m^3)	19.6	
K_0	1	
$C_u/\gamma D$	1.25	
V/D	1.5	

Table 6.3 Input Parameters for Finite Element Analyses of Tunnels with the Same H/D and with Homothetic Hyperbolic Stress-Strain Soil Model with $\phi=0$

was equal to 40.494 MPa.

Figures 6.9 to 6.11 present the ground reaction curves at the crown, springline and floor calculated for both cases. The curves are plotted in terms of radial displacements at these points relative to the ratio of current to in situ radial stresses. Distinct curves were obtained for each case. But if the displacements are again normalized to the tunnel diameter and to the ratio of in situ radial stress to in situ tangent modulus, as before, then single curves result for each point of the tunnel contour as indicated in Figure 6.12. As the in situ stress level at the deeper tunnel is twice that at the shallower one, and as the diameter of the former is also twice that of the latter, the displacements in the deeper tunnel are 4 times larger than those in the shallower position. The ratio of the displacements given by the numerical calculations is almost exactly equal to four.

Figure 6.13(a) furnishes the distributions of subsurface settlements along the tunnel cover calculated for a ground stress release of 50%. As in Figure 6.7, the settlements are plotted against the depth normalized to the tunnel diameter. The settlements at the deeper and larger tunnel are four times larger than those at the other tunnel. Therefore, if the settlements are normalized to the crown settlement of each case, then a unique distribution of normalized settlements with depth is found, as shown in Figure 6.13(b). Similar results are found for the surface

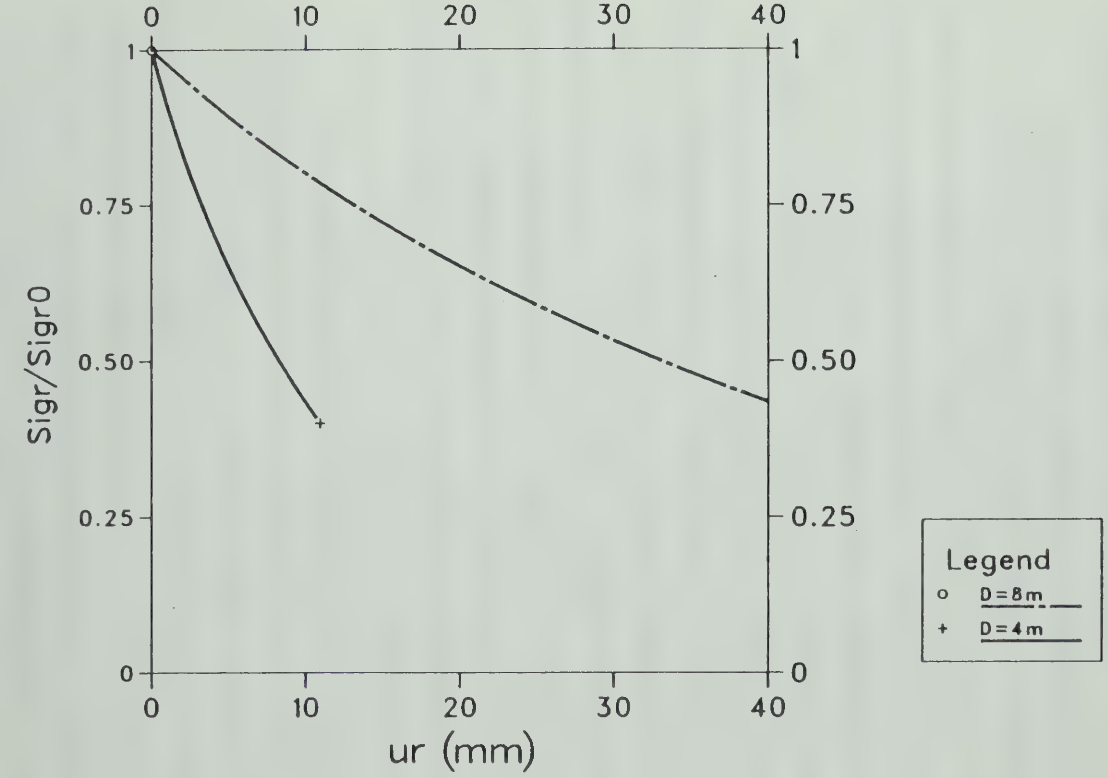

Figure 6.9 Ground Reaction Curve for the Crown of Geometric Homothetic Tunnels in a Soil with a Homothetic Hyperbolic Stress-Strain Relationship (frictionless model)

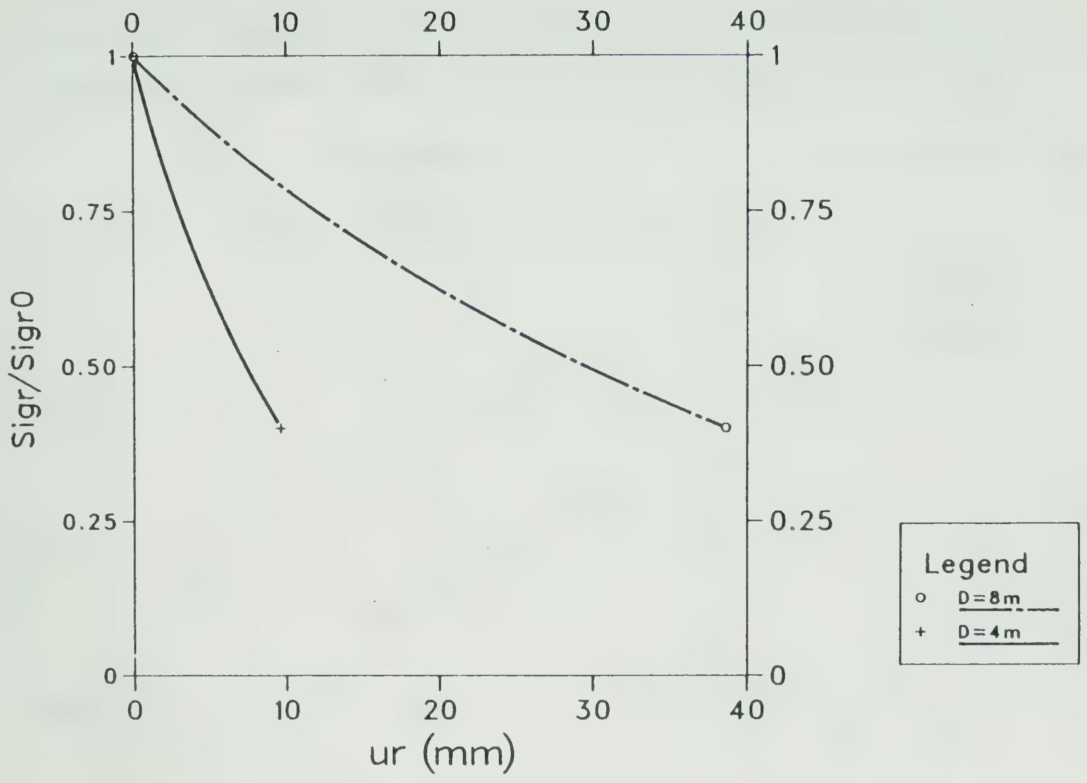

Figure 6.10 Ground Reaction Curve for the Springline of Geometric Homothetic Tunnels in a Soil with a Homothetic Hyperbolic Stress-Strain Relationship (frictionless model)

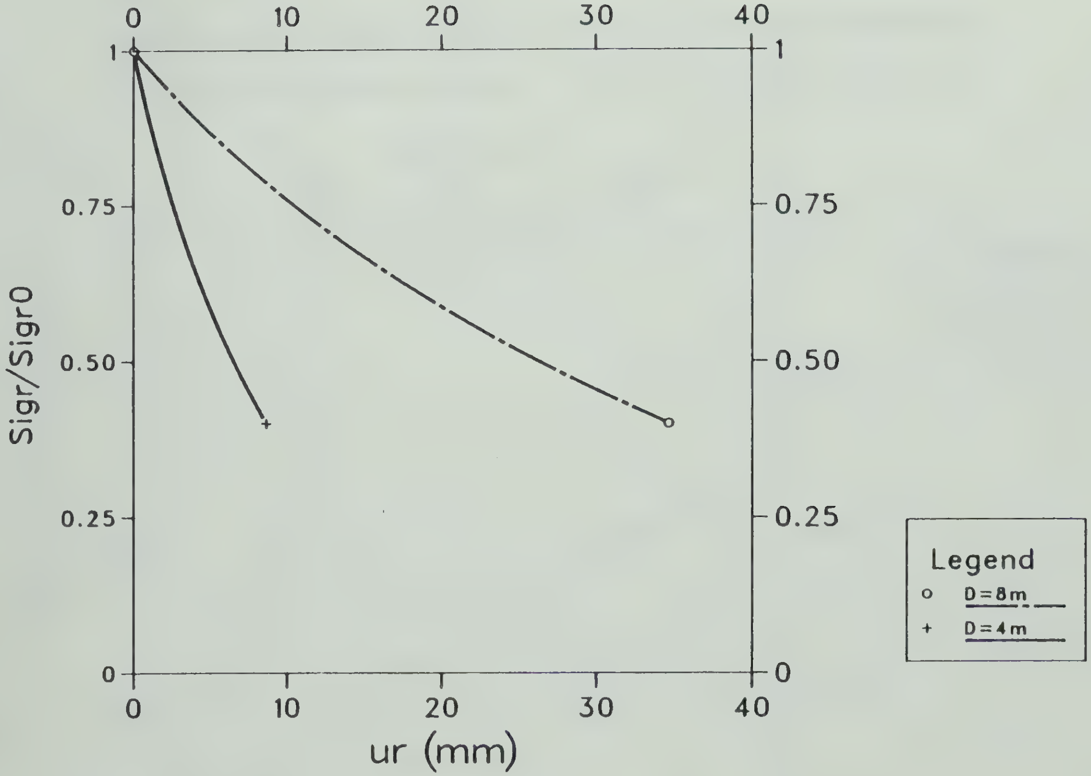

Figure 6.11 Ground Reaction Curve for the Floor of Geometric Homothetic Tunnels in a Soil with a Homothetic Hyperbolic Stress-Strain Relationship (frictionless model)

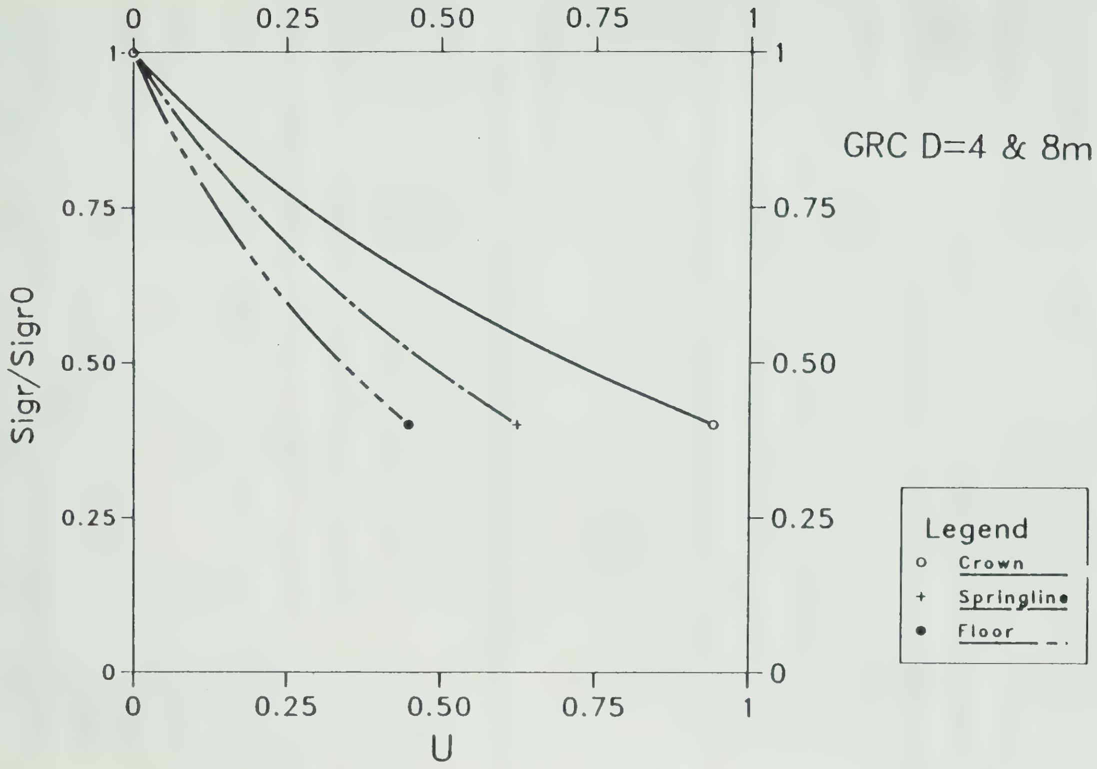

Figure 6.12 Normalized Ground Reaction Curves of Geometrically Homothetic Tunnels in a Soil with a Homothetic Hyperbolic Stress-Strain Relationship (frictionless model)

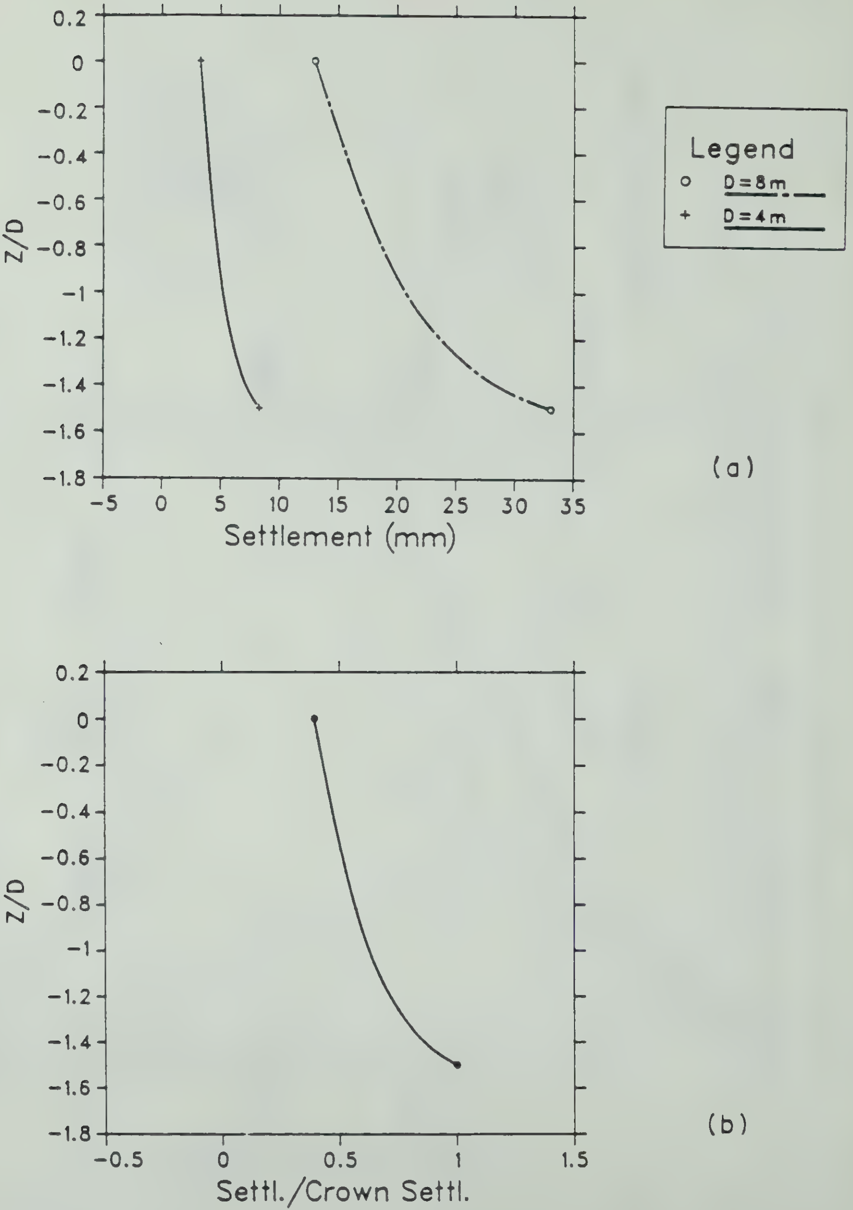

Figure 6.13 Subsurface Settlements along the Cover of Geometrically Homothetic Tunnels in a Soil with a Homothetic Hyperbolic Stress-Strain Relationship ($\phi=0$), for a Stress Release of 50%

settlements as indicated in Figures 6.14(a) and (b). When the surface settlements are normalized to the crown settlement calculated for a certain amount of ground stress release, a unique distribution is found.

As in the case of the cohesionless soil simplification (Section 6.2.2), the property of homothety will simplify the parametric analyses for this case, as the projected solution will not depend on the tunnel size, but simply on the ratio H/D. Obviously, it will depend on the ratio $c_u/\gamma D$, where it is sufficient to vary the values of c_u since, as in the former case, the unit weight of the soil of an homogeneous ground profile does not affect the normalized tunnel response.

Moreover with friction angle set equal to zero, there will be no need to vary the failure ratio, R_f, to obtain a general solution. This is because it is always possible to define an equivalent (undrained) cohesion c_{ue}, associated with a failure ratio (R_{fe}) equal to unity which gives the identical tangent modulus. If the tangent modulus given by equation 6.5 is to be the same, c_{ue} has to be selected in such a way that:

$$R_f \frac{1}{c_u} = R_{fe} \frac{1}{c_{ue}}$$

setting $R_{fe}=1$, then:

$$c_{ue} = \frac{c_u}{R_f} \qquad [6.7]$$

The stress-strain curve and thus the normalized ground response to tunnelling for the frictionless soil, with $R_{fe}=1$ and with an undrained cohesion c_{ue}, given by the equation

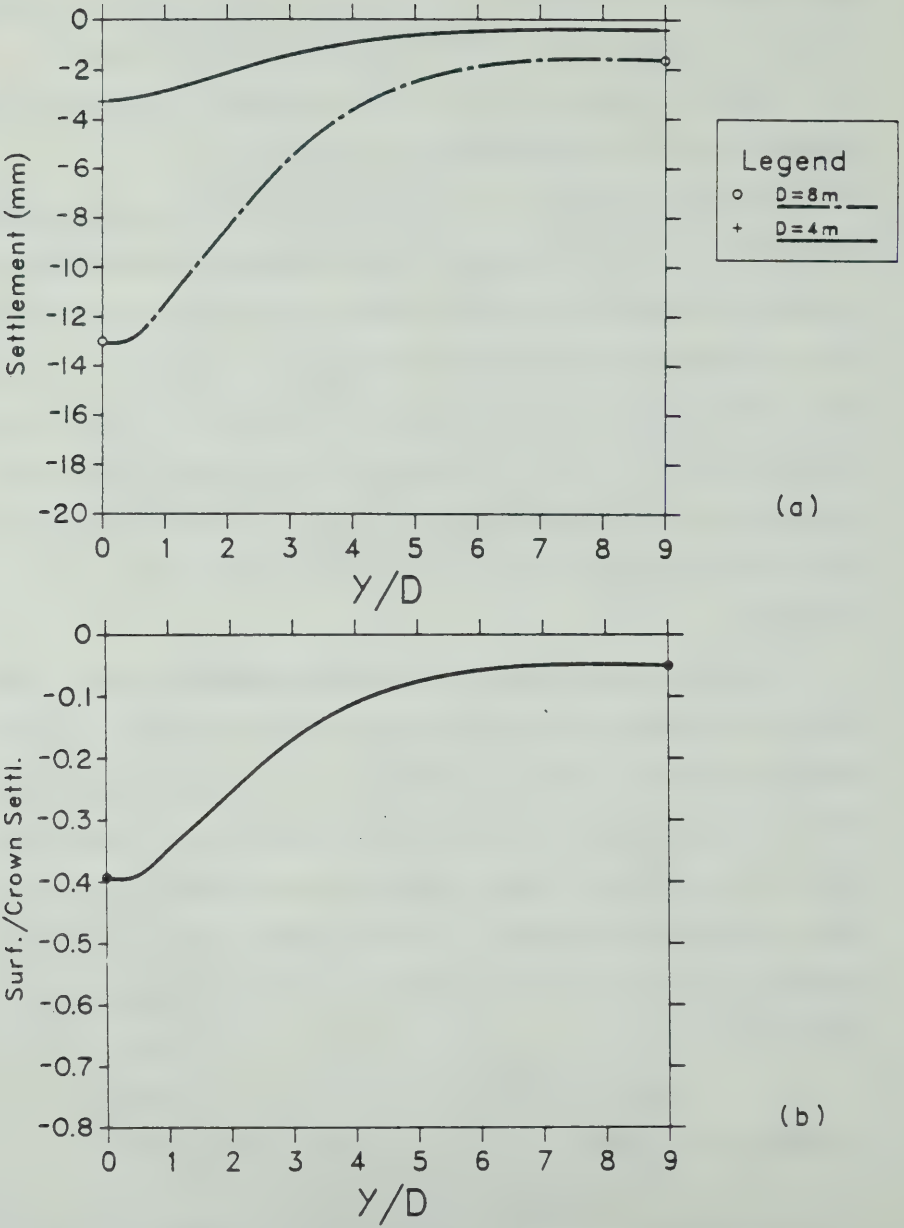

Figure 6.14 Surface Settlements over Geometrically Homothetic Tunnels in a Soil with a Homothetic Hyperbolic Stress-Strain Relationship ($\phi=0$), for a Stress Release of 50%

6.7, are identical to that of the frictionless soil, with R_f not equal to 1 and a cohesion equal to c_u.

The simplifications introduced so far allow equation 6.1 to be expressed in a more compact form, for this group of soil:

$$F= f(\theta , \frac{\sigma_r}{\sigma_{ro}} , \frac{u_r E_{ti}}{D\sigma_{ro}} , \frac{H}{D} , \frac{c_{ue}}{\gamma D} , \nu_u) \quad [6.8]$$

valid for $K_o=1$.

In this particular case, the variables in the above equation are mutually independent, with E_{ti} being solely a function of Janbu's modulus K and of the atmospheric pressure.

When the writer developed the simplifications described above regarding the homothetic soil models for a cohesionless soil (Section 6.2.2) and for a frictionless soil (present section), he was not aware that a similar approach has been used by other authors. In fact, the theoretical solution of settlements above tunnels by Resendiz and Romo, 1981 (see Section 4.3.3) also took advantage of the homothetic property of the hyperbolic model for $\phi=0$ and a c_u constant profile. Even earlier than that, these authors (Resendiz and Romo, 1972:819) used a similar soil model for the study of embankment deformations. In the latter case, a slightly different model was adopted in which the soil was assumed to be consolidated under its own weight and then sheared under undrained conditions, upon addition of subsequent embankment layers (hence a consolidated undrained condition). Resendiz and Romo (1972,1981) expressed their solutions using the original hyperbolic model formulation by Kondner (1963) for cohesive soils. The writer favoured the extended formulation by Duncan and Chang (1970) that makes use of more standard soil parameters. The novel development in the present work is, actually, the first soil model discussed (Section 6.2.2), representing a cohesionless soil. Despite the similarities between the models used by the writer and Resendiz and Romo (1981) for cohesive soils, the subsequent development of the design methods are quite different as will be seen in following sections of this chapter.

A final comment should be added to the present discussion. In section 5.2.2.1, it was pointed out than an incrementally reversible stress-strain relationship was assumed in the two dimensional numerical solution adopted herein. Consequently, no distinction is made between the loading, unloading and reloading behaviours. Had a different unloading - reloading response been specified, like the linear elastic response originally proposed by Duncan and Chang (1970), the uniqueness of the normalized ground response would cease to exist, even for the simplified soil models proposed. It was discussed earlier in this thesis, and especially in Section 5.2.2.2, that some points around the two-dimensionally represented tunnel may have their principal stresses rotating, or commuting directions. This unloading and reloading response may in fact happen around the shallow tunnel, depending on the in situ stress ratio.

It is easy to recognize that if a distinct stress-strain response had been specified for a decreasing principal stress difference, the stress-strain curves representing the soil behaviour would not result homothetic any longer. The similarity of the ground response or its independence on the scale of the problem (tunnel size) would not exist, except approximately.

This difficulty with similarity techniques applied to non-linear incremental laws, with distinct loading and unloading representations, was discussed by Winter (1982:1076). This author suggested that in order to apply these techniques to these types of constitutive laws, one is forced to neglect either the influence of the unloaded zones or of the loaded zones. In the first case, the similarity solution implies more stored energy than it should, and in the second case the converse is true. The last alternative implies in reducing the treatment of the problem to a linear elastic representation and this, as shown earlier in this thesis, is not an acceptable choice.

In order to avoid these difficulties, in the present work makes no distinction between the loading and unloading-reloading soil responses. The numerical model was therefore implemented accordingly. Despite this simplification, the model was tested and proved satifactory in matching the performance of three shallow tunnel case histories (Section 5.2.4). Although this cannot be claimed as proof of the validity of the simplification, it does stand as an indication that it may be acceptable in practical terms.

6.2.4 Comments on Some Simplifying Assumptions

6.2.4.1 The Effect of Janbu's Modulus K

The in situ tangent modulus is directly proportional to the Janbu's modulus K, as shown by equations 6.2 and 6.6. As the normalized displacements are invariant to E_{ti}, they should also be invariant to the modulus K. Figures 6.15 to 6.17 demonstrate this fact. The ground reaction curves shown were calculated numerically, using the cohesionless soil model described in Section 6.2.2 and assuming $\phi=30°$, $n=0$, $\gamma=19.6$ kN/m^3, $K_o=1$, $\nu=0.4$, D=4m, H=12 m and three different values for the modulus K. The ground stress release of the unlined circular opening was performed in ten equal increments.

If the displacements are expressed as:

$u_r/D.\sigma_{ro}$

the ground reaction curves are those shown by the solid lines. Clearly, as the K modulus decreases, the tunnel convergence increases proportionally, for the same amount of stress release.

If the displacements are normalized to E_{ti} and therefore to K, the ground reaction curves at each point of the tunnel contour are reduced to a single normalized curve shown by the dashed lines in Figures 6.15 to 6.17. Consequently, there will be no need to vary the value of K in the modelling step, in order to obtain the general solution to the problem.

6.2.4.2 The Effect of Janbu's Exponent n

A fairly restrictive assumption was made in the development of the cohesionless and of the frictionless soil models, presented in Sections 6.2.2 and 6.2.3. It refers to the value of the Janbu's exponent n, which was set equal to zero. This is the parameter controlling the rate of increase of the in situ tangent modulus of a soil deposit with depth. For instance, in a homogeneous and cohesionless deposit, if n is made equal to unity, the in situ tangent modulus increases linearly with depth. In this soil deposit, if n is set equal to zero, a constant modulus with depth is found. Except for some overconsolidated soil deposits, a constant in situ modulus profile does not generally correspond to reality.

The influence of the rate of increase of the in situ modulus with depth on the ground response to tunnelling, was thus investigated. Some typical results of this investigation are presented herein. They refer to three finite element analyses of a tunnel with D=4m and H=12 m, in soil with the following parameters: $\gamma=19.6$ kN/m³, $K_o=0.8$, $c=0$, $\phi=30°$, $\nu=0.4$, and Janbu's modulus K=400. Three exponents n were considered in these analyses: n=0, 0.5 and 1.0. These conditions yielded respectively, the following in situ tangent moduli at the tunnel axis elevation: 31.015 MPa, 45.672 MPa and 67.255 MPa.

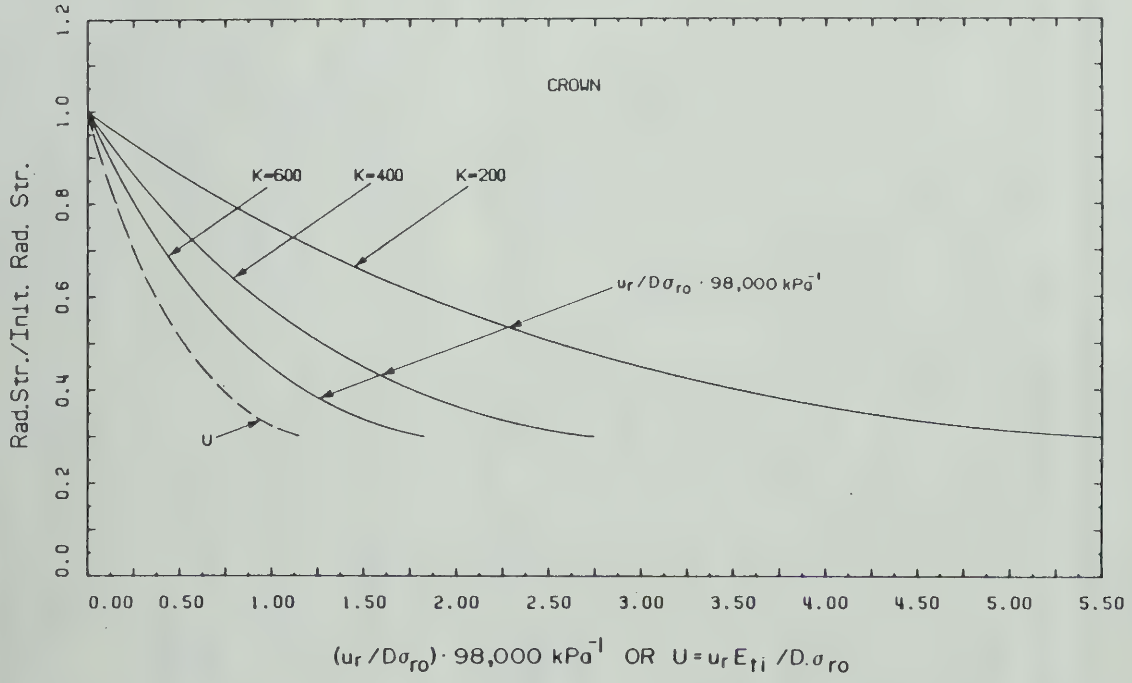

Figure 6.15 Influence of Janbu's Modulus K on the Ground Reaction Curve of the Tunnel Crown

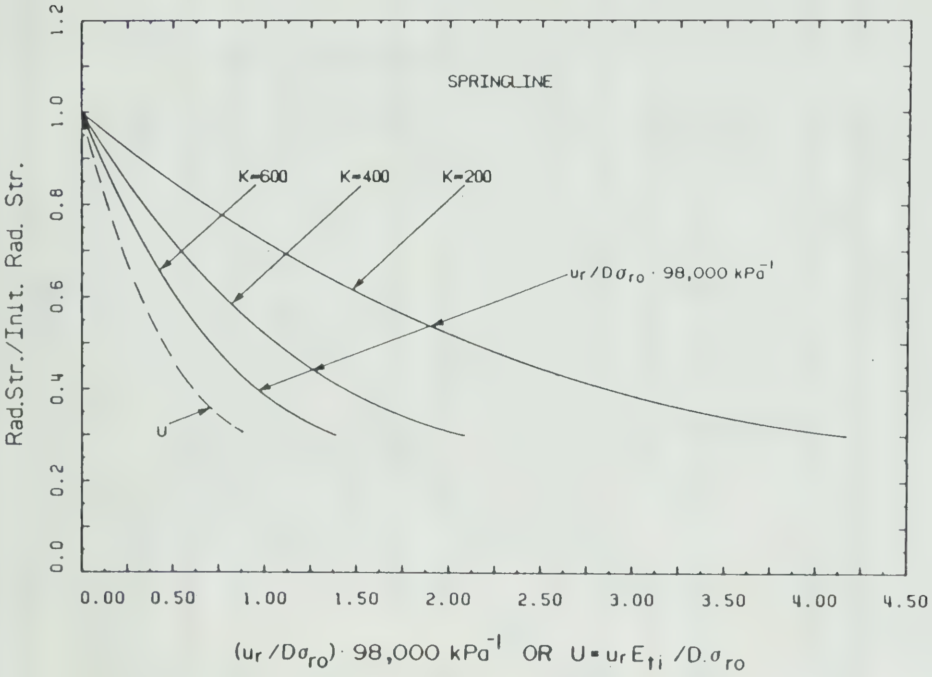

Figure 6.16 Influence of Janbu's Modulus K on the Ground Reaction Curve of the Tunnel Springline

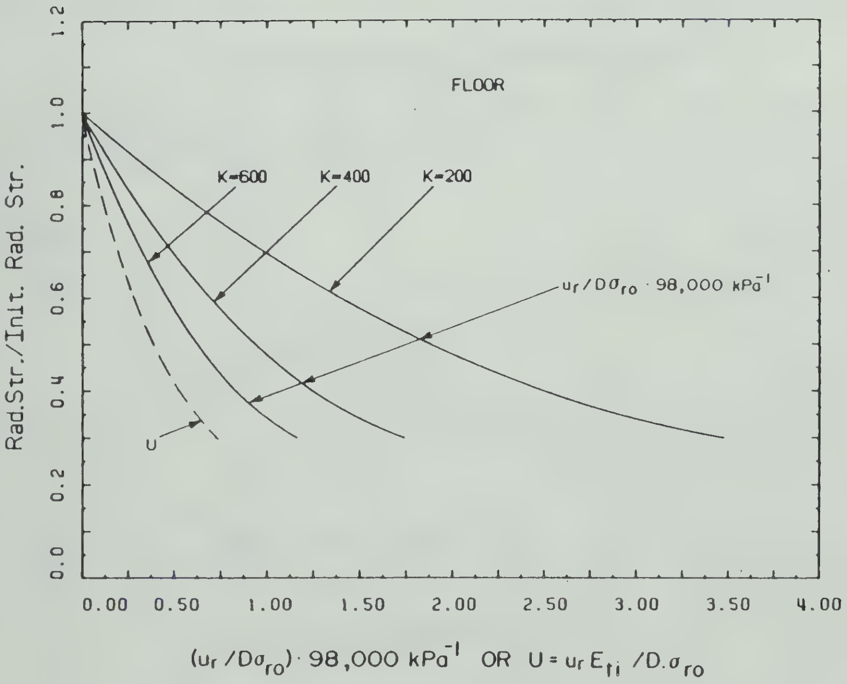

Figure 6.17 Influence of Janbu's Modulus K on the Ground Reaction Curve of the Tunnel Floor

If the in situ tangent modulus at the tunnel axis elevation is normalized to one, the variations of the modulus with depth, for the three cases considered are those shown in Figure 6.18.

The numerical analyses were performed with the gradual release of the ground stresses at the opening in ten increments. After the sixth unloading increment, some elements at the springline failed and the results thereafter were disregarded.

Figure 6.19 presents the calculated normalized ground reaction curves for the tunnel crown. In all cases, the displacements were normalized to the initial tangent modulus taken at the springline elevation. The ground reactions at the crown seem to be basically controlled by the soil cover stiffness. Since the displacements were normalized to the modulus at the tunnel axis, the resulting NGRC for the constant modulus profile (n=0) is stiffer than the other cases. An opposite trend is of course found at the tunnel floor. Figure 6.20 shows that when the modulus increases linearly with depth (n=1), a "stiffer" ground response is noted. The influence of the rate of increase in the ground stiffness with depth on the NGRC is less pronounced at the tunnel springline than elsewhere on the tunnel contour. This is illustrated in Figure 6.21, where the NGRCs appear fairly close together. Nevertheless, like the reponse at the crown, the resulting NGRC for n=0 is stiffer than the others, and this shows that the springline response of this shallow

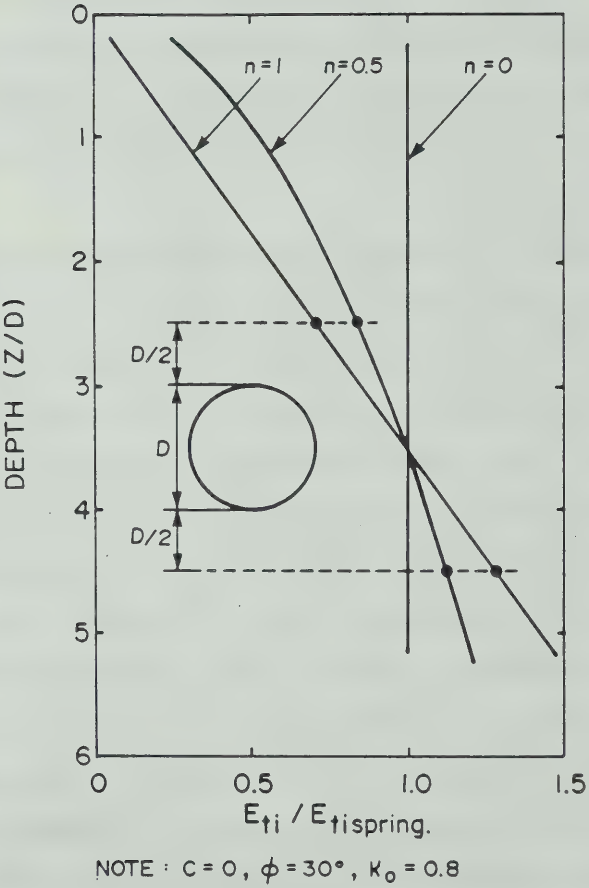

Figure 6.18 Variations with Depth of the In Situ Tangent Modulus for Three Values of Janbu's Exponent, n

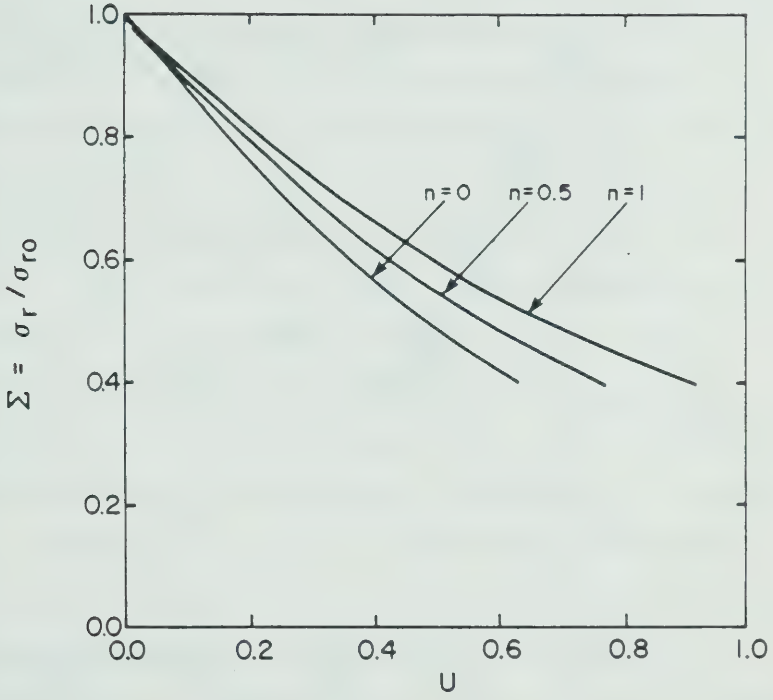

NOTE : C=0, ϕ=30°, K_0=0.8, ν=0.4, H/D=3

Figure 6.19 Normalized Ground Reaction Curves for the Tunnel Crown, Calculated for Different In Situ Tangent Modulus Profiles

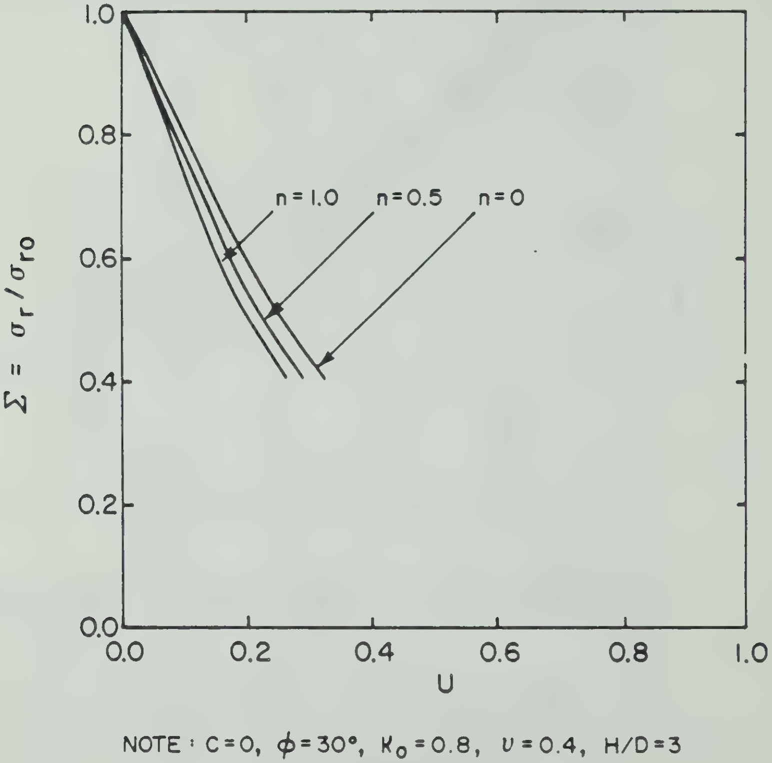

Figure 6.20 Normalized Ground Reaction Curves for the Tunnel Floor, Calculated for Different In Situ Tangent Modulus Profiles

tunnel is more affected by the stiffness of the ground above it than below it.

From the trends noted in Figures 6.19 and 6.20, it is observed that the NGRCs at the crown and at the floor reflect some sort of 'average' stiffnesses of the ground above and below the tunnel, respectively. If these average stiffnesses could possibly be determined and used to normalize the corresponding displacements, then a NGRC which would be independent of the rate of increase of the stiffness with depth, could eventually be found. After a few attempts, it was found that if the ground responses at the crown and at the floor were normalized to the in situ stiffness of the ground at points located half diameter above and below the tunnel respectively, the resulting NGRC would be practically independent of the rate of increase of E_{ti} with the depth. For n=0.5, these moduli are equal to 38.514 and 51.744 MPa, at half diameter above and below the tunnel respectively. For n=1.0 they are 47.530 MPa and 85.946 MPa. The new NGRCs for the crown and the floor are shown in Figure 6.22. As one notes, the newly defined response is virtually independent of the exponent n. This artifice thus allows the effect of E_{ti} increasing with depth to be approximately accounted for from the results of analyses where a constant in situ stiffness is assumed. The artifice was tested and found to yield approximately the same results for other geometric situations and soil parameters, within the ranges of variables considered in the

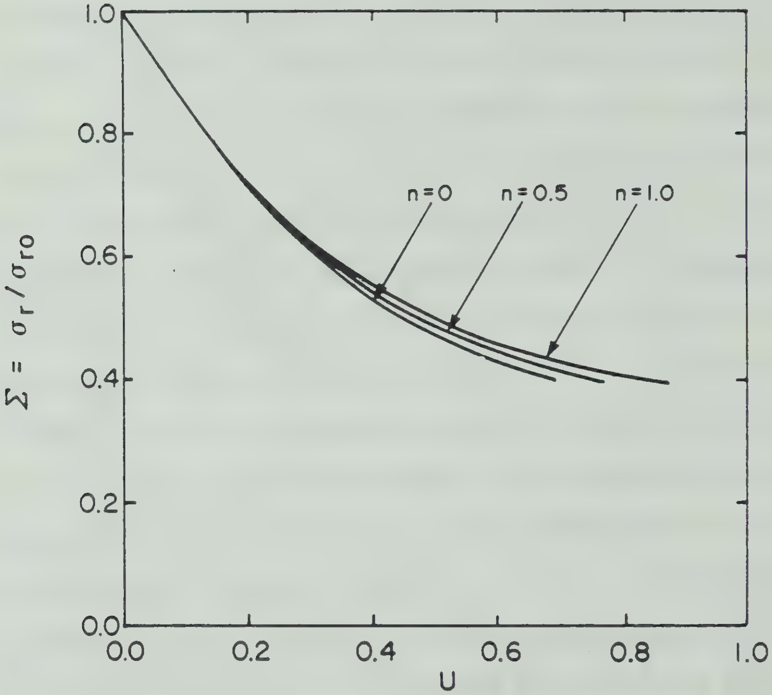

NOTE : C=0, ϕ=30°, K_0=0.8, ν=0.4, H/D=3

Figure 6.21 Normalized Ground Reaction Curves for the Tunnel Springline, Calculated for Different In Situ Tangent Modulus Profiles

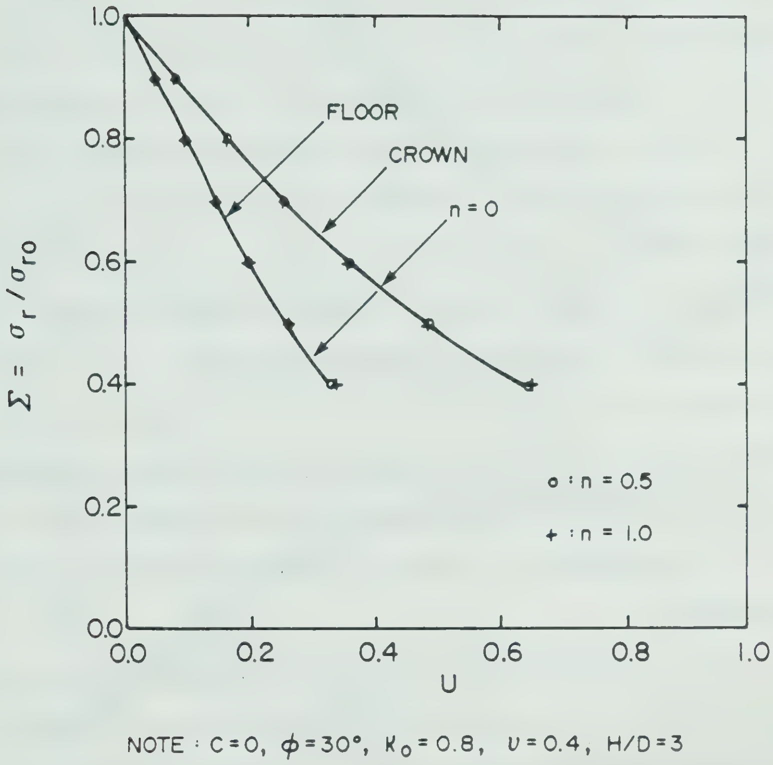

Figure 6.22 Ground Reaction Curves for the Crown and Floor, with the Displacements Normalized to the Soil In Situ Stiffnesses at Points Half a Diameter Above and Below the Tunnel Respectively

modelling step to be presented later.

If the resulting normalized ground reaction curves are nearly independent of n, one would expect the same with regard to the ground settlements. Figures 6.23 (a) and (b) present the distributions of subsurface and surface settlements normalized to the crown settlement, for n varying from 0 to 1, and for 50% of ground stress release at the opening. Indeed the resulting distributions are very close to each other, although the influence of n is clearly noted. Moreover, one observes that the assumption of n=0 implies a slightly smaller average strain in the tunnel ground cover, as in fact one would expect, and which leads to a marginally higher normalized surface settlement at the tunnel axis. Although the maximum normalized settlement is larger for n=0, the maximum normalized distortion at about 2D off the centerline seems to be insensitive to the exponent n.

The results shown in Figure 6.23 depend slightly on the amount of ground stress release allowed at the opening. Table 6.4 presents the values of normalized maximum surface settlements for different n and different stress releases. The number shown between brackets represent the ratios of normalized settlement for n=0 to n>0. Therefore they represent the amount of approximation involved in the constant modulus profile assumption. By making n=0, one observes that the normalized maximum surface settlement is overestimated by 4 to 11%, depending on the value of n and

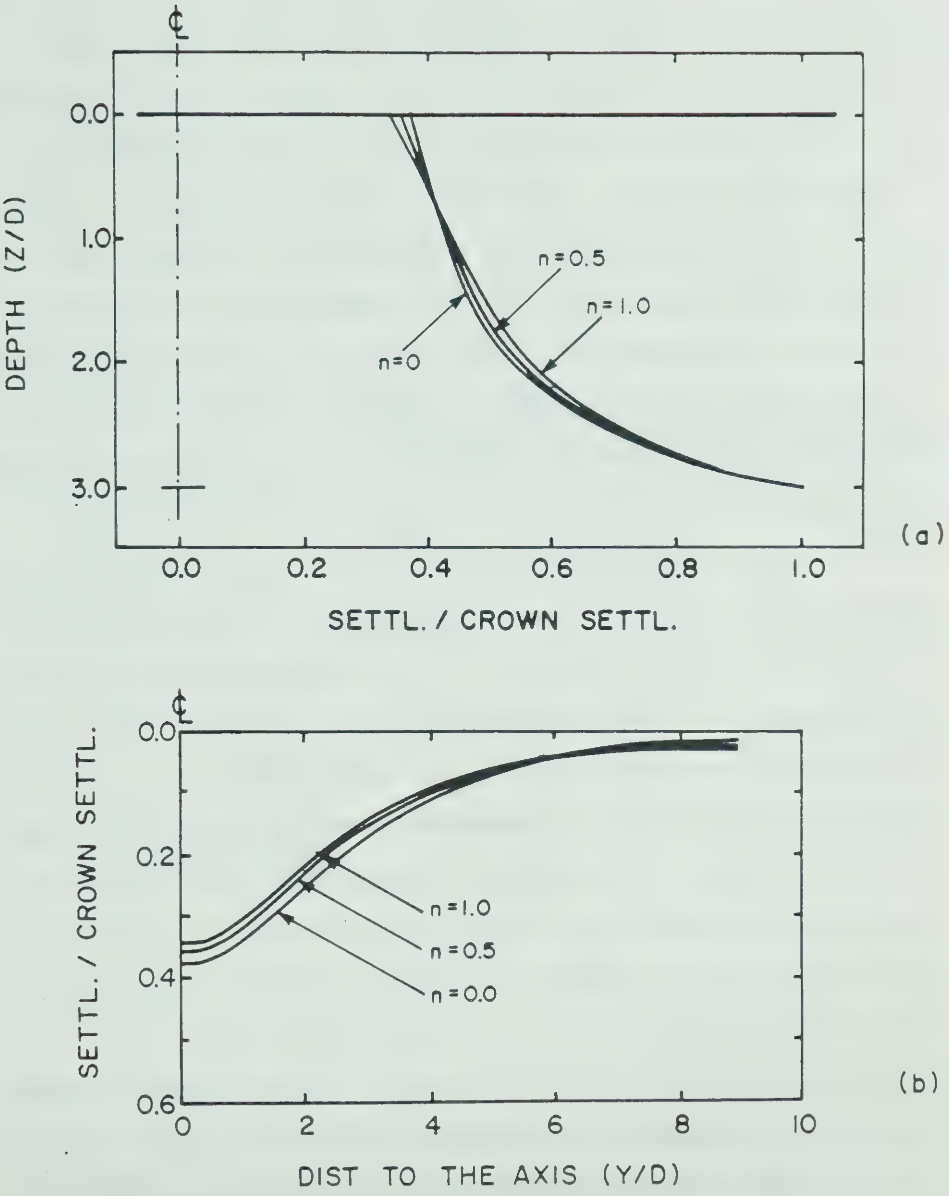

NOTE : C = 0, $\phi = 30°$, $K_0 = 0.8$, $\nu = 0.4$, H/D = 3

Figure 6.23 Normalized Subsurface and Surface Settlements for 50% Ground Stress Release at the Opening, for Different Exponent n Values

on the amount of ground stress release. The error seems to increase as n increases and as the stress release decreases.

To complete the picture, Table 6.5 was prepared. It shows the ratios of normalized crown displacements for n=0 to n>0. The assumption of n=0 may under or overestimate the normalized displacement for n>0, depending on the valaue of n and on the amount of stress release. As the stress release increases, the n=0 assumption tends to underestimate U for n>0. The error in the U estimate with n=0 varies within plus or minus 3%.

If the results of Tables 6.4 and 6.5 are combined one may estimate the final error in the actual maximum ground surface settlement estimate for the assumption of n=0. It will usually be overestimated by 2 to 14%. For n=0.5, the overestimate should not normally exceed 5%.

In summary, one may conclude that the exponent n does have an effect on the ground response to tunnelling. The soil models described in Sections 6.2.2 and 6.2.3 assume n=0. However, the effect of n on the normalized ground reaction curves can be taken approximately into consideration, by using the actual in situ tangent modulus at points located half diameter radially away from the point of the opening being considered. A lower E_{ti} is therefore selected for the crown curve, an intermediate one for the springline and a higher one for the floor.

The subsurface and surface settlements normalized to the crown settlement are not much affected by n, and the

	Maximum Surface Settlement/Crown Settlement		
Stress release	40%	50%	60%
n = 0	0.366 (1.000)	0.375 (1.000)	0.379 (1.000)
n = 0.5	0.350 (1.046)	0.359 (1.045)	0.363 (1.044)
n = 1.0	0.329 (1.112)	0.339 (1.106)	0.343 (1.105)

Note: The ratios of settlement ratios for n = 0 to n > 0 are shown between brackets.

Table 6.4 Variation of the Maximum Normalized Surface Settlement with the Exponent n and with the Amount of Stress Release Allowed in the Opening

	U (n = 0)/U (n > 0) at crown		
Stress release	40%	50%	60%
n = 0.5	1.000	0.990	0.980
n = 1.0	1.023	1.000	0.974

Table 6.5 Ratio of Normalized Crown Displacements for n=0 to n>0, for Different Exponents n and Different Amount of Stress Release at the Opening

assumption of n=0 seems to be a safe one in most cases. Moreover, the degree of overestimation is not excessive. The maximum normalized surface distortions are also not much influenced by n.

6.2.4.3 The Effect of the Cohesive Strength Component

Another fairly restrictive assumption made in the development presented in Section 6.2.2 refers to the zero cohesion assumed in the frictional soil model. Soil cohesion has a clear and important role in the stability of an underground opening as discussed in other sections of this thesis (for instance, Section 4.3.4). To neglect the cohesive component of soil strength may be an unduly conservative assumption.

To investigate the effect of the cohesion on the ground response to tunnelling, some finite element analyses were carried out. An unlined circular tunnel with D=4m and H=12 m was considered in a homogeneous soil profile, with the following properties: $\gamma=19.6$ kN/m^3, $K_o=0.8$, $\phi=30°$, $\nu=0.4$, n=0, and K=400. Three cohesive strengths were considered in these analyses: c=0, c=9.8 kPa and c=19.6 kPa (i.e., $c/\gamma D=0$, 0.125 and 0.250). For those conditions, the following in situ tangent moduli were obtained at the tunnel axis elevation, respecively: 31.015 MPa, 31.653 MPa and 32.211 MPa.

Once more the numerical analyses were performed with the gradual release of the ground stresses at the opening in ten constant increments. For c=0, after the sixth unloading increment, some elements close to the springline failed and the results thereafter were disregarded. In the other cases, the failure of elements close to the springline was noted only after the seventh unloading increment. The increased soil strength in these cases thus allowed a larger stress release to be applied at the opening, without inducing localized soil failure.

Figure 6.24 shows the calculated normalized ground reaction curves for the tunnel crown. The displacements were normalized to the initial tangent modulus at springline elevation. As would be expected, the increase in c, besides making the soil stronger which permitted a larger stress reduction without failure, it also makes the soil stiffer, thus leading to smaller U values for a given stress release. A similar behaviour is noted for the tunnel springline, as indicated in Figure 6.25. A more pronounced non-linear response is noted here which reflects the trend of soil elements at the springline to fail earlier than elsewhere when K_o is less than unity, as in this case. The influence of the cohesion on the ground reaction at the tunnel floor is less pronounced, as indicated in Figure 6.26. Unlike the response at the springline, soil elements close to the floor are likely to fail later, and require a larger stress reduction to cause local soil failure. The ground response shown is thus mainly controlled by the frictional strength of the soil rather than the cohesive component. The higher confining stress level below the tunnel, causes the

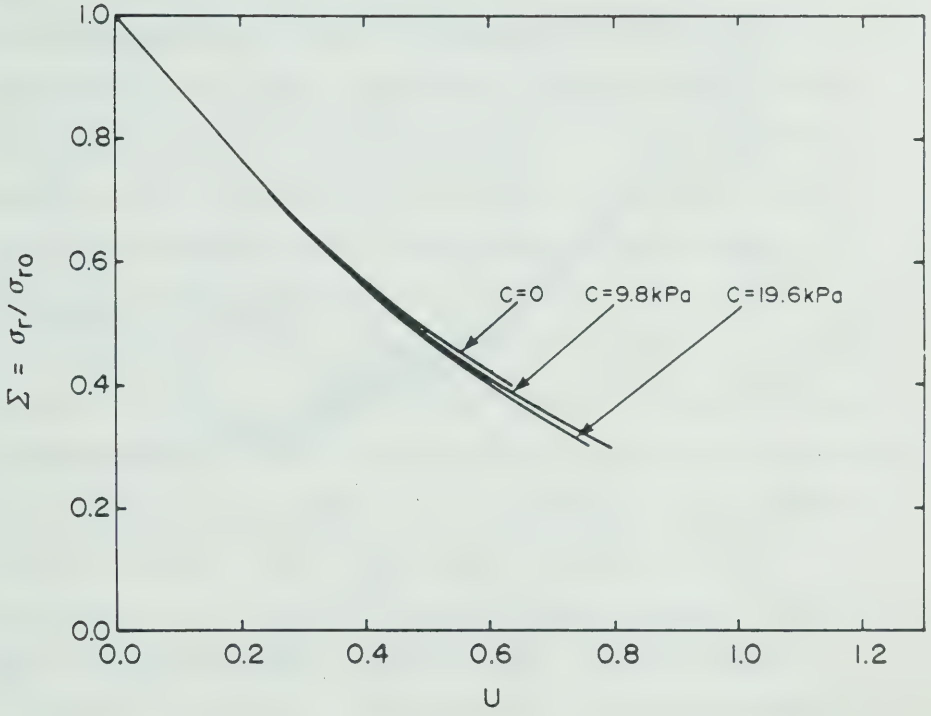

NOTE : $\phi = 30°$, $K_o = 0.8$, $\nu = 0.4$, $n = 0$, $H/D = 3$, $D = 4m$

Figure 6.24 Normalized Ground Reaction Curves for the Crown, Calculated for Different Cohesive Strengths of the Soil

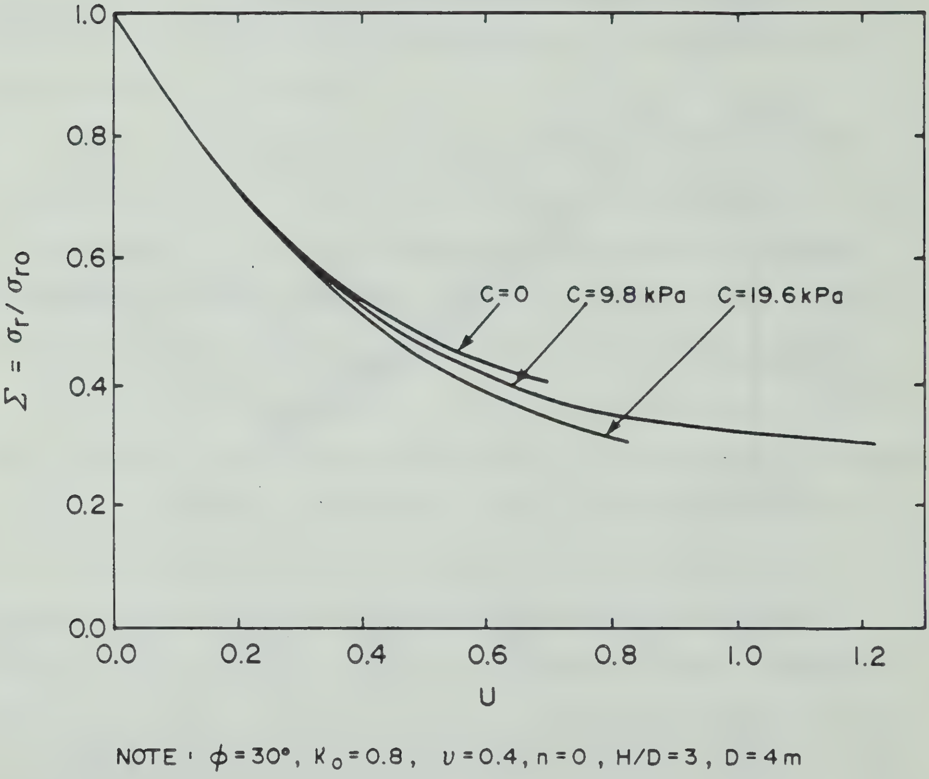

Figure 6.25 Normalized Ground Reaction Curves for the Springline, Calculated for Different Cohesive Strengths of the Soil

frictional component of strength to dominate the response, and the NGRC for different c values virtually coincide. Similar responses are noted at the crown and springline for smaller amounts of ground stress release (up to about 40% and 30% respectively).

Figures 6.27(a) and (b) present the distributions of subsurface and surface settlements normalized to the crown settlement, for c varying from 0 to 19.6 kPa and for a ground stress release of 50% at the tunnel. For these conditions and parameters, the influence of cohesion is basically immaterial. The maximum normalized ground distortion is virtually insensitive to the soil cohesion. The results shown in this figure depend on the amount of stress release. Table 6.6 presents the values of normalized maximum surface settlements for different c and different stress releases. The numbers shown between brackets represent the ratios of normalized settlements for c=0 to c=0. As for the NGRC, one notes that if the cohesive component of strength is neglected the normalized maximum ground surface settlement is overestimated by 1 to 3%, depending on the value of c and the amount of ground stress reduction. The error involved in neglecting c seems to increase as stress reduction increases and, of course, as the soil cohesion increases. If the cohesion is higher than the values considered herein, then the degree of overconservatism in the c=0 assumption might become excessive. To compensate for this and to get closer to the

	Maximum Surface Settlement/Crown Settlement		
Stress release	40%	50%	60%
c = 0	0.366 (1.000)	0.375 (1.000)	0.379 (1.000)
c = 9.8 kPa	0.362 (1.011)	0.369 (1.016)	0.373 (1.016)
c = 19.6 kPa	0.358 (1.022)	0.365 (1.027)	0.369 (1.027)

Note: The ratios of settlement ratios for c = 0 to c ≠ 0 are shown between brackets.

Table 6.6 Variation of the Maximum Normalized Surface Settlement with the Cohesive Strength of the Soil and with the Amount of Stress Release Allowed

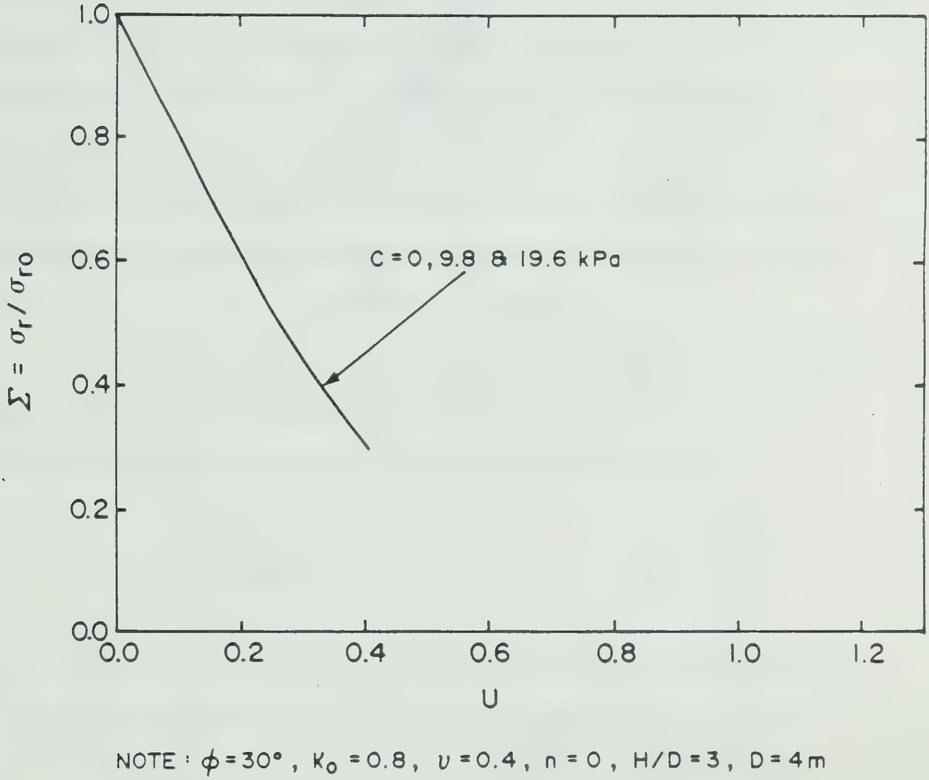

Figure 6.26 Normalized Ground Reaction Curves for the Floor, Calculated for Different Cohesive Strengths of the Soil

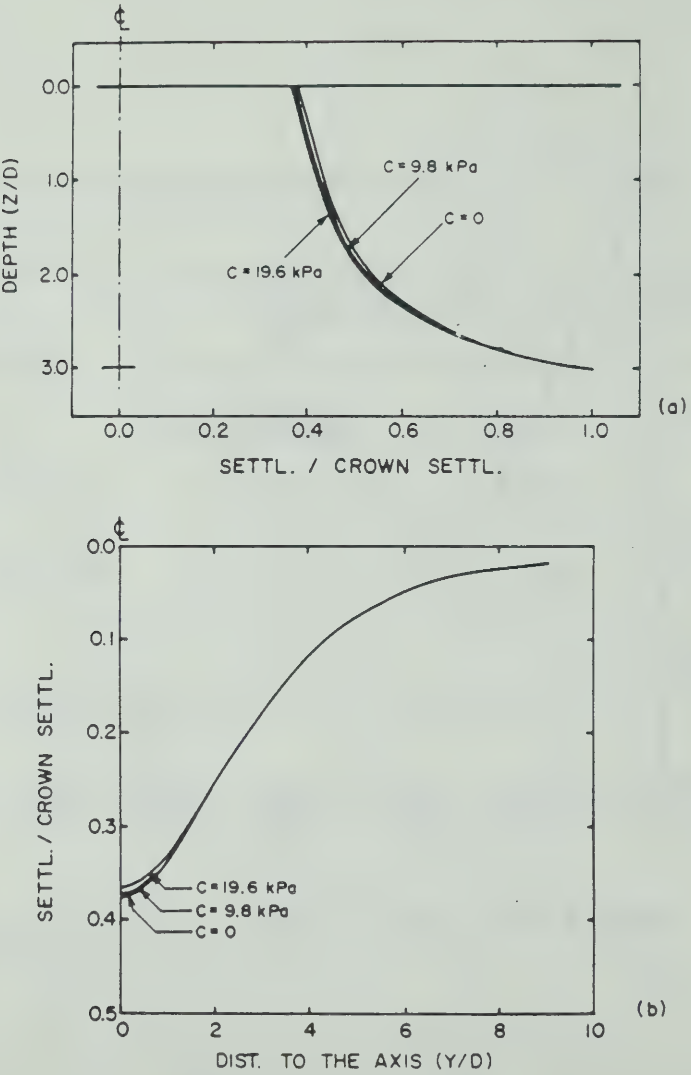

NOTE : $\phi = 30°$, $K_o = 0.8$, $\nu = 0.4$, $n = 0$, $H/D = 3$, $D = 4m$

Figure 6.27 Normalized Subsurface and Surface Settlements for 50% Ground Stress Release, Calculated for Different Cohesive Strengths of the Soil

response that includes the effects of both frictional and cohesive components of strength, an approximation can be devised. This consists of adjusting the friction angle of the soil with c=0 (so as to not depart from the cohesionless soil model) in such a way that the in situ strength defined in terms of the principal stress difference at the springline elevation, is made equal to the strength of the actual soil with a non-zero cohesion. A problem then emerges, as the stress difference at failure depends on the stress path leading to failure and this is not exactly known.

If it is assumed that at failure the normal stress is equal to the average in situ principal stress $(\sigma_1+\sigma_3)/2$, then the resulting adjusted friction angle is:

$$\phi_a = \arcsin\left[\sin\phi + 2c\cos\phi/\gamma(H+D/2)(1 + K_o)\right] \qquad [6.9]$$

On the other hand, if it assumed that failure is reached by keeping the minor in situ principal stress constant and by increasing the major principal stress, then the adjusted friction angle becomes:

$$\phi_a = \arcsin\left[\frac{1+(\sigma_3/c)\tan\phi}{1+(\sigma_3/c)\sec\phi}\right] \qquad [6.10]$$

If the results of the finite element analysis with the higher cohesion (c=19.6 kPa) is taken as an example, equation 6.9 for $\phi=30°$ will give an adjusted friction angle of 34.7°, while equation 6.10 leads to ϕ_a=32.4°. Two additional finite element analyses were then carried out both with c=0 and with each of the above adjusted values for friction. Figure 6.28 present the NGRC for the crown derived from these analyses. The use of the adjusted friction angles led to better approximations of the correct NGRC, compared to the result given by the assumption of c=0 and ϕ=30°. Actually, the assumption of c=0 and ϕ_a given by equation 6.10 led to a NGRC that virtually coincided with the correct curve. Figure 6.29, on the other hand, presents the NGRC for the springline obtained through these analyses. Once more the analyses with the adjusted friction angles yield better approximations than the c=0 and ϕ=30° assumption. In this case, however, it was noted that the adjustment given by equation 6.9 (constant normal stress) tends to slightly underestimate the dimensionless displacement U for a given amount of stress release. With regard to the tunnel floor, the NGRC obtained with ϕ_a given by both equations virtually coincided with the correct curve shown in Figure 6.26.

Other assumptions and adjustments of the friction angle were made and tested to conditions different than those considered herein. The best approximations to the correct response were always found using the friction angle given by equations 6.9 and 6.10. However, equation 6.9 sometimes may yield unsafe approximations of the NGRC (a stiffer response), especially for tunnels with small covers in soils with higher cohesion, where the cohesive component of

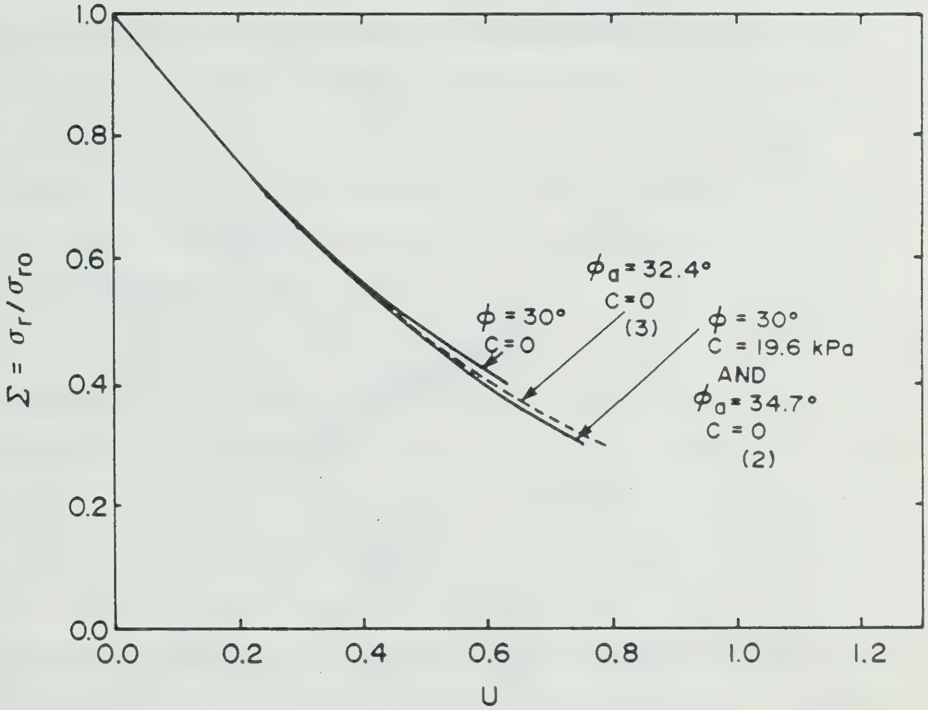

NOTES

1. $K_0 = 0.8$, $\nu = 0.4$, $n = 0$, $H/D = 3$, $D = 4$ m
2. ϕ_a BY EQUATION 6.9
3. ϕ_a BY EQUATION 6.10

Figure 6.28 Normalized Ground Reaction Curves for the Crown, Calculated for Different Soil Strengths

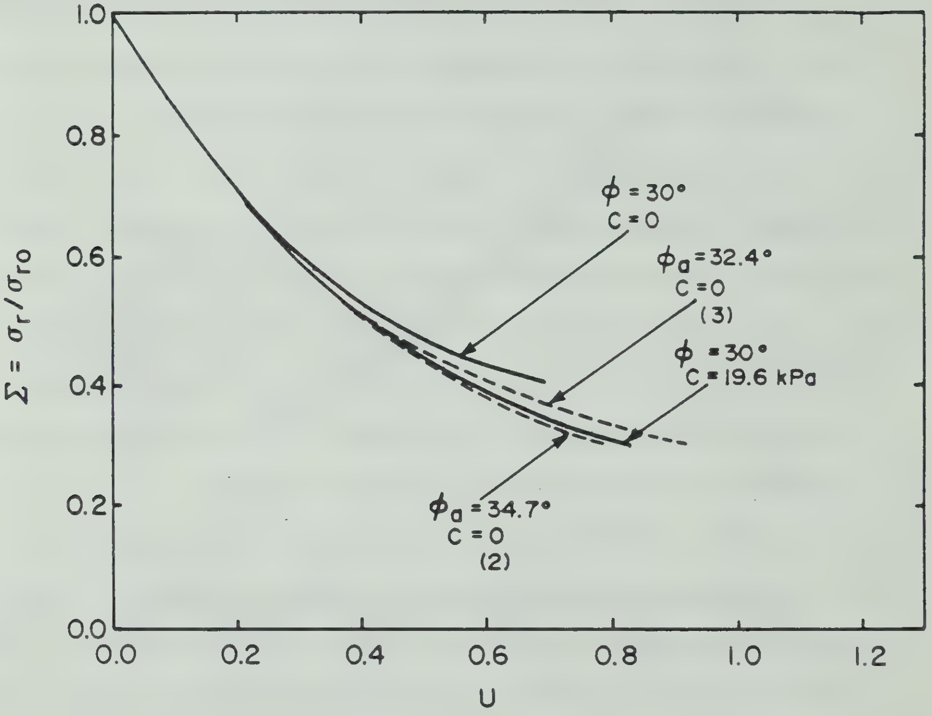

NOTES

1. $K_o = 0.8$, $\nu = 0.4$, $n = 0$, $H/D = 3$, $D = 4$ m
2. ϕ_a BY EQUATION 6.9
3. ϕ_a BY EQUATION 6.10

Figure 6.29 Normalized Ground Reaction Curves for the Springline, Calculated for Different Soil Strengths

strength therefore dominates the response. For this reason. equation 6.10 will be favoured hereafter. In some special circumstances where the cohesive component of strength predominates, another possible assumption could be made by disregarding the soil's frictional resistance and by using the frictionless soil model. As the adjustments proposed herein are, in fact, simple approximations, each practical situation should be investigated individually and the adjustments should be selected on a case by case basis. In most cases, the approximation given by equation 6.10 with c=0 should prove sufficient.

To summarize the above discussion, Table 6.7 was prepared. It gives the variation of dimensionless displacement at the tunnel crown for the different strength assumptions made and for different amounts of stress release. The numbers between brackets are the ratios correct U for c=0 to the corresponding approximate U for c=0, calculated according to the different assumptions. They give an indication of the approximations involved in each case.

6.2.4.4 The Effect of Poisson's Ratio

As indicated by equations 6.4 and 6.8, the ground responses depend on the values of the Poisson's ratio, ν. The frictionless soil model described in Section 6.2.3 was developed for soils under fully undrained conditions. Therefore, an undrained Poisson's ratio ν_u, of 0.5 should be considered. To avoid numerical problems a ratio close to

	U at the crown		
Stress release	40%	50%	60%
$c = 19.6$ kPa $\phi = 30°$ (correct)	0.354 (1.000)	0.465 (1.000)	0.595 (1.000)
$c = 0$ $\phi = 30°$ (1st approx.)	0.363 (0.975)	0.484 (0.961)	0.635 (0.937)
$c = 0$ $\phi = 34.7°$ (2nd approx., eq. 6.9)	0.350 (1.011)	0.460 (1.011)	0.589 (1.011)
$c = 0$ $\phi = 32.4°$ (preferred approx. eq. 6.10)	0.354 (1.000)	0.475 (0.979)	0.609 (0.977)

Note: The ratios of correct U for $c \neq 0$ to the approximate U for $c = 0$ are shown between brackets.

Table 6.7 Variation of the Dimensionless Crown Displacement for the Different Strength Assumptions made and for the Different Amounts of Stress Release

that value (ν_u=0.49) should be sufficient for the parametric finite element analyses to be carried out in the modelling step. On the other hand, the value of ν for the cohesionless soil model can vary typically from 0.2 to 0.4.

To assess the influence of the Poisson's ratio on the ground response to tunnelling, two finite element analyses were conducted. In both cases, an unlined circular tunnel with D=4 m and H=12 m was considered in a homogeneous soil profile, with the following properties: γ=19.6 kN/m^3, K_o=1.0, ϕ=30°, c=0, n=0,and K=400. One analysis was carried out with ν=0.2 and the other with ν=0.4. In both cases, the in situ tangent modulus of the soil was equal to 40.494 MPa. The analyses were performed with the gradual release of the ground stresses at the opening in ten increments. Local failure of soil elements at the crown, springline and floor was detected after the seventh unloading increment.

The resulting normalized ground reaction curves for the tunnel crown are represented in Figure 6.30. It is noted that for the same amount of stress reduction, ν=0.4 yields dimensionless displacements U usually larger than for ν=0.2, unless the stress release is greater than about 65%.

The normalized ground reaction curves for the springline are shown in Figure 6.31 and for the floor in Figure 6.32. Similar results are found, but the differences in the NGRC for ν=0.2 and 0.4 are less pronounced.

Figures 6.33(a) and (b) present the distributions of subsurface and surface settlements normalized to the

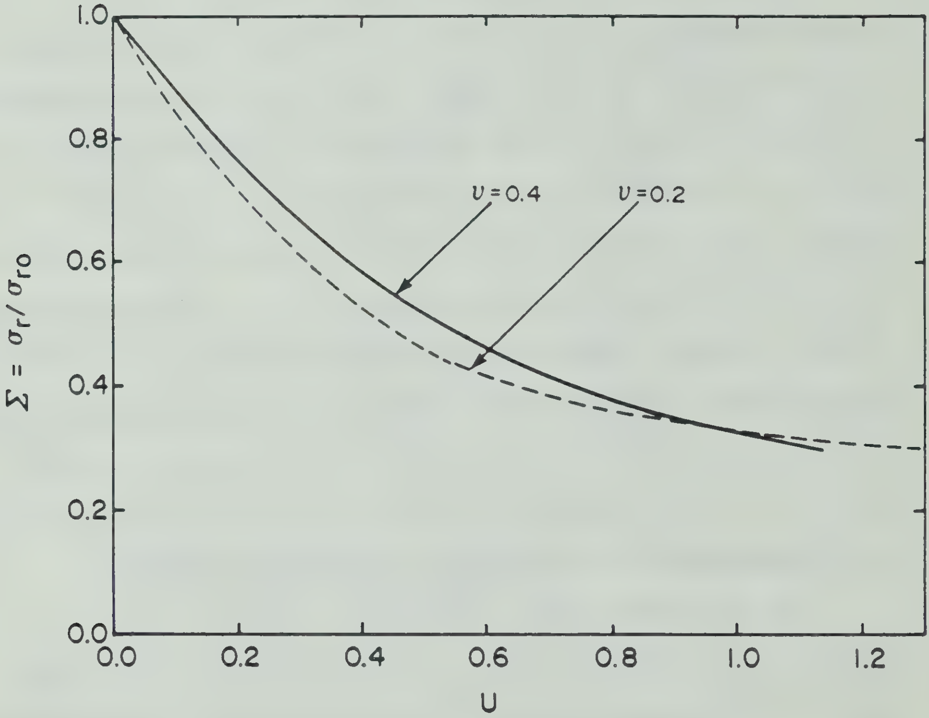

NOTE : C=0, ϕ=30°, K_0=1.0, n=0, H/D=3, D=4m

Figure 6.30 Normalized Ground Reaction Curves for the Crown, Calculated for Different Poisson's Ratios

corresponding crown settlement, for the two Poisson's ratios considered and for a ground stress release of 50%. Similar results are found for other amounts of stress reduction. One notes that the normalized subsurface settlement distribution is not much affected by ν and that the values for ν=0.4 are slightly larger than for ν=0.2.

The analysis with ν=0.4 yielded a maximum normalized ground surface settlement slightly larger than with ν=0.2 (Figure 6.33(b)). The difference between settlement ratios at points other than the centreline tend to increase, with increasing distance to the axis. As a result, the normalized ground distortion at the surface is greater for ν=0.2, than for ν=0.4.

With the exception of the distortion, one notes from Figures 6.30 to 6.33 that for ground stress releases varying between 30% and 65%, the ground displacements seem to increase for an increasing Poisson's ratio. This range of ground stress release can be taken as typical of that occurring before activation of linings in tunnels built under good ground control conditions. In order to reduce the number of independent dimensionless variables in Equation 6.4 and to simplify the modelling step, it was decided to select a single value for Poisson's ratio. In order to be generally on the safe side in terms of ground settlements, the higher value of Poisson's ratio (ν=0.4) will be used in the modelling step analyses. It should be remembered, however, that this simplification may result in unsafe

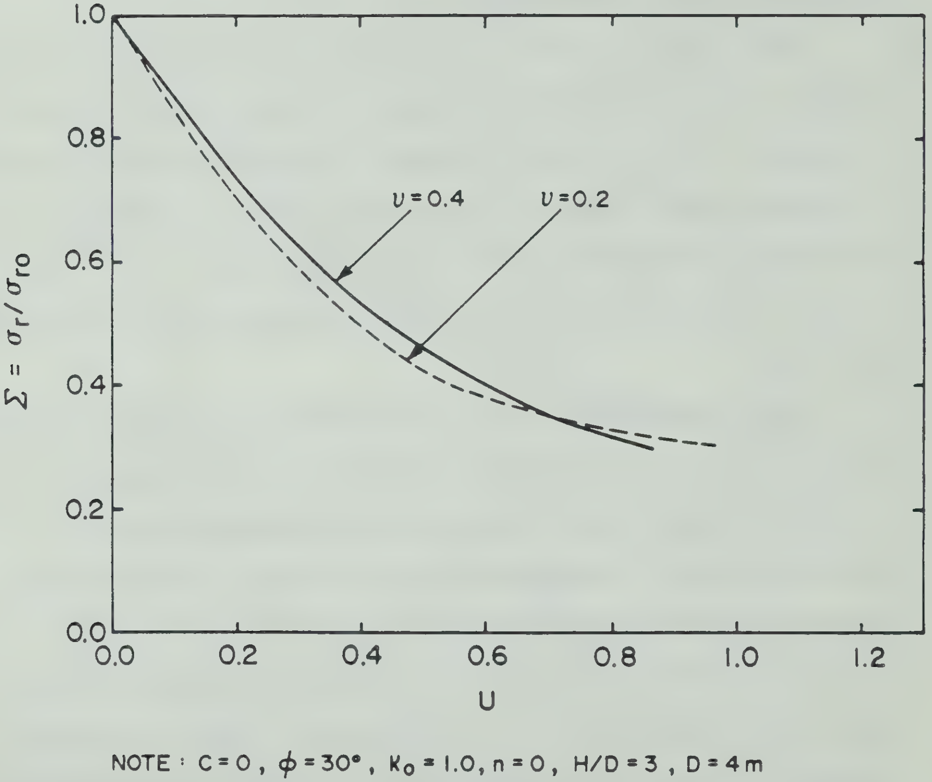

Figure 6.31 Normalized Ground Reaction Curves for the Springline, Calculated for Different Poisson's Ratios

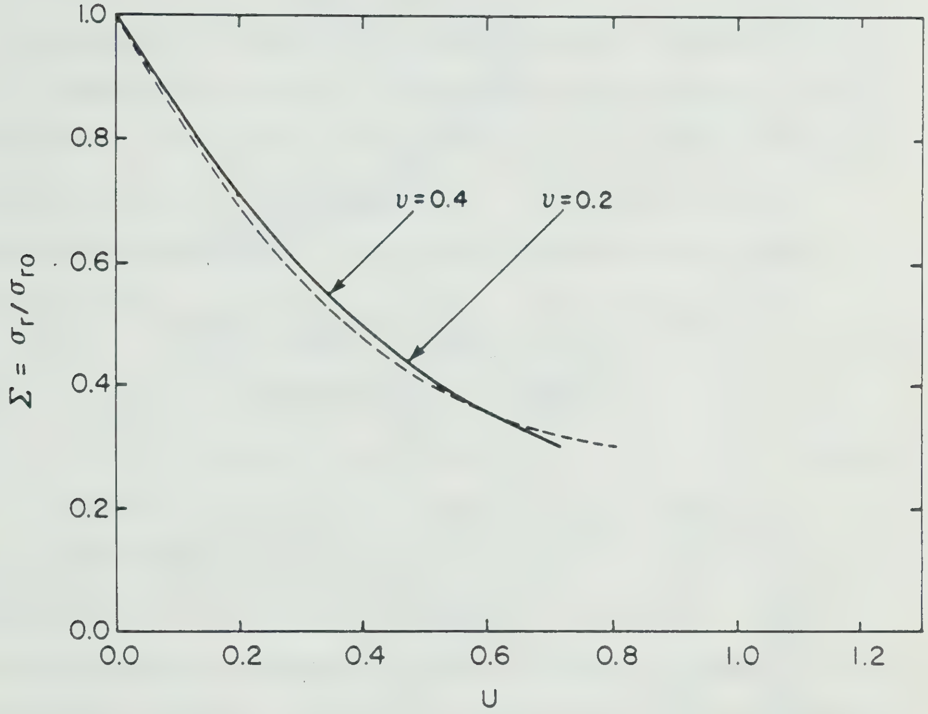

NOTE: $C = 0$, $\phi = 30°$, $K_0 = 1.0$, $n = 0$, $H/D = 3$, $D = 4m$

Figure 6.32 Normalized Ground Reaction Curves for the Floor, Calculated for Different Poisson's Ratios

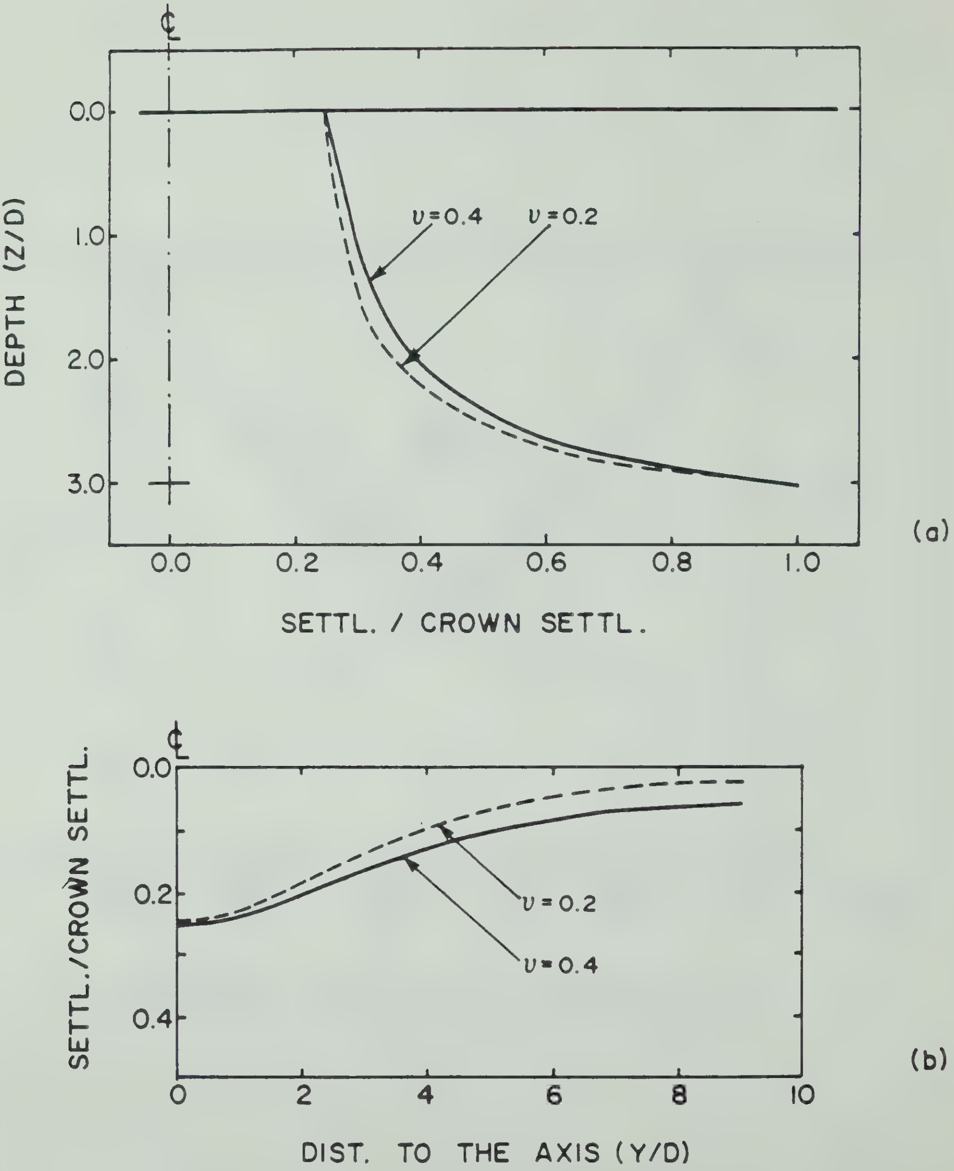

NOTE : C=0 , ϕ = 30°, K_0 = 1.0 , n = 0 , H/D = 3 , D = 4 m

Figure 6.33 Normalized Subsurface and Surface Settlements for 50% Ground Stress Release, Calculated for Different Poisson's Ratios

estimates of the maximum normalized surface distortion. As it can be seen from Figure 6.30, this simplification may imply overestimates of the dimensionless crown displacement of 16 to 23% for stress releases between 40% and 60%.

6.2.5 Ranges of Variables for the Parametric Analyses

The simplifications introduced in the previous sections allows the normalized ground reaction curves for a shallow tunnel in a soil whose behaviour is described by the cohesionless soil model presented in Section 6.2.2, to be written as:

$$F = f\left(\theta, \frac{\sigma_r}{\sigma_{ro}}, \frac{u_r E_{ti}}{D\ \sigma_{ro}}, \frac{H}{D}, K_c, \phi_e\right) \qquad [6.11]$$

Similarly for the frictionless soil model:

$$F = f\left(\theta, \frac{\sigma_r}{\sigma_{ro}}, \frac{u_r E_{ti}}{D\sigma_{ro}}, \frac{H}{D}, \frac{c_{ue}}{\gamma D}\right) \qquad [6.12]$$

The above equations, in these general forms, will be useful for the definition of the ranges of variables to be considered in the parametric numerical analyses. These ranges should be selected in order to cover the most common situations found in practice. To identify the latter, the data gathered in Tables 5.31 to 5.33 may be of some help. Data from some 53 case histories were included there. However, they may not be entirely representative of all practical situations to be encountered in practice for at least three reasons. The first refers to the fact that they include a fairly large number of tunnels built in certain locations, such as Frankfurt, London, Sao Paulo and Washington. This will have an effect on the conclusions drawn, since they will tend to be more representative of the conditions found at those locations. Secondly, the survey was conducted for a different purpose than the present one. It covered only case histories where substantial subsurface instrumentation data were available. Although this kind of instrumentation is fairly common in practice, it tends to be used only in relatively important projects. Therefore, the cases reviewed are typically large diameter tunnels, mainly for subway systems and only a few cases of smaller size tunnels, like those for sewerage or drainage, were analysed. Thirdly, the survey refers to tunnels that were predominantly built under good ground control conditions, which are normally found in good quality construction practices and in favourable grounds. Usually the cases did not entail ground collapses or pronounced time dependent responses. This is reflected in the review by the inclusion of a large number of tunnels driven through stiffer clays and only a few in softer clays or in other less stable grounds.

With these aspects in mind, the data contained in Tables 5.31 and 5.32 may be interpreted accordingly. Figure 6.34 presents the frequency distributions of the geometric variables. The majority of the cases reviewed had excavation diameters ranging between 5 and 7 m and soil cover between 10 and 14 m. Most frequently the ratio H/D varied between 1 and 2. It was shown, for both soil models proposed, that the NGRC does not depend on the size of the opening. Therefore, an arbitrary value of D, equal to 4 m, was selected and kept constant in the parametric analyses. The geometric variable to be considered is simply the H/D ratio. Three ratios of H/D were selected: 1.5, 3 and 6. These values cover most of the cases reviewed as noted in Figure 6.34.

Figure 6.35 shows the distributions of soil properties encountered in the case histories reviewed. As explained in Section 5.3.6.1, these properties represent average values for the ground around the tunnel profile. The E_{ti} values indicated represent drained as well as undrained moduli, depending on the type of ground response that was anticipated at each particular case history. This is explained in Section 5.3.6.1 and shown in Tables 5.31 and 5.32. The zero friction angle cases correspond to those tunnels driven through saturated clayey soils, where an undrained ground response may have developed. The non-zero friction angles correspond to cases classified as showing drained behaviour. The undrained cohesion values, of course, refer to those cases where the ground response was defined as undrained. About 28% of all tunnel cases reviewed were grouped in the undrained category.

As explained in previous sections in this chapter, particularly Section 6.2.4.1, the normalized ground response is independent of E_{ti} or of the Janbu's modulus K. Thus in the parametric analyses for the modelling step, it will be sufficient to arbitrarily choose any value of K. A constant K value equal to 400 has been therefore selected.

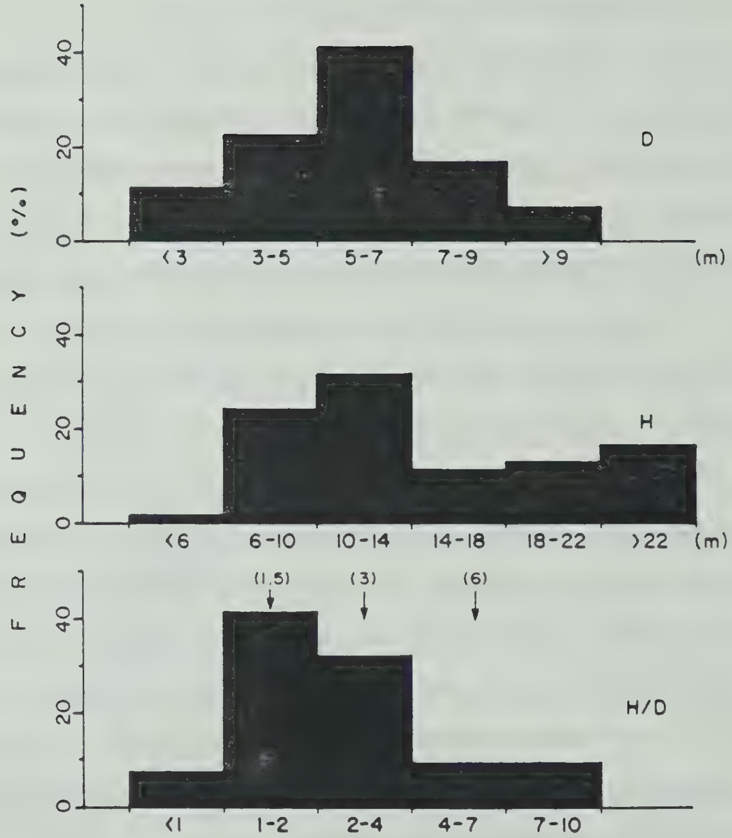

NOTES:
1. FREQUENCY FOR 53 CASES.
2. H/D SELECTED FOR THE PARAMETRIC ANALYSES, SHOWN IN BRACKETS.

Figure 6.34 Distributions of Sizes and Depths of Tunnels Reviewed

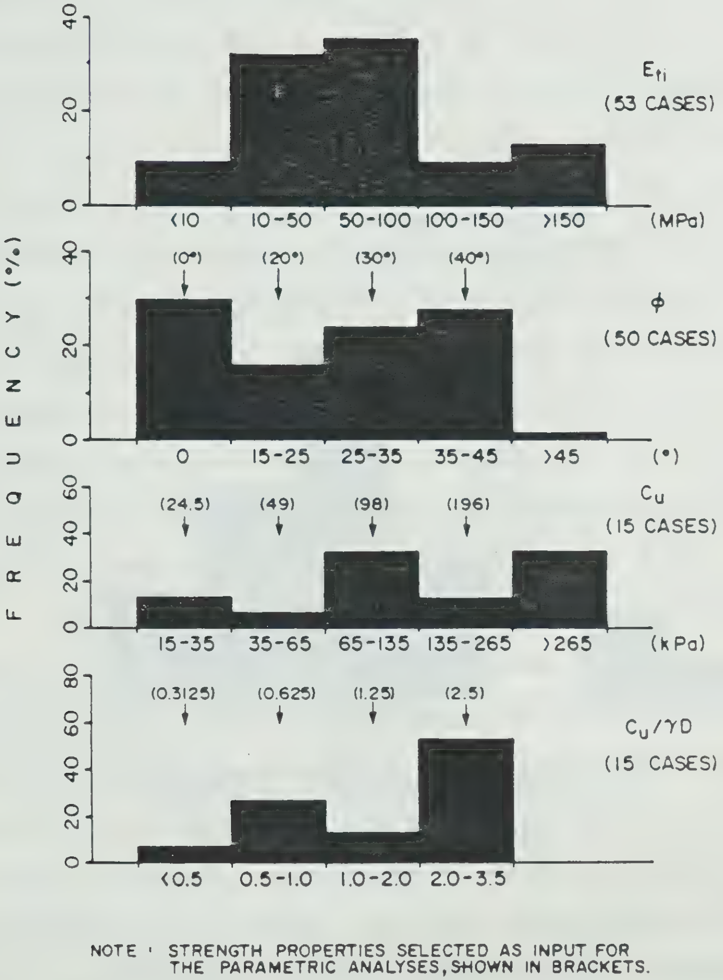

Figure 6.35 Distributions of Geotechnical Properties of the Grounds Through Which the Tunnels Reviewed were Driven

The friction angles found in the surveyed case histories varied considerably. Appropriately four values for ϕ were selected: zero (for the frictionless, undrained soil model), 20°, 30° and 40^0. These values almost entirely cover the ranges of friction angles likely to be encountered in practice, as indicated in Figure 6.34.

Four values of the undrained cohesion; c_u, were selected, covering almost the full range of c_u found in the survey (c_u=24.5 kPa, 49 kPa, 98 kPa and 196 kPa). More importantly, the undrained strength ratio, $c_u/\gamma D$, entirely covers the corresponding range found in the reviewed cases. Note that, as explained in Section 6.2.2, the normalized ground response does not depend on the unit weight of the soil. Thus a single and constant γ value equal to 19.6 kN/m^3 was selected and used in the parametric analyses.

Figure 6.36 shows the distribution of the in situ stress ratio, defined in terms of either total or effective stresses. Three values for in situ stress ratio have been selected for the parametric analyses: 0.6, 0.8 and 1.0. These values, as shown in the figure, typically cover more than 75% of the cases reviewed. Moreover, it was noted that the average in situ stress ratio for the undrained cases is close to unity, in support of the assumption made for the frictionless soil model set up in Section 6.2.3.

For completeness, Figure 6.37 was prepared in order to show the distribution of the construction methods used in the tunnels reviewed. It also includes the distance from the

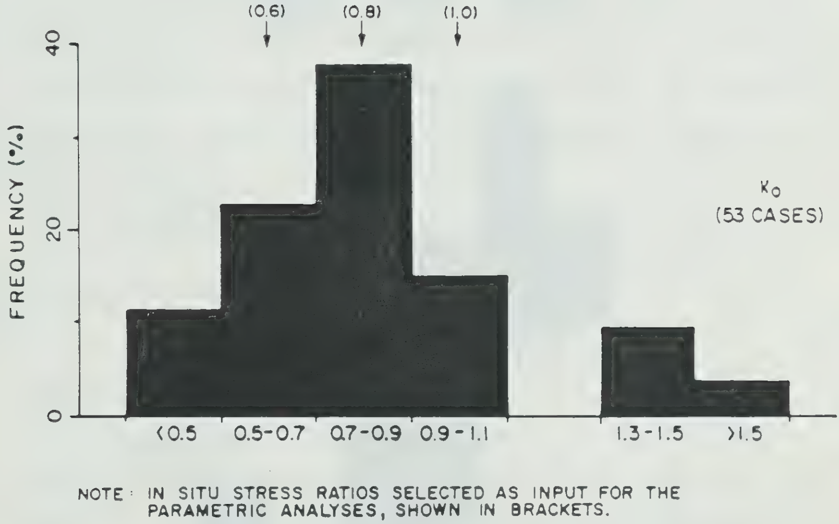

Figure 6.36 Distribution of the In Situ Stress Ratios in the Case Histories Reviewed

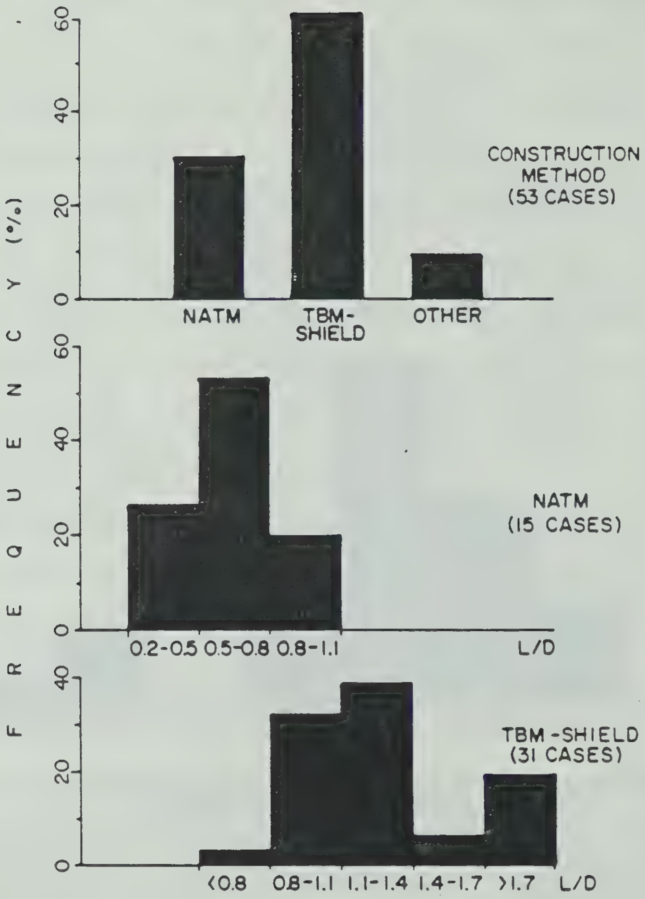

Figure 6.37 Distribution of Construction Methods and Distance of Support Activation in the Tunnels Surveyed

face at which the support was activated. One notes that while in the NATM cases, the lining is frequently closed at 0.5 to 0.8D behind the face, in TBM-shielded constructions the support is applied usually at 1.1 to 1.4D.

In summary, Table 6.8 lists the variables selected for the parametric analyses for both soil models. For the cohesionless soil model, 27 analyses were performed combining the parameters shown in the table. For the frictionless soil model, 10 analyses were conducted. The smallest undrained ratio $c_u/\gamma D$, was used only in connection with the smallest H/D case. These 37 parametric analyses were supplemented by some additional calculations which are described later on.

6.3 Parametric Analyses

6.3.1 Details of the Analyses

6.3.1.1 Number of Unloading Increments

All two dimensional finite element analyses were performed as described in Chapter 5 with full ground stress release in a single phase and with no lining installed. The number of steps adopted for the incremental unloading was defined after a number of trial runs, where different numbers of increments were tested, for different geometries and soil properties. To illustrate the influence of this factor, Figure 6.38 was prepared. It shows the NGRC for the

Cohesionless soil model

H/D	1.5	3.0	6.0
ϕ(°)	20	30	40
K_0	0.6	0.8	1.0
c (kPa)	0		
n	0		
K	400		
γ (kN/m^3)	19.6		
ν	0.4		
D (m)	4.0		
R_f	1.0		

Frictionless soil model

H/D	1.5	3.0	6.0	
C_u (kPa)	(24.5)	49	98	196
$C_u/\gamma D$	(0.3125)	0.625	1.25	2.5
K_0	1.0			
ϕ(°)	0			
n	0			
K	400			
γ (kN/m^3)	19.6			
ν	0.49			
D (m)	4.0			
R_f	1.0			

Table 6.8 Selected Variables for the Parametric Finite Element Analyses

tunnel springline for the case with H/D=3, $\phi=30°$ and $K_o=1.0$. The results of the two analyses are shown, one using ten constant increments to release the in situ stresses and another using twenty. In both cases, after 70% of the stress release, some elements at the crown, springline and floor failed and the numerical results thereafter were discarded.

It is noted that by increasing the number of steps, the ground response gets 'softer', with larger displacements being calculated for the same amount of stress release, as would be expected in an incremental solution of this kind. Unfortunately, the exact solution is not available for an assessment of the errors involved. A decision had to be made, therefore, balancing both technical and cost aspects.

Figure 6.39 furnishes the percentage by which the dimensionless displacement U at the tunnel contour calculated for 20 increments exceeds U calculated for 10 increments. For up to 60% of the stress release, the differences in U are typically less than 6%. However, as local failure is approached, that difference increases substantially. However, the differences in the calculated grounds settlement normalized to the crown settlement are appreciably smaller. Figures 6.40 (a) and (b) provide the differences in the normalized settlements along the depth of the cover and at the ground surface for a stress release of 50%. Although the absolute settlements for 10 increments are typically 4% smaller than that calculated for 20 increments, the normalized settlements for 10 increments are always

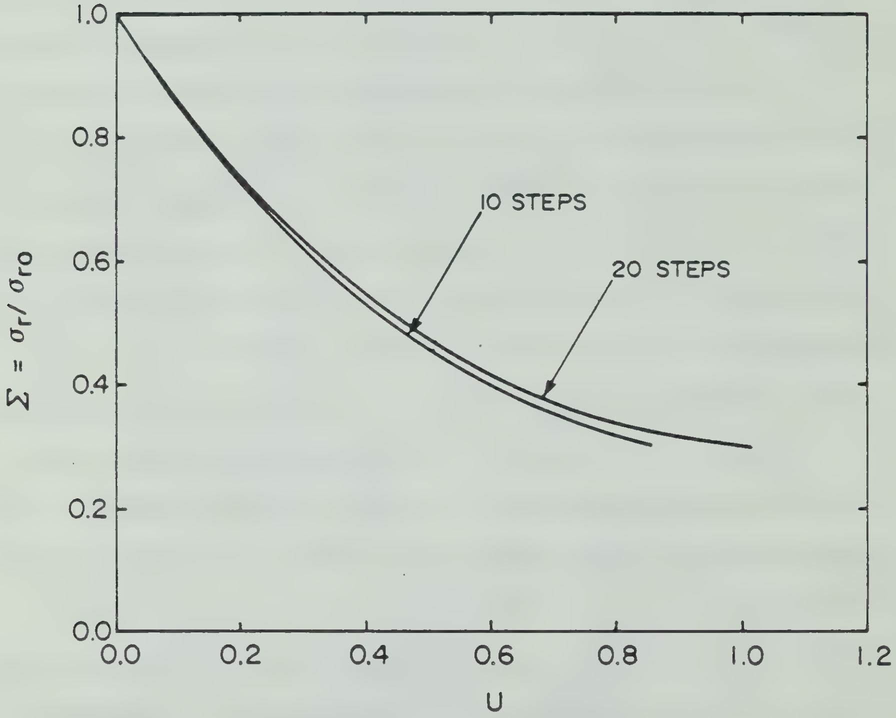

Figure 6.38 Normalized Ground Reaction Curve for the Springline Calculated for Different Numbers of Unloading Increments

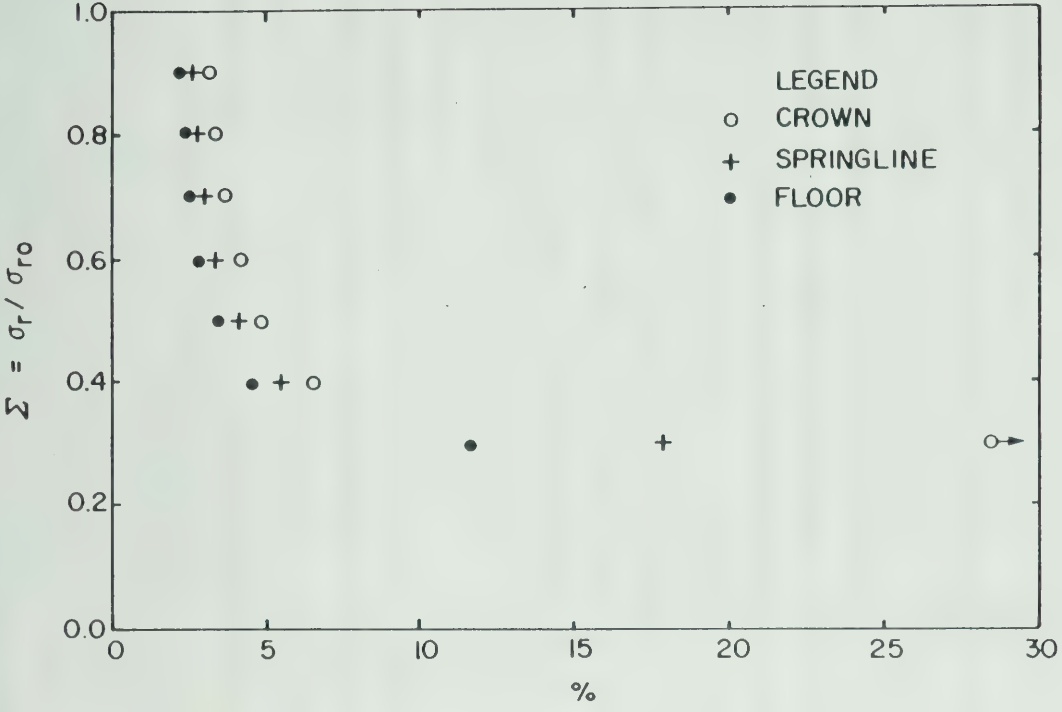

Figure 6.39 Difference in the Calculated Dimensionless Displacement U for Ten and Twenty Unloading Increments

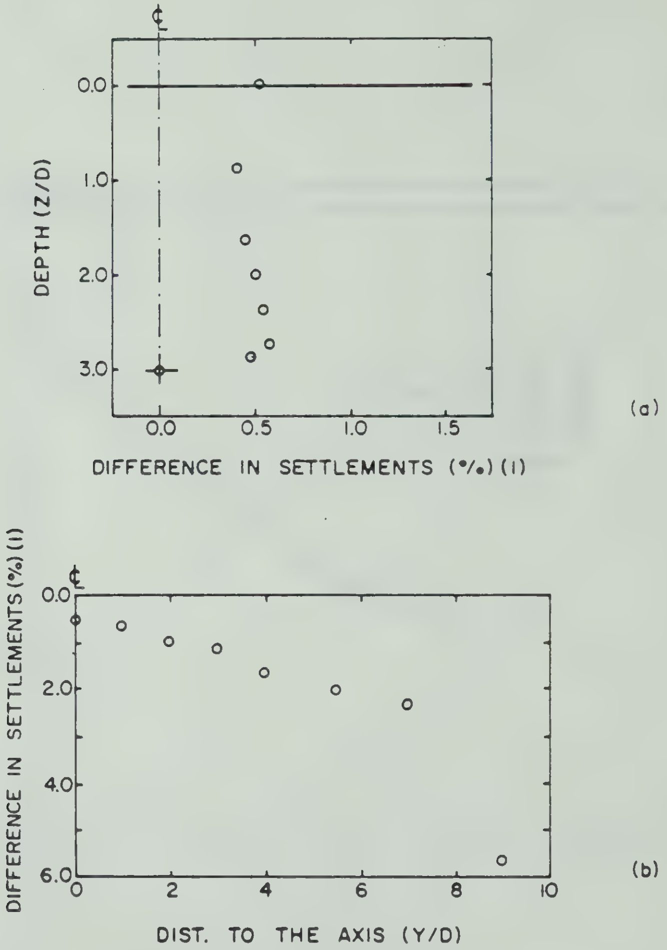

NOTE: DIFFERENCE IN SETTLEMENTS DEFINED AS:
$\{[\delta/\delta_c\ (N=10)] - [\delta/\delta_c\ (N=20)]\} \,/\, [\delta/\delta_c\ (N=20)]$
WITH N = NUMBER OF INCREMENTS, δ = SETTLEMENT,
δ_c = CROWN SETTLEMENT.

Figure 6.40 Differences in the Normalized Ground Settlements for Stress Release of 50%, Calculated for Ten and Twenty Unloading Increments

larger than for 20 increments. The subsurface normalized settlements for 10 steps exceed those for 20 steps by about 0.5%, as indicated in Figure 6.40(a). For the ground surface settlements, the difference is a minimum at the centreline and it increases with the distance to the axis, never exceeding 6% in this case.

Bearing in mind the other approximations introduced earlier and considering that the cost[14] of the analysis is directly related to the number of steps used, the 10 increment option was favoured and adopted. It should be remembered that the back analyses of case histories presented in Section 5.2.4 were all performed with five unloading increments for each construction phase, thus amounting to 10 increments altogether. Fairly reasonable results were obtained. The parametric analyses in 10 steps would thus roughly approximate the conditions met in the back analyses[15].

Regardless of the number of steps used, the incremental analysis will always yield an NGRC which will lie on the unsafe side where less displacement occurs for a given stress release. This error might be compensated for by other assumptions which led to conservative estimates of the NGRC (for instance, the c=0 and ν=0.4 assumptions), but this compensation cannot be assured. Some correction may possibly be introduced by considering a reduced soil strength.

---

[14] The unit cost of a 20 step computer run was about $45.00, at the low system rate. This was for a run involving 90 seconds of CPU time and 400 page-minute of CPU storage of virtual memory integral, at the U.of A. computer scheme, at 1984 costs. The ten increments run cost was about half that figure (Post-processing costs not included).

[15] Tan (1977:181) conducted similar non-linear analyses, also using a hyperbolic stress-strain model, and found it adequate to simulate the tunnel construction of a particular case history and to run parametric analyses using eight load increments.

6.3.1.2 Mesh Design and Influence of the Lower Boundary

The finite element mesh used in the parametric analyses was designed in accordance to the guidelines presented in Section 5.2.1.1 and as described in Section 5.2.2.1. A standard mesh, quite similar to that shown in Figures 5.12(a) to (c), was used. Layers of elements above the tunnel were removed or added according to the particular geometry of the problem being studied.

A major inconvenience resulted in adopting the constitutive soil models developed in Sections 6.2.2 and 6.2.3. This refers to the constant initial tangent modulus profile. While it provided potential generality to the projected solution, by ensuring similarity conditions not found otherwise, it made the calculated soil response to the tunnelling simulation sensitive to the position of the lower boundary of the finite element mesh. The influence of the position of this boundary on the surface settlements, calculated through a linear elastic soil model, was pointed out by Oteo and Sagesta (1982:654). When a non-linear elastic model is used, this influence is less pronounced but still discernible (see for instance, Tan, 1977:81). This is particularly true when the initial tangent modulus is constant with depth. All back-analyses of the case histories presented in Section 5.2.4 took into account the increase of the soil stiffness with depth. As explained in Section 5.2.1.1, for this condition, the position of the lower boundary does not have much effect on the results of the analysis.

To illustrate this aspect, some typical numerical results will be presented herein. They refer to finite element analyses carried out in ten unloading increments for the following conditions: $H/D=1.5$, $K_o=0.6$, $\phi=40°$, $c=0$, $n=0$, $K=400$ and $D=4$ m. In these analyses, the position of the lower boundary, where the nodal displacements were set equal to zero (rigid boundary), was varied. The vertical distance, V, between the tunnel floor and the rigid boundary was made equal to four distinct values: 0.5 D, 1.5D, 3D and 6.125D. In all cases, some elements at the springline failed after the ground stresses were released by 70%. The results after this event were disregarded. Figure 6.41 shows the NGRC of the tunnel crown, obtained through the gradual unloading of the unlined opening. As it is observed, as the rigid base is moved towards the tunnel floor (V/D decreasing), the crown response becomes "softer" and larger U values are obtained for the same amount of stress release. This behaviour does not reflect any "softening" mechanism of the tunnel cover. Rather, by reducing the thickness of the soil underlying the tunnel, the overall ground heave associated with the reduction of the ground stresses at the opening is reduced. The mechanism involved in the developement of such a heave

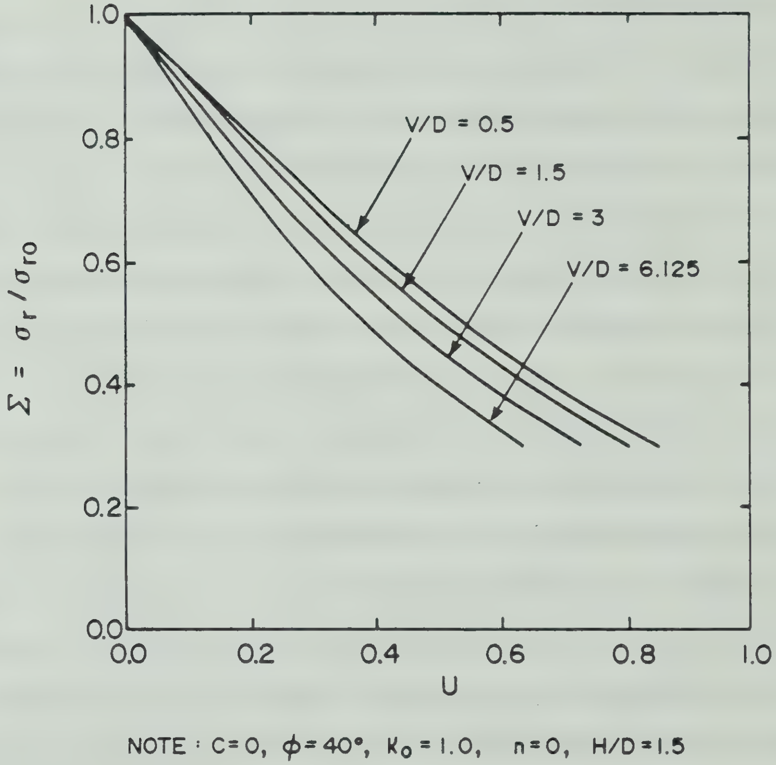

Figure 6.41 Normalized Ground Reaction Curves for the Crown, Calculated for Different Positions of the Lower Rigid Boundary

was discussed in Chapter 2, where it was explained to be a consequence of the gravitational stress gradient which is always active in a shallow tunnel. This heave is one of the components of the ground displacement. Thus, points above the tunnel which otherwise would move downwards as a result of the tunnel excavation, may show reduced net settlements. An infinitely thick layer of soil below the invert would theoretically lead to infinite upwards movement in the ground. Accordingly, by increasing V/D, the net settlement at the crown decreases.

By applying the same reasoning to the tunnel springline, one would conclude that its NGRC should not be much sensitive to V/D. Figure 6.42 does in fact demonstrate this: for all practical purposes the NGRC's do not change much for changes in V/D. A minor trend towards a "stiffer" response at this point is noted as the rigid base gets closer to the tunnel.

The strongest effect of the position of the lower boundary is noted, of course, at the tunnel floor. Figure 6.43 shows that as V/D decreases, the floor reaction gets "stiffer" and smaller invert heaves are noted for a given stress reduction.

The effect of the overall ground heave in partly compensating for the trend of the ground cover to settle is better illustrated in Figure 6.44. It shows the distinction between the normalized settlements of the ground cover along the tunnel axis, for a ground stress release of 50%. Note

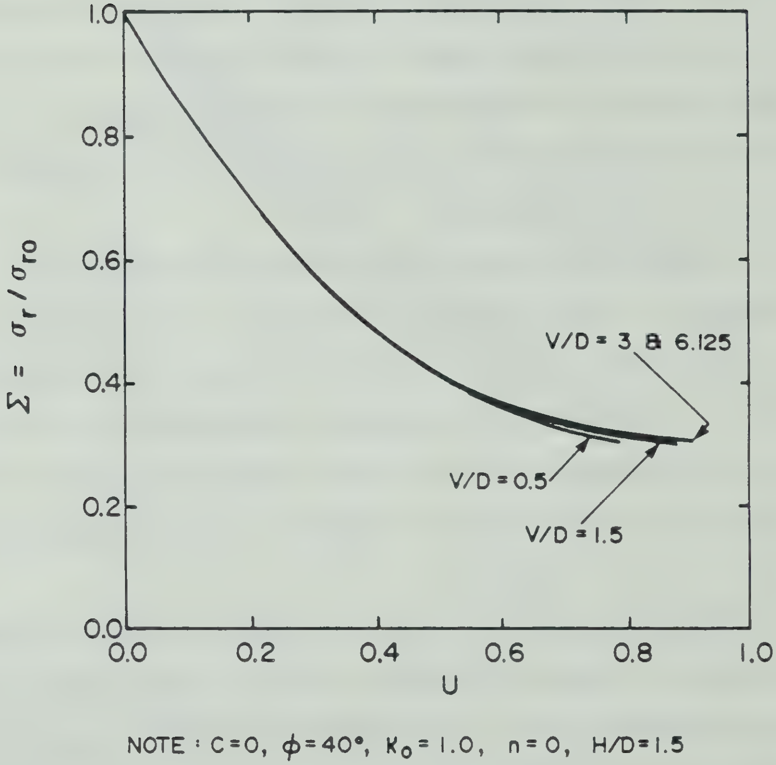

Figure 6.42 Normalized Ground Reaction Curves for Springline, Calculated for Different Positions of the Lower Rigid Boundary

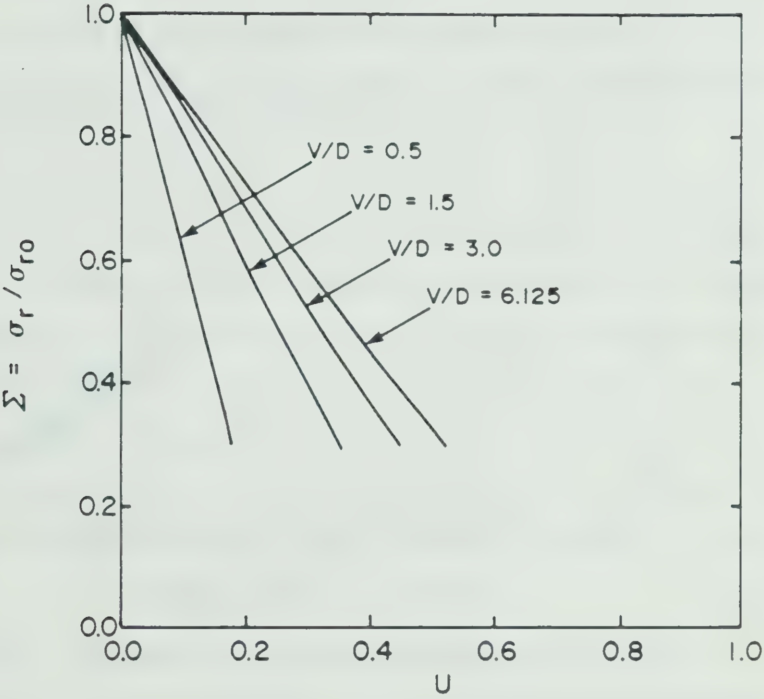

NOTE : C=0, ϕ=40°, K_0= 1.0, n = 0, H/D=1.5

Figure 6.43 Normalized Ground Reaction Curves for Floor, Calculated for Different Positions of the Lower Rigid Boundary

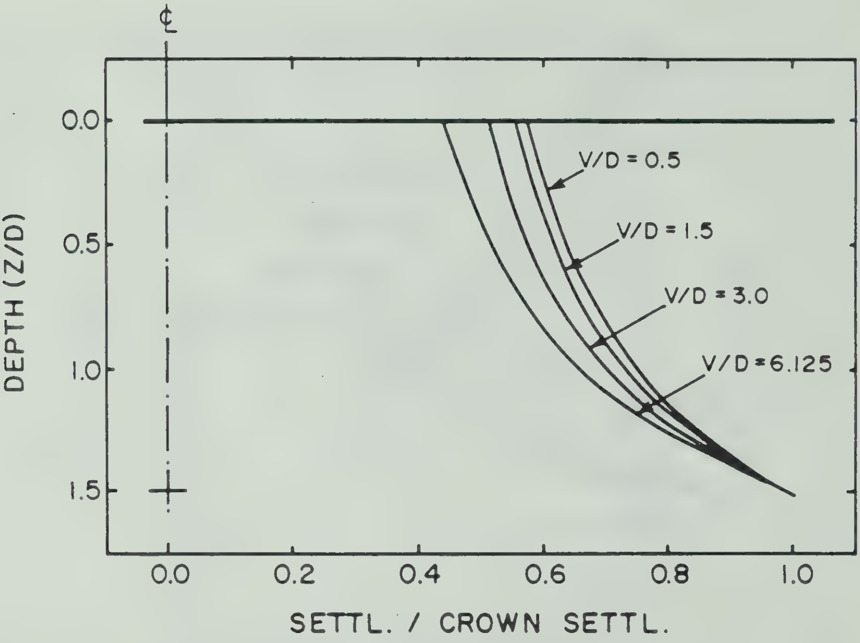

NOTE : C = 0, ϕ = 40°, K_o = 1.0 , n = 0 , H/D = 1.5

Figure 6.44 Distribution of Subsurface Normalized Settlements for 50% Ground Stress Release, Calculated for Different Positions of the Lower Rigid Boundary

that as before, the settlements were normalized to the corresponding crown settlement which leads to a settlement ratio of one at the crown. If the settlements are not normalized, as shown in Figure 6.45, the ground heave effect is perhaps clearer. The upward displacement components seem to act uniformly with depth in the cover along the tunnel axis, as the settlement difference at the crown and surface remains almost constant with V/D increasing.

Figure 6.46 presents the transverse profiles of the normalized ground surface settlements for a stress release of 50%, calculated for different V/D. The maximum normalized surface distortion does not appear to be affected much by V/D. However, the variation in V/D exerts considerable influence on the maximum normalized settlement and on the overall distribution of these settlements. The ground heave component does not seem to act uniformly over the ground surface and the resulting net distribution of settlements may depart considerably from the usual trough shaped profile. For certain conditions, the net surface movement beomes a heave, and again this is a very unrealistic result.

Other unrealistic results become evident as V/D increases. If it is remembered that in the present case where H/D=1.5, the ratio of radial in situ stresses at the tunnel floor and crown is equal to 5/3, an equal crown and floor displacement will be obtained when the ratio of dimensionless crown and floor displacements is also 5/3. It follows that by comparing Figures 6.41 and 6.43, one

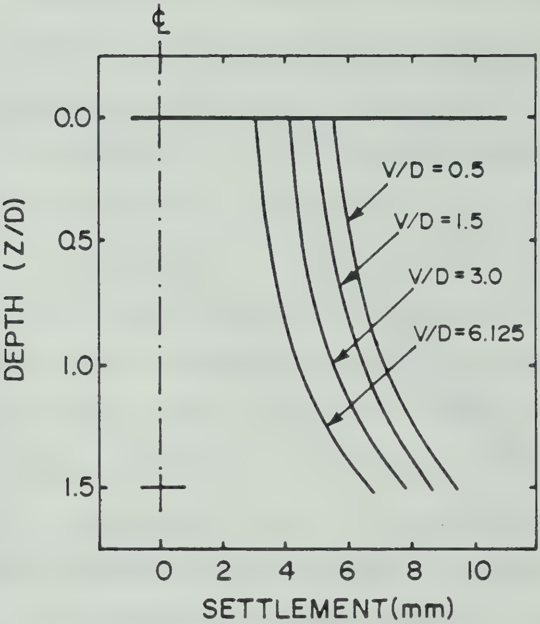

NOTE: $C=0$, $\phi=40°$, $K_0=1.0$, $n=0$, $k=400$, $H/D=1.5$, $D=4m$

Figure 6.45 Subsurface Settlement Distribution for 50% Ground Stress Release, Calculated for Different Positions of the Lower Rigid Boundary

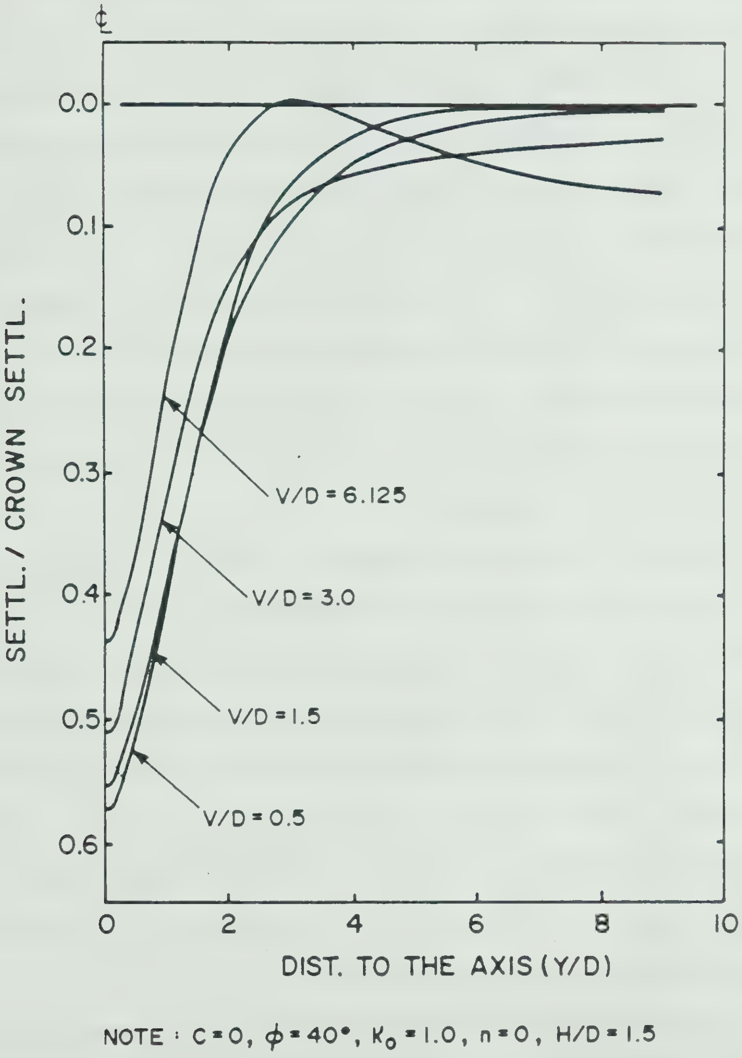

Figure 6.46 Transverse Profiles of Normalized Ground Surface Settlements for 50% Stress Release, Calculated for Different Positions of the Lower Rigid Boundary

concludes that for V/D equal to or greater than 3, the radial displacements at the floor are larger than that at the crown. This is also a result that is not substantiated in reality. To support this, Table 6.9 was prepared. It gives indications of final movements measured below the floor elevation in actual tunnels and in tunnel model tests. Unfortunately, it is not common practice to observe ground displacements in that region. Nevertheless, it is noted that the ratio of floor to crown displacements (u_f/u_c) is seldom greater than 0.5, and in particular, ratios exceeding 1.0 have never been recorded.

Table 6.9 also includes the location of points below the tunnel where no vertical movements were observed. The position of these points is given by y_o, the horizontal distance between the measuring point and the tunnel axis, and by z_o, the depth of this point below floor elevation. From this, one notes that ground movements were never observed at distances greater than 1.4D below the tunnel floor. Normally, the zero heave condition is noted at depths smaller than 1.0D below the floor.

From what has been discussed so far, one may conclude that by fixing the lower rigid base at distances greater than about 3D below the tunnel, unrealistic ground responses may result. These appear as excessive heave below the floor, and unlikely displacement fields above the crown. One would be thus tempted to reduce this distance to a minumum, and expect safer estimates of the ground movements above the

No.	Tunnel	Reference	D (m)	H/D	u_c (mm)	u_f/u_c	$y_0^{(1)}$ (m)	$z_0^{(2)}$ (m)	z_0/D	Notes
1	Frankfurt LH2	Brem (1981)	10	1.10	8.4	-	6.1	>1.8	>0.18	
2	Butterberg-Osterode	Meister and Wallner (1977)	11.5	1.27	$27.3^{(3)}$	-	7.5	1.9	0.17	
3	Regent Park (Sth B)	Barrat and Tyler (1976)	4.15	7.71	$25.2^{(3)}$	-	3.8	$5.8^{(4)}$	1.4	1st tunnel
4	Regent Park (Nth B)	Barrat and Tyler (1976)	4.15	4.29	$29.6^{(3)}$	-	4.0	$5.8^{(4)}$	1.4	2nd tunnel
5	Heathrow Cargo	Muir Wood and Gibb (1971)	10.9	0.67	$15.6^{(3)}$	$0.3^{(4)}$	0	$1.0^{(4)}$	0.1	
6	New Cross	Boden and McCaul (1974)	4.12	1.94	$29.1^{(3)}$	-	0	$4.0^{(4)}$	1	
7	Chinnor	McCaul et al (1976)	5.0	1.14	$26.8^{(3)}$	-	0	$5.0^{(4)}$	1	
8	Edmonton Experimental	Eisenstein et al (1981)	2.56	10.0	$56.3^{(3)}$	$0.4^{(4)}$	0	$2.5^{(4)}$	1	
9	Edmonton SLRT (Sth)	Branco (1981)	6.17	1.44	$39.4^{(3)}$	-	4.3	3.2	0.3	
10	S. Paulo ABV-NATM CC1	Negro and Eisenstein (1981)	4.04	1.54	8.8	0.8	0	4.2	1.04	
11	S. Paulo Horseshoe	Negro and Eisenstein (1981)	3.99	1.68	$17.7^{(3)}$	0.2	0	4.4	1.1	
12	S. Paulo - ARMCO	Negro and Eisenstein (1981)	3.66	1.58	20	≥0.15	0	2.8	0.77	
13	Thunder Bay II	Palmer and Belshaw (1980)	2.47	4.0	105	-	0	2.5	1	
14	Mulheim/Ruhr	Elmer (1980)	~9	1.2	26	-	6	≥4	≥0.44	Bentonite Shield in sand
15	Acton Grange (Sect. A)	Ryley et al (1980)	2.87	1.59	-	-	2	1.4	0.48	
16	Newcastle Sewer (BHJ)	McCaul et al (1983)	3.49	3.28	-	-	2.5	3.3	0.96	
17	Static Model Test (THI)	Casarin (1977)	0.038	1.20	6.5	0.38	0	0.015	0.4	Lining at X/D = 0.11
18	Static Model Test (THJ)	Casarin (1977)	0.038	1.28	1.5	0.4	0	0.015	0.4	Lining at X/D = 0.41
19	Static Model Test (No.3)	Cording et al (1976)	0.151	2.36	5.6	0.1	0	0.15	1	
20	Centrifuge Model Test (2DP)	Mair (1979)	0.060	1.60	7.0	0.14	0	0.06	1	LF=1
21	Centrifuge Model Test (2DV)	Mair (1979)	0.060	3.10	8.0	0.13	0	0.03	0.5	LF=1
22	Static Model Test (DC)	Seneviratne (1979)	0.060	0.95	1.5	0.27	0	0.03	0.5	LF=0.6
23	Munich U 519 B7 MQ1	Baumann et al (1985)	6.95	3.2	-	-	0	6.0	0.86	Sliding micrometer
24	Munich U 519 B6 MQ21	Amstad and Kovari (1984)	10.09	1.6	-	-	0	10.80	1.07	Sliding micrometer

Notes:
(1) Distance to the axis of point below tunnel floor where no ground movement was observed.
(2) Difference between floor elevation and elevation of point where no movement was observed.
(3) Extrapolated displacement to tunnel contour as indicated in Table 5.31.
(4) Estimated from displacement field around tunnel.

Table 6.9 Recorded Final Movements below Actual Tunnels and Tunnel Model Tests

opening. But this creates another difficulty which is explained in the following.

The general solution projected for the NGRC expressed by equations 6.11 or 6.12, would allow an estimate of the amount of stress release taking place before the lining activation, as explained in Sections 5.3.1, 5.4 and 6.1. Besides this, the NGRC could also provide an indication of the degree of ground "softening" taking place, while the ground stresses are reduced. This would be particularly helpful if the intended solution was to be used in connection with a ring-and-spring or a ring-and-plate model, in order to analyse the ground-lining interaction phase of the tunnel construction. The non-linear response of the ground could be partly taken into account in either of these models, by assigning elastic moduli to the soil that were compatible with the degree of straining taking place before the support is activated. In fact, this approach will be presented and discussed in following sections and in Chapter 7.

The slope of a ground reaction curve can be understood as corresponding to the radial spring constant or modulus of a ring-and-spring model. This type of model was reviewed in Section 4.3.2.4. If a single radial spring constant is to be used in this model to represent the ground, it was demonstrated in that section that, for tunnels in gravitational stress fields, with H/D between 1.5 and 6.0 and K_o between 0.6 and 1.0, a mean spring constant would be given approximately by:

$$\bar{k}_r = \frac{1}{1+\nu}\,\frac{E}{R} \qquad [6.13]$$

where E and ν are average elastic properties of the ground around the opening and R is its radius.

The development that led to the above equation assumed a gravitational stress field acting on a plate of infinite extent. In a shallow tunnel situation as the one being considered, the slope of the NGRC will of course reflect the limited depth of the cover or the presence of a rigid base. Hence, for a given set of elastic properties, k_r at the crown would decrease as H/D decreases and k_r at the floor would increase as V/D decreases. Not only would the local spring constant be altered by the position of the boundaries, but the average spring constant $\bar{k}_r$ would also be affected by them.

It was shown in Sections 5.2.4.2, 5.2.4.3 and 5.2.4.4 how the original in situ modulus of the tunnel is reduced as a result of stress release applied to the opening. It will be shown later in this chapter and in the following, how it is possible to obtain an estimate of the reduced soil modulus at the instant the lining is activated. Despite some degree of stiffening that may occur locally at the crown or floor due to the rotation of principal stresses, the ground modulus decreases on average as the in situ stresses are reduced at the opening. A reduced soil modulus should result even if the lining is installed right at the tunnel face (L/D=0).

If the rigid lower boundary is located too close to the tunnel floor, its effect on the floor NGRC can be so pronounced that the average ground modulus for a lining installed at the face may be greater than the in situ initial tangent modulus. This condition is not realistic and thus unacceptable. It was found to occur when V/D was set equal to 0.5 or less. After a very large number of trials covering different geometries, strength parameters and in situ stress ratios, it was found that the problem is avoided completely whenever V/D is set equal to 1.5 or more.

As a consequence of the above findings, it was decided to locate the lower boundary at a fixed distance below the tunnel floor equal to 1.5 D, in all parametric analyses. The results to be presented in the following sections are, therefore, strictly valid for a soil profile interrupted by a rigid horizontal base at 1.5 D below the tunnel. The results presented earlier in this chapter were derived from analyses where different V/D values were adopted: 1.5 (in Tables 6.2 and 6.3 and in Sections 6.2.4.2 and 6.2.4.3), 2.875 (in Table 6.1) and 3.0 (in Sections 6.2.4.1, 6.2.4.4 and 6.3.1.1).

6.3.2 Results of the Analyses

The large amount of data that was generated in the parametric analyses required a decision to be made regarding which aspects of the ground behaviour should be collated and interpreted. The need to relate tunnel closure to the amount of ground stress release at the opening called for the interpretation of the ground reaction curves at, at least three points of the tunnel profile (crown, springline and floor - represented shortly by C, S and F, respectively). Regarding the induced ground displacements, the minimum information required in the distribution of the ground settlements at the surface, and the distribution of subsurface settlements along the tunnel axis. The monitoring of these movements at these locations is the most frequently implemented activity in the observational control of shallow tunnel constructions.

Even after reducing it to a minimum, the numerical output data to be collated and interpreted amounted to something in excess of 5 000 pairs of data. This had to be classified and post-processed. To organize this information and to present it in a condensed form, a few routines were developed and included in the finite element program. The results to be presented and discussed herein refer to this post-processed output.

Recall that in all analyses after a certain amount of stress release had been imposed, soil failure developed locally at points adjacent to the opening. Whenever this happened, the finite element program assigned a very low tangent modulus to the failed elements. It was soon found that after this event, the ground stress-strain response ceased to be homothetic, and a unique normalized ground response could not be obtained. When the failure criteria was locally violated, the subsequent ground response, both in terms of NGRC or normalized settlement distributions, could not be reliably defined. This problem, in fact, was not unexpected, as the selected numerical model is actually unable to simulate this type of condition (see Sections 5.2.2.1 and 5.2.2.2). Accordingly, all numerical output after local failure occurred was disregarded.

In all analyses with the cohesionless soil model, failure was a consequence of excessive shearing. In some analyses with the frictionless soil model, tensile stresses developed. No attempt was made to numerically simulate the soil failure under tension and the resulting stress redistribution. As in the case of ground failure by shear, all numerical output after the local development of tensile stresses was disregarded.

The results of the parametric analyses in terms of normalized subsurface and surface settlements are included in Appendix C, in a compact graphic form. Some of these results are presented and discussed in the following sections.

6.3.2.1 Frictionless Soil Model Results

Effect of the Amount of Stress Release

Figures 6.47 to 6.49 present the results of an analysis for H/D=3 and $c_u/\gamma D=1.25$. One notes through the NGRC shown in Figure 6.47 a 'softer' response at the tunnel crown and a 'stiffer' one at the floor, due to the presence of the free stress ground surface closer to C, and to the rigid boundary